



ettc 2018

© Volocopter

© Italdesign

Conference Proceedings European Test and Telemetry Conference



©Audi

June 26th - 28th, 2018 in cooperation with
SENSOR+TEST 2018 Nuremberg, Germany

Proceedings

European Test and Telemetry Conference – ettc2018

26. – 28.6.2018, Nuremberg Germany

The European Test and Telemetry Conference – ettc2018 is organized by the European Society of Telemetry in cooperation with SENSOR+TEST 2018.

The European Society of Telemetry

Arbeitskreis Telemetry e.V.

Rudolf-Diesel-Straße 29a

82216 Gernlinden (Germany)

Tel.: +49 (0)8142-284582-0, Fax: +49 (0)8142-284582-2

info@telemetry-europe.org

www.telemetry-europe.org

President:

Renaud Urli – Airbus Helicopters Deutschland GmbH

Vice presidents:

Dr. Karen von Hünerbein – Lange-Electronic GmbH

Herb Wutz – Tel Data System GmbH

Treasurer:

Werner Lange – Lange-Electronic GmbH

This volume covers the proceedings of the European Test and Telemetry Conference – ettc2018, and contains the manuscripts of the lectures.

The authors are responsible for form and content of the papers.

AMA Service GmbH accepts no responsibility for the correctness and completeness of the details and the consideration of private rights of third parties.

Publisher:

AMA Service GmbH

Von-Münchhausen-Str.49 • 31515 Wunstorf / Germany

Tel. +49 5033 9639-0 • Fax +49 5033 9639-20

info@ama-service.com

www.ama-service.com / www.sensor-test.com / www.ama-science.org



Dear Telemetry Friends,

On behalf of the European Society of Telemetry, it is a great pleasure to welcome you to the European Test and Telemetry Conference 2018 in Nuremberg!

“Never touch a running system”: your feedback the previous years was so positive that we decided that the cooperation with SENSOR+TEST shall go on this year. The worldwide leading trade fair for sensing, measuring, and testing is the ideal platform for the conference participants to get inspired by the latest innovation in measurement technologies for all industries at the Nuremberg Convention Centre.

Urban mobility has left the concept phase and becomes now reality in many projects and products of our everyday life. Relying on telemetry technologies like data links, both Ground and Air Urban Mobility offer many technical and organizational challenges to our industries. The European Society of Telemetry is therefore proud to announce the presentations of Volocopter and Audi, two main actors in Urban Mobility, for the Opening Ceremony of ettc2018.

The ettc2018 technical program displays highly interesting presentations from authors across Europe and beyond. Networks, networks... and networks: they are everywhere. Papers focus this year on ground and airborne networks and on their architectures, but also show how security against interception / jamming / spoofing has to be considered.

This year's conference also features special technical sessions: AIM2018 – Advance In-Flight Measurement Symposium 2018, ICST General Session – International Consortium for Telemetry Spectrum, ETSC Open Meeting – European Telemetry Standardisation Committee.

Education and training in the fields of telemetry is one of the missions of the European Society of Telemetry. ettc2018 conference participants have the opportunity to attend a free Short Course on the new standard IRIG 106 Chapter 23, Metadata Description Language MDL.

The technical papers are merged in these Conference Proceedings. You can find here the latest and most promising methods but also hardware and software ideas for the telemetry solutions of tomorrow!

The ultimate success of the conference remains entirely dependent upon your continued patronage. So thank you very much for supporting ettc2018!

We are always seeking ways to improve the European Test and Telemetry Conferences. Please contact us with ideas, critiques, suggestions, and visit us on www.telemetry-europe.org.

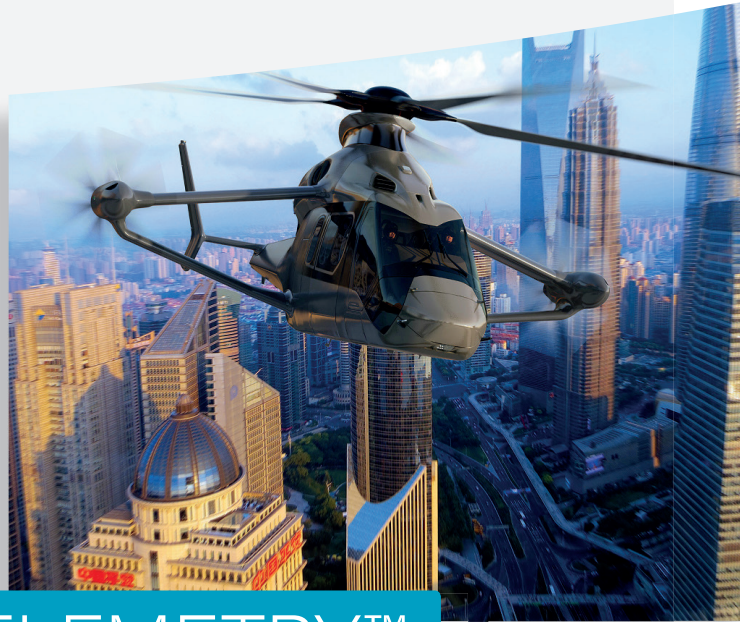
We're looking forward to meeting you!

A handwritten signature in blue ink, appearing to read 'R. Urli'.

Renaud Urli
President of the European Society of Telemetry

ZODIAC DATA SYSTEMS

 **ETTC, Booth 2-312**



WE ARE TELEMETRY™



ACQUIRE



RECORD



TRANSMIT



TRACK



RECEIVE



PROCESS



REPLAY



As a world leader in telemetry, Zodiac Data Systems is the only provider offering the entire IRIG106 & CCSDS datalink from data acquisition to decommutation and display for flight testing.

GLOBAL SALES

5, Avenue des Andes - CS 90101 - 91978 Courtaboeuf Cedex - FRANCE
Tel.: +33 1 69 82 78 00 - Email: sales.zds@zodiacaerospace.com

USA

11800, Amber Park Drive - Suite 140 - Alpharetta, GA 30009 - USA
Tel.: +1 770 753 4017 - Email: sales.zds@zdsus.com

ZODIAC DATA SYSTEMS

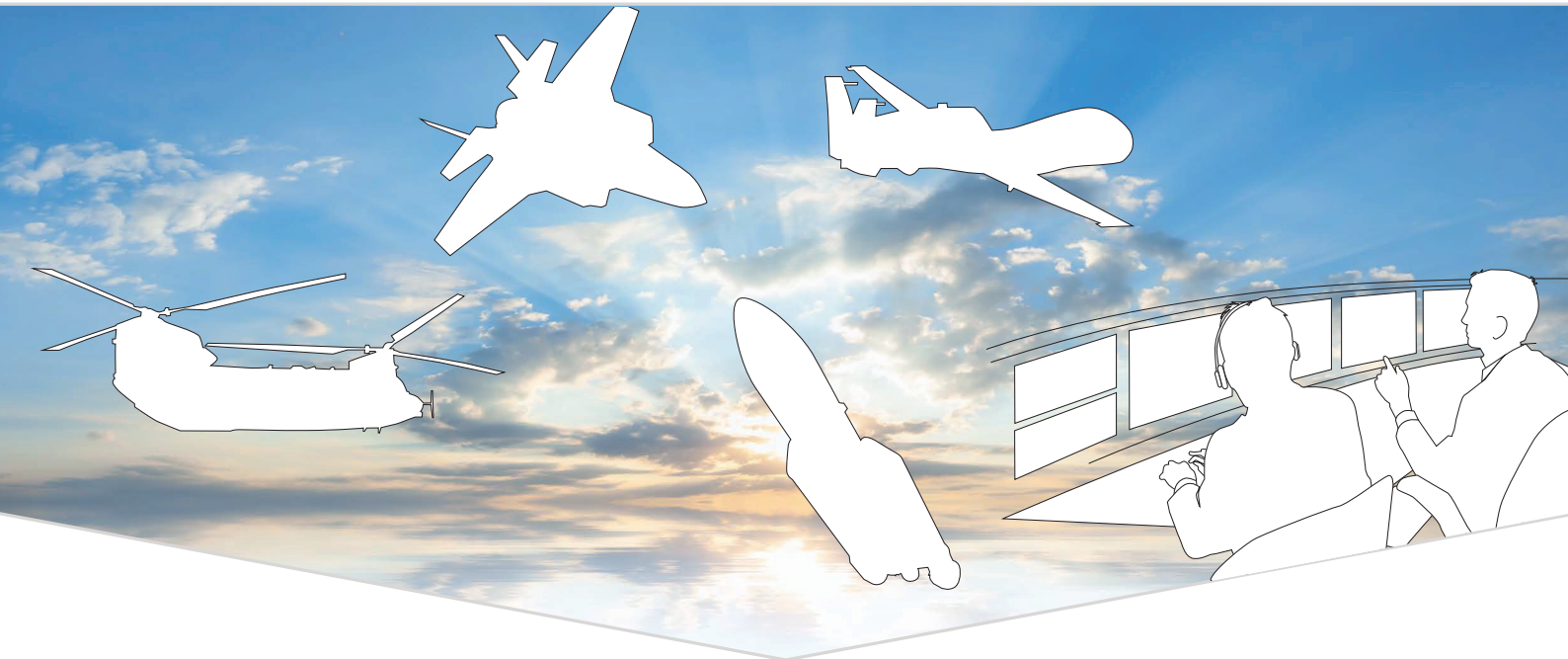
ZODIAC AEROSYSTEMS
Control Systems Division



With the courtesy of Lockheed Martin, Airbus Helicopters, Boeing, Thales Alenia Space

COMPLETER.NET

WE DEVELOP BUSINESS ...



... BY BUILDING ROADS BETWEEN MANUFACTURES AND USERS.

FLIGHT TEST INSTRUMENTATION



- + *Ground Station Recorder*
- + *Telemetry Receiver*
- + *Realtime-Processing Software*
- + *Post Mission Data Mining Software*



- + *Airborne Flight Test Instrumentation Recorders Fixed & Rotary Wing*
- + *Mission Recorders*
- + *Multi-purpose Integrated Airborne Routers, Processors and Recorders*

THE H145. MAKES LANDING IN A STORM A BREEZE.



FLY
WE MAKE IT

It's no surprise the H145 is the helicopter of choice for rescue missions. Whether at sea, on a mountain or in a blizzard, it can bring help to where it's needed. Compact and versatile, it provides outstanding flight performance under the most extreme conditions.

Resilience. We make it fly.



1. Sensors

Chairman: Stephen Lyons, QinetiQ, Ceredigion (Great Britain)

- | | | |
|------------|--|-----------|
| 1.1 | New high-temperature ICP®-vibration sensors with overload protection to improve measurement uncertainty and reduce measurement errors | 12 |
| | S. Meyer, PCB Synotech GmbH, Hückelhoven (Germany) | |
| 1.4 | Rotor Loading Test with Wireless Transmitting | 17 |
| | M. Yaping, L. Ming, H. Jing, G. Shipeng, L. Peng, Flight Test Establishment of China, Xi'an (China) | |
| 1.7 | Vibration Test of Airplane Moving Surface with Wireless Sensor | 24 |
| | H. Jing, M. Yaping, L. Ming, L. Tielin, Z. Xingchang, Chinese Flight Test Establishment, Xi'an (China) | |

2. Modulation & Coding

Chairman: Philipp Wager, Airbus Defence and Space GmbH Flight Test Ground Station (FTGS), Manching (Germany)

- | | | |
|------------|--|-----------|
| 2.1 | Transhorizon over-sea propagation tests with Line-of-Sight Lygarion® Data Link technology | 29 |
| | A. Fihef, J. Maillieux, J. Ernst, HENSOLDT France, Plaisir (France) | |
| 2.2 | Telemetry Standards That Improve Link Availability | 37 |
| | K. Temple, Air Force Test Center Edwards AFB, California (USA) | |
| 2.3 | History and Advantages of Best Source Selection for Today's Modern Telemetry Applications Along With the Benefits of Different Approaches | 48 |
| | S. Nicolo, GDP Space Systems, Horsham, Pennsylvania (USA) | |
| 2.4 | Launch Vehicle Electrical Power System Rocket-ground Wireless Interface Prototype | 55 |
| | J. Zhang, X. Bi, X. Wang, W. Zhu, Beijing Institute of Astronautic Systems Engineering, Beijing (China) | |

3. Data Management Standards

Chairman: Mahmut Kürsüd Arpacioğlu, TAI Turkish Aerospace Industries, Inc., Kazan-Ankara (Turkey)

- | | | |
|------------|---|-----------|
| 3.1 | Next Generation Vehicle Diagnostics | 61 |
| | J. Supke, emotive GmbH & Co. KG, Ostfildern (Germany) | |
| 3.2 | Configuring Applications based in XdefML | 68 |
| | J. A. Gonzalez Pastrana, Airbus Defence and Space, Getafe, Madrid (Spain) | |
| 3.3 | A JSON transactional data server for flight tests | 71 |
| | O. Gigato Rodriguez, Airbus Defence and Space, Getafe, Madrid (Spain) | |

4. RF Design

Chairman: Mark McWhorter, Lumistar, Inc., Carlsbad (USA)

- 4.1 Hardware Acceleration for Beamforming Algorithms based on Optimized Hardware-/Software Partitioning 78**
R. Schmidt, S. Blokzyl, W. Hardt, Technische Universität Chemnitz, Chemnitz (Germany)
- 4.2 Experimental Measurements and Antenna Isolation for TETRA Communication System in Underground Mining and decline 87**
B. Bazargur, O. Bataa, Z. Khurelbaatar, B. Battseren, School of Information and Communication Technology, Mongolian University of Science and Technology (Mangolia)
- 4.3 Design of Telemetry System for Low Orbit Satellite Based On Short Message Service of BeiDou III Navigation Satellite System 94**
S. Ding, Beijing Space Quest Ltd., Beijing (China)

5. Time-Space position technologies

Chairman: Pilar Vicaria Torralbo, Airbus Defence and Space, Pinto (Spain)

- 5.1 Position Tracking for Outdoor Sport Events with GNSS and LoRa 97**
J.-M. Gruber, B. Brossi, Institute of Embedded Systems, Zurich University of Applied Science, Winterthur (Switzerland)
- 5.2 LORA based Biotelemetry System for Large Land Mammals 101**
K. C. Grande, F. F. Hilario Gomes, E. L. Santiago, B. Schneider, P. M. Gewehr, V. H. Dambrat Bergossi, B. Schneider Jr, Federal University of Technology, Paraná (Brazil)
- 5.3 Testing Acquisition of GPS / GNSS Location and Velocity to Improve Safety in Autonomous Driving 106**
K. von Huenerbein, W. R. Lange, Lange-Electronic GmbH, Gernlinden (Germany)

6. Networks & Architectures

Chairman: Gerald Escriva, Safran Aircraft Engines, Coudoux (France)

- 6.1 MIL-STD-1553B and it's potential for the future 114**
H. Plankl, AIRBUS Defence and Space, Manching (Germany)
- 6.2 Sabotage and Disclosure of Flight Test and other reasons & methods to intercept, jam or spoof telemetry 123**
M. Niewoehner, COMPLETER.NET Sales & Engineering GmbH, Hamburg (Germany)

7. AIM 2018

Chairman: Fritz Boden, Deutsches Zentrum für Luft- und Raumfahrt e. V. (DLR), Göttingen (Germany)

- 7.1 Application of Fibre Optic Range-Resolved Interferometric Vibrometry to a Full-Scale Feathered Propeller in a Wind Tunnel 130**
N.J. Lawson, T. Kissinger, S.W. James, R.P. Tatam, School of Aerospace, Transport and Manufacturing, Cranfield University, Cranfield (Great Britain); M.V. Finnis, Defence Academy, Cranfield University, Shrivenham, Wilts (Great Britain)
- 7.2 Optoelectronics System for Estimating Measurement Error of Image Pattern Correlation Technique 136**
T. Kirmse, F. Boden, German Aerospace Center (DLR), Goettingen (Germany); A. Y. Poroykov, K. M. Lapitskiy, Y. V. Ivanova, I. A. Lapitskaya, National Research University "Moscow Power Engineering Institute", Moscow (Russia)

7.3	Application of Fibre Bragg Grating Sensors to a Stalled High Lift Wing	143
	E. Alcusa-Saez, S. W. James, S. Prince, E. Chehura, N. J. Lawson and R. P. Tatam, School of Aerospace, Transport and Manufacturing, Cranfield University, Cranfield (Great Britain)	
7.4	Optical Rotor-Blade Deformation Measurements using a Rotating Camera	147
	F. Boden, B. Stasicki, German Aerospace Center, Institute of Aerodynamics and Flow Technology, Göttingen (Germany), K. Ludwikowski, HARDsoft Microprocessor Systems, Kraków (Poland)	

8. Spectrum Efficiency

Chairman: Timothy A. Chalfant, COLSA Corporation, Palmdale, California (USA)

8.1	Integrated Network Enhanced Telemetry (iNET): Impact to the Telemetry Community for the ettc2018	155
	T. Young, USAF Air Force Test Center, California (USA)	
8.2	Creating the Future Test Range Infrastructure: Vision for a Wireless Inter-Range Network Environment	162
	T. O'Brien, U.S. Department of Defense Test Resource Management Center, Arlington (USA)	
8.3	Ninja Telemetry: AMT Survival in a Congested Spectral Environment	167
	T. A. Chalfant, COLSA Corporation, Palmdale, California (USA)	
8.4	Telemetry Network Standards Overview	175
	T. B. Grace, Naval Air Systems Command (NAVAIR), Patuxent River, Maryland (USA); B. A. Abbott, Southwest Research Institute® (SwRI®), San Antonio, TX, (USA)	

9. Data Acquisition

Chairman: Michael Tänzer, Airbus Defence and Space GmbH, Flight Test Ground Station (FTGS), Manching (Germany)

9.1	Telemetric acquisition of vitality parameters and classification of cognitive condition via machine learning	179
	M. Bussas, TROUT GmbH, Kassel (Germany)	
9.2	DASP Towards a Generic Data Acquisition Configuration System	185
	M. Gonzales Martin, J. A. Gonzalez-Pastrana, C. Behr, T. Brueggemann, C. Rominger, K. Keil, S. Montes-Sanchez, R. Paredes-Huertas, Airbus Defence and Space, Getafe (Spain)	
9.3	Integrated Data Acquisition Solutions for Aerospace Platforms with highly restrictive space and weight requirements and harsh environmental conditions	190
	P. Quinn, Curtiss-Wright, Aerospace Instrumentation, Dublin (Ireland)	
9.4	Design of a minimum weight/space/energy consumption instrumentation system	198
	F. Mertl, R. Urli, Airbus Helicopters Deutschland GmbH, Donauwoerth (Germany)	
9.5	Inflight-Measurements of Aircraft Undercarriage Vibration during Deployment	202
	J. Schwochow, J. Sinske, R. Buchbach, DLR Institute of Aeroelasticity, Goettingen (Germany)	

10. Imaging & Video

Chairman: Christian Herbepin, Airbus Helicopters, Marignane (France)

- 10.1 A400M. Flares trajectories calculation from a chase aircraft 210**
 F. Coll Herrero, I. Lopez Herreros, Flight Test Analysis Tools Team Leader/Development Flight Test, Airbus Defense and Space, Getafe, Madrid (Spain)
- 10.2 PARIS - Parallelisation Architecture for Real-time Image Data Exploitation and Sensor Data Fusion 217**
 M. Nagler, S. Blokzyl, R. Schmidt, W. Hardt, Technische Universität Chemnitz, Chemnitz (Germany)
- 10.3 Applications of Machine Vision in Flight Test 224**
 H. Ibaroudene, A. J. Whittington, B. A. Abbott, M. L. Moodie, P. M. Westhart, Southwest Research Institute, San Antonio (USA)
- 10.4 Method and Software to Perform Pitch Drop 228**
 N. P. O. Leite, A. Y. Kusumoto, Instituto de Pesquisas e Ensaios em Voo, Sao Jose dos Campos (Brazil), L. E. Guarino de Vasconcelos, C. M. Araujo Lopes, Instituto Tecnológico de Aeronautica, Sao Jose dos Campos (Brazil), L. Roberto, Instituto Estudos Avancos Espaciais, Sao Jose dos Campos (Brazil)
- 10.5 Low Level Flight Monitoring - High performance graphics 238**
 A. Rodrigo López Parra, Airbus Defence and Space, Sevilla (Spain)

11. Networks & Data acquisition

Chairman: Sergio Duarte Penna, EMBRAER, Sao Jose dos Campos (Brazil)

- 11.1 Intelligent Networked Flight Test Instrumentation for a new Fighter Prototype 243**
 G. Martinez Moran, Airbus Defence & Space, Getafe, Madrid (Spain)
- 11.2 Progress and Future Perspectives in Airborne Communication Networking 250**
 K.-D. Büchter, Bauhaus Luftfahrt e.V., Taufkirchen (Germany)
- 11.3 Design and Implementation of a Long Range Autonomous Wireless Critical System and its Application in Remote Hydroelectrical Infrastructure (Water Canals) for Risk Prevention and Hazards in Case of Hydraulic Canals Breaks. 258**
 Fco. J. Fernández Huerta, Fco. J. Alonso Caballero, KUNAK Technologies S.L., Noain (Spain), L. J. Etayo Pérez, Acciona Energía S.A. Sarriguren (Spain)
- 11.4 Real-Time access to past measurements using bidirectional communication (TmNS) 268**
 H. Körtzel, C. Büchner, Airbus Defence and Space GmbH Flight Test Instrumentation, Manching (Germany), G. Martinez Moran, Airbus Defence and Space S.A.U., Getafe (Spain)
- 11.5 System for Aircraft Data Value Demonstration 273**
 S. Martin, AIRBUS Operations SAS, Toulouse (France)
- 11.6 How to connect a sensor to the Internet 277**
 T. Schildknecht, Schildknecht AG, Murr (Germany)

12. Data Management Applications

Chairman: Pedro Rubio, Airbus Defence and Space, Getafe (Madrid) (Spain)

12.1	Real Time Data Validation Embedded System for Flight Test Using Common Portable Devices	279
	N. P. O. Leite, A. Y. Kusumoto, W. O. Lima, Instituto de Pesquisas e Ensaio em Voo, Sao José dos Campos (Brazil)	
12.2	A case study in creating flexible FTI configuration software	285
	A. Cooke, Curtiss-Wright, Aerospace Instrumentation, Dublin (Ireland)	
12.3	A Process Model for the Discovery of Knowledge in Sensor-Based Indoor Climate Data	293
	D. Gruedl, T. Wieland, Fraunhofer Application Center for Wireless Sensor Systems, Coburg (Germany)	
12.4	Machine Learning-Driven Test Case Prioritization Approaches for Black-Box Software Testing	300
	R. Lachmann, IAV GmbH, Gifhorn (Germany)	
12.5	Improving the efficiency of T&E for Aircraft and Mission Systems with more effective modeling and simulation	310
	P. Aves, J. Baxter, Analytical Graphics Incorporated, Exton, PA (USA)	
	Key Words	316

New high-temperature ICP®-vibration sensors with overload protection to improve measurement uncertainty and reduce measurement errors.

Stefan Meyer

PCB Synotech GmbH
Porschestrasse 20-30
41836 Hückelhoven

Abstract

ICP® technology is an integral part of electronic measuring technology combined with sensors. We find this two-wire technology in laboratories, test benches, in production, in monitoring systems and mobile test installations. Even if it is a simple and proven technique, you should pay attention to some parameters in the sensor selection. New developments provide additional protection against unwanted overloading and also offer higher temperature stability, which improves the values of the measurement uncertainty by a factor of 10.

In the lecture the problem of overloading will be discussed. With examples from practice regarding the reasons for a overloading, detection and prevention. Various application examples are shown. The use of newer generation piezoelectric materials such as the UHT-12™ industrial single crystal significantly improves the measurement uncertainty and quality of the measurement signals. The technical characteristics of this material are explained and the advantages of using it as a measuring element are shown.

Key Words

ICP®, UHT-12™, Low Temperature Coefficient (LTC), Ferroelectric Ceramics, Acceleration Sensors, Overload, Low Pass Filter,

The requirements for ICP® Vibration Sensors changed.

The ICP®-Technique was originally developed for modal- and structural analysis and was also used in vibration machine monitoring as well as applications in research and development. Here, more and more often the limits in temperature and frequency bandwidth were reached. The results are faulty measurement data or defective sensors.

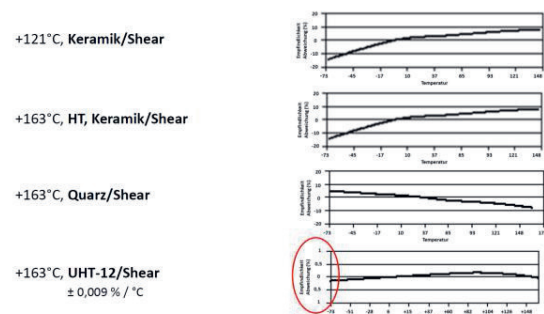
Particular attention must be paid to the materials used for use in space application in order to minimize the outgassing of materials in a vacuum. In addition, there has been a growing interest in being able to use ICP® Vibration sensors even at higher temperatures.

More than 40 years ago, when the ICP® piezoelectric sensor technology was introduced by Piezotronics, Inc., the upper temperature limit was 121°C for a long time. This changed with the development of ICP® models with special high-temperature amplifier electronics that could be used up to 163°C. Continuous development

allowed PCB® to expand its range of applications and improve precision. Current state of the art is the achievement of a continuous operating temperature for ICP® sensors of +180 °C with the three-axis measuring models HT356B01 and TLD339A37.

ICP® is a technology with many variations.

Looking at the circuit diagram of an ICP sensor, two components are visible (Figure 1). This is the piezoelectric measuring element and an amplifier or impedance converter. In the sensor part we have the possibility of mechanical design and selection of the piezoelectric material. The electronics offer the possibility of high integration and implementation of additional functions such



as filters, amplification and automatic parameterization (TEDS).

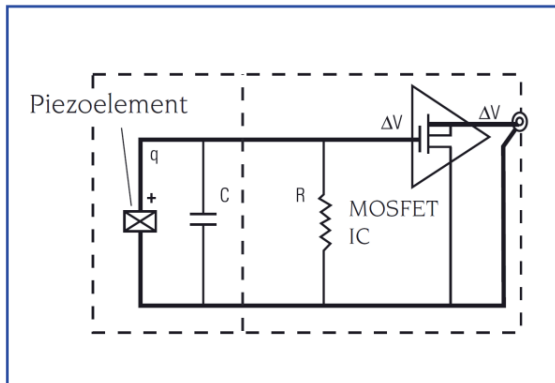


Figure 1: ICP®-Technology (IEPE)

The piezoelectric material is the cause of high measurement uncertainty.

The selection of the piezoelectric material depends on the size, the measuring range, the temperature range and the desired measurement uncertainty. As materials are available versions of the family of ferroelectric ceramics, quartz or industrial single crystals (UHT-12). In recent vibration sensor developments, single crystals such as UHT-12 are used, which have extremely good stability with larger temperature changes. This is an important feature when used in a climate chamber, engine test benches or gas turbines. If we compare the trend of sensitivity over temperature for equivalent sensors with different piezoelectric materials, we can see considerable differences (Figure 2).

Figure 2: Comparison: Temperature coefficients / sensitivity changes over temperature. Comparable vibration sensors with 10mV / g.

The range of measurement uncertainty has a bandwidth of 1.5 to 25% and more. The best results are achieved by the sensors with the UHT-12 single crystal. There is now a whole product family of uniaxial and triaxial vibration sensors available with this piezoelectric material, even in different sizes (Figure 3).

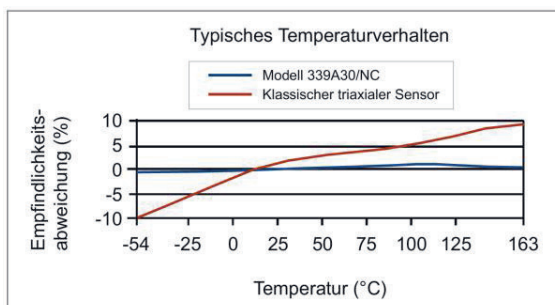


Figure 3: Temperature response of the sensitivity: standard vs. UHT-12 (339A30 triaxial).



Figure 4: Series 339 products

The relationship between operating temperature and sensitivity is called the temperature coefficient of sensitivity. Since the relationship between temperature and sensitivity is not linear, model-specific characteristics are shown on the data sheets of the sensors and in this brochure, which show the course over the entire temperature range. To minimize the temperature error, sensors with low temperature coefficients should be used, such as the M320C52 and 355M102 uniaxial models, and the 339 series triaxial types equipped with UHT-12™ sensor elements.

What is so special about UHT-12?

The piezoelectric synthetic single crystal (UHT-12™) has been developed for high temperature applications. It is very temperature stable and can be reliably used up to 650 ° C. The piezoelectric material is not pyroelectric and has a high internal resistance, even at high temperatures. The piezoelectric coefficient (pC/N) of UHT-12™ is about three times larger than that of quartz. It can therefore also be used in sensors with ICP-technology. Vibration sensors with such elements have an extremely low temperature coefficient (Series 339).

Examples of + 180°C ICP®- Accelerometers



Triaxial TLD339A37, 100mV/g, LP-Filter, TEDS



Miniatur Triaxial HT356B01

What's next in the high temperature range of ICP® sensors?

The +180°C are currently state of the art and are limited by the electronics. The further development of the electronics (ASIC) brings us further miniaturization with integrated temperature compensation. As a result, even very small sensors with ceramic elements can be considerably improved with regard to measuring inaccuracy. The first candidate with this technique is available with a weight of 0.9 grams, 10mV / g, + 163 ° C, TEDS and temperature response of $\leq 3\%$ (Figure 5).

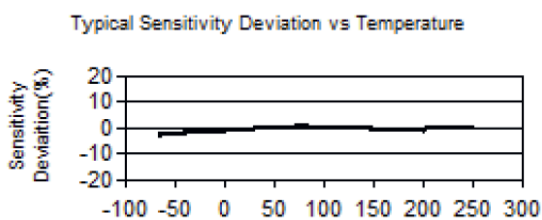


Figure 5: Temperature response Model 352A59



Figure 6: Sub-miniature model 352A59 with advanced electronics

Unusual measurement results with ICP® vibration sensors

After completing a test and evaluating data, test engineers may observe obvious signs of problems within the data that was collected. Many factors can affect the data from a PE accelerometer including measurement range, the measurement input amplitude, the measurand input frequency content, and the data acquisition sample rate. For example, input amplitude levels that are greater than the sensor's measurement range

will saturate the amplifier. Input frequency content at or near the sensor's resonant frequency may also saturate the amplifier. The high Q-factor at resonance will cause the sensor to enter an overload recovery state and no meaningful data can be acquired (even with post-process filtering in your DAQ).

Saturation of the amplifier by overload

Amplitudes greater than the measurement range can saturate the ICP® amplifier in the sensor. Frequency components in the signal, which are in the range of the resonant frequency of the sensor, can also lead to the saturation of the amplifier. The resonance effects in the sensor element mean that the sensor can't capture meaningful data. Filtering afterwards does not lead to useful measurement results.

Typical for overload conditions of the amplifier are exponential decay curves (Figure 7).

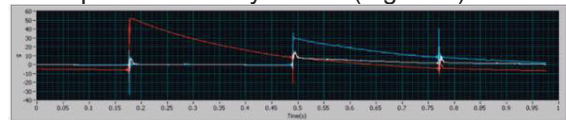


Figure 7: Saturated amplifier

Saturation of the amplifier due to resonance effects

In some applications, the sensor elements are excited in the region of the resonant frequency. The reason is high-frequency and high-energy pulses, usually caused by metallic shocks, or, more rarely, by high-frequency vibrations with high amplitude, which occur especially in random vibration tests. Input frequencies close to its resonant frequency can cause saturation of the amplifier, generating inaccurate readings. The solution against the problems described is a low-pass filter, between sensor element and amplifier, since a rework of the signal with filter is no longer possible. For applications where such conditions are expected, a filtered model should be selected (Figure 8).

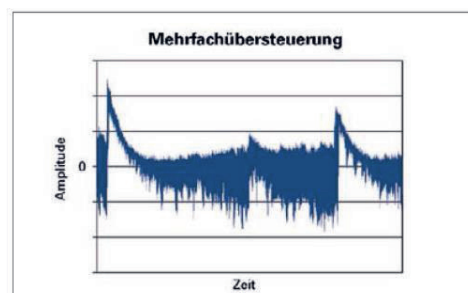
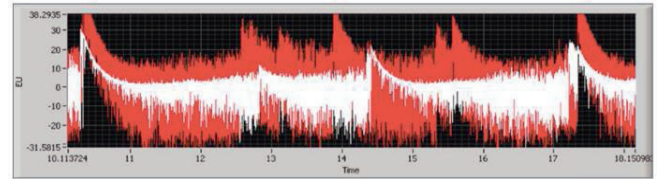


Figure 8: Multiple saturated amplifier

Internal filters help

Sensors with single or two-pole low pass filters will decrease the chance of amplifier saturation and increase the useable frequency range. Low pass filters will attenuate (suppress) signal generation at or near the resonant frequency of the sensor. This counteracts the gain (high-Q) factor caused by the sensor's mechanical resonance (Figure 9).



Saturated amplifier by resonance excitation

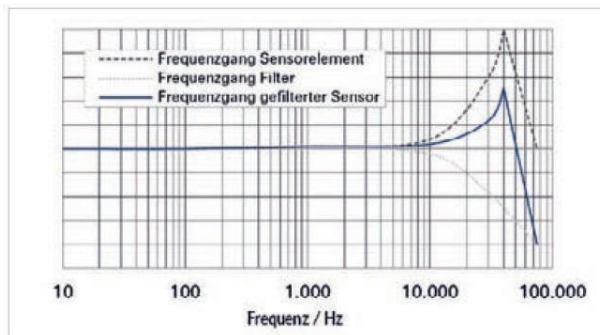


Figure 9: Influence of the filter on the frequency response

Where should sensors with low temperature coefficients and integrated low-pass filter be used.

- Ideal for component and component testing in climate chambers.
- Measurements on vehicle powertrain.
- HALT/HASS measurements.

Saturated amplifier; real-life examples.

Error image from the aviation industry.

Summary

- By using sensors with a particularly low temperature coefficient, thermal measurement errors can be reduced to a minimum.
- Such transducers use the temperature-stable sensor element material UHT-12™, which has been specially developed for piezoelectric high-temperature sensors.
- It delivers precise measurement results over the entire operating temperature range of -54 to 163 °C, even at changing temperatures.
- Many ICP® high-temperature sensors from the PCB® portfolio have integrated low-pass filters.
- They are always useful when high-frequency vibrations or high-energy pulses are exposed to the sensor.
- Such impulses are caused by metallic impacts, such as can occur in the combustion events in drive trains.
- The measuring element of an acceleration sensor is excited by such shocks in its resonance, which can cause saturation of the amplifier in unfiltered models.
- A correction of the signal data after a saturation is not possible, not even by filtering, since the raw data has already been recorded incorrectly.
- Filtered sensors eliminate this source of error.

References

- Technische Information TN-30 „Ungeöhnliche Messergebnisse bei piezoelektrischen Beschleunigungssensoren“ (PCB Synotech).
- Technische Information TN-051 „Piezoelektrische Aufnehmer mit eingebauer Mikroelektronik nach dem ICP®-Konzept“ (PCB Synotech).
- ICP®-Hochtemperatur-Beschleunigungssensoren (PCB Synotech).
- Sensoren für den Prüfstandsbaue (PCB Synotech).

Rotor Loading Test with Wireless Transmitting

MA Yaping, LIU Ming, HE Jing, GU Shipeng, LIU Peng
Chinese Flight Test Establishment, Xi'an 710089, China
E-mail address:myp_2008@163.com

Abstract: Helicopter rotor loading and strength flight test is the studying stress loading spectrum of airplane test in actual atmosphere. In the rotor loading test the test devices in the rotor should be strong anti-interference, small size, light weight because rotor high spin speed produces centrifugal force loading with high temperature gas and hot noise. Traditional rotor loading test solution of helicopter cannot meet present requirement due difficult balance between signal transmission reliability and test data real-time acquisition. This article propose a method for multi-channel, wide bandwidth and accurate synchronization rotor loading test with modular, redundancy and high integration design to modulate, transmit and demodulate the dynamic loading data.

Key words: Rotor system; Load; Wireless Transmitting; Time synchronization

1. Introduction

Helicopters are widely used in military and civilian fields because of the characteristics of vertical take-off and landing, hovering, and slow speed which are not available in fixed wing aircraft. As the key component of the helicopter, the rotor system not only provides lift and forward force for the helicopter, but also provides the longitudinal and lateral steering torque of the helicopter in order to achieve the helicopter's course operation. The aerodynamic characteristics of rotor system determine helicopter performance, quality and reliability, which are the main sources of vibration and noise of helicopters. The stress load spectrum of rotor system determines the safe service life of helicopter. Therefore, the load test of the rotor system in the helicopter flight test is the key subject. To obtain the rotor load test data

for the helicopter fatigue and life it is a necessary for the helicopter load and strength flight test. Improper handling of rotor system components will directly affect the aircraft control system and endanger flight safety. In the process of high-speed rotation, the rotor system produces very large centrifugal overload and is mixed with high temperature air, so the testing equipment installed on the rotor should be reliable, accurate and small. It is crucial not only to obtain real reliable, high precision flight data, but also to ensure flight safety.

This paper mainly describes wireless transmission technology to achieve data acquisition and transmission of rotating components in the flight test of rotor system.

2. Characteristics and key technologies of rotor load test technology

Helicopter rotor system is generally

composed of main hub, tilt plate, damper, elastic parts and blades and other components to achieve the helicopter's maneuvering flight. Rotor system is one of the most complex structures of helicopters, and many mechanical components are spin components. Rotating parts inevitably cause vibration in practical work. Excessive vibration will cause damage to helicopter structure. Therefore, the strength load test of the relevant components of the rotor system is a key subject in the helicopter flight test. At present, rotor system load flight test requires at least 80 test parameters, and the sampling rate is at least 1K Sa/s.

Rotor load test is a key test subject in helicopter flight test. The rotor will produce very large centrifugal overload and high temperature airflow in the process of high speed rotation, so the testing equipment installed on the rotor system needs to be reliable, accurate and small. It is crucial not only to obtain true, reliable and high precision flight data, but also to ensure flight safety. The contact measurement in early rotor system load test is to supply load strain power and send test signal through brush collector ring. The working principle of the brush collector ring is signal transmitting through the brush installed between the moving and static parts, it will produce a lot of noise in the process of high speed rotation of the rotor, which can easily lead to the distortion of the load strain signal waveform, and its anti-interference performance is poor. Later, to avoid distortion of the signal transmission the rotor load test is mainly to integrate acquisition and recording system

by installing the measuring equipment on the rotating parts, and then output signal of the load sensor is tested and recorded directly, without the conversion and transmission of any intermediate link. However, the scheme can not carry on the telemetry transmission to monitor the real-time load data, and it is difficult to synchronize the time for the airborne testing systems to guarantee the time correlation. Due to the limitation of the technology, the load parameters can not meet flight test requirement for the quantity and the sampling rate. Therefore, the key technologies of the rotor system load testing are non-contact wireless signal transmission technology, rotating component power supply technology and nonstandard component customization technology.

Non-contact wireless signal transmission is an innovation of contact measurement method, which overcomes a series of problems such as noise interference from the traditional contact test, and the technology has high maturity. It is also the inevitable trend of the measurement technology development of the rotor system in the future. The method uses signal wireless transmission or photoelectric technology to overcome the acquisition and transmission of strain signals, and the wireless connection of the test data between the dynamic and static parts of the rotor system is realized in the process of rotation of the rotor system. The technology of non-contact wireless signal transmission is to modulate the collected data through frequency and send it to a telemetry receiver at a specific frequency. The telemetry receiver sends the

demodulated strain signals to the airborne data acquisition system in a specific form. This can effectively overcome the data transmission problem of rotating parts.

At present, the more advanced technology is to install acquisition module in rotating parts installation, which has amplifying, acquisition, modulation and transmitting for the test signals. Through the installing receiving device in the cabin, the real-time data acquisition and recording are realized, with the Ethernet data extraction technology inserted into the airborne network test system of the helicopter flight test status can be real-time displayed to both pilot and the ground safety monitoring station.

The power supply technology of rotating parts and the nonstandard parts customization technology is the design for dual redundancy power supply for the rotor load testing system and the design of the testing mechanism for the high centrifugal overload environment basing on the mechanical structure characteristics of the rotating parts.

3. Design of load test system based on wireless transmission

3.1 Design principles

According to the requirements of flight test, the characteristics of the test signal type, range and frequency response of the measured signal, the reliability, advanced and extensibility of the rotating part load testing system are fully considered, and a test scheme for rotating parts to meet the requirements of the flight test environment is designed.

The main functions of the rotor load test

system used for flight test are as follows:

- 1) The system has the ability to test dynamic strain.
- 2) Considering the complexity and safety monitoring of rotor installation, the system has the capability of wireless signal transmission.
- 3) Wireless transmission channels are independent of each other and have fast migration capability.
- 4) Measurement accuracy of analog signals is better than 1%.
- 5) The system has precise time synchronization (better than 1ms).
- 6) With IRIG-B time signal input function, it ensures time consistency with the airborne networked test system.
- 7) The number of signal acquisition channels is greater than 80, and the sampling rate is more than 1KSa/s.
- 8) Double redundant power supply system to improve the reliability.

3.2 Wireless transmission protocol design

According to the design requirements of the helicopter flight test system, the protocol of the wireless signal transmission should have independent signal channels and the mutual exchange between channels to ensure the fast channel switching in the case of a single channel failure at flight test. At the same time, the wireless channel set up time should be short and signal transmission bandwidth should have enough bandwidth to meet the test requirements.

Digital modulation technology determines the performance of wireless channel. Digital modulation uses the carrier signal to modulate the discrete quantity. In

the current mainstream digital signal modulation technology, compared with their respective technical characteristics, the FSK (frequency shift keying) digital modulation for wireless transmission of data is adopted. The frequency shift keying FSK digital modulation accepted by the International Telecommunication Union is widely used in the field of network transmission. It has the characteristics of mature and reliable, the weak signal crosstalk ability, the small radiation power and the short channel setting time and so on.

FSK (frequency shift keying) modulation technology is the frequency of sine wave controlled by digital signal, so that the frequency of sine wave vary with digital signal. The mathematical expression of the FSK signal is:

$$S_M(t) = A \cos(2\pi m \Delta f t + \omega_0 t)$$

($m = 1, 2, 3, \dots, M; 0 \leq t \leq T$), Where Δf is the frequency difference between M frequencies.

The binary FSK signal is the sine wave of two different frequencies F1 and F2 corresponding to the "1" and "0" of the digital signal.

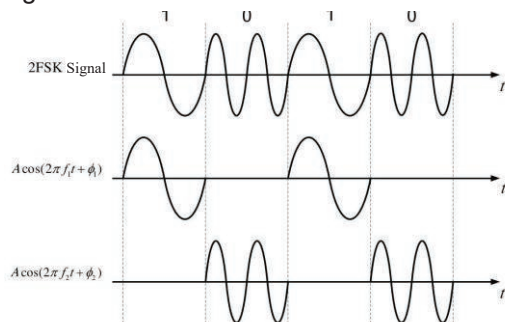


Figure 1 Binary FSK signal waveform diagram

3.3 Design of rotor load test system

The rotor load testing system mainly includes data acquisition and telemetry unit,

system installation disk, power supply unit and telemetry data receiving unit, Ethernet data extraction system and data monitoring on ground and on board. The system principle block diagram is shown in Figure 2. The data acquisition and telemetry unit complete the collection, modulation and wireless transmission of the load data. The customized system installation plate is the installation carrier of the data acquisition and telemetry unit. The installation disk has the installation base of data acquisition and telemetry unit and the related circuit of signal transmission and power supply. The power supply unit is supplied with double redundancy power supply, telemetry data receiving unit demodulates the received load data and sends it to the airborne networked data acquisition system in analog and Ethernet mode.

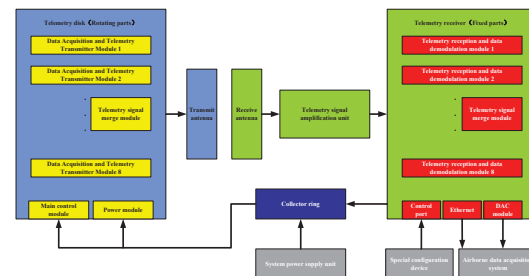


Figure 2 Principle block diagram of rotor load test system

3.3.1 Signal acquisition and processing unit

The data acquisition and processing unit is designed as shown in Figure 3.

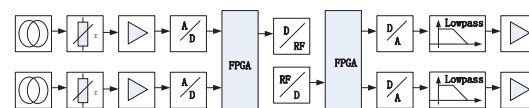


Figure 3 Signal acquisition table and processing

According to the accuracy requirements of the strain data, the strain data acquisition is designed with high precision constant

current source circuit, which can effectively reduce the nonlinear error of the circuit design and ensure the accuracy of the measured data. Each strain sensor can provide high precision current independently, and the user can set the current value. The sensor signal is amplified by an amplifier and then transformed by A/D. The processor (FPGA) converts the received A / D data and forms a serial data stream. The serial data stream is modulated and amplified by FSK (frequency shift keying) modulation technology. The carrier frequency can be set by the user to avoid interference with the original wireless signal.

The receiving antenna sends the received modulation signal to the receiver for demodulation. The receiver can filter the different channel signals according to the user's requirements, and the processed signals will be output to the general airborne acquisition system in the type of Ethernet or analog.

3.3.2 Design of system installation disk

The system mounting disk is the installation carrier of the rotor load test system. According to the requirement of the load test, the system installation disk needs to install signal acquisition and wireless transmitting module, double redundant power control module and backup battery package for strain signal acquisition, modulation and wireless transmission.

Due to the special structure of the rotor hub mounting bracket, the system mounting disk is specially customized according to the rotor hub structure. In particular, the weight and structural strength of the equipment

have special limitations. Through the relevant technical coordination in the early stage the design of the system installation disk adopts end face mounting and disc shape design. The installation disk is designed by using the mounting screws of the rotor hub with rain cover. The center is designed as a disc platform for mounting the telemetry disc. As shown in Figure 4.



Figure 4 System installation disk

The signal acquisition and wireless transmission module includes four functions of strain sensor power supply, signal conditioning, signal conversion and radio frequency transmitting. The module synchronizes all channels, the signal conditioning unit filters the input signal, the A/D converter oversampling it, and FSK (frequency shift keying) digital modulation to the sampled digital signal, and transmit it to the corresponding receiver by wireless communication.

Telemetry disk technical specification:

Signal input:	strain;
Number of channels:	80;
Sensor excitation:	constant current ;
Source excitation:	0mA to 10mA programmable;
Measurement range:	8 range adjustable;
Signal bandwidth:	DC to 19kHz (can be set);

Linearity: + 0.2% F.S.

3.3.3 Data extraction and security monitoring

In order to meet flight test requirements of safety monitoring, the helicopter rotor load testing system needs to transmit the rotor system load test data to the ground monitoring station and the pilot, providing a discriminant data for the flight safety. The telemetry receiver is inserted into the airborne network data acquisition system with analog connection and Ethernet communication, through the Ethernet extraction technology and then through the airborne telemetry system the load test data is sent to both the ground for safety monitoring station and the test pilots at the same time. As shown in Figure 5.

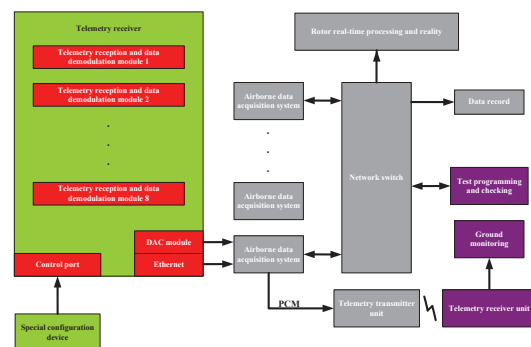


Figure 5 Data extraction and security monitoring

3.4 Laboratory debugging and verification

For the design of load test system, time synchronization is the key technology. The time delay of each channel and the time synchronization among channels is important to data analysis based on time history. The system uses IRIG-B time protocol to synchronize the processing units of the system, and the time synchronization accuracy design specification is 1 ms. Collecting and configuring each acquisition

channel through Ethernet, loading the programmed software to the rotor load test system. The airborne telemetry data receiving unit monitors the running state of the whole system, checks the time synchronism of each acquisition node of the whole test system, and finally guarantees the rotor load test system to meet the design specification.

3.4.1 Synchronization error test of acquisition channel

For the process of sampling, modulation, transmission, reception, demodulation and two sampling of different channel strain signals, the synchronization error between the channels is related to the requirement of the time correlation of the later data processing to the parameters.

The test results show that the synchronous interval is 940ns.

3.4.2 Time delay test of acquisition channel

The time delay of the test system mainly includes signal amplification delay, filter delay, A/D conversion delay, D/A conversion delay, wireless transmission delay, processing and buffer delay, etc. Two acquisition channels are chosen, by using the same standard signal source as input and a high precision oscilloscope to test the signal waveforms of the two channels to analyze the response time of the input signals and output signals of the two channels, the time delay of the two acquisition channels can be tested, which is the time delay of the load test system. The test results show the system delay 0.94mS

4. Conclusion

By using the key technologies such as multi-channel wireless communication and

dual redundancy rotating parts power supply, the seamless connection of the test system between rotating parts and static components during the high-speed rotation of the rotor is successfully realized, and a practical rotor load test scheme is provided. The technical scheme is stable and reliable, and it has been successfully applied at the present. The rotor load test data is accurate and reliable, and the real-time safety monitoring of the rotor load is realized for the first time. This technology has a certain reference and impetus for future helicopter rotor load test.

Reference

- [1] Zhang Xiao Gu. Helicopter dynamics design [M]. Aviation Industry Press, 1995.
- [2] Yang Yong. Design and implementation of spacecraft control system based on PD control. [J]. computer measurement and control, 2014.
- [3] Zhao Yaxing. FPGA principle, design and application [M]. first edition. Tianjin: Tianjin University press, 1999, p36-38.
- [4] Helicopter Main Rotor Telemetry User Manual, Telemetrie Elektronik GmbH.

Vibration Test of Airplane Moving Surface with Wireless Sensor

HE Jing, MA Yaping, LIU Ming, LI Tielin, ZENG Xingchang
 Chinese Flight Test Establishment, Xi'an 710089, China
 E-mail address: cfte_hj@126.com

Abstract: In flight test it is important to guarantee airplane flight safety through monitoring its structure vibration. But it is a challenge to monitor vibration for the airplane moving surface due to its large movement with composite materials and limited structure loading. It is difficult to use the conventional wire sensors and data acquisition system because of its large size and complicating wire routing. We design a test system based on micro-structure wireless sensor network with signal sensing, coding, storage and power supply to acquire data simultaneously through at several nodes with wireless time synchronization. The result of flight test show that the system is reliable with accurate data acquisition for vibration test of airplane moving surface.

Keywords: wireless network, vibration, time synchronization, MEMS, test technology

1. Introduction

The wireless network testing technology is considered as another hot spot in the field of industrial control after field bus and industrial Ethernet technology. As one of the most dynamic new technologies in the world, [1-3], its low cost, high integration, high flexibility and high reliability have solved the complicated connection, a lot of wiring, difficult installation and maintenance work for wired test. Therefore, all countries are competing for development in many application fields.

At present, the application of wireless intelligent testing technology is mainly focused on environmental monitoring and protection of medical care [4-5], large building structure [6-9] (such as Figure 1 bridge health monitoring) and military fields, and the application of state testing on aircraft structure is still applied less.

The health monitoring and structural state test of the aircraft is an important guarantee for the safety flight of the aircraft, and the wireless intelligent testing technology provides an effective method for the health monitoring and structural state testing of

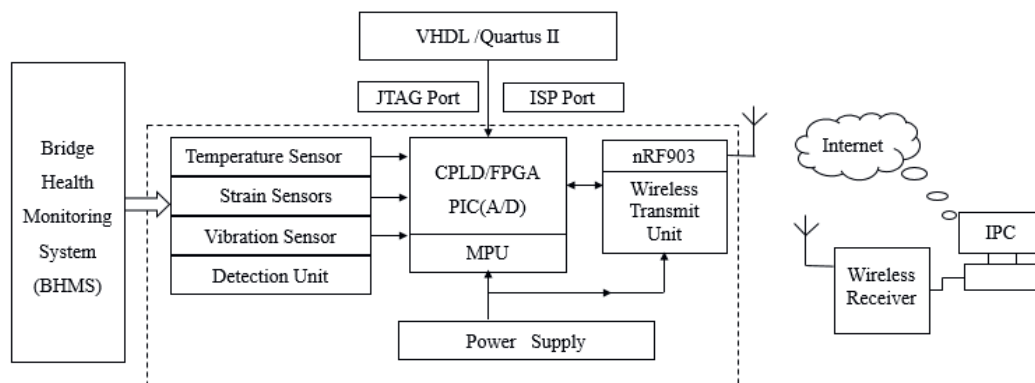


Fig. 1 Schematic diagram of wireless intelligent health monitoring for a large bridge

the aircraft. The vibration test of aircraft is an important basis for studying the strength, deformation, mechanical fatigue and impact resistance of aircraft key components, which is important to the flight safety of an aircraft. Therefore, it is important to acquire the data of the vibration which is used for the study of the characteristics of vibration on the aircraft structure.

In this paper, the vibration characteristics of aircraft flap surface are monitored. Due to the continuous movement of the plane's flap wing during the flight, and the material of the flap is complex, the bearing capability of the structure is limited. The traditional cable sensor and data acquisition system have large volume and cumbersome wiring, which limits its application. Therefore, the wireless intelligent vibration testing technology is adopted by the vibration characteristics test of the flap surface.

2. Vibration test with airborne wireless network

2.1 The diagram and main technical specifications of airborne wireless vibration testing system

2.1.1 Airborne wireless vibration testing system

The diagram of the airborne wireless vibration testing system is shown in Figure

2. The system consists of wireless intelligent sensor nodes, wireless control unit and measurement and control terminal. The wireless intelligent acceleration sensor node sends the data to the wireless control unit through the 2.4G wireless communication, and the wireless control unit can connect 50 wireless intelligent sensor nodes at most. The wireless control unit transmits the data to the ground test computer through the Ethernet interface. Besides test wireless control unit can also be connected to telemetry system through RS422 interface in flight test.

2.1.2 The main performance of the system

- 50 remote wireless sensors connection at the same time;
- Each wireless sensor records data according to data sampling time sequence;
- The system can receive time from external IRIG-B code, and the synchronization accuracy is better than 20 μ s;
- Wireless sensor integrates signal sensing, acquisition, recording and power supply;
- Continuous recording time: 15 hours;
- The measurement range and the sampling rate can be set up in software;
- Working status is displayed;

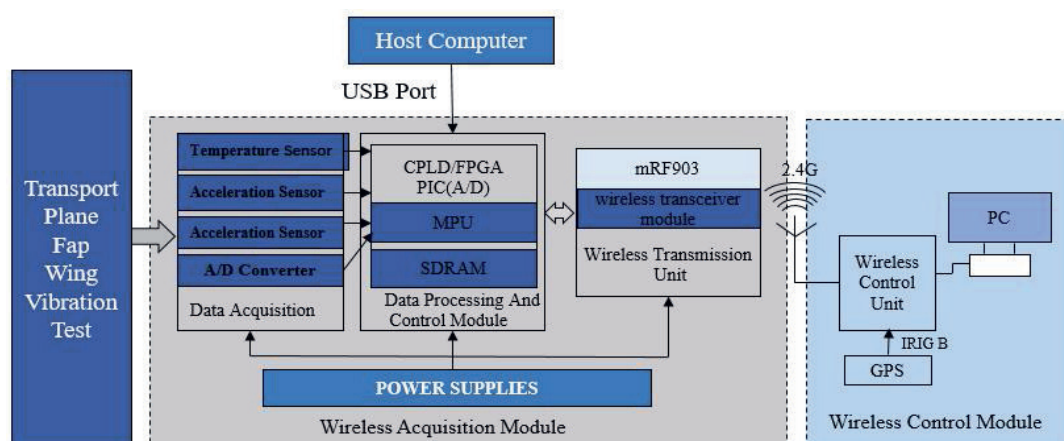


Fig. 2 Schematic diagram of airborne wireless intelligent vibration testing system

- Data logging supports the different type format for data, TXT, CSV format. Software should have online help, whose content is comprehensive and convenient to search. The contents should include description of system function, software usage and software function.

2.2 Wireless MEMS acceleration sensor

The research of wireless intelligent vibration testing technology is studied in this paper. The three axis MEMS accelerometer is used as a micro sensor unit for signal acquisition, data processing and data storage. It follows the module design. The sensor is divided into data acquisition module, CPU module, power module and wireless transmission module, as shown in figure 3.

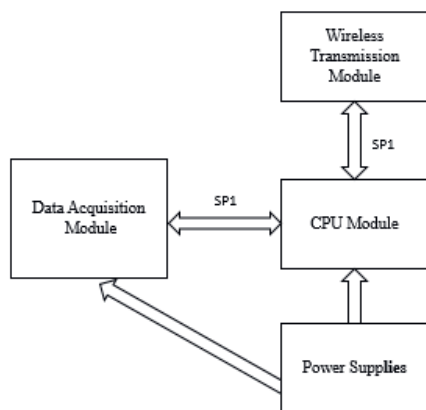


Figure 3 modular structure of wireless intelligence sensor

The sensitive device selects the MEMS acceleration chip, the signal conditioning part uses low power amplifier to build the two order of Butterworth low pass filter, and uses analog capacitor switching to realize the transformers of four different frequencies.

The CPU module is the core control part of wireless sensor, which completes data acquisition, data processing, data storage, power management, wireless communica-

tion protocol and so on.

2.3 Wireless control unit

The wireless control unit is mainly composed of CPU, power module, Ethernet communication module, wireless transceiver module and synchronization module. The schematic diagram is shown in Figure 4.

The wireless control unit synchronize the nodes through the IRIG-B code and synchronize with the airborne test system time. The 28V DC power of the aircraft is transformed into 5V and 3.3V by means of DC-DC conversion and linear regulator.

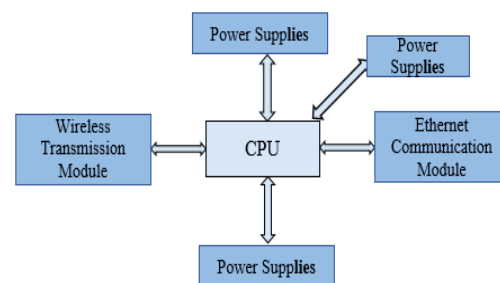


Figure 4. The schematic diagram of the wireless control unit

2.4 System time synchronization technology

In airborne wireless intelligent vibration testing system, time synchronization mechanism is a key technology, and each sensor node has its own local time. The sensor nodes use the crystal oscillator interrupt counter to get the local time. Because the frequency error and the initial timing time of the crystal oscillator are different, the local time between the nodes may be different, and the interference of the temperature and the electromagnetic wave etc. will also cause the time deviation between the nodes. The key to obtain the correct clock in time synchronization technology is how to calculate the frequency deviation correctly and phase deviation between the local time or the physical time and local clock. Usually the frequency deviation and

phase deviation are corrected by the transmission of synchronous information, but the time delay will be generated in the transmission of synchronization information. The uncertainty of the delay will affect the synchronization accuracy to a great extent. Therefore, calculating the delay of synchronization information correctly is the key step to improve the synchronization accuracy. The delay of synchronous information includes transmission delay, access delay, propagation delay and acceptance delay, as shown in Figure 3.

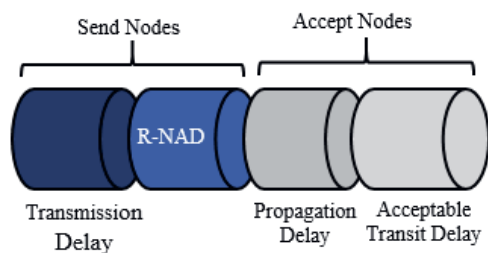


Figure 3 Time delay in a wireless channel

In order to solve the problem of asynchronous data time stamp in the test system, this project proposes a solution, which uses the DMTS method to broadcast synchronous information packets with time delay measurement, as shown in Figure 4. A synchronous packet is sent every second through the wireless base station control

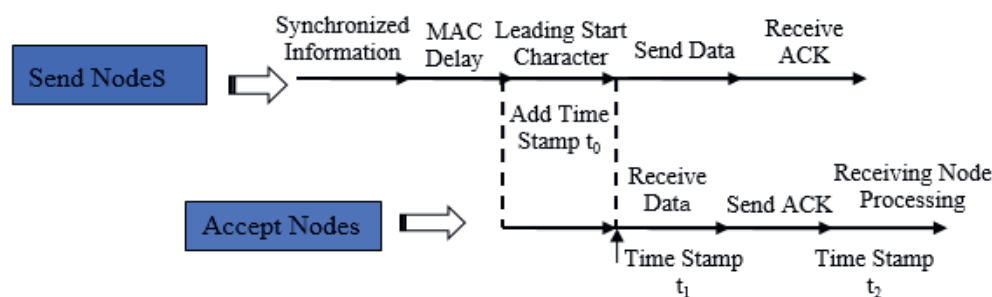


Figure 4 DMTS method broadcast synchronization packet delay measurement

unit, after the sensor node receives the synchronous packet, the initial value of the local timer is adjusted, thus the initial value of the local timer is adjusted. The time between each node is consistent, and the

synchronization accuracy can reach 20 microseconds.

3. System software

The wireless control unit is the control center of the wireless acquisition system. It operates the wireless protocol stack, controls all wireless sensor nodes, receives the synchronous clock from the airborne synchronization clock, sends the synchronization packets to the sensor nodes, receives all the data of the nodes, and runs the TCP protocol stack, and sends instruction and receives data through the Ethernet and the monitoring computer. The main functions are as follows:

- The functions of search, node query, parameter setting, data collection and sensitivity configuration;
- The functions of data storage query, data download, data erasure and so on;
- Supports Win7/Win10 operating system, downloads data through USB interface, and supports data format with data, TXT, CSV etc;
- Data analysis software: time domain, frequency domain analysis, batch processing, wavelet transform and other functions.

4. Test and Verification

By the design of wireless network measurement node (wireless acceleration sensor), wireless control unit and

measurement and control terminal software, the airborne wireless vibration testing system is constructed, and the time synchronization of wireless network nodes is studied by using the time delay measurement through synchronous packet broadcast based on DMTS method. The airborne wireless vibration test system can achieve 0 ~ 5KHZ sampling rate and 0 ~ 10g vibration measurement. The wireless vibration network realizes the measurement of 18 wireless vibration sensor nodes at the same time. The data acquisition of each node is completely synchronized and has no time delay. The airborne wireless vibration testing system is verified on the aircraft to meet the test requirements of aircraft movement surface vibration characteristics.

5. Conclusion

In this paper, the MEMS micro sensor signal testing system based on wireless network is proposed from the point of view of system structure, hardware design, time synchronization and measurement and control software. The system is proved stable by the test of flight, reliable and high time synchronization precision, which solves the wiring problem in some cases of tests. It has a certain value to promotion.

6. Reference

- [1]. Ren Zhi Ling, Zhang Guangquan, Lin Dong, et al. Overview of wireless sensor network applications [J]. sensors and Microsystems, 2018 (3).
- [2]. Ren Fengyuan, Huang Haining, Lin Chuang, et al. Journal of [J]. Software of wireless sensor network, 2003, 14 (7): 1282-1291.
- [3]. Potdar, Vidyasagar, Sharif, et al. Wireless Sensor Networks: A Survey[J]. Computer Networks-The International Journal of Computer and Telecommunications Networking, 2009, 38(4):393-422.
- [4]. Kung H Y, Hua J S, Chen C T. Drought Forecast Model and Framework Using Wireless Sensor Networks[J]., National Taiwan University biological resources and Agricultural Institute Experimental Forest Research Report, 2006, 20 (2):
- [5]. Hande A, Polk T, Walker W, et al. Self-Powered Wireless Sensor Networks for Remote Patient Monitoring in Hospitals[J]. Sensors, 2006, 6(9):1102-1117.
- [6]. Lee R G, Chen K C, Chiang S S, et al. A backup routing with wireless sensor network for bridge monitoring system[J]. Measurement, 2007, 40(1):55-63.
- [7]. Yuan S, Lai X, Zhao X, et al. Distributed structural health monitoring system based on smart wireless sensor and multi-agent technology[J]. Smart Materials & Structures, 2005, 15(1):1.
- [8]. Chintalapudi K, Fu T, Paek J, et al. Monitoring civil structures with a wireless sensor network[J]. IEEE Internet Computing, 2006, 10(2):26-34.
- [9]. Ye Weisong, Yuan Shenfang. Application of wireless sensor network in structural health monitoring. Journal of [J]. Sensing Technology, 2006, 19 (3): 890-894.

Transhorizon over-sea propagation tests with Line-of-Sight Lygarion® Data Link technology

Abderrahim Fihel, Joël Mailleux, Jérôme Ernst
 HENSOLDT France
 115, Avenue de Dreux
 78370 PLAISIR – FRANCE
abderrahim.fihel@hensoldt.net
joel.mailleux@hensoldt.net
jerome.ernst@hensoldt.net

Abstract:

This paper describes the experimental tests results of the transhorizon NLoS propagation over the sea, with Line-of-Sight Lygarion® Data Link technology, between an experimental ship and a low altitude ground station located on the coast border.

A series of experiments were performed in order to measure and to better understand the achievable performances (in terms of link coverage) for high data rate transmission over the sea and thereby to meet the needs of “command/control” and sensor data transmission for an unmanned marine vehicle systems USV.

The maximum range in NLoS conditions over the sea is a critical issue for major applications, such as the control of an USV for which the unavailability of the data link could be hazardous and, in some cases, catastrophic.

The experimental results have good agreement with the simulated values, obtained taking into account some propagation losses.

Our results and analysis show that some of the NLoS over-sea propagations phenomenon such as the reflection from sea surface and the multipath may be significantly overcome by the use of steerable directional antennas, double QoS double stream (DQDS) protected waveforms as well as efficient link management link acquisition functions.

Key words: transhorizon NLoS propagation, USV, experimental tests, steerable directional antennas, DQDS.

1. Introduction

Radio-wave propagation in maritime environments has been the focus of much theoretical and experimental research over the years for a wide range of military and commercial applications [1-2] for a seashore country. For military, these include Mine Counter Measures (MCM), Intelligence, Surveillance and Reconnaissance (ISR), Anti-Submarine Warfare (ASW), and Fast Inshore Attack Craft (FIAC) for combat training. For commercial, these include Oil and Gas Exploration and Construction, Oceanographic Data Collection, Hydrographic and Environmental Surveys.

For this type of applications, there is the requirement to transmit large sensor data to the ground station operator. The transmitted data

also includes command/control and telemetry and the status data. This information is necessary for the operator.

Classical maritime communication systems in coastal areas, mainly based on VHF and satellite communications systems, are not capable to satisfy these requirements because they suffer from one or more of the following weaknesses such low bandwidth or system capacity, short range and too expensive for many applications.

Recently, there are some growing interests in deployments of wireless systems in the maritime environments such as military maritime surveillance. Generally, these applications require the microwave radio systems to be operated in over-sea line-of-sight

(LoS) maritime environments (e.g., between a control station and a moving vessel).

In maritime environments, Unmanned Surface Vehicles (USV) are considerably used for a wide variety of military and commercial applications. They are remotely controlled and they perform their tasks autonomously with control from a host ship or on-shore-based station via high-data-rate communication links.

The main objective of the experimental tests is to measure and verify the maximum range obtained with NLoS conditions over the sea between an USV and a control station which is either on land or on a mother-ship.

This paper is organized as follows: Section II presents a brief description of the Lygarion® data link family used for unmanned aircraft systems (UAS), while Section III describes some key considerations for over-sea radio-wave propagations and some assumptions/requirements for such data link for maritime communication. The experimental tests details are given in section IV. Finally, Section V gives a conclusion and a summary of some results analysis.

2. Lygarion® Data Link Family Description

Lygarion® data link is a new generation, point-to-point, high data rate and programmable digital data link. This modular and compact solution is available in C and Ku bands for secure IP full duplex real-time wideband and C² data transmission, between two mobile platforms, up to 100 Mb/s data rate and 300 km range. It is primarily used for data transfer

between a ground data terminal and an airborne or surface data terminal through:

- Uplink data transfer: used to Command and Control (C²) the UAV/USV and/or the payload:
 - UAV/USV command include: high level command (speed, heading and altitude), new flight plan ...
 - Payload command include orientation and zoom
- Downlink data transfer:
 - Data provided by the Payload (video in case of observation payload)
 - UAV/USV state parameters (speed, position, attitude)
 - Payload state parameter

Lygarion® data link family is based on multi-platform-oriented product whose programmable and modular architecture allows to offer a large panel of datalink applications by configuration of:

- the antenna type,
- the tracking function,
- the programmable waveform type,
- the interfaces type.

Figure 1 illustrates the different product configurations allowed by the modular and therefore scalable design of the Lygarion® product family.

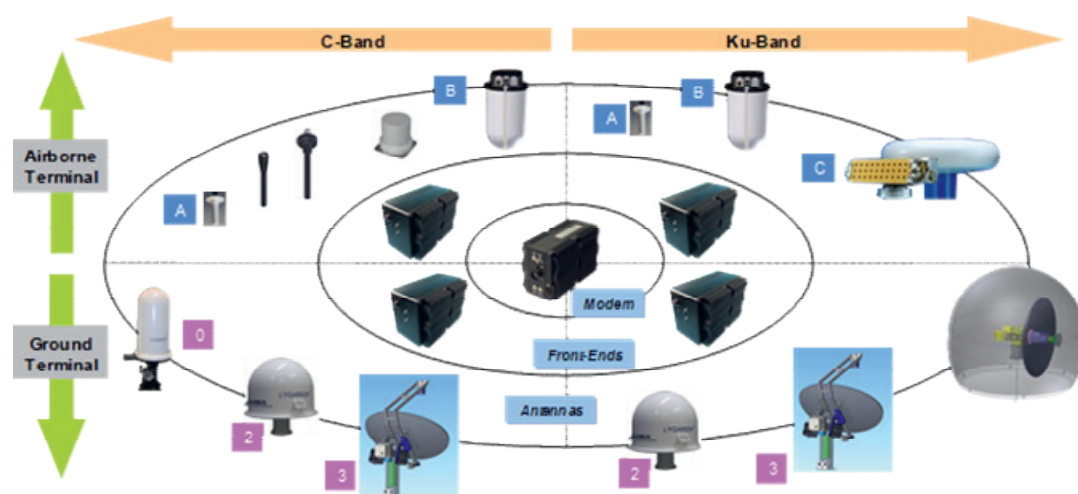


Figure 1: Lygarion® Product Family depending on the RF band application and the Data Terminal

3. Key Considerations for Over-Sea Radio-wave Propagations

3.1. NLoS Propagation over the Sea

The radio wave propagation over sea is very different from over land, as the atmospheric conditions over the sea are the dominant influence of the propagation characteristics.

From the literature, it is well recognized that near sea-surface radio wave propagation could be affected by the:

- sea-surface reflection,
- refraction caused by evaporation duct,
- diffraction,

- and other multipath propagation phenomena.

These propagating mechanisms (depending on the frequency, antenna height and sea state conditions) will cause path losses and finally limit coverage area.

3.2. Propagation Loss

Figure 2 shows an example of Fresnel ellipsoid diagram (Fresnel zone with some diffraction) for a transhorizon radio wave propagation at frequency of 5 GHz and distance of 37 km. The diffraction loss is estimated to 25 dB

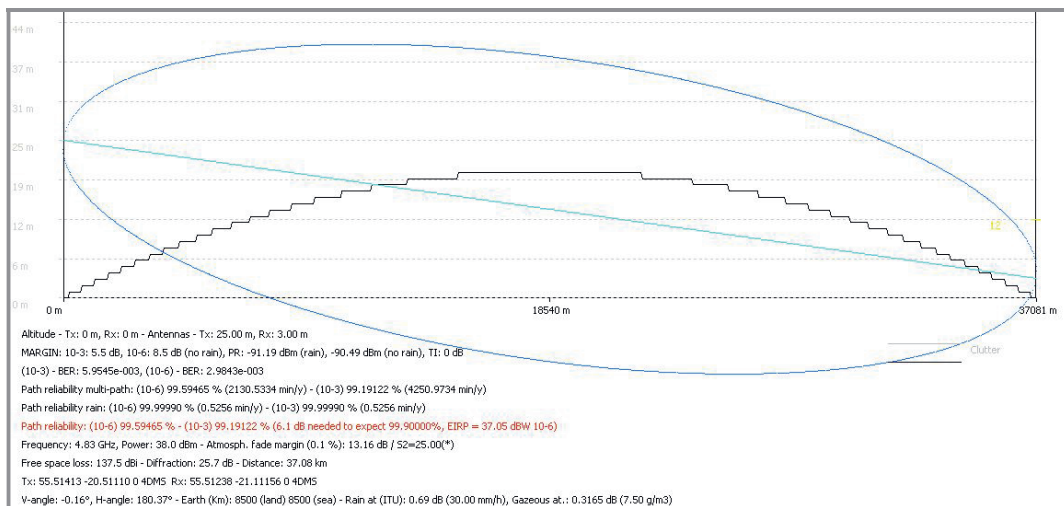


Figure 2: Fresnel ellipsoid for transhorizon radio propagation @ 5 GHz

C-band has been selected due to its technical characteristics that make it particularly attractive for high data rate transmission:

- It has less attenuation compared to other bands
- The lower frequencies that C-band uses, perform better under adverse weather conditions than the Ku-band frequencies
- More gain with directional antennas on both platforms (ground and ship)
- Fresnel ellipsoid not too narrow allowing to benefit from a not too strong diffraction in trans-horizon propagation
- Lower C-band available and compatible in all ITU regions.

3.3 DQDS Waveform Spectrum Occupancy

The Lygarion® datalink operates in Frequency Division Duplex (FDD). Therefore, the front-end incorporate a split of the C-band in order to achieve decoupling between transmit and receive part of the bidirectional link.

The operating frequency: C-band [4.4 -5.0] GHz

- Uplink (GDT → SDT): [4.4 - 4.6] GHz
- Downlink (SDT → GDT): [4.8 - 5.0] GHz

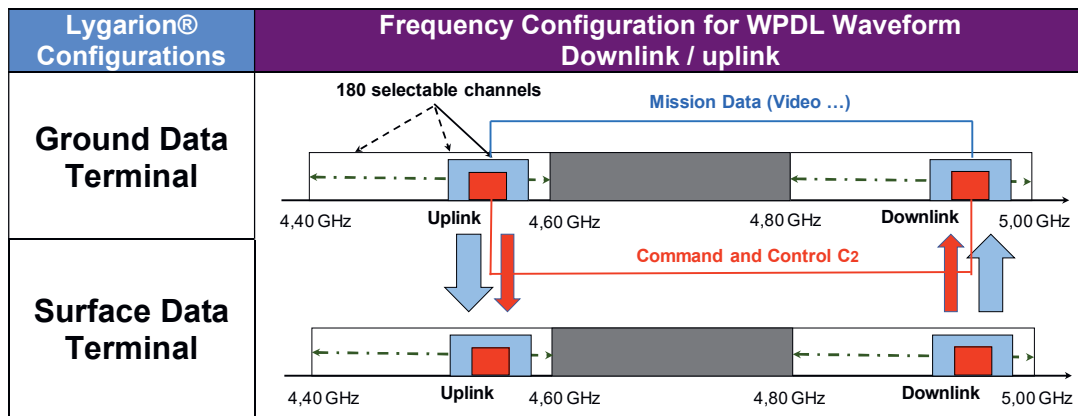


Figure 3: DQDS waveform spectrum occupancy

WPDL is a proprietary wide protected waveform based on BPSK modulation scheme and on the high jamming-resistance. The highly-protection and jam-resistance are achieved through:

- The use of several TRANSEC features including, Direct Sequence Spread Spectrum (DSSS), Frequency Hopping Spread (FHSS) and Forward Error Correction (FEC)
- Code Division Multiple Access (CDMA) C2 / high datarate stream segregation
- Extremely high C2 quality of service
- Two-stage channel coding.

As shown in Figure 3, the concept of this waveform permits :

- Real-time communication of double data stream C2 and wideband data (video)
- Double quality of service (QoS): each data stream ensures high QoS (with extremely high C2 quality of service) thanks to several Electronic Protection Measures.

That is why this protected waveform is denoted DQDS (Double QoS Double Stream) waveform.

In addition, the full duplex mechanism permits simultaneous and interference-free transmission of double stream from air/surface-to-ground and ground-to-air/surface enabling both sides to be in continuous communication.

3.4. Link Budget

The link budgets of the Lygarion® LOS Datalink System for waveforms WPDL and DVBS [3] are given below.

They take into account some provisions for the propagation attenuation loss:

- For WPDL waveform, the data rate for uplink is 19.2 kb/s and for downlink 5 Mb/s
- For DVB-S waveform, the data rate for uplink is 2 Mb/s and for downlink 10.71 Mb/s
- Operating frequency: C band
 - Up-link (GDT → SDT): 4.7 GHz
 - Down-link (SDT → GDT): 4.9 GHz
- Sea Data Terminal (SDT):
 - F-END of 6 W (38 dBm),
 - Directional antenna with gain of 13 dBi,
 - Omni-directional antenna with gain of 6 dBi,
 - SDT antenna height: 3 m
- Ground Data Terminal (GDT):
 - F-END of 6 W (38 dBm),
 - AZ/EL Directional antenna with gain of 23 dBi
 - GDT antenna height: 30 m

The following table provides a summary of the link budget of the Lygarion® LoS Datalink considering the ITU-R P.530 recommendation and the above assumptions. The link budget calculation incorporates atmospheric absorption and rain attenuations

.Data Rate		GDT Antenna	23 dBi	
		SDT Antenna	6 dBi	13 dBi
Downlink	5 Mb/s	Range	25.3 km (13.6 Nm)	30 km (16.2 Nm)
		Availability	98.6 %	96.5 %
		Link Margin	7.7 dB	6.1 dB
Uplink	19.2 kb/s	Range	25.3 km (13.6 Nm)	30 km (16.2 Nm)
		Availability	99.8 %	99.5 %
		Link Margin	16 dB	14.4 dB

Tab. 1: Lygarion® LOS Datalink link budget summary for WPD

Data Rate		GDT Antenna	23 dBi	
		SDT Antenna	6 dBi	13 dBi
Downlink	10.71 Mb/s	Range	25.3 km (13.6 Nm)	30 km (16.2 Nm)
		Availability	99.2 %	97.9 %
		Link Margin	10 dB	8.4 dB
Uplink	2 Mb/s	Range	25.3 km (13.6 Nm)	30 km (16.2 Nm)
		Availability	98.7 %	96.5 %
		Link Margin	7.6 dB	6 dB

Tab. 2: Lygarion® LOS Datalink link budget summary for DVB-S

3.5 Steerable Directional Antennas

Due to the movements (pitch, roll and yaw) of the ship in the sea, the use of a steerable directional antenna with tracking-pointing mechanism for both platforms (ship and costal station) has been considered. It should be noted that the steerable capability of ship and costal antennas, enables to compensate in real-time the sea wave moves thanks to INS/GPS compensation function implemented into the Lygarion® modem.

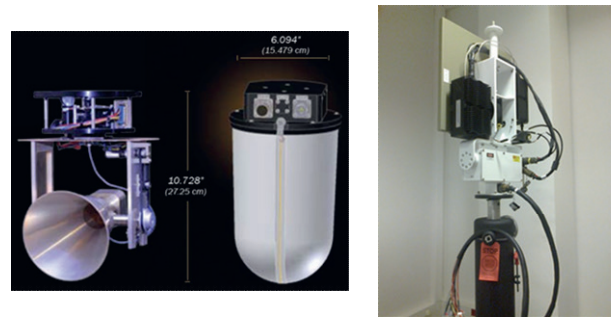


Figure 4: Steerable directional antennas for ship and costal station

In costal and marine environment, the use of a protection radome to shield the antenna from weather, improves the system availability since the antenna is not affected by winds, clouds and precipitation. It also improves the antenna performances since high winds or temperature variations can distort the shape and pointing direction of the antenna reflector.

Radome is also widely used to protect antennas which are continually in tracking while the ship undergoes pitch, roll and yaw movements.

Therefore, both directional antenna platforms (ship and costal station) have been equipped with a protection radome that also conceal the sensitive electronics of these antennas.

4. Experimental Tests Description

4.1. Tests Conditions

Experimental tests were carried out over-sea, between an experimental ship (Le CELADON) and a ground station located on the cost border in order to measure the maximum distance the USV can transmit high sensor data to the ground station depending of the sea state conditions

“Le CELADON” is an experimental ship suitable for sea trials, made available by “Sea Test Base” company.



Figure 5: The experimental ship (Le CELADON) from “Sea Test Base” company

The site is related mainly to the frequency authorization to transmit. It is also selected in order to ensure that the propagation is mainly over the sea surface and there is no blockage of the propagation signal. It is about the bay of Douarnenez which is located in the French county of Finistère in Brittany (in the Atlantic Ocean) north-western France. The tests were made continuously in November 2017. The location of the experiments is shown in Figure 6.

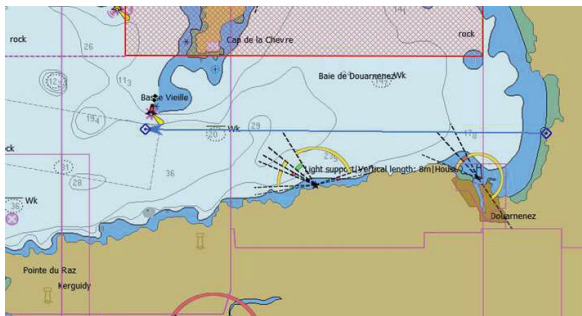


Figure 6: Location of the tests in the bay of Douarnenez

- Frequency band: C-Band,

The authorisation to transmit in C band, necessary for the Lygarion® data link deployment, was assigned by ARCEP (the French regulator of the electronic communications and postal sectors).

Two frequencies were allocated:

- 4.7 GHz for uplink direction,
- 4.9 GHz for downlink direction.

These frequencies were retained despite the center frequency for uplink direction is in limit of the Lygarion® modem band pass filter (with an impact of -10 dB on the link budget calculation).

Two waveforms were tested:

- WPDL: a secure proprietary TRANSEC waveform
 - the data rate for uplink is 19.2 kb/s
 - the data rate for downlink 5 Mb/s (SDT → GDT)
- DVB-S: a standard (ETSI) waveform
 - the data rate for uplink is 2 Mb/s
 - the data rate for downlink 10.71 Mb/s (SDT → GDT)

4.2. Tests Equipments

4.2.1 Sea Data Terminal (SDT) on the Chip

As shown in Figure 7, the SDT is installed in the experimental ship at a height of 3 m above sea level and it consists of:

- Lygarion® modem
- A high-power amplifier F-END in C-band of 6 W (38 dBm),
- Directional antenna with gain of 13 dBi, Equipped with Inertial Navigation System (INS)/GPS allowing to compensate the platform movement,
- Omni-directional antenna with gain of 6 dBi,



Figure 7: Lygarion® SDT on the experimental ship

Other equipment, necessary for setup and exploitation of the measurements, are housed within the boat cabin:

- Power supply unit 28 VDC-6A,
- An IP camera to generate a video stream,
- Two rugged laptops and display screen equipment,
- Associated cables.

4.2.2 Ground Data Terminal (GDT) on Shore

As shown in Figure 8, the GDT is located on the coast border (on shore) at an altitude of approximately 20 m and consists of:

- Lygarion® modem
- A high-power amplifier F-END in C-band of 6 W (38 dBm),
- Directional antenna with gain of 23 dBi
- Omni-directional antenna with gain of 2 dBi,
- 2-axis positioner allowing moving of Nx360° Azimuth and +/- 90° Elevation
- A height-adjustable tripod,

- A 19" rack containing a power supply unit 28 VDC-6A, interface board and some associated cables
- An electrical power generator.



Figure 8: Lygarion® GDT on shore

Other equipment (two rugged laptops and display screen equipment), necessary for the exploitation of the measurements, are housed within a small van.

The whole system was carefully calibrated on-site before the sea trials and checked again after the measurements. The system effect was minimized through the measurement of a back-to-back connection between the SDT and the GDT.

4.3. Measurement Routes

Measurements were carried out over-sea, between an experimental ship and a ground station located on the cost border (on shore: N 48°09'60.00", W 4°25'59.99"). The Measurements route and the location of the experimental ship are shown in the Figure 9.

During the trials, the experimental ship travelled with a maximum speed of 8 knots (speed between 4 to 8 knots). It was subjected to sea wave motion and variation.



Figure 9: Measurements route and the location of the experimental ship (22 Nm)

4.4. Sea State Conditions

The sea state varies with time, as the wind conditions or swell conditions change.

Three sea conditions were encountered in this experimentation:

- calm or near calm sea state: low wind speed (< 2 knots), clear and sunny weather
- moderate swell sea state: light wind (4 knots) with slight swell, clear weather
- rough sea state: high wind (22 knots) with swell of 2.5 m, cloudy and foggy weather.

5. Conclusion and Discussion

A campaign of experiments was conducted to measure the performance of the transhorizon NLoS propagation over the sea at the C-band, with Line-of-Sight Lygarion® Data Link, between an experimental ship and a low altitude ground station located on the cost border. This chapter presents the experimental tests results and gives some analysis and discussion of the results.

5.1 Summary of Results

Results have shown that the achievable performances (maximum range reached for the USV to transmit large sensor data to the ground station operator) depending of the sea state conditions are as follows:

- For WPDFL waveform:

Data Rate		GDT Antenna	2 dBi	23 dBi
		SDT Antenna	6 dBi	13 dBi
Downlink	5 Mb/s	Range	3.7 km (2 Nm)	36 km (19.5 Nm)
		Range		39 km (21 Nm)

Tab. 3: Maximum range reached for WPDFL waveform

- For DVB-S waveform:

Data Rate		GDT Antenna	23 dBi		
		SDT Antenna	6 dBi		13 dBi
Up/Down link	10.71 Mb/s	Range	8 km (4.3 Nm)	27.8 km (15 Nm)	40.7 km (22 Nm)
Up/Down link	44 Mb/s	Range			33 km (17.8 Nm)

Tab. 4: Maximum range reached for DVB-S waveform

The measured distances are found to agree with the simulated distances.

5.2 Analysis and Discussion of Results

Analysis of the measurements has revealed that when the ship is close to the shore the number of reflections is high and relatively strong and when the ship is further away in open sea, there is very few reflection. Moreover, the evaporation duct over the sea surface at 5 GHz frequency has negligible enhancement of signal strength for short-range.

Due to the frequency imposed by ARCEP (The French regulator of the electronic communications and postal sectors) in limit of the band pass filter for uplink direction (with an impact of -10 dB on the link budget calculation), certain measured performances are therefore below than those that would be possible to achieve in favourable conditions:

- Max distance for uplink @ 19.2 kb/s in WPDL reduced to 21 Nm
- Loss of the video in DVB-S at long distance whereas the downlink is still operating (camera in TCP-IP).

The performances achieved with omnidirectional antennas in both GDT and SDT, whatever the waveform used, are comparatively low, probably degraded by multipath and the reflection phenomena.

However, the performances achieved with directional antenna in GDT and an omnidirectional antenna in SDT, are very satisfying. It is thereby possible to envisage the use of an omnidirectional antenna in the USV as long as the use of a directional antenna is preferred in GDT.

It should be noted that, the use of a directional antenna overcome signal degradation due to the sea surface reflection and other multipath phenomena caused by a combination of reflections from the sea surface and vessels in maritime communications.

These experimental tests also allowed pointing out the impact of the sea state conditions on the data link performances:

- A perfectly smooth sea provides a mirror effect very disruptive for radio wave propagation over sea;
- A significant swell (heavy swell conditions) (wave height more than 2 m) may cause some masking problems at long range (above 10 Nm);
- A calm (glassy) sea with slight swell represents the best propagation condition.

6. Acknowledgement

The experimental tests presented in this paper were carried out with Sea Test Base company. The authors would like to express their thanks to Sea Test Base company for supporting these experimentations.

7. References

- [1] HEEMSKERK, H. J. M., BOEKEMA, R. B. The influence of evaporation duct on the propagation of electromagnetic waves low above the sea surface at 3-94 GHz. In Proceedings of the Eighth International Conference on Antennas and Propagation. Edinburgh (UK), 1993, p. 348 - 351.
- [2] MALIATSOS, K., CONSTANTINOPOULOS, P., DALLAS, P., IKONOMOU, M. Measuring and modeling the wideband mobile channel for above the sea propagation paths. In Proceedings of the 2006 First European Conference on Antennas and Propagation. Nice (France), 2006.
- [3] ETSI EN 301 210 V1.1.1 (1999-03) Digital Video Broadcasting (DVB) Framing structure, channel coding and modulation for Digital Satellite News Gathering (DSNG) and other contribution applications by satellite

TELEMETRY STANDARDS THAT IMPROVE LINK AVAILABILITY

Kip Temple

412TW-PA-18101

Air Force Test Center, Edwards AFB CA

Range Commanders Council Telemetry Group, RF Systems Committee - Chairman

kenneth.temple.2@us.af.mil

KEYWORDS - IRIG 106, coding, data quality metric, link availability, diversity

ABSTRACT

Inter-Range Instrumentation Group (IRIG) 106-17 is the latest release of the telemetry standard that defines many technologies that directly apply to increasing the link availability of aeronautical mobile telemetry (AMT) links. The Telemetry Group (TG) within the Range Commanders Council (RCC) has steadily worked with industry and government entities to develop standards that can be applied to the modern day serial streaming telemetry link that mitigate certain anomalies that exist in every airborne link in use today. Each of these technologies, or “tools” within the standard, are briefly addressed with real-world examples presented that directly show the benefit to the serial streaming telemetry link. The purpose of this paper is to not only increase awareness to the telemetry standard IRIG 106 but also provide some insight on when to apply these tools to increase link availability of a given telemetry link.

INTRODUCTION

Historically IRIG 106 has standardized best practices for modulation, recording, and multiplexing with the goal of ensuring interoperability. In response to decreasing AMT spectrum, recent additions to IRIG 106 have focused more on spectrally efficient modulations and techniques to increase the robustness of the link. Bandwidth efficient constant envelope modulation schemes Shaped Offset Quadrature Phase Shift Keying – Telemetry Group version (SOQPSK-TG) and Advanced Range Telemetry Continuous Phase Modulation (ARTM CPM) were included as were space-time coding, forward error correction, and smart diversity selection aimed towards increasing link performance. These technologies have all been laboratory and flight tested, standardized within the telemetry standard IRIG 106 [1], and productized by various vendors within the telemetry sector.

This hardware is now finding its way onto test ranges allowing the telemetry engineer to optimize the telemetry link for differing test scenarios and link conditions.

In addition to the technologies just mentioned, tried and true methods utilizing spatial and frequency diversity have not been widely implemented due to the lack of a key enabling technology, namely metric driven robust diversity source selection. Recent advancements in this area have lead the RCC/TG to standardize upon a metric to assess link quality and pass this information along to a diversity source selector.

All these tools are standardized within IRIG 106, can they be put to practice in a cohesive manner with the goal of not only increasing the efficiency and robustness of the telemetry link but also provide the test engineer with error-free data?

IRIG 106 TELEMETRY STANDARDS

The Range Commanders Council (RCC) is dedicated to serving the technical and operational needs of U.S. test, training, and operational ranges. The RCC provides a framework wherein:

- Common needs are identified and common solutions are sought
- Technical standards are established and disseminated
- Joint procurement opportunities are explored
- Technical and equipment exchanges are facilitated
- Advanced concepts and technical innovations are assessed and potential applications are identified

The vehicle that serves this RCC framework are standards that ensure test range interoperability. The RCC is comprised of 11 groups. Some of the more familiar groups are the Telemetry Group (TG), the Frequency

Manager Group (FMG), and the Telecommunication and Timing Group (TTG). IRIG 106 is maintained by the Telemetry Group. The TG is comprised of five committees: the RF Systems Committee, Data Multiplex Committee, Telemetry Network Committee, Vehicular Instrumentation Committee, and Recorder Reproducer Committee. The topics discussed in this paper can be found in Chapter 2 “Transmitter and Receiver Systems” which is dedicated to standardizing technical characteristics and methods of improving the performance of the serial streaming telemetry link.

The main focus of IRIG 106 is to ensure interoperability, at a certain level of performance, of telemetry hardware between test ranges. This is done through technical standards dealing with frequency bands of operation, frequency tolerances, modulation scheme definitions, spectral masks, phase noise limits, etc. There are also appendices that standardize mitigation techniques for many of the link anomalies that exist in every aeronautical mobile telemetry link such as multipath, transmit antenna patterns, and telemetry links with limited link budgets.

Modulation Techniques

Prior to the need for more radio frequency (RF) spectrum by the commercial sector, pulse-code modulation frequency modulation (PCMFM, a form of continuous phase modulation CPM) was the only choice for modulating an RF carrier for telemetering test data for many, many years. PCMFM is an extremely robust waveform offering excellent detection efficiency at the expense of spectral efficiency.

Today, IRIG 106 has two additional choices of modulation schemes that trade spectral efficiency measured in terms of the 99% occupied bandwidth using the bit rate R for comparison with detection efficiency measured in terms of the ratio of bit energy to noise density (E_b/N_0) versus a bit error probability of $1e^{-5}$. See Table 1 for this comparison showing this inverse relationship. Spectral occupancy goes down and detection efficiency goes up as you go down in the table. These additional waveforms are SOQPSK-TG and ARTM CPM. All three waveforms in IRIG 106 are constant envelope waveforms specifically created to operate with non-linear amplification, a typical power amplifier design used in telemetry transmitters to decrease overall current consumption.

Table 1 - IRIG 106 Waveform Comparison

Waveform	Spectral Occupancy (99% OBW)	Detection Efficiency (BEP= $1e^{-5}$)
PCMFM	1.16*R	9dB/12dB
SOQPSK-TG	0.78*R	11dB
ARTM CPM	0.56*R	13dB

Space-Time Coding

Space-Time Coding (STC) [2], a form of transmit diversity (spatial diversity coupled with temporal diversity), has been shown through theoretical studies [8, 9] and flight testing [13, 14] to mitigate the co-channel interference problem created by utilizing two antennas to transmit the same telemetry signal. This has also been referred to in literature as the “two antenna problem” and is a self-inflicted source of co-channel signal distortion. During a flight test mission, telemetry signal shadowing can exist under certain airplane-to-ground station geometries if only one transmit antenna is used. Conversely, using two transmit antennas mitigates shadowing but introduces another issue, a distorted composite transmit antenna pattern with deep nulls due to amplitude and phase imbalances between the transmitted signals. STC is designed to mitigate this distortion by space-time coding the baseband signal into two RF signals, S0 and S1. Each are at the same center frequency and transmitted each using two separate antennas. This specific Alamouti STC [12] is tightly coupled with SOQPSK-TG modulation and requires a specific transmitter than can construct the 128-bit pilot sequence coupled to a 3200-bit block of Alamouti-encoded data then provide the two RF signals (S0 and S1) for routing to the two transmit antennas.

Forward Error Correction Code

Forward error correction (FEC) is used to enhance transmitted data reliability by introducing redundant data (parity) prior to transmission. Forward error correction has been around for many years and comes in many different forms. The FEC code implemented within the telemetry community and standardized within IRIG 106 is Low-Density Parity Check (LDPC) [3] which is a “block” code. A block of information bits have parity added to them which aids in the correction of errors in the transmitted information bits once they are received at the ground station receiver/decoder. There are two information block sizes (1024, 4096) and three code rates (1/2, 2/3, 4/5) available in IRIG 106 which trade over-the-air bandwidth with coding gain. LDPC is a very powerful correction code offering gains in link margin exceeding 9dB

when compared to an uncoded telemetry link. [10]

Diversity Selection – Data Quality Metric and Encapsulation

Spatial and frequency diversity techniques are not new to the flight test community or to the wireless communication community in general. Both are mitigation techniques to fight the effects of multipath on the transmitted signal given one general concept, multipath will not occur at the same time with the same severity on two or more diverse telemetry signals. These multiple diverse signals can be created temporally, in frequency or in space (geographically). Frequency diversity is created on the test article; the same data stream is transmitted on two (or more) separate frequencies, for example F1 and F2. On the ground station both frequencies are received and a choice is made, either by a combiner (operating in the frequency domain) or best source selector (operating in the time domain), as to the best signal to use. Spatial diversity uses several ground stations placed around the test range(s) to receive the signal(s), route these demodulated signals to a main control center, then make a decision on the best signal to use. A combination of the two techniques can also be used to provide a greater level of multipath immunity. [15]

The key enabling technology that allows the combined use of these diversity techniques is smart source selection, commonly called Best Source Selection (BSS). Up until recently there was not a robust method to assess link quality, time-align or correlate each source, and then choose the best source on a bit-by-bit basis. The key here is not correlation or the bit-by-bit selection, but the accurate assessment of individual link quality done at the receive site. Bit errors are the one defining figure of merit for instantaneous link quality. In order to determine if a bit is in error, the original data must be known. Without this knowledge, the next best assessment is the probability that a bit is in error, or more commonly bit error probability (BEP) [6]. IRIG 106 contains a standardized method of assigning a Data Quality Metric (DQM) to a block of bits based upon a real-time assessment of BEP. Coupled with DQM is a standard way of transporting this information after reception for BSS consumption and processing [5]. This packaging of the metric and data together is known as Data Quality Encapsulation (DQE). [11]

To summarize, there now exists a method to assess data quality at the telemetry receiver and send this information along with a block of

data it applies to. A BSS can now take in many diverse telemetry streams with DQE, use DQM values to smartly decide which stream to choose, and present the best source to the end user. Diversity methods to fight telemetry channel anomalies can now be reliably implemented offering a huge step forward in end-user data quality.

FLIGHT TEST DESCRIPTION

The mitigation techniques standardized in IRIG 106 provide a means for the telemetry engineer to increase the efficiency and robustness of the telemetry link. Prior to any of these technologies appearing in IRIG 106, significant testing was accomplished comparing performance against a baseline. (Example: When new modulation schemes were being evaluated, PCM/FM was the comparative baseline.) But how do we know the affect these technologies can have on the telemetry link? The metric used to assess increased link performance or to evaluate the effectiveness of these technologies is known as Link Availability.

Link Availability

In addition to the random errors caused by receiver noise, error bursts due to multipath propagation, signal blockage, RF interference, receiver synchronization loss, antenna track loss, etc. are common occurrences during flight testing. Consequently, making an assessment of link quality based solely in terms of a bit error rate is not representative of link performance. The metric that best describes how well a telemetry link functions over time, or in this case during a test run, is called Link Availability (LA) [4]. This metric accounts for all sources of link outages. Link Availability, expressed as a percentage, is calculated using the following equation:

$$LA(\%) = \frac{[TotalTime - (SES + PLS)]}{TotalTime} * (100\%) \quad (1)$$

where:

TotalTime is the time of the test run in seconds

SES is Severely Errored Second, a second where the BER $\geq 1.0e^{-5}$

PLS is Pattern Loss Second, a second where synchronization was lost

Link Availability characterizes the data quality the end user observes and places a number to that observation. It is now the universal metric used for determining telemetry link performance and assessing link improvements.

Mitigation Techniques Put To Practice

The objective of any telemetry link design is to provide the control room user with the best possible data. Using the mitigation techniques now in IRIG 106, dedicated real-world flight testing has been accomplished providing the opportunity to systematically improve the data quality. At each stage of the testing, from a baseline configuration to a system configuration using all of the tools available to improve the link, data quality improvement was assessed so a clear progression of increased link availability could be illustrated.

In order to provide a challenging environment in which to test, a helicopter was chosen as the test platform coupled with a flight path designed to incorporate elements of the test range that stressed the transmission channel. The test range can be characterized as a valley with surrounding mountains enabling a multipath rich environment. Three geographically diverse receive sites were chosen throughout the range which were outfitted for signal reception, signal monitoring and data logging during the flight testing. Data reduction was accomplished at the end of each flight ensuring the data captured provided results justifying test progression to the next mitigation technique. [7]

The helicopter test platform incorporated an STC-enabled transmitter with LDPC forward error correction. One of the transmitters RF outputs was connected to an upper telemetry antenna and the other RF output to the lower telemetry antenna. An important feature of this particular STC-enabled transmitter, when not operating in STC mode, is that it can operate as two independent telemetry transmitters. This is important for this type of testing as it provides the capability to perform comparative link testing incorporating different mitigation techniques such as frequency diversity.

On the ground side, three geographically diverse telemetry sites (Site 1, Site 2, Site 3) were each outfitted with a dual channel telemetry receiver with data logging and bit error statistics capture and recording capabilities. When frequency diversity was implemented in the helicopter, each of the channels in the receivers were coupled to the same antenna polarization (RHCP). When STC was flown, channel 1 was coupled to RHCP, channel 2 to LHCP. In both cases each channel operated separately and the combined output was not used. Site 2 and 3 also had a telemetry over internet protocol (TMoIP) capability using existing range infrastructure to allow channel 1 and channel 2 received data to be sent to a central location via a dedicated IP connection.

Site 1 was the central location which housed the Best Source Selector with internal data logging, and a bit error rate tester (BERT) for logging error statistics of the output of the BSS. In addition, Site 1 housed all of the equipment necessary to control all of the remote ground station test assets located as Site 2 and 3. Though not sent to the BSS, each receiver's combiner bit error statistics were logged for later analysis. Figure 1 illustrates the entire test set-up.

A pseudo-random bit sequence, length $2^{23}-1$ (PRBS23) was used to simulate random data allowing bit error rate statistics to be captured at each site and at the output of the BSS. This information was then used for the calculation and determination of Link Availability enabling an assessment of link improvements for each flight. Table 2 shows the progression of flights starting with determining baseline telemetry link performance and progressing to applying diversity and coding techniques to mitigate channel impairments. The same flight path was flown for each flight, allowing comparisons of the results between flights, see Figure 2. The flight path selected was intended to stress the telemetry link and provide a means to show the benefits of each mitigation method. Data from each flight was not only viewed real-time at Site 1 but also logged, reduced, and analyzed after each flight. A diagram showing where and how the data was captured is included in Figure 1.

Table 2 – Flight Tests

Flight	Configuration
Flight 1 Test 1	PCMFM F1/F2 5Mbps
Flight 2 Test 1	SOQPSK-TG F1/F2 5Mbps
Flight 3 Test 1	SOQPSK-STC/LDPC F1 5Mbps

FLIGHT TESTING RESULTS

Baseline link performance testing for PCMFM modulation and SOQPSK-TG modulation both at 5Mbps were performed first. Since frequency diversity was one of the mitigating techniques under investigation, baseline link performance was further broken down on a per transmit antenna basis, upper versus lower transmit antenna. Once the baselines were determined, mitigation techniques to better the link performance were incrementally added. Test progression was as follows:

1. Baseline Link Performance – Link Availability on a per modulation and transmit antenna basis.
2. Single Site Frequency Diversity – Link Availability at each receive site utilizing frequency diversity.

3. Frequency Diversity coupled with Spatial Diversity – Link Availability using frequency diversity coupled with best source selection of spatially diverse receive sites.
4. Single Site STC coupled with LDPC – Link Availability at each receiving site on a per receive polarization basis using STC to mitigate the nulling in the composite transmission antenna pattern coupled with LDPC for error correction.
5. STC/LDPC coupled with Spatial Diversity – Link Availability using STC with LDPC coupled with best source selection of spatially diverse receive sites signals.

PCMFM Baseline

Tables 3-5 show the baseline performance of a PCMFM link operating at 5Mbps for each transmission frequency at each receive site. These results are typical PCMFM link performance in a helicopter environment without any mitigation techniques applied. These will be the LA numbers used for comparison purposes for PCMFM. At each receive site, channel 1 of the telemetry receiver was tuned to the upper antenna frequency (2240.5MHz) and channel 2 was tuned to the lower antenna frequency (2260.5MHz). Link Availability was then calculated for both of these signals at each site.

Table 3 - Site 1 PCMFM Baseline

PCMFM Baseline Link Availability		
Flight	Upper Antenna (F1)	Lower Antenna (F2)
PCMFM	86.1%	93.6%

Table 4 - Site 2 PCMFM Baseline

PCMFM Baseline Link Availability		
Flight	Upper Antenna (F1)	Upper Antenna (F1)
PCMFM	77.0%	87.0%

Table 5 - Site 3 PCMFM Baseline

PCMFM Baseline Link Availability		
Flight	Upper Antenna (F1)	Lower Antenna (F2)
PCMFM	83.3%	90.1%

SOQPSK-TG Baseline

The LA results in Tables 6 through 8 are the baseline performance of an SOQPSK-TG link on a per receive site basis. Again, at each receive site channel 1 of the telemetry receiver was tuned to the upper antenna frequency (2240.5MHz) and channel 2 was tuned to the lower antenna frequency (2260.5MHz). Link Availability was calculated for both of these signals at each site. The calculated LA numbers will be used as the baseline link performance

for SOQPSK-TG when assessing link improvement techniques.

Table 6 - Site 1 SOQPSK-TG Baseline

SOQPSK Baseline Link Availability		
Flight	Upper Antenna (F1)	Lower Antenna (F2)
SOQPSK-TG	76.7%	86.2%

Table 7 - Site 2 SOQPSK-TG Baseline

SOQPSK Baseline Link Availability		
Flight	Lower Antenna (F2)	Upper Antenna (F1)
SOQPSK-TG	72.9%	80.5%

Table 8 - Site 3 SOQPSK-TG Baseline

SOQPSK Baseline Link Availability		
Flight	Lower Antenna (F2)	Upper Antenna (F1)
SOQPSK-TG	81.4%	81.5%

PCM/FM Implementing Frequency Diversity

Table 9 tabulates Link Availability when frequency diversity is implemented using PCMFM modulation. Whereas Tables 3-5 show LA for each individual receiver channel, Table 9 shows the LA results when the receiver’s IF combiner at each site is allowed to choose between channel 1 and channel 2 as to the best signal. For this test, channel 1 of the telemetry receiver was tuned to the upper antenna frequency (2240.5MHz), channel 2 was tuned to the lower antenna frequency (2260.5MHz) and the receiver’s internal maximal ratio combiner was used to select the best signal.

Table 9 - PCMFM Frequency Diversity LA

PCMFM F1/F2 Combined		
Site 1	Site 2	Site 3
99.3%	96.2%	97.0%

SOQPSK Implementing Frequency Diversity

The numbers in Table 10 show Link Availability when frequency diversity is implemented using SOQPSK-TG modulation. For this test, channel 1 of the telemetry receiver was tuned to the upper antenna frequency (2240.5MHz), channel 2 was tuned to the lower antenna frequency (2260.5MHz) and the receiver’s internal maximal ratio combiner was used to select the best signal.

Table 10 - SOQPSK Frequency Diversity LA

SOQPSK-TG F1/F2 Combined		
Site 1	Site 2	Site 3
97.0%	95.1%	92.4%

PCM/FM with Frequency, Spatial Diversity

Building upon the results for single site frequency diversity, spatial diversity was then

added in an attempt to further increase LA. For this test, each channel (channel 1 for F1, channel 2 for F2) of each receiver at each site, totaling 6 telemetry streams, was assigned a DQM value at the receiver and sent using the DQE message structure to the Best Source Selector. Due to infrastructure constraints the combiner output for each receiver was not used. The BSS correlated the sources then made bit-by-bit source selection based upon the DQM value of each input stream. This combined stream was then sent to the BERT where bit error statistics were measured and logged. Link Availability of this configuration is shown in Table 11.

Table 11 - PCMFM Frequency/Spatial Diversity

LINK AVAILABILITY	
Flight	Frequency/Spatial Diversity BSS
PCMFM	99.4%

SOQPSK-TG with Frequency, Spatial Diversity

This test configuration is the same as the previous section with 6 sources being sent to the BSS but using SOQPSK-TG modulation. Link Availability of this configuration using both frequency and spatial diversity is shown in Table 12.

Table 12 – SOQPSK Freq/Spatial Diversity

LINK AVAILABILITY	
Flight	Freq/Spatial Diversity BSS
SOQPSK-TG	96.7%

SOQPSK-TG with STC and LDPC

This test combined SOQPSK-TG modulation with Space-Time Coding and Low Density Parity Check forward error correction. Because frequency diversity was no longer used, the single frequency transmitted was 2240.5MHz with one RF output (STC signal S0) of the transmitter connected to the upper antenna and the other RF output (STC signal S1) connected to the lower antenna. STC is being used to mitigate the self-imposed “two antenna problem” (previously mitigated with frequency diversity) and LDPC is being used to correct errors caused by the transmission channel. Since individual channels in the receivers were no longer tuning to individual frequencies, the receivers were configured to receive and decode the STC-LDPC signal and were reconnected to the antenna multicoupler, channel 1 to right hand circular polarization (RHCP) and channel 2 to left hand circular polarization (LHCP). LA numbers for this configuration at each site for each receive polarization are presented in Tables 13-15.

Table 13 - Site 1

SOQPSK STC/LDPC Link Availability		
Flight	LHCP	RHCP
SOQPSK STC/LDPC	96.3%	97.5%

Table 14 - Site 2

SOQPSK STC/LDPC Link Availability		
Flight	LHCP	RHCP
SOQPSK STC/LDPC	95.9%	96.7%

Table 15 - Site 3

SOQPSK STC/LDPC Link Availability		
Flight	LHCP	RHCP
SOQPSK STC/LDPC	97.7%	96.2%

SOQPSK-TG with STC/LDPC, Spatial Diversity

The final configuration built upon the previous results and combined STC/LDPC with spatial diversity utilizing best source selection. This configuration used all of the technologies currently standardized within IRIG 106 with the goal of providing the most robust telemetry link given the available mitigation technologies.

Each polarization (RHCP/LHCP) from each receiver at each receive site, totaling 6 telemetry streams, was assigned a DQM value at each receiver and sent with the DQE message structure to the Best Source Selector. The BSS performed its function on these 6 sources and sent the selected output to a BERT. Link Availability of the output of the BSS was calculated and is shown in Table 16.

Table 16 - SOQPSK STC/LDPC

LINK AVAILABILITY	
Flight	Spatial Diversity BSS
SOQPSK STC/LDPC	100.0%

ANALYSIS OF RESULTS

There are multiple ways to analyze the volume of data that was collected during the flight testing. The point of this paper is to highlight the systematic gains assessed in terms of Link Availability that are possible given the various mitigation techniques available today and standardized within IRIG 106. In addition to this, and perhaps more importantly, the analysis should emphasize the importance of assessing link quality at the telemetry receiver, i.e., the Data Quality Metric, and providing that information via Data Quality Encapsulation to a Best Source Selector to intelligently select the best data and provide that to the end user.

Modulation Comparison

Before mitigation techniques are analyzed, a quick comparison of modulation schemes shows PCMFM as the clear winner for a

helicopter operating in this transmission channel. This should be of no surprise as historically PCMFm is known as a very robust waveform with the receiver/demodulators exhibiting excellent detection efficiency and extremely fast receiver resynchronization properties. There is a reason it was used for over 40 years to telemeter data. Conversely, it is not nearly as spectrally efficient as SOQPSK-TG. As was stated above, historically the trade when determining modulation schemes is spectral efficiency versus detection efficiency, perhaps Link Availability should be added to this trade-off.

Another conclusion from the consolidated data presented in Table 17 is that the bottom antenna, regardless of the modulation scheme, always provided better LA. This was due in part to the flight profile and to the proximity of the rotary wing to the top transmit antenna. The flight profile led to portions of the flight where the upper antenna was shadowed from the receive site antenna due to the helicopter airframe. Also, the proximity to the rotary wing amplitude modulated the telemetry signal that at times caused the receiver to lose synchronization. Both conditions adversely affected overall Link Availability of the signal from the upper antenna.

Mitigation Technique Comparison with PCMFm Modulation

Systematic gains based on the mitigation technique for PCMFm are analyzed next. As IRIG 106 does not address PCMFm coupled with Space-Time Coding or LDPC forward error correction, these mitigation techniques were not implemented. Even so, frequency and spatial diversity techniques were tested and analyzed. Consider each one of the "Baseline" LA numbers in Table 18 to stand alone. In other words, during a "normal" flight test mission the data would be sent using one antenna at one center frequency and would be received using any one of the three receive sites.

Frequency diversity was the first mitigation technique explored. Each receive site configured the telemetry receiver to IF combine the two input signals, F1 and F2, and output the combined demodulated baseband signal to the BERT where LA was calculated using the captured statistics. IF combining, typically polarization combining and not frequency combining, is done every day on nearly every test range. In this case, significant gains in LA were achieved using frequency diversity with IF combining. At Site 1, LA increased from 93.6% to 99.3%, Site 2 increased from 87.0% to

96.2%, and at Site 3 an increase from 90.1% to 97.0% occurred.

The last of mitigation techniques for PCMFm used a combination of frequency and spatial diversity. For this test, the IF combiner in the receivers at each site was not used, instead each channel in the telemetry receiver (channel 1 for F1, channel 2 for F2) from each receive site was assigned a data quality metric and then sent via the range IP infrastructure using data quality encapsulation to the BSS resulting in 6 sources, each with a data quality estimate, to choose between. In this configuration resulting LA was 99.4%. In comparison, the telemetry link implemented in a fashion very similar to standard range practices today using a single frequency, a bottom-only antenna, and receiving at one ground station resulted in a best LA of 93.6%.

Coupling diversity techniques led to a very impressive gain in LA. Realizing this gain was achieved without the use of advanced techniques like Space-Time Coding, LDPC forward error correction, or even equalization. Rather, tried and true methods of frequency and spatial diversity were used and optimized by a link quality assessment made at the receive site and sent to a BSS using DQM/DQE for source selection.

Mitigation Technique Comparison for SOQPSK Modulation

A systematic approach in the application of mitigation techniques available for SOQPSK-TG modulation was applied to the telemetry link with the goal of clearly illustrating increasing LA with the results shown in Table 19. Baseline LA numbers from Table 17 are used for comparison. These baseline numbers can be considered as typical SOQPSK-TG link performance numbers, the configuration is representative of how a flight test mission would transmit and receive data. Best LA achieved under this baseline configuration was 86.2% using the bottom transmit antenna and receiving that signal at Site 1.

Frequency diversity was tried next with bit error statistics captured and analyzed for each receive Site 1, 2, and 3. Frequency diversity was achieved by configuring the telemetry transmitter to transmit the same information on two frequencies, F1 and F2. Each receiver at each site was configured to IF combine the two frequencies and output the demodulated combined signal. LA was calculated for each of the combined outputs shown in the row labeled "Frequency Diversity" in Table 19. Highest LA was 97.0% achieved at Site 1. Note: Most test ranges implement polarization diversity by IF

combining left-hand and right-hand receive antenna polarizations, this test differed from that by combined two separate signals containing the same information centered at F1 and F2.

Spatial diversity was then added to this configuration using each received signal from each receive site (F1 and F2 with no IF combining) resulting in 6 frequency AND spatially diverse signals being sent to the BSS. Combining frequency and spatial diversity resulted in a LA of 97.0%, shown in the row labeled "Freq/Spatial w/BSS" of Table 19. It is interesting to note this is the exact same LA achieved at Site 1 using frequency diversity suggesting Site 1 was selected most of the time by the BSS.

Applying advanced mitigation techniques as specified in IRIG 106 was the final step towards trying to achieve error-free telemetry. The first step towards this goal was to determine single site link performance by coupling together Space-Time Coding and Low Density Parity Check forward error correction to the telemetry link. Reiterating. STC is used with SOQPSK-TG due to the tight coupling between modulation and the code. Each site used RHCP and LHCP as channel 1 and channel 2 inputs to the telemetry receiver and LA was calculated for each of these signal paths and shown on row "STC/LDPC" in Table 19. Best LA that was achieved for this configuration was 97.1% receiving LHCP at Site 3. Note, this single site LA is greater than what was achieved using frequency and spatial diversity with uncoded SOQPSK-TG.

The last configuration again used a combination of STC/LDPC but this time coupled with best source selection. The received signals (STC/LDPC RHCP, STC/LDPC LHCP) had a data quality metric assigned to each signal accomplished at each of the three receive sites then encapsulated for transfer to the best source selector located at Site 1. This gave the BSS 6 coded, spatially diverse sources in which to make a bit by bit link selection based upon the assigned DQM for each source.

It is important to understand this last configuration for both the airborne platform and ground stations prior to taking an in-depth look at the results. Recapping, the STC-enabled transmitter had one RF output (S0) connected to the top antenna, the other RF output (S1) connected to the lower antenna and both STC and LDPC were enabled in the transmitter. In this specific case, the information block size for the LDPC code was 4096 and the code rate was 2/3. Data was PRBS23 at a rate of 5Mbps

(uncoded), over-the-air rate after applying LDPC and STC was 7.8125Mbps transmitted at a center frequency of 2240.5MHz. At each receive site the telemetry receiver had channel 1 connected to the RHCP RF multicoupler, channel 2 was connected to the LHCP RF multicoupler, and STC and LDPC decoding for SOQPSK-TG was selected for each channel. The receiver then applied a DQM value to each demodulated signal and encapsulated that information for transport via TMoIP to the best source selector located at Site 1. A total of 6 coded, diverse sources were applied to the BSS which first time correlated the sources then made bit by bit best source selection based upon the DQM value for each. The output of the BSS was connected to a bit error rate tester where bit error statistics were logged and displayed real-time.

The flight path shown in Figure 2 was flown and bit error statistics were captured at each site per Figure 1 throughout the flight. Referring to Table 19, LA for this flight and test configuration was **100%**. Equation 1 for Link Availability tells us this result means there were no severely errored seconds (SES) and no pattern loss seconds (PLS) throughout the flight. Because the BERT's used were able to log individual bit errors, a deeper look at the recorded bit error statistics revealed that the output of the BSS had zero bit errors throughout the flight.

Further investigation of this revolutionary result is justified. The underlying assumption of utilizing diversity for telemetry systems is that the channel distortion is uncorrelated with respect to the diversity method. For example, if diversity is used it is assumed that channel distortion including multipath, composite transmission antenna pattern nulling, ground station antenna pointing error, or threshold signal-to-noise ratio (SNR) do not occur at the same time at each receive station. Previous analysis has shown this can be illustrated by plotting the estimated bit error probability that each receiver assigned the signal throughout the duration of the test or during times of interest. This information can be captured at each receiver and then again at the BSS. If the distortion was time correlated these plots would show groupings of estimated BEP indicating that errors occurred at exactly the same time. If the plot was magnified, it would further show that there were groupings on a per site basis where degraded BEP was time correlated. If the receiving sites are truly diverse, there will be no correlation of multipath or channel distortion events. For this test we know this analysis to be true as the BSS always had an error-free source to select.

Table 17 – Comparison of Modulation Schemes

Flight	BASELINE LINK AVAILABILITY					
	Site 1		Site 2		Site 3	
	Upper Antenna (F1)	Lower Antenna (F2)	Upper Antenna (F1)	Lower Antenna (F2)	Upper Antenna (F1)	Lower Antenna (F2)
PCM/FM	86.1%	93.6%	77.0%	87.0%	83.3%	90.1%
SOQPSK-TG	76.7%	86.2%	72.9%	80.5%	81.4%	81.5%

Table 18 – Comparison of Mitigation Techniques, PCMFM

Flight	PCM/FM LINK AVAILABILITY					
	Site 1		Site 2		Site 3	
	Upper Antenna (F1)	Lower Antenna (F2)	Upper Antenna (F1)	Lower Antenna (F2)	Upper Antenna (F1)	Lower Antenna (F2)
Baseline	86.1%	93.6%	77.0%	87.0%	83.3%	90.1%
Frequency Diversity	99.3%		96.2%		97.0%	
Freq/Spatial w/BSS	99.4%					

Table 19 – Comparison of Mitigation Techniques, SOQPSK-TG

Flight	SOQPSK-TG LINK AVAILABILITY					
	Site 1		Site 2		Site 3	
	Upper Antenna (F1)	Lower Antenna (F2)	Upper Antenna (F1)	Lower Antenna (F2)	Upper Antenna (F1)	Lower Antenna (F2)
Baseline	76.7%	86.2%	72.9%	80.5%	81.4%	81.5%
Frequency Diversity	97.0%		95.1%		92.4%	
Freq/Spatial w/BSS	97.0%					
	LHCP	RHCP	LHCP	RHCP	LHCP	RHCP
STC/LDPC	96.3%	97.5%	95.9%	96.7%	97.1%	96.2%
STC/LDPC w/Spatial BSS	100.0%					

CONCLUSIONS

There are few transmission channels as challenging as a helicopter flying at low altitudes. This combination coupled with rotary wing effects on the transmitted signal led to a multipath rich environment causing Link Availability for the baseline configuration of 76.7%. The baseline configuration mimicked traditional transmission and reception methods used today throughout the airborne telemetry community. By coupling various standardized techniques together for both PCMFM and SOQPSK-TG modulation schemes, significant increases in link availability were achieved when compared to the baseline configuration. These gains in LA were achieved using tried and true frequency and spatial diversity methods as well as methods standardized within IRIG 106, Space-Time Coding, Low Density Parity Check forward error correction coding, and Data Quality estimation. The key enabling technology was the ability of the telemetry receiver to accurately estimate signal quality without a priori knowledge of the signal. With this quality estimate in the form of an

estimate of bit error probability, a best source selector with signal correlation capabilities could use the link quality estimates to intelligently select the best source on a bit-by-bit basis.

Once a baseline link performance was established, systematically stepping through frequency diversity, spatial diversity, STC, LDPC, and best source selection illustrated the gain associated with each method and ultimately showed how coupling these methods can significantly improve link availability.

*Ultimately, the combination of SOQPSK-TG modulation with STC and LDPC with DQM/DQE assigned to the received signals allowed the use of a BSS to intelligently choose the best telemetry signal to output. This configuration achieved a LA of 100%. Further investigation into this result led to the realization that not one bit error occurred at the BSS output, realizing the goal of **error-free telemetry**.*

The methods standardized in IRIG 106 have been shown to increase link availability either

individually or when used in conjunction. These standardized methods should be considered

when designing new telemeters if end user data quality is of ultimate importance.

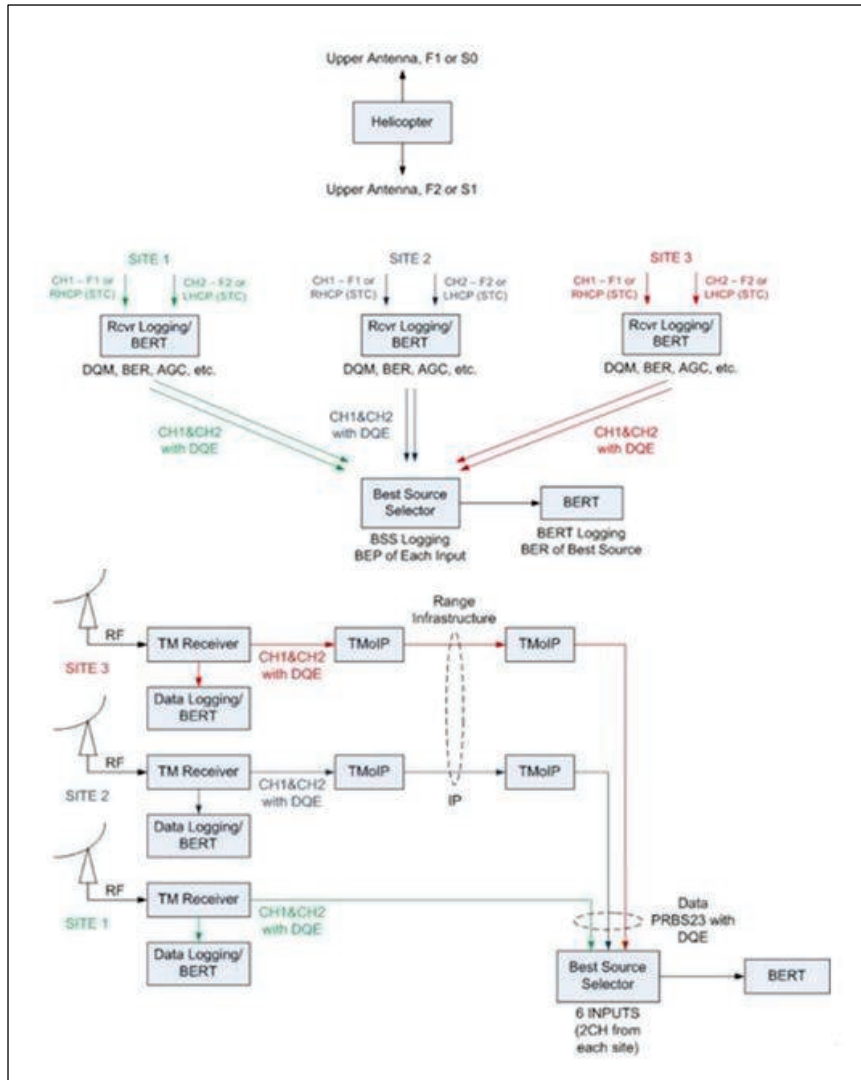


Figure 1 – Test Set-Up and Data Logging



Figure 2 – Flight Test Path

REFERENCES

- [1] Secretariat, Range Commander Council, “*Transmitter and Receiver Systems*”, RCC Document IRIG 106-17 Chapter 2
- [2] Secretariat, Range Commander Council, “*Low Density Parity Check Codes for Telemetry Systems*”, RCC Document IRIG 106-17 Appendix 2D
- [3] Secretariat, Range Commander Council, “*Space-Time Coding*”, RCC Document IRIG 106-17 Appendix 2E
- [4] R. Jefferis, “*Link Availability and Error Clusters in Aeronautical Telemetry*”, International Telemetry Conference Proceedings, Las Vegas, NV, October 1999
- [5] T. Hill, “*Metrics and Test Procedures for Data Quality Estimation in the Aeronautical Telemetry Channel*”, International Telemetry Conference Proceedings, Las Vegas, NV, October 2015
- [6] M. Rice, E. Perrins, “*Maximum Likelihood Detection from Multiple Bit Sources*”, International Telemetry Conference Proceedings, Las Vegas, NV, October 2015
- [7] M. Diehl, J. Swain, T. Wilcox, “*Rotary-Wing Flight Tests to Determine the Benefits of Frequency and Spatial Diversity at the Yuma Proving Ground*”, International Telemetry Conference Proceedings, Phoenix, AZ, November 2016
- [8] M. Rice, T. Nelson, J. Palmer, C. Lavin, K. Temple, “*Space-Time Coding for Aeronautical Telemetry: Part I – Estimators*”, IEEE Transactions on Aerospace & Electronic Systems
- [9] M. Rice, T. Nelson, J. Palmer, C. Lavin, K. Temple, “*Space-Time Coding for Aeronautical Telemetry: Part II – Decoder and System Performance*”, IEEE Transactions on Aerospace & Electronic Systems
- [10] E. Perrins, “*FEC Systems for Aeronautical Telemetry*”, IEEE Transactions on Aerospace & Electronic Systems, vol. 49, no. 4 pages 2340-2352, October 2013
- [11] Secretariat, Range Commander Council, “*Standards for Data Quality Metric and Data Quality Encapsulation*”, RCC Document IRIG 106-17 Appendix 2G
- [12] S. Alamouti. “A Simple Transmit Diversity Technique for Wireless Communications.” *IEEE Journal on Selected Areas in Communications*, vol. 16, no. 8, pp. 1451-1458, October 1998.
- [13] K. Temple, “*Performance Evaluation of Space-Time Coding on an Airborne Test Platform*”, International Telemetry Conference Proceedings, San Diego, CA, October 2014
- [14] M. Geoghegan, L. Boucher, “*Space-Time Coding Solution to the Two-Antenna Interference Problem*”, International Telemetry Conference Proceedings, San Diego, CA, October 2014
- [15] M. Geohegan, R. Schumacher, “*Performance Results Using Data Quality Encapsulation (DQE) and Best Source Selection (BSS) in Aeronautical Telemetry Environments*”, International Telemetry Conference Proceedings, Las Vegas, NV, November 2017
- [16] T. Rappaport, “*Wireless Communication, Principles and Practice*”, New Jersey: Prentice Hall, 1996
- [17] J. Proakis, “*Digital Communications*”, New York: McGraw-Hill, 1995

History and Advantages of Best Source Selection for Today's Modern Telemetry Applications Along With the Benefits of Different Approaches

Stephen Nicolo
 GDP Space Systems
 A Division of Delta Information Systems
 747 Dresher Road
 Horsham, Pennsylvania 19044-2247 USA
 Phone: (215) 657-5270
snicolo@gdp.space.com

Abstract:

Best Source Selection (BSS) has become a major topic at many modern telemetry ranges and ground stations around the world today. Best Source Selection techniques for telemetry applications, have been around for well over 25 years in one form or another. With the introduction of Next Generation Correlating Best Source Selection techniques a decade ago, the BSS function has evolved into an extremely powerful tool for the real-time and post flight recovery of telemetry data. These Next Generation techniques, currently operational at a variety of ranges around the world today, provide significant performance increases at these sites. As ranges continued to evolve, moving toward more network centric solutions, **Correlating Best Source Selectors** have also followed this trend while still dealing with the issues of encrypted data, latency and switching from stream-to-stream without dropping lock on downstream frame synchronizers.

This paper describes the evolution of Best Source Selection as well as the advantages and disadvantages of a variety of different approaches and **BSS** modes of operation that are available today.

Key words: Data Acquisition, Best Source Selection, Correlating Best Source Selectors, DQE

What is a Best Source Selector?

In the telemetry world there are many situations where there is a transmitting device sending telemetry information to several ground antenna receiving sites. In these types of applications, the transmitters are typically moving (i.e. aircraft, ground vehicle or missile). At any point in time the best received signal with the minimum amount of interference is changing as a result of noise, obstructions and / or signal reflections. These applications require an automatic and dynamic method of selecting the best source of data (best receiving site) at every point in time during the mission. One of many examples of this is a flight test application. In this application the aircraft under test continually transmits the test data to several receiving sites on the ground. These receiving sites are typically located at various points along the path of the test aircraft (refer to

Figure 1). In Figure 1, the transmitted signal from the aircraft (#1) is received by three antennas (# 2, 3 & 4). The received signal is then routed through receivers and bit synchronizers to a Best Source Selector unit (#5). The Best Source Selector (BSS) then selects the best signal for output (#6). At any point in time, based on the position of the transmitter on the aircraft with respect to a particular receiving site, one or more receiving sites has a better signal than the others. In these applications, a system (Best Source Selector) that can quickly detect and react (i.e. switch to the best signal) is required so that the end result is Best Source Selector data output that is better than any individual input over time.

This document explores the evolution of Best Source Selection in the telemetry world. It also points out the pros and cons of a variety of different approaches and modes, and describes

the many different modes that are available to solve this challenging problem as well as the significant performance gains that can be

achieved with the latest FPGA technologies that are available today.

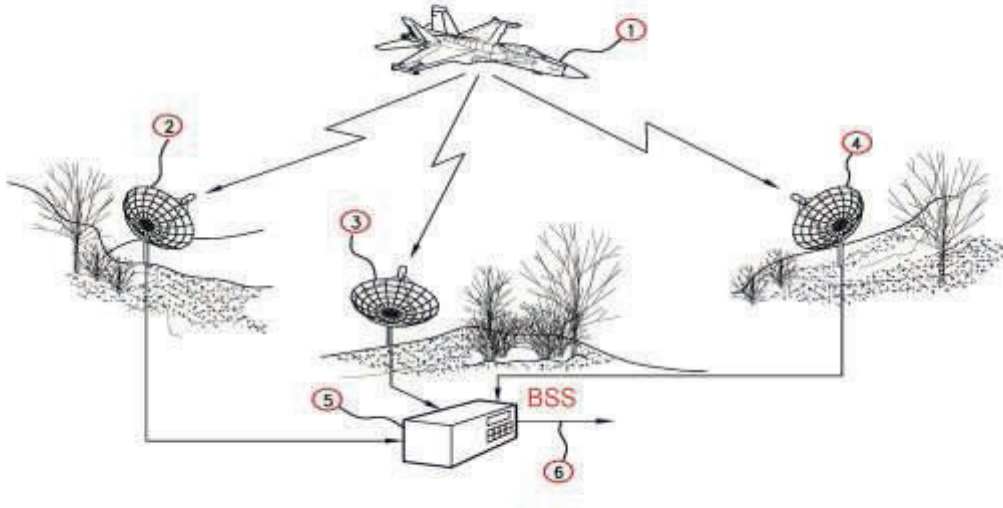


Figure 1. Example Flight Test Best Source Selector Application

Definition of the Problem

As streams are received from different sources they are routed to a central location for processing and Best Source Selection. Since time delays can vary from source to source, based on transmission distance and a variety of different equipment delays, data is skewed in both phase and time as it is received at the Best Source Selector. Probably, the most serious problem is that of data loss due to the switching process and / or noise bursts. These error bursts typically happen at the worst possible time (during the test maneuver), when critical data is required (i.e. aircraft / vehicle maneuver in the flight test example). Figure 2 depicts the misalignment of the streams as seen by the Best Source Selector. Because of these skews between streams, if the Best Source Selector does not handle this properly, the BSS switches from stream to stream resulting in time jumps and drop-locks on downstream frame synchronizers from the selected BSS output. This was one of the drivers in the evolution of Best Source Selectors toward correlating the streams in time to each other (Correlating Best Source Selectors). A second problem is the ability to do Best Source Selection of encrypted data.

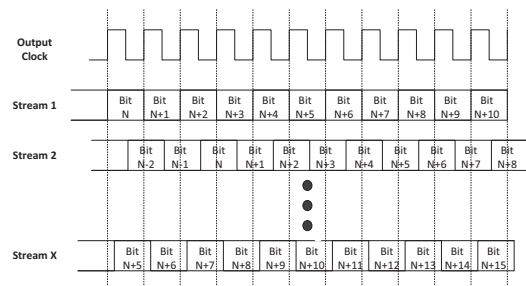


Figure 2 Raw Data (Not Phase or Time Aligned)

In Figure 2 the clock associated with the Best Source Stream is used as the Best Source output clock. In Figure 2 this happens to be Stream 1 at this point in time. Note however that any of the streams could have been the primary stream if it had been deemed to be the best stream based on quality metrics that are discussed further in this document. Notice that each rising edge of the output clock is lined up (synchronous) with the data transitions in Stream 1 (Stream 1 is in phase with the output clock). Since time delays can vary from source to source, based on transmission distance and a variety of different equipment delays, the phase and data content of the other streams are not lined up with the output clock (i.e. they do not switch synchronously with the rising edge of the output clock). Since in a Correlating Best Source Selector we regenerate the Best Source output bit stream on a bit-by-bit basis, all candidate streams must be

synchronous and time aligned with the output clock. This is one of the key problems that a modern BSS had to overcome. Methods of dealing with this problem for both clear and encrypted data are discussed in further detail in the following sections of this document.

History/Evolution of Best Source Selectors

In the late 80's and 90's Best Source Selectors were basically frame synchronizers with a selector switch on the output. The user had to have some knowledge of the path of the aircraft for best results. Each stream in a group was assigned a priority based on the path of the mission. The Best Source Selector logic basically started with the highest priority stream that was in lock. When the current stream dropped lock, the Best Source Selector output would switch to the next highest priority stream that was in lock. This is illustrated in figure 3 below.

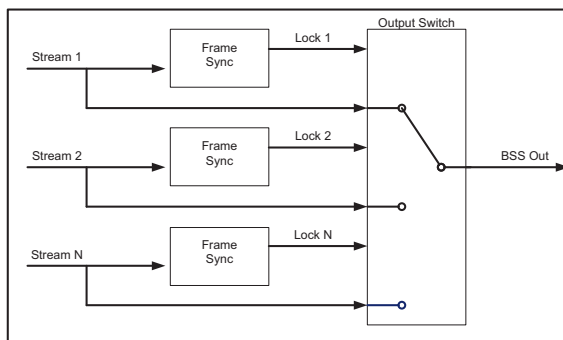


Figure 3 Non-Correlating Legacy Best Source Selector

Frame Sync lock was used as the indicator that the received stream was good or bad. As with most frame synchronizers, lock strategies (Allowable Search, Check, Lock & Flywheel Errors) could be programmed for each stream allowing them to ride through short bursts of errors in the stream without dropping lock, which would cause the unit to switch to another stream. This is because in early Best Source Selectors the streams were not correlated in time to each other and frequent switching was not desirable. At switch time, jumps and loss of lock on downstream frame synchronizers would occur. Another issue with this approach was that the BSS could not handle encrypted data because a clear frame sync pattern was required for switch decisions.

In the 2000's, as higher density FPGAs became more prevalent and as PC processing power increased significantly in the industry, they were adapted to Best Source Selector applications. There was a major push to correlate the streams in time to each other in the Best Source Selector. This is because once the

streams were correlated, there would be no interruption in the downstream data from the BSS output when the BSS switched from stream to stream. This made it acceptable to switch more often as the data quality of each of the streams dynamically changed. There was also a push for more complex modes of operation and algorithms for establishing quality of the streams for better performance of the BSS. With data stream correlation now possible, a next generation of Correlating Best Source Selectors was born.

For the correlation of the streams and the implementation of new BSS algorithms there are several different approaches from different vendors to accomplish this task. These approaches basically fell into two main categories: the PC Based Approach using PC hard drives and the hardware based FPGA approach using high density FPGAs, and solid state memories for the temporary storage and processing of BSS data. In the PC approach, frame synchronizers were again used to synchronize to the incoming streams and store these streams in buffers on the hard drive in the computer. The PC correlated the data streams in time to each other based on the framed data on the drive. This was again very processor intensive and although the PC could handle an individual stream at rates of up to the required 40Mbps, there was a maximum total aggregate rate for all streams together (all streams could not simultaneously operate properly at maximum rate). In a 16 stream system example, there was a limit to how many streams could be processed based on rates and number of streams. This was because the PC would reach its processing limit. Like the other legacy frame synchronizer based units, these units could not handle encrypted data until the introduction of RCC Encapsulated streams in late 2017. The RCC DQE/DQM is discussed further later in this document.

In the high density FPGA based solution; a completely different approach was taken from day one. The FPGA introduced a new correlation method based on the data content itself, which is totally independent of the frame synchronizer pattern. In this approach, state machines continually matched patterns in the actual data itself to correlate the streams in time to each other. Once the streams were correlated, the state machines would continually check correlation every 256 bits. This high speed, OS independent, FPGA based approach allowed the Correlating Best Source Selector to handle correlation of all streams at maximum bit rate simultaneously with no maximum aggregate rate limit and no

requirements for high speed PCs, PC Operating Systems and hard drives. With this FPGA approach for correlation of data based on data content and not frame synchronizer pattern, this approach could handle encrypted data from the start. In fact, due to the randomized nature of encrypted data, the FPGA approach of correlating on data content worked better with encrypted data (it is totally unique and easier to correlate). This FPGA based approach was the first approach that was able to support encrypted streams and it was introduced in the 2008 time-frame.

Figure 4 illustrates the incoming candidate streams for Best Source Selection both phase aligned and time aligned. With this new phase and time alignment of the streams, lossless switching between streams was now possible opening the way for more complex algorithms and modes of operation. These modes and methods of BSS are discussed in more detail later in this document.

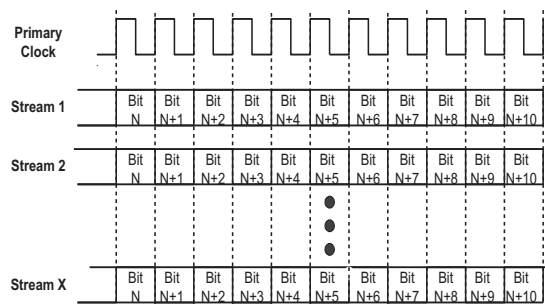


Figure 4 Streams Aligned in both Phase and Time Allowing Lossless Switching

Data Transport

Early Next Generation Correlating Best Source Selectors (CBSS) either used digital modes for data quality (quality based on errors in the frame sync pattern) or they used analog modes in which signal quality was assigned at the bit level (data quality for each bit) in bit synchronizers located in the Correlating Best Source Selector. These modes of operation are discussed in more detail later in this document. Around 2010 the bit synchronizers with Best Source Selector capability were not only available in the Correlating Best Source itself but were located at remote sites. At these remote sites bit synchronizers locked to the incoming data stream and assigned quality metrics at the remote site based on distortion of the received analog output of the receivers. Data, along with quality information, was then sent to the Correlating Best Source Selectors in a transfer frame and Data Quality Encapsulation (DQE) was born. This DQE transfer frame had a frame sync pattern along

with data and interleaved quality information. This allowed more flexibility in the CBSS system implementation and allowed further separation of the antennas. With DQE, the antenna could be over 50 miles away and still used in the Correlating Best Source Selector (CBSS) mix. The data along with quality information from the remote site were sent back to the CBSS as data and clock. In recent years, DQE was moved from the stand-alone bit synchronizer to the bit synchronizer in the receiver. This allowed receiver and bit synchronizer parameters in the receiver to generate data quality information, which today is called Data Quality Metrics (DQM). Today there are still several different modes for DQE and DQM (both legacy bit-by-bit and the newer RCC type based on thousands of bits). They each have their application and their benefits. Better Correlating Best Source Selector units support all of the available BSS modes and additionally support mixed modes. The support of mixed modes is a very important feature. With mixed modes operators can use different modes at the same time for optimum performance in any application. Having several different modes in their toolbox allows the user the flexibility to handle any application. Modes are discussed further in the next section.

Early Data Quality Encapsulation (DQE) implementations output data and clock which was transported over a variety of transport media at ranges (i.e. Ethernet, Multiplexers, Microwave, etc.) from remote sites to the CBSS. More recently, several types of DQE/DQM are able to be output directly from receivers in both Data/Clock format and also Ethernet transport. Better CBSS units accept data along with quality from transport streams in both Data/Clock and also from Ethernet directly.

Data Quality and Next Generation Correlating Best Source Selector Advanced Modes of Operation

With the availability of new technologies (Larger FPGAs and Higher Speed Computers) along with the challenges from industry to provide better more powerful implementations of Best Source Selection, telemetry manufacturers came up with a variety of new modes and algorithms. These could be utilized along with the new types of Correlating Best Source Selectors that provided lossless switching and additional performance gains. The CBSS output stream could now perform several dB better than the best input stream. Lossless switching (Correlating Best Source Selectors) was huge in the evolution of Best Source Selectors. These new advancements, which

went along with Best Source Selection, included new methods for determining the quality of the stream. One vendor (GDP) even determined quality down to the bit level for maximum performance in multipath situations. The data and the quality information was then stored into memory to be used by these new algorithms. The challenge was to do this in real time with minimal impact on latency.

The initial legacy systems used in the 90's depended on Frame Sync Lock for the determination of a good or bad stream. This was simple and straight forward. Progressions over the next two decades introduced a variety of different modes and algorithms. They include the initial digital modes and later analog modes along with a variety of different metrics all of which, in one way or another, come back to the error rate or error rate probability of the candidate streams for CBSSs. Several key modes utilized today are discussed in further detail in the following paragraphs.

Digital Pattern Mode (Pattern Eb/No):

In the Digital Pattern (Pattern Eb/No) mode, frame sync lock is still used in the Correlating Best Source Selector algorithm. In addition to frame sync lock, additional quality information is also gathered based on statistical errors in the frame sync pattern. This mode, by itself, can be used when legacy receiver and bit synchronizer hardware is being used that do not have the ability to provide the newer additional quality information to the Correlating Best Source Selector. It is not as fast to react as other modes because quality is determined on a small number of bits in each minor frame (frame sync pattern). Because of this, it takes many frames of data to calculate a useful quality measurement as a stream degrades or gets better. If three or more streams are available this mode can be used in conjunction with Majority Vote for several additional dB of performance gain (depending on the number of available streams). The switchover to Majority Vote should be quick and automatic as soon as three or more streams are available. This mode cannot be used when the stream is encrypted but is a very useful mode to have in your toolkit for situations when legacy hardware is being used that does not support some of the newer modes of best source selection.

RCC Mode DQE/DQM Mode:

In late 2017, the Range Commanders Council came up with a method to assign a Data Quality Metric (DQM), which was basically a Bit Error Probability (BEP) of each consecutive block of data from the incoming stream. This Data Quality Metric (16 bit quality value), which

translated directly to Bit Error Probability (BEP) from a defined table, was assigned to a block of data to be used in best source selection. A 16 bit quality value for each block of data (the DQM) was included in a special Data Quality Encapsulation (DQE) transfer frame to get the data blocks from the receiver to the Correlating Best Source Selector. The header for each block was 48 bits. The header contained a 16 bit frame sync pattern, the 16 bit DQM value for that particular block of data and some other information bits. Although the block size is programmable (minimum 1K bits / maximum 16K bits), the size that was initially qualified and used was 4K bits. The DQE transfer frame with data, allowed other BSS implementations that did not have the ability to measure quality of the analog baseband signals in their internal bit synchronizers, to now be able to handle encrypted data streams. This was because the quality information was passed to the BSS via the DQE stream. This is a solid mode of operation which is much better than the straight digital mode that looked for errors in the sync pattern. It could also be used in conjunction with a Majority Vote mode, when three or more streams are available, for performance gain on the BSS output. This mode has less overhead than the GDP bit-by-bit mode. However, with 2 streams there is no performance gain and it still has only 1 quality value for a very large block of data. Since this mode is fairly new, additional performance testing must still be done to further quantify this mode of operation. Further definition of this mode is provided in IRIG106-17 Chapter 2, Appendix 2-G.

CRC Mode:

The cyclic redundancy check or CRC is a technique for detecting errors in received digital data. CRC information is a code word containing a fixed number of bits that is appended to a defined block of transmitted data bits. The CRC information is based upon the multiplication of a polynomial with the data contained in the data block. By processing the received data blocks with the same polynomial in the same way as the transmitting system, the receiving system is capable of determining if errors exist in the received data. If the block of data has no errors, it can be used in the CBSS output.

When added to a telemetry frame that is passed over a data link, the CRC may be used to determine the quality of the transmitted bit-stream. The CRC word is appended as the last word contained in each minor frame of the telemetry stream produced by the transmitter. Pad bits (zeroes) may be added after the CRC, if needed, to permit decommutation of the

frame in a fixed number of bits per word. Calculation of the CRC is based upon the data block beginning with the first bit of the Frame Synchronization Pattern and ending with the last bit of the word preceding the CRC word (the entire telemetry payload). Since it is possible for a highly errored frame to be reported by the CRC test as OK, bit errors found in the frame synchronization pattern are also measured.

When the data stream is received by the CBSS, an error check is performed based upon the received CRC word. The received CRC is compared with the calculated CRC at the receiver. If a CRC error is detected, a "flag" bit is set to indicate this situation. The error bit (flag) is used by the best source selector as a part of its decision making process. Since a single bit error will cause a bad CRC value (stream is in error) this mode should also be used in conjunction with other modes like Majority Vote. When all streams are bad and there are more than 3 streams a Majority Vote will be performed. CRC mode is not widely used, but it is another available tool in the CBSS toolkit.

GDP Weighted Majority Vote /Analog Bit-by-bit Mode with GDP Data Quality Encapsulation (GDP DQE):

This mode is the most powerful mode in the Correlating Best Source Selector toolset and it should be utilized in any situation where it can be used. It has been available and operational for well over 10 years now. It is unique because it provides a quality measurement for each bit. This mode of operation has three configurations. The configuration that is used depends on the application. The first implementation includes full-up bit synchronizers as part of the Correlating Best Source Selector (CBSS) unit itself. The bit synchronizer takes the raw analog video output from the receiver. From this raw analog output signal, quality is determined based on distortions in the analog signal. The second implementation is where the bit synchronizer is located external to the CBSS. In this mode, the legacy receiver is typically at a remote location. A bit synchronizer with Data Quality Encapsulation ability is placed at the remote site. It measures the quality of the analog signal from the receiver and sends the data along with interleaved quality information to the CBSS. The third more recent implementation is to send this information with the data directly out of the receiver (via data/clock and/or Ethernet). When data is received, quality of the

stream is determined and the data along with interleaved quality information is sent to the Correlating Best Source Selector. Because this mode determines quality of the received analog signal it does not matter if the data is encrypted or clear.

In all cases there are two quality measurements made on the data. The first is a Long Term Signal Quality, measured over 256 bits. This is used in the validation of the stream and tells the CBSS the basic health of each received stream. The second measurement is a bit-by-bit Short Term Signal Quality (Quality of each bit). This information is then stored in the CBSS in solid state memories along with the data for each of the candidate streams. To achieve the full benefit of the Weighted Majority Vote mode, three or more data streams are needed. However, significant performance gain is still achieved with only two streams utilizing the bit-by-bit signal quality information alone. This ability to get a performance gain (greater than 2dB) with 2 streams and the fact that the data can be encrypted is huge. With this mode enabled, when there are only two valid streams present, they are automatically correlated in time. The bit-by-bit output is then determined based on the bit-by-bit signal quality. Figure 5 illustrates, at a high level, how this algorithm works. For example: if one of the two streams has a signal quality which is 5dB better than the other stream in a particular bit location, the bit value of the better stream is output in that bit location. Although error correction occurs in this mode, maximum error correction performance is achieved when three or more valid sources are present.

When a third source comes on-line, the FPGA state machines automatically correlate this stream with the other two sources and full majority voting (weighted by the short and long term Quality) is invoked. For example, with three sources, the corresponding bit location in each of the sources is examined and a vote occurs with the signal quality bits present to determine the validity of the data bits. This mode corrects the output data stream when error bursts occur due to receiver fades and / or multi-path interference. In this mode, a substantial link performance gain is achieved of better than three times the error rate squared. For example three sources with an error rate of 10^{-3} result in an output error rate better than 3×10^{-6} . This translates to performance gains of better than 2dB for two streams, better than 3 dB for three streams and better than 5 dB for four streams.

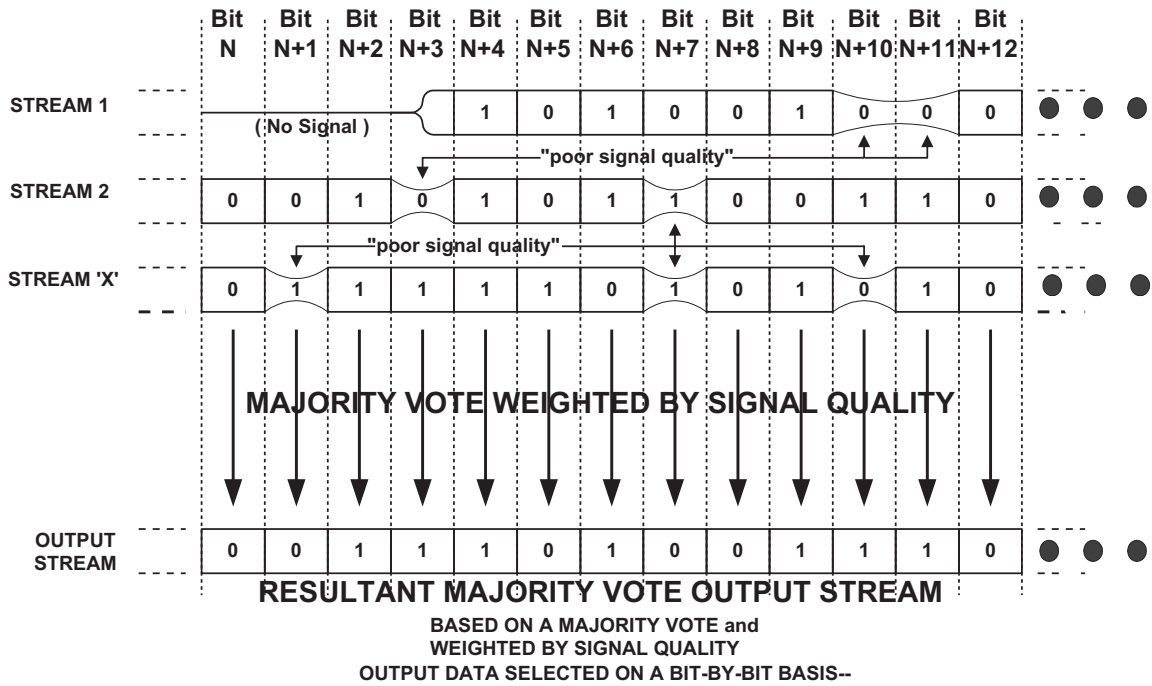


Figure 5 Best Source Selector: Majority Vote Mode (Weighted by Signal Quality)

In the GDP DQE mode, data and quality information is again sent to the CBSS in an encapsulated stream. The encapsulated stream includes a frame sync pattern along with data and interleaved Long Term and Short Term (Bit-by-Bit) data quality. Because the encapsulated stream includes quality data for each bit, the link between the remote site and the CBSS requires a bandwidth of 2.1 times the bit rate. For situations where bandwidth is an issue, there is another GDP encapsulation mode that provides quality for every 4 bits. This mode requires a bandwidth of 1.6 times the bit rate.

Conclusion:

Best Source Selection has come a long way over the past 25 years. Today's modern Correlating Best Source Selectors (CBSS) are

extremely powerful and not only pick the best source but also provide significant performance gains (in some cases over 5dB). CBSS units allow the user to take advantage of spatial diversity with multiple antennas each having a different view angle of the test vehicle. The signals from these antennas can be summed for maximum performance. CBSS units that can simultaneously use a variety of different modes and algorithms, as needed, not only provide performance gains but also provide the best bit-by-bit output solution at any instant in time. Modern units support the data / clock inputs and outputs as well as Ethernet links between the hardware. Correlating Best Source Selectors are here to stay and are at the heart of any new modern test range or launch facility.

Launch Vehicle Electrical Power System Rocket-ground Wireless Interface Prototype

Xianting Bi, Jingang Zhang, Xinglai Wang, Wei Zhu

Beijing Institute of Astronautical Systems Engineering, Fengtai Strict, Beijing, China

Zhangjg2009@126.com

Abstract:

To realize unattended test for launch vehicle, we design and implement the electrical power system rocket-ground wireless interface prototype by means of a short distance high speed wireless communication and high power wireless power supply integration technology that is adapted to test and launch mode. This work gives the overall design and application scheme. The wireless laser power supply and wireless communication integration system consists of high power laser, transmit optical antenna, receive photoelectric conversion array and wireless laser communication equipment (transmit and receive). The transmission and conversion efficiencies of wireless power supply and communication are promoted by optimization design of transmit and receive device, the performance of 2kw power supply at 25m with 500Mbps bidirectional wireless communication capability can be achieved.

Key Words: rocket-ground wireless interface, laser, unattended test, optimization

I. Introduction

Launch vehicle electrical power system rocket-ground interface is used for power supply, instruction and data interaction between on-vehicle electrical system and ground test and control system during testing and launching. The traditional connection-separation devices used in launch vehicle electrical power system rocket-ground interface are pull-off connector and separation connector, which are complicate to operate, have low connection reliability and cannot realize automatic connection, therefore are unable to meet the front end unattended test demand of new launch vehicle^{[1]-[5]}. With the rapid development of high speed wireless communicate technology represented by laser^{[6],[7]}, microwave communication and high power wireless power supply technology represented by electromagnetic

coupling and laser, the rocket-ground interface of launch vehicle can be upgraded from wire connection to wireless connection. The electrical system adapts wireless interface to realize wireless power supply and wireless communication integration, consequently, the mechanical connection can be cancelled and the operation is greatly simplified. In abnormal situation, rocket-ground control and power supply can be rapidly recover and launch vehicle safety are remarkably improved.

This program aimed at unattended operation in test and launching phase of launch vehicle, breaking through short distance high speed wireless communication and high power wireless power supply integration technology adapted to launch vehicle test and launching mode, and finally realizing electrical system rocket-ground wireless.

II. Wireless rocket-ground interface description

To realize wireless power supply from ground to rocket and bidirectional communication, every section of the launch vehicle is installed with a wireless rocket-ground interface, as shown in figure 1. Electrical system can be powered through this interface during ground test phase, meanwhile, the bidirectional wireless communication between ground and rocket

downlinks the digital data of electrical system states information(single equipment built-in test information, sensor information, navigation and guidance information, sequence control information, power supply and distribution information and et. al) and uplinks ground instructions(power supply and distribution instruction, test procedure control instruction, fault injection instruction, data setting, software setting and et. al).

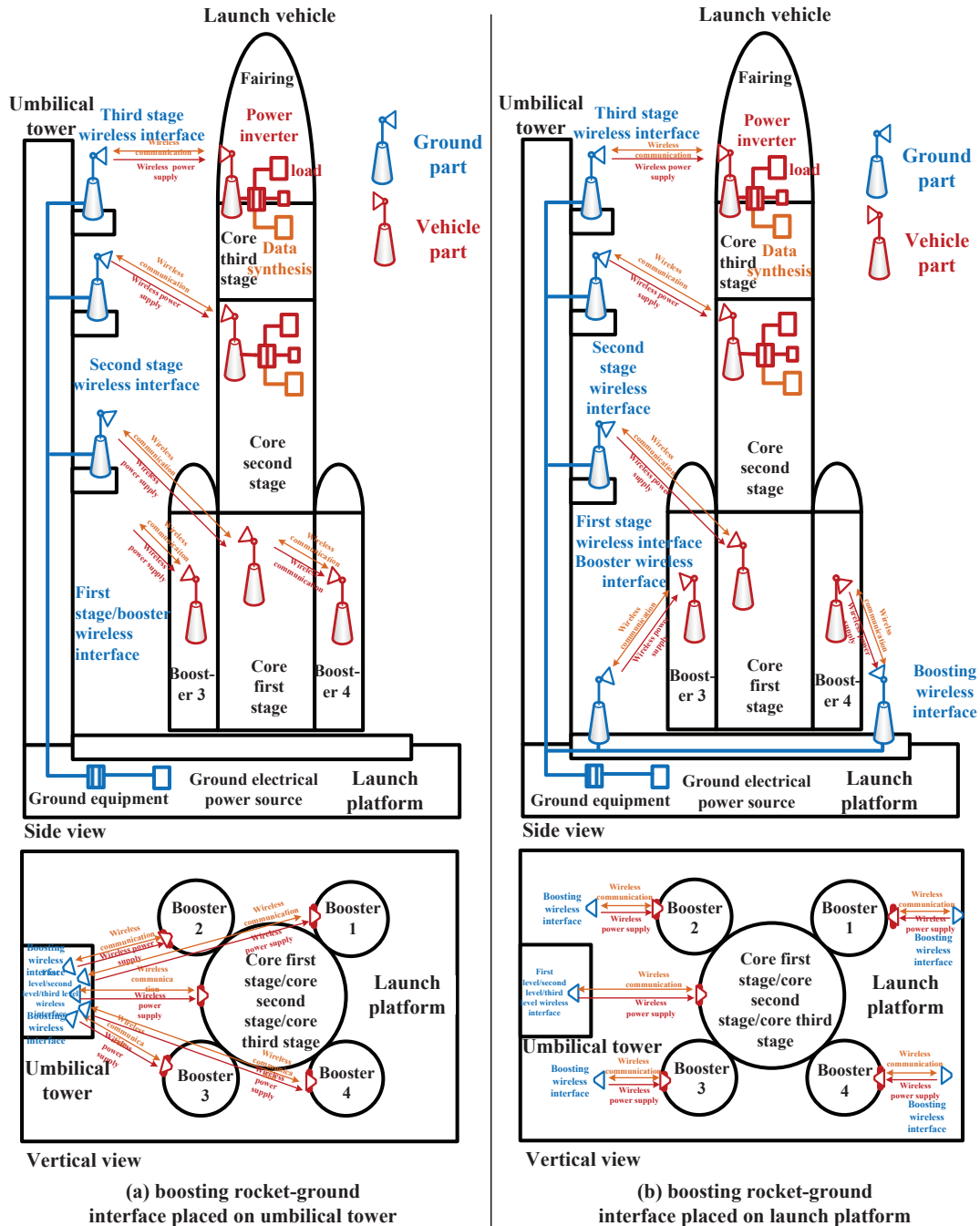


Fig. 1 wireless rocket-ground interface application

The ground part of booster stage wireless interface can be placed on umbilical tower or launch platform, and the onboard part can be placed on the outside of booster cabin wall, laser is employed for wireless power supply and rocket-ground communication. For the first, second and third stage, the ground parts are placed on the umbilical tower of launching platform, the onboard

parts are placed on interstage or the outside of instrument cabin, the ground power supply and rocket-ground communication are also realized by laser. The ground part are connected to power source and communication equipment inside the launching platform with cable.

III. Application Mode

During ground testing, the rocket-ground

wireless interface automatic connection, aided by optical aiming method to minimum the power loss of wireless power supply and communication, is firstly performed. The test instructions and data are transferred by wireless interface, and then distributed to related equipment. There are three application modes of wireless power supply:

(1) charge while using: in ground test, fill and prelaunch prepare phase, the relation between battery and wireless power supply is similar to mobile phone battery and charger. When onboard load is lower than wireless electric supply power, onboard equipment is powered by wireless power supply and the battery is simultaneously charged until full. when onboard load is higher than wireless electric supply power, both wireless power supply and battery provide energy to onboard equipment. The battery and wireless power supply are balanced by battery management system. (2) no charge while using: traditional analogy cable is replaced with rocket-ground wireless power supply, onboard battery is not used while ground testing, only wireless power supply provide energy to onboard equipment. (3) charge without using: to simplify up- and down-rocket operation, battery is used to provide energy during ground testing and charged with wireless

power supply during intermittency.

Before igniting, rocket-ground wireless power supply and communication are disconnected consequently, onboard equipment is then powered by onboard battery after power mode switching. If emergency cut-off happens after igniting, onboard equipment communication can be immediately recovered, ground can thus monitor and control of onboard equipment, onboard pyrotechnics short-circuit protection and key equipment power-off operation are performed according to the situation.

To get into the optimum work state, initial aiming is needed from ground to onboard receiver. Aiming error generated by rocket and ground sloshing and other external factor is compensated.

IV. Laser wireless power supply scheme

Basic principle of laser wireless power supply scheme is shown in figure 2. It consists of two parts. The ground part, constructed with ground power supply, high power laser and optical lens, transmits high power wireless laser. The onboard part, constructed with photovoltaic convert array, power supply management equipment and load, is used to receive high power wireless laser signal.

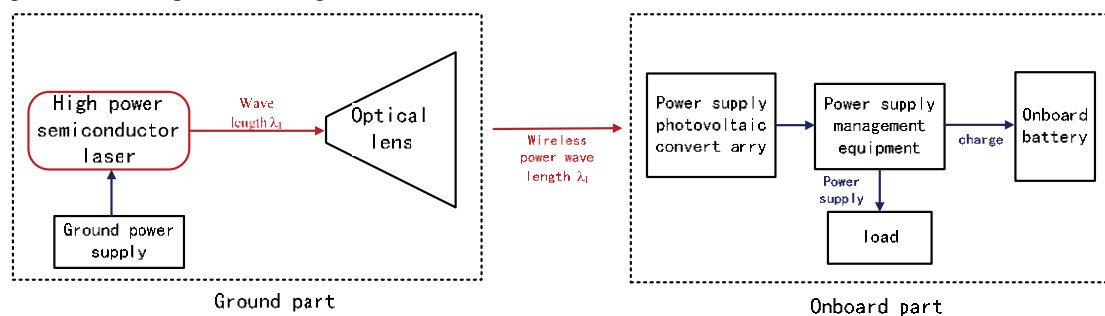


Fig. 2 laser wireless power supply basic structure

The ground power supply provide energy so that the high power laser can output high power laser. The cyber and transmit optical lens are coupled to output laser beam, which

is then transmitted to onboard receiver through space chain after collimating of the optical system. To transform input optical energy to electrical power, the light spot

received by onboard receiver is projected to the photovoltaic converter array constructed by laser photoelectric cell. Voltage transformation and filter are also needed.

To promote the received electrical power, both the transmitted power and the receive efficiency should be improved. For this reason, researches including multi-beam energy transmit, optical spot homogenization, multi-beam cooperate simulation and photovoltaic converter array optimization are conducted.

V. Wireless power supply transmission efficiency optimization

The overall electrical-optical-electrical transmission efficiency are as follows:

$$\eta = P_S/P_R = \eta_1 \cdot \eta_2 \cdot \eta_3 \cdot \eta_4 \cdot \eta_5 \cdot \eta_6$$

where η_1 represents laser electro-optical conversion efficiency; η_2 is antenna transmission efficiency; η_3 is laser transmission efficiency in space; η_4 is incident spot utilization efficiency; η_5 is pointing deviation efficiency; η_6 is optical-electrical conversion efficiency.

a) Laser optical-electrical conversion efficiency

The optical-electrical conversion efficiency of the present semiconductor laser are 35%, which is the efficiency of common commercial lasers.

b) Antenna transmission efficiency

The transmit light path is constructed by a series of lens to shape, collimate and astigmatism correct the input beam. The

transmittance of one lens surface can reach up to 99.9% with added reflection reducing coating.

This system includes transmission and reflection homogenization transmit antenna. Considering the homogenization effect and center spot energy area, the efficiency of the present transmission type homogenizer can reach up to 95%, of reflection type can reach up to 97%.

c) Atmosphere scattering attenuation

The experiment transmission distance is 25m, the atmosphere scattering attenuation is ca. 99.7% for 0.92/km ground atmosphere transmittance.

d) incident spot utilization efficiency

The key component of receiver is optical-electrical conversion unit, on which the photocell panel convert laser energy to electrical energy. The incident spot utilization efficiency is affected by two main factors: the battery arrangement duty ratio and the area ratio of photocell panel to incident spot.

To increase energy coverage, small photocell package are chosen in this design. The photocell slice is 10*10mm, the electric conduction electrode is 1mm, the gap between adjacent photocell is 0.5mm, therefore the actual area of every photocell 10.5mm*12.5mm(132.25mm²) and the irradiation efficiency of single slice is 76.19%. Array lens package can effectively increase the coverage efficiency to 91.4%.

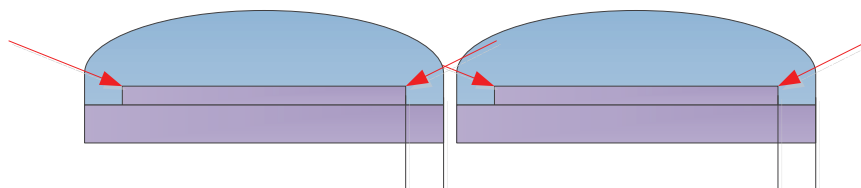


Fig. 3 photocell slice package

For a 400mm diameter target surface, the photocell distribution efficiency is 92%

without considering laser communication antenna, 90% considering laser communication antenna.

e) photo-electrical conversion efficiency

By measuring the open circuit voltage and short circuit current of GaAs battery, the conversion efficiency is acquired as 40%.

f) Aiming adaption error

The light spot coverage efficiency will decrease when the incident energy beam deviation happens. For the present stepper motor turntable, a 2cm deviation at 25m will decrease coverage efficiency to 97.5%.

g) Transmission efficiency synthesis

According to the above analysis, the total electrical-electrical conversion efficiency is 13.4%, the total optical-electrical conversion efficiency is 33.59%. The data is shown in table 1.

Tab. 1: Transmission efficiency

Num.	item	efficiency
1	Laser optical-electrical conversion efficiency	40%
2	Optical transmission antenna efficiency	95% or 97%(avg. 96%)
3	Atmosphere scattering attenuation efficiency	99.7%
4	Incident spot utilization efficiency	80%
5	Pointing deviation efficiency	97.5%
6	Photoelectrical panel optical-electrical conversion efficiency	45%

VI. Conclusion

This program provides an integrated design

of short distance high speed wireless communication and high power wireless power supply, thus realizes electrical system rocket-ground wireless interface. On this basis, future launch vehicle rocket-ground connection can be more flexible and be further simplified, which is important for unattended test and rapid test.

Reference

- [1] Z. S. Liu, Z. Zhang. LM-2F Manned Launch Vehicle. Missiles and space vehicles, 2004, 1(267): 6-12.
- [2] C. Q. Du, J. L. Pan. Integrated Design of Ground Test Launch and Control System for New Generation Launch Vehicle. Aerospace Control, 2004, 22,2:50-52.
- [3] D. Li, J. Wang, W. Hei, et al. The General Scheme and Key Technologies of CZ-5 Launch Vehicle. Missiles and space vehicles, 2017, 353(3): 1-5.
- [4] Y. LU. Space Launch Vehicle's Development in China. Astronautical Systems Engineering Technology, 2017, 1(3): 1-8.
- [5] Z. Y. Wang, H. P. Chen, Y. Q. Zhu, et al. Survey and Review on Rapid Test Technology of Launch Vehicle. Journal of North University of China(natural science edition), 2017, 38(3): 307-315.
- [6] Spaceward Foundation. Power Beaming(climber) Competition[EB]. <http://www.spaceward.org/elevator2010-pb>(accessed December 08).
- [7] V. Khvostikov, S. Sorokina, N. Potapovich, et al. AlGaAs Converters and Arrays for Laser Power Beaming. International Conference on Concentrator Photovoltaic Systems, 2015, 1679(1): 187-194.

Next Generation Vehicle Diagnostics

Dr. Jörg Supke

EMOTIVE GmbH & Co. KG, Pfingstweideweg 17, D-73760 Ostfildern, Germany, www.emotive.de
contact@emotive.de

Abstract:

The next generation vehicle diagnostics have to master the ever-increasing complexity in automotive electronics. Due to its integrative and harmonizing effects, the new OTX standard plays a key role for this challenge. As a meta-language, OTX can bring together different, previously separate standards more effectively than any other standard. OTX is a platform and tester independent exchange format for executable test sequences. The XML-based test sequence language offers the opportunity to exchange test knowledge across departments, tools and process boundaries. The paper shows the practical experiences and benefits of cross-sectoral use of OTX at a German vehicle manufacturer in development, production, service and within the vehicle. It will demonstrate the leading role OTX plays in solving diagnostic tasks inside the new end-to-end electronic architecture [5].

Key words: test language, test knowledge, exchange format, vehicle diagnostics, OTX

Introduction

We live in a connected world. The worldwide availability of a secure broadband and cross-system communication, the increasingly demanding customer requirements and the ever-growing global competition result in a permanent pressure on all operational procedures and processes. The well-known trends in automotive electronics

- Onboard diagnostic tester,
- Onboard high-performance computer,
- Onboard gigabit ethernet,

- Standardized webservice interface for access to the vehicles,
- Service-oriented architecture replaces component-oriented architecture,
- Cloud-based outsourcing of services,
- Future integration of functions currently unknown

as well as the resulting complexity (see Fig. 1), challenges companies to continually improve their operations. The degree of the "relaxed" mastery of complexity makes the quality of operational processes visible.

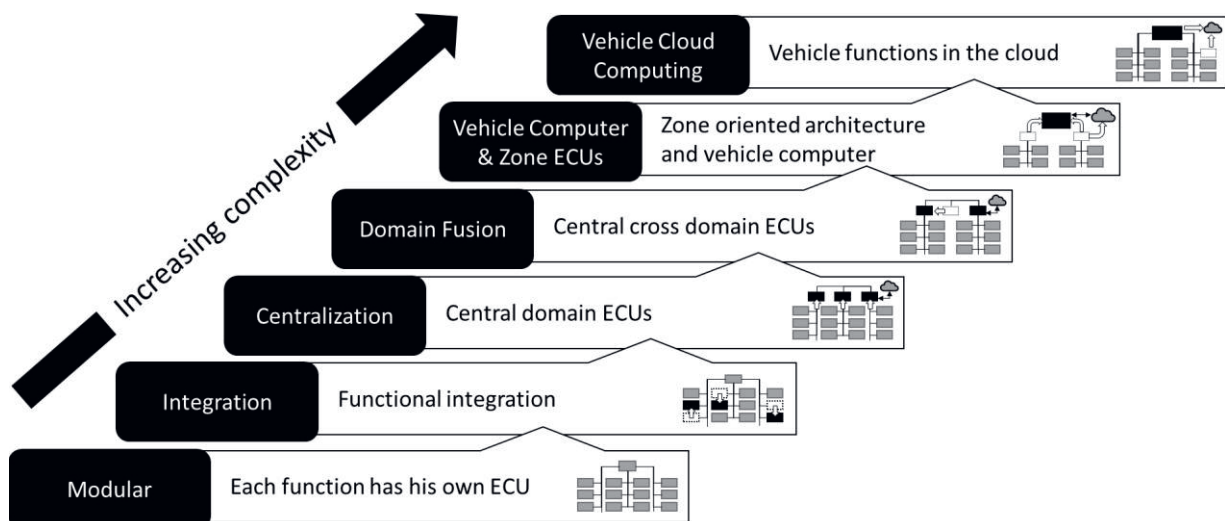


Fig. 1. Evolution of E / E architecture

So-called end-to-end processes have become a leading principle. An end-to-end process is a process that consists of all consecutive sub-processes that are necessary to fulfill a specific customer need. The emphasis on end-to-end is to make people aware that this process extends from the needs of the client to the delivery of services. This process is typically cross-departmental. A holistic end-to-end process organization is therefore the key to operational excellence [4].

Standards play a key role in this development. They establish uniform fundamentals for the exchange of components worldwide. They are based on provable scientific arguments and target macroeconomic purposes. The benefit for all is beyond the benefit of individuals or institutions. Basically, a standard is a recommendation and the use is optional. Because of the significant importance for the interplay of technical and economic solutions, the widest possible acceptance and application of standards is necessary and useful.

The cross-linking of the vehicle and the resulting technological leap offers the opportunity to establish consistent and standardized end-to-end processes. In this evolution standardization should be promoted and existing standards should be strengthened. This is a requirement for the continuous improvement, the consistency of value generation and the avoidance of redundancies.

OTX Standard

Due to its integrative and harmonizing effect, the OTX standard is of particular importance. OTX stands for Open Test sequence eXchange and it is standardized in ISO 13209. As a meta-language, OTX seamlessly integrates with existing diagnostic communication standards such as ODX and MVCI (see Fig. 2). Like no other standard OTX can bring together previously separate standards such as ASAM GDI, ASAM XIL or MCD3-MC. With OTX test knowledge can be exchanged between different departments in development, production and after-sales.

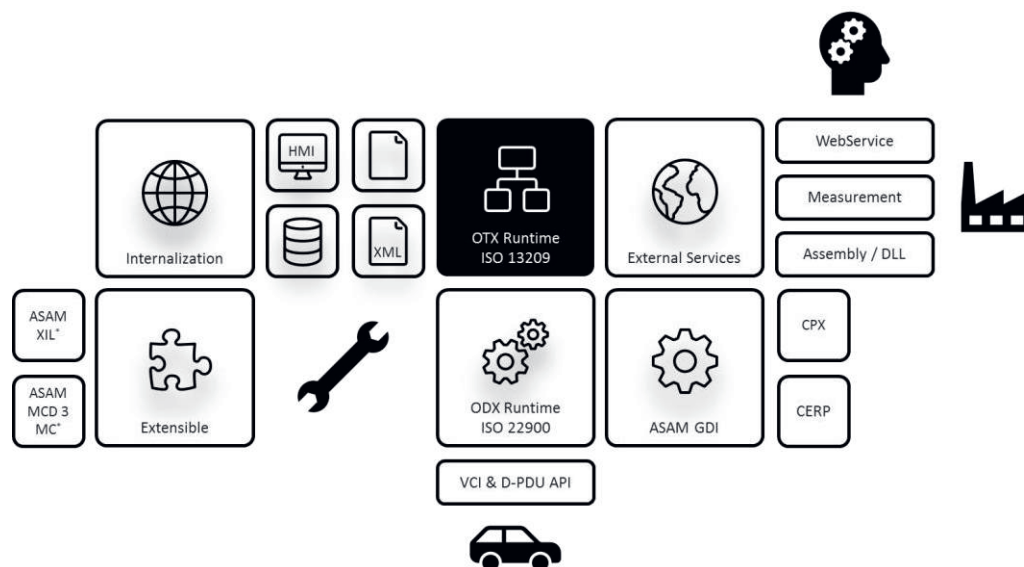


Fig. 2. OTX can connect standards and applications in other areas

The target of OTX is the process-reliable exchange, archiving and execution of test knowledge. With the support of appropriate software tools, it makes the diagnostic development process easier and more productive. OTX describe executable test logic with testable quality. OTX is machine and human readable. It stores test knowledge and is independent of the technology, the service provider and the tool manufacturer. OTX is open and stable. OTX has a strict separation of test logic and runtime implementation. Therefore, OTX is platform independent. OTX is

actively developed within the ASAM and the ISO/DIN and has a broad tool support.

An OTX sequence consists of one or more activities. All activities are thematically grouped in OTX libraries so called OTX Extensions. The OTX core library [1] contains all the activities for the general test logic, such as procedure calls, assignments, branches, loops, activities for parallel execution, error handling and furthermore. All 36 extensions (see [2] and [3]) extend the stand-alone executable core by specific functionalities (see Fig. 3). Besides extensions for vehicle diagnostics, the HMI or

the access to an arbitrary external system via the "External Service Provider" extension, there are a lot of extensions, which can cover almost

every aspect of testing in the automotive industry. Furthermore, OTX can be expanded easily and standard compliant.

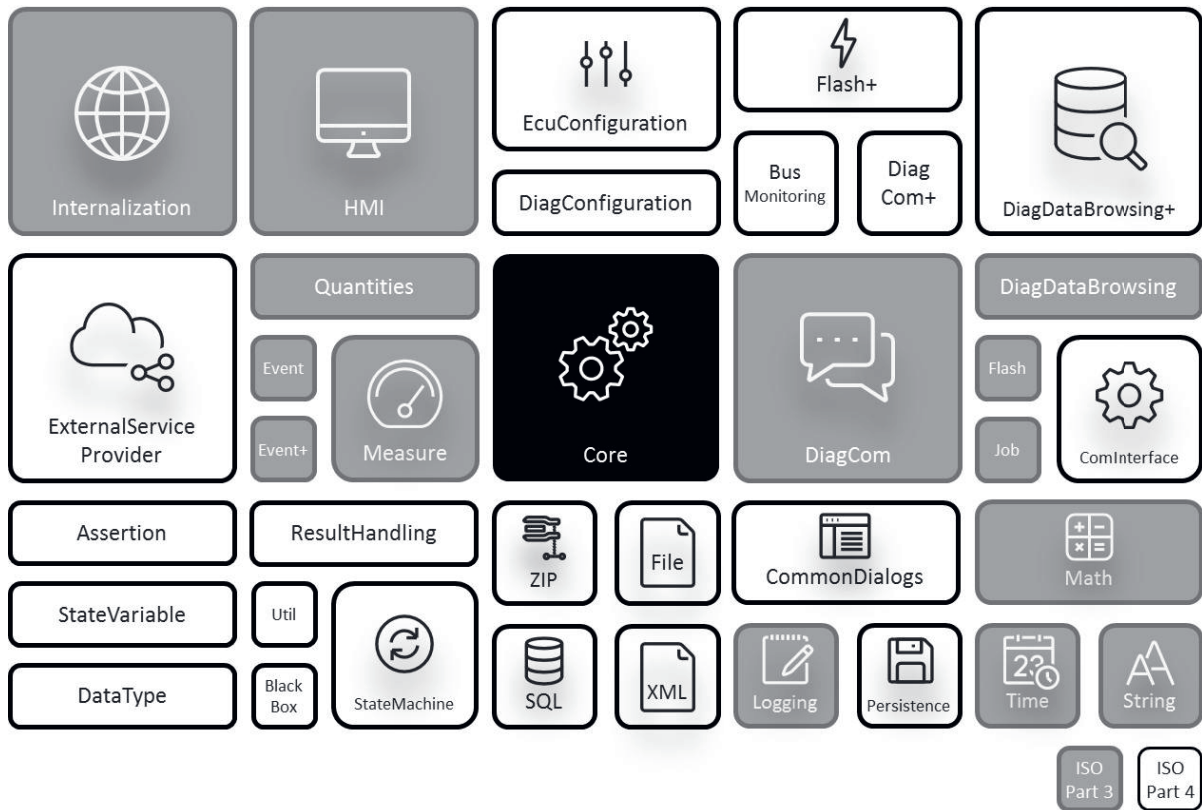


Fig. 3. Overview of the latest 36 standardized OTX Extensions

OTX is stored in XML documents. The following picture shows a very simple example of an OTX sequence (see Fig. 4). Within the procedure named "main", the value "Hello World" is assigned to "Variable1". The same procedure is shown on the right as OTL. OTL is a Java-like scripting language based at the OTX data

model. In the EMOTIVE development environment Open Test Framework (see Fig. 9), an author can develop the sequences in a graphical workflow designer or in the OTL Code Editor. Designer and Code Editor synchronize themselves continuously.



Fig. 4. OTX "Hello World" sample in XML and OTL

Access to external Systems – OTX Mapping

One of the biggest advantage of OTX is the ability to separate test logic and runtime implementation. This allows an access to any external system in the environment. Together with a German vehicle manufacture, EMOTIVE has developed the so-called OTX Mapping. The aim was, that simply by exchanging a mapping file, the same OTX sequence should be

executed in different environments. Because of that, the OEM was able to use the same OTX sequence without changing the test logic in development, production, after-sales and inside the vehicle. This significantly reduces the effort required to create, edit, validate and maintain the test logic. It reduces the dependency on suppliers and by the way a uniform, standardized documentation without additional effort is available.

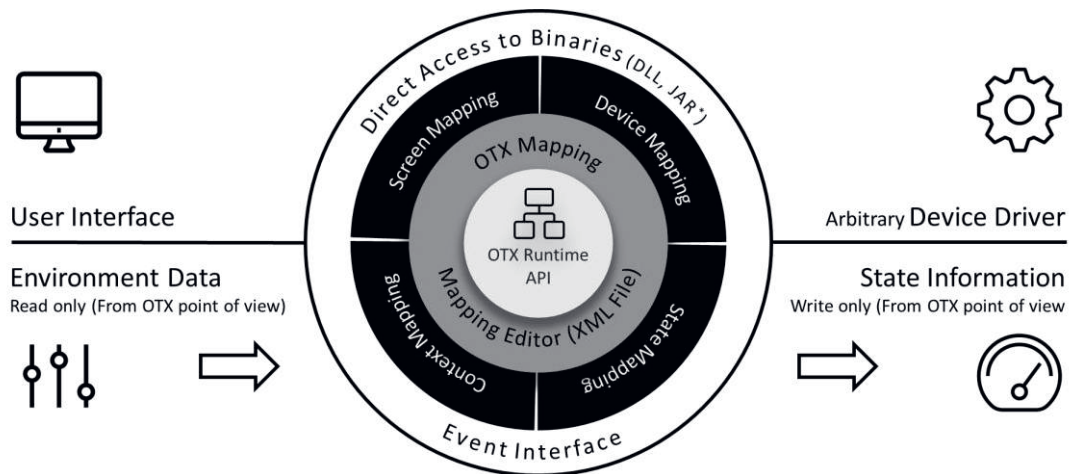


Fig. 5. Access to external systems – OTX Mapping

The OTX Mapping consists of four parts (see Fig. 5): The Screen Mapping for the interaction with any user interface. With the Screen Mapping the parameters of a so-called OTX “Screen Signature” are bound to the properties of GUI controls. With the Device Mapping, any function in an external system can be called via a so-called OTX “Device Service Signature”, such as reading the terminal-15 state. Via the Context Mapping values from the environment can be read and via the State Mapping status information into the environment can be transferred.

The following simplified example for the calibration of tire pressure sensors should illustrate the OTX Mapping for different target systems (see Fig. 6).

At first the ID of a tire pressure sensor must be entered for three different environments via the Context Mapping. Inside the production the ID will automatically entered via the test system. Within the development it will entered via a barcode scanner and for a service station it will entered manually. At next the entered value must be validated. After then a routine will be started via a diagnostic service to calibrate the sensors. The routine will be monitored and parallel the calibration process will be visualized in three different ways via the Screen Mapping:

Within the production via a screen inside the test system. In the development via a simple generic screen and in the after-sales via a screen inside the infotainment system of the car. The last two steps calculate, log and print out the result.

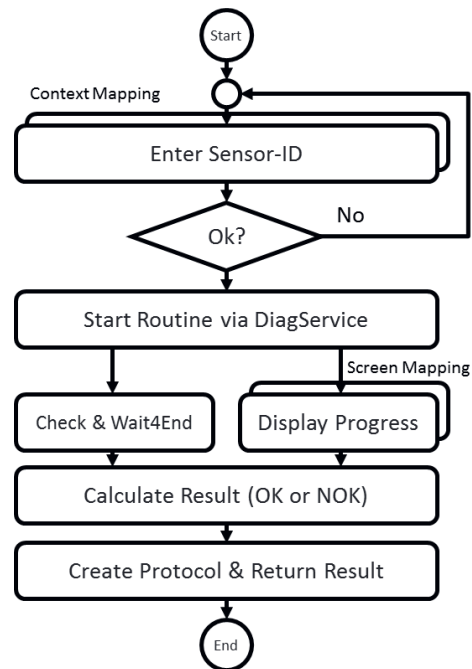


Fig. 6. Use case example – tire pressure sensor calibration

Fig. 7 shows the process for developing this setup sequence. It starts with an abstract specification of the simple test logic like in Microsoft Visio. The result is an initial OTX document. In the following implementation phase, all specifications will be implemented using an OTX test step library. A completely executable OTX document will be generated and tested in the next step. The result is a standardized PTX file, which can be transferred to other departments. Each department adds its environment-specific OTX Mapping and creates a so-called PPX file. While a PTX file is platform-neutral, a PPX file contains platform-specific information in the form of the OTX Mapping file. The PPX file can be executed on

different target systems. In application 1, the sequence is executed within an existing system in production or after-sales. Application 2 executes the same PPX within a generic pilot tester within the prototype workshop of the development.

In summary, it can be said that with the new OTX Mapping it is possible to exchange test knowledge through adaptation and enrichment across departments in an efficient way never seen before. A test sequence is specified, implemented and tested in the development. It is adapted and enriched for production, after-sales and for the use inside the vehicle without changing the test logic.

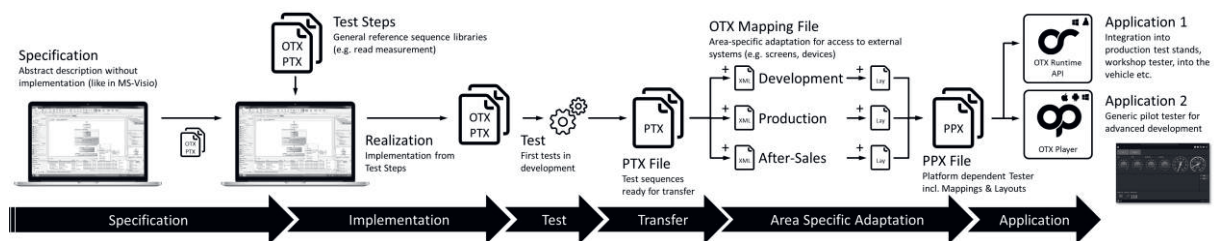


Fig. 7. Development of a start-up sequence step by step

OTX Tool Chain

Due to the standardization process and the resulting possibilities, a complete OTX tool chain was developed by EMOTIVE (see Fig. 8).

The tool chain is in productive use at several OEMs in development, production, after-sales and inside the vehicle. It mainly consists of the OTX development environment "Open Test Framework", the OTX Runtime API and the OTX Player.

The Open Test Framework (OTF) is a complete development environment for designing, maintaining, and testing a new generation of process-reliable tester applications that run on Windows and Linux (see Fig. 9). The OTF has a clear and intuitive user interface. It helps sequence designers and project managers to create and deliver tester solutions faster and without any programming skills. All relevant standards such as ISO 13209 (OTX), ISO 22900 (MVC) and ISO 22901 (ODX) are supported.

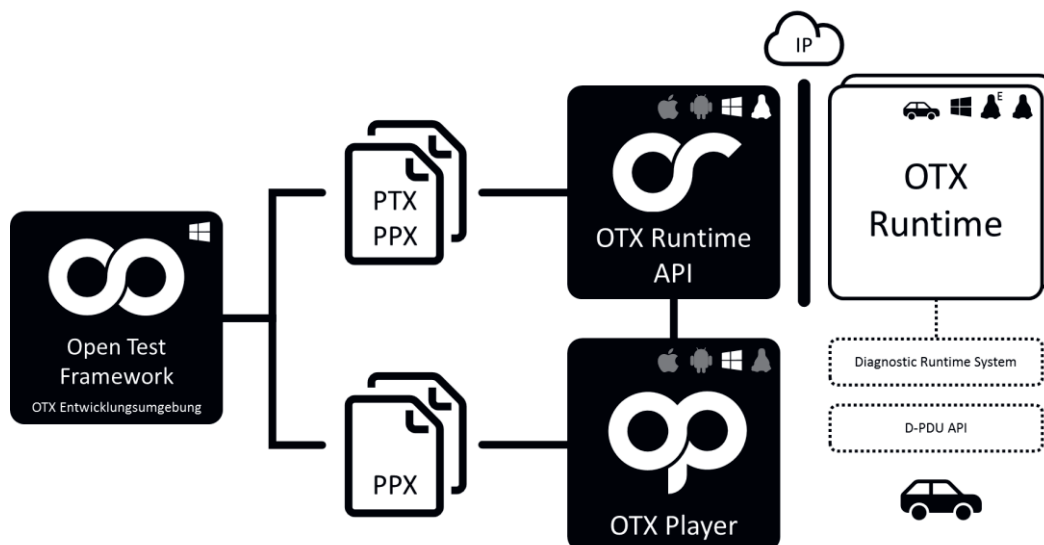


Fig. 8. OTX tool chain of EMOTIVE

The areas of application of the OTF are the basic work with standardized test sequences, the creation of redistributable players etc. Applications inside off-board vehicle diagnostics are in the foreground. Examples are a universal

and quickly adaptable Flash tool, a tool for checking the ECU protocol conformity, simple and complex development and production testers or even a simple scan tool in the OBD environment.

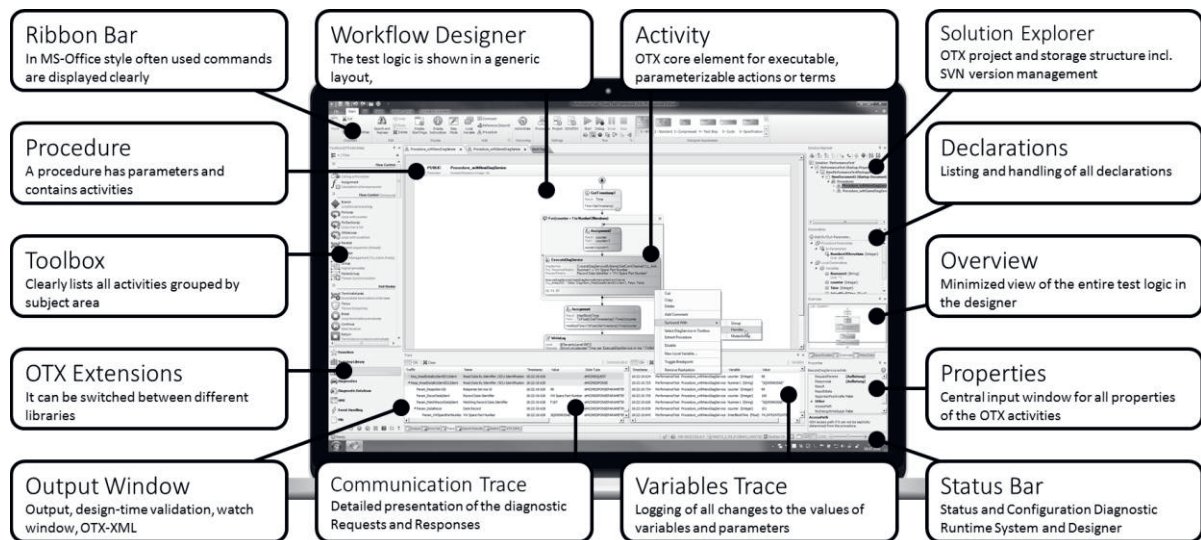


Fig. 9. OTX development environment Open Test Framework

The Open Test Runtime API (OTR) is a programming interface for the simple execution of OTX procedures in own applications. It works independently even without the development environment and is available for Windows, Linux and Embedded Linux. It has comprehensive possibilities for seamless integration into existing systems and infrastructures (see Fig. 10). The key features of the OTX Runtime API are:

- Enables users to use OTX in their own applications
- API for Java, DotNet and COM
- Runs on Windows, Linux and Embedded Linux
- Synchronous and asynchronous execution of OTX sequences
- Multi-threading and multi-instance capable
- Long-term stable and performant
- Remote capable

The application areas of the Open Test Runtime API range from the simple execution of

PTX files through the integration in test benches of different manufacturers to the complete and seamless integration of OTX into own applications.



Fig. 10. Open Test Runtime API (OTX runtime) for seamless integration into existing systems

The Open Test Player (OTP) is a complete generic, OTX based tester for the simplest distribution and execution of test sequences (see Fig. 11). It is completely based on the Open Test Runtime API and can be easily adapted to the company look and feel. It works with Windows. Implementations for iOS and Android are planned. A player project (PPX) can be graphically created and tested in the Open Test Framework without any programming skills.



Fig. 11. Open Test Player with theme support

The key features of the OTP are:

- 100% generic OTX based tester
- For the simplest distribution and execution of test sequences
- Modern interface with company CI
- Based completely on the OTX Runtime API
- A player project (PPX) is created in the OTF without programming skills
- Install player, load PPX, run ... Done!

Due to the easiness of development of a player without programming knowledge, the OTP is used especially when established testers, which cannot be adapted quickly and flexibly enough for new ECUs or test sequences. For example, in the prototype workshop of development and production: Together with the OTP, ECUs can be setup quickly and easily without the use of numerous special tools. Component owners can also use the Open Test Player to deliver their ECU together with a player project that provides the basic functions of the ECU.

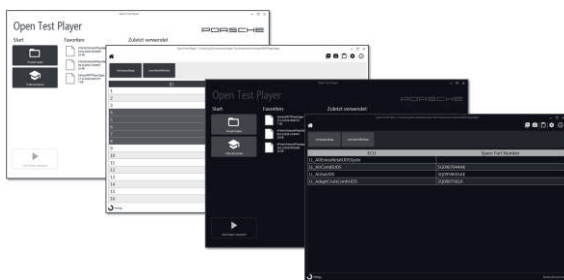


Fig. 12. Open Test Player with company CI

The design of the Open Test Player can easily be changed via themes (see Fig. 12). The user can adapt the logo, the colors, the fonts and the

icons inside the Theme Manager of the Open Test Framework. A theme file with the company CI can be created, transferred and loaded into the OTP.

Summary

The new standard OTX (Open Test sequence eXchange) is an executable, platform and tester independent exchange format for test sequences, standardized in ISO 13029. It leads to a substantial simplification of the processes to create and maintain standardized test logic. OTX enables the reliable archiving of testing knowledge, it can bring together different standards and promotes integrated end-to-end processes. This next generation of vehicle diagnostics significantly reduces time and cost to master the increasing complexity.

References

- [1] ISO 13209-2:2011, Road vehicles — Open Test sequence eXchange format (OTX) — Part 2: Core data model specification and requirements, 2011
- [2] ISO 13209-3:2012, Road vehicles — Open Test sequence eXchange format (OTX) — Part 3: Standard extensions and requirements, 2012
- [3] ASAM Base Standard OTX Extensions, Open Test eXchange format, Interface Definition, Version 2.0.0, 2017
- [4] Operational excellence, Wikipedia, https://www.wikipedia.org/wiki/Operational_excellence
- [5] Dr. Jörg Supke, Next Generation Vehicle Diagnostics (German), Diagnose in mechatronischen Systemen XII, Thelem Universitätsverlag, 2018

Configuring Applications based in XdefML

*José Antonio González Pastrana
Airbus Defence and Space, Getafe-Spain,
Jose.o.gonzalez@airbus.com*

Abstract:

Developing applications to configure instrumentation is a never ending task as new equipment is constantly coming up in the market. Embedding this new instrumentation to existing software can be tricky if you have to deal with every single characteristic of the equipment. XdefML files facilitate adapt these new instrumentations in your internal developed configurations tools.

Key words: MDL [1] , XML [2], Open Standards, DAS[3], XidML [4], XdefML[5].

Introduction

A XdefML file is a kind of XML file that contains all possible values that an instrument can have. It is an open standard, so everybody can use it freely. As any other XML file, it is based in its own schema. This schema represents all possible fields that a XdefML file can support.

The aim of a XdefML file is to have available all possible settings, parameters, channels, etc, that an instrument can have to create another file, which represents the real configuration of the instrument. This file that contains the configuration of the instrument can be written in different ways, such as XML or text files.

What is XdefML?

XdefML is a metamodel that permits us to define the features supported by a card or equipment. We need it because configuration files tell us which the configuration of an equipment is. But in its schema there isn't a way to define what characteristic have to be set or which values are permitted for certain equipment/card.

So, for writing a XidML, MDL or any other kind of configuration file we need previously to know which are the features that an equipment have. A XdefML file give us the features and the values valid for such an equipment.

XdefML files characteristics

There are different standards to define configurations for data acquisition systems as it can be XidML and MDL, also there are vendor dependent files too. Any of them need a file to describe which are the settings, parameters,

specifications, etc, necessary for define a card or equipment configuration. Usually these kind of files are not supplied because it is intended that the configuration software supplied with the equipment is in charge of this. If you have to create configuration files by yourself, beforehand you need to know which the admitted values are for each one of the named features. This is why you need XdefML, to create your own configuration files, instead of using the vendor's tools. If you are dealing with big data acquisition systems or you need to manage a great quantity of projects, you'd better use an automatic system to create the configuration files.

XdefML Schema have three main nodes 'InstrumentIdentification', 'InstrumentSpecifications' and finally 'InstrumentConfiguration'.

So, in any XdefML file all these three will be shown. The necessary information to identify the instrument as Manufacturer, PartReference, Serial Number, etc. is displayed in the 'InstrumentIdentification' node.

Under the 'InstrumentSpecifications' node, mainly information about mechanical characteristics and related documentation as its datasheet is shown.

Under the 'InstrumentConfiguration' node, the information that contains all possible channels, settings and parameters characteristics is displayed. It must be taken into account that some of the characteristics are recursive. For example, an instrument can contain another instrument and this one another one, and so on. A parameter can have subparameters, settings can have subsettings, etc. This recursion makes to deal with XdefML schema even more

difficult. Recursive schemas can't be imported with the libraries that can be used in most languages as C# and similar ones.

So, there is a SDK [6] that helps you to deal with XdefML files. This SDK is available from CW-Controls (former ACRAControl).

Working with XidML SDK

XidML SDK contains libraries that help you to work with XidML and XdefML files. In this case our main concern is with XdefML related library. This library can load a XdefML file and navigate through it to extract all necessary information in order to fill-in data in your database or to generate XidML files, or any other kind of configuration file you may need to use.

A function of this SDK can load a XdefML file and from it generate a new XidML file, filling all its parameters with default values. This configuration file (XidML) can only be used by one vendor configurations. When you have this XidML file in your computer memory you can change default values for other ones you may prefer.

However, any developer can take all the features of a card/equipment from a XdefML file. Having them in the computer memory and then create a configuration file for any other vendor.

Obviously this way is harder than using the function already in the SDK, anyway you can always build your own function which outputs the file you need. To build your own classes/functions there is a library called LINQ (Language Integrated Query) from Microsoft that helps you to query xml files.

Tools based in XdefML

Two tools have been developed based in XdefML files and on the library XidML SDK. These are the DASp and DAC_TOOL3.0 tools, another one is under construction and several other will be developed in the near future.

DASp is a tool that generates configurations for any kind of acquisition systems, based on plugins that get the input as xml files which have been obtained, in our case, from our database.

DASp extracts all necessary data for cards/equipment from XdefML files, it processes all this information and writes the output in the way that is needed. The first plugin creates configurations for XidML 3.0 files. These files are compiled to check if they are correct, to be loaded on the equipment.

DAC_TOOL3.0 is a tool to save the card's configuration in our database. It gets a XdefML file from a card/equipment and present all its settings and parameters. This way the engineer can change the default values for any other useful for certain application. There is another tool under construction (FTIForm3.0) to check that instrumentation information corresponds with the one of the DAS [8]. Fairly, the information of the aircraft's parameters is displayed in an easy way, to check where exactly a parameter is connected to the DAS.

The ranges of the card's channels and the calibration can be correctly set. It queries the values from the database, if they are null it takes the default values from XdefML file that corresponds to the card.

In a near future some other tools will be developed. The main one is a suite of tools to manage all instrumentation processes, from requirements coming from the customer to DAS configurations, sensors calibration and storage. All this will turn up to be an integrated tool called FIDA. FIDA will use XdefML files to get all the information necessary to know which the features of equipment and the admitted values for them are. It will be a graphical tool that will contain objects linked to each XdefML file. Therefore for including a new acquisition system the only thing we will need to do, it'll be to copy the new XdefML files to the computer directory where all the others are stored.

Conclusions

XdefML files are going to be a key technology for instrumentation and DASes in ADS [7]. These kind of files are suitable to define the characteristics for any type of acquisition system, no need to worry about the vendor, as they are not vendor dependent and are an open standard.

However, having these types of files supplied by the vendor is an advantage. As XdefML files are vendor agnostic all software needed to create configurations for different kind of acquisition systems is almost the same for all of them.

Therefore most of the software developed internally to create data acquisition systems configurations is the same for all vendors.

These characteristics make updating the tools to support new acquisition systems faster and easier.

References

- [1] MDL - <http://www.irig106.org/docs/106-17/Chapter23.pdf>
- [2] XML - <https://www.w3.org/XML>
- [3] DAS – Data Acquisition System.
- [4] XidML - <http://www.xidml.org>
- [5] XdefML - <http://www.xidml.org>
- [6] SDK – Software Development Kit
- [7] ADS – Airbus Defense and Space
- [8] DAS – Data Acquisition System

A JSON transactional data server for flight tests

A. Óscar Gigato Rodríguez¹
¹ Airbus Defence and Space Sevilla-SPAIN
oscar.gigato@airbus.com

Abstract:

Airbus Defence and Space has been using a protocol for gathering Flight Tests data, called FxS (Flight Test Data Exchange Service), based on XML and transactions among clients and servers. An evolution of this protocol is proposed, covering current implementation desired characteristics, like being **object-oriented**, **metadata support**, **encryption** and/or **compression**, and based on **JSON** instead of XML (more lightweight).

Key words: object-oriented, JSON, encryption, metadata, compression.

Introduction

In Airbus Defence and Space we use a client/server model for gathering data from a Flight Test, because of its tremendous advantages, such as centralized store of data, ease of backup's processes, access control and so. Since beginning of 2000's, we have been developing a protocol called FxS (Flight Tests Data Exchange Service), in order to use the same layer for access different data formats stored on heterogeneous systems.

After more than 15 years after entry into production of FxS data servers, we think that it's time to an evolution of this concept, keeping the good ideas, and introducing some new technologies, in order to fix a few drawbacks detected during this period, so we can maximize performance and reliability of our systems, and give the best possible service to our users.

In general lines, we can proudly say that FxS data servers works very well and stable, but we want to polish it even more.

A bit of history

Before the developing of FxS, access to data from flight tests was performed using proprietary applications developed in-house, with direct access to data. That is, tools used by analysis team had to have visibility of stored data, with no intermediary. And each ground station had its own suite of applications, being incompatible among them.

In this situation, former CASA and DASA ground stations teams met and agreed the development of a new interoperable protocol, so that an engineer of one team can connect to data of the other team without problems. Then FxS was born. The key of this concept was to create a new layer over stored data, and harmonize the way data is accessed by both ground stations teams.

The concept of „Data server“

With the development of FxS, data server architecture was also deployed. Instead of access data directly, so that each client had to have visibility of stored data, from now on, a new actor enters into scene. The data server is the only application that has access to all data repository, and clients have to connect with it, if they want to gather stored data.

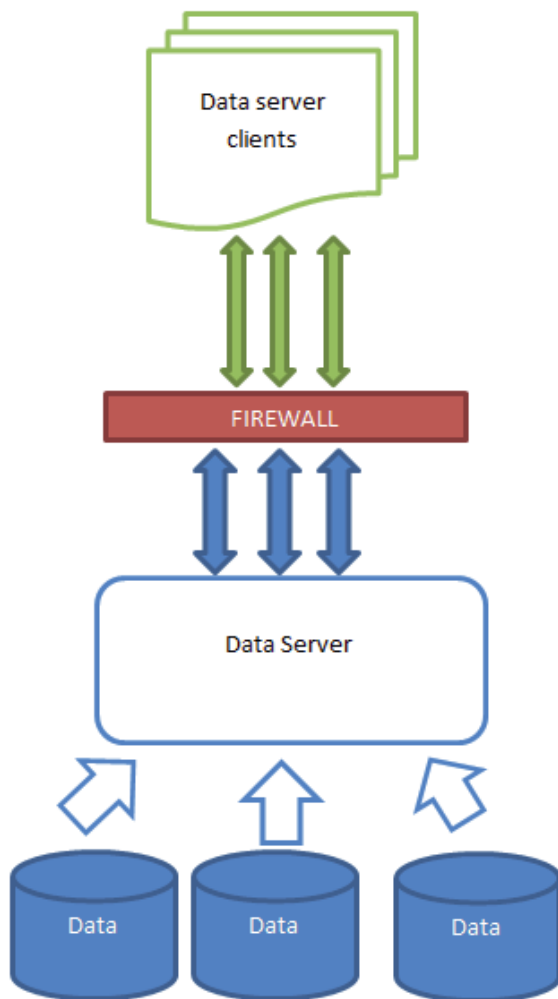


Fig.1: Data server architecture.

Among the multiples advantages of this philosophy, we have:

- Permissions management is now centralized on data server itself. This simplifies this task enormously.
- Clients only need to “speak” FxS. It permits access to different formats of data, in different systems.
- Clients read only the data they need. They have no longer to access all the data for gathering, for example, 4 parameters. The data server have access to all test, but only delivers required parameters, at the required rate during the required period of time. This saves enormous bandwidth and time.
- Some data of flight tests have been recorded in “raw format”, and need to be converted to engineering format. This is called “calibration”. Before data server deployment, calibrated parameters can be either directly stored in calibrated units, or having to be

calculated by clients. Now, it is normally the data server who performed these calculations.

- Use of this architecture permits to be independent from Operating System and hardware. Clients only have to know the FxS protocol. No more.

However, during all this time, we have detected some lacks or drawbacks that have to be fixed:

- Use of metadata is mandatory. In some situations, we have to reserve some valid values to indicate that data is not valid, for example. Metadata shall avoid this problem.
- Full support of strings. Actually, we need to make some workarounds in order to use strings.
- Opaque parameters native support. Sometimes, data recorded in one parameter is the traffic from one data bus, and thus it does not have a fixed size.
- In offline mode, use of only one socket will simplify passing through a firewall.
- Compression and/or encryption is also desirable when using offline data server from a remote location.
- User identification can be stronger.

Today: The FxS protocol

FxS (Flight Test Data Exchange Service) protocol is based on XML transactions among server and clients. All messages are validated before processed, using XML schemas. This makes all transactions consistent, and prevents use of messages that don't fully respect FxS specification.

The following transactions are defined:

- Status Announcement.
- Client Identification.
- Special parameter.
- Data File List.
- Data File Info.
- Parameter List.
- Tag-Size List.
- Program/Setup.
- Offline Test.
- Start.
- Stop/Close.

- Pause.
- Resume.
- Remove.
- Rate.
- Refresh.

Current data server uses two channels with the client. The first one, TCP, is reserved for transactions, and the second one, UDP unicast or multicast, is reserved for data transmission.

Introducing a new data server architecture

Keeping in mind all the advantages of FxS data server, I propose a new (evolutionary) architecture for the data server. It tries to overcome all the drawbacks of current software, as well as maximize both speed and network bandwidth efficiency. It also tries to simplify both transactions and connections management. The way it addresses these points is:

- Use of JSON instead of XML (lighter messages, faster transactions generation).
- Use of only one TCP port in OFFLINE mode (it eases tunnel traffic forwarding for use behind a firewall).
- In ONLINE mode, it uses an UDP connection for data, just like the current data server. But this connection is made by the client to the server (in current data server, is the server who opens this port). This avoids some problems with local firewalls (in client equipment).
- Use of compression is supported in OFFLINE mode. Although LZMA2 is recommended, there is no obligation to use that one.
- Redesign some transactions.
- Permit the use of TTD and CVT data in the same connection (current data server needs two different connections for this purpose).
- Things that work quite well will be maintained, like XML use for configuration files. In this case, XML files are more readable for a human, hence this decision.
- Time for samples sent by data server will be in PTP time format, an 8 byte time specifications who allows precisions of nanoseconds, while specifying the year too.

The JSON Data Interchange Syntax

JSON (JavaScript Object Notation) is a lightweight, text based, independent syntax for defining data interchange formats[1]. Is like XML, but simpler and lighter. It is harder to read for a human, but in this case, these messages will not be read by persons. It is also faster to parse and generate, and there are too many libraries in many programming languages that support this standard. Possibility of validation (just like XML schemas) exists, as there is a draft of a standard for validation.

An example comparing XML and JSON:

```
{
  "firstName": "John",
  "lastName": "Smith",
  "age": 25,
  "address": {
    "streetAddress": "21 2nd Street",
    "city": "New York",
    "state": "NY",
    "postalCode": "10021"
  },
  "phoneNumber": [
    {
      "type": "home",
      "number": "212 555-1234"
    },
    {
      "type": "fax",
      "number": "646 555-4567"
    }
  ],
  "gender": {
    "type": "male"
  }
}
```

Fig.2 A sample JSON definition.[2]

```
<person>
  <firstName>John</firstName>
  <lastName>Smith</lastName>
  <age>25</age>
  <address>
    <streetAddress>21 2nd Street</streetAddress>
    <city>New York</city>
    <state>NY</state>
    <postalCode>10021</postalCode>
  </address>
  <phoneNumber>
    <type>home</type>
    <number>212 555-1234</number>
  </phoneNumber>
  <phoneNumber>
    <type>fax</type>
    <number>646 555-4567</number>
  </phoneNumber>
  <gender>
    <type>male</type>
  </gender>
</person>
```

Fig.3 A sample XML definition.[2]

As shown in previous figures, for the same definition JSON uses less character, thus making it faster for transmitting it over the network. Clearly XML is powerful than JSON, but in our case, is enough with JSON, and so we can worth its advantages over XML.

Transactions for the new data server

Some of the transactions defined in the new data server will be redesigned. One of them disappears, while a new one is created. Transactions contents might vary in its final implementation.

Tab 1 Comparison between transactions.

FxS Transaction	New transaction
Status Announcement	Status Announcement
Client Identification	Client Identification
Special Parameter	-
-	Connection Options
Data File List	Tests List
Data File Info	Test Info
Parameter List	Parameter List
Tag-Size List	-
Program/Setup	Program
Offline Test	Offline Test
Start	Start/Retrieve
Stop/Close	Stop/Close
Pause	Pause
Resume	Resume
Remove	Edit Parameter List
Rate	Modify Rate
Refresh	Refresh

There is something more than a change of names. Special Parameter has no sense since now we have metadata sent associated to parameters values. Let's explain these transactions:

- Status Announcement: This one does not change. Data server sends, each second, a broadcast message for announcing itself.
- Client Identification: This transaction identifies the client in the data server. It is useful for both audit and access control purposes.
- Connection Options: Used for negotiating connections aspects, like compression (only for OFFLINE), local UDP port for ONLINE mode, etc.
- Tests List: In OFFLINE mode, this transaction returns the list of available tests, according with access permissions of the user.
- Parameter List: The client asks the server for the list of parameters using this transaction. Regular expressions can be used.
- Program: This transaction tells the server the list of parameters that have to be sent to the client. It also specifies each parameter mode (CVT, TTD), and rate (only for CVT).
- Offline Test: Specifies the server the test to work with, and the time span to be used (within test time limits).
- Start (ONLINE)/Retrieve (OFFLINE): Makes the data server start sending the data to the client.
- Stop (ONLINE)/Close (OFFLINE): Makes the data server stopping the data transmission. After data stop, connection with the client is closed.
- Pause: Pauses data sending.
- Resume: Resumes data sending.
- Modify Rate: Changes the rate for one or more parameters (CVT mode).
- Refresh: Forces the send of last value for all programmed parameters, in CVT mode. Normally, only changed values are sent.

Transfer of data

Due to the great amount of data that can be transmitted over the network, binary connection is the most efficient one. We define two different frames, although in the same channel, for both CVT and TTD modes. This allows the use of these two modes in the same connection. In OFFLINE mode, only one port is used by each client, for both transactions and

data connection. Each message specifies the type of information before the payload. That is, for a transaction, a TRANSACTION identifier is prepended. For data, a DATA identifier is also prepended. All information is sent in a TCP connection. Here is the frame definition, for both CVT and TTD modes.

Tab. 2: CVT DATA frame definition

	SIZE (IN BYTES)	DESCRIPTION
FRAME TYPE	1	VALUES: TRANSACTION, DATA, STATUS
FRAME SIZE (IN BYTES)	2	-
CURRENT TIME	8	PTP TIME
NUMBER OF PARAMETERS	2	NUMBER OF TAG/VALUE PAIRS
TAG 0	4	FIRST TAG SENT
METADATA 0	1	FIRST VALUE METADATA
SIZE 0 (OPTIONAL)	2	SIZE OF FIRST VALUE
VALUE 0	VARIABLE	FIRST VALUE SENT
...
TAG N-1	4	LAST TAG SENT
METADATA N-1	1	LAST VALUE METADATA
SIZE N-1 (OPTIONAL)	2	SIZE OF LAST VALUE
VALUE N-1	VARIABLE	LAST VALUE SENT

Tab. 3: TTD DATA frame definition

	SIZE (IN BYTES)	DESCRIPTION
FRAME TYPE	1	POSSIBLE VALUES: TRANSACTION, DATA, STATUS
FRAME SIZE (IN BYTES)	2	-

CURRENT BASE TIME	8	PTP TIME
TAG 0	4	FIRST TAG SENT
DELAY 0	2	DELAY OVER BASE TIME (ns)
SIZE 0	2	SIZE OF VALUE 0
METADATA 0	1	FIRST VALUE METADATA
VALUE 0	VARIABLE	FIRST VALUE SENT
...
TAG N-1	4	LAST TAG SENT
DELAY N-1	2	DELAY OVER BASE TIME (ns)
SIZE N-1	2	SIZE OF LAST VALUE
METADATA N-1	1	LAST VALUE METADATA
VALUE N-1	VARIABLE	LAST VALUE SENT

When sending transactional data, first byte indicates that it is a transaction, next two bytes gives frame length, and just after this information, JSON serialized message is appended.

The only difference between ONLINE and OFFLINE frames, is that the first one does not use TRANSACTION type of frames.

There are two aspects that I want to emphasize:

- Strings and variable size data are permitted. When necessary (in CVT mode), a size field will be used. The existence of this field can be checked in metadata.
- Metadata includes some flags, like Valid Data Flag, No Data Flag, Size field present flag, etc.

ONLINE (real time) mode

We must say “quasi real time” mode, so we are using neither a real time device nor Operating System. In this mode, we use two connections per client. The first one, TCP, will transmit transactions between client and server. And a second one, UDP, will be used to send data.

This is due to TCP connections are designed for reliability, but not for quick response. In order to avoid problems with local firewalls, both connections will be open by the client.

As this mode will be used mainly in local area networks, compression algorithms shall not be provided.

Once the client sends the Start transaction, data server begins sending programmed data at the desired rate. Only the data that has changed since the last data sent is delivered. This saves both bandwidth and CPU resources in client and server.

If the client wants the server to send all parameters values, it can send a Refresh transaction to the server. Upon the reception of this message, the server delivers last acquired parameters values.

Client can also pause and resume data delivering to itself, by sending both Pause and Resume transactions.

During the receiving of data from the data server, client can send an Edit Parameter List transaction, adding/deleting parameters to program. Upon the receipt of this transaction, data server will refresh all data to his client.

Once the client no longer needs data from the server, it sends a Stop transaction, making it to finish data sending, and the subsequent close of connection.

OFFLINE (processed) mode

In this mode, clients will require previously stored and processed data for its study by specialists. As we can be connected from both LANs and remote locations (remote location means other center, for example), only one TCP port will be used. This eases port forwarding over a SSH tunnel, for example.

In addition to this, compression can be enabled using the Connection Options transaction.

The usual lifecycle for OFFLINE data servers starts receiving a Client Identification transaction from one client, then a Connection Options one. After this, normally a Test List Request is made, and then a Parameter List can be made (is optional). Next step is an Offline Test Request, specifying test and time slices required, followed by a Program request.

Once the client sends the Start transaction, the server will send it all required data, at the fastest speed permitted by both client and server.

Like in ONLINE mode, when a Stop transaction is sent, data server will close its connection to the client.

Frame Type field is used to distinguish among TRANSACTIONS, DATA or STATUS messages.

Future: SSH tunneling and Web Services

Tunneling over a SSH connection could be made by OFFLINE data server. This approach is useful for encrypting data and facilitates its pass through a firewall. Moreover, this tunnel can also provide compression, avoiding the use of it directly in the protocol.

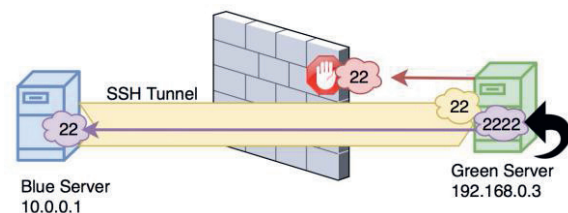


Fig. 4 An example of a SSH tunnel.

A Web Service is a technology that enables interchange of information between two applications, using WEB standards. The client is normally run inside a web browser, which eases enormously deployment of client applications (every computer has a browser installed), security restrictions and so on.

Technologies like SOAP, JSON, AJAX, REST and others are used in web services.

The idea is to embed data server functionality into a web service, adapting the way it works to offer its services and make them accessible from web clients.

Making a data server operate as a web service opens a world of interoperable services, and the possibility of development of thin clients, that can be run from a laptop to a smartphone or tablet. For example, a light client for checking live parameters could be easily deployed in a tablet, or opened from a web browser. This would allow us checking parameters inside an aircraft in real time, from any place of it.

Today it's possible to implement this scenario, but web services make rather simple deploying clients in any site. Firewalls are not a problem using this approach.

Among drawbacks of using a web service, the main one could be performance loss, due to overhead created by HTTP/SOAP layers to transmit data to the clients.

References

- [1] <http://www.ecma-international.org/publications/files/ECMA-ST/ECMA-404.pdf>
- [2] Wikipedia: <https://en.wikipedia.org/wiki/JSON>

Hardware Acceleration for Beamforming Algorithms based on Optimized Hardware-/Software Partitioning

*René Schmidt, Stephan Blokzyl, Wolfram Hardt,
Technische Universität Chemnitz, Straße der Nationen 62, D-09111 Chemnitz, Germany,
{rene.schmidt, stephan.blokzyl, wolfram.hardt}@informatik.tu-chemnitz.de*

Abstract:

Beamforming techniques are widely used in many fields of research like sonar, radar, wireless communication and speech processing applications. Beamforming algorithms are mainly used for signal enhancement and direction of arrival estimation. In applications for tracking mobile communication partners like speaker or aircrafts, beamforming algorithms are employed to estimate the direction of arrival.

Beamforming processing is always accompanied by high computational costs, which are challenging for embedded devices. Recent approaches process the calculation in frequency domain to reduce the processing time. However, in many cases the processing is still very slow and cannot be used for real-time processing. Alternative real-time solutions based on FPGAs face the drawback of long development processes and restricted communication interfaces.

This paper introduces a novel implementation approach based on System on Chip (SoC) technology with optimized Hardware-/Software Partitioning for real-time delay and sum beamforming. Basis for evaluation is a runtime measurement of software implementations to determine computation steps with high processing time and parallelization capabilities. Extracted computation steps are implemented on an associated FPGA with full pipelined architecture for high data throughput and fast processing speed. The complexity of the deduced architecture is evaluated regarding data length and data width with respect to computational accuracy.

Key words: Beamforming, System on Chip, Hardware-/Software Partitioning, Parallelization

Introduction

Nowadays, beamforming algorithms are used in numerous fields of applications. One field of application is the data generation as it is done in sonar systems to isolate ocean waveguide information [1]. As another example, the automotive industry uses beamforming algorithm for data fusion approaches to merge signals from distinct short range radar systems [2]. However, a main application for beamforming algorithms is signal quality enhancement. On this account, beamforming methods are used in wireless applications [3] and RF designs [4] to enhance the signal quality. Another field of application is spatial filtering focusing on separation of mutually effecting frequencies. In result the signal quality is increased as well [5]. Furthermore, beamforming algorithms are used in speech processing applications to improve speaker signal quality from a certain direction. In result, the signal quality increases and suppressing unintended influencing signals generated by sound sources in different directions like background noises [6].

However, beamforming algorithms can be used in opposite direction. The previous fields of application mainly focused on signal enhancement while another main application of these algorithms is direction of arrival estimation [7]. On basis of beamforming the direction of arrival is identified and used for speaker localization and tracking [8] or determining the position of aircrafts [9]. For this applications steered beamformers are used accompanied by high computational effort challenging embedded devices.

In the following, possible hardware acceleration techniques for beamforming algorithms determining the direction of arrival are analyzed and advantages and disadvantages of the distinct approaches are discussed. Basis for further considerations is the analysis of runtime and calculation complexity of a common delay and sum (DAS) beamformer. For elucidation of the theoretical values an exemplary implementation of the beamformer is used. On this basis, a novel System on Chip (SoC) design will be derived. The novel approach will be

described in detail and evaluated with respect to runtime and hardware utilization. Finally, the results are presented and critically discussed in conjunction with a summary of the paper and possible improvements in future works.

Related Work

As previously mentioned, the main problem of beamforming algorithms is the high computational complexity. One possibility to realize a beamforming algorithm for direction of arrival estimation is the calculation in time domain providing simple implementation effort, but reducing the angle accuracy drastically. This raises from the direct proportional dependency of sampling rate F_s and angle resolution represented by following equation:

$$\Delta_i = \left\lceil F_s \frac{i \cdot b \sin(\theta)}{c} \right\rceil \quad (1)$$

with Δ_i representing amount of delayed samples, intermediated sensor distance b , input angle θ , signal speed c and $i \in \{1, 2, \dots, M\}$ where M is the amount of sensors. This implies the increasing of accuracy can just be obtained by increasing the sampling rate. For time domain calculation all input signal are delayed by Δ_i in respect to input angle θ_n with $n \in \{1, 2, \dots, N\}$ where N represents the measurement window size. In time domain each sample of the measurement window represent an angle according to equation (1) (comp. Fig. 1). Afterwards the delayed signals according to θ_n are summed up. This procedure is repeated for all N . The maximum amplitude of the summed values represents the direction of arrival. Considering the described computation a calculation complexity of $O(N^2)$ can be identified.

Because of the high computational costs accompanied by low accuracy the calculation is transferred to frequency domain. In this context the convolution in time domain is reduced to a multiplication in frequency domain in conjunction with less computational effort. Another benefit is the representation of the time delay Δ as phase shift in frequency domain defined as steering vectors. In consequence an arbitrary angle resolution can be achieved restricted by computational power only. Therefore, the calculation complexity in frequency domain results in $O(N_A \cdot N_{FFT})$ where N_A represents the amount of angles with respect to angle resolution and N_{FFT} represents the amount of frequency components resulting of FFT usage and defining FFT resolution.

The previously discussed arguments are universally valid for beamforming algorithms. However, in last decades numerous versions of beamforming methods have been developed. Each of this algorithms rely on additional non

trivial calculations effecting the calculation complexity. One example is Minimum Variance Distortionless Response (MVDR) beamformer depending on an inverse calculation of $M \times M$ matrix [10]. Another example is the Multiple Signal Classification (MUSIC) beamformer depending on calculation of eigenvalues of an equal sized matrix [11].

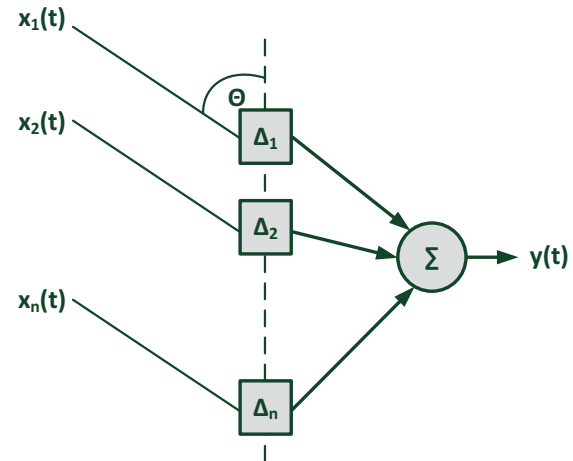


Fig. 1: Standard beamformer with delay Δ and input angle Θ .

Consequently, the transfer in frequency domain alone is not sufficient to solve the computational effort problem. On this account, the algorithms has been realized on specialized Hardware like Field Programmable Gate Arrays (FPGA) [12] or Graphics Processing Units (GPUs) [13] beside powerful PCs.

FPGA based realizations provide a high degree of flexibility with regards to correlated requirements as well as maximum parallelization capabilities. Another big benefit of FPGA usage is the low power consumption leading to a variety of possible applications. On the contrary, FPGA development is accompanied by long development times reasoned by specialized hardware implementation for the specific use case. Furthermore, there is a reduction of usability through additional specialized interfaces for data transfer reducing the throughput of FPGA designs.

On the other hand, GPUs have very high power consumption, but offer high performance and good parallelization characteristics with high throughputs and high processing speed.

In summary, a normal PC is powerful and can handle the specified algorithms in acceptable computing time, but is not suitable for mobile use due to the lack of mobility and high power consumption. FPGAs have low power consumption and high parallelization capabilities, but facing the drawback of long development times. GPUs, on the other hand,

have high power consumption but offer enormous throughput and acceleration possibilities.

A compromise between power consumption, mobility and hardware acceleration is represented by the SoCs from Xilinx and Altera. The combination of ARM Processor and FPGA provides high flexibility and parallelization capabilities with low power consumption and provides novel possibilities for hardware/software partitioning due to standardized flexible communication interfaces. For this reason, this architecture provides a suitable basis for accelerating beamforming algorithm for the usage on embedded devices.

For identification of potential task for hardware acceleration, the following chapter provides a detailed description and run time analysis of a standard beam scan algorithm represented by the DAS beamformer.

Algorithmen Analysis

To analyze the most popular representative of the beam scan algorithms, the DAS beamformer, the input signal of the sensors is defined as follows:

$$x_i(t) = g_i(t) * s(t) + n_i(t) \quad (2)$$

Where g represents the spatial response of signal source s with adaptive gaussian noise n at time t . The beamformer output can be represented as:

$$y(t) = \omega^H x(t) \quad (3)$$

Where $\omega = [\omega_1, \omega_2, \dots, \omega_M]$ defines the weights of the input channels and H is the Hermitian transpose. Transforming the input signal x_i to frequency domain equation (2) has to be rewritten as:

$$X_i(k) = G_i(k)S(k) + N_i(k) \quad (4)$$

With X_i representing the result of applying a SFFT to the corresponding input signal x_i . Furthermore, S is the signal spectrum of signal source s and noise spectra N . This leads to beamformer output definition:

$$Y_i(k) = W^H(k)X(k) \quad (5)$$

With spatial filter W describing the time delay of equation (1) in frequency domain by a phase shift with respect to input angle θ .

The Delay and Sum Beamformer determines the direction of arrival by successively scanning of the power spectrum. Input angle θ is defined by the maximum magnitude of the power spectrum defined by [14]:

$$P(\omega) = \frac{1}{K} \sum_{k=1}^K |X(k)|^2 = W^H X(k)X(k)^H W \quad (6)$$

$$= W^H R_{xx} W \quad (7)$$

Where R_{xx} is the well-known covariance matrix of input signal $X(k)$ defined by $R_{xx} = X(k)X(k)^H$. Spatial filter W represents the steering vectors defined by [14]:

$$S(\theta) = [s(\mu_1(k, \theta)), \dots, s(\mu_M(k, \theta))] = \quad (8)$$

$$\begin{bmatrix} 1 & 1 & \dots & 1 \\ e^{j\mu(1,\theta)} & e^{j\mu(2,\theta)} & \dots & e^{j\mu(K,\theta)} \\ \vdots & \vdots & \vdots & \vdots \\ e^{j(M-1)\mu(1,\theta)} & e^{j(M-1)\mu(2,\theta)} & \dots & e^{j(M-1)\mu(K,\theta)} \end{bmatrix}$$

In this context, term $e^{jq\mu(k,\theta)}$ represents the phase shift of input signal X with respect to input angle θ , frequency bin k and sensor q . On this basis μ has to be defined as:

$$\mu(k, \theta) = \frac{-2\pi}{\lambda_k} b \sin(\theta) \quad (9)$$

Where λ is the wavelength of frequency k . In consequence the direction of arrival is described by the maximum amplitude of equation (7):

$$\operatorname{argmax}\{P(\theta)\} = \operatorname{argmax}\{S(\theta)^H R_{xx} S(\theta)\} \quad (10)$$

The described algorithm results in the process flow depict in Fig. 2.

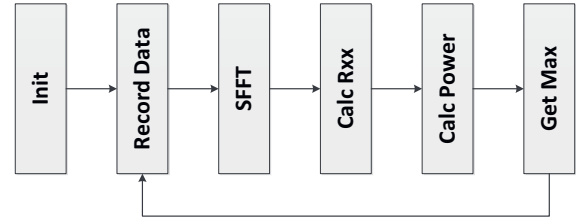


Fig. 2: Process flow for Beamforming computation.

At begin of the process all constants are determined including the steering vectors, since they just depend on angle granularity and FFT resolution. The "Init" process will be ignored in the further analysis, since the initiation costs just appear ones and effect the startup of the system only. The second step is the acquisition of data consisting of data sampling and copying in a predefined buffer. The runtime has complexity of $O(MN_{FFT})$ because every sample of the measurement window has to be copied ones for each input channel. Therefore, N_{FFT} is the length of measurement window defining FFT length and FFT resolution respectively. The following block is SFFT describing short-time Fourier transform of length N_{FFT} . If $N_{FFT} = 2^p$ with $p \in \mathbb{N}$ it can be shown that the complexity of SFFT is $O(N_{FFT} \log(N_{FFT}))$ and the accumulation for all channels results in $O(MN_{FFT} \log(N_{FFT}))$.

Afterwards, the calculation of the $M \times M$ matrix $R_{xx} \in \mathbb{C}$ takes part. According to definition of $R_{xx} = X(k)X(k)^H$, M^2 complex

values has to be determined. For the determination of one component of matrix R_{xx} M complex multiplications and $M-1$ additions has to be executed leading to a runtime complexity of $O(M^4)$ for one frequency component. The process has to be repeated for each frequency bin successively conducting in runtime complexity of $O(\frac{N_{FFT}}{2}M^4)$. According to the master theorem, if $M \ll N_{FFT}$ the complexity for R_{xx} determination can be estimated by $O(N_{FFT})$.

The final power calculation from equation (7) is realized in the subsequent ‘‘Calc. Power’’ block. Therefore, the steering vectors given by equation (8) are multiplied with the determined matrix R_{xx} to archive the power level corresponding to input angle θ . The computation of equation (7) has to be repeated for each possible input angle and for each frequency component resulting in runtime complexity of $O(\frac{N_{FFT}}{2}N_A) \cdot O(W^H R_{xx} W)$. The computational costs for $W^H R_{xx} W$ can be estimated by $O(M^3)$. The result of this matrix multiplication is a vector of length M which has to be multiplied by the steering vector as well. In consequent, the vector multiplication has to be estimated by $O(M^2)$. Subsequently, the absolute value of the result has to be determined. The calculation is accompanied by two multiplications for square computation, one addition and one square root determination resulting in $O(3n_b \log n_b^{2O(\log^* n_b)})$ with n_b defining number of bits [15]. In consequence the total runtime complexity is $O(\frac{N_{FFT}}{2}N_A) \cdot (O(M^3 + M^2 + 3n_b \log n_b^{2O(\log^* n_b)}))$. Following the master theorem the complexity can be reduced to $O(N_{FFT}N_A)$. The last task is the maximum detection with a trivial runtime of $O(N_A)$.

For clarification of the theoretical time estimation, the system has been implemented on a Cortex A9 ARM Processor with the purpose to measure the time for each described task. For evaluation a FFT resolution of 1024, an angle granularity of one degree and three input sensors have been chosen. The results are depict in Tab.1.

Tab. 1: Results of runtime measurement for DAS with 3 Sensoren, N_{FFT} 1024 und N_A 180 implemented on ARM Cortex A9 Prozessor.

Task	Complexity	Time (ms)
Record Data	$O(MN_{FFT})$	1,313
SFFT	$O(N_{FFT} \log(N_{FFT}))$	1,668
Calc Rxx	$O(\frac{N_{FFT}}{2}M^4)$	5,124
Calc Power	$O(N_{FFT}N_A)$	533,181

The results show that the runtime of $O(N_{FFT}N_A)$ in combination with the expensive constant costs for square root calculation effecting the overall runtime massively. In consequence the theoretical consideration and the exemplary time measurement identifying the power calculation as bottleneck in the localization process.

The following chapter describes a novel approach for hardware acceleration bases on SoC Architecture with the aim of dissolving the bottleneck.

System on Chip Architecture

To handle the identified bottleneck a Xilinx Zynq SoC is used. The SoC combines a Cortex A9 ARM Processor and FPGA with the standardized AXI-Interface as communication medium. The Aim of the design is to use the parallelization capabilities of the FPGA to dissolve the bottleneck and improve the throughput of the power calculation but also keep the most possible flexibility to compensate the FPGA development costs.

A localization system bases on beamforming algorithms usually depends on the amount of sensors M , the scanning region defined by angle range, the granularity of the angles resulting in number of steering vectors N_A and length of measurement window N_{FFT} given by FFT resolution. To ensure the greatest possible flexibility and reusability of the FPGA design, the realization should be independent from this parameters as fare as possible.

By considering equation (7) and the corresponding runtime complexity it is clear that all this parameters influencing the calculation. The amount of angles and angle granularity are indirectly given by the amount of steering vectors. The steering vectors depend on the frequency components and possible input angles only whereby a calculation in the initialization phase is sufficient. On the other hand, the calculation of R_{xx} has to be adapted with each measurement window. Nevertheless, the amount of steering vectors has a huge memory complexity since there is one complex steering vector for each frequency component, input angle and sensor. This leads to a memory usage of $O(\frac{N_{FFT}}{2}N_A M)$ which represent a big challenge for FPGAs and the limited Block RAM resources to store all steering vectors initially. For this reason, the steering vectors has to be transferred from the DDR RAM separately.

On this account, the task of the process flow depict in Fig.2 are mapped to the software part until task ‘‘Calc Rxx’’, the other tasks are mapped to the hardware part connected by DMA controller and AXI-Lite interface. The resulting

system architecture is shown in Fig.3. The maximum detection has been moved to the hardware part to reduce communication costs. After power calculation N_A values have been generated and have to be transferred to the software by a DMA Controller with subsequently maximum detection. However, usually just the direction of arrival is needed which is represented by one angle with maximum magnitude. Based on this just one angle need to be transferred if the maximum detection is realized on hardware.

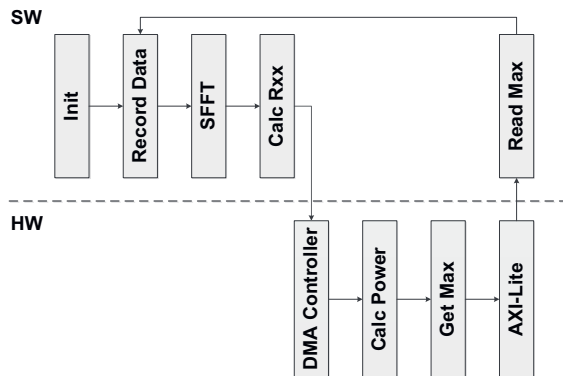


Fig. 3: System architecture with HW-/SW-Partitioning.

Since a huge amount of data has to be transferred between processor and FPGA a DMA controller is used to transfer all necessary data from DDR RAM to FPGA by direct memory access sequentially. Reversely, an AXI-Lite interface is used, since it provides less hardware utilization and simple usability for transferring low amount of data. After finishing the calculation process, the angle indicating the direction of arrival has to be transferred only, reasoning the usage of AXI-Lite interface. Additionally the AXI-Lite interface acts as configuration interface as well.

Reviewing equation (7) in detail it is evident, that the matrix multiplication can be divided in three parallel vector multiplications. This vector multiplications can be efficiently implemented with shift registers. The following vector multiplication proceeds in parallel with one clock cycle delay (see Fig.4).

$$\begin{pmatrix} R_{11} & R_{12} & R_{13} \\ R_{21} & R_{22} & R_{23} \\ R_{31} & R_{32} & R_{33} \end{pmatrix} \begin{pmatrix} W_1 \\ W_2 \\ W_3 \end{pmatrix} = \begin{pmatrix} x_1 \\ x_2 \\ x_3 \end{pmatrix} \quad (P(\alpha))$$

Fig. 4: Schematic power calculation of equation (7) with parallel vector multiplication (gray) for $M=3$.

This calculation has to be carried out N_A times without changes of the R_{xx} values. For this reason, the values for R_{xx} are transmitted once for each frequency component to subsequently

stream the steering vectors through the calculation architecture. This approach has been realized in the following FPGA design depicted in Fig. 5.

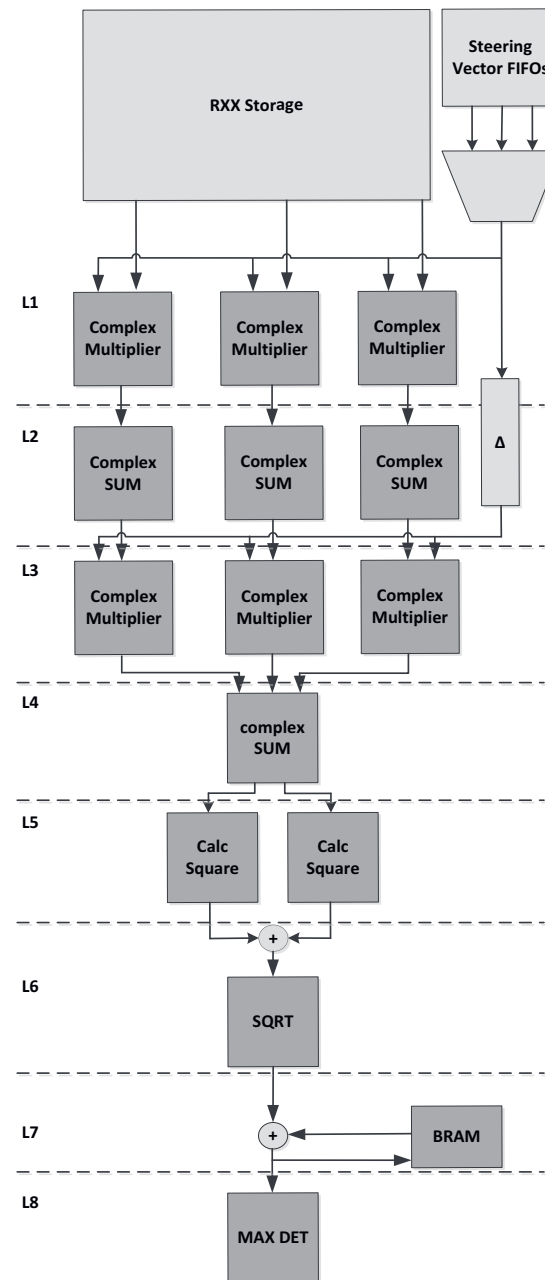


Fig. 5: Block diagram of FPGA Design for parallel computation of equation (7) with maximum detection for $M=3$. Calculation instances are displayed dark gray routing and storing instances light gray divided in computation level L1 to L8.

The data are transmitted to the FPGA by a simple streaming protocol, whereas the first M^2 data are identified as R_{xx} entries. The R_{xx} entries are stored in RXX Storage. All other incoming data are steering vectors which are stored in M separated FIFOs. The FIFOs representing one row of the matrix depicted in equation (8). For

communication reduction the first row is not transmitted since it is constant one. The DMA Controller supports 32bit and 64 bit interfaces. For this implementation, 64bits are used which is logical divided in two 32bit values. The two values representing the real and imaginary part of one complex number. For this reason an arbitrary amount of sensors can be supported since they can be identified by a simple modulo calculation.

After the R_{xx} values and the steering vectors have been transferred, the data according to formula (7) and the schematically represented calculation in Fig.4 are transferred into the calculation architecture by a multiplexer.

The first level of the calculation architecture (L1) is formed by M complex multipliers, which as the name implies, realizes a multiplication of complex numbers. To reduce the number of DSP cores, which are used to perform the multiplications, the calculation is realized as follows:

$$z1 = (a + bi) \quad z2 = (c + di)$$

$$R(z1 \cdot z2) = ac - bd \quad (11)$$

$$I(z1 \cdot z2) = (a + b)(c + d) - ac - bd \quad (12)$$

The advantage over the traditional variant is the reduction of four multiplications to three multiplications leading to a reduction of M DSP cores per calculation level. The resulting calculation tree is depicted in Fig.6.

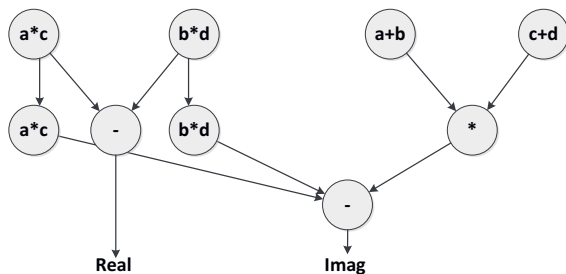


Fig. 6: computation flow for complex multiplication for $z1 \cdot z2$.

The realization requires three clocks for one complex multiplication until the result is obtained, but offers a full pipelined structure with maximum throughput.

The multiplexer passes the corresponding matrix components from Fig. 4 one after the other to the complex multipliers. The multiplication results are transferred to level 2 (L2). In L2 the summation of the intermediate results takes place ending the parallel matrix calculation shown in Fig.4. The result of L2 is the row vector (x_1, x_2, x_3) in Fig. 4. In L3 the multiplication of row vector x and steering vector takes place. For this reason the incoming steering vectors are

delayed in such way so that they are present at the appropriate time at L3. The resulting summands are summed in level 4 leading to the sum representing the complex value of $P(\Theta)$. In L5 the square of the real and imaginary part transferred from L4 is calculated summed and forwarded to L6 for square root determination. For square root computation the Cordic-IP core is used, provided by the vendor. Result of L6 is the power value of the dedicated frequency component at input angle Θ . Since the results must be added over all frequency components, each value is stored in a BRAM. In each subsequent iteration the values are read and summed up in parallel. For this purpose, the number of angles N_A must be transferred once during the initialization phase via AXI-Lite interface. In the last step, the maximum is determined by storing the current maximum and the associated angle index for each iteration, which can be accessed via the AXI-Lite interface after completion of the calculation.

To determine the latency of the system, the respective latencies of the described blocks have to be added for each processing level. The multiplication in L1 and L3 requires three clock cycles while the summation in L2 and L4 takes one clock cycle only. Squaring the real and imaginary part in L5 is calculated in one clock cycle the subsequent summation requires one additional cycle. The calculation of the square root is more complex and requires 13 clock cycles until the result is available. The summation in L7 and the determination of the maximum in L8 are processed in one cycle respectively. In summary the latency of the design results in 25 clock cycles. The determination of the total runtime is given by the behavioral description of the system. To determine one power value, N_A steering vectors must be shifted through the calculation architecture. All N_A steering vector have to be active for M clock cycles since all M components of matrix R_{xx} have to be shifted through the complex multipliers. This results in a runtime of $N_A M + 25$ clock cycles for one maximum determination of a frequency component. The process has to be repeated $\frac{N_{FFT}}{2}$ times for each frequency component. The total runtime results in $\frac{N_{FFT}}{2} (N_A M + 25 + T_{com})$ with T_{com} defining the communication time for transferring the steering vectors from DDR RAM to FPGA. T_{com} can be estimated by N_A clock cycles, but includes additional communication costs for DMA controller processing leading to inaccuracies in the estimated total runtime. The conversion from clock cycles to time units depends on the individual configured FPGA base frequency.

The correctness of the design has been verified by simultaneous simulations in Matlab and Vivado simulator.

Results

For evaluation purpose of the design architecture, the design has been implemented on a Zynq ZedBoard according to Fig.3. Correspondingly, the data acquisition, the determination of the SFFT and the calculation of the R_{xx} matrix were implemented in software. On hardware the power computation and maximum detection have been realized with FPGA base frequency of 100 MHz.

Reviewing, the FPGA design from Fig. 5 is independent of the number of steering vectors, the definition of the steering vectors and the resolution of the FFT. However, the design architecture still depends on amount of sensors M since each column in Fig.5, at level 1 to 3, represents one Sensor. For the usage of M sensors M complex multiplier and M summations have to be implemented in L1 to L3 influencing the resource utilization massively. The following figure depicts the used Look Up Tables (LUT) and Flip Flops (FF) in respect to the amount of sensors.

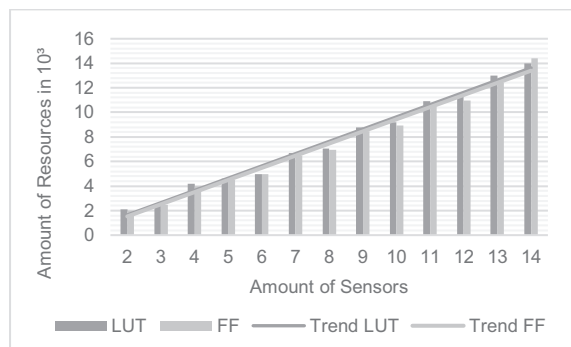


Fig. 7: Resource utilization of FFs and LUTs in dependency of used Sensors and linear trend (light and dark grey lines).

It can be observed that a linear correspondence between resources and amount of sensors has been achieved. This can be explained by the linear relationship between the number of sensors and the required complex multiplier and summations. An additional observation is the constant relation between amount of LUTs and FFs, furthermore the amount of resources is almost equal.

For the realization of the multipliers DSP cores are used. The usage of the DSP cores depending on amount of sensors is shown in Figure 8. For the same reasons, a linear trend is identified for DSP usage. However, the number of DSP cores is twice as high as instantiated multipliers reasoned by DSP core input vector width. The calculation bases on the multiplication

of 32 bit values while the DSP cores supporting a 25bit multiplication only. During synthesis, this is resolved by using 2 DSP cores reasoning the higher utilization.

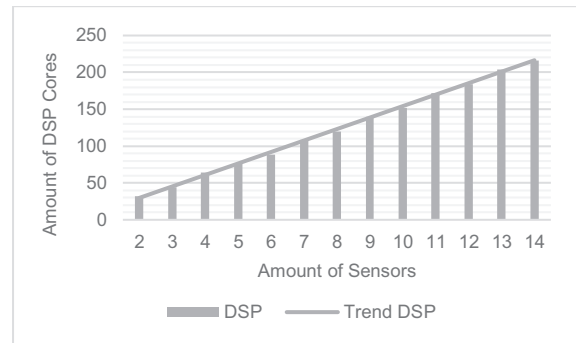


Fig. 8: Amount of used DSP Cores in dependency of used Sensors and linear Trend.

The parameters N_A and N_{FFT} have no influence on the hardware resources, but determining the overall processing time mainly. As derived in the previous chapter, a linear dependency of the runtime $\frac{N_{FFT}}{2}(N_A M + 25 + T_{com})$ is expected. To evaluate the processing time, the design from Fig. 5 was used to proceed varying amounts of data, to measure the necessary runtime. The procedure was repeated 500 times to ensure the statistical significance. The data variability is the result of the variation of the parameters N_A and N_{FFT} . The measurement results are illustrated in Figure 9 confirming the linear dependence on amount of steering vectors N_A and processing time. Figure 10 shows the measurement results for different FFT resolutions. The linear relationship between amount of frequency components and processing time can be confirmed by the measurements as well.

The number of sensors have a linear influence on the processing time of the calculation as well since it defines the size of matrix R_{xx} . However, the high influence of (M^3+M^2) of the sensor count has been cancelled out by the parallelization of the matrix calculation.

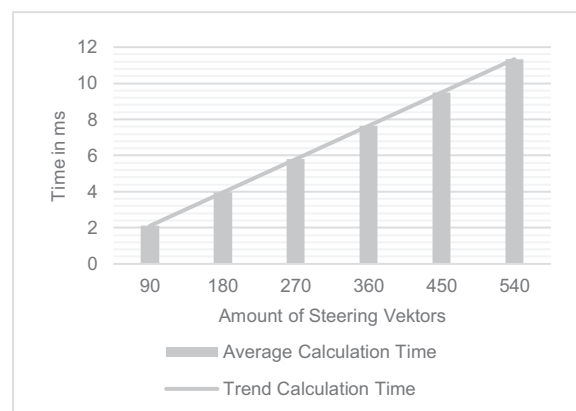


Fig. 9: Dependency between angle resolution and average processing time with trend line.

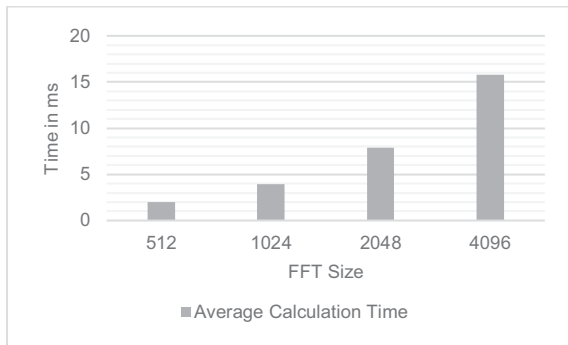


Fig. 10: Dependency between processing time and FFT resolution.

Even in a numerical comparison of runtimes, the design has significantly accelerated the processing time to the pure software solution. Compared to the software solution in Table 1, the processing time has been reduced from ~500 ms to ~4 ms. Even at four times higher resolution a processing time of ~15ms was achieved which is much faster than a standard embedded processor. For illustration, the used ARM processor has a frequency of 700 MHz and needs approximately 500 ms for calculation. This is equivalent to approx. 350 million clock cycles, to achieve the same processing time of 4 ms a processor with a frequency of 87,5 GHz has to be used. The explanation can be derived from the comparison of runtime estimations. For Software solution a runtime of $O(\frac{N_{FFT}}{2} N_A) \cdot O(M^3 + M^2 + T_{root})$ has been identified on the other hand a runtime of $O(\frac{N_{FFT}}{2} (N_A M + 25 + T_{com}))$ for hardware solution have been achieved. Comparing both results it is clear that the big factor of $O(M^3 + M^2 + T_{root})$ has been reduced to $O(M)$ reasoned by the parallelization of matrix calculation. Furthermore the calculation time of square root estimation has been canceled out reasoned by pipelining the root determination.

In summary, the presented design is flexible in terms of angular granularity, scan region and FFT resolution. Only a change in the number of sensors has an effect on the FPGA design. Furthermore, the processing time scales linear to all depending parameters.

Conclusion and Future Work

This paper presented a novel approach to hardware acceleration of beamscan algorithms for localization of signal sources. The algorithm class was analyzed and calculation bottlenecks identified. Based on the analysis, a Hardware-Software Co-Design design was derived resolving the bottleneck. The design works in the frequency domain and is independent of the FFT resolution, the angle resolution, as well as the scan region. Only changes in sensor count leads

to an adaption of the FPGA design. By the novel integrating of the FPGA into the localization system, the complexity of the system could be reduced leading to a linear scalability of all hardware resources and total runtime.

Future work will deal with further reduction of DSP cores and optimization techniques to reduce the hardware resources.

Acknowledgment

The authors gratefully acknowledge funding by the DFG (GRK 1780/1).

References

- [1] G.E. Allen, B.L. Evans, Real-time sonar beamforming on workstations using process networks and POSIX threads, *IEEE Transactions on Signal Processing* 48.3, 921-926 (2000); doi: 10.1109/78.824694
- [2] K. Schuler, et al, Array design for automotive digital beamforming radar system, *Radar Conference, 2005 IEEE International. IEEE*, 2005; doi: 10.1109/RADAR.2005.1435864
- [3] J. Litva, and T. K. Lo, Digital beamforming in wireless communications. *Artech House, Inc.*, 1996. ISBN:0890067120
- [4] R. Kohno, Spatial and temporal communication theory using adaptive antenna array, *IEEE personal communications* 5.1: 28-35 (1998); doi: 10.1109/98.656157
- [5] B. D. Van Veen, K. M. Buckley, Beamforming: A versatile approach to spatial filtering, *IEEE assp magazine* 5.2,4-24 (1988); doi: 10.1109/53.665
- [6] J.-M. Valin and et al., Robust sound source localization using a microphone array on a mobile robot, *Intelligent Robots and Systems, 2003.(IROS 2003). Proceedings. 2003 IEEE/RSJ International Conference on, vol. 2. IEEE*, 1228–1233 (2003); doi: 10.1109/IROS.2003.1248813
- [7] V. Krishnaveni, T. Kesavamurthy, and B. Aparna, Beamforming for direction-of-arrival (doa) estimation-a survey, *International Journal of Computer Applications, vol. 61, no. 11*, 2013; doi: 10.5120/9970-4758
- [8] I. Markovi'c, et al., Speaker localization and tracking with a microphone array on a mobile robot using von Mises distribution and particle filtering, *Robotics and Autonomous Systems, vol. 58, no. 11*, pp. 1185–1196 (2010); doi: /10.1016/j.robot.2010.08.001
- [9] U. Michel, History of acoustic beamforming, *1st. Berlin Beamforming Conference*. 2006.
- [10] J. Capon, High-resolution frequency-wavenumber spectrum analysis, *Proceedings of the IEEE*, 1408-1418 (1969); doi: 10.1109/PROC.1969.7278
- [11] R. Schmidt, Multiple emitter location and signal parameter estimation, *IEEE transactions on antennas and propagation*, 276-280 (1986); doi: 10.1109/TAP.1986.1143830

- [12] A. Ahmedsaid, A. Amira, and A. Bouridane, Accelerating MUSIC method on reconfigurable hardware for source localization, *Circuits and Systems, 2004. ISCAS'04. Proceedings of the 2004 International Symposium on. Vol. 3*, IEEE, 2004; doi: 10.1109/ISCAS.2004.1328760
- [13] V. P. Minotto, et al., GPU-based approaches for real-time sound source localization using the SRP-PHAT algorithm, *The International Journal of High Performance Computing Applications*, 291-306 (2013); doi: 10.1177/1094342012452166
- [14] S. N. Bhuiya, F. Islam, M. A. Matin, Analysis of Direction of arrival techniques using uniform linear array, *International Journal of Computer Theory and Engineering*, 931 (2012).
- [15] M. Fürer. Faster integer multiplication. *SIAM Journal on Computing*, 979-1005 (2009); doi: 10.1137/070711761

Experimental Measurements and Antenna Isolation for TETRA Communication System in Underground Mining and decline

Batzorig Bazargur¹, [Otgonbayar Bataa](#)¹, Zagarzusem Khurelbaatar¹, Batbayar Battseren¹
¹ School of Information and Communication Technology,
 Mongolian University of Science and Technology
batzorigbazargur@gmail.com, otgonbayar_b@must.edu.mn, zagarzusem@must.edu.mn,
nano.batbayar@gmail.com

Abstract:

Mining industries play an important role in the economic development of Mongolia. In mining operations, truly reliable and robust communication systems play a vital role in ensuring personnel safety, enhancing operational efficiency and process optimization. In this thesis, we have carried out the calculation of RF amplifier wave propagation in mines and in special-purpose tunnels, in tunnel entrance and in box cut declines of tunnel entrance. UHF radio frequency radiation tests have been carried out in the 16-degree box cut declines at a depth of 30 meters and in the 150m long tunnels beneath it. In this case, it is necessary to create significant isolation between the donor antenna and the service antenna of RF amplifier. Our results are useful to understand the isolation of antennas and implications of the physical environment, signal radiation characteristics in underground mine communication system.

Key words: tunnel, propagation calculation, UHF frequency, RF amplifier, decline.

Introduction

We need to provide reliable radio communication services in tunnels for different purposes and in the decline (underground mines, subway tunnels etc.) or in small-diameter, deep holes where the radio communication signal strength is so weak. Installing fiber optic amplifier or a base station is highly reliable and easy to install in such environments, but it leads to prohibitive cost and time. There is no ready to use model for calculating and modelling radio wave propagation as well. So, radio wave propagation modeling plays a vital role to solve such problems which is possible with RF amplifier. RF amplifier model utilized in underground mines is shown in Figure 2.

The Scope of works is for the provision of civil construction and tunneling services for the associated portal structures, twin parallel declines and conveyor transfer and drive station excavations to facilitate installation of ore handling system and service access to underground shaft mine, and associated services.

- 6.6km long twin parallel tunnel

- 16.6 km tunneling

The decline is a dual heading system with parallel declines each consisting of three legs required for conveyors and mine access.

- 16.6km tunnels & 34,000 cu.m large chambers
- Leg length approx. 2200m
- Final depth 1120m
- Gradient max 18.5%
- Crosscut every 200m
- Safety bay every 30m

10.2 angle is the maximum grade range of decline which can provide safest working condition in order to reach 1300m deep.



Fig. 1. Decline and tunnel

RF amplifier is used in order to meet the radio communication needs during the Phase 1 construction work means early stage of this project (150-200m tunnel). It is comprised of the following main components such as donor of amplifier, service antenna, isolation and amplifier. RF amplifier is developed to provide radio communication network in the decline of conveyor transfer and in the decline of the first 150-200m depth.

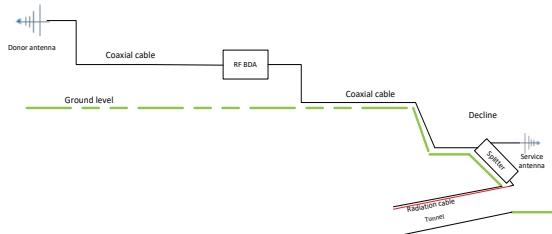


Fig. 2. Geometric modelling of RF amplifier connection diagram for decline and tunnel

Background

In this thesis, we have carried out the calculation of RF amplifier wave propagation in tunnels, radiating cable modelling and wave propagation modelling in tunnel entrance and in the declines. In order to provide effective construction activity as well as safety control, executive should have reliable radio communication coverage around the decline construction area. Before two-way radio coverage couldn't cover under the surface level and decline tunnel therefore additional radio coverage expansion requires around the construction area. Radio coverage will be expanded by step by step to align with construction activity:

Phase 1.

- To cover decline area
- To cover extended range (100-150m) of decline tunnel construction. RF amplifier is used as a temporary solution at a depth of 150-200 meters in the decline. RF amplifier test has not been carried out in longer tunnels. Permanent solution to this is DAS based solution connected to BTS. We have used RF amplifier, donor and service antenna (both are Yagi antenna), coaxial and leaky radiation cables for the temporary solution.

In [1], repeater amplifiers, also known as signal boosters, are specialized RF systems that extend radio coverage into enclosed or shadowed areas where abrupt propagation losses impair communication.

Materials such as soil or rock, brick, cement, reinforced concrete, metals, and metal-coated thermal glass panes are notorious for their

ability to block electromagnetic radiation in the radio frequency range. In the interior of structures made of those materials, and in areas where natural or man-made structures block radio propagation, radio frequency levels may be 30 to 100 dB or more below unobstructed levels (nothing but cosmic ray particles and neutrinos penetrates into deep mines, for example). Repeater amplifiers boost radio signals to levels sufficiently high to provide reliable communication in those enclosed or blocked areas.

Repeater amplifiers have acquired great prominence in the radio communication industry in the last few years, due to a rapidly growing demand for extended communications services inside all types of urban structures. However, they made their first appearances several decades ago, as a part of "leaky feeder" or "leaky coax" radio communication systems in underground mines, vehicular and railroad tunnels. One-way repeater amplifiers were used in various configurations for simplex and semi-duplex radio communication in underground tunnels. In another paper, the authors looked the tunnel propagation model, and in this paper a fully vector finite element base propagation model is developed for blocked straight and curved tunnels. Effect of different vehicles, location of vehicles and number of vehicles inside tunnels is analyzed [2]. Some researcher studied to look at the frequency band techniques in Indian underground mining case. The paper discusses different radio frequency communication techniques being employed for Indian underground mines. Experiments were conducted in the laboratory as well as in the underground coal mines for medium wave frequency (MF), very high frequency (VHF) and ultra-high frequency (UHF) electromagnetic propagation as well as induction technique to meet different types of mining conditions [3]. On the other hand, they looked the trends of the tunnel propagation model. The authors developed current and future trends in technology, applications and propagation modeling are also identified. About ninety relevant references have been reviewed that consider: 1) the emergence of technology and applications, 2) analytical, numerical and measurement based propagation modeling techniques, and 3) implications of the physical environment, antenna placement and radiation characteristics on wireless communication system design. Affected systems include narrowband, wideband/ultra-wideband (UWB) and multiple-antenna systems. The paper concludes by identifying open areas of research [4]. To put it another way, above researchers have presents that results showing the

accuracy of the ADI technique when used to model the parabolic equation for (a) square (b) circular and (c) semi-circular cylindrical PEC tunnels. For each tunnel, we compare the numerical solution with the known analytical solution for different discretization along the transverse plane and propagation axis [5]. They are also maintains that explores extend the analysis of this method by including the realistic cases of branching tunnels and tunnels with rough walls [6]. The paper [7], concludes that the ADI-PE, shows simulation results for tunnel test cases with known analytical solutions. The author propose that configure a radio transceiver, designers must understand the performance parameters and tradeoffs of the RF amplifiers being used. A multitude of system requirements must be considered to choose an optimal amplifier from the many devices available by suppliers in the marketplace [8]. The paper notes that focuses on the modern linearizing techniques for the high power transmit amplifiers and reports on efforts to evolve system and behavioral level performance measures and quantifying techniques which will aid processes such as the design, specification and evaluation of linearizers and their overall contribution to transmit channel performance [9]. In [10] this doctoral thesis has focused on Doherty amplifiers (dynamic load technique) and high efficiency class-E amplifiers (main amplifier in EER) applied to WiMAX at 3.5GHz. This paper investigation that the amplifier requirements, the proposed solutions and their status [11]. All cavities work at 88 MHz, are independently phased and powered by amplifiers whose power ranges from few kilowatts to 250kW. Research in tunnel wireless communication [12], the author describes the various assumptions used in the design and analysis of distributed antenna system (DAS) for trains, tunnels and in-building wireless radio coverage. The design includes handover overlap design, base station connectivity, signal reticulation using splitters, couplers, bidirectional amplifiers, attenuators, discrete antennas, radiating cables and optic-electric couplers etc.

Radio Frequency (RF) Isolation

In this section, we focus our attention on the RF isolation between donor and service antenna. Obtaining isolation between donor antenna and service antenna is one of the most important factors to provide radio network in tunnels and decline using RF amplifier. However, it provides acceptable results when such tunnels and declines are located close to the base station (Receiver antenna gain and a donor antenna gain of RF amplifier can be -75dB and more). Antenna isolation is a key consideration in the

design of any radio communications system. Sufficient isolation is required to ensure that interference between systems is kept within acceptable levels (levels at which the equipment can operate effectively).

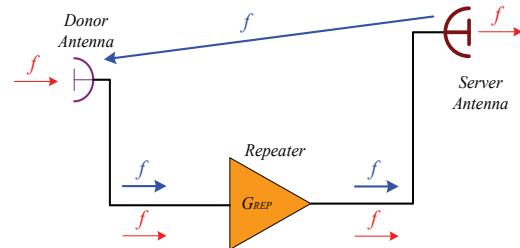


Fig. 3. Radio frequency (RF) amplifier isolation.

To let repeater works well, $F > G + 15\text{dB}$.

F: Isolation between the Donor antenna and service antenna.

G: Gain of the repeater

$$I_h = 22.0 + 20 \log_{10}(d/\lambda) - (G_d + G_r) + (X_d + X_r) + C \quad (1)$$

G_d , G_r is the gain of donor and server

X_d , X_r is the Front to Back ration for antennas.

In Oyu Tolgoi mine, we suppose $f=400\text{MHz}$, $\lambda=0.75\text{m}$.

Suppose $G_d = 10\text{dB}$, $X_d = 20\text{dB}$, $G_r = 10\text{dB}$, $X_r = 16\text{dB}$. C is the loss by obstacles. Suppose $C=0$ here.

Tab. 1: Radio frequency (RF) horizontal isolation

D (distance)	3	5	8	10	15	20
horizontal isolation(dB)	50	54	59	60	64	67
maximum gain(dB)	35	39	44	45	49	52

The calculator provides an estimate of the horizontal and vertical isolation provided by two 2-3m separated antennas. The spacing between a donor antenna and a service antenna is 3-58m.

$$I_v = 28.0 + 40 \log_{10}(d/\lambda) + C \quad (2)$$

C is the loss by obstacles. Suppose $C=0$ here

In OT, suppose $f=400\text{MHz}$, $\lambda=0.75\text{m}$

Tab. 1: Radio frequency (RF) vertical isolation results

D (distance)	3	5	8	10	15	20
vertical isolation(dB)	52	61	69	73	80	85
maximum gain(dB)	37	45	54	57	65	70

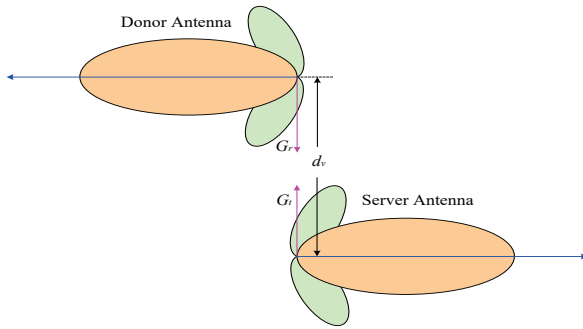


Fig. 4. Radio frequency (RF) vertical isolation

With same distance, vertical isolation is larger than horizontal isolation. So it is better to use vertical isolation [13].

Modelling of radio wave propagation in tunnels

Radiating cables are widely used to ensure radio communication in tunnels, but they have no amplifier like antennas. Attenuation coefficient of radiating cables is different from antenna’s attenuation coefficient. There are two main types of losses: Longitudinal loss and transmission loss. Transmission loss has 2 different measurements: C95 (95% percentile of the coupling loss) and C50 (median value of the coupling loss). These are predicted measurements of received signals via radiating cables [13].

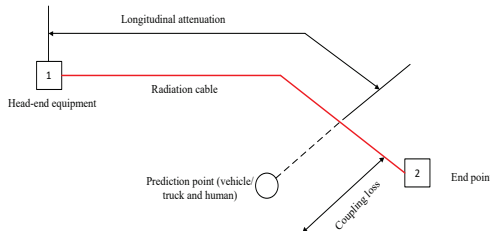


Fig. 5. Geometric modelling of radiating cables propagation

Calculating of RF amplifier wave propagation in tunnels

The RF amplifier radio communication network in tunnel entrance is provided by the service antenna isolation under the decline and in tunnels, radio communication network is enabled by radiating cables via two-way splitter. The calculation of this wave propagation modelling is carried out as follows:

$$P = P_i - L_1 - L_2 \tag{3}$$

For leaky cable, suppose cable was install tunnel side wall, and following:

- Suppose P is the signal power at a tunnel point 2 meters away from leaky cable.

- P_i is the RF power input the leaky cable
- L_1 is the cable transmission loss from cable input point to the point of testing location (P point)
- L_2 is the leaky cable coupling loss (95% coupling loss)

If mobile locate far from 2 meters, then additional small loss will have, but if the mobile is inside a vehicle, then about additional more 15dB loss must be considered on 800MHz (for our case we supposed the 17dB loss considered on our TETRA band 400Hz) [14].

We used RLK78-50JFNA model radiating cable in this calculation. Following that, we have carried out the line and cable calculation in tunnels. Based on the results of a calculation, we have determined how many meters of radiating cables are needed in tunnel.

$$Link\ Budget = TX\ power + abs(Rx\ sensitivity) - (all\ additional\ attenuations) - Coupling\ loss \tag{4}$$

$$Cable\ Length = Link\ Budget / Longitudinal\ Loss\ (dB/100m) * 100 \tag{5}$$

Calculation of radio wave propagation modelling in the decline of tunnels

Okumura-Hata model is used to calculate wave propagation in the tunnel entrance as it is shown in (see Fig. 2).

$$L_u = 69.55 + 26.16 \log_{10} f - 13.82 \log_{10} h_b - C_H + [44.9 - 6.55 \log_{10} h_b] \log_{10} d \tag{6}$$

- L_u -is the path loss (dB)
- h_b -is the base station antenna height (in meters)
- C_H -is the antenna height correction factor (dependent of environment, frequency and mobile height)
- f -is the transmission frequency (MHz)
- d -is the distance between transmitter and receiver (in kilometers).

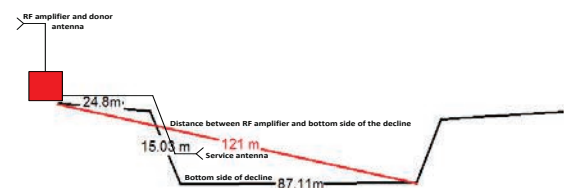


Fig. 6. Geometric modelling of decline flat area

We used service Yagi antenna specification, the antenna horizontal beam width is 65 degree, vertical beam width is 105 degree, and gain is 6dBd/8dBi. The area service antenna covered could be regarded as a flat area, so, free space propagation formula could be used. Assuming antenna height is 15.03 meters, repeater output power is 43dBm.

Comparative data of 400MHz and 800MHz frequencies of RF amplifier isolation and signal power in tunnels is illustrated in Figure 7 and Figure 8 respectively.

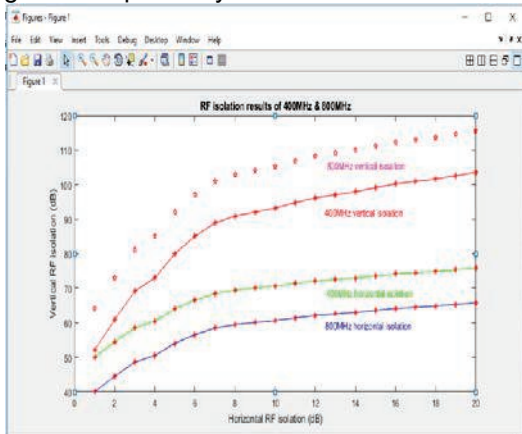


Fig. 7. Horizontal and vertical RF isolation results both on 400MHz & 800MHz

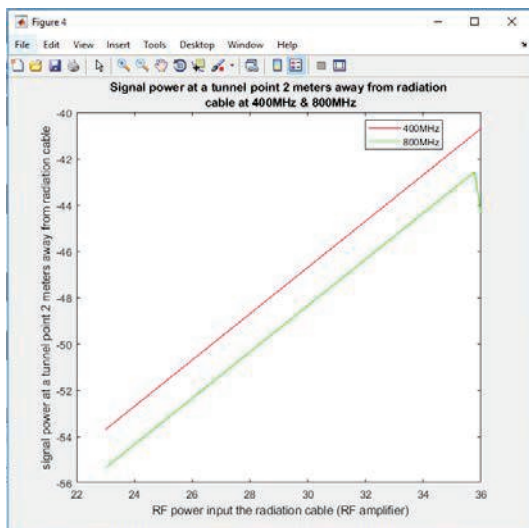


Fig. 8. Horizontal Signal power at a tunnel point 2 meter away from radiation cable at 400MHz & 800MHz

This was successfully tested and deployed in the decline of Oyu Tolgoi mining in 2016.

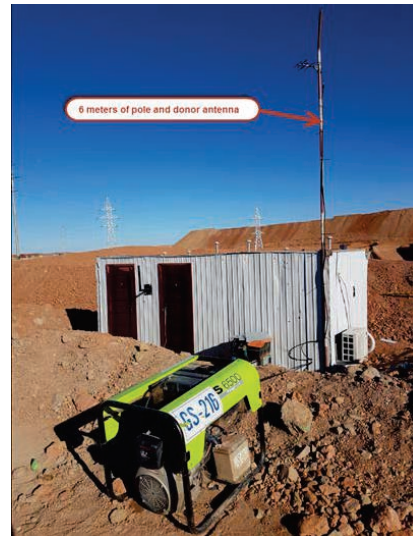


Fig. 9. RF donor antenna location

In order to provide radio communication network below the decline of tunnel entrance, we used a service antenna isolation with metal board.



Fig. 10. RF metal isolation between donor and service antenna

In tunnels, we used radiating cables fixed on the wall of a tunnel and Yagi antenna was utilized at the end of radiating cables.

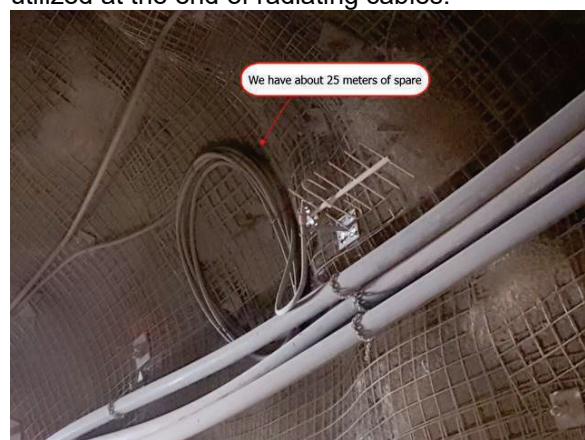


Fig. 11. End point of the radiation cable

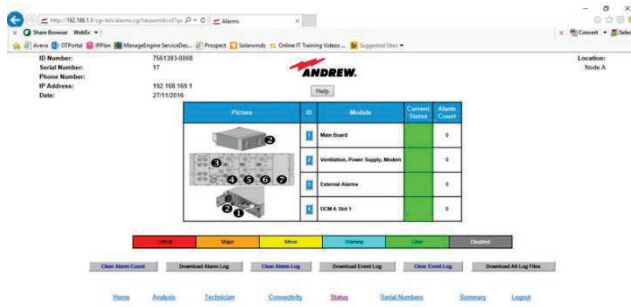


Fig. 12. RF amplifier's normal status

After utilizing RF amplifier, signal strength received by the user TETRA handheld radio terminal has been improved from -89dB to -64dB. This outcome is shown in Figure 13.



Fig. 13. TETRA handheld radio's RSSI results before and after

CONCLUSION

In this thesis, the calculation of wave propagation has been carried out to utilize RF amplifier in tunnels. One of the most important thing is to provide isolation between a donor antenna and a service antenna of RF amplifier. Because the better the isolation is provided, the higher antenna gain there will be on a service antenna. Particularly, it would be more effective when we provide horizontal isolation. It is clearly seen from Figure 5 and Table 1.

Besides that, we have carried out calculation of tunnel wave propagation based on RF amplifier. In order to provide better isolation, we can increase spacing between a donor antenna and a service antenna, use metal wall or large buildings if possible. In case if a service antenna is not utilized, it would be easier to calculate wave propagation in tunnels using RF amplifier and to provide radio communication network. Because the spacing between a tunnel and a donor antenna would be a good isolation. RF amplifier enables radio communication network in the declines and tunnels. It provides low cost and more reliable services compared to base stations and optical amplifier. Further we need careful and accurate calculation of influence of obstacles on wave propagation in tunnels. It plays an important role in predicting radio wave propagation in tunnels.

References

- [1] Ernesto A. Alcivar, Repeater Amplifier Systems: Principles and Applications, 1994 TX RX Systems Inc. p.1.
- [2] Kamran Arshad, Ferdinand Katsriku, Aboubaker Lasebae, MODELLING OBSTRUCTIONS IN STRAIGHT AND CURVED RECTANGULAR TUNNELS BY FINITE ELEMENT APPROACH, *Journal of ELECTRICAL ENGINEERING*, VOL. 59., NO. 1, 2008, p.9.
- [3] L. K. Bandyopadhyay, P. K. Mishra, Sudhir Kumar and A. Narayan, RADIO FREQUENCY COMMUNICATION SYSTEMS IN UNDERGROUND MINES", p.1.
- [4] Arghavan Emami Forooshani, Shahzad Bashir, David G. Michelson, Senior Member, IEEE, and Sima Noghianian, Senior Member, IEEE, A Survey of Wireless Communications and Propagation Modeling in Underground Mines, 1553-877X/13/\$31.00 © 2013 IEEE, p.1.
- [5] Richard Martelly and Ramakrishna Janaswamy, Propagation in Tunnels Using the Parabolic Equation and the ADI Technique, 1-4244-0878-4/07/\$20.00 ©2007 IEEE, p.45.
- [6] R. Martelly, R. Janaswamy, Propagation Prediction in Rough and Branched Tunnels by the ADI-PE Technique, 978-1-4244-3386-5/09/\$25.00 ©2009 IEEE, p.596.
- [7] Richard Martelly and Ramakrishna Janaswamy, Fellow, IEEE, An ADI-PE Approach for Modeling Radio Transmission Loss in Tunnels, 0018-926X/\$25.00 © 2009 IEEE, p.1759.
- [8] Tuan Nguyen, Choosing the Proper RF Amplifier Based on System Requirements, *WJ Communications, Inc., San Jose, CA*, p.1
- [9] M. O'Droma, N. Mgebrishvili, A. Goacher, LINEARITY AND EFFICIENCY ISSUES IN RF POWER AMPLIFIERS FOR FUTURE BROADBAND WIRELESS ACCESS SYSTEMS, *ECE Dep., University of Limerick, Ireland*, p.1.
- [10] Manuel Yarlequé, RF POWER AMPLIFIERS FOR WIRELESS COMMUNICATIONS, *PhD-thesis, June 2008*, p.v.
- [11] Marco Di Giacomo, Bernard Ducoudret, RF POWER AMPLIFIERS FOR THE SPIRAL 2 DRIVER: REQUIREMENTS AND STATUS, *Proceedings of LINAC08, Victoria, BC, Canada*, p.897.
- [12] S. K. Palit, DESIGN OF WIRELESS COMMUNICATION SENSING NETWORKS FOR TUNNELS, TRAINS AND BUILDINGS, *INTERNATIONAL JOURNAL ON SMART SENSING AND INTELLIGENT SYSTEMS*, VOL. 2, NO. 1, MARCH 2009, p.118.
- [13] Telco Authority, Antenna Placement and Isolation Guideline, March 2015, p.4 and p.14.
- [14] Simon R. Saunders, Alejandro Aragon-Zavala, Antennas and Propagation for Wireless

Communication Systems: *2nd Edition*, (May 7, 2007).pp.315-317

Design of Telemetry System for Low Orbit Satellite Based On Short Message Service of BeiDou III Navigation Satellite System

Suquan Ding

Beijing Space Quest CO., LTD., Room 207, Building B, No. 28, Xijiekouwai Street, Xicheng District, Beijing, China
ddssqq@sina.com

Abstract:

The first two BeiDou III satellites were successfully launched on Nov. 5, 2017. Eight BeiDou III satellites have been launched in Xichang, China. The BeiDou III navigation satellite system is plan to provide basic services to countries along the Belt and Road by launching 18 satellites around 2018, and achieve global coverage by 35 satellites around 2020. In addition to navigation services, the BeiDou III system also provide short message service, which can be used for telemetry of low orbit satellites.

The telemetry system of low orbit satellite is designed based on the short message service of BeiDou III system. The onboard telemetry system consists of short message terminals and antennas. The terminal include power module, serial interface, short message processing module, and power amplifier module. The two-layer patches antenna is designed for the onboard telemetry system. Simulation results show that gain of the antenna is above -3 dBi in the field of 60 degrees. Simulation results also show that time delay of the telemetry data is less than 1 minute. The link budget shows that the link margin is great than 3 dB.

Key words: BeiDou III satellites, short message service, telemetry, short message terminal, two-layer patches antenna

Introduction

After successful constructions of BeiDou I and II navigation satellite system, the goal of China's BeiDou III navigation satellite system is to provide basic services to the countries along the Belt and Road and in neighboring regions by launching 18 satellites around 2018, and to complete the constellation deployment with launching of 35 satellites by 2020 to provide services to global users^[1]. The BeiDou space constellation shall gradually take a transition from BeiDou II to BeiDou III and provides open services for users worldwide.

The first two BeiDou III satellites were successfully launched on Nov. 5, 2017, while the third and fourth satellites launched on Jan. 12, 2018, the fifth and sixth satellites launched on Feb. 12, the seventh and eighth satellites launched on March 30, in Xichang satellite launch center of China.

The space segment of Beidou III system is a hybrid navigation constellation consisting of 3 Geostationary Earth Orbit (GEO) satellites, 3

Inclined Geosynchronous Satellite Orbit (IGSO) satellites and 24 Medium Earth Orbit (MEO) satellites^[2]. According to actual situation, spare satellites may be deployed in orbit. The GEO satellites operate in orbit at an altitude of 35,786 kilometers and are located at 80° E, 110.5° E, and 140° E respectively. The IGSO satellites operate in orbit at an altitude of 35,786 kilometers and an inclination of the orbital planes of 55 degrees with reference to the equatorial plane. The MEO satellites operate in orbit at an altitude of 21,528 kilometers and an inclination of the orbital planes of 55 degrees with reference to the equatorial plane. In comparison with other navigation satellite systems, the BeiDou system operates more satellites in high orbits to offer better anti-shielding capabilities, which is particularly observable in terms of performance in the low-latitude areas. The BeiDou III constellation is shown in Fig. 1 and their sub-satellite track are shown in Fig. 2.

The BeiDou system integrates navigation and communication capabilities for the first time,

and has five major functions: real-time navigation, rapid positioning, precise timing, location reporting and short message communication services. The short message service can send up to 120 Chinese characters which correspond 240 English letters for a single message^[3]. The short message service provide a way for low cost telemetry system of low orbit satellites. The low cost telemetry system can meet the development of commercial satellites which require to reduce cost greatly.

Design of on board Telemetry system for low orbit satellite based on short message service of BeiDou III system

Both BeiDou II and BeiDou III system can provide short message services for users. As the BeiDou II is a regional navigation system while BeiDou III system aims to provide global services, it is natural to use the BeiDou III system to provide global coverage for the satellite whose telemetry based on short message service.

The system diagram of the onboard telemetry system based on the short message service of BeiDou III system is shown in Fig. 3. The onboard telemetry system consists of short message terminals and antennas. The terminal include power module, serial interface, short message processing module, and power amplifier module. The serial interface receives the telemetry data and connects to the short message processing module which converts the telemetry data based on the short message service protocol. The power amplifier amplifies the output signals of the short message processing module and transmits the signal to the antenna. The power module provides appropriate powers for the serial interface, short message processing module and the power amplifier.

The short message service of BeiDou III system work in L band. The antenna for the onboard telemetry system is selected according to the antenna radiation pattern, polarization characteristics and installation considerations. The two-layer patches antenna is designed for the onboard telemetry system.

Simulation results and link budget

Simulation results show that gain of the antenna is above -3 dBi in the field of 60 degrees. The performance of the antenna can meet the requirements of link budget and onboard installation. Simulation results also show that time delay of the telemetry data is less than 1 minute.

The link budgets are computed both for the GEO and MEO satellites. The requirements for the EIRP of short message terminals for BeiDou system is between 3.5 dBW to 19 dBW^[4]. Link budget shows that the link margin is great than 3dB when the EIRP is 6dBW for GEO satellites while the EIRP is 16dBW for MEO satellites.

Conclusions

The onboard telemetry system is designed for low orbit satellites based on the short message services of China's BeiDou III navigation satellite system. As the BeiDou III system aims to provide global services around 2020, it is reasonable to achieve good coverage for telemetry of the user satellites. Simulation results show that the performances of the telemetry system can satisfy the requirements for low orbit satellites. It provides a low cost, space based telemetry solution for commercial low orbit satellites.

References

- [1] China's BeiDou Navigation Satellite System, the State Council Information Office of the People's Republic of China, June 2016
- [2] BeiDou Navigation Satellite System Signal In Space Interface Control Document Open Service Signal B3I (Version 1.0), China Satellite Navigation Office, Feb. 2018
- [3] Development report on BeiDou navigation satellite system (V2.1), China Satellite Navigation Office, Dec. 2012
- [4] General standard of BeiDou navigation satellite system location reporting & short message communications terminal, China National Administration of GNSS and Applications, Aug. 2014

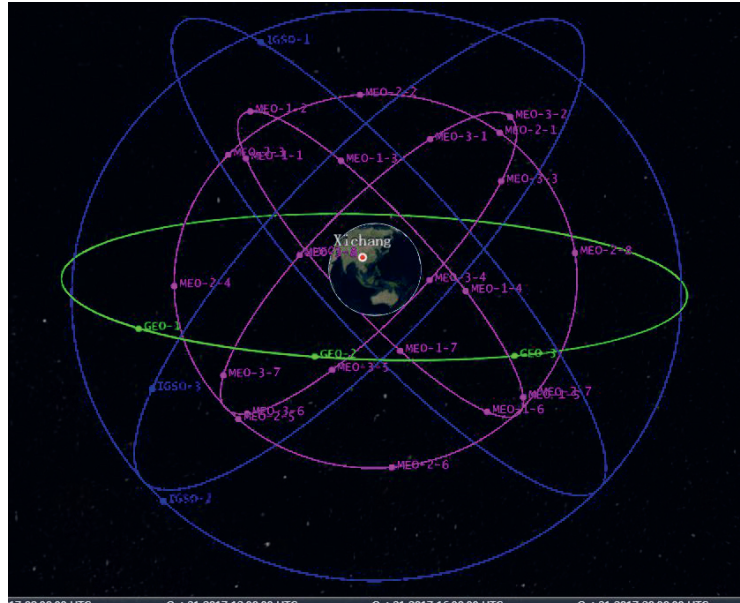


Fig.1.Constellation of BeiDou III navigation satellite system

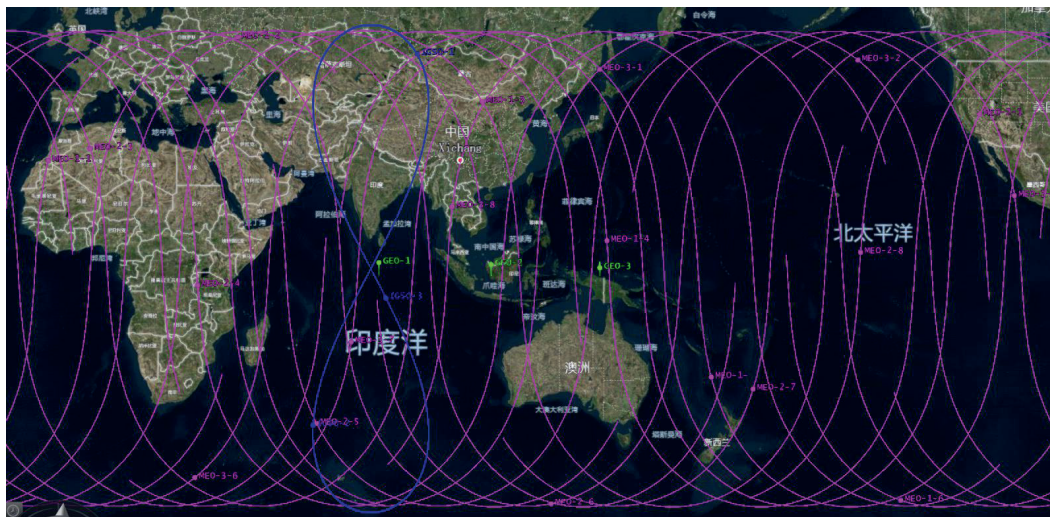


Fig.2.Sub-satellite points of BeiDou III navigation satellite system

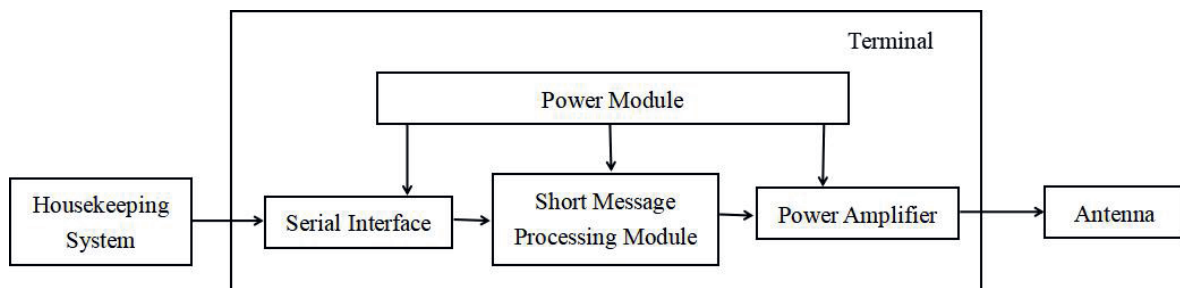


Fig.3.system diagram of the onboard telemetry system

Position Tracking for Outdoor Sport Events with GNSS and LoRa

Juan-Mario Gruber¹, Benjamin Brossi¹
¹ Institute of Embedded Systems (InES)
 Zurich University of Applied Sciences (ZHAW)
 8401 Winterthur, Switzerland
 gruj@zhaw.ch, broi@zhaw.ch

Abstract

Outdoor sport events often require a real time tracking of the position of participants or equipment within a defined area in real time. Global navigation satellite systems (GNSS) determine the position with great accuracy. In addition, using the LoRa radio technology, data is transmitted under optimal conditions over a distance up to 4 km.

Key words: LoRa; GNSS; Real-Time Position Tracking; Low Power; Energy Harvesting

Motivation

Outdoor sport events often need position tracking of participants.. Since the participants are often spread over a wide area, the data must be able to be transmitted over a large distance.



Fig. 1. Position tracking at a sailing regatta

A new system has been developed to transmit real-time position data from a global navigation satellite system (GNSS) live over a long distance to a base station. The base station visualizes the data on a map. By defining a finish line, the crossing of the finish line can be detected. For data transmission the LoRa wireless standard is used. The whole system is to be optimized for low energy consumption, so that it can be operated for several hours by rechargeable batteries or energy harvesting. In summary, the following objectives can be defined:

The system is optimized for low energy consumption, live data from a GNSS is used, the data is transmitted via LoRa, the trackers are inexpensive to produce and the position data is displayed in real time.

Concept

The system tracks the position of up to 255 independent objects in a large-scale area. It consists of multiple position trackers and a central base station (Position Tracker Manager).

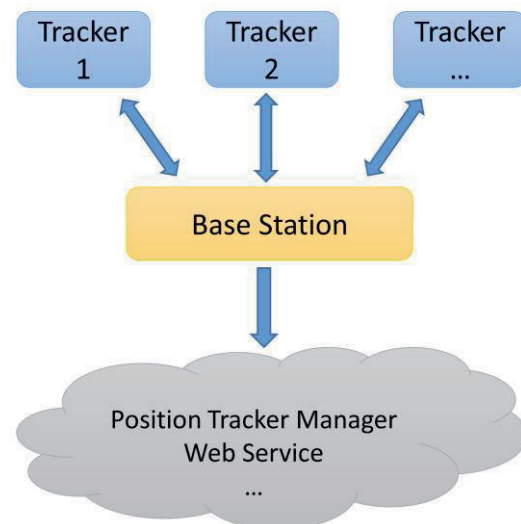


Fig. 2. System block diagram [1]

The system implements a standard LoRa functionality and uses the 868 MHz band. The position trackers are built with latest very low power components and are optimized for low power consumption. This means that they are ready to be powered by energy harvesting.

The system communicates bidirectionally. Thus the base station can configure and control the

trackers at every time. The data package consists of object number, position data and time stamps. This has to be done because only a certain amount of data per hour can be sent through the LoRa band. The system can automatically perform position-based evaluations such as crossing the finish line.

Tracker device

The tracker devices (Fig. 3) use GNSS to determine time and position data send them via LoRa.



Fig. 3. Tracker device prototype

The GNSS module L86-M33 from Quectel is used to determine the time and position. GPS, GLONASS and QZSS can be used with this module. The LoRa module iM880B-L from IMST is used for the data transfer. This is a certified module for wireless communication via the LoRa radio standard. The module features a STM32L151 microcontroller with an ARM Cortex M3 core and a SX1272 LoRa chip from Semtech.

Fig. 4 shows the software state diagram for the tracking device. When switching on the track device, the required peripheral modules of the microcontroller, the LoRa radio and the GNSS module are initialized first. After the initialization, a valid time of the GNSS module is waited for and then the RTC is synchronized to this time. This may take a few minutes, depending on the signal quality of the satellite signals. When the RTC is successfully synchronized, the log and TDMA counters are started. The software changes to idle state.

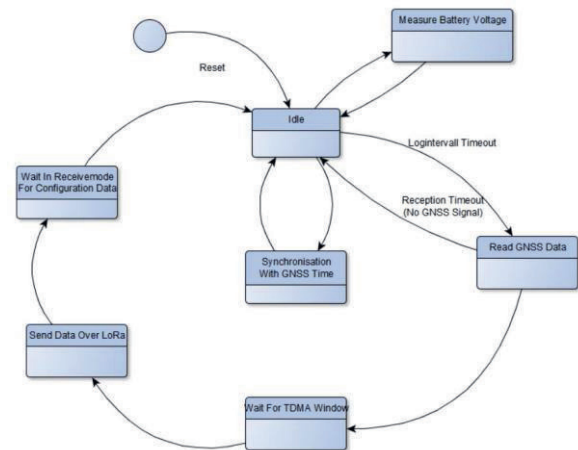


Fig. 4. State diagram tracker device

The software changes to the log state by an event, in which the UART is set to receive the data of the GNSS module. If the data has been successfully received, the data is buffered. The data in the buffer is sent to the base station via LoRa. When transmission is complete, the software switches to receive mode in which it is possible to receive configuration data from the Base Station. The reception time window is 30 milliseconds according to the TDMA protocol. If configuration data is received, the new log interval is set and the log and TDMA counters are restarted.

If a low battery event occurs, the log and TDMA counters are deactivated. An attempt is made to determine a last position within 30 seconds. If successful, this position is transmitted in Low Power Mode. All components are then switched to the low power mode in order to consume as little power as possible. The Tracker Device must then be recharged and restarted with the switch.

For the transmission the smallest possible log interval has to be determined. Also the sending interval for the data packets is to be defined. In order to increase the reliability of data transmission, the current and previous position data are transmitted during each transmission. It turned out that the best results are achieved with 3 seconds log interval and 9 seconds transmission interval.

Base station

The base station uses a Raspberry Pi with a LoRa hat. The Raspberry is running a data logger and provides data for the web interface and for the Position Tracker Manager.

When the base station is turned on, it is in the idle state. Receiving data triggers an interrupt. The system checks whether the data is valid. If this is the case, the new log interval is saved so that it can be configured via LoRa when

receiving data from the corresponding tracker device.

The system communicates bidirectionally, so if data has been received, the software switches to transmit mode in which the new log interval is sent to the tracker device, if a new log interval has to be configured. If there is no new log interval, the software switches to the data processing mode. The data received via LoRa are stored in this module. In this state the times of the positions are reconstructed, assigned to the corresponding tracker device ID and stored. The system then uses the time to check whether the position has already been received. If this is not the case, the position is sent via the UART interface. The software then changes back to the idle state.

PC software (Position Tracker Manager)

The base station is connected to the Position Tracker Manager via a virtual COM interface via USB. The data is transferred to the computer via UART. The Position Tracker Manager evaluates the data and displays the device trackers on an embedded map. In the software, two trackers can be defined as start and end points of the finish line. The software automatically calculates the distance to the finish line and detects when it is crossed. The transferred raw data and the ranking list can be exported from the software into a CSV file for further use.

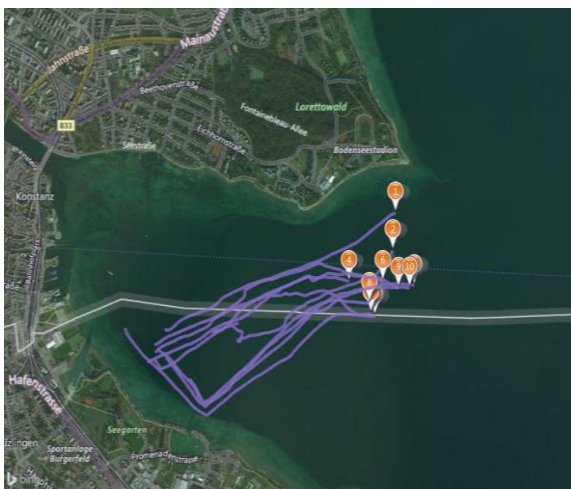


Fig. 5. Life visualization

Energy Consumption

A Li-Ion battery powers the tracker device. Additionally, a charging circuit with integrated buck converter and 3.3 VDC output is used to charge this battery. The charging circuit is supplied by a 5 VDC plug from a power supply unit.

To determine the current consumption of the LoRa module iM880B-L, the following values of

the current consumption are taken from the data sheet [2]:

Tab. 1: Current consumption iM880B-L

State	Current
Idle	5 mA
Transmit	90 mA
Receive	11.22 uA
Low Power Mode RTC ON	1.85 uA
Low Power Mode RTC OFF	0.8 uA

The module can transmit a maximum of 36 seconds per hour at 14 dBm in worst case scenario. This corresponds to the maximum permitted values issued by the Federal Office of Communications (OFCOM). The time for the receiving state is shorter than that of the sending process and in this case is specified at 10 seconds per hour. The remaining time the module is in Low Power Mode RTC ON. These values result in an average current of 0.933 mA.

To calculate the total power consumption of the tracker device, the current consumption of the individual components is added together. Based on the capacity of the battery used, a battery life of 16.6 h can be estimated [1].

Tab. 2: Current consumption tracker device

Item	Current
Quectel L86-M33	26 mA [2]
iM880B-L	0.933 mA
LEDs	2 mA
LTC4080	1.9 mA [3]
Total	30.833 mA
Estimated battery life	$500 \text{ mAh} / 30.1 = 16.6 \text{ h}$

Test Results

Field tests at sailing regattas have shown that the device trackers work reliably. The positions are resolved with an accuracy of a few meters or less and the data transfer works in good conditions up to 3 km. The battery life of over 16 hours is sufficient for most sports and competitions. It should also be possible to operate the device trackers with an outdoor solar panel. The device trackers are ideal for use in open terrain. In built-up areas, both the

accuracy of the position and the maximum transmission distance are reduced.

Conclusion and outlook

It has been proven that it is possible to operate the device trackers with a very small energy budget. The accuracy of position and transmission distance is sufficient for most applications.

In future, the base station will be replaced by a Raspberry Pi with a LoRa hat. The Raspberry Pi should be able to perform the data evaluation without the need of a PC. In addition, a web server and a JavaScript application should replace the position Tracker Manager.

References

- [1] T. Eigenmann, R. Gubler, Echtzeit-Positionstracker mit LoRa (Bachelor Thesis, advisor J. Gruber), Zurich University of Applied Science, 2017
- [2] iM880B Datasheet, v1.3, IMST GmbH Wireless Solutions, 2016
- [3] L86 Hardware Design, Rev. V1.0, Quectel Wireless Solutions, 2014
- [4] LTC4080 Datasheet, Rev C, Linear Technology, 2015

LORA based Biotelemetry System for Large Land Mammals

*Karin Cristine Grande*¹, *Fausto Fernando Hilario Gomes*², *Eduardo Lino Santiago*³, *Pedro Miguel Gewer*⁴, *Victor Hugo Dambrat Bergossi*⁵, *Bertoldo Schneider Jr*⁶
^{1 2 3 4 5 6} Federal University of Technology - Paraná, Brazil
Karincristine13@gmail.com
bertoldo@utfpr.edu.br

Abstract

The best way to understand the environment and its actors is monitoring them. Brazil has the two most biodiversified forests in the planet, the Amazon and the Atlantic forests, a vast field for biotelemetry. Biotelemetry is still made in the most part of the world with obsolete technologies, causing animal stress and demanding a lot of extra field human work. A good biotelemetric system must have quasi-real time, no animal stress, channels for biological, climate, meteorological, and positional data, low power, shorter antenna, and low cost as possible characteristics. It was designed a LORA® technology based animal tracking device, small enough to fit in a collar of a large mammal (e.g., *Panthera onca*), capable to provide real-time position information and other physiological parameters. Tests was made where a volunteer, with the device rode a bicycle through a large urban area and the real time data, collected by a fixed base, were successfully compared with reference GARMIN GPS® device data. Additionally, several Arduino based circuits for physiological, positional and meteorological data measurements can provide extra information for the biotelemetric system proposed. The system is ready to field biological tests and needs improvement and integration with other GPS, GPRS and UHF technologies.

Key words: biodiversified forests, biotelemetric system, *quasi-real* time, animal tracking, LoRa systems.

Introduction

Biotelemetry is a technology system that allows to supervise, locate and collect information from forms of life from a distance using radio communication, satellite, GPS, wireless, and others. The relevant data are geographical coordinates (latitude, longitude, altitude, date and time), physiological parameters (heartbeat rate, body temperature, velocity, etc) [1, 2], climatic data (light, temperature, humidity, pressure), and anyone other for study of species in natural (or not) habitat. Biotelemetry is a remote system, by definition, and can collect data from isolated places on the planet.

An important work was made in Minnesota University with the white-tailed deer (*Odocoileus virginianus*) [3], and it is probably the first animal tracking work ever. Another of the first works observing animals was made in 1960's by Craighead brothers, in Yellowstone

American Park. They studied the behavior of the grey bear (*Ursus arctos horribilis*) in his habitat [4, 5, 6]. For this, a tracking device was created using an UHF transmitter device in a collar placed in the bear. A team of researchers using three or more antennas localized the animal by goniometry triangulation. The hibernation place and period was discovered in that work. After that many others works with animals was made, opening the way for ecology, animal behavior, and animal routes and habitats research.

When an animal is extinct there is an unbalance in its influence area. This unbalance can promote unbalance in the animal and vegetal spheres including serious environment and economic instability for human being. A lot of species are in the extinction risk and many are the reasons for this. Illegal hunt is the principal, followed by human occupation, natural

disasters, sicknesses, among others. In the last years humanity could see many extinctions, like the North white rhinoceros (*Ceratotherium simum cottoni*) declared extinct in march 20, 2018, after the dead of the last male in Kenya. Its correlated black rhinoceros (*Diceros bicornis*) was extinct in 2011. These are examples of animals that were extinct by illegal hunt. Others species suffer with this and bad management and bad policies, like the famous Cecil lion, which was killed by an illegal hunter in its sanctuary, the National park of Hwange. In this case, even using a track system, there was no time to save it, because the no-real-time technology did not enable fast reactions. The International Union for Conservation of Nature (IUCN) is the institution that elaborates the red lists of endangered species, showing to the world the problem created by human beings. Animals are in constant movement, searching for environmental resources, food, protection, and mating. This movement can beneficiate the man and the nature by carrying seeds and pollen, or bad things like illness, like the case of the migratory birds. Tracking these animals generates new understanding to prevent and protect, or stimulate, when necessary [2]. Aiming the preservation and conservation of the species, the better understanding of the world and its relation with the man, as well as the sustainability and economic exploration of the natural resources, many scientists had developed several animal tracking technologies.

The biological research depends on the precision of the data collected [7]. Those technologies can be simple system like monitoring by photo machines or complex ones, like real time monitoring [6]. The most used system are those based on very high frequency (VHF) and Ultra high frequency (UHF) bands. Those systems were less expensive and were largely used [8]. They need two components, the transmitter and the receiver. The transmitter is placed next to the animal, fixed by collars, vest, glue, implants, hook, ring, and the receiver is used by the researcher. Usually, this researcher or team need to stay closed the animal, directing the antenna to the right place. This field action could take several hours, or even days for encounter the signal position [9]. This technology had survived till nowadays by using additional technologies like drones [9], or telephone towers, or internet. Another adaptation was made by the University of Wisconsin-Milwaukee scientists, which put tags with transmitters in sturgeon fishes of sea and rivers, using drones to overfly to keep the sturgeon signals [10]. Some systems has no transmission and use a local memory to store

data. It is the case of greater animals like monkeys and apes, and these animals need to be captured and their collars removed for the scientists to access the data [11].

Another method uses the sound. Echolocation systems use a source of sound or ultrasound and analyses its reflection, locating or measuring animal trajectories. Acoustic localization is different, because in this case only the animal makes sounds. Those sounds when analyzed can identify the species, localize individuals or even count them (object of studies of our Biomedical Engineering research team in UTFPR). Some teams add radio devices to acoustic localization [12]. In a study with killer whales or orcas (*Orcinus orca*), in Oregon, USA, it was possible, by passive acoustic observation, using subaquatic sound sensors, to know the area of activity and migration routes of this animals [13].

When the animal is a bird the system must be slim and weightless [7]. Some scientists use tags with memory and (Global position system) GPS embedded, but it is necessary capture the bird to read the data, causing stress in the animals e arising the cost of the research [16]. The use of the GPS is very important for the animal tracking because its high precision data [14]. The problem is that GPS systems has no transmission devices, so it is common to use the Global system for mobile & General packet radio service (GSM/GPRS) where the telephone services are present. Systems using satellites are very efficient and the great advantage is the global service covering, even over oceans. The Argus service, initiated in 1978, with 12 active satellites over each hemisphere, works like an auxiliary system for animal and ships tracking, and maritime safety [8, 15, 16]. Sometimes there is no Argus satellite over the observed animal, causing a lack of contact which can remain for hours.

The proposed system developed by Biotelemetry team of the Federal University of Technology – Paraná, Curitiba, Brazil, was designed to be a quasi-real time system.

Methods

The developed system has a LORA RN2903 working with a microcontroller PIC18LF45K22-I/PT and a GPS Integrated circuit, like shown in Fig. 1. In Brazil this IC, the same used in Europe, is homologated for 14 dB, differently of the Europe and USA. The program was made with C language and the data is transmitted in ASCII code, for minimize transmission energy. Some additional systems based on Arduino platform can measure temperature, humidity,

velocity, light and physiological parameters (heartbeat rates, oxygen saturation, and internal temperature when an implant could be made), working like parallel and auxiliary sensors.

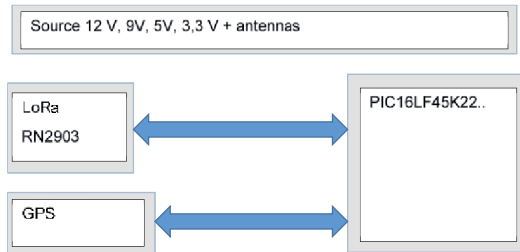


Fig. 1. Block diagram of the tested system. A LoRa RN2903 and an ordinary GPS IC working with a microcontroller PIC16LF45K22-I/P. A battery is used to source the voltages necessary for the circuit and appropriated common antennas for GPS reception and LoRa Transmission.

For testing the device it was focused in demonstrate its capability of transmit the precise position in bad conditions, i.e., near to the end of life of battery conditions, or when the source of energy is almost depleted. Thus, an area of a big urban park was choice to test the system, using a battery with less than 30% of charge. The points was processed using the TrackMaker software version 13.9. The software access the satellite photo of the Google Earth shown in Fig. 2.

Results

The Barigui Park of the Curitiba city in south Brazil was used to test the performance in bad conditions of energy. The mobile part was put in a bicycle basket and a button was pressed to transmit a position. Each position successfully received is marked in Fig. 2 with a circle with a central dot and in Fig. 3 with a diamond. In the same basket, a Garmin GPS reference device model E-trex 30 was programed to keep the way points automatically. The way of the GPS E-trex device is shown in Fig.2 with continuous line.

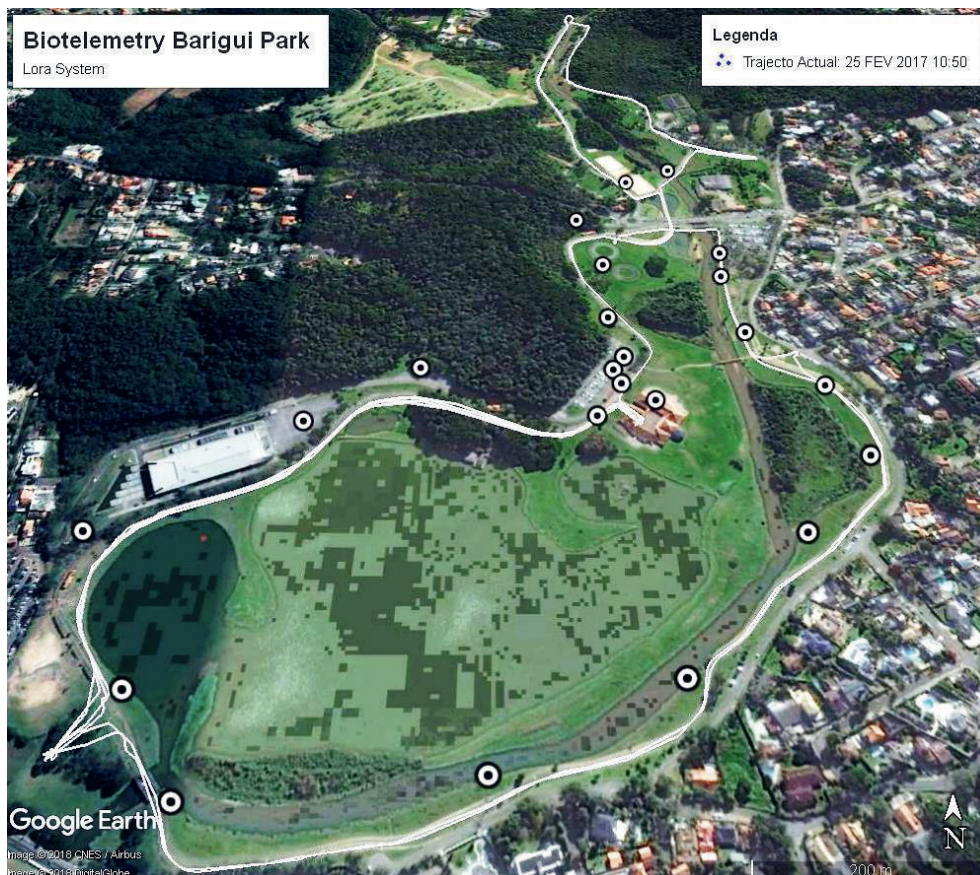


Fig. 2. The continuous line represents the way marked by the GPS E-trex reference device. The circles with a center dot shows the successfully received positions. The photo is a satellite photo, in a non-orthogonal

perspective, of the Barigui park in Curitiba, South Brazil, license of the Google Earth. The software used for integration of these data was the TrackMaker software version 13.9.

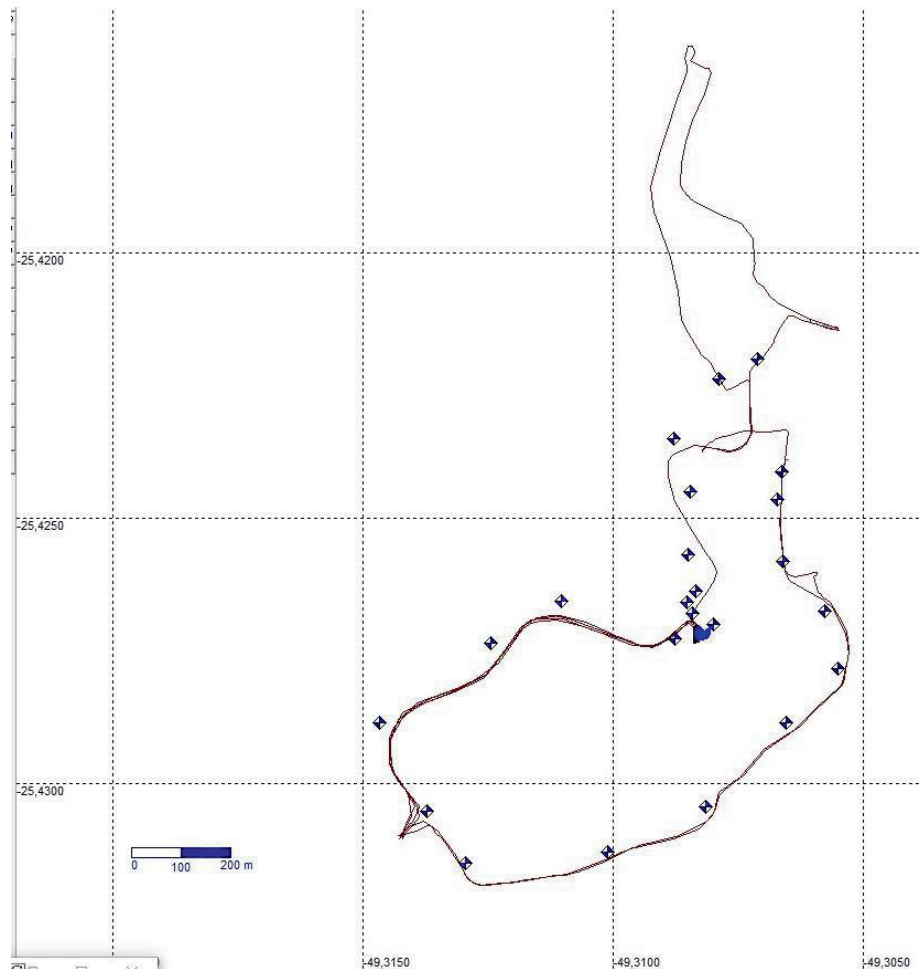


Fig. 3. Image of the TrackMaker software. The continuous line represents the way marked by the GPS E-trex reference device. The diamonds shows the successfully received positions. Orthogonal point of view.

Conclusion and Discussion

It is possible to note the great error, sometimes near 30 m in a relative plain terrain. Although this error is not so big for animal tracking application, it is necessary to consider about its fonts. First of all, there is the low battery problem. Our methodology demanded an almost depleted battery. This can account to imprecision of the points. Besides, points farther than 800 m was not successfully received. In Fig. 2, there would be points in the right upper corner of the figure. This problem is certainly related with battery condition, because tests in plain terrain with full charged battery and the same antennas achieved a distance of 1.8 km in urban area. Other font of error is the datum used in the GPS integrated with the LoRa circuit. Theoretically, the position of a point in the Earth surface depends on the ellipsoid of revolution used to model the curvature of the planet surface. The set of measurements and conditions of this model is called datum in

geodesy and cartography [17]. Datum must be configured for each region of the planet, to enhance accuracy. Generally it is used the WGS84 world standard datum. In Brazil the official datum was changed from the SAD-69 to SIRGAS-2000 in 2005. A little tens of meters of error can be attributed to difference between datums used.

It was used the interchanged ICs NR2903 (American standard) for 915 MHz and the NR2483 replacing the 2904 of the Fig. 1. The frequency used for the data set shown here was the 686 MHz, using the NR2483. The proposed device demonstrated appropriated performance to animal tracking purpose and new experiences are made with other technologies and systems, like gateways, GPRS, UHF repeater, as well as the field work with mammals like the guará wolf (*Chrysocyon brachyurus*) and some kind of wild felines, like the jaguar (*Panthera onca*). The program of the system was enhanced and now is immune to

unsuccessful reception and works full automatically. The redesign seeks very low power consumption and lighter device. The microcontroller can be anyone with I2C and enough analogue and digital entries.

Acknowledgements

The authors would like to thank the support received from the CAPES (Coordination for the Improvement of Higher Level Personnel), the Graduate Program in Electrical and Computer Engineering (CPGEI) and Graduate Program in Biomedical Engineering (PPGEB), both in UTFPR.

References

- [1] V. R. Jain, R. Bagree, A. Kumar & P. Ranjan. wildCENSE: GPS based animal tracking system. In *Intelligent Sensors, Sensor Networks and Information Processing*, 2008. ISSNIP 2008. International Conference. Pp. 617-622. (2008). Doi: 10.1109/ISSNIP.2008.4762058
- [2] R. Kays, M. C. Crofoot, W. Jetz & M. Wikelski. Terrestrial animal tracking as an eye on life and planet. *Science*. V. 348, n° 6240, aaa2478. (2015). Doi: 10.1126/Science.aaa2478
- [3] J. R. Tester, D. W. Warner, & W. W. Cochran. A radio-tracking system for studying movements of deer. *The Journal of Wildlife Management*. Pp. 42-45. (1964). Doi: 0.2307/3797933
- [4] J. J. Craighead, & F. C. Craighead Jr. Grizzly bear-man relationships in Yellowstone National Park. *BioScience*. V. 21 n° 16, pp. 845-857. (1971). Doi: 10.2307/1295811
- [5] F. C. Craighead Jr, & J. J. Craighead. Data on grizzly bear denning activities and behavior obtained by using wildlife telemetry. *Bears: Their Biology and Management*. Pp. 84-106. (1972). Doi: 10.2307/3872573
- [6] C. S. Miller, M. Hebblewhite, J. M. Goodrich & D. G. Miquelle. Review of research methodologies for tigers: telemetry. *Integrative Zoology*. V. 5, n° 4, pp. 378-389. (2010). Doi: 10.1111/j.1749-4877.2010.00216.x
- [7] N. Sobajic, J. Gutierrez, R. Kraemer & M. Krstic. Using wake-up receivers in bird telemetry-Viability study. In *Telecommunication in Modern Satellite, Cable and Broadcasting Services (TELSIKS)*, 11th International Conference on. V. 2, pp. 530-533. (2013). Doi: 10.1109/TELSKS.2013.6704434
- [8] S. Erdogan, T. Shaneyfelt & A. Honma. Integrated Knowledge Base for Environmental Research. *Autonomic and Autonomous Systems and International Conference on Networking and Services ICAS-ICNS 2005. Joint International Conference on. IEEE*. Pp. 54-54. (2005). Doi: 10.1145/1095242.1095267
- [9] G. A. M. Dos Santos, Z. Barnes, E. Lo, B. Ritoper, L. Nishizaki, X. Tejada, A. Ke, H. Lin, C. Schurgers, A. Lin & R. Kastner. Small unmanned aerial vehicle system for wildlife radio collar tracking. In *Mobile Ad Hoc and Sensor Systems (MASS)*, 2014 IEEE 11th International Conference. Pp. 761-766. (2014). Doi: 10.1109/MASS.2014.48
- [10] T. R. Consi, J. R. Patzer, B. Moe, S. A. Bingham, & K. Rockey. An unmanned aerial vehicle for localization of radio-tagged sturgeon: Design and first test results. In *OCEANS'15 MTS/IEEE Washington*. Pp. 1-10. (2015). Doi: 10.23919/OCEANS.2015.7404448
- [11] C. P. Juarez, M. A. Rotundo, W. Berg & E. Fernández-Duque. Costs and benefits of radio-collaring on the behavior, demography, and conservation of owl monkeys (*Aotus azarai*) in Formosa, Argentina. *International Journal of Primatology*. V. 32, n°1, pp. 69-82. (2011). Doi: 10.1007/s10764-010-9437-z
- [12] S. Fregosi, H. Klinck, M. Horning, C. P. Costa, D. Mann, K. Sexton, L. A. Hückstädt, D. K. Mellinger & B. L. Southall. An animal-borne active acoustic tag for minimally invasive behavioral response studies on marine mammals. *Animal Biotelemetry*. V. 4, n°1, pp. 4- 9. (2016). Doi: 10.1186/s40317-016-0101-z
- [13] H. Matsumoto, A. Turpin, J. Haxel, C. Meinig, M. Craig, D. Tagawa, H. Klinck & B. Hanson. A Real-time Acoustic Observing System (RAOS) for killer whales. In *oceans 2016 mts/ieee monterey*. Pp. 1-6. (2016). Doi: 10.1109/OCEANS.2016.7761032
- [14] F. Urbano, F. Cagnacci, C. Calenge, H. Dettki, A. Cameron & M. Neteler. Wildlife tracking data management: a new vision. *Philosophical Transactions of the Royal Society B: Biological Sciences*. V. 365, n°1550, pp. 2177-2185. (2010). Doi: 10.1098/rstb.2010.0081
- [15] R. Lopez, J. P. Malarde, F. Royer & P. Gaspar. Improving Argos doppler location using multiple-model Kalman filtering. *IEEE Transactions on Geoscience and Remote Sensing*. V. 52, n°8, pp. 4744-4755. (2014). Doi: 10.1109/TGRS.2013.2284293
- [16] J. M. Martin, G. W. Swenson & J. T. Bernhard. Methodology for efficiency measurements of electrically small monopoles for animal tracking. *IEEE Antennas and Propagation Magazine*. V. 51, n° 2. Pp. 39-47. (2009). Doi: 10.1109/MAP.2009.5162015
- [17] R. M. Friedmann. Fundamentos de orientação, cartografia e navegação terrestre. *Fundamentos de Orientação, Cartografia e Navegação Terrestre*. Curitiba: UTFPR ed. (2008).

Testing Acquisition of GPS / GNSS Location and Velocity to Improve Safety in Autonomous Driving

Karen von Hünerbein¹, Werner R. Lange¹

¹ Lange-Electronic GmbH, Rudolf-Diesel-Str. 29a, 82216 Gernlinden, kvh@lange-electronic.com

Abstract:

GPS (Global Positioning) and GNSS (Global Navigation Satellite Systems) yield very accurate positioning, velocity and timing, which are crucial for many ADAS (advanced driver assistance systems) and in autonomous driving. 3D locations can be as accurate as a few decimeters, with the help of additional correction methods. In addition a wide range of different sensors, among them optical, LIDAR and RADAR are used to detect obstacles and street marks, GNSS location and trajectory data can be exchanged via wireless data links with other cars (Car2Car) or sent to infrastructure (Car2X), in order to improve early detection of possible accidents, avoid drastic breaking events on the road ahead, traffic jams and detect vehicles around the corner, which are not visible to the driver due to obscuration. This element of telemetry in ADAS and autonomous driving serves to improve safety of all traffic participants and efficiency of driving. In order to guarantee safety of ADAS and autonomous driving, millions of test km need to be driven on different roads in diverse environments. Especially in city centers and mountainous areas, GNSS reception can be impaired by obscuration of signals by buildings, bridges, vegetation and mountains and by signals reflected on even surfaces, called multipath. Furthermore, there are many sources of interference, potentially jamming, spoofing and meaconing GPS/GNSS receivers, especially on motorways and in cities. Testing can become very time consuming and costly, especially when driving all the required kms. Thus, it is more efficient to record the GPS/GNSS and interference signal environment during test drives with advanced record and replay systems, to be able to reproduce the realistic signal environment inside the laboratory, enabling repeatable and realistic tests. Such new record and replay systems are able to record GNSS signals on all frequency bands with a high bandwidth and resolution plus many additional sensors synchronously. In this paper we will present the use cases of GPS/GNSS data in autonomous driving, Car2Car and Car2X, sources of errors and vulnerabilities for GPS/GNSS and appropriate test systems to allow for repeatable and realistic tests in the laboratory. The aim is to decrease time and money spent on testing and to improve the safety of driver assistance systems and autonomous driving.

Key words: GPS/GNSS locations, errors and vulnerabilities, safety in autonomous driving, record and replay systems, interference signal environment

Introduction

In recent years the importance of GPS/GNSS positioning and navigation has grown dramatically in civilian applications, due to the world-wide availability and high accuracy of positions and velocity calculated from GPS/GNSS signals, which can be obtained almost anywhere under the open sky. The positioning, navigation and timing functions (PNT) are widely used, especially in mobile phones and in-car navigation systems, to show the way and the current location. In the last few years, more and more research and development effort have been invested into Car2Car (V2V), Vehicle to Infrastructure (V2X),

Driver assistance functionality (ADAS) applications, and more recently into fully autonomous driving. PNT provided by Global Navigation Satellite Systems (GNSS) is key for most of these applications and technologies [1,2,4,5].

Car to Car communication (C2C or V2V), is a technology under development, employing the IEEE 802.11p standard at 5.9 GHz in Europe, for the exchange of messages in between cars, about location, heading, trajectory, special events of the current vehicle, which are being broadcast to all vehicles in the vicinity. The goal of this technology is to increase awareness and safety for each vehicle on the road by allowing to foresee dangerous situations and issue alerts

to the driver in case of incidences, e.g. on a motorway, a car fully breaking on the road ahead that may be concealed by bigger transport lorries. Other goals of V2V are to enhance traffic flow, eco-driving, efficiency and gaming/entertainment. One important component of the messages is the location calculated from GPS/GNSS signals. Accuracy needs to be very high in the 1-2 m range in order to be able to distinguish on which lane a car is moving, breaking or static. [2,3]

A similar technology concept is vehicle to Infrastructure communication (V2I) and vice versa, e.g. informing drivers ahead of time about obstacles, red traffic lights and other vehicles or pedestrians approaching sideways on a crossing, possibly invisible by buildings and vegetation. Again, accuracy of location needs to be high for the prediction of dangerous situation, and for distinguishing between critical and non-critical events [2,3]. Both types of communication represent special, challenging cases of telemetry by using remotely acquired and transferred data to improve driver awareness, traffic flow and traffic safety.

ADAS, Advanced Driver Assistance Systems, are electronic applications in cars to assist the driver in all sorts of driving situations, some of them potentially dangerous, where additional information can be helpful, e.g. blind spot monitoring, lane departure warning, Collision Avoidance System, Parking Assistant, wrong way driving warning [4]. These systems can operate stand-alone in the car and are based on an array of different sensors, such as cameras, LiDAR (light detection and ranging) [7], automotive RADARs, ultrasound, odometers, accelerometer, gyroscopes, and GNSS. Cameras provide an all round view to the driver. LiDAR, ultrasound sensors and RADARs serve to measure distances to obstacles and objects around the vehicle. Wheel speed sensors, called odometers, deliver information about speed, and dangerous states, such as blocked wheels, or wheels, which lost their grip. Accelerometers provide accelerations, speed changes in different directions, and gyroscopes indicate heading and heading changes. The latter two are also called inertial sensors used for inertial navigation [5,6,12]. In order to integrate all these different type of sensor information, intelligent sensor fusion algorithms have been developed with the challenge of correctly interpreting the measurement results of various sensors and to deal with conflicting information [8].

In autonomous driving a great variety of different sensors is employed, for gaining maximum information. GNSS positioning is a

crucial source of location information with extremely demanding requirements, such as non-stop availability (24h/7d a week), very high accuracy of location, and fail-safe-operation. All of these conditions need to be fulfilled even in challenging environments to ensure the safety of passengers, other vehicles, pedestrians, cyclists and infrastructure. Many environments pose particular challenges to GPS/GNSS signal reception, as these signals are transmitted by moving satellites, which are distributed across the visible sky. Some satellites are located at a low elevation, so that their GPS/GNSS Signals can be attenuated or blocked by vegetation, buildings and mountains. In certain environments a lot of multipath is present, caused by reflections of GPS/GNSS signals by even surfaces such as glass, metallic and water surfaces. In this case, there are several signals for the same satellite arriving from various directions, they are weaker in signal power than the LOS signals, travel longer non-direct paths, and they contain exactly the same information in the navigation message as the other signals [9]. In this case, the receiver algorithm has to decide, which of the multiple signals from each satellite it should use for the PNT fix.

GPS/GNSS signals are vulnerable, because they arrive at the surface of the Earth with a very low signal power of -120 to -130 dBm, so low that it is usually buried inside the thermal noise. Thus GNSS signals are easy to interfere with and vulnerable to different types of effects, including atmospheric disturbances, multipath and malicious spoofing. Interfering radio signals in the L-band can be emitted and generated unintentionally, e.g. by defect devices or intermodulation effects of several RF transmitters, or different transmitter antennas installed on top of roofs of large sea vessels for a variety purposes, e.g. for mobile satellite communication and RADAR. They can also be emitted with the intention of jamming or spoofing, which is providing false signals to the receiver, providing misleading information [9, 20,21]. All these disruptive effects and degradations need to be considered, mitigated and verified at all development stages by thorough testing.

To increase accuracy, availability and integrity, GNSS correction data are used and additional sensors are integrated into the onboard navigation system. Much higher accuracy can be achieved by a method called Real Time Kinematic (RTK), using carrier phase measurements, where a mobile reference station transmits GPS/GNSS correction data to a rover receiver over the air. It is based on "carrier-based ranging and provides ranges and

positions that are orders of magnitude more precise than those available through code-based positioning.” [19] The horizontal position accuracy can be improved to about 2-3 cm in real-time. Correction data are also provided by national CORS Networks (Continuously Operating Reference Station), with stationary reference stations, which continuously monitor all GNSS satellites and gather integrity information and pseudorange corrections for their specific location. These data can lead to a significant improvement of the accuracy and integrity of the position fixes up to 200 km from the reference station. “Rovers determine their position using algorithms that incorporate ambiguity resolution and differential correction. Like DGNS (Differential GNSS), the position accuracy achievable by the rover depends on, among other things, its distance from the base station (referred to as the “baseline”) and the accuracy of the differential corrections. Corrections are as accurate as the known location of the base station and the quality of the base station’s satellite observations. Site selection is important for minimizing environmental effects such as interference and multipath, as is the quality of the base station and rover receivers and antennas.” [19]. RTK is a method for real-time correction. There are also methods for post-processing data to improve accuracy, if it is not needed in the field, such as postprocessed kinematic, allowing for more convenient calculation in the lab. However, in autonomous driving highly accurate positioning is required in real-time during the drive so that post-processing is not an option.

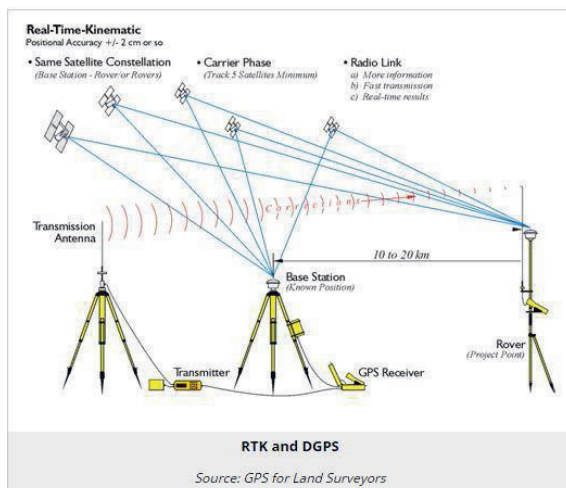


Fig. 1. Overview Real Time Kinematic [13]

Another type of correction data are broadcasts from special geostationary satellites. These systems are called Satellite Based Augmentation Systems (SBAS). Some provide data in the public domain free of charge [e.g. EGNOS

the European Geostationary Overlay Service, 16], others are commercial systems, e.g. Starfire or Omnistar [17,18]. Correction data of the publicly available SBAS can improve accuracy to 1-3 m, which is sufficient for some ADAS, but not for autonomous driving. The commercial SBAS systems are able to provide accuracy in the sub-dm range, down to 5 cm [22].

Higher availability, accuracy and integrity of positioning can be achieved by a combination of GPS/GNSS with inertial measurements units (IMU), containing different inertial navigation sensors (INS). “Inertial navigation is a self-contained navigation technique in which measurements provided by accelerometers and gyroscopes are used to track the position and orientation of an object relative to a known starting point, orientation and velocity. Inertial measurement units (IMUs) typically contain three orthogonal ... gyroscopes and three orthogonal accelerometers, measuring angular velocity and linear acceleration respectively. By processing signals from these devices it is possible to track the position and orientation of a device.” [citation from 10]. “GPS/Inertial systems combine the interference mitigation, high bandwidth and low noise benefits of inertial measurements with the long-term stability of GPS into a self-calibrating, higher accuracy blended navigation solution” [11]. Inertial systems alone are not able to maintain a stable accurate position fix over a long-time, as they drift too much. They are well able to bridge short gaps caused by GPS/GNSS outages lasting several seconds to a few minutes. Thus INS provides greater continuity and full availability, while GPS/GNSS provides stability of PNT accuracy. Both systems complement each other with their respective strengths [5, 6, 11, 12]. According to automotive experts, GNSS/INS Positioning, Navigation and Timing will be a major building block for highly automated driving [1].

Importance of Testing

Because of the GPS/GNSS vulnerabilities, and in order to check the performance of the integrated sensor system and sensor fusion algorithms, thorough testing of all components and of the complete autonomous vehicle with all integrated sensors and algorithms is required. Test of components and sub-systems can be carried out in the laboratory. To verify safety, the fully integrated autonomous vehicle must successfully complete millions of km driven on real roads around all sorts of different environments: urban, sub-urban, mountainous area, motor-ways, small streets, and many more.

In order to maintain correct navigation and timing, it is crucial that the receiver algorithm has functions to detect and cope with dangerous and unexpected events. These functions need to be tested, too, to guarantee continued operation, even in case of external error sources. When improving software algorithms or installing other countermeasures, systems need to be retested to verify and quantify and the improvement.

The easiest way of testing is a live sky test with live GNSS signals outside buildings. Advantages are immediate availability and realistic signal environment. Disadvantages are high time consumption, high cost and lack of repeatability, because all GNSS signals vary a lot with time, as the GNSS satellites are moving fast in their orbits. They also vary with weather, 3D terrain and different disruptive factors, as described above. Thus the tests under live-sky conditions can only convey part of the picture and do not allow for controlled and repeatable testing.

More systematic testing can be performed in the laboratory. A lot more tests can be run in the laboratory than in the field, improving the results and giving a chance to fully assess the strengths and weaknesses of the GNSS based positioning and navigation [26].

Testing in the lab can save a lot of time and will improve the overall reliability and functionality of the GNSS based navigation unit and answer questions like: How quickly does the navigation unit recover after coming out of a tunnel? How well does it hold on to a signal, e.g. near buildings and under significant tree cover? How robust is the PNT solution when stressed by real-world threats? How accurate is the PNT solution in different types of environments? [26].

Record and Replay of GNSS signals

Record and Replay of GNSS signals has been established as a valuable test method, with signals being received and captured in a static or dynamic measurement like a test drive. The signals are then converted to IF and stored on a hard disk, and later replayed in the lab after up-conversion from the IF back to the RF signals, faithfully reproducing any propagation effects. [9, 15].

The advantages are that the recordings can fully capture real signal environments with complex errors including obscuration and multiple reflections, called multipath, real-world fades and in-band interference. Signals from multiple test drives at difficult locations, with a known GPS/GNSS reception problem, can be captured and used for tests, with no need to revisit the real location. The replay tests are

fully repeatable, as the same signal environment is reproduced during each replay, at the same time and date [9,14, 15].

On the other hand there is virtually no control over the signals and the error conditions in the recording, except that some attenuation can be applied. Contrary to GNSS simulators, time and date of the test drive cannot be changed, nor the amount of satellite signals present in the recording, nor the signal parameters and the navigation message.

For every new location or date a new test recording is required. The recorded error conditions captured in the recording are usually unknown, unless the user has additional information about special conditions from external sources, like space weather reports. Test drives and recordings are easy and cost effective for stationary and land vehicle based receiver and allow Software and Hardware testing including system trials, algorithm studies and iterative algorithm development, interference and jamming recording and monitoring.



Fig. 2. Front view of Record and Replay System

One example of a record and replay system is the Spirent GSS6450 [14,24,25]. The record / replay system (RPS) GSS6450 is a portable unit with a weight of 2.2 kg capable of recording 4 GNSS bands simultaneously at all L-band frequencies, including IRNSS (Indian Regional Navigation Satellite System) L5, SBAS L1 and L5, Inmarsat based correction services, QZSS (Quasi Zenith Satellite System) L1, L5, L6, Beidou B1, B2, B3, GLONASS L1,L2,L3 and Galileo E6. In short it will record all major GNSS bands via 1 RF input port and many SBAS and regional service signals. The latest version of the GSS6450 is capable of recording signals in the GNSS, WIFI and LTE band, simultaneously, via 3 RF input ports, the second RF port records 690-2400 MHz and the third one records 100 MHz – 6 GHz for WiFi bands at 2.4 GHz and 5.0 GHz [24]. During recording, the RF signals, are downconverted, digitized and stored at IF. During playback, the IF signal is recreated and then up-converted to RF at the relevant GNSS frequency using the same built-in oven controlled local oscillator (OCXO) as used to record the data for minimum phase

noise.” [9,14]. RF signals can be recorded at 4, 8 or 16 bit for quantization and at 10, 30, 50, 60 MHz and 80 MHz bandwidth [24]. There are throughput limitations at 8 and 16 bits together with the 50, 60 and 80 MHz bandwidth, limiting the amount of channels that can be recorded simultaneously to 1-2 [14]. The record and replay system contains an OCXO for record and playback for high frequency stability. It is very small with a size of 21*20 cm, with a large storage capacity of 2-4 TB internal and external SSD [14]. USB 3.0 is supported allowing data transfer to or from external drives [24].

The major advantage of this record and replay system is the 16 bit depth for quantization of I and Q each, allowing to capture GNSS signals even at high jamming powers. Most other portable record and replay systems have a 2 bit quantization, which is suitable for general GNSS signals with a 12 dB dynamic range. “However it will not be good under jamming / interference scenarios as the interference ‘soaks’ up the dynamic range reducing GNSS resolution as described” and it is also “limited in the ability to capture Multipath and Fading effects for Real environments where small signal perturbations cannot be captured by the 4 levels of 2 bit sampling... 16 bit sampling overcomes this by increasing the 4 levels to 65536 levels.” [personal communication by Julian Kemp]. Greater bit depth allows better resolution of GNSS signals and greatly increases this dynamic range both for jamming and for multipath and fading effects, to 21 dB at 4 bit I and 4 bit Q, to 45 dB at 8 bit I and 8 bit Q and to 80 dB at 16 bit I and 16 bit Q.

Sampling rates are 10.23, 30.69 or 51.15 MHz, synchronous recording rate for external data is 300 kbps at 10.23 MHz, 900 kbps at 30.69 MHz and 1500 kbps at 51.15 MHz, asynchronous recording rate for external data is 4800-115200 baud. [14] The reference oscillator is an OCXO with a frequency of 10.23 MHz, to allow direct generation of the wanted GNSS frequencies. There are two RF outputs: one normal RF output with a standard GNSS RF signal strength (nominal -130 dBm for GPS L1), and one high power output at the back of the test system with around -80 dBm nominal [14]. In addition there is a 10 MHz Reference IN port, allowing to input a source of precise timing. The better the timing, the better the accuracy of the GNSS Position, Navigation and timing solution.

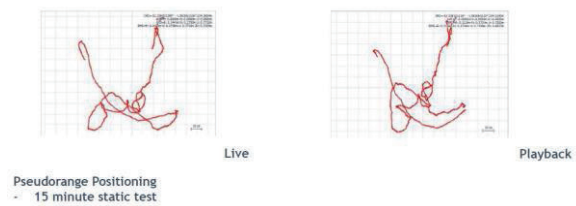


Fig. 3. Comparison of pseudorange position fixes with live sky signals and replayed GNSS signals measured with a Novatel GNSS receiver at 10 Hz update rate. Each grid cell's width and height corresponds to 10 cm [25]

The system contains two types of attenuators for replay: single channel attenuators with a total attenuation of 9 dB in 0.5 dB steps and a general attenuator for all channels with a total attenuation of 31 dB in 1 dB steps [9,14].

“The GSS6450 is fully integrated and no PC or external drives are required” [14]. It can be controlled from the front panel, over WiFi, from the webserver or via scripts. “Scripts allow inclusion of automatic test routines” [14]. Major actions and settings are available from the front panel with a LCD touch screen. Remote control is possible via a VNC (Virtual Network Computing) server and HTTP (Hypertext Transfer Protocol) messages. VNC is a software displaying the screen display of a remote computer on a local computer. This record/replay system can be controlled by devices like ipad, iphone, tablet and Laptop via a WiFi interface.” [14]. Additional control options are inclusion of event markers in the recorded file and the option to start replay at any point in the file.

Two units can be joined together to run in a master/slave configuration and thus can record/playback 8 GNSS frequencies synchronously.

External data can be recorded synchronously and asynchronously. The wide range of external data sources includes: audio, CAN (Controller Area Network) bus data, timing pulses, NMEA (National Marine Electronics Association) data, IMU (Inertial Measurement Units) and other sensors. Up to 8 synchronous inputs can be stored, that is two per recorded GNSS frequency [9,14]. Synchronous recording of external data, such as CAN bus data and IMU data, is possible as serial datastreams. Such data are stored inside the GNSS file with GNSS raw data, and can be replayed synchronously, but not retrieved separately. In addition, recording of 4 different video streams parallel to GNSS signals is possible via webcams, and the video signals can be replayed within 0.5 sec of the GNSS signals,

with a potential drift rate of 0.25 seconds per hour. [14]

External data can be also stored asynchronously, via the serial port, resulting in additional files, stored separately from the GNSS signal data, which can be easily edited and modified, e.g. NMEA data or WiFi data. Timestamps can be added to the serial data [14]. In the new model there is an integrated High Speed CAN bus interface for 2 highspeed CAN interface devices, eliminating the need for an external box. It provides physical recording of the signals without acknowledgements and bus arbitration. [24].

In addition, the RPS GSS6450 contains an L1 only GPS/GNSS receiver, integrated together with an internal LINUX controller, allowing to cross check visible satellites and carrier to noise levels. The internal GSS receiver uses GPS and Galileo L1 signals with either Beidou L1 signals or GLONASS L1 signals and is able to record NMEA and display C/No levels on the front panel display [14].

The GSS6450 can be used for testing of highly accurate PNT: a) by recording any corrections b) by using 2 RPS units, one as a rover and one as a base station. The RPS unit serving as basestation can replay the GNSS signals to a high quality geodetic GNSS receiver, which calculates the corrections and transmits the correction data to the rover. For this procedure carrier phase positioning is used, which relies on high quality carrier phase measurements. In two test campaigns it was shown that RPS units provide high quality carrier phase observations, and can be used for RTK and post processing carrier phase purposes [25, 27].

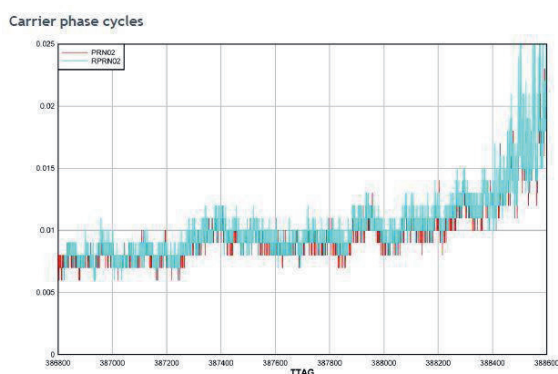


Fig. 4. Comparison of phase noise measurements of live signals (red) and recorded and replayed signals (blue) Plot for GPS SV02 measured with a Novatel receiver, parameter ADRStd on y-axis from 0-0.025 [25]

Advantages for autonomous driving:

As described above, a multitude of sensors is employed in autonomous driving, in order to

ensure comprehensive awareness of the environment. This record and replay test system, allows to record signals of many different key sensors in parallel, synchronously with the GPS/GNSS signals, and replay them repeatedly in the laboratory.

The advantages are that the recordings can fully capture real signal environments with complex errors including obscuration and multiple reflections, called multipath, real-world fades and in-band interference. Signals from multiple test drives at difficult locations, with a known GPS/GNSS reception problem, can be captured and used for tests, with no need to revisit the real location. The replay tests are fully repeatable, as the same signal environment is reproduced during each replay, at the same time and date.

Benefits

- Recording of all GNSS bands with a high bandwidth in combination with inertial sensors
- All in-band signal effects, external factors, and interference signals are captured like multipath, obscuration, atmospheric delays, interference signals
- Synchronous recording of external sensors and units, e.g. IMUs, CAN bus data [14]
- Highly synchronous replay of synchronously recorded data
- Additional data can be sampled via serial port and stored internally
- Video and audio data
- Connection of two RPS units for recording even more frequencies and sensors in parallel
- Internal GPS receiver records NMEA data for comparison, with laboratory results
- Full repeatability
- High dynamic range, due to high bit depth of digitization
- High quality of signals, low phase noise
- Portability, relatively low power consumption, so that it can be run on a car battery without exhausting it, as observed in test drives by TU Braunschweig.

Drawbacks

- No control over GNSS signals: signals cannot be modified, only attenuated
- Error effects are uncontrolled and unknown – except that it is possible to set event markers (e.g. passage through a tunnel or deep valley) and to cross check the data with a video

stream, so that external structures can be seen.

- Throughput limitations at high digitization bit depth, when combined with high bandwidth
- Large recorded data volume
- Small losses in signal power due to digitization

Recording the GNSS signals together with the external sensors takes a lot of storage space, so that recording time is fairly limited when using the internal SSD only and when recording 3 or 4 frequencies of GNSS signals simultaneously with a bandwidth of 30 or 50 MHz each. This limitation can be mitigated by the option to use 2 SSDs with 2 TB each and by the possibility to attach a 8 TB external memory. However, attaching external memory makes the setup more bulky and less easy to handle during a test drive [23].

There is a certain loss in GNSS signal strength due to digitization. When 2 bits are chosen for digitization 2 bits for I and Q component of each frequency, this results in a 1.5 dB loss of signal strength overall. This loss is much smaller, when recording with 8 or 16 bit digitization. In addition loss can be compensated for by replaying the GNSS signals with +10 dB or +20 dB amplification. Alternatively, it is possible to switch on an AGC compensation to replay the signal within 3 dB of the original signal level. [24].

Examples of Test Use Cases:

- Interference and Jamming
- GPS/INS sensor fusion
- Algorithm proving
- Multipath

References

- [1] M. Baus, Safe GNSS/Inertial Positioning for Highly Automated Driving. Presentation. Munich Satellite Navigation Summit (2018)
- [2] Car2Car Consortium, The Car-2-Car Communication Consortium Roadmaps beyond Day-1. Presentation. (2016) Retrieved from <https://www.car-2-car.org/index.php?id=214>
- [3] VW press release: https://www.volkswagen-media-services.com/en/detailpage/-/detail/With-the-aim-of-increasing-safety-in-road-traffic-Volkswagen-will-enable-vehicles-to-communicate-with-each-other-as-from-2019/view/5234247/7a5bbec13158edd433c6630f5ac445da?p_auth=I98AdbHg, 28th June, 2017

- Sensitivity
- Genuine Equatorial Scintillation
- Testing for BeiDou-2 B1 and GPS, GLONASS, Galileo [25]

Conclusions

In this paper we have described the crucial role of GNSS positioning and navigation for Car2Car, Advanced Driver Assistance Systems and autonomous driving. Multisensor systems and GNSS correction data are necessary to achieve the stringent requirements for safety, accuracy and reliability. In a navigation unit for autonomous driving, a major building block will be a combination of GNSS and inertial sensors (INS). GNSS signals are vulnerable and there are many different error sources, degrading or even preventing GNSS signal reception. Thus, thorough testing is required. Drive tests are necessary, but time-consuming and not repeatable. A GNSS Record and Replay System is capable of recording and replaying signals from all GNSS bands with a high signal quality and low phase noise, including all in-band error effects on the GNSS signals such as interference, multipath and atmospheric effects. Additional signals, e.g. inertial sensor data, can be recorded and replayed synchronously. This allows repeatable testing in the laboratory with different sensors and can save a lot of test drives speeding up development and verification.

Acknowledgements

We would like to thank Dave Belton, INS, for permission to use figures 3 and 4, Jan van Sickle for permission to use figure 1, Ali Soliman and Romain Zimmermann, Spirent, for valuable advice.

- [4] L. Junge, FAMOS Galileo for Future Automotive Systems. Conference AAET2012, 13th Braunschweiger Symposium, 8th-9th Feb 2012 Retrieved from http://www.dlr.de/rd/Portaldata/28/Resources/dokumente/rn/satnav/4.GalKonf05_Junge.pdf
- [5] M. Gäb, Ein Beitrag zur Stützung eines Software GNSS Empfängers mit MEMS-Inertialsensoren. PhD Thesis, May 2016, Institut of Navigation of the University Stuttgart (2016)
- [6] G. Falco, M. Pini, G. Marucco, Loose and Tight GNSS/INS Integrations: Comparison of Performance Assessed in Real Urban Scenarios. Sensors (2017), 17, 255; doi:10.3390/s17020255
- [7] Y. Gao, S. Liu, M. Atia, A. Noureldin, INS/GPS/LiDAR Integrated Navigation System for Urban and Indoor Environments Using Hybrid Scan Matching Algorithm. Sensors (2015), 15, 23286–23306; doi: 10.3390/s150923286.

- [8] B. Reuper, M. Becker, S. Leinen, Performance Assessment of Automotive Localization Algorithms via Metrics on a Modular Level. International Symposium on Certification of GNSS Systems & Services, 05-06 July 2017, Darmstadt, Germany (2017)
- [9] K. v. Huenerbein, W. Lange, Monitoring of the interference environment on large vehicles with a network of highly accurate record and replay systems synchronised by a very precise timing unit, European Navigation Conference, Lausanne, Switzerland, 9th -12th May, 2017
- [10] Retrieved from https://en.wikipedia.org/wiki/Inertial_navigation_system
- [11] N. Fedora, C. Ford, P. Boulton, A Versatile Solution for Testing GPS/Inertial Navigation Systems, Proceedings of the 21st International Technical Meeting of the Satellite Division of The Institute of Navigation, September 16 - 19, 2008, Savannah International Convention Center: 1227 – 1236 (2008)
- [12] A.D. King. "Inertial Navigation – Forty Years of Evolution" (PDF). GEC Review. General Electric Company plc. 13 (3): 140–149 (1998). Retrieved from: http://www.imar-navigation.de/downloads/papers/inertial_navigation_introduction.pdf
- [13] Jan Van Sickle, GPS for Land Surveyors. Book. Taylor and Francis Group. (2008) Figure 1 retrieved from: <https://www.e-education.psu.edu/geog862/node/1828>
- [14] Spirent Communications GSS6450 Multi-Frequency Record&Playback System. MS3098 Datasheet with Product Specification. Issue 2-03, (2018)
- [15] S. Hickling, T. Hadrell T, "Recording and Replay of GNSS RF Signals for Multiple Constellations and Frequency Band" Proc. of ION Conference, Nashville, TN; (2013)
- [16] U. Celestino et al. "Expanding EGNOS Horizons in North Africa and the Middle East", Inside GNSS March/April 2015, vol. 10(2), pp. 44-52; (2015)
- [17] T. Sharpe, R Hatch, F. Nelson. "John Deere's Starfire System: WADGPS for Precision Agriculture", (2006) Retrieved from: <https://web.archive.org/web/20060711194114/http://www.navcomtech.com/docs/StarFireSystem.pdf>
- [18] <http://www.omnistar.com/>
- [19] Novatel: <https://www.novatel.com/an-introduction-to-gnss/chapter-5-resolving-errors/real-time-kinematic-rtk/>
- [20] K. Hünerbein, W. Lange. Real Life Evidence for Spoofing and Jamming of GNSS Receivers, Conf. Proc. of CerGal, DGON Conference, Darmstadt, Germany, 7th-8th July, 2015.
- [21] M. Stanisak, K. Hünerbein K, U. Bestmann, W. Lange, "Measured GNSS Jamming Events at German Motorways", Proc. of POSNAV ITS, DGON Conference, Berlin, Germany, 5th-6th July, 2016.
- [22] Spirent Communications, Testing Multi-Frequency, Survey-Grade GNSS Receivers. Case Study (2014)
- [23] K. Huenerbein, W. Lange (2015) Multi-Sensor vehicle testing: Recording Inertial Sensors via CAN bus in Combination with Recorded GNSS RF signals. DGON Conference Proceedings: Inertial Sensors and Systems, 22th-23th Sept 2015, Karlsruhe.
- [24] Spirent Communications, GSS6450 - 3RF- V3 SW Improvement - Automotive Focus. Presentation, Issue 1.00 (2018).
- [25] Spirent Communications, GSS6450 Performance Analysis Summary. Presentation, (2018).
- [26] Spirent Communications. How to construct a GPS/GNSS Test Plan. A guide for engineers integrating GPS/GNSS capabilities into new devices. Whitepaper (2016).
- [27] C. Fuente, "GSS6425 Multi-Frequency Record\playback - 50MHz RTK Results", Presentation (2016).

MIL-STD-1553B and it's potential for the future

*Helmut Plankl
Airbus Defence and Space
Rechliner Strasse
85077 Manching, Germany
helmut.plankl@airbus.com*

Abstract:

MIL-STD-1553B (MILBUS) as a network standard for military systems – with a data rate of 1 Mbps – comes across as (and is) a little out-dated, but is still well-known for its reliability, safety and the strong determinism of a real time bus protocol. The strong electromagnetic immunity of MILBUS has given rise to a number of new applications for military and civil programmes, as well as some lightweight applications with unshielded cables.

But the future will lead to higher speeds and we have made several efforts to implement the excellent MILBUS command/response protocol in modern and faster physical networks. The data rate capability for EFABUS / STANAG 3910 was raised by means of a parallel network. The result was the optical EFABUS Express. MIL-STD-1760E for stores defines a switched electrical Fibre Channel interface for mapping MIL-STD-1553 messages and for 1 Gbps mass data transfers. A fibre optic interface will follow. Another concept is the implementation of a collision- and delay-free protocol at Ethernet level.

Another option, especially for upgrade programmes, is E1553 / STANAG 7221, whereby available MILBUS cables are retained for a Broadband Real-Time Data Bus (B-RTDB) with Multi-Carrier Waveform (MCW) protocol for higher data rates.

Key words: Data Bus, MIL-STD-1553B, MIL-STD-1760, Fibre Channel, Fibre Optical

MIL-STD-1553B (MILBUS) introduction

Conceptual studies for the MIL-STD-1553 started in the 70s for the F-16 weapon bus. The idea was a robust and electromagnetic immune command/response data bus that can work in harsh environments to replace dedicated analogue or discrete connections between multiple avionics equipment within a military aircraft (A/C).

MIL-STD-1553B is now an international networking standard for the integration on military platforms and also for some applications on civil programmes. The revision of MIL-STD-1553B + Notice 2 [1] has been adopted by NATO as STANAG 3838.

The key element is a Bus Controller (BC) and various subsystems that function as Remote Terminals (RT). A Bus Monitor (BM) function is optional. Information data transfers are initiated by commands on a command/response protocol that can address up to 31 different RTs individually. Each RT (0...30) retains up to 30 Sub-Addresses (SA 1...30) for transmitting and 30 for receiving messages. Each message has maximum 64 bytes in 16 bit of data word format. (Fig 1, 2, 3). A status word indicates

possible failure states. Command and status words differ from normal data words through a dedicated sync. Each word ends with a parity bit.

Broadcast transfers (RT 31) are also provided. Special mode commands (SA 0, 31) and programme-specific protocols for mass data transfer complement the protocol. The data code is Manchester II bi-phase. MILBUS has a very limited data rate of 1 Mbps.

The network is a shielded twisted pair wire with optional isolation couplers, the terminals are connected via bus-stubs (Fig 1).

Some parameters of the MILBUS network are:

- Z_0 : 70 – 85 Ω (cable impedance)
- R_A : $Z_0 \pm 2\%$ (bus termination)
- R_i : 0.75 Z_0 (fault isolation resistor)
- Cable (bus, stub): max 1.5dB/100ft (1 MHz)
max 30 pF/ft

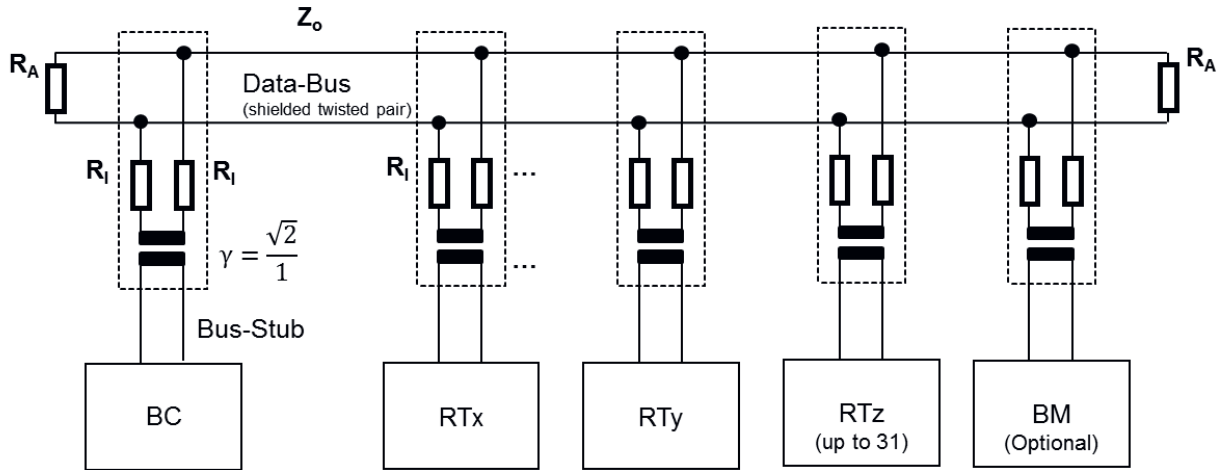


Fig 1: MIL-1553-B Data-Bus with isolation couplers for transformer coupled Bus-Stubs

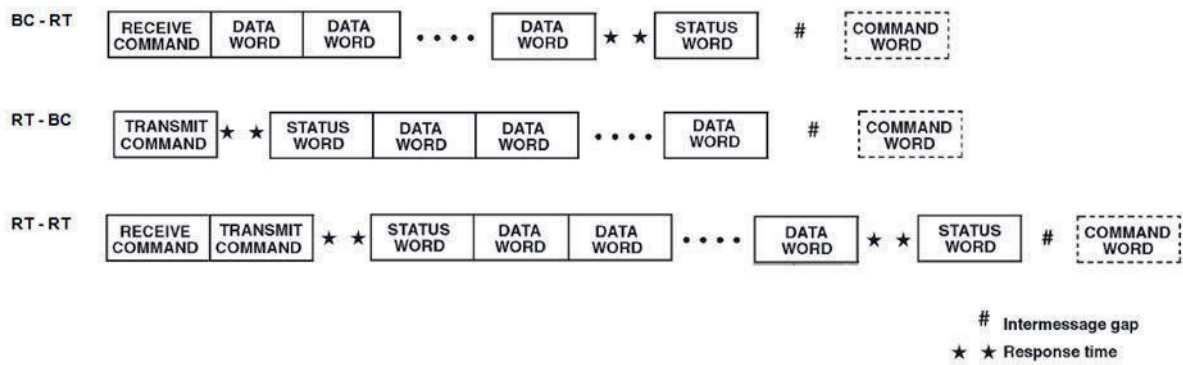


Fig 2: Typically information data transfer types [1].

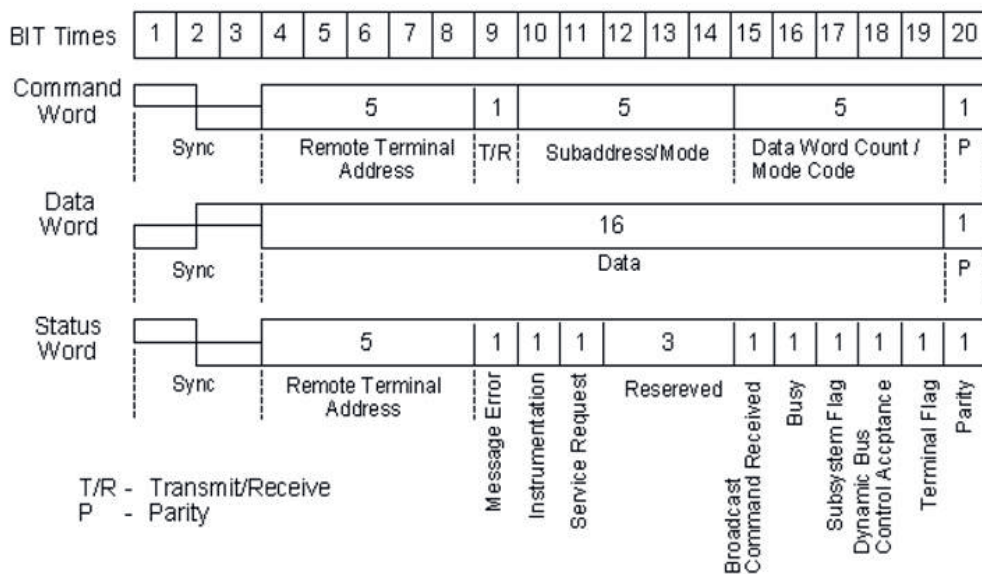


Fig 3: Command-, Data- and Status Word format [1].



Fig 4: A typical MILBUS-Message (Teledyne LeCroy WaveRunner with 1553 TD Trigger and Decode package)



Fig 5: Eurofighter A/C [2]

Special characteristics of MILBUS are:

- A physical layer with high electromagnetic immunity and therefore a very low error rate. Robust, for harsh environments. Technically mature by more than 40 years of service history.
- A deterministic strong synchronous operation for cyclic messages with very low timing jitters. The terminals synchronise themselves on the bus protocol. This results in high stability of the control circuit in an A/C. Acyclic messages are also possible.
- Immediate reaction to changes in operational situations, critical events or failures is possible by a fast command overwrite function.
- The direct and passive bus structure provides very easy access directly to the physical data transmission of the flight control and avionic subsystems. This structure enables rapid diagnostics and facilitates qualification- and certification activities.
- For safety reasons, a different redundancy concept was considered – in most applications the network is dual redundant and there is also redundancy of the BC

function. Quadruplex bus concepts are also known; for example for the safety-critical Eurofighter Flight Control System (FCS).

- The electrical bus network concept (impedance, termination resistors, isolation couplers and fault isolation resistors) determines a minimum system attenuation of 12dB. The bus length (Fig 1, Data bus) is not specified in MIL-STD-1553B. Our experience is 100m or even longer, if necessary.

Known problems with some new MILBUS applications:

In new applications, customers often do not consider the large variation in specified cable impedance for the MIL-STD-1553B standard, which is defined between 70 – 85Ω. This often leads to a negative effect of an undefined cable and a mixture of different bus terminations and isolation resistors. The consequence is often a very diverse impedance matching and a data bus with very limited performance. For this reason, the impedance of the bus system and all its components should be clearly defined. For the Eurofighter and many other programmes, for example, impedance was strictly defined at $77\Omega \pm 2\%$.

Then, the standard retains the option for directly coupling a bus stub without the use of bus couplers. That sounds cheap, but in this case, the protection is lost in the event of a shortcut on a terminal. (Fig 6.). All terminals of the entire data bus are then affected by an invalid Manchester code. In addition, practical experience in electromagnetic compatibility (EMC) shows that a symmetric (twisted pair) and transformer coupled electrical bus connection has significantly better EMC interference immunity (noise-, common mode rejection and electrical DC isolation) than a bus without couplers for isolation.

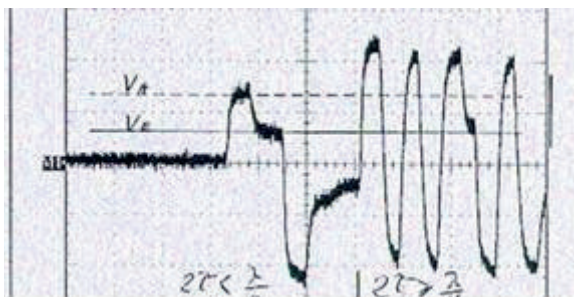


Fig 6: Signal distortion by a distant shortcut

These are the reasons why in MIL-STD-1553A the maximum permitted stub length for directly coupled stubs has been limited to 1ft (0.3m). In addition, MIL-STD-1553B + Notice 2 only permit

transformer-coupled stubs for US Army and Air Force applications. In most A/C programmes, including the Eurofighter, direct coupling is prohibited in any case.

However, the fault isolation resistors of correct transformer-coupled stubs (Fig 1) protect the data bus from the effect of a single shortcut on a terminal. Only the directly affected terminal will fail in this case – other terminals are not affected.

But there is also a frequent problem with transformer-coupled stubs: Very often applicants try to 'save bus length' by exceeding the stub length (Fig 1, Bus stub). If a data bus is terminated correctly, the bus length is not a very critical factor; while the back reflection and the capacitive load of a long stub cable will degrade the whole bus signal.

For example, a transformer-coupled bus terminal on a bus stub of up to a maximum of 10ft (3m) causes an electrical load of $>800\Omega$ on the data bus, while the electrical load of a bus stub of more than 20ft (6m) is often 500Ω or less (see [2], figure I-1.7).

For this reason, the MILBUS standard recommends transformer-coupled stubs should not exceed 20ft [1]. However, in many A/C programmes, including the Eurofighter, stub length for transformer-coupled stubs is strictly limited by definition to a maximum of 10ft, except for longer test ports that are not connected during flight operations.

There is also a complex situation with upgrade programmes:

- Do we really need an upgrade from MIL-STD-1553B – or is it an earlier version like MIL-STD-1553A, which is quite different. (see [2], table II-2 and II-4.5.1.5.3)
- Then we have the known problem with the variation of cable impedance. An upgrade or extension should be performed with cables and components of the same impedance (Z_0) as the original system.

As MILBUS is very reliable and failure tolerant, there is often a sloppy design approach with many small failures and over-tolerances – one argument for this is, why? It works!...

With upgrade programmes, there is often a small change and suddenly a limit is overdue. In this case very often a bus length over 10m is critical and the entire bus design has to be revised.

Based on this experience at Airbus Defence and Space, we found good practice by comparing the bus attenuation with an

arithmetic bus model. The attenuation of critical bus components is additionally analysed during the design phase at a frequency of 0.2 to 5 MHz.

The assessment of signal quality (Fig 4, 6, 7) with an oscilloscope is also a relevant step in maintaining or reconstructing the physical signal quality. In case of reasonable doubt, we use a Time Domain Reflectometer (TDR) for additional fault analysis and determination of the existing cabling (Fig 8).

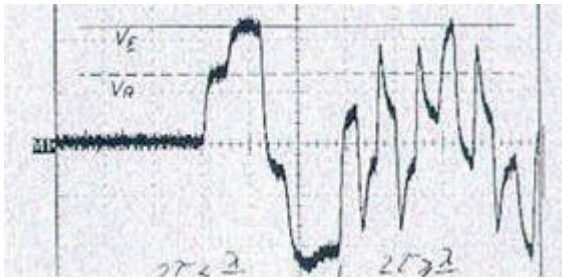


Fig 7: Signal distortion by a missing bus termination or a disruption of the cable (invalid Manchester code)

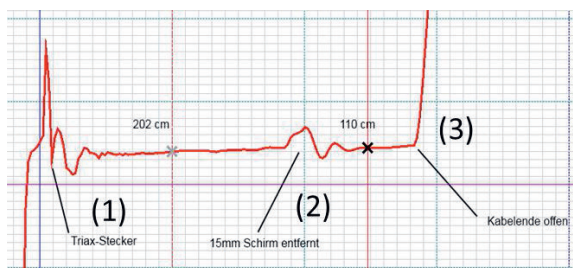


Fig 8: TDR for fault analysis: See wrong impedance of test adaption (1), fault on screen continuity (2) and missing bus termination (3)

In addition to wiring tests, our laboratory is one of only a few labs worldwide capable of performing the complete MILBUS RT Validation Test Plan to verificate the design of remote terminals. This includes protocol tests and physical tests such as signal level, waveform, zero crossing and noise immunity test.

We offer automatic or manual MILBUS configurations and patches for test rigs and benches.

Then our AIDASS® (Advanced Integrated Data Acquisition and Stimulation Systems) test support system family is suitable for subsystem and system tests.

These services and products are also for the German 'System Support Centre' (SUZ). The SUZ in Manching provides support for the entire range of Tornado and Eurofighter needs in

cooperation between the German Air Force on the national customer side and Airbus Defence and Space on the engineering and industry side [10].

Lightweight applications with unshielded cables

Lightweight applications with unshielded cables were sometimes in demand.

It is not possible to replace the shielded twisted pair directly with a simple twisted pair cable without shielding, as this has a cable impedance of about 110Ω in most cases.

A simple way to use unshielded lightweight cable is to replace the termination and isolation resistors with correctly calculated resistors for the actual cable impedance (Z_0).

Concepts for enhanced speeds for the future

MILBUS with 1 Mbps data rate is out-dated in many cases and we need significantly higher speeds, and there have been several efforts to implement the excellent MILBUS protocol in modern and faster physical networks. However, most commercial data bus products do not fulfil the reliability and determinism of MILBUS without modifications.

STANAG 3910 / EFABUS / EFEx

An early attempt to increase data rate was STANAG 3910. The idea was to improve the MILBUS command/response protocol and wiring by adding an additional high-speed data transfer network.

In this way, the data rate capability for the Eurofighter avionic and attack bus was raised to 20 Mbps by an additional optical network with a star coupler. The first issue was EFABUS. This was followed by EFEx (EFABUS Express), now with the command/response protocol and the data transfers on the fibre optic, without necessarily using an electric network. The number of potential messages and the data block length has also been increased to 8 kbytes.

Fibre Channel (copper/electrical)

Fibre Channel is a deterministic protocol that guarantees the provision of information. Fibre channel enables copper and optical connection.

Fibre Channel is in the meantime the primary avionics bus for the latest A/C fighter programmes in the US arsenal, including the F-35 Joint Strike Fighter, F-18E/F and F-16 Block 50+ [5].

MIL-STD-1760E Class I for weapons and storages defined a switched electrical Fibre Channel interface for mapping MIL-STD-1553 messages and for mass data transfers at 1 Gbps for the high-speed weapon bus in SAE-AS5653B on the high bandwidth lines (HB) with PINs 2 and W [5], [6].

SAE-AS5653B [7] also describes the command and control protocol FC-AE-1553 on Fibre Channel.

FC-AE-1553 sub-addresses 1 to 30 are reserved for legacy MIL-1553 data transfers with a payload of up to 64 bytes. Known broadcast transfers, mode commands and error handling protocols are also available.

Another transfer type is for MILBUS with an extended payload of up to 2 kbytes. Extensions for large file are about 4 Gbytes.

The switch is non-blocking to ensure minimal transport delays. The cable is a copper 75Ω coaxial.

SAE-AS5725B for miniature mission store interface (MMSI), which will be relevant for military UAVs in the future, is also considering a Fibre Channel interface.

Ethernet

Ethernet has great potential in commercial applications, but Ethernet and IP-based networking is not deterministic enough to replace MIL-STD-1553B.

However, commercial off-the-shelf (COTS) systems and thus Ethernet-based communication systems are increasingly being introduced for non-real-time and non-safety-critical mission systems, image processing and sensor fusion. The same applies for example to cabin entertainment systems on commercial A/C.

MILBUS is not very common in commercial aviation and Avionics Full Duplex Switched Ethernet (AFDX® / ARINC 664, part 7) as a protocol who guaranties a calculable maximum latency has been established mainly as replacement for ARINC 429 serial data links [8].

In Airbus Defence and Space technology programmes, additional an Ethernet-based collision- and delay-free and therefore deterministic command/response protocol,

internally called MILBUS via Ethernet, was examined and patented. The principle is comparable with the FC-AE-1553 protocol on Fibre Channel or EFEx. MILBUS via Ethernet protocol is also planned for legacy MIL-1553 data transfers and for additional messages with increased address space and block lengths.

FireWire / IEEE1394

FireWire is mainly used as a COTS mission data communication system on some A/C designs, including the F-35. SAE-AS5643B has established FireWire as a military and aeronautic standard. The standard does not consider a real-time protocol for legacy MILBUS data transfers.

Fibre optic interfaces

Fibre optic has excellent electromagnetic immunity and allows data rates of significantly more than 1 Gbps with a potential of up to 1 Tbps.

Therefore some current activities are in the field of fibre optic interfaces.

EFABUS and EFEx was a very early fibre optic application. This was also a time in which we had our first experiences with operating an A/C with fibre optic cables, connectors and interfaces. An additional OM 3 fibre connection with an Ethernet protocol is planned for the next generation Eurofighter.

In commercial aviation (Airbus A380 / Boeing 787) and in military transport A/C A400M, an interconnection system based on an OM 1 62.5/125 graded index fibre for point-to-point connections was established for bidirectional data transfer on 850/1300nm wavelength. Protocol is a fibre optic Fibre Channel.

MIL-STD-1760E Class I also reserved two bi-directional fibre optic interfaces between the aircraft and stores on PINs U and Y as a growth potential for future applications. At the moment, 'the use of fibre optic interfaces by a mission store shall not occur until the optical and logical (protocol) characteristics of the fibre optic interfaces are added to this standard' (see MIL-STD-1760E, 5.2.11 [6]).

Airbus Defence and Space technology has been investigating programmes for HSDN (High-Speed Data Network) optical bus protocols for several years. The investigation led to a mature product family of fibre optic data transmission (and optical sensing) technologies Highspeed Optical Reconfigurable NETWORK (HORNET®), which are protected by several

patents. Data rates of 1 Tbps are realistic for non-DAL implementations in laboratory environments, while data rates of more than 10 Gbps are realistic for DAL-A use. Initial product applications on A/C have already been implemented, combining the HSDN and Basic Mission Chain (BMC) functionalities to enhance customer experience throughout the operational chain. Airbus Defence and Space currently defines Maintenance, Repair and Operation (MRO) guidelines and concepts for standard installations of high-speed optical networks on any A/C.

The results of these investigations will have an impact on future MIL-STD-1760 fibre optic interfaces and are currently the subject of international standardisation.

E1553® / STANAG 7221

E1553® / STANAG 7221 (AAVSP-02, Edition A) [9] is a high-speed network designed for using the same wiring as MIL-STD-1553B. The motivation was to retain existing cables by adding a B-RTDB (Broadband – Real-Time Data Bus) on an existing MILBUS.

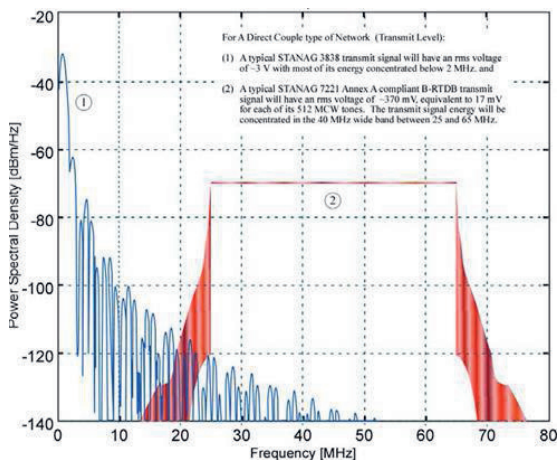


Fig 9: Typical B-RTDB Waveform representation [9]

Fig 9: Blue is the low band (1) of the legacy MILBUS operation. B-RTDB (in red) will operate on the high band (2) within a frequency between 25 and 65 MHz.

The principle is similar to the use of Digital Subscriber Lines (DSL) on an analogue telephone line for internet connection at home

The high band can alternatively be used for an additional high-speed MILBUS with BC and RTs, or for mass data transfers (example videos). The theoretical data rate is 100 Mbps when MIL-STD-1553B transfers on the low band are enabled.

250 Mbps should be possible on E1553 on an extended high band and without transfers on the low band (information is not conformed).

For evaluation purposes we used the E1553 demonstrator from Edgewater. The evaluation system worked well with the demonstrator's reference bus couplers.

For a random selection of bus couplers in an existing A/C, the transfer rate (bandwidth) was than less than 100 Mbps, in one case only 50.2 Mbps (Fig 10, 11.)

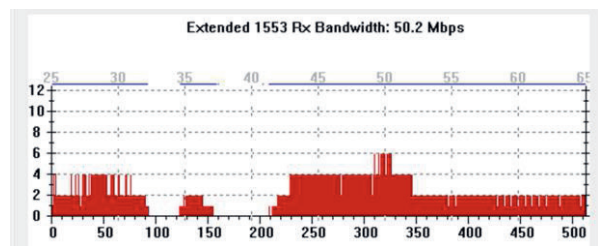


Fig 10: A B-RTDB tone map from the high band

The evaluation on an existing A/C (cockpit and weapon bus) was in the range of between 40 and 75 Mbps.

To find the discrepancy, we analysed the MILBUS couplers at a frequency of between 0.2 and 100 MHz, red (25 – 65MHz) is the relevant high band.

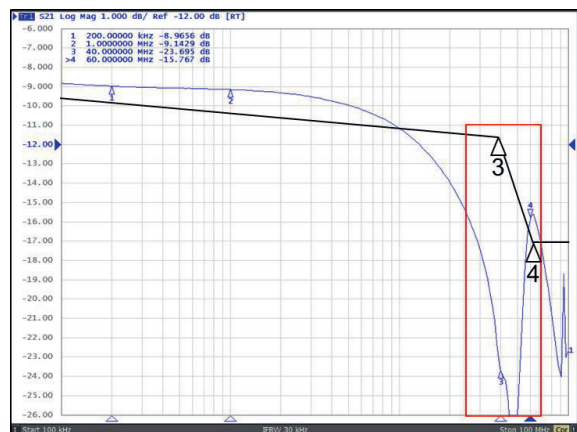


Fig 11: Coupler of an existing A/C

Explanation:

Coupler of an existing A/C (Fig 11): The specification of STANAG 7221 is not fulfilled; the deviation was up to 10 dB more attenuation at the relevant high band. This is the reason for a reduced data rate (Shannon Criteria).

The reference coupler from the evaluation kit is fully STANAG 7221 compliant (Fig 12).

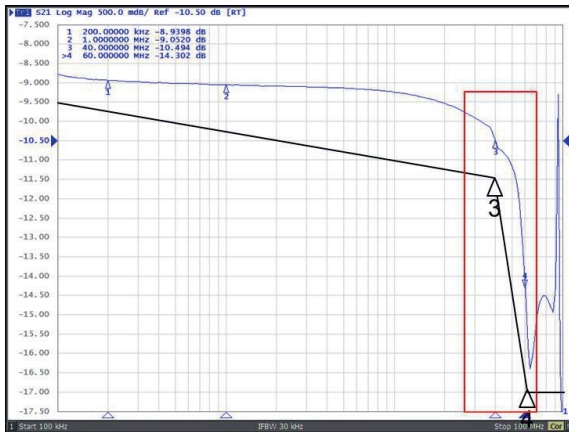


Fig 12: Reference coupler from the E1553 evaluation system

Remark: All couplers were fully compliant with MIL-STD-1553B, but not necessarily compliant with STANAG 7221.

See also the note in STANAG 7221 / AAVSP-02 A.3.2.1: 'These specifications do not apply to components used in actual legacy platforms. Expected baseline performance from an existing legacy platform can only be established by carrying out a system characterization' [9].

Other test results:

The attenuation of all newer MIL-STD-1553B compatible cables evaluated was no problem.

A B-RTDB protocol on the high band had almost no influence on bus performance and the bit error rate (noise immunity) on the legacy MIL-STD-1553B bus transfers on the low band.

If it is critical to install new cables, STANAG 7221 is an interesting approach to implement a data mass transfer between two systems by using an existing MILBUS network with a realistic data rate of about 20 to 75 Mbps on the high band. Replacing all legacy MIL-STD-1553 LRUs by keeping the old cables and couplers was not considered as an option.

Currently we have no activities on STANAG 7221.

Conclusion

MIL-STD-1553B remains relevant for military A/C product upgrade programmes. MILBUS will also be a relevant communication system in the next generation weapon systems. Due to the very long product life cycle on military A/C, we do not expect MIL-STD-1553B to be replaced in the coming decades.

With new programmes, however, a partial replacement by modern products has already taken place.

Electric Fibre Channel has been established as an avionics bus in the new US fighter programmes and the FC-AE-1553 protocol is a direct replacement and high data rate upgrade of MILBUS. This protocol is already part of the MIL-STD-1760E for the military aircraft/store interconnection system.

However, for non-safety critical mission systems, image processing and sensor fusion, the trend in Europe is clearly towards Ethernet. The technology for MILBUS via Ethernet is also of interest for military avionics.

For both technologies, Fibre Channel and Ethernet based, an improvement by an increasing amount of fibre optics (instead of copper cables) is the foreseeable future. There has already been considerable progress made in standardisation.

EFABUS/EFEx for Eurofighter has not been used in any other programme.

STANAG 7221 B-RTDB will certainly find a place in some upgrade programmes in my opinion.

MILBUS without shielding was a question that came from space industry and from commercial consumer market. It is not known whether this technology is actually supported.

In commercial aviation I know of some applications where MILBUS with its high electromagnetic immunity was installed instead of ARINC 429 on modern carbon fibre composite laminate A/C structures. One application was for parts of the Airbus A350-XWB Wide Body Jet Airliner flight control system.

The author

Dipl.-Ing. Helmut Plankl is expert in data communication and test systems at Airbus Defence and Space Military Aircraft in Manching, which is located between Nuremberg and Munich, Germany.

In this position, Helmut has 30 years of experience in the field of system design verification and validation, technical problem solutions and aspects of continuous product and process improvement.

He is responsible for technology projects to improve economy and efficiency of ground testing facilities for civil and military air systems.

In the field of electrical and fibre optic communication systems, he is a recognised specialist for MILBUS and deterministic communication protocols and has been consulted on many European programmes. He was involved in the development of EFABUS/EFEx. He was one of the first to conduct studies on E1553 in Europe.

One focus of his work is the improvement of methods, engineering tools and diagnostic systems to improve the safety and reliability of wired and fibre optic airborne communication systems.

Helmut and his extended team hold some patents and are members of global standardisation groups. The AIDASS® test support system is one of the products developed by this team.

References

- [1] MIL-STD-1553B + Notice 2 INTERFACE STANDARD FOR DIGITAL TIME DIVISION COMMAND/RESPONSE MULTIPLEX DATA BUS; Department of Defense, United States of America, 1986
- [2] MIL-STD-1553 Designer's Guide; Data Device Corporation; doi:10.1108/aeat.1999.12771dab.055
- [3] EFABUS - SP-J-403-V-1146 / EFABUS Express (EFEx) - SP-J-403-V-1156 are program specific Standards for Eurofighter (Typhoon) Fighter Aircraft
- [4] Stefan Gygas, Luftwaffe: Eurofighter-GAF, <https://theaviationist.com/2012/04/11/gaf-typhoon-scrumble/> (09.05.2017, 07:24).
- [5] Weapon Standards; J. Kutka; Airbus Defence and Space, 2018
- [6] MIL-STD-1760E; DEPARTMENT OF DEFENSE INTERFACE STANDARD Aircraft/Store Electrical Interconnection System; Department of Defense, United States of America, 2007
- [7] SAE-AS5653; High Speed Network for MIL-STD-1760 Rev. B; 2014; Society of Automotive Engineers, SAE International
- [8] ARINC 429 / ARINC 664 are Standards from Aeronautical Radio Incorporated, USA
- [9] NATO Standardization Agreement (STANAG 7221) / AAVSP-02 Broadband Real time Data Bus (B-RTDB) Edition A Version 1, 12 May 2015
- [10] Abstract: Ground Test Facilities and Integration Concepts for Combat Air Systems at Airbus Defence and Space; European Test & Telemetry Conference – ETTC 2014 in Nuremberg , H. Plankl; Airbus Defence and Space

® E1553 is a registered Trademark of EDGEWATER COMPUTER SYSTEMS, INC.

® AFDX is a registered trademark of Airbus

® HORNET is a registered trademark of Airbus

® AIDASS is a registered Trademark of Airbus

Sabotage and Disclosure of Flight Test and other reasons & methods to intercept, jam or spoof telemetry

Michael Niewöhner
COMPLETER.NET Sales & Engineering GmbH,
www.completer.net,
Michael.Niewoehner@completer.net

Abstract

The paper deals with the reasons for jamming and spoofing telemetry and GPS, but also with methods from the world of electronic warfare, which may not (yet) be relevant or known in the domain of flight test. The lecture will also give a closer look at and deeper insight in the possibilities of intercepting and evaluating telemetry data and the possibilities that arise from this, even if the contents are encrypted. FISINT (Foreign Instrumentation Signals Intelligence) is an area of signals intelligence (SIGINT), that plays a subordinate role in electronic warfare and military intelligence but is very interesting to intelligence agencies and beneficial to other organizations.

Key words: Jamming, Spoofing, Telemetry, GPS, FISINT

The world of Electronic Warfare (EW) and Signals Intelligence (SIGINT)

Electronic warfare (EW) is any action involving the use of the electromagnetic spectrum or directed energy to control the spectrum, attack of an enemy, or impede enemy assaults via the spectrum. The purpose of electronic warfare is to deny the opponent the advantage of and ensure friendly unimpeded access to the EM spectrum.

EW can be applied from air, sea, land, and space by manned and unmanned systems, and can target humans, communications, radar, or other assets. Electronic Warfare has several subdivisions.

Electronic Attack (EA)

EA involves the use of electromagnetic energy, directed energy, or anti/radiation weapons to attack personnel, facilities, or equipment with the intent of degrading, neutralizing, or destroying enemy combat capability. In the case of electromagnetic energy, this action is referred to

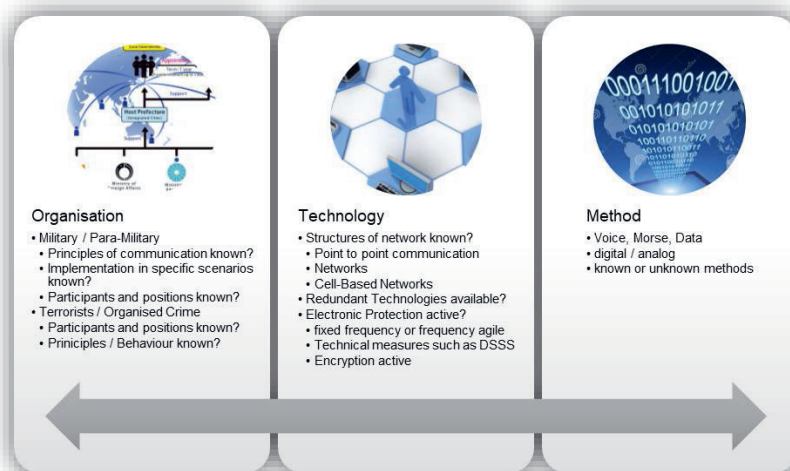


Figure 1: Taxonomy for Electronic Attack Measures

as jamming and can be performed on communications systems or radar systems.

Electronic Protection (EP)

EP involves actions taken to protect personnel, facilities, and equipment from any effects of friendly or enemy use of the electromagnetic spectrum that degrade, neutralize, or destroy friendly combat capability.

Electronic Warfare Support (ES)

ES is involving actions tasked by, or under direct control of, an operational commander to search for, intercept, identify, and locate or localize sources of intentional and unintentional radiated electromagnetic energy for immediate threat recognition, targeting, planning, and conduct of future operations.

These measures begin with systems designed and operators trained to make Electronic Intercepts (ELINT) and then classification and analysis broadly known as Signals intelligence from such detection to return information and perhaps actionable intelligence to the commander.

The purpose of ES tasking is threat recognition and other tactical actions such as threat avoidance and homing. However, the same assets and resources that are tasked with ES can simultaneously collect intelligence that meets other collection requirements.

Signals Intelligence (SIGINT)

SIGINT is derived from the direction finding, processing, and analysis of intercepted enemy communications, electronics and foreign instrumentation signals. It provides the commander valuable, near-real-time intelligence on enemy intentions, readiness status, and disposition by intercepting and locating enemy command, maneuver, fire support, reconnaissance, and logistic emitters.

Any nation has a political interest to gain information superiority against its potential threats. Therefore, most of them operate strategic intelligence systems with monitoring and locating capabilities as well as evaluating and reporting functions.

The vital interest of nations is formation of strategy, policy, and military plans and operations at the national and theatre levels. Strategic intelligence concentrates on the national political, economic, and military considerations of states or nations. It identifies the support for governments, the ability of states or nations to mobilize for war, the national political objectives, and the personalities of national leaders. It predicts other nations' responses to own theatre operations.

Intercepting and Locating Telemetry emissions

Foreign instrumentation signals intelligence (FISINT) was formerly known as TELINT or telemetry intelligence. FISINT entails the collection and analysis of telemetry data from a missile or aircraft tests.

Telemetry communication is mainly one-directional transmission from instrumented device to a telemetry receiver in a control station (mobile/fixed). Different applications are Meteorology, Oil and gas industry, Motor racing, Transportation, Agriculture, Water management, Swimming pools, Energy monitoring, Resource distribution, Medicine/Healthcare, Fishery and wildlife research and management, Retail, Energy providers, Falconry, Law Enforcement and Mining. All of those are of minor interest for intelligence authorities. Of more interest are the usage in the Aerospace, Defense and Space Domain.

Telemetry is used in complex systems such as missiles, RPVs, spacecraft, oil rigs, and chemical plants since it allows the automatic monitoring, alerting, and record-keeping necessary for efficient and safe operation.

Space agencies such as ISRO, NASA, ESA and other agencies use telemetry and/ or telecommand systems to collect data from spacecraft and satellites. Telemetry is vital in the development of missiles, satellites and aircraft because the system might be destroyed during or after the test. Engineers need critical system parameters to analyze and improve the performance of the system. In the absence of telemetry, this data would often be unavailable.

Space Science

Telemetry is used by manned or unmanned spacecraft for data transmission. Distances of more than 10 billion kilometers have been covered, e.g., by Voyager 1.

Rocketry

In rocketry, telemetry equipment forms an integral part of the rocket range assets used to monitor the position and health of a launch vehicle to determine range safety flight termination criteria. Problems include the extreme environment (temperature, acceleration and vibration), the energy supply, antenna alignment and (at long distances, e.g., in spaceflight) signal travel time.

Flight testing

Today nearly every type of aircraft, missiles, or spacecraft carries a wireless telemetry system

as it is tested. Aeronautical mobile telemetry is used for the safety of the pilots and persons on the ground during flight tests. Telemetry from an on-board flight test instrumentation system is the primary source of real-time measurement and status information transmitted during the testing of manned and unmanned aircraft.

Intercepted telemetry was an important source of intelligence for the United States and UK when Russian missiles were tested. Telemetry was also a source for the Russians, who operated listening ships in Cardigan Bay to eavesdrop on UK missile tests performed in the area.

Telemetry communication in aircraft / missile testing is according to IRIG 106 standard an FQPSK / SOQPSK signal with a PCM signal encoded. Such telemetry mainly operates in L-Band, S-Band and C-Band. Nowadays it moves more and more in the direction of C-Band. Due to the fact, that transmission is one-directional, there is no possibility for error-correction. Consequently, the requirements for the quality of the signal are high.

The users of this sort of telemetry are Air Force Bases, Aircraft Industry and general defense industry.

Evaluating Telemetry emissions

Telemetry emissions are mainly encrypted. This should secure the content of the transmitted data. What is not known widely is, that this does not protect against interception, analysis and evaluation. Putting together several intelligence sources, a clear picture of the monitored emitter could be put together.

By triangulation, the position of an emitter can be identified very accurate. By comparing different

positions over time, the flying speed can be calculated and tracked. With some intelligence systems, even the flying height (elevation of the signal compared to position) can be found out.

The fact, that a telemetry emission is sending continuously makes it easy to track the exact flying route of the aircraft. If communication is bi-directional, the structure and setup of ground stations could be disclosed. As transmitted power is relatively high, and the object is transmitting from a high position, the interception station can be far away from the aircraft.

Coming back to the encryption, the content is relatively safe against real-time decryption. Nevertheless, all traffic can be recorded and decrypted with high performance computers later.

Finally, all such information helps enemy forces to plan jamming and spoofing procedures for future flight tests.

Electronic Attack (EA) for telemetry and GPS

Jamming is the deliberate radiation, re-radiation, or reflection of electromagnetic energy for disrupting enemy use of electronic devices, equipment, or systems. It degrades communications by reducing or denying the enemy's ability to pass key information at critical times and can cause enemy operators to become irritated, confused, or misled during offensive, defensive or retrograde operations. When applied successfully, jamming can contribute to the failure of those actions which depend on communication using the electromagnetic spectrum.

ES is the primary source of information used to identify and develop jamming targets. It helps to

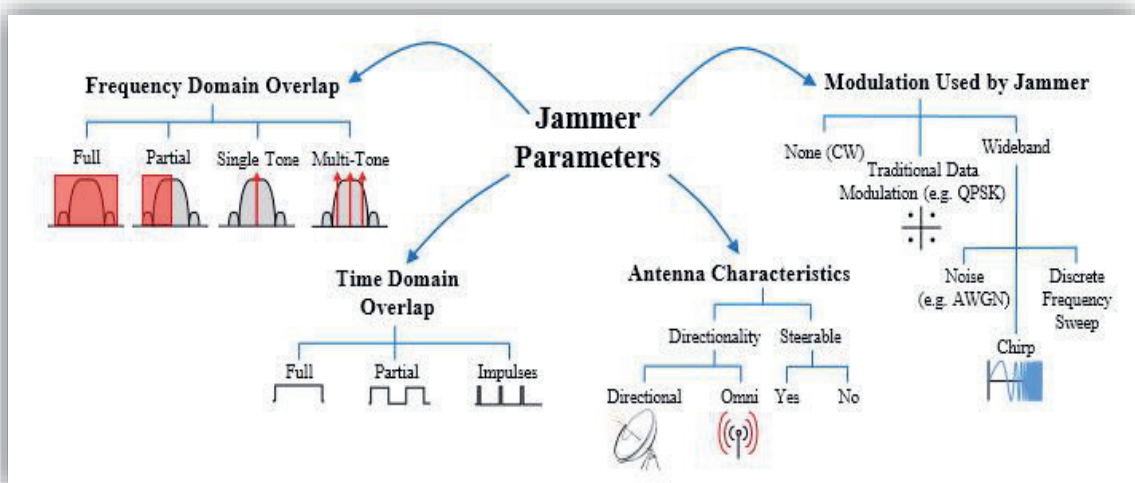


Figure 2: Jammer Parameters

identify the enemy's locations and intentions and thereby identify valuable jamming targets. Indiscriminate jamming wastes resources could impede friendly communications or could attract countermeasures such as artillery fire. Consequently, jamming operators/ systems need to know exactly who, what frequency, where and when to jam.

Enemy nets, which routinely pass information of intelligence value, should be identified and monitored, other nets, such as those having a highly tactical value to the enemy but little or no intelligence value to friendly forces, could be attacked with jammers. Enemy secure communications may also be jammed with the intention of drawing the enemy into clear voice communication.

The process may be along the following lines. An intercept DF network picks up a transmission that is determined not to be from own forces or from neutral operators. Analysis identifies specific parameters for the situation such as:

- transmission central frequency
- 3-dB and IO-dB bandwidth
- modulation scheme in use
- signal strength at the detecting receiver(s)
- direction or localization position if known
- times of transmissions
- how frequently the channel is used
- duration of transmissions
- association with other systems (activity analysis)

This is where the behavior of an enemy network is studied to determine its structure specific identifying features such as frequency instability, operator Morse behavior, the same voice on successive intercepts or transmission of formatted messages.

These factors can be analyzed with the benefit of knowledge already known, such as association with known weapon systems and technical parameters of known enemy systems. The detected transmission may for example be associated with a specific air defense command system or be of a type known to be used for command and control. Transmission behavior may also reveal the relative importance of the channel. If is frequently used, then it may be an important command and control channel. If it is noticed before artillery shells arrive, then it may be the artillery command network. If troop movements are correlated with the transmissions, then again it may be a command net. If other transmissions on other frequencies

follow on quickly after the initial transmission, then again it might be part of the command network and so on.

For effective jamming operations, the planning function needs all information about function, position in a net, position on the battlefield and ability to affect the combat plan. For those reasons, the planning of jamming operations shall be in responsibility of the tactical leader.

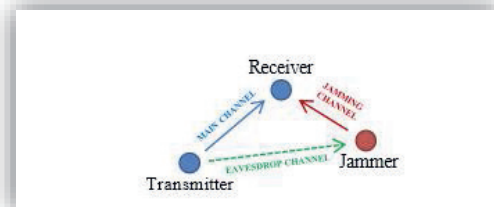


Figure 3: Jamming Principles

One main principle that regularly gets forgotten is that it is possible to deny the interception of a signal by jamming, but not the transmission.

Different methods of jamming are briefly explained in the following section.

Spot Jamming

Spot jamming occurs when a jammer focuses all its power on a single frequency. While this would severely degrade the ability to track on the jammed frequency, frequency agile radar would hardly be affected because the jammer can only jam one frequency. While multiple jammers could possibly jam a range of frequencies, this would consume a great deal of resources to have any effect on frequency-agile radar and would probably still be ineffective. Spot jamming is used to jam a pre-selected frequency that has been determined as a target of interest.

Once the transmission is determined to be a high priority target, an EW tasking mission may be issued to the spot jammer. This will include the technical parameters and any other pertinent information, such as the duration of the jamming task. The actions of the jammer detachment will be to tune the jammer to the required frequency and bandwidth if this is adjustable. The antenna will be pointed in the direction of the enemy receiver. Before jamming, the channel can be listened on to determine whether it is still transmitting (there is no point in jamming an unoccupied channel). If it is still in use, then jamming can commence. The jamming can consist of un-modulated or modulated noise. Un-modulated noise will raise the noise floor of the enemy receiver, preventing them being able to communicate. Modulated noise does the same thing but also disrupts audio reception of the

transmission signal making it impossible for the receiving operator to hear the message. Periodically, the jamming signal will be turned off so that the jammer operators can listen to determine whether the enemy is still using the channel or have changed to a different one.

Sweep Jamming

Sweep jamming is when a jammer's full power is shifted from one frequency to another. While this has the advantage of being able to jam multiple frequencies in quick succession, it does not affect them all at the same time, and thus limits the effectiveness of this type of jamming. Although, depending on the error checking in the device(s) this can render a wide range of devices effectively useless

Barrage Jamming

Barrage jamming is the jamming of multiple frequencies at once by a single jammer. The advantage is that multiple frequencies can be jammed simultaneously; however, the jamming effect can be limited because this requires the jammer to spread its full power between these frequencies, as the number of frequencies covered increases the less effectively each is jammed.

Barrage jamming is the simplest form of jamming and is usually defined as a jammer which transmits noise-like energy across the entire portion of spectrum occupied by the target with 100% duty cycle in time. Thus, it is non-correlated and non-protocol-aware. Barrage jamming has been shown game theoretically and information theoretically to be the best a jammer can do in the absence of any knowledge of the target signal.

Barrage jamming is used to deny the enemy of the use of a portion of spectrum. This can be because enemy forces are frequently changing channels or that they are using full frequency hopping systems. Compared to spot jammers, barrage jammers need to supply jamming power into many channels rather than just one. On the rather simplistic assumption that the barrage jammers deliver the same jamming power into each jammed channel and that the effective jamming power has the same effect as the spot jammer, it is easy to calculate the power reduction for the number of channels jammed.

Partial Band Jamming

When jamming a single-carrier signal, it has been shown that jamming gains can be achieved by not jamming the entire signal in the frequency domain, but rather jamming a fraction of the signal. This is known as partial-band jamming, and it is usually considered a non-correlated jamming attack because the jammer transmits

continuously in time. Performing partial-band jamming against an Orthogonal Frequency-Division Multiplexing (OFDM) waveform does not make sense because strong forward error correction could allow the data to be reconstructed from the unjammed subcarriers.

Responsive Jamming

Responsive jammers have an RF detection capability that allows them to scan for threats and jam those of interest.

Adaptive Jamming

Adaptive jamming is an extension of responsive jamming but with the potential to jam several targets at the same time. It provides an improved method to achieve the same effects as barrage jamming but in a far more focused manner.

Repeater Jamming (Follower Jamming; Responsive Jamming; Reactive Jamming)

Repeater jamming is the simplest form of correlated jamming when the jammer has no knowledge of the protocol. In repeater jamming, the jammer transmits when it senses energy on the channel. This may be in the form of the jammer re-transmitting what it receives with noise added or sensing a series of subchannels and transmitting noise when it senses energy on one or more subchannels.

Smart Jamming (Pilot jamming; Equalization Jamming)

Smart jamming is the term used to describe jamming aimed at network vulnerabilities rather than simply raising the noise floor or causing unacceptable audio or data performance. Methods of smart jamming are aimed at types of network such as GSM, UMTS, paging systems and many others.

A smart jammer designed to attack GSM will have less or even no effect against other networks that may be present, so it is important to be able to identify the exact type of network for it to work. Some network vulnerabilities include: pilot channels; synchronization channels, time slots or data; paging channels or time slots; error correction checksums; acknowledgement or Not Acknowledged messages.

The purpose of smart jamming is to prevent normal performance of a network. This may be by denying subscribers the ability to log on to the network by causing base station overload, disrupting signals telling subscribers that they have a call, preventing successful call initiation or disrupting communications once a link is established by causing the system to successively re-send packets of data due to Not Acknowledged or error checksum faults. This

type of jamming is relatively new compared to the other methods.

Equalization jamming involves targeting any mechanism related to equalization. Known data symbols (reference symbols) are inserted into the transmitted waveform to estimate the channel's frequency response and equalize the effect of the channel at the receiver prior to demodulation. These known symbols are called pilot symbols in multicarrier communications such as OFDM or single-carrier frequency division multiple access (SC-FDMA) and channel sounding symbols in multiple-input and multiple-output (MIMO) systems. For example, in OFDM, pilot tone jamming is simply the process of jamming pilot tones, which may reside on certain subcarriers (in the case of 802.11) or may be multiplexed in time and frequency with data (in the case of LTE).

Pilot jamming is protocol-aware because the jammer must know where the pilots are located. If the pilots occur on a dedicated subcarrier then the attack is non-correlated, but if they are multiplexed in time then it must be correlated to surgically jam the pilots. It was found that pilot jamming can be energy efficient and similar degradation in target receivers Bit Error Rate (BER) can be achieved using roughly one-tenth of the energy.

The pilot jamming process is similar in the case of SC-FDMA, which is the single-carrier variant of OFDM and used in the uplink of the LTE air-interface. In MIMO systems, known reference signals are used for channel sounding and thus can be jammed if they are known by the jammer a priori. Another special kind of equalization jamming attack involves jamming the cyclic prefix (CP) of a multicarrier waveform such as OFDM or SC-FDMA. These waveforms use a CP to mitigate inter-symbol interference (ISI) and inter-channel interference (ICI). CP also ensures that the convolution of the channel impulse response with the modulated symbols has the form of a circular convolution, which is essential for simple one-tap equalization in the receiver. These crucial roles played by the CP make SC-FDMA particularly vulnerable to jamming attacks through CP.

Synchronization Jamming

For a communications link to function, the receiver must synchronize to the incoming signal in both time and frequency. To aid in this task, a synchronization signal, or synchronization symbols, are usually designed into the PHY layer protocol. For example, in LTE there are two different synchronization signals that each appear every 5ms. Synchronization jamming is simply the process of surgically jamming one or

more synchronization signals. This jamming technique is unique in the sense that it may only prevent radios from establishing a communications link, and thus it won't cause immediate Denial of Service (DOS).

However, synchronization signals tend to be very sparse with respect to the entire signal, thus providing a significant jamming gain. Synchronization jamming must be protocol-aware, to know where the synchronization signal is located. It must be time-correlated, assuming the synchronization signal is multiplexed in time with data and other signaling.

AGC Jamming

The automatic gain control (AGC) mechanism in a receiver adjusts the input gain in such way that the received signal comes in at a proper level to best utilize the range of the analogue-to-digital converter(s).

A jamming attack that targets the AGC mechanism is one that uses a very low duty cycle (e.g., 2%) but with extremely high instantaneous power. By not transmitting continuously, the jammer can save power and remain harder to detect in some situations. AGC jamming is non-correlated, although the specific period and duty cycle used are important parameters. Aside from the assumption/knowledge that the target receiver uses AGC, it is non-protocol-aware.

Protocol-Aware Jamming

The term protocol-aware simply means the jammer is aware of the protocol of the target signal. Information about the signal's protocol is obtained during the Signal Awareness step and used in the Attack Selection decision-making. For example, the jammer may identify that a signal is a Wi-Fi or LTE signal, which due to the open nature of specifications allows the jammer to know almost everything about the PHY and MAC layers.

A jammer could use a priori knowledge of the protocol to exploit weaknesses in the protocol and launch a jamming attack that is more effective and may be harder to detect than non-protocol-aware jamming. For example, the jammer may only know a signal uses OFDM with pilots in certain locations, which would be considered protocol-aware if it knew exactly where the pilots were placed.

In most wireless protocols, the data takes up the largest portion of time and frequency resources. Thus, when targeting something besides the data, it will likely result in an attack that uses less power and is harder to detect (if the targeted mechanism is essential for communications). Possible mechanisms that could be targeted in a

protocol-aware attack (taken from open literature) include Control channels/subchannels, Control frames or packets (e.g., ACKs), Pilots (reference symbols), Synchronization signals and Cyclic prefix in OFDM.

Possible protection measures

There are different possibilities to protect own flight tests against jamming and spoofing. First, the level of confidentiality should be very high. As explained, jamming should be planned and if planning time is reduced by missing a priori knowledge like flight plans, the probability of being jammed is reduced significantly. But this is probably not new knowledge.

Technically it is most beneficial to have alternative communication means on board, as every military unit should do. If one is jammed, the system can take evasive measures and switch to another communication means.

Also, it is helpful to raise own power of the received signal. As explained, the jammer can deny receiving but not transmitting. So, if the original signal is much stronger than the jamming signal, the probability of being jammed is lower. This could be done by high power emitters, but on other hand, this would make it easy to intercept and thereby evaluate your flight test. Another possibility is, to operate a receiver network in the flight test area, so that the aircraft has a short distance to the receiver station. Therefore, you would need more small, remote controlled and transportable receivers/ antennas for reasonable prices.

Resume

Military intelligence and intelligence agencies are interested in monitoring telemetry communication, as they gain insight on new weapon system development, the structure and capabilities of foreign forces and generate target knowledge at a very early state. Jamming and Spoofing are methods to deny beneficial usage of the electromagnetic spectrum.

In Flight Test Surrounding, currently the risk of being jammed is much smaller than the risk of being intercepted and analyzed. However, sometimes you have malfunctioning in your flight test campaigns it might also be a smart, protocol-aware jammer and you will be wondering what

happened. Especially as the occurred problem is not reproduceable in the lab.

Expressions

- [1] **Intelligence collection management (ICM)** is the process of managing and organizing the collection of intelligence from various sources. The collection department of an intelligence organization may attempt basic validation of what it collects but is not supposed to analyze its significance.
- [2] **Signals Intelligence (SIGINT)** results from collecting, locating, processing, analyzing, and reporting intercepted communications and non-communications (for example, radars) emitters. SIGINT provides the commander with valuable, often NRT intelligence and targeting information on enemy intentions, readiness status, and dispositions by intercepting and locating enemy command, maneuver, fire support, reconnaissance, air defense, and logistics emitters. SIGINT operations require efficient collection management and synchronization to effectively overcome and exploit enemy efforts to protect his critical communications and weapons systems through emissions control, communications operating procedures, encryption, and deception. SIGINT is subdivided into: communications intelligence (COMINT); electronic intelligence (ELINT); and Foreign instrumentation signals intelligence (FISINT).
- [3] **FISINT (Foreign instrumentation signals intelligence)** is a sub-category of SIGINT, monitoring primarily non-human communication. Foreign instrumentation signals include (but not limited to) telemetry (TELINT), tracking systems, and video data links. TELINT is an important part of national means of technical verification for arms control.
- [4] In military telecommunications, the terms **Electronic Support (ES)** or Electronic Support Measures (ESM) describe the division of electronic warfare involving actions taken under direct control of an operational commander to detect, intercept, identify, locate, record, and/or analyze sources of radiated electromagnetic energy for the purposes of immediate threat recognition (such as warning that fire control RADAR has locked on a combat vehicle, ship, or aircraft) or longer-term operational planning. Thus, Electronic Support provides a source of information required for decisions involving Electronic Protection (EP), Electronic Attack (EA), avoidance, targeting, and other tactical employment of forces. Electronic Support data can be used to produce signals intelligence (SIGINT), communications intelligence (COMINT) and electronics intelligence (ELINT).

Application of Fibre Optic Range-Resolved Interferometric Vibrometry to a Full-Scale Feathered Propeller in a Wind Tunnel

Lawson N.J., Kissinger T., Finnis M.V.; James S.W., Tatam R.P.*
 School of Aerospace, Transport and Manufacturing
 Cranfield University
 Cranfield MK43 0AL
 U.K.

*Defence Academy, Cranfield University, Shrivenham, Wilts SN6 8LA. U.K.
 n.lawson@cranfield.ac.uk
 +44-1234-758245

Abstract:

The vibration characteristics of a full scale Jetstream 31 turboprop propeller blade are analysed using a fibre optic range-resolved vibrometer. Using this vibrometer, a 1.2m length propeller blade was interrogated on the low pressure surface at selected spanwise positions. The spectral characteristics of the surface were recorded over wind tunnel speeds ranging from 5m/s to 30m/s in an attempt to decouple an expected aerodynamic shedding frequency from the natural structural frequency of the blade. However, the dominant frequency was found to be the natural frequency and no evidence of shedding aerodynamic frequencies were found using subsequent hot-wire anemometry measurements. Further work is planned to isolate structural and aerodynamic effects, including measurements adjacent to the aerofoil surface and a computation model.

Key words: laser vibrometer, hot-wire anemometer, propeller aerodynamics.

Introduction

The aerodynamics of aircraft propellers appears very mature, with the first designs dating back to the early 1900's [1]. One of the most significant developments in this field was the hydromatic propeller in 1938 which allowed the pitch of the propeller to be finely controlled in order to set engine speed at any flight speed [2]. This control system also allowed an arrangement known as feathering when, under engine failure conditions, all the propeller blades on the hub are rotated 90° to the flow to minimize drag (See Figure 1).



Fig.1. Feathered propeller configuration

Little detailed aerodynamic work has been published on this feathered configuration, as manufacturers own the design data. When feathered at low flight speeds, however, it has been observed that the blades vibrate [3], which implies potentially high blade drag and structural interaction of the blades with the aerodynamics. This paper applies an advanced optical technique, a fibre optic range-resolved vibrometer [4,5], with traditional measurement methods, including hot wire anemometry [6] and surface flow visualization, to establish whether there is an interaction of the aerodynamics of a feathered propeller blade with the structure of the blade.

Experimental Rig

The experimental rig was based on a full sized, 1.2m length production Dowty Jetstream 31 propeller blade, mounted in a 2m open jet wind tunnel (see Figure 2). The blade was held on a milling machine chuck at the blade hub to allow twist and tilt of the blade so that appropriate relative wind conditions could be obtained. In these experiments, a set of spanwise pitch, ϕ , and angle of attack, α , conditions (see Figure 3) were tested over a range of wind tunnel speeds

varying from 5m/s to 30m/s. The pitch angle ϕ was based on flight test data [3] and ranged from 3.3° to 9.5°. The angle of attack was fixed at 5°. Both the pitch angle ϕ and angle of attack α were set using a reference line, obtained by insertion of a bar into a hub datum hole. This datum system is used by aircraft engineers to set the blade angles up on actual aircraft. At 30m/s, the tunnel achieved a maximum Reynolds number condition of around 50% of the flight Reynolds number. As will be outlined in the following section, initial flow visualization tests showed the blade to be insensitive to Reynolds number and so it was assumed the general characteristics of the blade under these conditions were representative of flight conditions.

The wind tunnel was controlled through a serial interface to the motor and achieved stable tunnel speeds, typically within 0.1 m/s. Centreline tunnel turbulence intensity was less than 0.5% and the propeller blade was mounted in the centre of the jet, with the hub positioned just on the edge of the jet (see Figure 2).

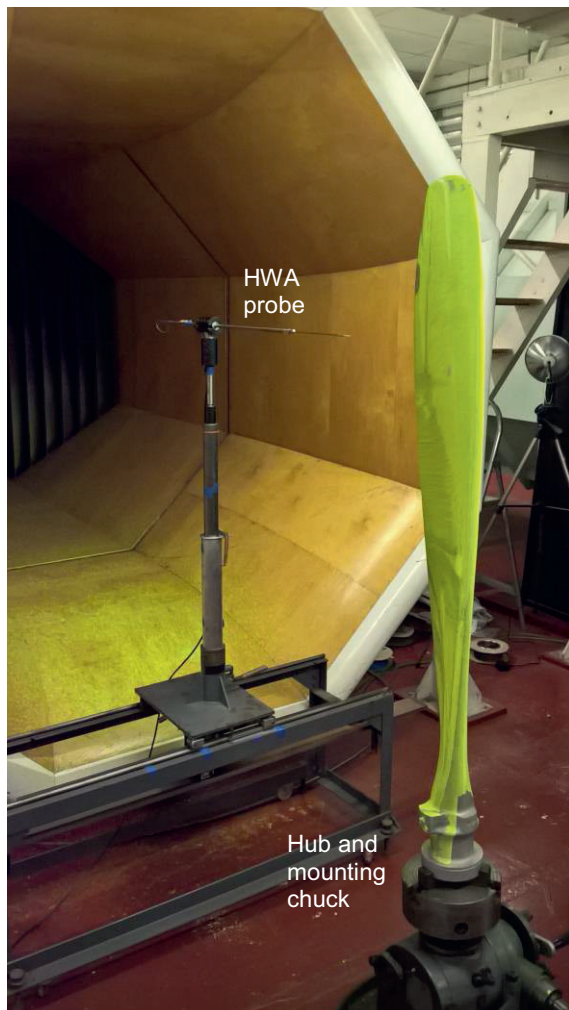


Fig.2. Wind tunnel set-up with hot wire anemometer

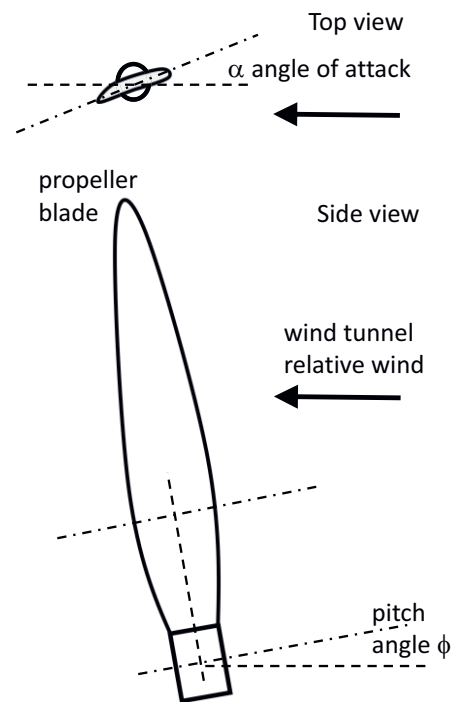


Fig.3. Wind tunnel propeller setting angles

Surface Flow Visualisation

In order to establish the general flow characteristics around the propeller blade, initial tests were completed using surface flow visualization. Through a range of test conditions, the blade was first coated with an oleic oil and fluorescent pigment emulsion. The wind tunnel was then run at a fixed condition until the flow pattern stabilized and the emulsion dried on the propeller surface. Images were then taken of the resulting flow pattern using a digital camera, while the blade was illuminated by ultra-violet light. A typical black and white image with key flow features is shown in Figure 4.

The result shows the surface flow to be highly three dimensional, with a number of key features including a separation line towards the top half of the propeller, which is confined by a region of attached flow in the middle section of the blade. Below this attached region the flow has even greater 3D complexity, including a node and a further separation line that extends to the hub at the bottom of the blade.

To establish the sensitivity of the flow features to Reynolds number, the tests were repeated at wind speeds of 15m/s, 20m/s and 25m/s at fixed pitch angles and angles of attack. Results showed the general surface flow features to be consistent across these test conditions.

Changes in pitch angle also showed no significant change in the general flow features and, therefore, it was concluded at this stage of testing that increases in Reynolds number or pitch did not appear to have a major effect on the flow structure.

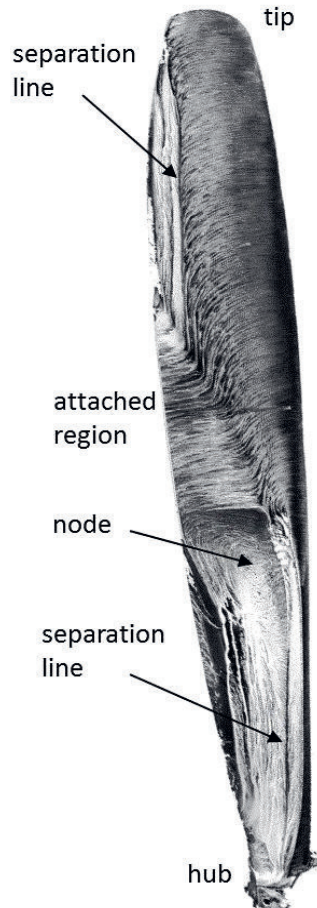


Fig.4. Surface flow visualization ($\phi = 7^\circ$, $\alpha = 5^\circ$, 25m/s)

Range Resolved Fibre Optic Vibrometer Measurements

Using the flow visualization results, an area was selected in the top section of the blade, near the separation line, to examine the vibration characteristics of the propeller blade using a fibre optic, range-resolved vibrometer. At this stage, the study was expected to establish a relationship between wind tunnel speed and shedding frequency off the rear section of the blade tip. Previous work on 2D aerofoils has suggested that a distinct shedding frequency may exist, which varies with tunnel speed, consistent with a fixed Strouhal number [7,8]. Therefore if the shedding frequency has a dominant effect on the blade structure, vibrometer measurements would show a strong

frequency behavior that matches the aerodynamic Strouhal number.

The fibre optic range-resolved vibrometer is based on a 1551nm laser diode source with beam modulation and demodulation carried out using a low cost programmable gate array (FPGA). Fresnel fibre tip reflection is used as an interference reference source, providing a system with a compact sensor head and with complete download insensitivity. This system provides an estimated resolution of 5 nm at a 21kHz bandwidth, in this case with the sample rate of 49kHz, downsampled to 1.5kHz [4,5]. Figure 5 and 6 shows the basic vibrometer set-up used for these tests.

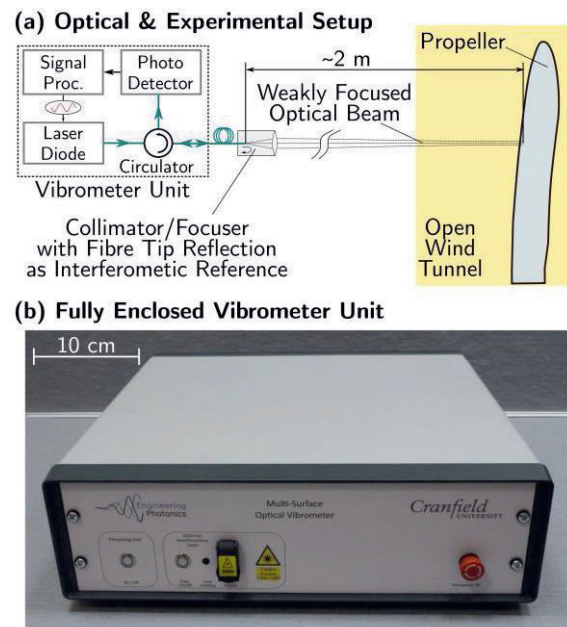


Fig.5. Basic schematic of the fibre optic range-resolved vibrometer set-up

Spectral plots of the data obtained from the propeller over a range of wind tunnel speeds from 15m/s to 25m/s are shown in Figures 7 and 8. The contour plot in Figure 8 illustrates the spectra over the full tunnel speed range. The results show a consistent spectrum with a dominant peak at a frequency of around 23 Hz. Further energy in the spectrum is found in the region of 35 Hz, 50Hz, 65 Hz and 90 Hz. However, the general characteristics of the spectra do not change with wind tunnel speed, which suggests that there is no influence of an aerodynamic characteristic on the blade structure. If there was such an aerodynamic driver, the spectral peaks would be expected to shift proportionally with wind tunnel speed.

A further experiment was undertaken with the wind tunnel turned off by pinging the blade to obtain the natural frequency of the structure and to record the spectrum with the vibrometer.

In this case, the natural frequency matched precisely the 23 Hz dominant frequency seen in the spectra in Figure 7. Further decomposition of the spectral data using wavelet methods did not lead to any additional evidence of an aerodynamic influence on the blade. Therefore it was concluded, at this stage, that the blade's structural behaviour was independent of the aerodynamic flow over the blade.

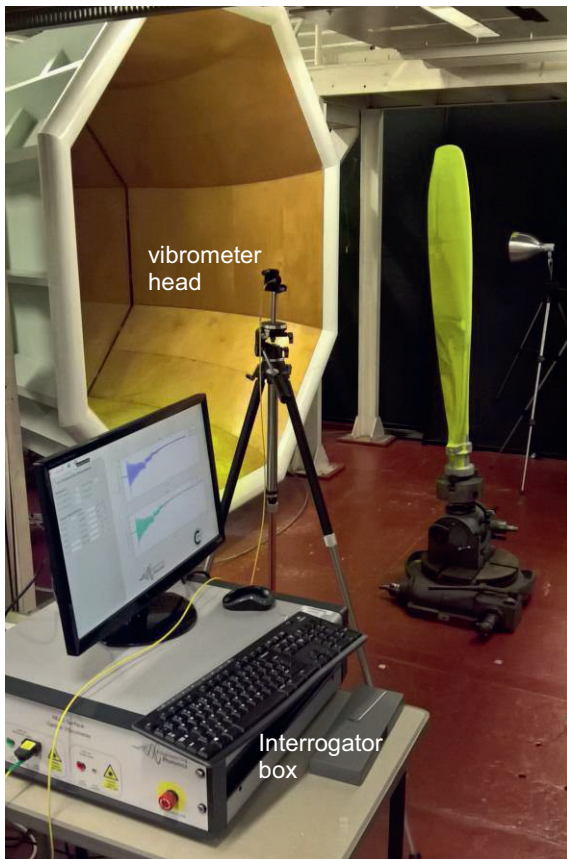


Fig.6. Fibre optic range-resolved vibrometer set-up in the wind tunnel

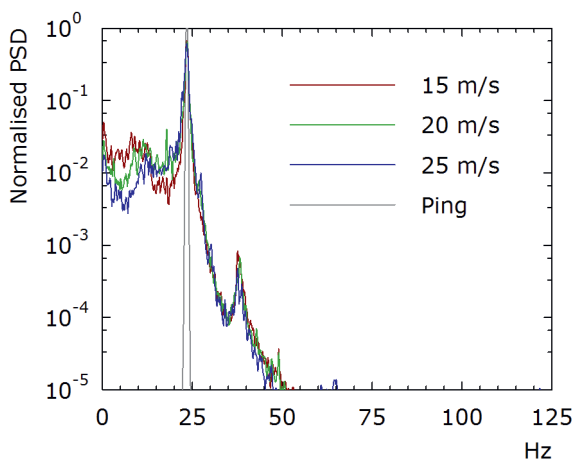


Fig.7. Vibration spectra obtained using the fibre optic range-resolved vibrometer (333mm from tip, 70mm from leading edge, ping is natural frequency)

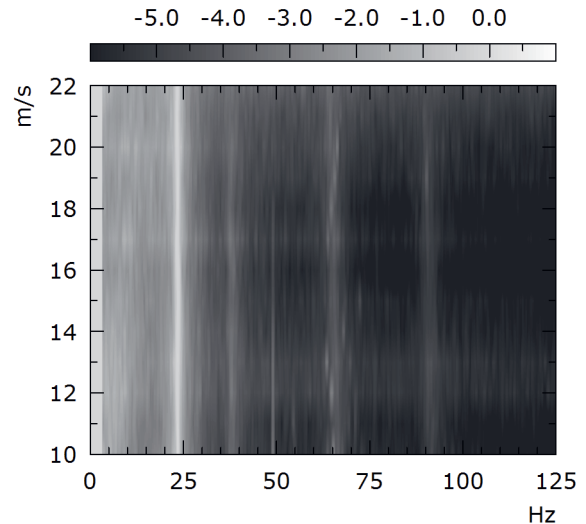


Fig.8 . Contour plot of spectra of data obtained using the fibre optic range-resolved

Hot Wire Anemometry Measurements

To investigate whether an aerodynamic shedding characteristic was present on the propeller blade, one dimensional hot wire anemometry (HWA) measurements were taken adjacent to the trailing edge at the mid-span position. The HWA set-up consisted of a Dantec 55P05 gold plated probe mounted on a Dantec 55H22 probe support and connected to a Dantec 56C01/56C17 CTA / bridge combination with a 4m probe cable (see Figure 2). The bridge output was measured using a Dewetron signal-processing voltage module connected to a National Instruments 6036E 16 bit A/D convertor. The Dewetron voltage module was set with its low pass filter at 1 kHz. Sampling was at 2 kHz for typically 30s and the wire was mounted in a vertical position to capture any streamwise wake fluctuations.

Horizontal traverses were initially completed to capture the mid-point of the wake, as shown in Figure 9. The spectra were then examined at the mid-point, as shown in Figure 10, for two wind tunnel speeds.

One of the wind tunnel speeds chosen was lower than the range tested for the vibrometer and the surface flow visualization, as previous work has reported changes in shedding characteristics at the lower Reynolds number range [7,8], corresponding in this case to a wind speed of 5 m/s. However if the spectra are examined for both speeds, there is no significant change with tunnel speed and there is no dominant frequency at any of the spectral peaks found in the vibrometry measurements, for example the 23 Hz mode.

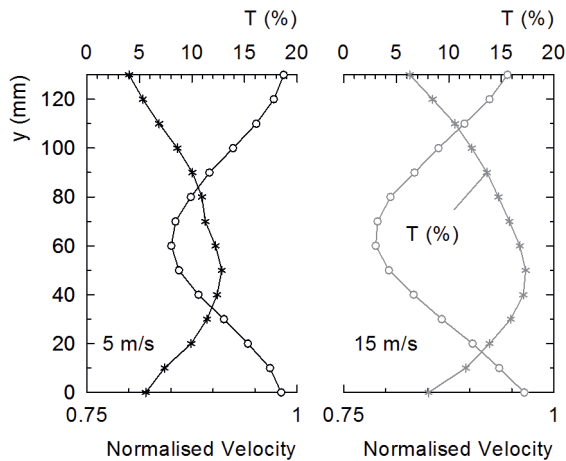


Fig.9.HWA wake data at a mid-span, trailing edge position

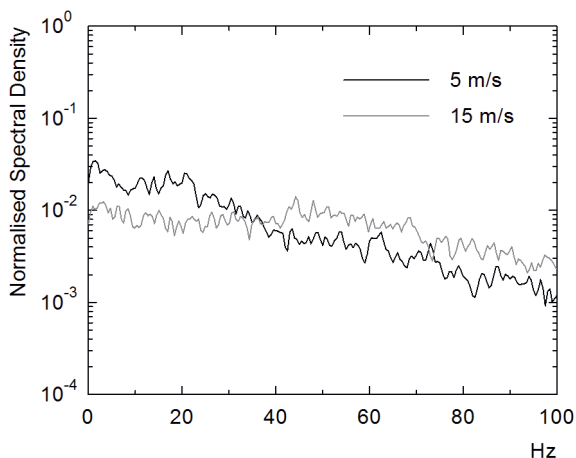


Fig.10.HWA wake spectra at a mid-span, trailing edge position (mid-point wake position, $T(\%)$ – turbulence intensity)

Discussion

The initial motivation for the measurements was to see if it was possible to decouple aerodynamic and structural frequencies by using the high sensitivity of the vibrometer. In a stalled aerofoil, shedding frequencies are often generated and generally follow well-presented characteristic Strouhal numbers. However, in all the measurements made here, although the surface flow visualization indicated separation regions on the aerofoil, the vibrometer consistently showed that the structural frequency of the blade dominated the results, without any evidence of aerodynamic shedding.

In an attempt to isolate this finding, given that the wake behind an aerofoil contains information on the flow upstream on the upper surface of the aerofoil, HWA measurements were then made at an area downstream of the blade which was thought to have the highest probability of separated flow. However, these results still did not allow the identification of any

dominant shedding frequencies, leading to the conclusion that, although the flow is stimulating the natural frequency of the blade, any local separation on the upper surface potentially leads to reattachment before leaving the leading edge of the blade. This effect would then both cause the blade to vibrate, but would also suppress significant fluctuations in the wake.

Hence future work could include more local HWA measurements adjacent to the top surface of the blade to confirm the reattachment phenomena. Alternatively, the vibrometer may be adapted for point wise measurements of density gradient near the trailing edge to interrogate the flow optically, particularly at the higher wind tunnel speeds. This may allow a more detailed investigation of both structural and aerodynamic frequencies. A further investigation may also include the use of a flow diagnostic method such as particle image velocimetry (PIV) [9] in selected regions, to examine wake structure or pressure side blade structure.

Conclusions

A fibre optic range-resolved vibrometer has been used to measure the vibration characteristics of a full scale Jetstream 31 propeller blade in a feathered position in a low speed wind tunnel. The measurements were made in an attempt to isolate the structural modes of the blade from the expected aerodynamic shedding frequencies, usually seen on a stalled aerofoil. However, although surface flow visualization indicated areas of separation on the aerofoil, the vibrometer spectra did not reveal any aerodynamic frequencies and subsequent hot-wire anemometry measurement also could not find any aerodynamic shedding characteristics.

Further work is now planned to interrogate the flow near the aerofoil surface and to develop an unsteady computational model to isolate any potential unsteady flow effects. The fibre optic vibrometer may also be adapted to measure density gradients, allowing more in-depth spectral characterization.

Acknowledgements

The authors would like to acknowledge the Cranfield University workshop staff at Shrivenham Defence Academy.

References

- [1] H.C. Watts, The Design of Screw Propellers: With Special Reference to Their Adaptation for Aircraft, Longmans (1920)

- [2] American Society of Mechanical Engineers, Historic Mechanical Engineering Landmarks, Hydromatic propeller, web reference <https://www.asme.org/about-asme/who-we-are/engineering-history/landmarks/149-hydromatic-propeller>, accessed April 2018
- [3] H. Jacques, Simulation of Propeller Effects on the Jetstream 31 Aircraft, Cranfield University, *MSc Thesis* (2014)
- [4] T. Kissinger, T.O.H. Charrett, and R.P. Tatam, Range-resolved interferometric signal processing using sinusoidal optical frequency modulation, *Opt. Express* 23(7), 9415–9431 (2015); doi: 10.1364/OE.23.009415
- [5] T. Kissinger, T.O.H. Charrett, S.W. James, A. Adams, A. Twin and R.P. Tatam. Simultaneous laser vibrometry on multiple surfaces with a single beam system using range-resolved interferometry, *In Proc. SPIE*, vol. 9525, p. 952520 (2015); doi: 10.1117/12.2183281
- [6] H.H. Brun. Hot-Wire Anemometry: Principles and Signal Analysis, OUP Oxford (4 May 1995), ISBN 978-0198563426.
- [7] S Yarusevych, SH Boutilier, Vortex Shedding of an Airfoil at Low Reynolds, *AIAA Journal* 49(10), 2221-2227 (2011); doi: 10.2514/1.J051028
- [8] K.B.M.Q. Zaman, D.J. McKinzie, C.L. Rumsey, A natural low-frequency oscillation of the flow over an airfoil near stalling conditions, *J.Fluid Mech.* 202, 403-442 (1989); doi: 10.1017/S0022112089001230
- [9] M Raffel, C.E. Willert, S. Wereley, J. Kompenhans, Particle Image Velocimetry: A Practical Guide, *Springer* Berlin (2007)

Optoelectronics System for Estimating Measurement Error of Image Pattern Correlation Technique

A.Yu. Poroykov¹, T. Kirmse², F. Boden², K.M. Lapitskiy¹, Yu.V. Ivanova¹, I.A. Lapitskaya¹

¹ National Research University "Moscow Power Engineering Institute"(MPEI), Krasnokazarmennaya 14, Moscow, 111250 Russia,

² German Aerospace Center (DLR), Bunsenstrasse 10, 37073 Göttingen, Germany
poroykovay@gmail.com

Abstract:

Photogrammetric methods for in-flight deformation measurements have undeniable advantages: e.g. contactless measurements, measuring the entire surface and the relative simplicity of the setup. During the European research projects Advanced In-Flight Measurement Techniques (AIM and AIM2) an implementation of the photogrammetric method – Image Pattern Correlation Technique (IPCT) has been proposed. It had been successfully applied in several flight test campaigns.

To evaluate the measurement error of photogrammetric methods either opto-geometric evaluations or digital modeling of synthetic images are commonly used. Some works indicate only error estimation, but without the explanation of its origin. The paper presents an approach for estimating the measurement error for the IPCT. An experimental system is developed including an imitator of the surface deformation and an additional optical sensor for measuring the present surface profile. The error is determined as a difference between the results of the optical sensor and the IPCT. The system allows to simulate a deformation with an amplitude of ± 25 mm on a surface area of 380×380 mm² in increments of 0.5 mm horizontally and 0.001 mm vertically, with a measurement accuracy of 0.075 mm. The system will be outlined in the paper and measurement results are presented.

Key words: optoelectronics system, deformation measurement, accuracy estimation, photogrammetry, IPCT.

Introduction

The problem of surface deformation measurement occurs in many branches of science and technology. It can be found in the automotive industry, construction and aviation.

Different methods can be used to solve this problem. All of them can be conditionally divided into three groups: methods using strain-gauge, piezoelectric and mechanical sensors, optical and photogrammetric methods.

The principle of operation of the first group of methods is based on effects like tensor resistive effect, direct piezoelectric effect and others. To measure deformations surface-distributed sensor arrays can be used. Disadvantages of such methods are the locality of the measurements, direct contact of the sensing element with the test sample, the need for calibrating the sensors, and the influence of environmental factors on the measurement results.

The methods of the second group - optical methods, have an important advantage over the methods of the first - they are non-intrusive. The second group includes many different optical methods: the grid method [1], the moiré method [2], the photoelasticity method [3], the method of holographic and speckle-interferometry [4-5]. The shortcomings of optical methods include the need to make exact copies of the test samples, the complexity of processing the obtained results, and the need to use complex optical systems.

So for in-flight measurements most methods of the first and the second group involve a large installation effort. The third group – photogrammetric methods can be partially attributed to optical methods. However, it is based on digital signal processing with minimal use of optical systems.

The Image Pattern Correlation Technique (IPCT) is a modern implementation of the photogrammetric methods for measuring deformations based on digital image processing

[6-8]. This non-intrusive method captivates by its simple experimental setup. It requires two digital cameras, a correlation pattern on the surface to be measured and a computer for image acquisition and processing using modern image processing algorithms. Therefore, this method is well suited for the use in field experiments such as in-flight measurements.

To determine the deformation of the object a special correlation pattern is applied to the investigated areas. Generally, the pattern consists of randomly placed dots. Images of pattern are obtained with digital cameras before and after deformation. Further cross-correlation processing of the registered images allows to calculate the displacement field of the pattern. This field can be used to reconstruct the deformed surface profile by means of triangulation.

Although the method itself is relatively easy to implement, the analysis of its measurement error is difficult because of the multiple parameters which influences the accuracy of the method like the calibration of the camera and the use of cross-correlation to determine point correspondences in the stereo views. Therefore, it is difficult to estimate the error

using direct calculations. In general, either opto-geometric evaluations [9-13], or digital modeling of synthetic images [14-15] are commonly used for its estimation. However, these approaches cannot take into account all the factors that arise in real experiments. This problem can be solved by comparing the results of IPCT measurements with the results of measurements obtained by another reference method. This approach will allow to take into account all the factors influencing the error, and to estimate it within the frame of the accuracy of the reference method.

Measurement Techniques

For the automation of measurements, a software and hardware optoelectronics system was created to estimate the IPCT measurement error by MPEI. It is based on the simple idea to use a surface whose deformation occurs in a given way (an imitator of a deformable surface) and a high-precision optical sensor which can precisely measure surface deformation. Comparing the results obtained by sensor and by IPCT we can estimate the absolute error of the photogrammetric measurements within the scope of the error of the optical sensor.

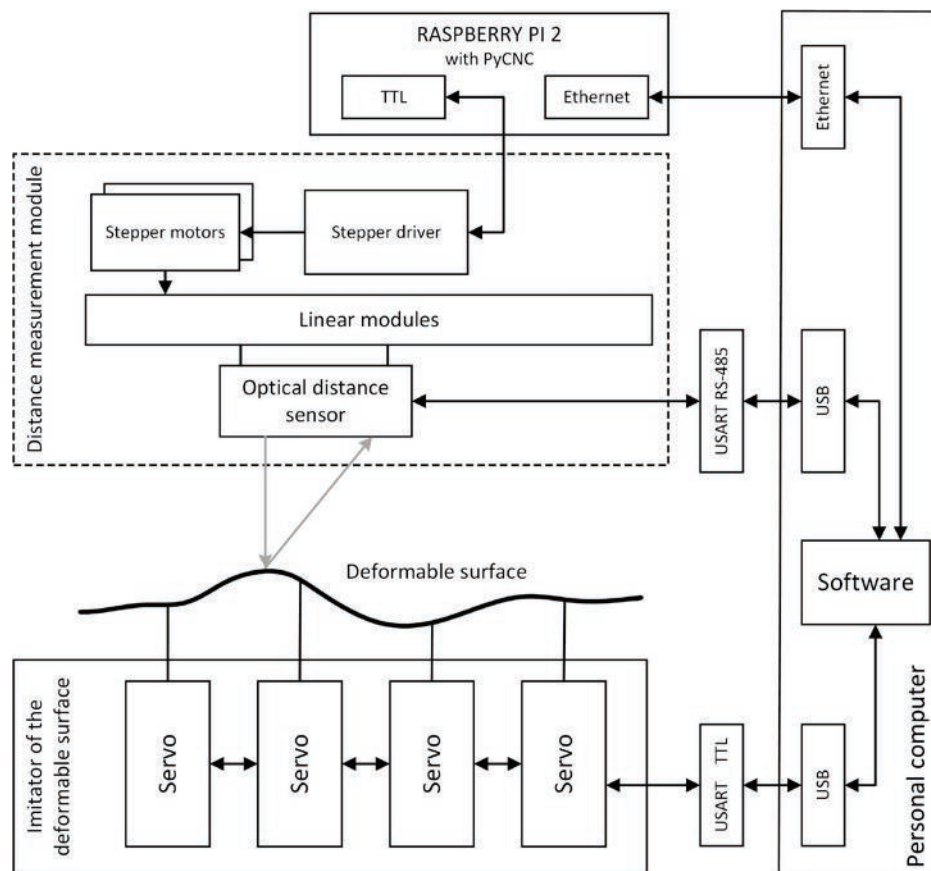


Fig. 1. The functional scheme of the optoelectronics system for estimating IPCT measurement error

To measure the entire surface by one sensor, linear displacement modules with stepper motors were used. The sensor measures the distance to the surface at a grid of points of a defined distance by moving above the surface in two perpendicular directions. Stepper motors allow to control the position of the sensor with increments of 0.1 mm and error no more than 0.5 mm.

The proposed system consists of three main components: an imitator of a deformable surface, a module for measuring the distance to the surface and software for a personal computer. The functional scheme of the system is shown in Fig 1.

The imitator of the deformable surface consists of an aluminum base and several servos fixed on it. Each servo is rigidly connected to a section of a flexible plate located above the servos. The plate acts as a deformable surface with an area of $380 \times 380 \text{ mm}^2$. The total number of servos is 16. They are evenly distributed under the plate. Changing the position of the servo arm leads to a proportional displacement of the plate part above it in the vertical direction. The amplitude of the displacements for each servo is $\pm 25 \text{ mm}$. Appearance of the imitator of the deformable surface is shown in Fig. 2.

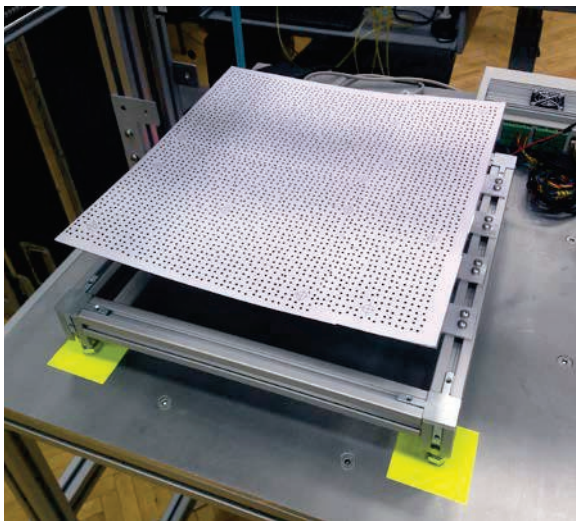


Fig. 2. Appearance of the imitator of the deformable surface

The module for measuring the distance to the surface consists of two linear displacement modules perpendicular to one another and optical sensor. Their lengths are 500 mm for X direction and 400 mm for Y direction. The optical sensor LS5-40/50 "NPP PRIZMA" measures distance based on the triangulation of the laser beam reflected from the measured surface. Sensor has a resolution of 0.001 mm and an error of not worse than 0.075 mm in the range of distances of 50 mm and the minimal

distance to the sensor of 40 mm. The spot size of the laser beam of the sensor in the middle of the measurement range is $175 \mu\text{m}$ and does not exceed $300 \mu\text{m}$ in the entire range.

The software part is designed to control the entire installation as a whole: setting the positions of the servos (deformation of the object) and displaying the results of the distance measuring unit to the surface using a graphical interface.

The software part of the test setup was developed in C# and Python language for a personal computer. The program allows to set the positions of each servo separately and displays the distances to the surface measured by the sensor.

System Distance Measurement Accuracy

An experimental investigation was carried out to estimate the accuracy and repeatability of the optical sensor data for the complete measurement volume. For this purpose we used a granite surface plate with grade 00, which provides non-flatness no more than $3 \mu\text{m}$ on its area of $400 \times 400 \text{ mm}^2$.

The method of investigation consisted in the multiple measurement of the same points on the surface of the plate at different moments of time. 400 points were uniformly distributed over the entire surface of the plate. Every day from 5 to 20 measurements of the entire surface of the plate were carried out. For all measurements for one day, the average deviation from the mean for each point was calculated, and then they were averaged. The obtained data is presented in Fig. 3.

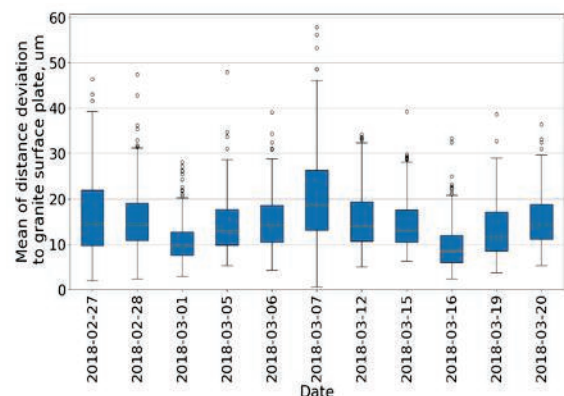


Fig. 3 Mean of distance deviation to granite surface plate

Results show us that accuracy and repeatability of measurement by the optical sensor are lower than the declared value of instrumental error of the sensor. Thus, the developed system can be successfully used to measure the surface of a deformed surface to estimate error of photogrammetric methods.

Stereo System Calibration

To obtain reliable information about the error of the photogrammetric method, it is necessary to calibrate the cameras as accurately as possible. Another important thing is to link the object coordinates (in which the measurement is carried out by IPCT) with the coordinates in which optical sensor is moving above the surface.

The calibration process is to align points of the three-dimensional coordinate space with two-dimensional points on the image. We suggest to use an optical sensor for allocating a point in space. The coordinates x and y of the light spot from the sensor are set in the three-dimensional coordinates (Fig. 4a) by changing optical sensor position above the surface.

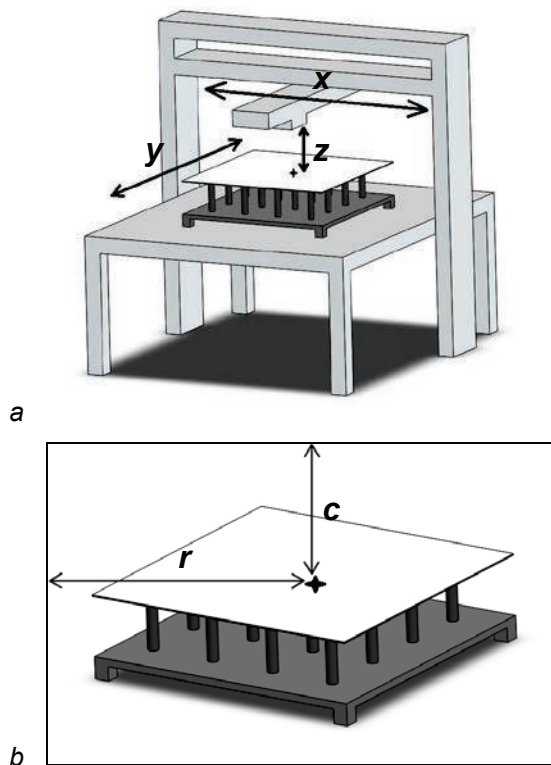


Fig. 4 Scheme of stereo system calibrating in proposed optoelectronics system:

a – scheme of determine three-dimensional coordinates; *b* – scheme of determine two-dimensional coordinates on image

The coordinate z corresponds to the measured value of the distance to the surface, which can be varied with the imitator of the deformable surface. On the images obtained from the cameras (Fig. 5) we can determine the two-dimensional coordinates r and c (Fig. 4b) by means of digital processing.

In experimental investigations a small value of the aperture diaphragm is used to increase the depth of field of the imaged space. This

requires the use of additional lighting to obtain high-quality images for the IPCT. The additional illumination is not used during the calibration process which facilitates the determination of the spot light position of the optical sensor within the camera image.

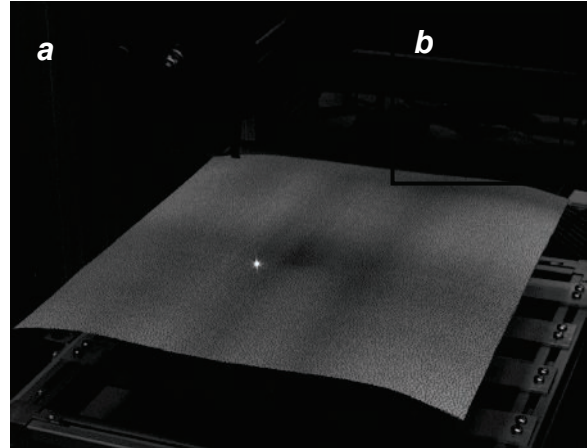


Fig. 5 Experimental image of a background pattern with a light spot:

a – image obtained by camera; *b* – enlarged image of a light spot

The image processing searches for an associated object with total intensity greater than the specified value by means of threshold filtering to filter glares on the parts of the experimental setup. In a next step the object coordinates are calculated by center of mass method. The calibration procedure is fully automated by the software written in Python using the OpenCV library. As a calibration model the Hall method is used [16].

Experimental results

We used the following scheme of the experiment for estimating IPCT measurement error. One cycle of the experiment consists of the following steps:

1. The software randomly sets the position of the servos forming a deformation of the test surface on the imitator.
2. A stereo camera system captures images of the deformed surface and transfers them to a personal computer, where they are processed by the developed IPCT evaluation software, which delivers the surface as result.
3. The optical sensor moves by linear modules with stepper motors above the surface and measures the distance to it at several specified points.
4. The distances to the surface at these points are compared with the position of the points on the reconstructed surface profile. Thus, the desired error is estimated.



Fig. 6. The appearance of the optoelectronics system for estimating IPCT measurement error:

a – cameras stereo system; *b* – the imitator of deformable surface; *c* – linear modules with stepper motors; *d* – the optical distance sensor; *e* – the computer with developed software

After storing the results of the steps 1-4 are repeated. The random deformation of the surface and many repeated measurements deliver a good statistical basis for the error estimation of an IPCT-setup.

In the first step the focus of the work was set to the development of the test bench consisting of the imitator of the surface deformation and an additional optical sensor. In the next step the IPCT evaluation software has to be improved. Nevertheless for the demonstration of the principle functionality of the complete system a simple IPCT evaluation routine was already implemented.

In the experimental investigation the stereo system of two Baumer VLG-24M video cameras were used. The cameras are equipped with a 1/1.2" CMOS Sony IMX249 sensor with a resolution of 1920×1200 pixels and a pixel size of 5.86×5.86 μm. For the control and image acquisition of the cameras the Baumer API and special designed C++ Python extension were used. The processing of the obtained images was carried out using fast Fourier transform algorithms [17].

The appearance of the system for automatic IPCT error determination is shown in Fig. 6.

In the experiment the distance from the cameras to the center of the surface was 1350 mm. The inclination of the cameras to the surface was 20°. Fujinon HF25HA-1B lenses

with a focal length of 25 mm and a relative aperture of 1:1.4 were used.

The example of the system measurement results is presented in Fig. 7. The profile of the deformed surface reconstructed by IPCT is shown in Fig. 7a. It was obtained by calculating 568 displacement vectors with a window of 128×128 pixels. The profile of the deformed surface reconstructed by optical sensor is shown in Fig. 7b. It was obtained by measuring at 121 points in 38 mm steps.

The difference between these two profiles (shown in Fig. 7c) is the result which allows estimating the error of the IPCT-measurement. The average value of the difference was 0.617 mm and its standard deviation was 0.358 mm.

Conclusions

The paper presents an approach for estimating the measurement error for the IPCT. An experimental system is developed including an imitator of the surface deformation and an additional optical sensor for measuring the present surface profile. The error is determined as a difference between the results of the optical sensor and the IPCT. The system allows to simulate a deformation with an amplitude of ±25 mm on a surface area of 380×380 mm² in increments of 0.5 mm horizontally and 0.001 mm vertically, with a measurement accuracy of 0.075 mm.

The accuracy of the IPCT is influenced by many factors like the camera calibration, the stereoscopic setup and the accuracy in the determination of point correspondences in the

stereo views. The presented optoelectronic system enables a detailed investigation of different influence factors to the accuracy of IPCT for a further improvement of the method.

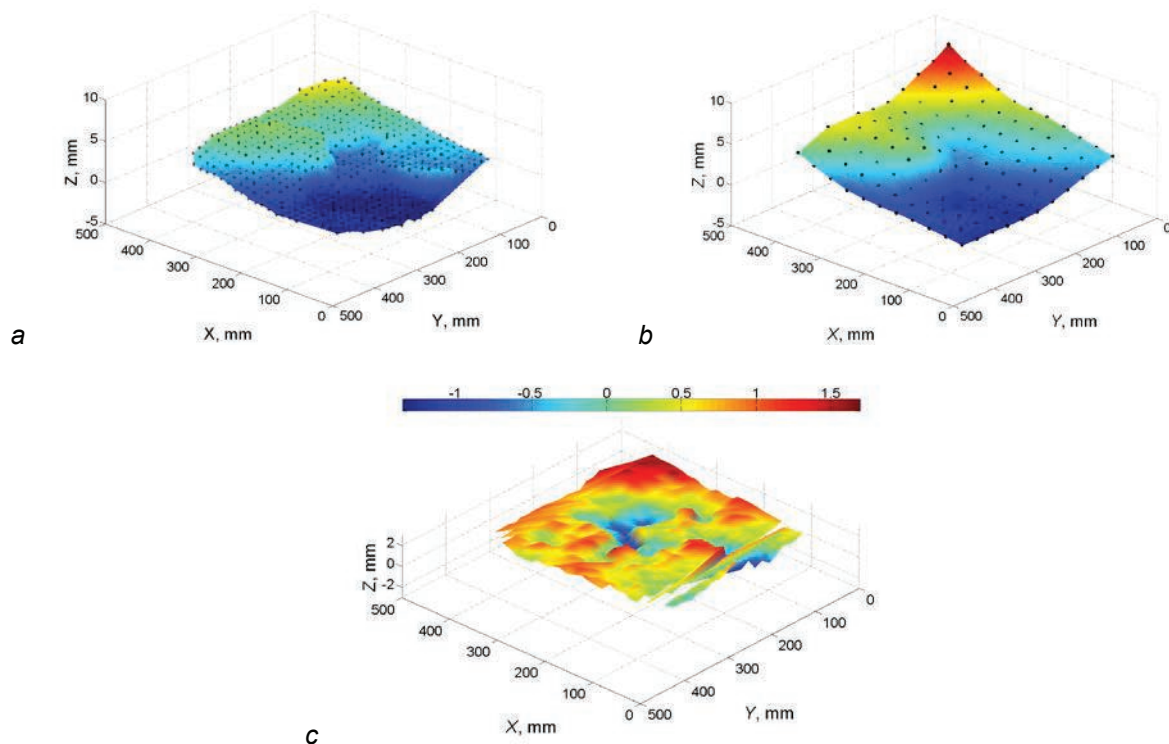


Fig. 7. The example of the system measurement results:

a – The profile of the deformed surface reconstructed by IPCT; b – The profile of the deformed surface reconstructed by optical sensor; c – The difference between reconstructed profiles

References

- [1] M. Grediac, F. Sur, B. Blaysat, The Grid Method for In-Plane Displacement and Strain Measurement: a Review and Analysis, *Strain*, 53(3), 205-243 (2016); doi: 10.1111/str.12182
- [2] D. Tomita, M. Fujigaki, Y. Murata, Deformation Distribution Measurement from Oblique Direction Using Sampling Moire Method, *Advancement of Optical Methods in Experimental Mechanics*, 3, 197-204 (2015); doi: 10.1007/978-3-319-06986-9_22
- [3] N.K. Raghuwanshi, A. Parey, Mesh Stiffness Measurement of Cracked Spur Gear by Photoelasticity Technique, *Measurement*, 73, 493-452 (2015); doi: 10.1016/j.measurement.2015.05.035
- [4] A. Sánchez, H. Manuel, F.M. Santoyo, T. Saucedo-A, D. Reyes, Simultaneous 3D Digital Holographic Interferometry for Strain Measurements Validated with FEM, *Optics and Lasers in Engineering*, 52, 178-183 (2014); doi: 10.1016/j.optlaseng.2013.06.013
- [5] Y. Arai, Simultaneous In-Plane and Out-of-Plane Deformation Measurement by Speckle Multi-Recording Method, *Measurement*, 91, 582-589 (2016); doi: 10.1016/j.measurement.2016.05.037
- [6] F. Boden, N. Lawson, H.W. Jentink, J. Kompenhans (Eds), *Advanced In-Flight Measurement Techniques*, 344 (2013); doi: 10.1007/978-3-642-34738-2
- [7] R. Meyer, T. Kirmse, F. Boden, Optical In-Flight Wing Deformation Measurements with the Image Correlation Technique, *New Results in Numerical and Experimental Fluid Mechanics IX*, 124, 545-553 (2014). Springer, Cham; doi: 10.1007/978-3-319-03158-3_55
- [8] A.Y. Poroikov, Reconstruction of 3D Profile of a Deformed Metallic Plate by Means of the Image Pattern Correlation Technique, *Measurement Techniques*, 57(4), 390-395 (2014); doi: 10.1007/s11018-014-0466-4
- [9] B. Wieneke, PIV Uncertainty Quantification from Correlation Statistics, *Measurement Science and Technology*, 26 (7), 074002 (2015); doi: 10.1088/0957-0233/26/7/074002
- [10] N.J. Lawson, J. Wu, Three-Dimensional Particle Image Velocimetry: Error Analysis of Stereoscopic Techniques, *Measurement Science and Technology*, 8(8), 894-900 (1997); doi: 10.1088/0957-0233/8/8/010

- [11] N.J. Lawson, J. Wu, Three-Dimensional Particle Image Velocimetry: Experimental Error Analysis of a Digital Angular Stereoscopic System, *Measurement Science and Technology*, 8(12), 1455-1464 (1997); doi: 10.1088/0957-0233/8/12/009
- [12] F. Boden, T. Kirmse, A.Yu. Poroikov, B.S. Rinkevichyus, N.M. Skornyakova, I.A. Shashkova, Accuracy of Measurement of Dynamic Surface Deformations by the Image Pattern Correlation Technique, *Optoelectronics, Instrumentation and Data Processing*, 50(5), 474-481 (2014); doi: 10.3103/S8756699014050057
- [13] V.P. Kulesh, Measurements of Deformation of the Adaptive Wing Leading Edge in a Wind Tunnel by the Videogrammetry Method, *TsAGI Science Journal*, 45, 993-1006 (2014); doi: 10.1615/TsAGISciJ.2015013557
- [14] F. Scarano, M.L. Riethmuller, Iterative Multigrid Approach in PIV Image Processing with Discrete Window Offset, *Experiments in Fluids*, 26(6), 513-523 (1999); doi: 10.1007/s003480050318
- [15] C. Willert, The Fully Digital Evaluation of Photographic PIV Recordings, *Applied Scientific Research*, 56(2-3), 79-102 (1996); doi: 10.1007/BF02249375
- [16] J. Salvi, X. Armangué, J. Batlle, A Comparative Review of Camera Calibrating Methods with Accuracy Evaluation, *Pattern recognition*, 35(7), 1617-1635 (2002); doi: 10.1016/S0031-3203(01)00126-1
- [17] M. Frigo, S.G. Johnson, The Design and Implementation of FFTW3, *Proceedings of the IEEE*, 93(2), 216-231 (2005); doi: 10.1109/JPROC.2004.840301

Application of Fibre Bragg Grating Sensors to a Stalled High Lift Wing

*Erica Alcusa-Saez, Stephen W. James, Simon Prince, Edmond Chehura,
Nicholas J. Lawson and Ralph P. Tatam*

*School of Aerospace, Transport and Manufacturing, Cranfield University, Cranfield, MK43 0AL, UK
s.w.james@cranfield.ac.uk*

Abstract

An array of optical fibre Bragg grating strain sensors attached to a high lift wing configuration in a low speed wind tunnel has been used to monitor successfully the steady flap deflection and the fluid shedding frequency generated by the flap. The shedding frequencies match closely those obtained previously using hot wire anemometry.

Key words: Optical fibre sensors, fibre Bragg gratings, shedding frequencies, high lift wing, flap deflection, wind tunnel.

Introduction

The aerofoils of unmanned aerial vehicles and small scale wind turbines often operate at low chord Reynolds numbers, making them prone to the development of a separated shear layer arising from boundary-layer separation. Depending on the Reynolds number and the angle of attack, this can lead to the formation of separation bubbles and vortex shedding, which negatively affect aerofoil performance [1] and can impart unsteady forces to the aerofoil, causing flutter. There has been interest in characterizing such flow features by measuring the surface pressure distribution along the span, determined using a number of pressure taps [1], and by monitoring the wake using hot wire anemometers and the structural vibration of the aerofoil using accelerometers [2].

Optical fibre sensors (OFS) are becoming viable replacements for traditional wind tunnel and flight test sensors. OFS systems capable of measuring geometry, strain, pressure and temperature - the main measurement variables of interest for basic aerodynamic analysis - are becoming well established in industrial sectors such as oil and gas and wind energy, and there is a long-standing interest in their use in wind tunnel and aircraft structural health monitoring [3-7] and wing shape measurement [8, 9].

The key benefits of OFS that drive this interest include their immunity to electromagnetic interference, the low weight of the sensor elements, the ability to embed optical fibres into composite materials or to surface mount, with a low profile, to metals, and the ability to perform

multiplexed or distributed measurements within a single length of optical fibre.

The focus of this paper is on the use of optical fibre Bragg grating sensors (FBGs) to undertake measurements of the dynamic aerodynamic loading on a high lift wing in a wind tunnel in order to determine parameters of aerodynamic interest; the steady flap deflection and the shedding frequency.

Optical Fibre Bragg Gratings

An FBG consists of a periodic modulation of the refractive index of the core of an optical fibre, which reflects a specific wavelength the Bragg wavelength, back along the optical fibre, all other wavelengths pass through the grating [10]. The Bragg wavelength, λ_B is dependent upon the period of the grating, Λ and the refractive index of the propagating mode, n_{eff} , according to

$$\lambda_B = 2n_{\text{eff}}\Lambda \quad (1)$$

Typically, the refractive index modulation is introduced to the optical fibre by illuminating the fibre from the side with a spatially modulated UV laser beam [11]. The reflected Bragg wavelength is sensitive to perturbation of the grating structure by parameters such as strain and temperature. The measurement of the Bragg wavelength forms the basis of FBG sensing [12]. The strain sensitivity of an FBG arises from a combination of the physical change in the period of the grating and the change in the refractive index of the fibre via the elasto-optic effect

$$\Delta\lambda/\lambda_B = (1-p)\epsilon \quad (2)$$

Where p is the elasto-optic coefficient (0.22 for silica), ε the strain, and $\Delta\lambda$ is the change in Bragg wavelength. For an FBG fabricated in standard telecommunications optical fibre (SMF28), the sensitivity is $1.2 \text{ pm}/\mu\varepsilon$.

A major advantage of FBG technology is that an array of uniquely identifiable sensors can be multiplexed within a single length of optical fibre by fabricating each FBG in the array with a different grating period, and thus a different Bragg wavelength at quiescent conditions [12]. While a number of approaches to the interrogation of FBG sensor arrays have been reported, the majority of commercially available interrogation units employ a wavelength-swept laser to illuminate the sensors, and a photodiode to detect the reflected signals.

Experiment

5 FBGs were fabricated in a length of SMF-28 optical fibre that had been hydrogen loaded to increase its photosensitivity. The fibre was side-illuminated via a phase mask using the output at a wavelength of 266 nm from a frequency quadrupled flashlamp pumped Nd:YAG laser. A different phase mask was used for the fabrication of each FBG, such that, in their quiescent states, the FBGs were of different Bragg wavelengths, and thus could be multiplexed in the wavelength domain. Prior to exposure, the polyacrylate buffer jacket was removed from the sections of fibre into which the FBGs were to be written. Each FBG was of length 4 mm with a typical reflectivity of 50% and 3 dB bandwidth of 0.5 nm. The sections of optical fibre containing the FBGs were not subsequently recoated.

The 2D, 3 element high lift wing configuration, comprising a single slotted leading edge slat, a main element and a single slotted trailing edge flap is shown schematically in Figure 1.

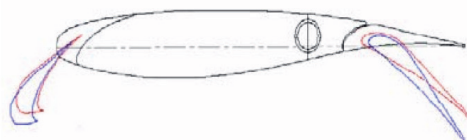


Fig. 1. 2D 3 element high lift wing

The wing has a stowed chord of 0.6 m and a span of 1.4 m. The FBG sensors were bonded to the surface of the trailing edge flap, having chord length of 180 mm, oriented along the spanwise direction, 140 mm from the trailing edge, using cyanoacrylate adhesive. The physical arrangement of the FBGs is illustrated in Fig. 2, where FBG 3 was positioned at the

mid-point of the span of the slat. The fibre was terminated with an FC/APC connector to allow connection to the FBG interrogator.

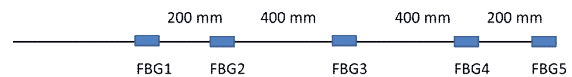


Fig. 2. Arrangement of FBG sensor array

The FBG sensor array was interrogated using a SmartScan Aero Interrogator (Smart Fibres, UK). The interrogator has a data rate of 2.5 kHz, a wavelength scan of 40 nm, a resolution of 1pm and can monitor 16 wavelength division multiplexed FBGs in a single optical fibre. The interrogator can be used to monitor up to 4 fibres simultaneously.

The wing was suspended between two 1.2 m diameter circular end plates, as is shown in Figure 3, to facilitate its mounting vertically in an 8x6 foot wind-tunnel such that its angle of attack was adjustable. The wind speed could be changed from 0 m/s to a maximum of 42 m/s.



Fig. 3. The 2D 3 element high lift wing mounted in a 8x6 foot wind-tunnel

Wing angles of attack in the range 0° to 20° were selected to initiate a stall characteristic off the flap section, allowing the use of the FBGs to detect the excitation of the slat at the fluid shedding frequencies. For each angle of attack the wind speed was varied from 16 m/s to 40 m/s, giving a Reynolds number range based on flap chord of 195,000 to 488,000. The signals from the FBGs were acquired over a duration of 10s at each wind speed and subsequently filtered to reduce the noise. The frequency content of the strain data was calculated using a fast Fourier transform.

Results and Discussion

Figures 3(a) and (b) show the changes in load experienced by the slat at the locations of the 5 FBG sensors at two angles of attack; 0° and 20° as the wind speed was increased from 0 to 40 m/s, held at 40 m/s and subsequently reduced to 0 m/s. This illustrates the ability of the sensors to monitor the steady flap deflection. The distribution of the strain shows that for the steady measurement the strain is largest at

center of the slat, and the loads are larger for high angles of attack. This is consistent with an aerofoil up to a stall condition.

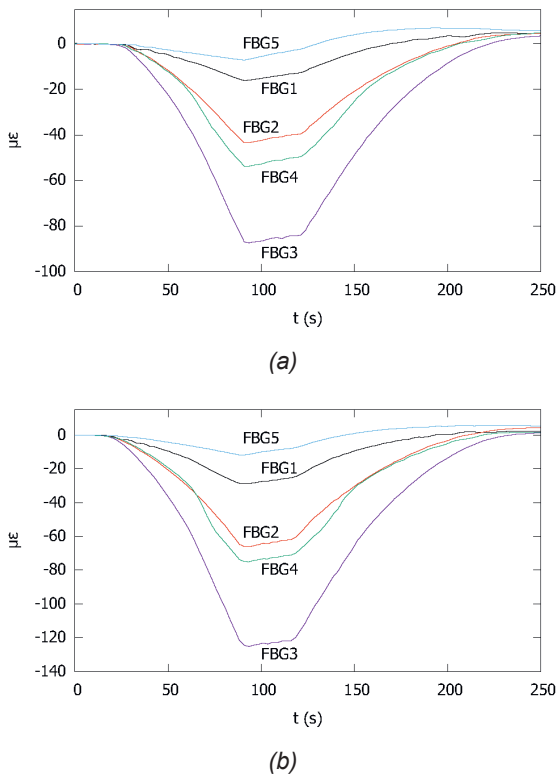


Fig. 3. Strain measured by the FBG sensors with increasing wind speed, at angles of attack (a) 0° and (b) 20°

Fig. 4 shows the power spectra of the signals obtained from FBG 3 for an angle of attack of 20° at three wind speeds, 16 m/s, 20 m/s and 24 m/s. Each spectrum exhibits a dominant frequency, which increases with increasing wind speed.

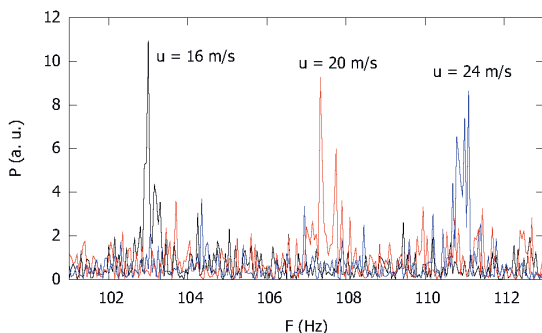


Fig. 4. Power spectrum of the strain data obtained from FBG 3 with increasing wind speed (u), at an angle of attack 20° .

Figures 5 (a) and (b) show the variations in the shedding frequency with wind speed for 0° and 20° angles of attack. The frequency shows a sigmoidal dependence upon wind speed, and the frequency increases with increasing angle of attack. This is consistent with previous

reports [1,2]. The amplitude of the frequency component was dependent upon the location of the sensor (data not shown here), suggesting that the FBGs were sampling the vibration mode shape in the span-wise direction. This is the subject of further investigation.

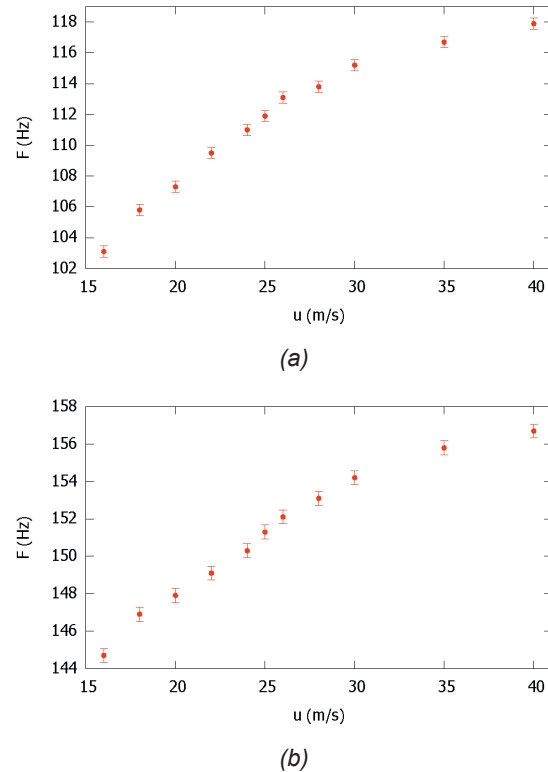


Fig. 5. Variation in shedding frequency (f) plotted as a function of wind speed (u) for angles of attack (a) 0° and (b) 20°

From Figure 5, if the Strouhal number (St) is calculated based on flap chord, it is equivalent to St in the range 0.1 – 0.5. This compares with previous work on aerofoils with a similar Reynolds number range [1,2], where reported Strouhal numbers were in the range 0.15 – 0.25. The higher upper limit of the Strouhal number measured in the present tests, which occur at the lower wind speeds at the highest angle of attack, is thought to be due to separations on the main element and possibly high frequency oscillations of a separation bubble on the flap. A second set of tests together with a study using high resolution computational fluid dynamics aims to shed more detail on this complex flow physics.

Summary

An array of five FBG sensors was bonded to the slat of a high lift wing configuration, and used to monitor the static and dynamic loads experienced by the slat when the wing was subject to wind speed of 0 – 40 m/s in a low speed wind tunnel. The FBGs were able to

detect the excitation of the flap at the fluid shedding frequencies characteristic of the aerofoil stall at angles of attack between 0° and 20° . Shedding Strouhal numbers were consistent with those reported in the literature for flows at similar Reynolds number, but more study is needed to properly interpret these results.

Thus, the preliminary results presented here show that the FBG system has successfully detected both the steady flap deflection and the associated shedding frequency in a stall, with dominant spectral frequencies ranging from around 100Hz to 160Hz, which closely matches expected frequencies reported from previous hot wire anemometry data.

References

- [1] Yarusevych S and Boutilier M S H, Vortex Shedding of an Airfoil at Low Reynolds Numbers *AIAA J.*, 49, 2221 – 2227 (2011);doi: 10.2514/1.J051028.
- [2] Zaman K, McKinzie D J and Rumsey C L, A natural low-frequency oscillation of the flow over an airfoil near stalling conditions, *J. Fluid Mech.* 202, 403-442 (1989); doi: 10.1017/S0022112089001230
- [3] Read I J and Foote P D Sea, and flight trials of optical fibre Bragg grating strain sensing systems *Smart Mater. Struct.* 10, 1085–94 (2001); doi: 10.1088/0964-1726/10/5/325
- [4] Lee J-R, Ryu C-Y, Koo B-Y, Kang S-G, Hong C-S and Kim C-G, In-flight health monitoring of a subscale wing using a fiber Bragg grating sensor system *Smart Mater. Struct.* 12 147–155 (2003); doi: 10.1088/0964-1726/12/1/317
- [5] Papageorgiou A W, Karas A R, Hansen K L, Arkwright J W, Monitoring pressure profiles across an airfoil with a fiber Bragg grating sensor array, *Proc. SPIE*, 10539, 105390C (2018); doi: 10.1117/12.2288024
- [6] Singh D B and Suryanarayana G K Application of Fiber Bragg Grating Sensors for Dynamic Tests in Wind Tunnels, *J. Indian Institute of Sci.*, 96, 47-52 (2016).
- [7] Correia R, Staines S E, James S W, Lawson N, Garry K and Tatam R P Wind tunnel unsteady pressure measurements using a differential optical fiber Fabry-Perot pressure sensor, *Proc. SPIE* 9157, 915708 (2014); doi: 10.1117/12.2059631
- [8] Lawson N J, Correia R, James S W, Partridge M, Staines S E, Gautrey J E, Garry K P, Holt J C and Tatam R P Development and application of optical fibre strain and pressure sensors for in-flight measurements, *Meas.Sci.Technol.* 27, 104001 (2016); doi: 10.1088/0957-0233/27/10/104001/.
- [9] Ko W L, Richards W L and Fleischer V T, Applications of Ko displacement theory to the deformed shape predictions of doubly tapered ikhona wing NASA/TP-2009-214652 (2009).
- [10] Jutte C V, Ko W L, Stephens C A, Bakalyar J A, Richards W L and Parker A R Deformed shape calculation of a full-scale wing using fiber optic strain data from a ground loads test NASA/TP-2011-215975 (2011).
- [11] Kashyap R, *Fibre Bragg Gratings* (2nd Edition) Academic Press (2009).
- [12] Bennion I, Williams J A R, Zhang L, Sugden K and Doran N J, UV-written in-fibre Bragg gratings *Opt Quant Electron* 28, 93-135 (1996); doi: 10.1007/BF00278281.
- [13] Othonos A, Fiber Bragg gratings, *Rev. Sci. Instrum.* 68, 4309 (1997); doi:10.1063/1.1148392

Optical Rotor-Blade Deformation Measurements using a Rotating Camera

Fritz Boden¹, Bolesław Stasicki¹, Krzysztof Ludwikowski²

¹ *German Aerospace Center, Institute of Aerodynamics and Flow Technology, Göttingen, Germany*

² *HARDsoft Microprocessor Systems, Kraków, Poland*

fritz.boden@dlr.de

Abstract:

For the design of rotors for helicopters or wind turbines, the knowledge of movements and deformations of the rotor blades is important. Measuring these parameters in the rotating system is difficult, because the number of sensors is limited due to their impact on the aerodynamics and the modification of the structure. Strain gauge measurements furthermore can be affected e.g. by the sensor location or temperature effects. To avoid those problems and in addition enable direct shape measurements, optical methods have been applied to rotor deformation measurements in the past. These attempts have been done out of the rotating frame observing either only small rotors or the blade passing the field of view. DLR and Hardsoft developed a rotating 3D imaging system for helicopter rotors and performed tests on the whirltower of Airbus Helicopters in Donauwörth (GER). The system is mounted on the hub and co-rotates with the rotor. It is able to record images of the whole blade at each azimuth angle. Those images later are processed with an Image Pattern Correlation Technique (IPCT) software tool and deliver the 3D surface shape and location of the observed blade. The paper briefly describes the rotating camera system, the non-intrusive deformation measurement method IPCT and the measuring setup, as well as the obtained data and a discussion of the measurement results.

Key words: IPCT, rotating camera, blade deformation, optical measurements, stereoscopic imaging

Introduction

For the proper design and the secure operation of rotor systems the occurring blade deformations and movements are of great importance. Especially for blades with a high aspect ratio like on helicopter main rotors or wind turbines the knowledge about the flapping motions and the blades behavior at the natural frequencies is crucial.

Usually for modal analysis and testing accelerometers and strain gauges are applied. For measurements on the rotating blades commonly strain gauges are preferred, because any sensor placed on the surface should affect the aerodynamic properties as little as possible and thus the sensor size should be very small. The measured strains can be twice integrated in order to obtain the blade twist and bending. To perform this calculation insufficient accurate way, a large number of measuring stations is required. If the expected mode shapes are known (e.g. by numerical calculations) and the strain gauge bridges are placed in a clever way the so called strain pattern analysis (SPA)[1] can be applied in order to identify the blade

deformation with less sensors. In order to obtain good measurement results, strain gauge measurements should be performed accurately by experienced and skilled staff to minimize the main error sources such as the mounting procedure, transverse sensitivity, temperature effects, humidity effects, strain cycling, fatigue and cable effects [2]. For increasing the accuracy and enabling a little bit larger number of measurement locations fiber Bragg grating (FBG) sensors can be used for a strain-based modal analysis [3]. But also those sensors are effected by the ambient conditions and require an accurate installation by experienced staff.

To avoid the problems mentioned above and in addition enable direct shape measurements contactless optical methods have still been applied to rotor and propeller deformation measurements in the past [4]-[8]. These attempts have been done with measurement devices out of the rotating frame observing either only small rotors or the blade passing within the field of view. Former recordings with rotating camera devices on helicopter rotors have been performed just to visualize the flow

over the blades [9] or to determine the motion of the rotor blade [10].

Based on their experience from the in-flight application of a rotating camera on an aircraft propeller [11], DLR in cooperation with Hardsoft developed a rotating 3D image acquisition system for helicopter rotors [12] and performed first tests on the whirltower of Airbus Helicopters in Donauwörth, Germany. The system is mounted on the hub and co-rotates with the rotor. It includes four CMOS camera sensors and a complete data acquisition system and is able to record images of the whole blade at each azimuth angle. Later, those images are processed with an IPCT software tool and deliver the continuous 3D surface shape and location of the observed blade. From the comparison of the 3D surfaces for different recordings, the bending and torsion of the blade can be obtained. In what follows this rotating camera system, the IPCT method as well as some example results are given.

Design of the rotating camera system

In the simplest case a rotating camera system can be realized by a single motion picture camera mounted on the hub co-rotating with the rotor and observing a part of one blade [9]. For qualitative observation of the flow or the blade movements such a system fulfils all requirements, but if quantitative shape and deformation measurements are intended to be performed, such a system should comprise digital imaging sensors best in a stereoscopic arrangement. Such a rotating stereo camera system for 3D blade deformation measurements has been realized by the authors in the past on a propeller aircraft [11].

To observe a complete helicopter main rotor blade, being an object with a high aspect ratio viewed under a flat viewing angle, it was decided to build a double stereo vision system consisting of four lightweight Ximea XiQ MQ042MG-CM global shutter cameras in two stereoscopic arrangements with overlapping fields of view (Fig. 1) in order to enable imaging with sufficient resolution for optical deformation measurements. The cameras each have a resolution of 2,048 pixels x 2,048 pixels with a maximum frame rate of 90 fps. The applied lenses as well as the positions of the cameras including the height above the rotor and the base distance between the two cameras of each stereoscopic system iteratively have been chosen in order to obtain an optimum between the size of the field of view and the inaccuracy of the deformation measurements. In Fig. 2 the estimation of the measurement inaccuracy of the final camera setup calculated according to [13] is depicted.

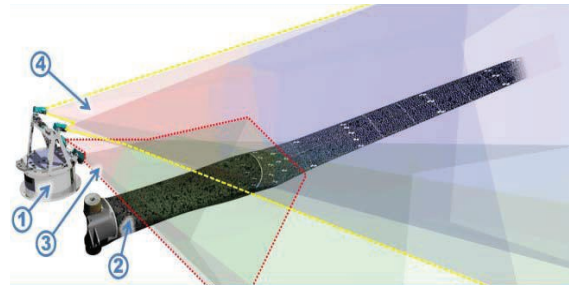


Fig. 1. Fields of view of the rotating camera system for rotor blades (1 - rotating camera system, 2 - observed rotor blade, 3 - field of view of the lower cameras, 4 - field of view of the upper cameras).

The cameras of the lower stereo-system have C-mount lenses with a focal length of $F = 12$ mm, a base distance B of around 250 mm and are located approximately 400 mm above the rotor. They observe the control cuff and the rotor blade attachment with an estimated measurement inaccuracy of 0.4 to 0.55 mm. The cameras of the upper stereo-system are around 600 mm above the rotor and have lenses with $F = 25$ mm, a base distance $B = 280$ mm. They observe the complete blade from the attachment to the tip. The estimated measurement inaccuracy goes from 0.2 mm (in the area overlapping with the lower camera system) up to 1.4 mm at the blade tip. Because all devices located in the rotating system of a helicopter are exposed to enormous centrifugal forces and vibrations, the cameras as well as the required recording hardware need to be mounted on the rotor hub in a compact and rigid way. Furthermore it should be enabled to perform a fine adjustment of the camera viewing angles in-situ. The final design of the rotating camera system is shown in Fig. 3. The system has a maximum diameter of 340 mm and is approximately 370 mm high. The lowest part is an interchangeable connecting flange (item 1 in Fig. 3) enabling the mounting of the rotating camera system on different rotor hub geometries. The big aluminum cylinder (item 2 in Fig. 3) contains all electronics required for the image acquisition.

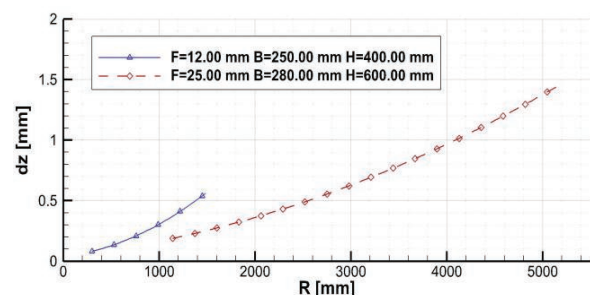


Fig. 2. Estimated measurement inaccuracy of the designed rotating camera system according to [13] (dz - inaccuracy, R - rotor radius, F - focal length of the cameras, B - base distance between cameras, H - height of camera system above rotor).

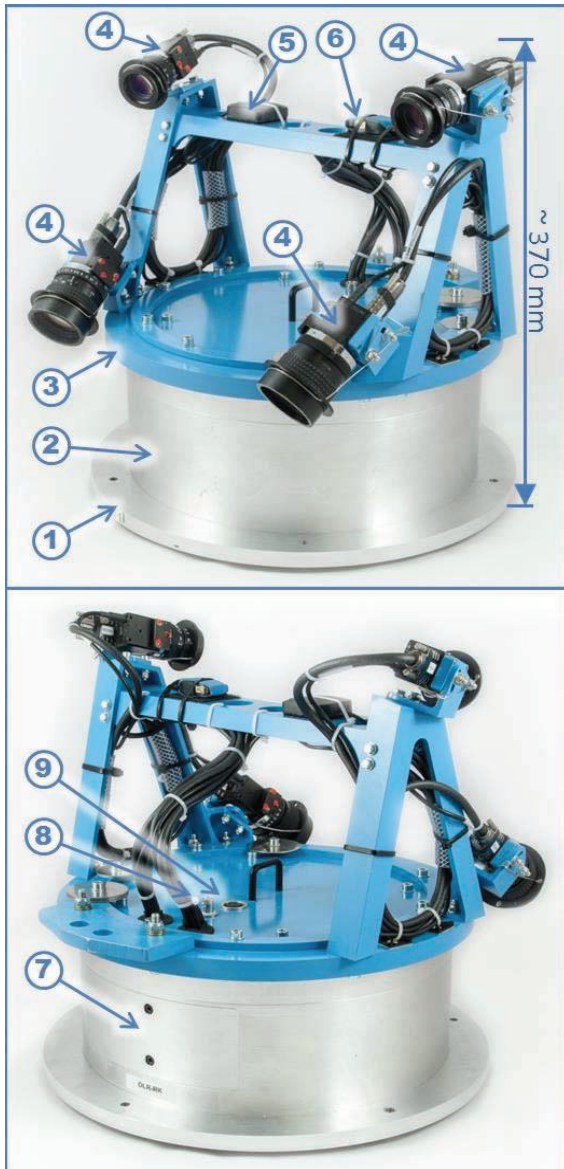


Fig. 3. The rotating camera device (1 – interchangeable mounting flange, 2 – electronics enclosure, 3 – adjustable camera mounting support, 4 – cameras including optics, 5 – GPS antenna, 6 – WLAN antenna, 7 – service connector compartment, 8 – trigger connector, 9 – connector for external power supply).

one embedded PC as control computer, a multichannel contains all electronics required for the image acquisition - one embedded PC as control computer, a multichannel phase shifter card [14] for accurate triggering at multiple phase angles during each revolution, four removable solid state drives (SSD) for the operating system and storing the data as well as two battery packs (optional for autonomous operation). The printed circuit boards (PCB) are mounted in single stages inside the cylinder prevented against rotational forces and vibrations like in a corset. On top of the cylinder the lightweight rigid camera support (item 3 in Fig. 3) is seated.

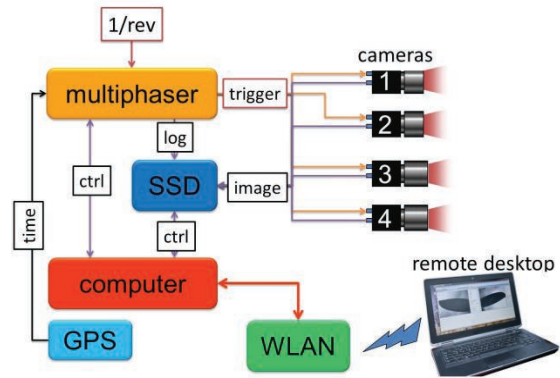


Fig. 4. Schematic sketch of the rotating camera system.

When releasing the clamping mechanism the complete support can be rotated around the vertical axis enabling the observation of different blades without dismantling the rotating camera from the rotor hub. The four cameras (item 4 in Fig. 3) are affixed at this camera support on folded sheets allowing a fine adjustment of ± 20 degree around the vertical axis and the line of sight of each single camera. Antennas for GPS (item 5 in Fig. 3) and a WLAN (item 6 in Fig. 3) are used for time synchronization and remote control, respectively. Connectors for an external trigger signal (item 8 in Fig. 3) and external power supply (item 9 in Fig. 3) are situated on the detachable cover of the aluminum cylinder. Behind a cover plate (item 7 in Fig. 3) at the side of the cylinder additional connectors for a monitor and USB devices are located for the purpose of a test and general setup of the system on ground. The working principle of the rotating camera system schematically is shown in the flow chart in Fig. 4. A TTL signal, e.g. an index pulse occurring once per revolution (1/rev), is provided to the multichannel phase shifter [14] (based of the previously developed digital phase shifter [15]). This "multiphaser" uses the 1/rev signal to calculate the present rotor speed and exactly triggers the four cameras to take images at the rotor azimuth angles programmed with the computer. The images are directly stored on the removable SSDs together with a log file containing the image number, the phase or azimuth angle, the rotational frequency, the GPS time and position as well as the camera settings. The recording of such single images in combination with the log file eases the later processing of the image data compared to the recording of video data where usually only fix frame rates are possible and the access to dedicated single frames is difficult. Furthermore these log files ease the synchronization of the image data with other events and measurements happening in parallel to the image recording.



Fig. 5. The rotating camera system mounted on the experimental rotor (left – view on the mounted camera system, right – view along the patterned blade).

To allow a remote control of the camera system, e.g. for starting recording sequences, changing the camera exposure settings, or checking recorded images, a laptop computer is linked to the rotating camera system using a WLAN connection and a remote desktop application. After the performed test, the SSD with the gathered image data can easily be removed from the rotating camera device and used for offline data processing

An example measurement campaign

During a measurement campaign within the German national project CHARME (CHallenge in AeRoThermoMEchanics) the developed rotating camera system was tested on the Airbus Helicopters whirletower in Donauwörth (Germany). A standard rotor measurement program was performed including static deformation as well as vibration measurements. Besides the measurement by means of the rotating camera additional deformation measurement systems have been applied during the test, such as an instrumentation of the blade with strain gauges and another optical measurement system standing on ground. In addition transition measurements by means of Infrared-Thermography have been performed.

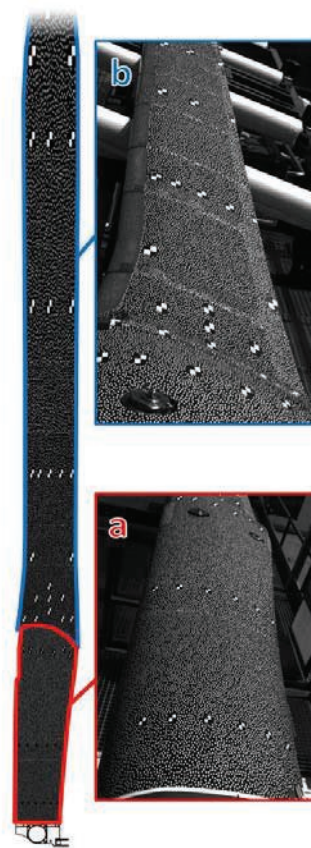


Fig. 6. Overview on the designed IPCT pattern for the control cuff and rotor blade (a - sticker with printed pattern on control cuff, b - pattern painted directly on the blade surface).

For the optical deformation measurements using the image pattern correlation technique (IPCT) the rotating camera was mounted on the rotor hub (see Fig. 5) observing one of the rotor blades covered by a stochastic dot pattern. Two types of pattern application method have been tested - a printed pattern on a sticker on the control cuff and the pattern painted on the blade using a paint mask. The advantages of the sticker method are the high quality of the printed pattern and the fast and easy application and removal of the sticker. As a drawback the sticker can be peeled off by the flow especially at locations with high pressure gradients. Therefore in those regions the pattern should be directly painted on the blade surface. For a proper painting a paint mask manufactured with a cutting plotter is recommended. The design of the pattern has been done with the help of the known 3D CAD geometry and a digital mock-up tool (DMU) [11], [16]. In Fig. 6 an overview of the pattern as well as the two different regions (sticker and paint) are given. It is clearly visible that the sticker provides a much better reproduction of the pattern design - on the painted part inhomogeneities (e.g. due to the covering material on the strain gauge instrumentation)

are also seen in the pattern whilst the sticker covers that different backgrounds. Taking a look to the pattern itself, it can be seen, that beside the stochastically distributed dots additional checker board markers are included. Those markers serve as reference points to merge the results of the lower and upper camera systems, to correct unwanted camera movements and to get initial information about corresponding areas between the two cameras of each stereoscopic system. Furthermore the designed pattern and the markers are increasingly stretched towards the blade tip. This ensures a similar size of all parts of the pattern on the camera sensors, as it can be seen on the camera images in Fig. 6 and Fig. 7. Prior to the mounting on the rotor the rotating camera system had been balanced in order to avoid unwanted vibrations in the rotor system. After a successful first functional test with running rotor the real measurement campaign started. Before each run a 3D camera calibration has been performed by placing a checker board calibration target in front of the cameras and record images whilst moving the target along the blade. The recorded images are later used for the determination of the intrinsic and extrinsic camera parameters [17]. Fig. 7 shows a set of sample recordings taken during the measurement campaign - on the left side the images recorded by camera 1 and camera 2 (upper stereoscopic system) and on the right side the images recorded by camera 3 and camera 4 (lower stereoscopic system). The high resolution images show sufficient contrast and sharpness of the IPCT pattern and the markers. The background behind the blade is naturally blurred due to the high rotational speed. The overlapping area between both stereoscopic systems located around the blade attachment is well represented in all images.

Image processing by means of IPCT and example results

After the test, the recorded stereoscopic image pairs are processed by means of the image pattern correlation technique (IPCT) using a software tool developed by DLR. Fig. 8 delivers a short overview on the main steps from stereoscopic images to measured 3D surfaces. First of all the calibration images (Fig. 8-1) are evaluated in order to deduce the transformation matrix between image and world co-ordinates. Next a marker detection algorithm is applied to the measurement images (Fig. 8-2) to find the image coordinates of corresponding markers (Fig. 8-3). If those image co-ordinates are triangulated utilizing the 3D calibration, the 3D positions of the markers can be obtained as a first result.

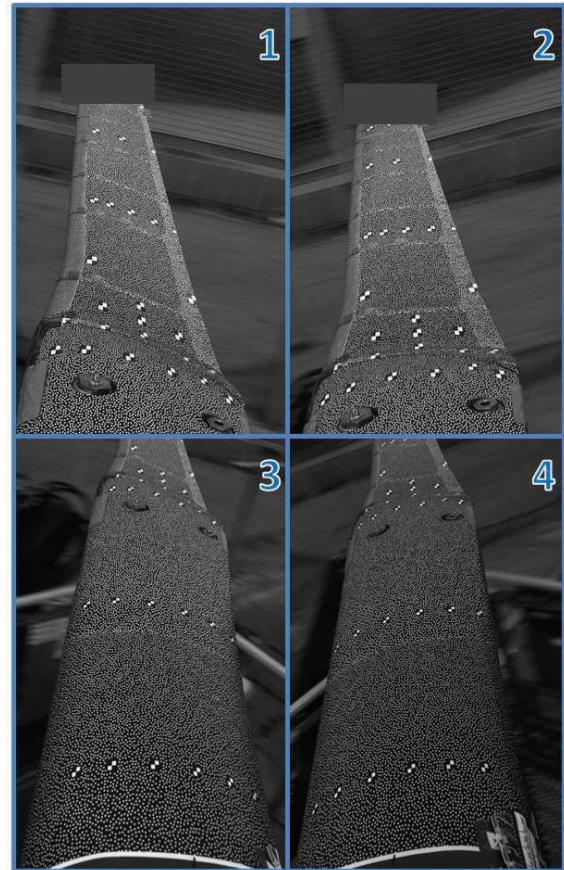


Fig. 7. Example recordings taking at full rotor speed (1 + 2 = upper stereoscopic system (camera 1 and camera 2), 3 + 4 = lower stereoscopic camera system (camera 3 and camera 4)).

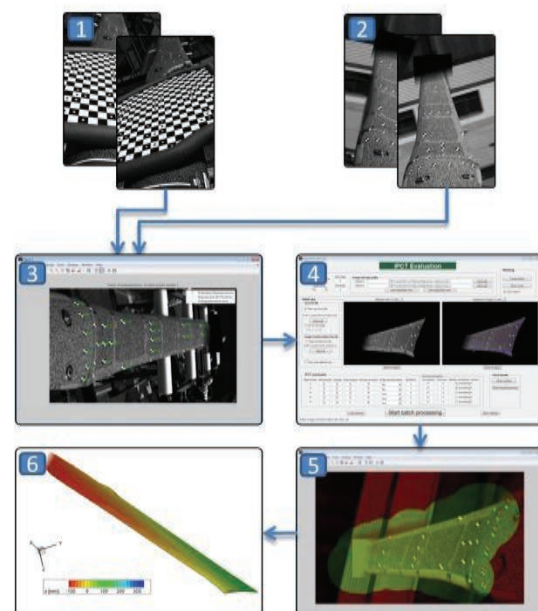


Fig. 8. Scheme of IPCT processing (1 - images for stereo camera calibration, 2 - stereoscopic measurement images, 3 - Marker detection procedure, 4 - image pattern correlation, 5 - overlay of successfully deformed images, 6 - triangulated resulting surface).

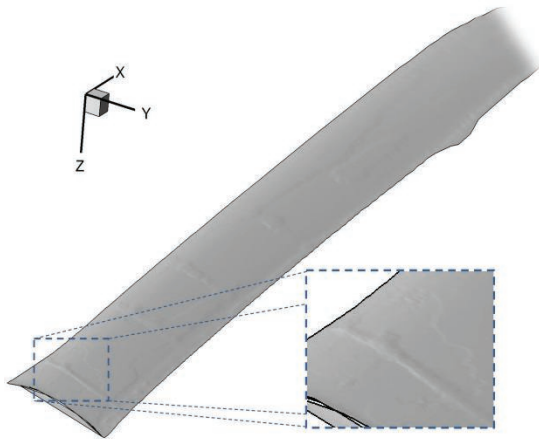


Fig. 9. Example surface of the rotor blade obtained from IPCT processing with zoomed detail (remark: the blade tip is faded out due to confidentiality reasons).

For the following image pattern correlation (Fig. 8-4) the image co-ordinates of the markers are used to get start values for an initial image deformation. By means of an iterative cross correlation more and more corresponding points are identified in the two stereoscopic images and the image deformation is improved until both images are matching as shown in Fig. 8-5 by an overlay image. In the last step the corresponding points are triangulated using the 3D calibration resulting in the reconstruction of the measured 3D surface of the blade (Fig. 8-6). In the references [13], [16], [17] further information about the IPCT processing can be found.

An example surface obtained from the measurement images by means of IPCT is depicted in Fig. 9. The surface is smooth and in agreement with the shape of the investigated blade. Like shown in the zoomed box even small details on the blade surface can be reconstructed - in that case the raise due to the covering material of the strain gauge installation.

If the IPCT processing is performed for different measurement points, the movement and the deformation of the observed blade can be determined. Fig. 10 shows the surfaces for a measurement sequence with nine different collective pitch settings. For each collective pitch setting ten surfaces are taken. The small graphs on the right side show lines extracted in spanwise and chordwise direction identifying the blade bending and the local change of the pitch angle as well as the local heave. As expected the increasing heave with increasing blade pitch angle and increasing spanwise location is clearly visible. Furthermore the growing lag of the blade for higher pitch angles can be seen.

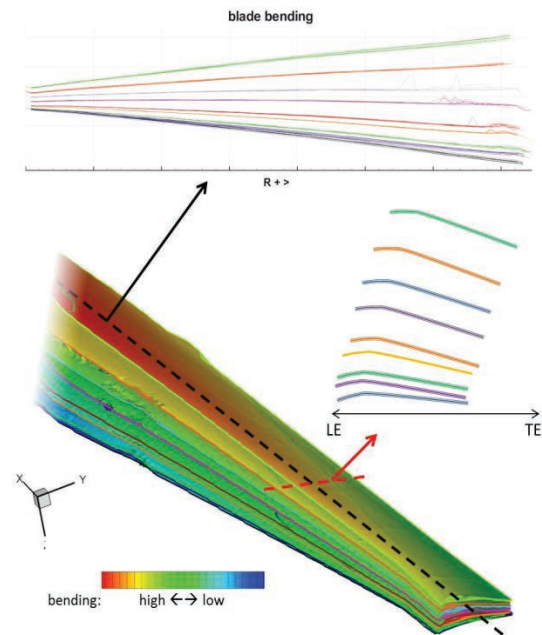


Fig. 10 Example surfaces (left) for different measurement points including spanwise extracted blade bending curves (top right) and chord wise extracted profiles (bottom right) (remark: the blade tips are faded out and the graphs are not to scale due to confidentiality reasons).

Beside the big displacements between the nine sets of measurement points with different pitch settings, a small flapping motion can be observed for the ten lines with the same pitch setting.

Conclusion

Based on the experiences in optical deformation measurements in rotor systems gained from the application of a rotating camera system mounted on an aircraft propeller a remote controlled rotating camera system with four imaging sensors has been successfully applied to optical rotor blade deformation measurements. The system was able to record the complete main rotor blade (including control cuff, blade attachment and the overall blade) during its full revolution under real operation conditions.

During the measurement campaign the rotor system was recorded under different loading conditions including different rotor speeds, different collective and cyclic pitch settings as well as excited natural frequencies of the rotor resulting in a huge amount of valuable image data processable by means of IPCT. The preliminary processing of some of these images demonstrated the feasibility of the application of IPCT measurements with a rotating camera system.

Even without the IPCT processing the recorded images deliver a novel and valuable insight in

the behavior of the running rotor system that can not directly be observed with classical methods or with camera systems on the ground. The recorded images can also be used in order to check if movements observed from the non-rotating frame are due to e.g. trigger jitter or if they are real movements of the rotor system.

Compared to a classical strain gauge setup, the instrumentation for optical deformations measurements with the rotating camera system was relatively easy - only a pattern had to be applied on the blade and the camera system had to be mounted on the hub. In addition (if a pattern sticker or washable paint is applied) the installation can be removed after the test and the investigated blade can then be used like a normal production blade.

As the system is co-rotating with the blade the camera exposure times can be much longer than for cameras watching the passing blade from the fix frame. Thus the background illumination (e.g. the sunlight) is sufficient for image recording i.e. no additional strobe light is required. Nevertheless reflections of the sunlight on the investigated surface should be avoided, because they disturb the measurements.

Like mentioned above, the images taken during the test and the first IPCT processing of the data look very promising and deliver a first proof of concept. In the next step all image data has to be processed with the IPCT and shall be compared to the strain gauge measurements, the parallel applied optical measurement from the non-rotating frame, as well as the existing numerical simulations for the blade behavior. In case of the very probable successful comparison the authors are looking forward to test the helicopter camera in flight in the near future.

Besides the in-flight application of the imaging technique, the method is applicable for other fast rotating objects like wind turbine rotors, ship propellers or wheels, either in combination with deformation measurement techniques like the IPCT or with other measurement techniques for optical flow or pressure measurements.

Acknowledgement

The performed measurement campaign was part of the project CHARME (funding code 20H1501A) funded by the German Federal Ministry for Education and Research (BMBF) where DLR has been subcontracted by Airbus Helicopters to perform measurements with a rotating camera.

The authors furthermore would like to thank the personnel of Airbus Helicopters for the realization of the whirltower test at their premises in Donauwörth.

References

- [1] N. Tourjansky, E. Szechenyi, The measurement of blade deflections - A new implementation of the strain pattern analysis, *ONERA TP – 92-127* (1992).
- [2] K. Papadopoulos, E. Morfiadakis, T.P. Philippidis, D.J. Lekou, Assessment of the strain gauge technique for measurement of wind turbine blade loads, *Wind Energy* 3(1), 35-65 (2000)
- [3] F.L.M. dos Santos, B. Peeters, B., On the use of strain sensor technologies for strain modal analysis: Case studies in aeronautical applications, *Review of Scientific Instruments* 87 (10), 102506 (2016); doi: 10.1063/1.4965814
- [4] J. Sicard, J. Sirohi, Measurement of the deformation of an extremely flexible rotor blade using digital image correlation, *Measurement Science and Technology* 24 (6), 065203 (2013); doi:10.1088/0957-0233/24/6/065203
- [5] G.A. Fleming, S.A. Gorton, Measurement of rotorcraft blade deformation using projection moiré interferometry, *Shock and Vibration* 7(3), 149{165 (2000);
- [6] F. Boden, C. Maucher, Blade deformation measurements with IPCT on an EC 135 helicopter rotor, *Advanced In-Flight Measurement Techniques*, ch. 13, 195-213, Springer Verlag, Heidelberg New York Dordrecht London (2013); doi: 10.1007/978-3-642-34738-2_13
- [7] C. Lanari, B. Stasicki, F. Boden, A. Torres, Image based propeller deformation measurements on the Piaggio P 180, *Advanced In-Flight Measurement Techniques*, ch. 9, 133-153, Springer Verlag, Heidelberg New York Dordrecht London (2013); doi: 10.1007/978-3-642-34738-2_9
- [8] P. Beaumier, B. van der Wall, K. Pengel, C. Kessler, M. Gervais, Y. Delrieux, J.-F. Hirsch, P. Crozier, From ERATO basic research to the Blue Edge™ rotor blade: an example of virtual engineering?. *Rotorcraft Virtual Engineering Conference* (November 2016). LIVERPOOL, United Kingdom. HAL Id: hal-01413109.
- [9] F.B. Gustafson, G.C. Myers, Stalling of helicopter blades, *NACA TN No. 1083* (1946).
- [10] E. Zappa, L. Trainelli, R. Liu, A. Rolando, F. Rossi, P. Cordisco, E. Vigoni, M. Redaelli, Real time contactless sensor for helicopter blade angle measurement, *Metrology for Aerospace*, IEEE pages 239-244 (2016); doi: 10.1109/MetroAeroSpace.2016.7573219
- [11] F. Boden, B. Stasicki, M. Szypuła, P. Ružička, Z. Tvrdik, K. Ludwikowski, In-flight measurements of propeller blade deformation on a VUT100 cobra aeroplane using a co-rotating camera system, *Measurement Science and Technology* 27.7,

- 74013-74025 (2016); doi:10.1088/0957-0233/27/7/074013
- [12] Involved DLR-patents: DE4309353.1, DE195 44 642, DE10 2011 001 268. B4, DE 10 2014 117 655.3.
- [13] T. Weikert, Basic optics and camera modelling, *AIM² Advanced Flight Testing Workshop – HANDBOOK of ADVANCED IN-FLIGHT MEASUREMENT TECHNIQUES*, ch. 3, 37-48, BoD - Books on Demand, Norderstedt (2013);
- [14] F. Boden, B. Stasicki, K. Ludwikowski, Multikanalphasenschieber, *Patent DE 10 2014 117 655* (2014).
- [15] B. Stasicki, G.E.A. Meier, Digital phase shift method, *Patent DE 195 44 642* (1997).
- [16] T. Kirmse, F. Boden, H. Jentink, Image pattern correlation technique (IPCT), *AIM² Advanced Flight Testing Workshop - HANDBOOK of ADVANCED IN-FLIGHT MEASUREMENT TECHNIQUES*, ch. 6, 63-85, BoD - Books on Demand, Norderstedt (2013).
- [17] T. Kirmse, Recalibration of a stereoscopic camera system for in-flight wing deformation measurements, *Measurement Science and Technology* 27(5), 054001 (2016); doi:10.1088/0957-0233/27/5/054001

Integrated Network Enhanced Telemetry (iNET): Impact to the Telemetry Community for the ett2018

Tom Young

*USAF Air Force Test Center, 61 N. Wolf Ave., Bldg. 1633, Edwards AFB, CA., USA
Tommy.Young.1@us.af.mil*

Abstract:

The enormous increase in the complexity of modern aircraft, coupled with the Department of Defense's (DoD) spectrum reductions, has created a growing gap in DoD's ability to collect all the data needed from a flight test in real-time. Over the past 50 years, aircraft flight test performance has been monitored using a unidirectional telemetry link for the test article to the ground, sending only pre-planned data to Mission Control. iNET will provide the capability to access and transmit onboard data in a packetized [Internet Protocol (IP)-based] format. This will enable flight test engineers to access aircraft data in an on-demand fashion using a duplex datalink. Without iNET, DoD ranges will be unable to meet near-term rapidly expanding test data throughput requirements, in the face of increased competition for limited radio frequency (RF) spectrum/bandwidth. Initial deployment will be at Edwards Air Force Base, California USA, and Naval Air Station (NAS) Patuxent River, Maryland USA.

This capability will provide to the test community unprecedented control from the ground over the instrumentation system on board the test article, in real-time. Based on the architecture of the system and its intended implementation, the ability to share spectrum over the radio frequency network is one of iNET's key features in support of spectral efficiency. While spectrum efficiency is a primary driver for the next generation telemetry capability, additional benefits will be realized with a two-way RF link. These benefits might initially be described as data efficiencies, however under the surface the impacts to spectrum efficiency will be extensive due to the enabling architecture. The ability to control the airborne instrumentation system from the ground, provides access not only to the data recorder but the data acquisition unit that controls data format and sample rates. This ability for dynamic real-time adjustment of information flow to the ground will change the face of flight testing in the very near future.

Key words: (bi-directional, telemetry, serial, dynamic, real-time).

Background

A continual challenge for the Aeronautical Mobil Telemetry (AMT) community is dealing with the increased data acquisition requirements imposed by aircraft information systems. With the complexity of aeronautical systems increasing, the test ranges are ever challenged to respond to this growing requirement. The pressing need to transmit massive quantities of data in real-time is the trend when supporting these next generation weapons systems. In turn the AMT system infrastructure needs to be capable of scaling to support the needs of these, high tech test articles. In addition to these traditional challenges, new challenges exist for AMT. The singular most significant

challenge is the availability of protected test and evaluation RF spectrum allocations for AMT.

To operate in a reduced AMT spectrum environment, the end-user will need the capability to change the measurements telemetered in-flight. This capability lets the end-user start/stop the measurements associated with a specific phase of the test. To do this a two-way connection with the AMT system in the test article is needed and that does not exist in current systems. Also, once the two-way connection with the test article is established, the AMT system must be capable of accepting and responding to configuration changes. This capability also does not exist in current systems today.

Finally, reduced spectrum means that AMT system needs to move away from command and control spectrum management. In this scheme, spectrum is allocated for each specific telemetry signal transmitted with white space between signals to avoid interference. To maximize the spectrum available, a group of test articles need to share the same spectrum with the white space recycled for use. A network enhanced AMT provides the means to modify the data telemetered to the ground in-flight.

The current AMT systems architecture (see Fig. 2) does not support in-flight changes to the telemetry stream. The ability to make changes in-flight give the end-user the ability to manage what measurements are telemetered at any given time. If future AMT systems must operate with reduced spectrum then the current architecture must have the capability to make in-flight changes, the traditional architecture for AMT needs vast improvements; a shift in paradigm.

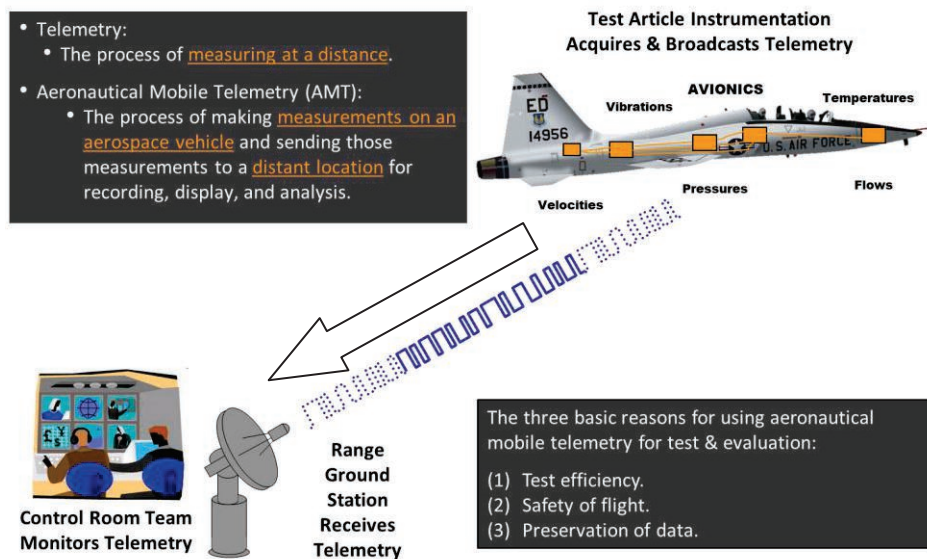


Fig. 1. Current AMT Condition.

Introduction

Network telemetry is the main ingredient to ensure the shift in T&E capability contains the needed answers to continue manned flight test at the ranges. iNET is the building block to achieve supportability of next generation weapons systems development. Without the introduction of network telemetry, many components of the T&E infrastructure will likely be out paced by the very systems they are in place to support. Thankfully the iNET capability is nearing completion and its maturity has been tested in flight. iNET's architecture describes the standard for network telemetry within the DoD ranges, now and for the foreseeable future.

The iNET capability will provide to the test community unprecedented control of the aircraft instrumentation system, from the ground in real-time. Based on the architecture of the system and its intended implementation, the ability to share spectrum over the radio frequency

network is one of iNET's key features in support of spectral efficiency. Spectrum efficiency is a primary driver for the next generation telemetry capability; additional benefits will also be realized with a two-way RF link. But iNET doesn't stop there, upgrading both the System Under Test (SUT) along with the ground components complete the iNET capability. Enhancing the acquisition site with duplex communication to the aircrafts instrumentation system and providing the capacity to deconstruct TmNS network packets in a mission control room, completes the iNET system upgrades. Once the range architecture mods are in place, the full benefit of network telemetry can be realized (see Fig. 2). These modifications are the backbone of the iNET capability and provide the benefit of, spectrum efficiency, data efficiency as well as the added advantage of upgrading aging components. This, a hidden gem of the program is the requirement to provide a path to an open

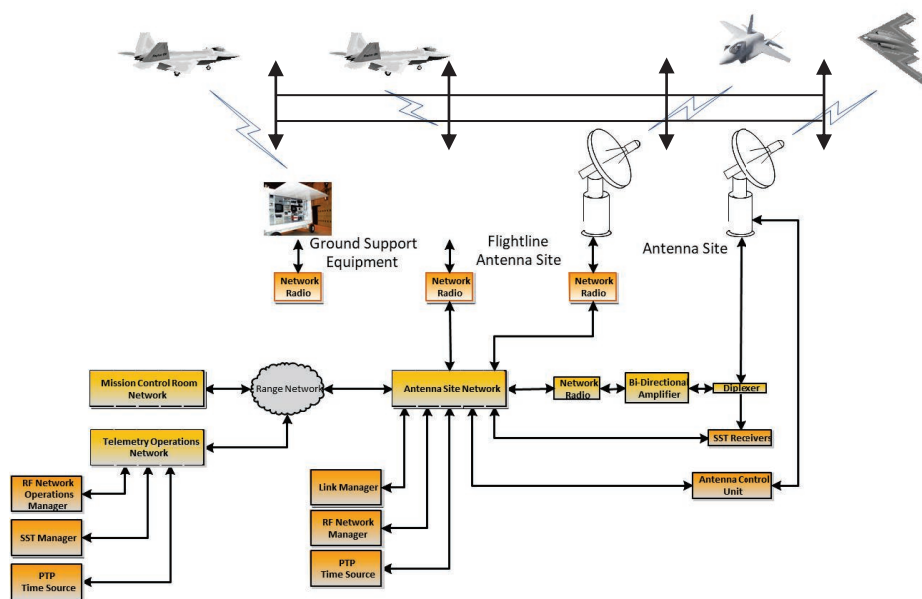


Fig.2.iNET TM Network Architecture.

architecture and move away from stove pipe proprietary solutions. By leveraging commercial standards and establishing standardized components, the goal of a low cost, interoperable system with benefits of increased spectral density and improved test data efficiency is reachable.

Impacts to spectrum efficiency will be extensive due to the enabling architecture. The ability to control the airborne instrumentation system from the ground, provides access not only to the data recorder but the data acquisition unit that controls data format and sample rates. This ability for dynamic real-time adjustment of information flow to the ground will change the face of flight testing in the very near future. Many of the technology investments being made today can enhance the DoD capability while supporting strategies to share resources without compromising test capabilities.

Networked Telemetry

The Integrated Network Enhanced Telemetry (iNET) program has developed a new approach to telemetry for the airborne environment. iNET has developed a network architecture for airborne platforms that will replace the current serial instrumentation bus with industry standard Ethernet and add a bidirectional network channel from the aircraft to the ground. While iNET will utilize Serial Streaming Telemetry (SST) links for safety of flight and other telemetry data, the addition of a network-based communication channel will provide

additional functionality that is not possible today. iNET will support command and control of the instrumentation systems while the aircraft is in flight, which will enable capabilities such as:

- Requesting data from the onboard recorder to “backfill” or replace lost or corrupt data initially transmitted over the SST link
- Changing of original SST data package or data format during flight
- Selecting the telemetry data sent down on the network link vice initial load
- Monitoring the health and status of the instrumentation system throughout the mission
- Control Airborne instrumentation system from the ground
- Requesting data from the recorder that was not originally being telemetered

iNET will use a standard network architecture that leverages the existing ground station infrastructure with minor modifications to support two-way communication. By network enabling the instrumentation systems on the aircraft as well as adding capabilities to the MCR systems supporting interactive access to testing data, the iNET program has laid the cornerstones for the modernization of AMT. This paper will build upon the enabling technologies of iNET and examine possible implementations that will enhance the duplex wireless telemetry paradigm.

Spectrum Efficiencies

Spectrum sharing is a key aspect to iNET to reduce the spectrum requirement by introducing the concept of block allocations. The use of a Time Division Multiple Access (TDMA) architecture uses time slots versus independent frequency bands. This concept elevates the need for much of the scheduling and resource overhead associated with SST system and allows the telemetry networking tools to manage the independent links. Not only does this increase spectrum sharing but increases productivity by using the automated tools instead of manual processes. The iNET Network can be shared by up to ten test participants simultaneously, through a mix of dynamic bandwidth sharing and quality of service priority schema. Twenty Megahertz is the current agreed upon baseline network allocation, with the maximum throughput for any one link restricted to eight Megabits. The reduction in spectrum works as a function of eliminating the required guard bands between test participants, adding players increases the efficiency gained.

Another component to spectrum reduction is based on the availability of a network link; this will lead to a reduction in the SST link with a decreased amount of "critical" parameters sent down the serial link. This shift away from SST will encourage testers to reevaluate the required information being telemetered to the ground, due to having access to all the aircraft data. Throttling bandwidth based on the need or priority of the participant can also impart a reduction in spectrum required for a mission. If a priority user of the network may opt to use less bandwidth between test points knowing that bandwidth will be there when needed, allowing lesser priority testers a chance to fly and gather data.

Other artifacts of the iNET system provide command and control of the SST device allowing for power, frequency tuning and additional opportunity for enhanced modulation techniques. This in itself can reduce the spectrum footprint twenty to forty percent on the serial link by utilizing a more efficient schema. The ability to be frequency agile can additionally impact the availability of frequency resources when specific allocations become available; the transmitter can be re-tuned to the available frequency. Never before in the flight test environment has this been possible, bringing to bear usable spectrum to a test platform on demand. Automated inter-range handoff is a feature of iNET that can free-up spectrum resources and make them available to other users that much faster. Due to the

manual nature of the frequency assignment process it could potentially be hours before the resource is again available for use. Not only does this autonomy provide newly released spectrum back to the resource manager quicker but also increases the opportunity for re-use.

While the above stated iNET enablers will assist the test community with the reduction of this mission critical resource, by far the most significant impact is the decrease in data being transmitted. Of course, this sounds very straightforward but until it is put into context does it sound like a revelation. In the unidirectional paradigm of current test programs, a transmitted data format is built to encompass all of the requirements of the program, from start to finish. The beauty of a two-way link is that you can organize your test program based on the spectrum needs of the specific mission, test card, test point. In other words, dynamic access to the data on the test article and only transmitting to the ground what is needed and when. That's a PARADIGM shift!

Test Data Efficiencies

Just recently, spectrum efficiency has become an extremely hot topic and has received much attention from the decision makers. Test / data efficiency has always been a recognized metric that has received considerable scrutiny. To that end an ample amount of focus has been spent increasing those metrics. Until now the previous work pales in comparison to the improvements incorporated into the Telemetry Network System (TmNS) known as "iNET". Discussed earlier as a key spectral efficiency factor, manipulation of the transmitted test data is a formidable test and data efficiency. The immediate correction of corrupt data due to link outages is the gold standard when it comes to RF communications. This pristine data is provided to the tester via the network data recorder in near real-time, ten to twenty milliseconds after the event. Proving to the disciplined test engineer with pristine recorder data, that the test point does not need to be re-accomplished. This technique is known as Data Backfill or SST backfill.

As important to the tester as Data Backfill, Data on Demand is the premier data efficiency feature that iNET employs. Providing the ability to request data in real-time from the onboard data recorder without interrupting recording; down to the parametric level. Access to the recorded data in real-time provides the entire data set, previously unavailable until the aircraft landed. The ability to evaluate this pristine data set in real-time can improve test efficiency by

ensuring test points/ cards were performed to expectations; thus reducing expensive re-fly's. With the added capability of the duplex link another component that increases test efficiency is the ability to control the onboard instrumentation components. Having the ability to control instrumentation from the ground enables moving that control out of the cockpit, freeing up the pilot for more important things, flying. Additional controls allow dynamic re-configuration of components ensuring less reflys, decreased time between missions and increased access to data more rapidly.

Due to the architecture of TmNS, managing the spectrum in chunks versus individual test frequencies significantly eases the burden of resource management. Schedulers as well as Frequency Managers will benefit from the ability to manage additional functionality with a less resources. Using the automated network tools and the TDMA building blocks increases opportunities for test and data efficiencies.

Sustainability and Interoperability

An overlooked advantage of using the open architecture, standards-based approach is cost saving, by leveraging commercial investment. Using the available network tools and standards instead of developing purpose-built tools saves time and money. The use of commercial communication standards (e.g. Ethernet, TCP/IP, UDP/IP, SNMP, RTSP, FTP, XML, PTP1588) and standard interfaces significantly decreases the acquisition, implementation and operations costs, as well as maintenance and replacement costs. These improvements alone will save the ranges considerable investment but the ability to interoperate is just as important.

The concept of test ranges being interoperable has been the charter of the Range Commanders Council (RCC). The RCC committees have done a fantastic job working together, encouraging standardization. Moving away from costly one-off proprietary solutions, building and maintaining common standards for the ranges to interoperate. Much thought was given by the initial iNET developers to develop standards for a common approach for network telemetry, defined as TMNS. These standards are captured, published and maintained by the RCC Telemetry Group and the baseline standards were released in August of 2017. These Inter-Range Instrumentation Group (IRIG) 106-17 Chapters 21-28 contain the new telemetry network standards. With the above standards the various test ranges can build, purchase, integrate and test interoperable components / systems. Interoperable capability

is an enormous benefit for the test customer however cost savings is at the heart of standardization. This is the key that all members of the range community must strive to achieve when developing new capabilities.

Lastly, the vendor community involved to support interoperability. Not only are they involved in standards development but many build the components and systems to the standards. It is important to realize from a customer perspective how important it is for competition in the marketplace. Indeed, it decreases cost but also reduces the risk to the test mission support community. The reduction in risk is due to multiple vendor solutions targeting a singular problem space. Bringing the commercial community into the RCC creates cooperation and teaming for solving tough problems for the ranges. Its in the best interest for all involved to meet mission goals and at the same time be as financially responsible as possible.

Implementation Considerations

Based on the enormous change to the telemetry system that iNET provides, substantial attention needs to be focused on the Concept of Operations (ConOps). How you implement the specific network telemetry system to meet a ranges needs will certainly need consideration. A primary factor to consider is the physical placement of the control interface to the TmNS. This powerful interface will have the ability to control the instrumentation system onboard the test aircraft anytime. Concerning as this may be, determining the best location, based on the ranges needs and mission are the primary factors. Locations that have already established physical security measures in place will most likely be the locations of choice, e.g. Range Control or Mission Control Room.

An additional vital topic to be considered is where the responsibility for making control decisions will reside. Access to the network for the purpose of manipulating the transmitted data should be given to a select few. Commands requesting large amounts of data simultaneously could be detrimental to the telemetry network. Ensuring proper control of the mission data flow is essential for a successful implementation of iNET. Other considerations that need to be addressed are the modified functions of both the Resource Schedulers and the Frequency Managers. Both of these functions will be impacted by the operational network telemetry capability. Not that either of these functions will be impacted negatively, on the contrary, there is opportunity

for increased productivity. Training on the new systems and capabilities will be an important factor for a successful transition into network telemetry. There are many new capabilities that are available with iNET and they will need specific understanding from the support organizations. System level control from a single Graphical User Interface (GUI) is a powerful concept that will introduce new factors for consideration. This single system interface can also provide the capability of the current the Ground Support Equipment. Will the need for such an interface to the aircraft still exist if the GUI in the Control Facility can provide the same function? Additional opportunities to learn will present themselves as we install and learn about this new game changing capability.

Soon the test ranges will be faced with unlocking the true potential of this bi-directional telemetry architecture. Much like the advent of the internet and the cell phone, iNET has the potential to be as impactful for the telemetry community. To use an example from cellular technology; would you have guessed that the cell phones primary function is all but forgotten by today's cell phone customer. iNET provides the capacity for an application-based capability. This capability has the potential to provide unlimited test capability for the customer. Limiting the telemetry downlink because most of the decision making is taking place on the SUT, autonomously. This concept will also have an impact to instrumentation systems ultimate configuration and the acquisition sites as well. Automated tools are increasingly being used in instances where the processing horsepower was previously not available. The days of being resistant to change because its uncomfortable are over, get comfortable with these new capabilities.

Conceivable Implementations

TmNS is the platform to build upon to achieve the test capabilities required by the next generation, complex weapons systems. Without the capacity and flexibility of the TmNS, supporting telemetry requirements into the future is questionable. DoD spectrum allocations continue to decline, increasing the need for network telemetry. By continuing to apply network capability, it is possible to establish the two-way connection out to the test sensors. Enabling dynamic control out to the sensor for real-time calibration, modifying sample rate or adjusting sensitivity. Establishing real-time control out to the edges creates the environment of smart sensors.

Another conceivable implementation is on board real-time validation of models. This

powerful test concept is within the art of possible, with an established duplex link. Time and cost savings can be realized as models are validated in real-time and the information is fed back to the test team. This has the implications of significantly reducing the time to test.

A distributed test capability is yet another possible implementation that is enhanced by a two-way link. The ability to send packets to any location in near real-time has great potential for cost savings. Sending test teams to various locations to conduct a test is no longer required. Sending telemetry data in real-time to a distributed test team saves time, money and possibly engineering support.

But possibly the most controversial topic to end the paper, is the ability for real-time decision automation. To potentially automate and augment the information received by the test team, increasing the speed in making engineering judgement calls. This in turn could reduce the required amount of safety information being telemetered to the ground; reducing the spectrum requirement. The possibility exists that test engineers may only have the need for 2nd & 3rd generation processing / analysis in real-time; the rest is automated. Similar concepts are being flown today, e.g. the automated flight termination systems on unmanned vehicles.

Global Ranges and Over the Horizon Coverage

Network telemetry will also allow the realization of a "Range-less Range" or "Global Range" capability. When test articles use a packet-based infrastructure instead of the serial systems of today, testing will be conducted anywhere network connectivity is available. Options like commercial / government satellites, commercial wireless / cellular providers could be leveraged to support test missions conducted across the globe. The utilization of airborne routers and mesh or Mobile Ad-hoc Network (MANET) protocols could be used to extend the network where the use of satellites might not be suitable. In this case, a series of aircraft and/or surface vessels could act as mobile network routers that extend coverage over the horizon by relaying network telemetry data through each mobile node and down to the ground.

Conclusion

Clearly the current telemetry environment is ripe for technology advancement to keep pace with the next generation weapons systems development. The initial operational capability provided by iNET is the crucial building block necessary for the DoD to modernize the test

range telemetry infrastructure. Bi-directional communication with the instrumentation system provides the improvement for the growth in capability. Controlling the data transmission to the ground is the primary driver for influencing spectrum and test efficiency goals. iNET is the capability that the DoD test community has invested in for the future of network telemetry.

Creating the Future Test Range Infrastructure: Vision for a Wireless Inter-Range Network Environment

Thomas O O'Brien

*U.S. Department of Defense Test Resource Management Center, 4800 Mark Center Dr Suite 07J22,
Arlington, VA 22350*

Abstract:

Radio frequency spectrum is a vital resource to Test & Evaluation (T&E) and is used to support nearly every test in every environment, yet the availability of RF spectrum to support testing has diminished since the 1990s. A major testing challenge is balancing the development of complex systems requiring the transmission of increasingly large amounts of data with a diminished amount of spectrum available to test facilities and ranges. This inverse relationship creates spectrum congestion at test facilities and can delay test activities.

In order to continue testing systems efficiently and adequately, a major test infrastructure paradigm shift is being developed looking toward a bi-directional, highly integrated, wireless, inter-range network environment that seamlessly supports any and all range operations and data types with even greater spectrum efficiency than currently possible. The implementation of a wireless, inter-range network environment relies on leveraging current efforts to develop a network-based telemetry capability and applying a mobile wireless "cellular" paradigm. While the T&E environment differs from the mobile wireless environment, adaptation of certain wireless technologies to the testing environment might provide significant benefits that satisfy increasing testing requirements.

This paper highlights the spectrum availability issues facing the major Department of Defense test ranges and the vision developed by the Department of Defense Test Resource Management Center to implement a wireless inter-range network environment to support test data transmission requirements. The ultimate goal is to garner support and awareness for the effort both domestically and abroad and show U.S. commitment to invest in spectrally efficient technologies, methodologies, and paradigms to support data transmission requirements.

Key words: Telemetry, Test and Evaluation, Test Infrastructure, Network Environment, Network Based Telemetry, Test Resource Management Center

Introduction

Radio frequency (RF) spectrum is a vital resource to the Test and Evaluation (T&E) community and is used to support nearly every test in every environment, yet its availability to support these tests has been decreasing. Beginning in the early 1990s, the spectrum available to the Major Range and Test Facility Base (MRTFB) has significantly decreased. The widespread development and use of wireless communications devices (WiFi- and WiMAX-enabled), as well as cellular and satellite services, has led to commercial entities seeking increasing amounts of spectrum to support their communication services. Spectrum bands affected domestically in the U.S. are typically those used for T&E purposes, such as flight test telemetry (e.g., reallocation of the 1710-1755 MHz, 1755-1780 MHz, & 2310-2360 MHz bands).

Spectrum access is further complicated by increasing demand from other DoD users to support new or

modified military systems. These complex military systems require the telemetering of a large amount of data to effectively characterize system performance during testing—an exponential growth in data transmission requirements over the past twenty-five years. RF spectrum availability affects test programs in many regards, most importantly cost and schedule. Insufficient access to RF spectrum leads to test scheduling delays which in turn lead to increased program costs.

To address the inverse relationship between decreasing spectrum availability and increased telemetry data requirements, the DoD Test Resource Management Center (TRMC) has developed a vision for a wireless, highly integrated, network to support all range data transmission in the most spectrally efficient manner possible. This vision represent a major shift in the test infrastructure paradigm, moving from a point to point link in which an omnidirectional antenna or wrap around antenna on the SUT is used

to broadcast telemetry data to one or more parabolic, mechanically steered tracking antennas on the ground, each of which are only capable of tracking one test article at a time. In order to build towards this vision for test range infrastructure, the TRMC established several efforts to address spectrum resource issues. These technology development efforts focus on achieving greater efficiencies in the use of the available spectrum, pursuing additional spectrum in different frequency bands, implementing a robust networked telemetry capability, and leveraging cellular based technologies to support telemetry operations. For example, TRMC sponsored programs including Integrated Network Enhanced Telemetry (iNET), Cellular Based Range Telemetry (CRTM), Cellular Range Telemetry Network (CeRTN), and Flightline Radio Network (FRN) to build towards this vision and better use the spectrum that is available for T&E.

Spectrum Availability

Spectrum is a limited commodity, just like oil, and its availability to the MRTFBs for testing has been constantly decreasing. In recent years, a disturbing trend has surfaced—increasingly complex systems requiring a large amount of data to be transmitted are being developed while the amount of spectrum available to the test range has been steadily decreasing—making it very difficult for test ranges to operate (Figure 1).

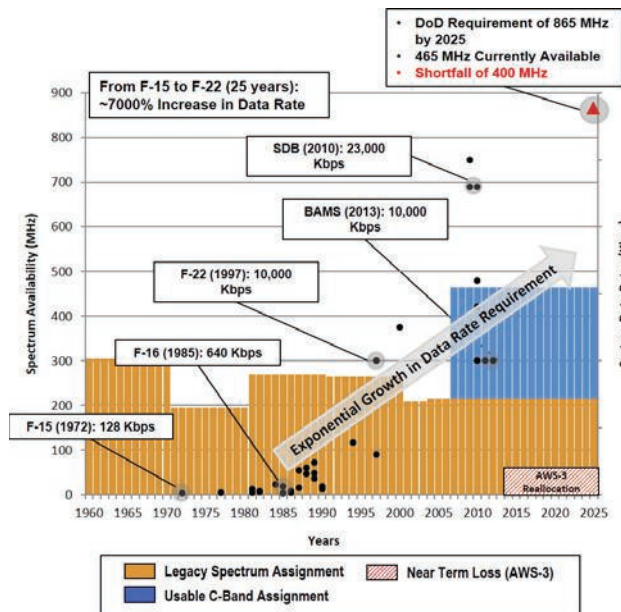


Figure 1- Spectrum & Data Rate Trends

Domestic repurposing of RF spectrum in the U.S. has drastically changed the amount of spectrum that is available for testing. Figure 2 shows the historic allocations given the U.S. test ranges versus the RF spectrum currently available for testing.

Historic Frequency Allocations, MHz	Current Frequency Allocations, MHz
Lower L Band (TSPI)	1350-1390

1350-1400 & 1427-1436	
Lower L Band 1435-1535	1435-1525
Shared Upper L Band 1710-1850	1780-1850
Lower S Band (UAS) 2200-2300	2200-2290
Upper S Band 2310-2395	2360-2395
Sum : 484 MHz	Spectrum Lost : 159 MHz (~33%)

Figure 2- Spectrum Allocations

This chart shows the effects that spectrum repurposing activities has on the testing environment—33% of the spectrum that was once allocated for testing has been re-allocated to support other uses.

The loss of spectrum, increasing demand for spectrum to test complex systems, and the threat of future losses of spectrum have snowballed into a larger problem for test ranges—band congestion. The issue that has arisen is that as the amount of spectrum decreases, scheduling becomes more and more difficult and the telemetry bands are becoming heavily congested. As a result, it is estimated that 17% of all scheduling requests are denied due to insufficient spectrum as a result of band congestion¹. Spectrum availability, and the prospect of future limitations on spectrum access are a driving factor towards a bi-directional wireless inter-range network environment.

Current Range Telemetry Paradigm

The test infrastructure at MRTFB sites is currently configured to support unidirectional point to point link in which an omnidirectional antenna (or wrap around antenna on a missile) on the test article is used to broadcast telemetry data to one or more parabolic, mechanically steered tracking antennas on the ground which are only capable of tracking one test article at a time. While this approach has traditionally supported telemetry operations, a new approach is necessary to adapt to the complex spectrum environment created by the growth in personal wireless devices and commercial cellular equipment. Furthermore, the current telemetry paradigm limits the spectral efficiencies that can be gained when compared to a bi-directional networked telemetry approach.

Shortfalls with the current test range telemetry paradigm include²:

¹ Information taken from the Sarnoff “RDT&E Spectrum Requirements Assessment”, 5 August 2004; Estimate of the shortfall is for the Western Range facilities

² Young, Tom and Radke, Mark, “An Innovative Approach to Modernizing Telemetry” ITEA Journal, 2016

- Limited flexibility in transmitted data format

Currently, test data is acquired by the instrumentation system on the test article and encoded into formats that are pre-defined and referred to as a “data package”. These data packages are composed of fixed length frames containing data along with synchronization words to delineate the beginning of each frame. These frames are then transmitted over a fixed bandwidth, fixed frequency (both configurable, but not changed during a test) from an omnidirectional blade antenna (or wrap around antenna on a missile) to a parabolic, mechanically steered tracking antenna at one or more ground stations.

- Transmission of less urgent test data

Often when conducting test missions, a series of “test cards” are created to test specific aspects of the aircraft during that flight. Test cards are generally conducted with the same data package that includes all parameters needed to be monitored for the entire mission, or a particular aspect of the current test phase.

- Allocation of infrastructure resources

During a test mission, ground station resources are allocated to receive the telemetry signal and relay it to the mission control room. Since parabolic antennas only track one target at a time, they have to be dedicated to a test article for the duration of a mission. These telemetry ground stations (GS) are expensive to construct and maintain, most requiring to be manned during missions.

- Non-optimized spectrum scheduling and usage

Spectrum assignments for test operations are planned days in advanced to allow sufficient time for manual coordination and de-confliction. There are tools available to visualize spectrum occupancy and conflicts, but resolution of conflicts is a manually intensive process. Since the telemetry links can operate at distance of up to 150 nautical miles, frequencies are typically not re-used in instances where there is the potential for interference. This scheduling paradigm often requires frequencies for a single mission to be allocated across multiple ranges to prevent interference due to the power of the transmitter and gain of the ground antennas. The scheduling of frequencies across test ranges and facilities does not allow test planning tools to employ spatial diversity to reduce the probability of interference from adjacent signals and provide frequency re-use.

The TRMC is developing the core set of networked telemetry capabilities, including implementing a bi-directional telemetry link, as part of the Integrated Network Enhanced Telemetry (iNET) project. These capabilities are enabling components for the Wireless Inter-range Network Environment. The iNET program is developing a new telemetry system,

employing a network architecture for airborne platforms that will replace the current instrumentation systems with industry standard Ethernet and add a bidirectional network channel from the aircraft to the ground. iNET project status and changes to the current telemetry paradigm are found in the conference proceedings as part of the technical paper titled “iNET: Impacts to the Telemetry Community”.

Wireless Inter-Range Network Environment

The implementation of a wireless, inter-range network environment focuses on leveraging current efforts to develop a network based telemetry capability and mobile wireless “cellular” technologies. The wireless, cellular approach has been in use since the 1980s for commercial applications and has evolved and improved to the point where wireless voice and data services have become ubiquitous allowing instant communication. Commercial wireless carriers have challenges that are similar to those experienced by the MRTFB facilities and ranges, specifically how to cost effectively support increasing numbers of high bandwidth users over large geographical areas with a limited amount of spectrum. While the T&E environment differs from the mobile wireless environment, adaptation of current wireless technologies to this environment provides significant benefits and efficiencies.

Shifting the focus from the use of point to point links to a networked architecture will require changes in the terrestrial range infrastructure—specifically moving from parabolic, mechanically steered tracking antennas to an arrangement of smaller less network enabled ground stations which could be deployed across a range to provide the necessary coverage to flight line areas, hangars, and flight areas. To accommodate the existing range infrastructure, current long range antenna systems could be modified to provide additional coverage over ocean ranges and large expanses of open terrain where it might be impractical to deploy cellular based ground stations.

For example, in a wireless, inter-range network environment, multiple ground stations arranged in a manner similar to Figure 3 that cover a majority of range areas and provide additional capacity based on frequency re-use. In this scenario, these ground stations would be connected with either a wireless point to point, wireless mesh network, or fiber backhaul to transport data back to the mission control room. Each ground station would have a smaller coverage area to maximize spectrum re-use.

The test article transmit power can be automatically controlled to provide the optimum power required to maintain a stable link while minimizing interference to adjacent ground stations. When additional coverage is needed in a remote location, a mobile ground station could be deployed to provide the needed coverage. Each color in Figure 3 denotes a different frequency range in which a ground station would operate.

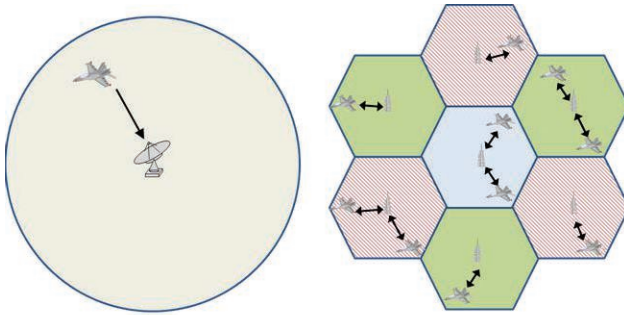


Figure 3- Example of Traditional data transmission method versus a Cellular Based Approach

Additionally, the commercial wireless industry invested heavily in developing various data modulation/transmission schemes to enable access to wireless channels by multiple users. Each of these schemes have benefits and shortcomings, and all would have to be adapted to the test range environment (e.g. increased Doppler shift due to higher velocities, different operating frequencies). The T&E community has invested in the technology to leverage one such modulation scheme, Orthogonal Frequency Division Multiple Access (OFDMA). In addition to OFDMA, other industry developed multiple access schemes like Single Carrier Frequency Division Multiple Access (SC-FDMA), which is being employed in the latest wireless standard of Long Term Evolution (LTE), could be leveraged and are typically more suitable for channels with high speed users. Additionally, different access schemes may prove more appropriate for use on the uplink portion of the communication channel as opposed to the downlink. When using OFDMA as a multiple access scheme, each test article would be allocated a set of subcarriers, enabling each ground station to support multiple test articles in each "cell". Supporting multiple simultaneous users with OFDMA will also save spectrum that would normally be lost to guard bands between single carrier signals. When channel conditions are suitable, more advanced modulations (e.g., SOQPSK-TG, ARTM-CPM, QAM16, QAM64) could be used to modulate the subcarriers providing even more throughput per unit of spectrum.

As a test article moves from one ground station to another, the network infrastructure system would need to execute a "handoff" of the test article to maintain connectivity. These handoff mechanisms would also be leveraged from the mobile wireless industry, which seamlessly allow movement from one cell to another while maintaining both voice and network connectivity. In addition to handing over data channels from cell to cell, additional handover mechanisms at the network level would need to be employed. As a test article moves to another range's network, it registers with a home agent on its home network and provides a "care of address".

In terms of resource scheduling, ground stations and spectrum that are required to support a test mission are scheduled days in advance. This is mainly due to the limited number of ground stations (which only

supports a single test article each) on a range, as well as the manually intensive process of frequency de-confliction often requiring cooperation between several ranges. By using a cellular-based approach, frequency assignments and de-confliction is done once during the planning and deployment phase of the ground stations or when modifications are required (ground stations added or removed). Ground station scheduling is also eliminated because each ground station can support multiple test articles simultaneously.

The TRMC is sponsoring several efforts to leverage, develop, or modify commercial cellular technologies to operate in the testing environment to support telemetry. The first such effort, the Flightline Radio Network with Seamless handoff (FRNSH) effort, is leveraging commercially available cellular technologies operating in the 1710-1755 MHz 3GPP band to support pre-flight test telemetry requirements and instrumentation check out in the hangar, flightline, and taxiway environments. Currently, AMT systems are turned on pre-test when an aircraft is in the hangar or flightline to ensure that onboard instrumentation systems are functioning properly. Unfortunately, this situation uses RF spectrum allocated for flight testing and consumes spectrum that could otherwise be used to support an additional flight test mission. By shifting this pre-test instrumentation telemetry requirement onto non-AMT spectrum, such as LTE or 3GPP commercial spectrum, an additional flight test mission can be conducted using the AMT dedicated spectrum. Additionally, the Cellular Range Telemetry (CRTM) and Cellular Range Telemetry Network (CeRTN) efforts are modifying commercial cellular components, such as eNodeB and user equipment, to operate in portions of spectrum allocated for AMT in the U.S. These efforts are developing the initial ground infrastructure required to implement a wireless inter-range network environment and are investigating technical components of the future vision for a test range infrastructure such as Doppler effects using cellular ground stations and cellular handover mechanisms and techniques. These technology development and demonstration efforts will lay the ground work to build on the CTEIP iNET project towards a wireless inter-range network environment to support all range data transmission requirements in the most spectrally efficient manner possible.

Conclusion

In order to fully realize a robust a wireless range network, continued investment in spectrally efficient technologies will be required. There are several thrusts within the DoD to invest in technologies that support more efficient usage of the RF spectrum and enable spectrum sharing opportunities.

Once the iNET project is completed and delivers the core networked telemetry components and the technology demonstrations and development efforts from the FRNSH, CRTM, and CeRTN projects are completed, the TRMC, in conjunction with the MRTFB facilities and ranges, will need to explore future investments to optimize cellular technologies

for use in the testing environment. Once the appropriate investments are made to tailor the cellular technologies to the testing environment, budgetary decisions can be made to fully implement a cellular telemetry capability across the MRTFB.

References

- [1] Sarnoff Corporation: “*RDT&E Spectrum Requirements Assessment*”, 2004.
- [2] Young, Tom and Radke, Mark, “An Innovative Approach to Modernizing Telemetry” ITEA Journal, 2016.

Glossary

AFB: Air Force Base

AMT : Aeronautical Mobile Telemetry

CTEIP: Central Test and Evaluation Investment Program

DoD: U.S. Department of Defense

iNET: Integrated, Network Enhanced Telemetry

MRTFB: Major Range and Test Facility Base

SUT: System Under Test

T&E: Test and Evaluation

TRMC: Test Resource Management Center

Ninja Telemetry

AMT Survival in a Congested Spectral Environment

Timothy A. Chalfant
COLSA Corporation, 41240 12th St. West, Palmdale, CA USA
tchalfant@colsa.com

Abstract:

Spectrum encroachment affects Aeronautical Mobile Telemetry (AMT) in many bands and many regions throughout the world. AMT users have found themselves with less spectrum in which to operate, and in some instances, spectrum once allocated exclusively for telemetry, has been opened to sharing with other users. This paper establishes a need for better tools and methodologies to accommodate AMT operations in this “unfriendly sky” when the AMT operator must operate in bands where they may lack a primary allocation (International Telecommunication Union (ITU) and/or domestic), and its associated protection. Of course, any operations on such a (secondary) basis would be for non-safety-of-flight and other non-high-value missions.

In these cases, we must function with the stealth of the ancient Ninjas to avoid causing interference while in turn avoiding interference from primary users in the band. This paper, directed to the Range or Facility executive management, presents a new philosophy and call to adapt to this new paradigm. The telemetry community needs to aggressively research and develop new technology to remain effective in shared spectral environments.

Key words: Aeronautical Mobile Telemetry, Radio Frequency (RF) Spectrum, Spectrum Encroachment, Spectrum Efficiency, Quality of Service, Spectrum Sharing

Early Telemetry

“Those were the days my friend, we thought they’d never end...”

- Song “Those Were the Days” [1]

Aeronautical Mobile Telemetry (AMT) has a long history in aerospace. Early aerospace telemetry dates back to its space inauguration with the Soviet satellite Sputnik, launched in 1957. The famous “beeping” of Sputnik-1 was in reality a Pulse Duration Modulated telemetry signal, encoding internal pressure (pulse length) and temperature (length between pulses) in the signal.

Telemetry systems advanced rapidly but were limited in their utilization by the technology of the day (large, heavy, lots of power). Early telemetry’s unreliability was such that Wernher von Braun once claimed that watching the rocket through binoculars was a better idea [2].

At this time the technology, not radio frequency (RF) spectrum, was the limiting factor.

In the United States (US) early telemetry system were assigned to an allocation in the 2-meter band at 225-260 MHz (sometimes referred to as “P” band). A government directive issued in 1958 required telemetry users to vacate this band and move to the 1435-1535 MHz and 2200-2300 MHz bands (L and S band) by 1970. We lost 35MHz but gained 200MHz. Life was good.

Telemetry systems grew to accommodate the increasing need for real-time data. The bands accommodated that growth very well through the 1960’s and 70’s. The available spectrum was able to accommodate the growing utilization. The slow advances in telemetry technology only limited telemetry growth at that time.

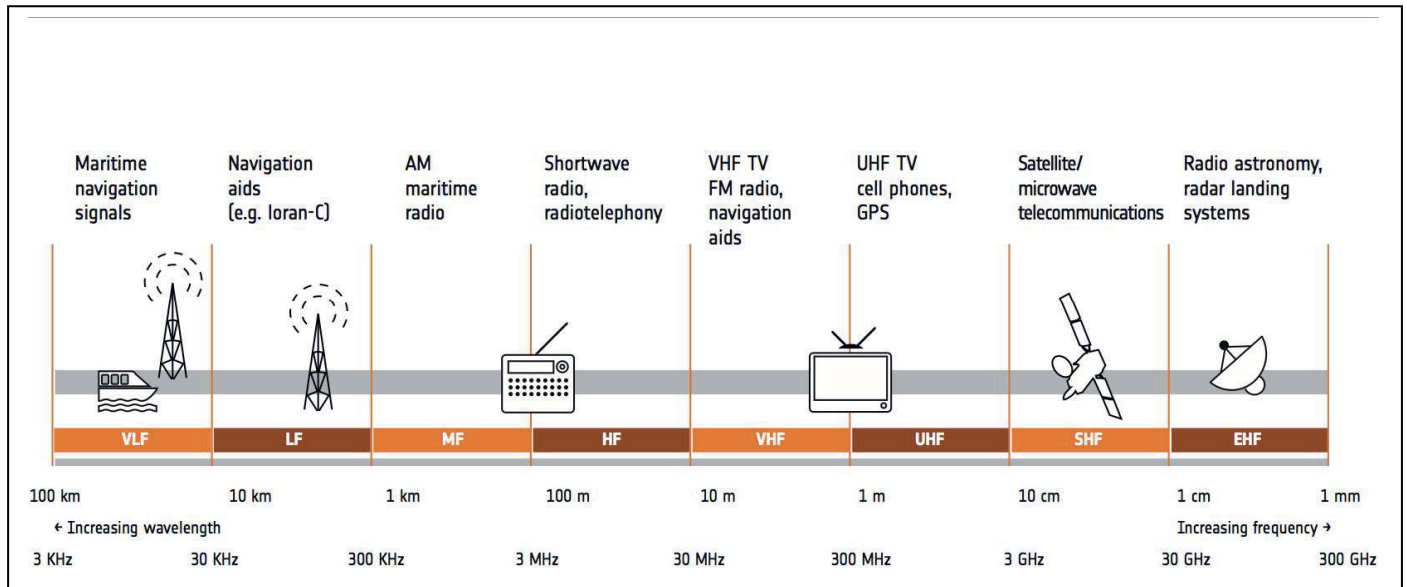


Fig. 1. RF Spectrum

US telemetry bands, managed and controlled by the US Government, were shared with the aerospace industry. Scheduling was done cooperatively between the Government and the aerospace industry (via the Aerospace and Flight Test Radio Coordinating Council [AFTRCC]) [3]. Scheduling was simple with projects being de-conflicted by assignment of dedicated center frequencies, bandwidths, and guard-bands. There were enough frequency assignments to accommodate all users. Once you had your assignment, you could use it whenever you needed.

At that time, flight test telemetry was protected from interference by the frequency coordination with AFTRCC and the government's frequency assignment system. The safety-of-flight needs associated with aerospace vehicles require protection to provide an interference-free environment, as do other high-value missions. AMT is very susceptible to interference. Due to the small size and power restrictions of aeronautical test articles, flight test telemetry is a low-power signal not very far above the noise floor. This meant that large antennas and clean spectrum was needed to find the telemetry "needle in the haystack". These signals were well protected from co-channel and adjacent channel interference by restricted access to these bands per US government's Federal Communications Commission (FCC) and the National Telecommunications and Information Administration (NTIA) regulations and the intelligent scheduling of center frequencies between guard-bands.

Then several things changed....

Growth of Wireless Communication

The growth of the internet, social media, and wireless communications created a new need for RF spectrum. Over the past 20 years, the world has seen the birth and adolescence of a rapidly growing commercial mobile service industry that has an insatiable appetite for spectrum. This growth has only accelerated. By the end of 2010, there were 5.3 billion mobile cellular subscriptions globally, including 870 million active mobile broadband subscriptions [4].

This has resulted in many national administrations taking a new look at RF spectrum. Increasingly, both industry and governments are viewing spectrum in economic terms, as an input to the production of telecommunications services and a source of revenue.

RF spectrum, once only of interest to scientists and engineers, has become the means to allow users to socially connect and download music and movies. The connected-generation has taken root globally and spectrum is now a limited commodity frequently auctioned for revenue and shared as a constrained resource.

The protection and abundant bandwidth once enjoyed by the flight test community is eroding. The scientific community is losing ground to social networks and cell phones. The new economic value of spectrum, and the politics of economic growth and voter appeasement, are the new norm.

Telemetry in the Wireless Sweet Spot

RF spectrum covers a lot of ground. It starts around 3 KHz and ends around 300GHz (Fig. 1) [5]. For many services, especially broadband

and cell phones, the unique characteristics of RF propagation and atmospheric distortion create a “sweet spot” below 3 GHz (Fig 2) [6]. Those characteristics serve telemetry well (low signals, long distances...).

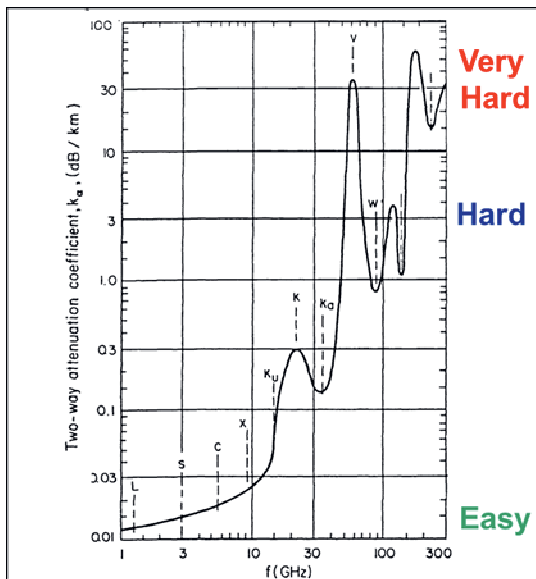


Fig. 2. Atmospheric Propagation Sweet Spot

This sweet spot also presents a unique aspect for wireless services. The best frequencies for mobile broadband are bands that: 1) can penetrate terrain and buildings (as much as possible) and 2) be received on small antennas. The range 300 MHz-3.5 GHz meets these criteria well.

This sweet spot is also the home to our AMT bands (for many of the same reasons). Many commercial services (cell phones, broadband) are aggressively seeking to displace AMT and locate in this sweet spot. It is like “waterfront” property in real estate, demanding high prices due to its short supply. The telemetry practitioner, once alone in this sweet spot, must learn to protect its property and, in some cases, involving non-safety/high-value tests, learn to share.

Telemetry Economics

The wireless service versus AMT economic comparison is difficult. A study on the economic value of telemetry in the US completed in 2006 placed a value on the 215 MHz of available telemetry spectrum in the US at approximately \$105 billion, generating 15% of the US gross domestic product (GDP), and providing over 11 million US jobs [7]. While AMT spectrum is in the critical path for the U.S. aerospace industry, and while the data above represent a set of very strong statistics, the spectrum value when used for AMT might be challenged by its value for broadband. Several past auctions in the US has shown the virtually untapped value of

spectrum as a revenue source. In 2015, the US auctioned 25 MHz of L-Band (AWS-3 spectrum auction, known as auction 97) at a record \$44.9 billion [8]. That is far more “\$ per Hertz” than raised in any previous spectrum auction in the US.

Surrounded by Unfriendlies

While there are many other economic variables to consider, to the growing wireless services, to them the next step is simple: their governments should seek to auction more spectrum. AMT is surrounded by unfriendly competing services seeking our spectrum. AMT needs to survive in a congested environment.

Telemetry Ninja’s

A lesson in survival techniques in unfriendly environments can be drawn from the Ninjas of ancient Japan. A Ninja was a covert agent that excelled in waging irregular warfare during the 12th-15th centuries. Ninjas figured prominently in legend and folklore, where they were associated with abilities such as invisibility and control over the natural elements. Historian Kiyoshi Watatani states that the Ninja were trained to be particularly secretive about their actions and existence [9]. Using “ninjutsu” techniques, they aim to ensure that one’s opponent does not know of one’s existence.

The safety issues that accompany flight test telemetry will protect our existing dedicated/primary spectrum, but the spectrum allocated for AMT is not likely to accommodate growth. Many administrations are pushing AMT to operate in shared bands. Sharing studies between AMT and other services show AMT is a difficult partner. AMT, as a small-signal service, is very sensitive to interference. Regardless, to accommodate AMT growth, we need to pursue a future that includes both dedicated and shared spectrum allocations. We must be able to survive in a shared environment, and in some cases the sharing may have to be on a secondary (non-interference) basis.

To survive outside our dedicated spectrum fortress we need to acquire new tools. Like a Ninja, the telemetry community needs to take action to survive in these commercially-driven political times. We must learn to operate in shared spectrum. We need to adopt ninjutsu techniques to ensure that our signal is not harmed by others.

To survive, telemetry ninjutsu techniques need to be developed in three main areas; DEFEND what we have, DEVELOP new ways to operate, and DISCOVER new approaches and solutions to meet our customer needs (Fig 3).

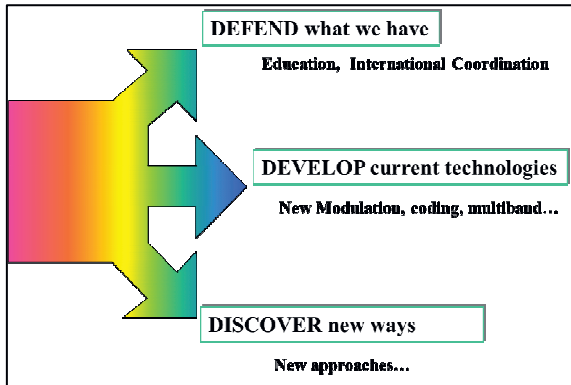


Fig. 3. 3 prongs needed for Survival

DEFENDING Telemetry Spectrum

The telemetering community needs to continually educate its decision makers. We need to tell an effective story to those in our management chains and national administrations so they have a solid appreciation for the importance of AMT spectrum. We need to make sure they have a good understanding and current information so they can make informed decisions and inputs.

Calling All Ninjas

To aid in “getting the message out” the International Consortium for Telemetry Spectrum (ICTS), chartered by the International Foundation for Telemetering, was created to “establish an international information exchange of telemetry practitioners to promote the benefits and enhancement of electromagnetic spectrum for telemetering applications” [10]. The main goal of the ICTS is to prepare the international telemetering community to address international concerns and threats presented at the World Radiocommunication Conferences (WRCs), the forum chartered by the ITU. The ICTS outreach effort was very effective in supporting the campaign to secure additional telemetry spectrum that resulted in the new C-Band telemetry band we recognize today at WRC-07 [11].

The ICTS is able to help defend AMT spectrum by working within the grass-roots scientific telemetry community. The ICTS needs to effectively engage the affected industries, manufacturers, academia, and government agencies that work with, and rely on, telemetry. Organizations like the ICTS needs to expand as a resource library that will help the telemetry community stress their needs to their management and national administrations, and eventually, the WRC.

DEVELOPING Current Technology

The telemetering community cannot rest on their current technology or spectrum. In the past we have relied on high walls (primary

assignments) and few enemies (very little commercial wireless) for our protection. Now we must learn to live closer to the enemy’s camp (other users). The flight test telemetry community has been working in this area for a long time. In the US, the Test Resource Management Center (TRMC) has funded several major projects (Advanced Range Telemetry (ARTM) [12], Integrated Network Enhanced Telemetry [iNET] [13]) and research efforts (Spectral Efficient Technologies) [14] that have paid off many times over in efficiencies and agility increases. Much more is needed.

Ninja Efficiency; Doing More with Less

While the telemetry need has grown (Fig 4) the US has been able to avoid significant cancellations and impacts by implementing these new technologies developed by several research programs. Even with the available telemetry spectrum shrinking by 35% (previous to WRC 07) they have accommodated an exponential data growth by increasing the bits/Hz efficiency of RF telemetry. The implementation of higher order modulations (like Shaped Offset Quadrature Phase Shift Keying (SOQPSK) and Continuous Phase Modulation (CPM), via the ARTM program) has

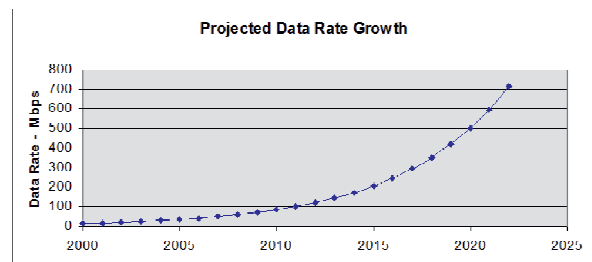


Fig. 4. Projected Telemetry growth in the US

resulted in many users achieving a 200% increase in data efficiency [15]. Without this and other improvements in quality of service, there would have been serious consequences to telemetry users. The US has achieved a major cost avoidance by the implementation of these new telemetry technologies. These efficiencies can be seen in the Yuma, California tests of an error-free AMT link on a helicopter recently accomplished by the Army [16]. The cost of delays, aborts, or cancels in a test program can be significant. One delayed or canceled test mission due to the unavailability of telemetry spectrum could cost a US program manager in excess of \$1 million [17].

We need to develop more techniques, like higher order modulation, to make telemetry more efficient, to be able to transmit more data with less spectrum.

Ninja Flexibility; Adapting and Adjusting

Another ninjutsu skill – the “telemetrist” (a user, supplier, or customer of telemetry) needs to develop is the Ninja’s ability to improve their use of existing weapons in their arsenal. Ninja’s were known for developing new techniques to increase the agility of their current weaponry in new and different ways.

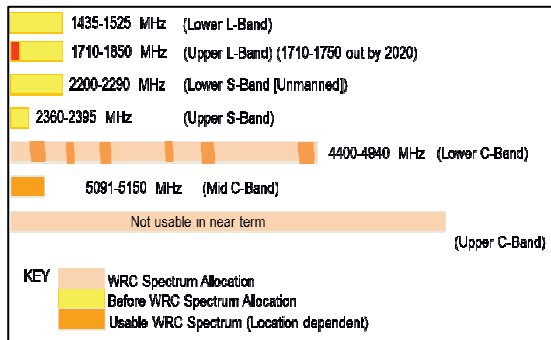


Fig. 5. RF Telemetry Bands Available (ITU Region 2 Shown)

One new weapon is telemetry frequency agility. We need the agility to access all spectrum bands available for telemetry. At WRC-07 we gained access to several new bands (Fig 5). To exploit these widely scattered telemetry bands we need to build more frequency agile technology. The development of multiband transmitters, antennas, cabling, and associated components is critical for exploiting these bands. The ability to tune, in real-time, to multiple bands will not only allow us to schedule more missions, but to avoid conflicts before they affect our mission. Additional research into software-defined radios and wide-band components is critical to achieve this desired telemetry frequency agility.

Telemetry Honor; Sharing and Respect

The sweet spot spectrum is congested. In areas where there are limited AMT authorizations (like Asia and the Pacific), AMT spectrum use for non-safety of life/non-high value purposes might be on a secondary basis. The telemetrist must give preference in such cases to the primary service by preventing interference. With Ninja-like honor, we need to accept interference from others, and not interfere with them.

Telemetry is by its low spectral power density nature an interference-limited technology. Our test articles typically have significant size, weight, and power limitations that restrict our transmission options. As a “small-signal-service”, we are sensitive to interference even from low-power components (such as cell phones). A cell phone near a telemetry dish will over-power reception from a test article

telemetry signal when the antenna is 100 miles away or even less.

Recent research into Low Probability of Detect Codes (LPDC), Space-Time-Coding (STC), error-correction, and other solutions can increase our noise tolerance and preserve our quality of service (QoS). As seen in several papers presented at telemetry conferences and other venues (European Test and Telemetry Conference, International Telemetering Conference [18], International Test and Evaluation Associations [ITEA] Test Instrumentation Workshop [19]) these technologies are maturing rapidly and many are now available commercially.

Risk Aversion as a Barrier

Telemetry executives need to manage risk better and become less new-technology averse. Once a technology is proven and reliable, they typically do not want to change it. Their job is not to test telemetry systems, but to use them to test something else. Telemetry is a critical tool that needs to be sufficiently mature (robust and reliable) so it can be relied on to do the real test job (air vehicles, rockets, and other aeronautical product development). Telemetry systems need to be low-risk to do a high-risk mission. This has caused many to be too comfortable with old style telemetry such as pulse code modulation/frequency modulation (PCM/FM), and current systems. We need to get comfortable with a new slew of acronyms (SOQPSK, CPM, LPDC, STC...).

The best way to do this is plan to implement them earlier than when you may need them. As a sailor, my Dad told me the “best time to reef the main is before you need it” [20]. This can also be true of new technology. Ranges and Test Facilities need to implement frequency agile, spectral efficient and robust technologies before the spectrum congestion demands it. We know our future will be more spectrally congested and sharing of frequency bands will become the new norm. Range and facility managers who rely on telemetry today need to make proactive investments in new technology to reserve the utility of their telemetry tools in the future.

DISCOVERING New Telemetry Frontiers

“... and now for something completely different...”

-Monty Python

The modern Ninja does not look or act like his 12th century relative. Today’s Ninjas are called Special Ops, Rangers, or many other terms that

denote the progression and development of the ninjutsu skill-set. They have been constantly redefined and reinvented. Telemetry needs to be “reinvented” also.

As cell phone technology can be categorized into multiple generations, the telemetry community is rapidly approaching a similar evolutionary path. As our 4G smart phones bear little resemblance to the 2G flip phones of just 10 years before, tomorrow’s telemetry system will diverge also. This can be visualized as “Telemetry Generations” (Fig 6).

- **1st Generation - frequency modulation (1960’s)**
- **2nd Generation –digitally encoding (1970’s)**
- **3rd Generation –advanced modulation (2000’s)**
- **4th Generation – Network-packets (2020’s)**
- **5th Generation - ??**

Fig. 6. *Telemetry Generations*

In figure 6 each generation had a significant change in architecture from the previous. Each generation has implementation challenges but can achieve increased capabilities as a result. In some cases, generational leaps can be caused by “disruptive technology”. A disruptive technology is a technical innovation that eventually displaces an existing technology. Not all technical innovations are disruptive, even if they are revolutionary. Telephone technology was a disruptive technology that eventually replaced the telegraph for long distance communication. In telemetry, we need more of these “disruptive technology” to move forward.

Ranges typically have a hard time adopting new technologies due to a legacy sensitivity that can slow the introduction of distributive technology. This is due impart to the sizable capital investment in test article instrumentation and range infrastructure. This investment cannot be easily ignored and discarded (as is done with cell phones). As a result, Ranges will typically overlap technologies via downward compatibility. The Ranges need for compatibility with legacy systems constrain the introduction of beneficial disruptive technology. On some of the largest Ranges, the period for these generational leaps has been measured in decades.

Some examples of what could be that disruptive technology that drives 5G telemetry may be new bands and commercial technology.

New Bands; Ninja Climbing Skills

Can telemetry survive outside the less-than 3 GHz “sweet spot”? Sometimes to avoid conflict with an enemy, a Ninja needs to climb up to freedom.

Aggressive research should continue to enable telemetry systems in higher spectral bands (one way to avoid the high cost of waterfront property is to move to the desert). The higher RF bands (X, Ku, K, KA, V, W) present many atmospheric and physical challenges that need aggressive research and innovation. Managers of test ranges and facilities should be promoting and leading this research.

New Technology; Ninja Weaponry Advances

As a Ninja adopts new weapons, the innovative telemetrist needs to look beyond the current telemetry paradigm. In the early years of telemetry, the telemetrist was a driving force in wireless communication. Today we are a small niche market for a handful of (awesome) companies. The telemetry stakeholders (suppliers and customers) need to promote research into new technologies and concepts that can operate in a shared spectral environment.

One of these disruptive technologies to telemetry maybe Long-Term Evolution (LTE) [21]. Joining the 4G cell phone industry maybe a future step for flight test telemetry. Research is ongoing in the US and several other countries on the utilization of LTE and 4G technology to take the next generational leap for telemetry. Using this concept of cells and LTE networks to collect and distribute real-time data from fast vehicles presents many interesting challenges (Doppler shifts, multipath, handoffs, QoS, security,...) that should be studied by the Ranges and Test Facilities.

Better Ninja Stealth

Taking the Ninja allegory (maybe too far?), what if telemetry went completely stealth? Additional research and testing of stealth telemetry technologies (directional antennas spread-spectrum, burst, LASER ...) could preclude the need for telemetrist to be seen (and schedule) with others. As the potential for interference is reduced, we may achieve complete Ninja stealth, the ability to operate in any band at any time, no need to schedule or manage outside the telemetry community.

Going “directional” shows potential telemetry promise. One of the nice features of many of our test articles is we know where they are (typically we have good time-space positioning information). If we know the test article position, and the ground antenna position, could we derive a predicted pointing solution for antenna tracking? Research outside the omnidirectional antenna model can have significant payback. Also, with a directional beam, power draw is reduced, interference reduced, and scheduling can be simplified. Research into directional antennas, phased-array applications, and

lobe/null tuning is showing great promise and needs to be matured.

Several other “stealth” techniques have been explored and should be developed. Pseudo-random noise-based spread spectrum signals allow the telemetry signal to hide in the noise floor. Systems that collect the data on-board and burst the signal over a high-capacity (microwave/LASER) link periodically needs further investigation. This application of “we can see them, but they can’t see us” telemetry technology should be pushed and developed.

The Need for Innovation

The Range and test facility management needs to respond to the congested spectral environment pro-actively. Telemetry is in need of massive influxes of innovation. Some of these innovations presented in this paper are under development. The threat (spectrum congestion, spectrum encroachment, spectrum sharing) is real and will grow. Like a Ninja, we need to adapt to the enemy at hand.

We cannot expect change if we always do what we have always done (that is the definition of insanity).

AMT FUTURE; A call for Super-Ninja Action

The international telemetering community is facing very aggressive threats that will shape a new Super-Ninja paradigm.

AMT users have found themselves with less spectrum in which to operate.

This community has a critical need for better stealth telemetry tools and methodologies to accommodate this new “unfriendly skies” paradigm. When we must operate in bands where we lack a primary allocation, we must develop Ninja-like skills.

Our safety aspects will always require interference protection, as will other flight tests which, while not necessarily involving safety-of-flight, may entail other high value factors. This protection is restricted to a few AMT bands. The new paradigm presented in this paper is that of secondary AMT uses (non-safety-of-flight/non-high-value tests) in shared bands—something new to the telemetry community. This could present itself as a significant spectrum model in the future.

In this future, we must function with the stealth of a Ninja to avoid causing interference while in turn avoiding interference from primary users in the band. We must share with honor and respect in this new age. The Range and test facility managers need to aggressively seek new research and develop new “super Ninja” technology to remain effective in congested

shared spectral environments. Without their direct involvement, the AMT community will be unprepared to react to the new paradigm.

References

- [1] [1] “Those Were the Days” song lyrics by Gene Raskin, who put English lyrics to the Russian song “Dorogoi dlinnoyu” (“дорогой длинною”), written by Boris Fomin (1900-1948) with words by the poet Konstantin Podrevskii.
- [2] History of Telemetry, <http://www.orielsystems.com/short-history-telemetry/> (as of 3/20/2018)
- [3] Aerospace and Flight Test Radio Coordinating Council , <https://afrcc.org/>
- [4] Exploring the Value and Economic Valuation of Spectrum, John Alden, ITU Broadband Series Report , 2012 <http://www.itu.int/ITU-D/ict/material/FactsFigures2010.pdf> .
- [5] http://www.esa.int/var/esa/storage/images/esa_multimedia/images/2013/11/satellite_frequencies (as of 3/20/2018)
- [6] The Great Radio Spectrum Famine, Institute of Electrical and Electronics Engineers Spectrum Magazine, <http://spectrum.ieee.org/telecom/wireless/the-great-radio-spectrum-famine>
- [7] Economic Impact of Telemetry and Its Essential Role in the Aerospace Industry, Darrell E. Ernst and Carolyn A. Kahn, MITRE TECHNICAL REPORT Project No.0703D110-AA, 2006
- [8] IT’S OVER: FCC’s AWS-3 spectrum auction ends at record \$44.9B in bids , Phil Goldstein , <https://www.fiercewireless.com/wireless/it-s-over-fcc-s-aws-3-spectrum-auction-ends-at-record-44-9b-bids>
- [9] [9] From Wikipedia, “Ninja” <https://en.wikipedia.org/wiki/Ninja> (as of 3/23/2018)
- [10] International Consortium for Telemetry Spectrum. <http://www.telemetryspectrum.org>
- [11] Resolutions 416 and 418 in the FINAL ACTS of the World Radiocommunication Conference (WRC-2007), Radiocommunications Sector, International Telecommunications Union, , Geneva, 2007
- [12] The Advanced Range Telemetry (ARTM) program is described in RANGE TELEMETRY IMPROVEMENT AND MODERNIZATION, Chalfant, Timothy A.; Irving, Charles :Edwards Air Force Base, Proceedings from the International Telemetering Conference, 1997
- [13] The integrated Network Enhanced Telemetry (INET) program is described in INTEGRATED NETWORK-ENHANCED TELEMETRY , Skelley, Dan S., Naval Air Warfare Center, Issue Proceedings from the International Telemetering Conference.

- [14] The Spectrally Efficient Telemetry program is under the Test and Evaluation Science and Technology effort managed by the Test Resource Management Center (DOD AT&L), US Department of Defense.
- [15] Description and Performance Results for the Advanced Range Telemetry (ARTM) Tier II Waveform, M. Geoghegan, Proceedings of the International Telemetry Conference, 2000
- [16] ROTARY-WING FLIGHT TESTS TO DETERMINE THE BENEFITS OF FREQUENCY AND SPATIAL DIVERSITY AT THE YUMA PROVING GROUND, Diehl, Michael; Swain, Jason; Wilcox, Tab, US Army Air Combat Systems Directorate, Proceedings from the International Telemetry Conference, 2016
- [17] Economic Impact of Telemetry and Its Essential Role in the Aerospace Industry, Darrell E. Ernst and Carolyn A. Kahn, MITRE TECHNICAL REPORT Project No.0703D10-AA, 2006
- [18] International Foundation for Telemetry www.telemetry.org
- [19] International Test and Evaluation Association. www.itea.org
- [20] Attributed to George A. Chalfant MD (1924-2012), of the sailing vessel WindSwift
- [21] Long Term Evolution, in 3 GPPP standard for cell phones

Telemetry Network Standards Overview

Thomas B. Grace¹, Ben A. Abbott²

1: Naval Air Systems Command (NAVAIR), Patuxent River, Maryland, USA

2: Southwest Research Institute® (SwRI®), San Antonio, TX, USA

Abstract: In recent years, flight test systems have increasingly used network technologies to benefit from the capabilities that have driven the growth of the Internet and other industries. Seeing the power of network technologies, the Central Test and Evaluation Investment Program (CTEIP) established the integrated Network-Enhanced Telemetry (iNET) project to develop an interoperable air to ground network telemetry capability. The standards developed by the iNET project have recently been adopted as Chapters 21 through 28 of the Range Commanders' Council (RCC) IRIG-106 standards. This paper introduces the new IRIG Telemetry Network Standards and provides insight into the new capabilities that systems using these standards provide.

Keywords: TmNS, iNET, RCC, IRIG-106, Networking

1. Introduction

In 1948 a working group on telemetry was created such that “a large amount of development effort could be saved by standardization” [1]. In 1953, versions of the resulting standards began evolutionary sequencing that lead to (after approximately ten updates/revisions) active use by multiple ranges in 1969. Many decades later, both commercial and military telemetry communities reap the benefits of having invested in these standards. The Telemetry Network Standards (TmNS) pose a major enhancement to the sequence of evolving RCC standards.

The TmNS guide the development of network-based telemetry systems. They support leveraging network system design methodologies in order to enhance existing telemetry systems. The goal is to support development of telemetry systems that provide general-purpose networking capability meeting the majority of flight test needs of the United States Air Force, Army, and Navy, and that are interoperable among test ranges. Systems built in this fashion can efficiently support programs with both large and small numbers of measurands, including the Test Article (TA) components that provide the measurands. The philosophy can be used to specify systems that are small enough to be accommodated in fighter-sized aircraft.

The development of the architecture was a result of studies and workshops assessing the need for and implementation of network telemetry. The study team visited five Major Range and Test Facility Base (MRTFB) sites. The following capabilities were identified as being needed for networked aeronautical telemetry:

1. The need to dynamically share spectrum resources among many concurrent activities based on instantaneous demand for telemetry resources.
2. The need to manage this sharing appropriately through defined “quality of service” rules to ensure both defined priorities and fairness.
3. The need to provide real-time or near real-time access to all of the test article measurements either directly from the sensors or from data recorded and stored on the TA, significantly increasing the access to available information during a test compared to that available via the current legacy telemetry systems.
4. The need to command and control TA equipment, sensor parameters, legacy telemetry formats, and other functions from the test/training command and control center.
5. The need to provide effective over-the-horizon telemetry including access to test articles on a worldwide basis.
6. The need to provide additional telemetry communications to support systems-of-systems test and training involving large numbers of test articles (e.g., test article-to-test article communications, chase vehicle to test article).
7. The need to efficiently interconnect ground based systems with TA systems to support the use of simulation and stimulation.
8. The need to protect the integrity of all telemetry communications with the appropriate government approved information assurance technologies for classified information and/or commercially accepted technologies for company proprietary information.

Additionally, qualities that drove the philosophy of the TmNS standards include:

- Scalability
- Flexibility in operation
- User friendliness
- Complexity reduction concerning the networking concepts

The TmNS system architecture supported by the standards provides transformational interoperability enhancements for existing telemetry systems by leveraging networking technologies that can be used to increase test efficiencies. At its core, a TmNS-based system mimics general-purpose Internet protocol (IP) networks, but it also

provides specialized protocols to support flight test capabilities. The technologies leveraged enable capability growth as the market place evolves.

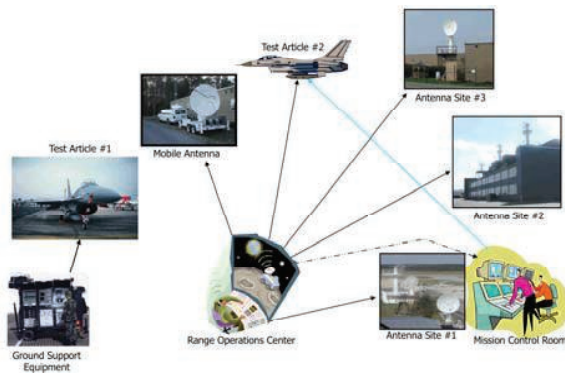


Figure 1: An example of typical TmNS subsystems

TmNS system architectures supports five major subsystems, the general functional areas (see figure 1 for an example). While the overall architecture does not mandate all five areas be utilized by every instance of a TmNS-based system, it is expected that typical system deployments will incorporate concepts from each of the subsystems. The five subsystems are described below.

1. **TA Subsystem:** The airborne TA provides functionality associated with network-based interfaces for transport, health and status information, configuration, and control of data sources, recording devices, and telemetry transmission devices. The TA also provides the means to interface into existing Pulse Code Modulation (PCM) systems.
2. **Ground Antenna Sites Subsystem:** A Ground Antenna Site supports the connecting of TAs with Range Operations. It provides a mechanism for routing data between a TA network and the range network. It relies on existing tracking mechanisms, such as a Serial Streaming Telemetry (SST) signal coming from a TA.
3. **Range Operations Subsystem:** The Range Operations functionality is focused on interfacing the RF-based components within antenna sites (e.g. radios) with the Range Operations Center (ROC). The Range Operations functionality provides the ability to remotely manage the resources within the Ground Antenna Sites (or Ground Stations) such as the tracking antennas, network devices (switches and routers) and the range network infrastructure, which provides the means to interconnect the range facilities.
4. **Mission Control Subsystem:** The Mission Control architecture concepts provide a means for interfacing into existing telemetry processing systems. The Mission Control consists of the resources necessary for processing TmNS data messages, communicating with the data side of the TA, and communicating with the telemetry processors.

5. **Ground Support Subsystem:** The Ground Support functionality supports various functions necessary to maintain the TmNS system's metadata, to perform maintenance and pre-flight checkout of the TA components, and to perform limited data reduction on the network data.

The bi-directional nature of the TmNS is fundamentally different from the historic approach. That is, devices on a TA may be accessed remotely during a test. When used in a typical military scenario, encryption-based separation of TA and mission control room portions of the network from the range and RF portions of the network is required. As such, there exists what we call a red side and a black side. We call the TA and Mission control room the red side.

2. IRIG 106 Chapters 21 through 28 Overview

The TmNS Standards comprise chapters 21 through 28 of IRIG-106. They are hosted for public download at www.wsmr.army.mil (see Figure 2).

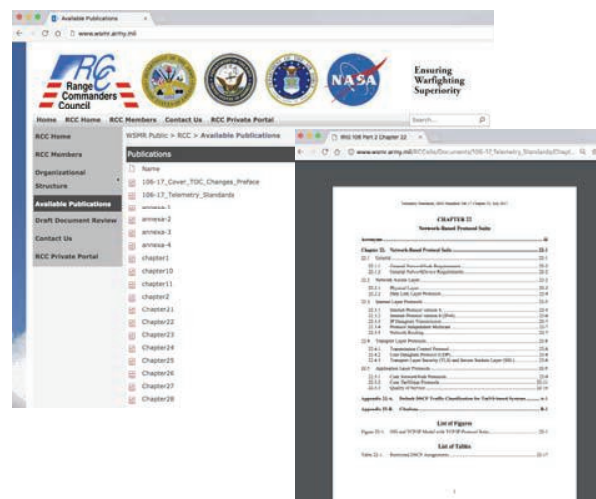


Figure 2: www.wsmr.army.mil is the official site hosting the TmNS Standards (chapter 22 is shown)

IRIG Chapter 21: Telemetry Network Standards Overview, introduces the overall concepts and introduces the remaining seven chapters. Abbreviated and slightly annotated versions of these descriptions is provided below [2].

IRIG 106 Chapter 22: Network-Based Protocol Suite. The TmNS approach leverages existing standardized Internet protocols to serve as the core set of communication. The TmNS's Network-based protocol suite and a large portion of the TCP/IP Protocol Suite (also known as the Internet Protocol Suite) along with other supporting technologies (e.g., underlying data link and physical layer technologies) are described in this chapter.

IRIG 106 Chapter 23: Metadata Configuration. This chapter describes system configuration data for TmNS based systems. It allows them to be described in a common fashion, and provides the means for describing the configuration of the components in a telemetry system, as well as their logical and physical interrelationships. This chapter defines a language, the Metadata Description Language (MDL). The MDL syntax defines vocabulary and sentence structure, while the MDL semantics provide meaning. MDL provides a common exchange language that facilitates the interchange of configuration information between telemetry system components.

IRIG 106 Chapter 24: Message Formats. The TmNS has defined several message structures unique for its use. This chapter describes the message formats of TmNS specific messages.

IRIG 106 Chapter 25: Management Resources. The TmNS defines Management Resources as resources that contain application-specific data accessible via an application layer protocol. Each TmNS Application defines a set of common resources and a set of application-specific resources. This chapter provides details concerning the standardized application resources.

IRIG 106 Chapter 26: TmNSDataMessage Transfer Protocol. The TmNS has defined several data transfer protocols unique for its use. This chapter defines how TmNS-specific messages (TmNSDataMessages) are transferred between TmNSApps.

IRIG 106 Chapter 27: RF Network Access Layer. This chapter defines the standard for managing the physical layer of RF links with the RF Network. The RF Network implements an Open Systems Interconnect (OSI) model approach to data transmission, where data moves through the OSI stack from the application layer to the physical layer, from physical layer to physical layer through some transmission medium, then back up the stack to another application on the receiving side.

IRIG 106 Chapter 28: RF Network Management. This chapter defines the standard for managing RF links within the RF Network.

3. TmNS Core Technologies

The TmNS utilizes an IP network, based on the success and description of the Internet Engineering Task Force (IETF) hourglass approach, which is shown in Figure 3. The IP layer is the basic interoperability between networked components. Figure 3 also shows a TmNS specialization of the classic IETF IP hourglass figure.

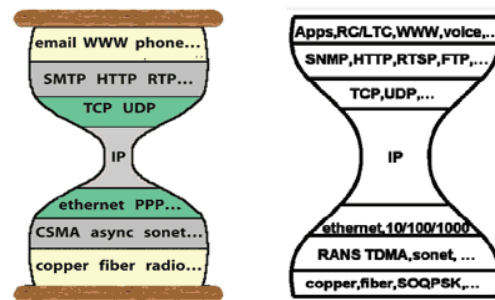


Figure 3: IETF vs. TmNS-Specific Hourglass

3.1 Network-Based Data Messages

Test data is delivered in TmNS Data Messages, which contains a header and a payload. Actual measurements are contained in the packages within a TmNS Data Message and the mapping of measurements in a TmNS Data Message is defined in a system configuration file, the MDL file. The MDL file describes the configuration for a particular device that is transmitting or consuming a given TmNS Data Message. Chapter 24 provides details concerning message shapes.

3.2 System Configuration and Management

System management within the TmNS is based upon the ISO Telecommunications Management Network model FCAPS, which stands for fault, configuration, accounting, performance, and security.

System Management is used across the TmNS to manage TmNS components, providing a view of fault, configuration, utilization, performance, and security configuration information on the network. Essentially, a TmNS system is composed of two types of components when it comes to management and configuration:

1. Managed devices: Any TmNS component that provides a management interface as defined by the System Management Standard and therefore can be managed.
2. TmNS Managers: An entity which manages TmNS Components. Managers implement the interfaces necessary to manage TmNS components in accordance with the System Management Standard.

All components within the TmNS are managed devices (including managers). As such, they can be managed by TmNS Manager(s). Figure 4 shows the building blocks of TmNS System Management. The core technologies used are Simple Network Management Protocol (SNMP) to pass management information through the system. SNMP Management Information Bases (MIBs) provide dictionaries for management information. Managed devices execute applications called agents which use the TmNS MIB to provide their internal status and accept controls and configuration. FTP, HTTP, and ICMP (ping)

play supporting roles related to file transfer, discovery and configuration.

The Metadata Description Language (MDL) is used for describing system configuration (Metadata) in a common fashion. The eXtensible Markup Language (XML) schema defined for the TmNS provides the means for describing the configuration of the components in the TmNS as well as their logical and physical interrelationships. MDL is expressive enough to describe a wide variety of systems: large and small, simple and complex, from the low-level transducer-to-measurement association for an acquisition card on a Data Acquisition Unit (DAU) up to network topology of multiple test mission networks.

By using the system management capabilities, TmNS components can be configured, reconfigured, controlled and statused in an interoperable way. Chapter 25 provides details on system management.

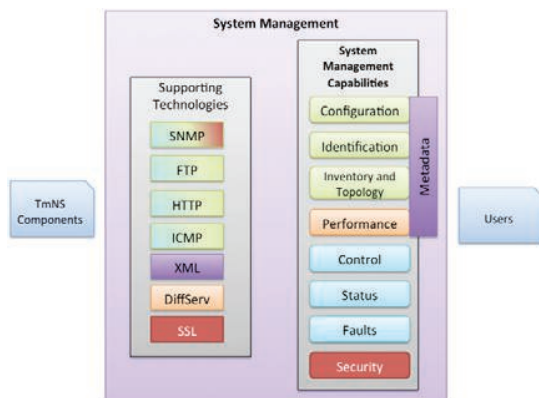


Figure 4: System Management Technologies

3.3 Time

Time within an entire TmNS based system is distributed using IEEE 1588-2008, also known as Precision Time Protocol (PTP) Version 2. Time within the TmNS is delivered without the addition of any wires. Chapter 22 provides details on 1588 time.

3.4 Quality of Service (QoS)

The TmNS annotates a typical Differentiated Services (DiffServ) architecture, a standard IP Quality of Service (QoS) mechanism for coordination of the delivery of competing data and command and control network traffic. Chapter 22 provides details on QoS functionality.

3.5 Routing

Routing is the process of selecting best paths in a network. The TmNS annotates IETF standards concerning a typical routed IP network. Using the classic routed IP architecture enables a variety of advanced capabilities, including relay, and other capabilities that have not yet

been explored. Chapter 22 provides details on routing technologies.

3.6 Source Selection

When RF propagation from one TmNS transmitting radio source arrives at two or more TmNS receiving radios, it is possible using routing and source selection to choose any one of the network packets. This support is provided through TmNS interfaces, data message formats, and management concepts. Collectively, the portions of the standard that describe these concepts are called the TmNS Source Selector portion of the standard. Chapter 28 provides details on source selection technologies.

4. Conclusion

The TmNS architecture is, by design, a communications and data delivery system that is partitioned into abstraction layers. As in the Open Systems Interconnection (OSI) model, a layer serves the layer above it and is served by the layer below it. The layers are in general independent, so that a layer can be changed with little to no impact to the other layers. This layered architecture in turn allows different technologies to be used in each layer.

6. Acknowledgements

The authors acknowledge the contribution of their colleagues to with respect to this work. There are too many SwRI, other contractors, and DoD personnel who have participated to count, so thanks everyone.

6. References

- [1] Reynolds, R. Stanton, "IRIG Telemetry Standards 1969," *Proceedings of the International Telemetry Conference*, Volume 5, 1969.
- [2] IRIG 106 Chapters 21 through 28 found at www.wsmr.army.mil

7. Glossary

CTEIP: Central Test and Evaluation Investment Program

DoD: Department of Defense

IETF: Internet Engineering Task Force

iNET: integrated Network-Enhanced Telemetry

IP: Internet protocol

IRIG: Inter-range instrumentation group

MDL: Metadata Description Language

OSI: Open Systems Interconnection

QoS: Quality of Service

RCC: Range Commanders' Council

RF: Radio Frequency

SwRI: Southwest Research Institute

TA: Test Article

TmNS: Telemetry Network Standard

XML: eXtensible Markup Language

Telemetric acquisition of vitality parameters and classification of cognitive condition via machine learning

Dipl.-Phys. Martin Bussas
TROUT GmbH, Parkstr. 28, D-34119 Kassel
m.bussas@trout-gmbh.de

Abstract:

The ability to acquire vital parameters and classify cognitive conditions opens doors to new technologies in diverse areas such as medical technology, automation, aerospace, fitness/wellness and security. TROUT gained considerable expertise in biometric data processing during automotive and medical technology developments which focused on machine learning and AI (Artificial Intelligence). With variations in the heartbeat, the organism can respond optimally to changing endogenous and exogenous influences and thus adapt to the current needs of the blood supply. Heart rate variability (HRV) provides not only information on the degree of stress on the cardiovascular system, but also on the quality of cardiovascular regulation and has also become established in other areas in recent years, due to ever smaller measuring instruments and lower costs, as well as applications in clinical research. [1]

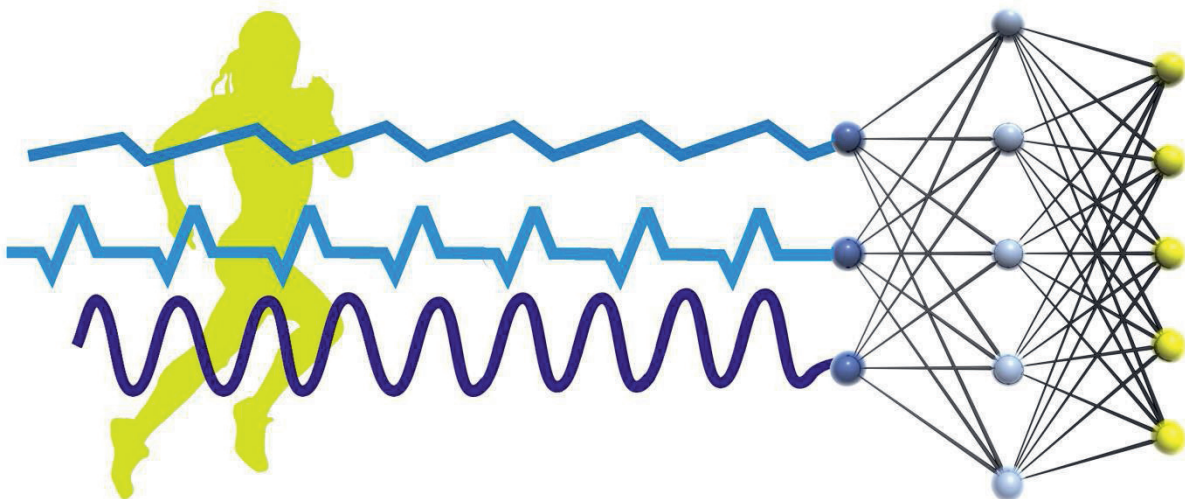


Fig. 1. Telemetric Acquisition of vitality parameters and classification

If we add information about the activities of an individual in correlation with their vital data, and process both data through a machine learning system, we are now able to achieve very good results concerning the individual's cognitive state such as stress level and fatigue. The system is adjusted by a feed-back loop mapping the individual's self-estimation of their cognitive state.

Key words: Artificial Intelligence, Machine Learning, Cognitive State, Stress Level.

Introduction

TROUT's R&D project VitaB focuses on the telemetric acquisition of vital data. VitaB is the German abbreviation of 'Determination of Vitality Parameters – Vitalitätsdatenbestimmung'. Telemetric sensors are e.g. video cameras, IR sensors and high frequency probe heads for heart rate and respiration rate.

VitaB was initiated by TROUT, and is funded in the framework of Hessen ModellProjekte (HA project no. 545/17-27), by LOEWE – Landes-Offensive zur Entwicklung Wissenschaftlich-ökonomischer Exzellenz, Förderlinie 3: KMU-Verbundvorhaben (State Offensive for the Development of Scientific and Economic Excellence).

One major focus is on investigating the relation between internal tension and external workload. Another objective of the R&D project is to establish a driver's state management system by classifying the driver's emotional and mental state and determining needs-based influencing measures targeting an optimal state. Machine learning algorithms detect relevant patterns in physiological and visual data. These patterns are used to classify the driver's condition at different levels of cognitive workload, arousal, valence and vigilance.

To support the development of a multilevel algorithm, an analysis application has been established which visualizes data and detects and evaluates apparent conspicuities. Several filters and evaluation functions are used to normalize and smooth the data for plausibility checks. The initial assumption is verified and optimized with technical and scientific support from the medical field, including a cardiovascular center amongst others. The resulting multilevel classification showed the desired high quality results, which were then further evaluated.

The objective of VitaB is to develop a cross-sectional, parameter-driven system that evaluates user vitality in order to classify the corresponding cognitive condition. Manifold products can be derived from the functional prototype. Using a closed-loop function, the estimated user state is continuously inspected and if necessary, positively influenced by downstream of adaptive systems. Depending on the estimate, an adaptive system can act in different ways in order to positively support the user.

Simulation Environment

3D goggles – not visible in the picture below – are used for perfect immersion into the driving environment.



Fig. 2. Simulator, photo HA – Jan Michael Hosan

Furthermore, we use a steering wheel equipped with motion sensors which detect acceleration and velocity of the steering motions of the

driver. Gear stick and pedals complete the driving environment.

ECG Sensor

The electrocardiogram (ECG) recording above illustrates beat-to-beat variability in R–R interval (top) and heart rate (bottom). Heart rate variability (HRV) is the physiological phenomenon of variation in the time interval between heartbeats. It is measured by the variation in the beat-to-beat interval.

Other terms used include: "cycle length variability", "RR variability" (where R is a point corresponding to the peak of the QRS complex of the ECG wave, and RR is the interval between successive Rs), and "heart period variability". The analysis of heart rate variability (HRV) has evolved in recent years to an established non-invasive detection of the level of exercise of the cardiovascular system. Thus, the HRV describes the interaction between the sympathetic and parasympathetic nervous system, which controls the activity of the heart, and allows the investigator to mathematically attribute the influence of the autonomic nervous system to the regulation of the cardiovascular system. This review is concerned with the analysis methods of HR-related, frequency-related and non-linear methods. Notes on the selection of the meaningful detection period are discussed and the visual values are presented for selected HRV parameters. [2] [3] [7].

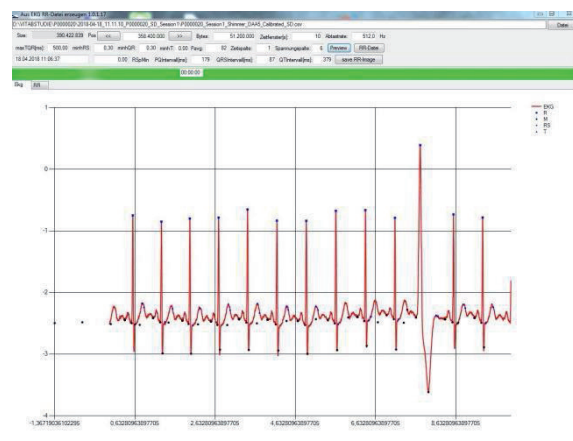


Fig. 3. ECG software to extract the R-R intervals

The ECG software, which extracts the R-R intervals from the signal, has been developed by TROUT. As the diagram above shows, the software has to deal with irregularities in the heart beat which occur once in a while.

Telemetric ECG sensor

In the previous study, we were able to evaluate a telemetric radar based ECG sensor from HF Systems Engineering GmbH & Co. KG with great success.

The basic idea of the radar based accurate heartbeat estimation method consists of time-domain signal processing applied on the electromagnetic waves reflected from the chest of the subject. A wideband signal in the middle region of the mm-wave band is used as the sounding signal, which is coherently recorded at the transceiver. Hence, the signal does not propagate through the tissue. Instead it scans precisely the skin movement due to respiration and micro skin vibration due to the heartbeat. Thus, a superposition of the strong chest signal and the weak heart signal resembles the raw data.

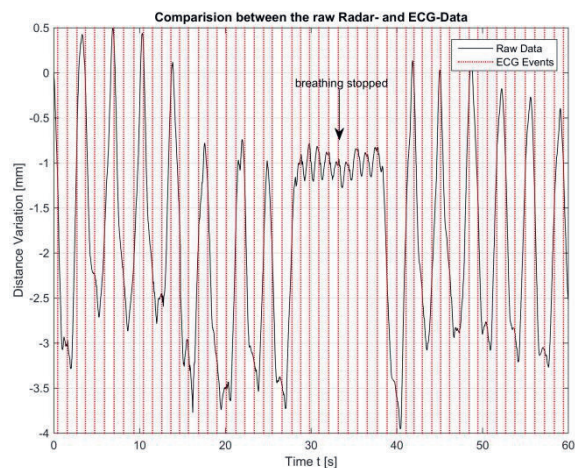


Fig. 4. Radar pulse versus ECG pulse

Super-resolution methods for highly accurate distance estimations are well known from specialist journals and documentation and are applied here to extract distance information of the range cell in the air-skin boundary. Subsequently, the distance vector is processed with spectral estimation methods and time domain parameter estimation methods to finally separate the breathing contamination from the heart beat content.

The radar signal reaches sufficient precision to be used for stress level evaluation below.

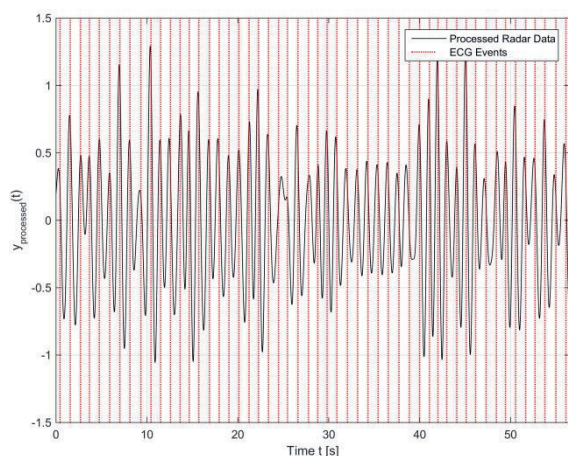


Fig. 5. Processed radar data

Acceleration Sensor in the Steering Wheel

Besides breath and heartbeat signals, we evaluate speed and acceleration via the steering wheel. This information is fed into the machine learning algorithms after processing the physiological data through a physiological model.

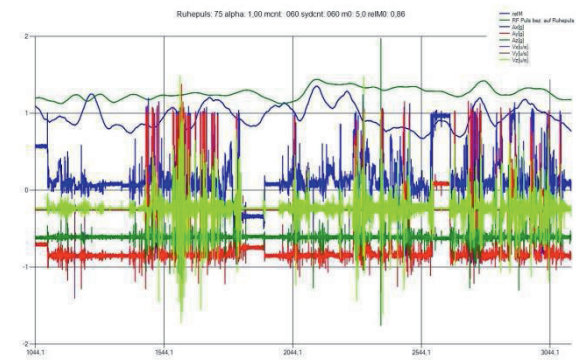


Fig. 6. Paired pulse ratio, steering wheel velocity and steering wheel acceleration versus time [s]

Physiological Model

The following features are extracted from available ECG data:

1. Actual pulse related to the resting pulse of the subject.
2. Average change in heart rate in percent per second averaged over 60 seconds, based on the average value determined for the subject.
3. Ratio of the velocity of pulse acceleration to the velocity of pulse deceleration averaged over 60 seconds, which is an indicator of the relationship between sympathetic and parasympathetic activity. This value is then calibrated according to the subject.
4. Ratio LF / HF from the Fourier Analysis determined ratio of the amplitude sums for LF and HF.

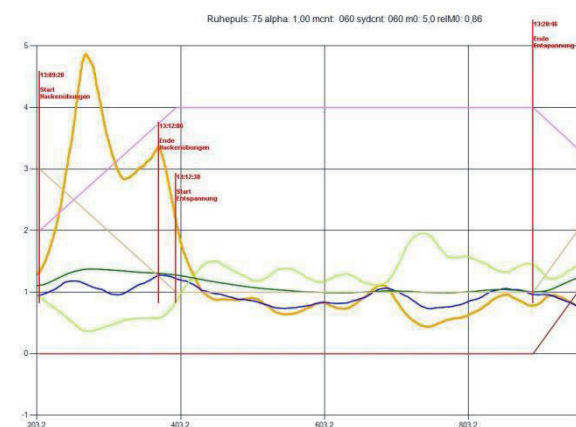


Fig. 7. Relaxation exercise

Legend for fig. 7 to 10: Heart rate based on the resting heart rate (green), ratio of pulse increases to pulse decreases (blue), HRV – Heart Rate Variability (light green), Event Marker (red – in German language), Calculated Stress Level (yellow) in a relative scale from 0 (no stress) to 7 (maximum stress) on the ordinate, the abscissa shows the time in seconds.

The drive simulation starts with a relaxation exercise in order to allow the subject to lower his pulse rate to the rest pulse rate.

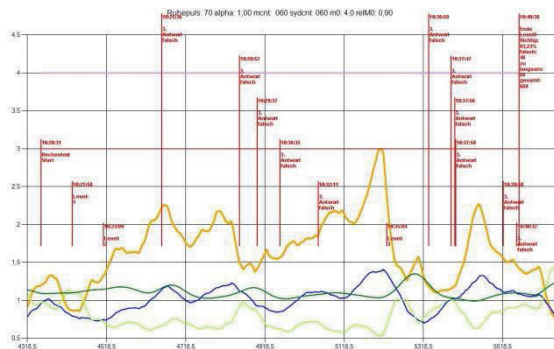


Fig. 8. Math Test

To increase the stress level, we start a math test after a couple of minutes until the subject has become accustomed to the operation of the simulation stand. The calculation starts with very easy tasks. With each level, the tasks become more difficult and the required response times are reduced. Each achieved level is logged along with frequent incorrect answers and a buzzer signal is activated.

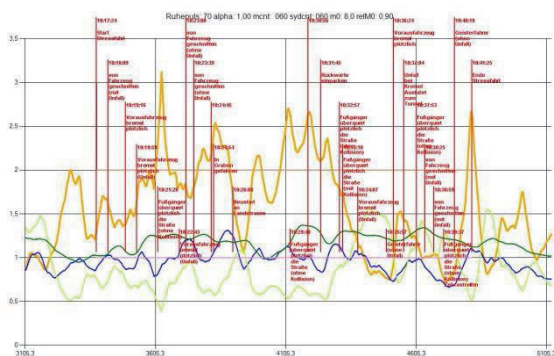


Fig. 9. Rush Hour

After the math test, the subject drives along a quiet mountain road before entering the rush hour traffic of a busy city. As the event markers above indicate, there are tasks waiting such as cars on the wrong side of the road or children running behind parked cars.

It is obvious that the calculated stress level – yellow line – meets the expectations such as high stress level shortly after 'near accident' situations and low stress level after the

mountain ride tour and when the rush hour events terminate.

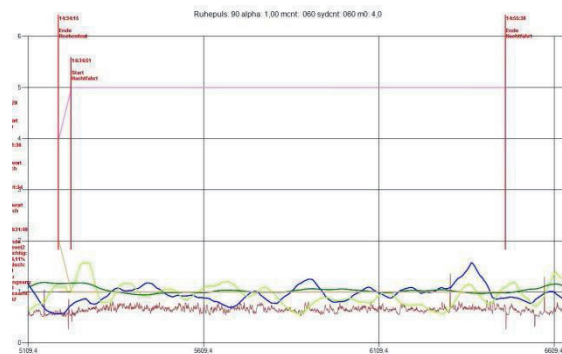


Fig. 10. Night Ride

Towards the end of the drive study, after almost two hours of strain, there are twenty more minutes to go on an empty motorway in the twilight which trigger tiredness in the end.

Machine Learning

The sensor signals and outcome of the physiological model are classified by means of various methods from the field of machine learning. The accuracy is enhanced by applying ensemble techniques, i.e. a dynamic combination of the following techniques. [4]

Artificial Neural Networks

Artificial Neural Networks (ANNs) are artificial neuron networks. Artificial neural networks, like artificial neurons, have a biological role model. They are juxtaposed with the natural neural networks that form nerve cell networks in the brain and spinal cord. However, ANNs are more about abstraction (modeling) of information processing.

Convolutional Neural Networks

Convolutional Neural Networks (CNNs) employ a variation of multilayer neurons designed to require minimal preprocessing. They are also known as space-invariant artificial neural networks based on their shared weights architecture and translation invariance characteristics. Here CNNs are used for feature classification after preprocessing the raw vital data using a physiological model. [5]

Random Forest

The method of Random Forest is a classification procedure consisting of several uncorrelated decision trees. All the decision trees have developed under a certain type of randomization during the learning process. Decision trees are ordered, directed trees that serve to represent decision rules. The graphical representation as a tree diagram illustrates successive decisions hierarchically.

Support Vector Machines

In machine learning, Support Vector Machines (SVMs) are supervised learning models with associated learning algorithms that analyze data for classification and regression analysis. In a series of training examples, each labeled as belonging to one of the two categories, an SVM training algorithm creates a model that assigns new examples to one or the other category, thereby creating a non-probabilistic binary linear classifier.

A Support Vector Machine serves as a classifier and regressor. It subdivides a set of objects into classes so that the broadest possible range remains free of objects around the class boundaries, the so-called large margin classifier. This is a mathematical method of pattern recognition from the field of machine learning. The basis for building a Support Vector Machine is a set of training objects, each of which knows which class to belong to. Each object is represented by a vector in a vector space. The task of the Support Vector Machine is to fit a hyperplane into this space that acts as the interface and divides the training objects into two classes. The distance of those vectors closest to the hyperplane is thereby maximized. This wide, empty border will ensure that even objects that do not correspond exactly to the training objects are classified as reliably as possible. [6]

Derived Values

After feature extraction, an automatic feature selection was used. Filter or wrapper approaches can both be used for feature selection. Filter approaches evaluate features based solely on characteristics that can be calculated from the data. Wrapper approaches use a classification algorithm (often the target algorithm that is also used in the final application) and evaluate features according to their contribution to the performance. The former approaches have the advantage that they are easy to calculate, while the latter have the advantage of providing very problem specific results.

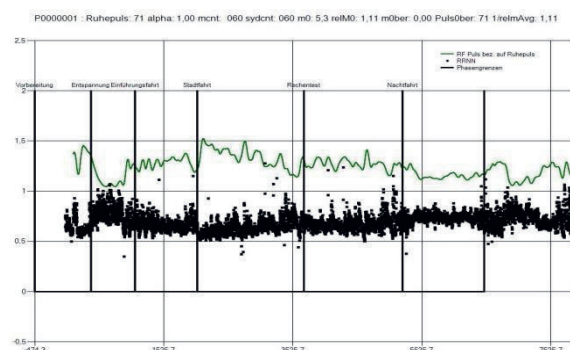


Fig. 11. RF and normalized R-R intervals RRNN

Fig. 11 shows the pulse related to the resting pulse of the subject RF and the normalized R-R intervals. At rest, RF is lowest, it is heavily elevated during physical activity and slightly increased in mental activity.

Fig. 12 shows the average change in the heart rate in percent per second averaged over 60 seconds based on the average value determined for the subject (m). It is low during activity. The value is related to the average pulse value of the subject.

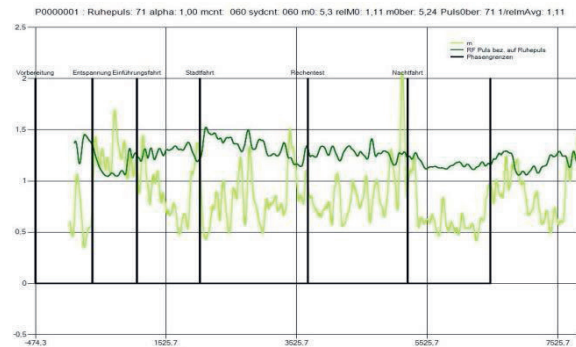


Fig. 12. m

The ratio of the rates of pulse acceleration to the rates of pulse deceleration averaged over 60 seconds (ReIM). Measurement of the relationship between sympathetic and parasympathetic activity. The value is set by a factor that averages a value of 1.

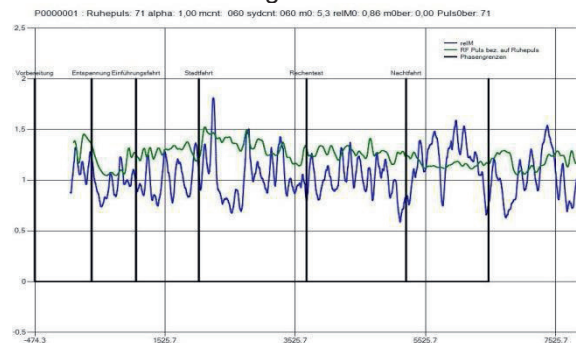


Fig. 13. ReIM

Strong fluctuations indicate increased activity and stress. When tired, it is below 1 and does not fluctuate much.

Stress is likely with pulse higher, ReIM higher and m lower. Fatigue can be expected with pulse lower and reIM not fluctuating so very much.

Results

Fig. 14 on the next page shows an example of the trend of the vital parameters, derived parameters and calculated stress level and fatigue for a test period of more than two hours.

The concordance with the subjects' self-assessment is greater than 80%.

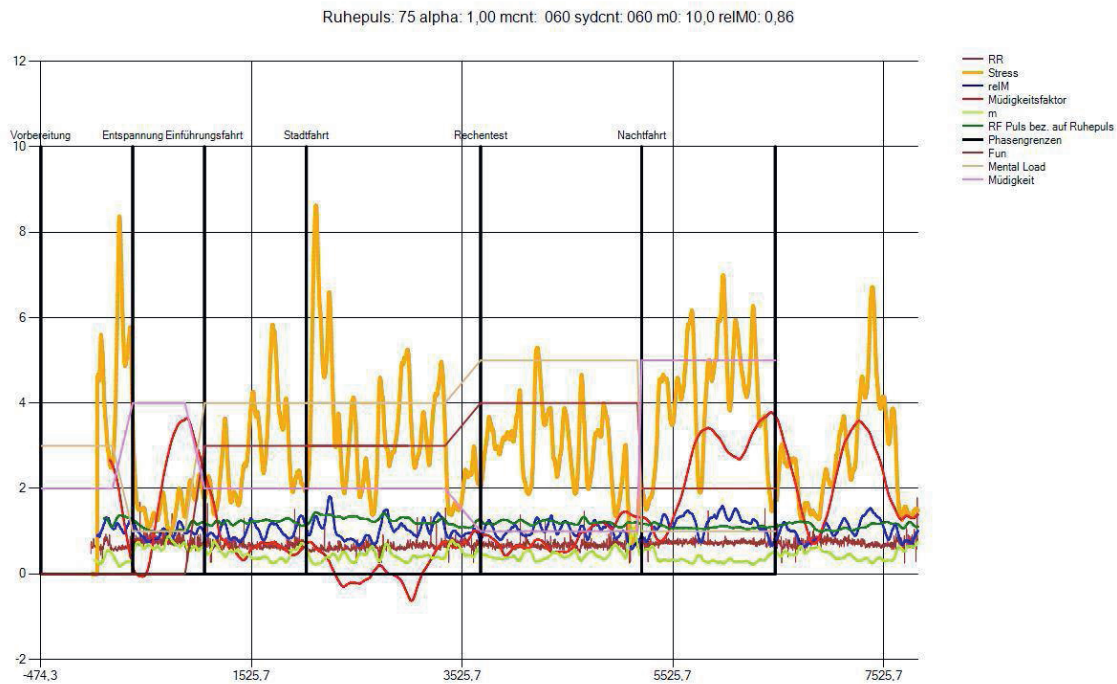


Fig.14. Stresslevel (yellow) and Fatigue (pink) versus drive time and events

Conclusions

Adaptations to new requirements, sensors and interfaces are easily implemented and the embedded environment features low current consumption and hardware costs, thus meeting applicable standards (e.g. electromagnetic compatibility, software and hardware development, safety and security). Furthermore, a real time learning feature has been developed and implemented.

Products or derivatives will be based on the functional prototype. In this context, the following areas pose further fields of application: automation, aerospace (e.g. 'intelligent' pilot and / or passenger seats or seats for tower staff), medicine, wellness / fitness, as well as security (person recognition, state evaluation).

Using a closed-loop function, the estimated user state is continuously inspected and, if necessary, positively influenced by downstream of adaptive systems. Depending on the current estimate, an adaptive system can act in different ways in order to assist the user to

regain a good state. For instance, one such action is to adapt the interior air conditioning of a vehicle.

References

- [1] Prof. Dr. med. Kuno Hottenrott – Herzfrequenzvariabilität im Sport; Hamburg; Czwalina, pp. 9-26
- [2] S. Sammito / I. Böckelmann: Analyse der Herzfrequenzvariabilität Herz 2015-40576-S84-DOI 10.1007/s00059-014-4145-7; Urban & Vogel 2014
- [3] Task Force of The European Society of Cardiology and The North American Society of Pacing and Electrophysiology (Membership of the Task Force listed in the Appendix) European Heart Journal (1996) pp. 17, 354- 381
- [4] Christopher Bishop, Pattern Recognition and Machine Learning, Springer, 2006
- [5] TensorFlow: OpenSource Machine learning framework; <https://tensorflow.org>
- [6] OpenCV: OpenSource Computational Vision Library; <https://opencv.org>
- [7] PhysioNet: the research resource for complex physiologic signals; <https://physionet.org>

DASP towards a generic Data Acquisition Configuration System

González-Martín Moisés, Gonzalez-Pastrana Jose Antonio, Behr Christian, Brueggemann Thomas, Rominger Claude, Keil Karsten, Montes-Sánchez Sergio, Paredes-Huerta Roberto

Flight Test – Airbus Defence and Space

moises.gonzalez, jose.o.gonzalez, christian.behr2, thomas.brueggemann, claude.rominger, Karsten.keil}@airbus.com, [@altran.com](mailto:Sergio.montes, Roberto.paredes)

Abstract

Flight Test Instrumentation is a process where multiple measurements must be acquired by means of different equipment and acquisitions systems. With the Ethernet adoption, multiple vendor solutions can be connected to the Flight Test acquisition network. As a consequence, vendor-specific systems configuration is not enough for the control and generation of a global FTI configuration.

Having in mind the requirement of flexibility and compatibility, Flight Test in Airbus Defence and Space is working on the implementation of a generic architecture capable to set up complex Ethernet architectures using a business-model-agnostic paradigm. This document explains the main steps in the programming generation process: definition of the input interfaces, design of a core solution based on a plug-in philosophy (allowing an easy integration of new components/manufacturers/protocols), and output generation.

Key words: DASP, FTI, Plug-in, XML, Database, Data Acquisition Configuration

Introduction

Until now, acquisition systems have been programmed by using manual processes, combined with ad-hoc tools which have to be updated every time a manufacturer changes its systems or releases new hardware components. This tailor-made solution implies a constant evolution and is definitely vendor-dependent.

DASP is an all-in-one tool to generate the programming and configuration files for the acquisition systems given a prototype.

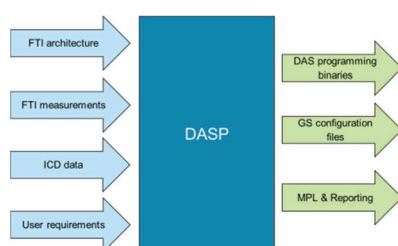


Fig. 1.DASP schema

The main benefit of DASP is to have a common normalized starting point for generating FTI configurations for heterogeneous acquisitions systems. There is a global need of having a tool for supporting multi-vendor FTI architectures and handling large flight test programs with a huge set of parameters and measurements.

The new approach for generating configurations allows facing all the challenges considered as big difficulties in the past:

- Ensure backward compatibility with the current supported vendors.
- Adopt and maintain new manufacturers with specific hardware.
- Mitigate the problems derived of manual processes, such as human-errors and delays in programming schedules.
- Support a huge amount of data. Often dozens of thousands parameters have to be acquired and doing this with manual processes is not affordable.

- Provide an appropriate preliminary feedback to final users about errors or warnings which can derive in future problems difficult to detect causing delays and the need of releasing new configurations.
- Give a fast response to constant changes requests during a test campaign

DASP architecture design

Common data model design

The tool is based on a shared common data model for supporting all the data acquisition systems features but also parameters, hardwired measurements and user requirements have to be programmed.

The information can be provided by means of XML files or retrieved from a database (standalone mode vs database integrated mode). All this data is managed by DASP which is in charge of loading in the internal data model to be analyzed before generating the expected outputs.

Having a common data model reduces the compatibility problems between different vendors, allows the reusability of SW modules and promotes the simplicity of the solution.

The different models have been defined avoiding specific features or restrictions; the definition is generic and flexible. This concept guarantees the agnosticism of the application which is essential in DASP philosophy.

Plug-in philosophy (Low level shared API)

The plug-in architecture solves the complexity of having different acquisition system vendors with their own features and restrictions. By means of a generic interface definition DASP manages the different plug-ins on the same way. From the shared FTI architecture data model (flexible and generic) is possible to support all the manufacturer relevant information.

The different vendor plug-ins must implement the following methods:

- Set inputs: How DASP data models are received and checked by the plug-in.
- Build: Each plugin specific model must be loaded and acquisition system sources generated from it.
- Generate binaries: The vendor compiler has been also integrated in the

solution, having a full-row tool which generates also the acquisition system binaries with the required parameter programming.

This design allows the tool extensibility, the application can be dynamically extended to include new vendors and capabilities, as features can be implemented as separate components they can be developed in parallel without having cross dependencies, and therefore an agile environment is guaranteed. The plugin framework ideally provides simplicity with a well-defined interface and documentation for plugin implementation, developers have a clear roadmap.

By means of using a generic plugin loader (direct access to build folder), DASP is able to know how many plug-ins are available to be used whenever the plugin name matches with the manufacturer name defined in the FTI architecture data model.



Fig. 2. Plug-in interface

The plug-in architecture is not only intended to be used for acquisition systems management, also configurable FTI equipment and Data Processing generation is considered as a plugin-able feature in order to support multiple FTI modules (recorders, switches, Data processing files...).

Configurable application

Using configurable models allow the user to change internal capabilities and execute different configurations without changing the source code. There is no need to know about low level implementation details or having programming skills, final user can easily change configuration parameters.

DASP has been implemented as a console application, in the future it will be included as a service in the framework FIDA, for managing the tool some configuration files (currently XML files but in the future it will be handled by forms in FIDA) have been implemented where the user can define configuration parameters, input paths, constant values...

A general configuration file (for DASP) and other specific ones (each plug-in has one) are provided. The idea is not to force the user to

provide all the configuration values so DASP has those parameters internally defined with default values according to the most used configurations.

Required inputs building & integration

Input data models

All the data is serialized into DASP model from the different input data sources. The model is divided in four layers:

- ICD data: Includes all the information about bus parameters (currently Arinc-429, Serial, CAN, Mil-Std-1553, Ethernet and Stanag-3910 buses are supported)
- Hardwired measurements: Defines the analog and discrete measurements installed on the A/C such as sensors, on/off signals and so on.
- User requirements: Defines the parameters to be programmed and where to send them. This input is based on the defined hardwired measurements and also on the ICD data so this model is directly correlated with the previous ones. After considering the requirements we could have a subset of measurements and bus parameters.
- FTI architecture: Includes all the information about the HW acquisition architecture installed on the A/C; the location of the acquisition cards, internal card settings, channel parameters configuration, bus and measurement connections as well as how the input data is linked to the outputs.

The main reason of having these layers is because there are different actors involved in the FTI configuration definition process: design offices, HW specialists and FTI departments. Each layer has its own restrictions and can be validated apart from the others making easier the process of reporting preliminary errors or warnings.

Database approach & XML file generation

DASP supports two different ways for providing the required information: Directly from a database or by a set of defined XML files, in this case the information can be stored in a database as well, but it is translated into a structured file by means of an auxiliary tool.

Although there is no difference between both approaches (from the final user point of view), there are some considerations to be taken account:

- Using XML files allows DASP to be compatible with different databases, making it possible sharing information between different sites. Most of FTI departments have its own database models and it is a hard challenge to define a common model for every organization or department, ensuring the lack of backward incompatibilities and the backup of the legacy data into this new model.

The use of these auxiliary files solves this problem with the disadvantage of having the need of defining some tools or methods for generating the files but with the advantage of avoiding the need of a database connection in DASP (standalone execution) and the need of retrieving the information from a database which is a less efficient process.

- DASP can be integrated with a Database and retrieve the data directly from it. This way of working implies the implementation of specific modules (based on database model) for querying the information. Despite the fact that a database promotes centralization (different applications connected to the same data source), data security and minimizes data inconsistency it requires a dedicated connection and more computational resources.

Manufacturer support & implementation

Current challenge

The lack of a common language for different manufacturers and acquisition equipment configuration, and the wide casuistic due to the multiple vendor restrictions, derives into a complex scenario difficult to be managed and maintained.

Using a manufacturer common model

Each manufacturer has its own standard and format but the required information is the same for all of them. Starting from a common input model (FTI architecture data model) is possible to support different data formats.

Each plugin has its own data model and is in charge of loading it from the provided common model. The conversion restrictions and

particularities have to be implemented and known at the plug-in level, isolating vendor dependencies between them, but also with DASP that does not need to know specific considerations. One of the benefits of having the plug-in based architecture is the fact that we can manage this complex scenario without compromising the design of the whole application. Specific tasks can be performed at the plug-in level, by doing this, only the plug-in will depend on third-party libraries, for example, a development toolkit provided by a manufacturer to program acquisition cards, or generate binaries for specific hardware architectures.

Plugins could also implement its own data models in order to generate the required source files to be compiled for generating specific binary files.

Acquisition system Datasheet automatization (by using a common HW description model)

Some automated processes have been implemented promoting the application maintainability, regarding the different acquisition system vendors, a procedure has

been defined for avoiding code modifications every time a new card or HW is released.

In the case of CW-Controls (formerly ACRA), the use of XdefML (similar to .xsd schemas) allows an easier way for supporting the different cards provided by this manufacturer. This file includes all the information for configuring a specific card (allowed ranges, data types, properties to be configured...) with the same structure. This schema is the translation of the system data sheet into an open-standard format file. The implementation of generic parsing method (in the plugin level) allows the support of new cards without modifying the code, just by managing this datasheet files (in most cases provided and supported by the vendors). This philosophy allows to know in a simple way how to configure the acquisition cards, set default values or validate the given data.

In other cases, vendors do not provide any file or format to be automated, we've seen that investing time and effort in generating and maintaining this information really worth it instead of implementing vendor-specific solutions sensitive to changes or updates of existing components.

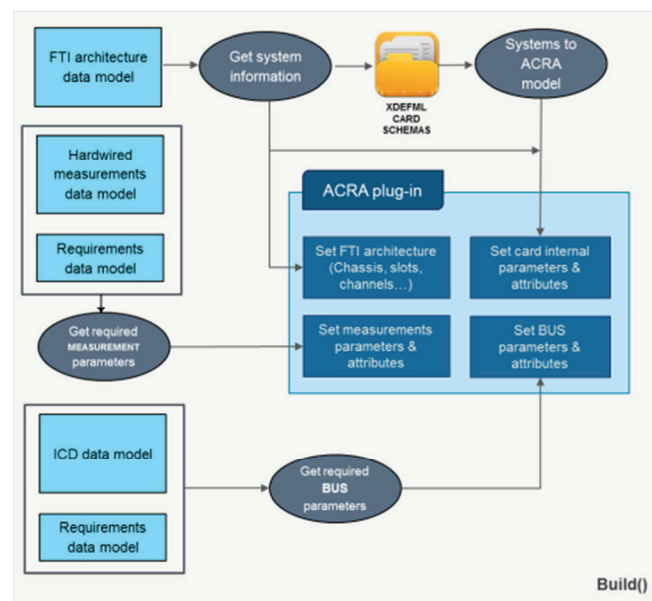


Fig.3. ACRA Plug-in building process diagram

DASP output generation

Output description

DASP generates multiple outputs, in some cases these outputs are not directly generated by DASP but by the plug-ins:

- DAS binaries: As a process of each plug-in, the required binary files are

generated in order to configure the different acquisition systems (this process depends directly on the compiler provided by the manufacturer).

- Data Processing configuration files: In order to know how to decode the information programmed in the

acquisition systems which is sent to the recorder and telemetry facilities, some configuration files are generated based on Data Processing Software Implementation (this procedure is implemented as a plug-in).

- General architecture configuration files: DASP has a global picture of the whole FTI design so it generates a configuration file which includes not only information for the programmable systems, but also includes non-programmable sources (i.e. GPS signals) which also belongs to the architecture too.
- User report files: An ad-hoc information module has been implemented in order to provide information about the execution process (detected errors and warnings), the programmed parameter list (for monitoring purposes) and some other information considered as relevant for debugging purposes. Modular design and multi-format support (plain text, .csv, .xlsx etc.) allows an easy way for generating reports and logs.

Preliminary data validation & error handling is considered as a key feature for reducing time and costs while generating parameters programming,

This is a module in permanent progress.

Future capabilities

Integration with diagnosis & analysis tools

An important phase is the verification phase when all the raw data has to be processed and analyzed. To perform this task, some tools are used, such as the network sniffer Wireshark, so all the traffic must be dissected and processed in order to know the internal characteristics of the received parameters.

The most important problem is that these applications cannot analyze deep enough the UDP packets because they do not have information about the structure of each message. This structure depends on the nature of parameters which have been programmed in the acquisition systems, so DASP can take the advantage of having all this information and provide an auto-generated script allowing the filtering and a deep analysis of the data.

In the case of Wireshark, the tool is ready to be integrated with LUA scripts, which can be a new

output in DASP, but also it is possible to build dynamic libraries or any other ad-hoc module to be integrated with any monitoring tool.

A/C DAS binary deployment

The process of installing the configuration files in the acquisition systems is a manual process done by the specialist in the A/C. In order to automate this procedure, DASP will provide an installation script for uploading the binary files directly in the A/C facilitating the installation process. The script needs to be executed in the FTI A/C network.

Sanitization of Data Processing configuration files

DASP will support the process of removing sensitive information from the generated outputs. As an optional input defines a list of specific parameters which have to be programmed but filtered from GS configuration files and parameter reporting, DASP will be able to deal with classified information, reducing the generated outputs classification level.

Automatic unitary test generation

An important stage while programming all the acquisition systems is to verify the configuration in the laboratory before installing the binaries in the A/C. Until now, this process is manually performed, DASP is able to generate unit test or applications for validating the expected behavior of every acquisition component reducing the scheduling time

Conclusions

DASP will be the future tool in FTI configuration programming tasks in Airbus Defence and Space, its greatest success will depend on the participation of the different actors involved in the process. Since it has been developed as a scalable modular tool it allows new features implementation in an easy-way. Having a multidisciplinary normalized and compatible programming tool will reduce costs and timing.

Acronyms

A/C: AirCraFt

DAS: Data Acquisition System

DASP: Data Acquisition System Programmer

FIDA: Flight Instrumentation DAtabase

FTI: Flight Test Instrumentation

HW: Hardware

ICD: Interface Change Document

XML: eXtensible Markup Language

Integrated Data Acquisition Solutions for Aerospace Platforms with highly restrictive space and weight requirements and harsh environmental conditions

*Patrick Quinn,
Product Line Manager, Data Acquisition
Curtiss-Wright, Aerospace Instrumentation, Dublin, Ireland*

Abstract

Space and weight are key factors in designing, mounting and installing data acquisition systems on UAV and missile development programs. Additionally, there are an increasing number of measurements and avionic busses that must be captured reliably and transmitted to the ground. This paper discusses the challenges faced by the current generation of solutions and proposes and integrated and expandable solution that addresses these challenges, meeting the requirements while future proofing the platform architecture for additional data acquisition requirements.

Key words: Data Acquisition, Missile Test, UAV Test, Integrated Solutions, Miniature-DAU

The components of Missile Data Acquisition Systems

Missile Data Acquisition Systems (DAS) are generally made up of 5 key component groups:

1. Data Acquisition Unit (DAU)
2. PCM transmitter
3. Multi-band antenna
4. Flight Termination Receiver (FTR)
5. Battery pack

The DAU is usually required to gather data from multiple input sources and encode them into a PCM frame for transmission to the ground during test. The type of data generally gathered includes

- Vibration
- Acceleration
- Temperature
- Pressure
- Strain
- Voltage
- GPS parameters
- Seeker information
- Video

A PCM transmitter is generally chosen to meet the specific needs of the flight test program. A dual band wrap around antennae mated with PCM transmitters and FTRs meeting the required RF and operating frequency power for the flight test environment are commonly chosen for missile test programs. UAV programs will have different requirements for a multiband antenna, but RF power and operating frequency are still key considerations. FTR systems are generally kept separate for safety of flight considerations although FTR systems usually monitor some key parameters from the DAU and the battery system onboard.

Given the restricted space and weight requirements of missile and UAV platforms, typical aircraft power of 28V is not available. Battery packs are generally used for power, but these can need to be large depending on the platform requirements and duration of flight required for the test programs. Different components of the system will also require different voltages and current capabilities, making the battery pack complicated.

Optional components

Missile systems are often used in very short test flights, placing tough requirements on the amount of data that can be gathered during the flight. Typically, a sub set of the data is all that can be transmitted, therefore, where possible, a rugged, crash survivable recording unit is an ideal solution for missile systems to record the all the data that is required to be gathered as part of each missile test firing.

Integrated Solutions

Leveraging new technologies and integrating the major components into reduced SWaP packaging offers a new paradigm in data acquisition solutions for UAV and missile applications. The following section discusses desirable features of DAUs and batteries.

DAU

A miniature, rugged, expandable DAU is the ideal solution. In comparison the traditionally available systems, it would be advantageous to have one that has added new functionalities, increases the number of signals and measurements acquired while reducing the size of the box¹.

Modular DAUs are typically available in different sized chassis lengths depending on the solid chassis chosen or how many modules are stacked in a slice of bread design (one where modules are bolted together to form the chassis). Slice of bread form factors are more flexible for altering size whereas a solid modular chassis is more rigid and makes the addition of new modules to meet new requirements easier to achieve.

Another two features that would make a DAU better suited to UAV and missile programs are the ability to daisy chain chassis and to field remotely mounted modules. Daisy chaining of chassis allows users to add multiple DAUs without the need for external switches to synchronize and gather data from slave DAUs into the master DAU for transmission PCM.

The ability to place modules closer to the sensors removes the need for long cable runs from the sensors to the DAU which lowers weight and improves the accuracy of the readings. Such can be achieved using a point to point link between each user slot and the chassis controller. This technology makes it possible to virtually extend the chassis backplane, allowing a signal conditioning module to be placed into the tightest of spaces. This also offers better heat dissipation due to the relative surface area the module has to draw the heat away from the module.

Battery

Traditional battery solutions have many draw backs when it comes to UAV and missile test applications. They can be bulky, heavy, slow to charge, have a slow power up time when turned on and require DC-DC converters to turn the voltage into the correct supply levels for each part of the telemetry system.

A DAU generally requires 28V supply capable of driving up to 80W of power. Transmitters require +/-4V to +/-6V DC 1-2 ampere supplies – these can generally be driven off the same 28V power as the DAU, but require DC-DC converters built into the transmitter.

FTRs typically share power off its own battery power as well as off the 28V power as the DAU, consuming up to 5.7W. But these systems are generally run off a separate battery pack for safety of flight considerations.

The latest generation of thermal batteries offer substantial improvements over the traditional battery solutions. They are totally inert before their activation, they can store power indefinitely, offer substantial savings in weight and size, and they can be used for short or long operating runs (95 seconds to 1 hour, making them ideal for missile applications). They are extremely robust and maintenance free without self-discharge for up to 10 years. They can be configured to give out multiple current and voltage outputs from a single battery, removing the need for bulky DC-DC converter assemblies on board for the different elements of the system.

But one of the main advantages of thermal batteries over traditional battery solutions is their fast activation. With traditional battery applications, the data acquisition system would have to be activated well before firing to allow the DAU to power up. This results in requirements for longer running batteries and therefore heavier systems. Thermal batteries activate almost instantly, which, along with an ideal near zero DAU boot time, is an advantage for missile test.

Integrated Solution Options

This section will walk through various options of a flight telemetry system for missile test programs, highlighting how improved DAU topologies can offer an improvement in SWaP and performance over more traditional data acquisition systems and how the various components of the full system can be integrated into a very compact package, without compromising on performance or functionality.

Missile and UAV test programs generally go through various stages of test flights, where the data gathering requirements vary depending on the tests being performed. During the initial unguided test shots, data from vibration, accelerometers, temperature, strain, pressure, voltages and calorimeter and radiometer inputs are required. As the test program progresses the requirement for these decreases and more guidance and video data is required. The DAU should be able to capture any of the above, in any combination, and be easily configurable to meet all requirements.

System Assumptions

There will be a concentration on a missile application, due to the tighter space and weight constraints this will place on the system. The data acquisition system is to be mounted in the warhead section of the missile.

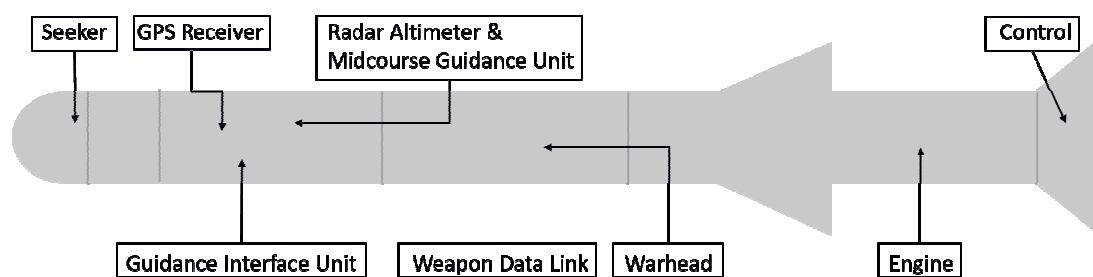


Fig. 1. Cross Section of Typical Guided Missile

GPS, seeker, pressure and video data all come off the front end of the missile. Vibration, acceleration and strain are all measured off the control and stabilizing surfaces. Voltage measurements are taken from the battery pack and off various other missile components throughout the missile. Temperatures are measured mostly at the engine stages of the unit. In this example, the system will be configured to gather the following signal list:

- Vibration – ICP sensors 6 channels sampled at 2,048 Hz
- Acceleration – single ended voltage, 2 x 3 axis accelerometers, 6 channels sampled at 2,048 Hz
- Temperature – 4 channels RTD, 4 channels thermocouple samples at 32 Hz
- Pressure – RS-485 data, 4 channels, Honeywell PPT sensors – sampled at 128 Hz
- Strain – full bridge, half bridge, 8 channels sampled at 256 Hz
- Voltage – 16 channels – monitoring battery voltages etc. sampled at 64Hz
- GPS NMEA data – RS-232 data, 1 channel, 115,200 bps, 1 Hz sampling rate
- Seeker Data – RS-485, 1 channel, 5 Mbps, sampled at 2048 Hz
- Video Data – HD-SDI H.264 compressed, 2 Mbps input, sampled at 2,048 Hz
- PCM encoder – Takes data from all of the above, transmitting out at 6 Mbps

Option 1: 13 user slot Acra KAM-500 chassis

This would have a size envelope of (H x L x W) 98.5 mm x 280 mm x 80 mm and an estimated weight of 2.9 kg². The transmitter would be a separate unit, wired to the PCM encoder for the input data and the output wired to the wrap around antenna. This would have a size envelope of (H x L x W) 33 mm x 83 mm x 57 mm. The transmitter generally requires 5W, drawing 1A. The FTR will be considered as a separate component for safety of flight reasons.

The battery pack would be required to supply up to 4.5A to the DAU, up to 1A to the transmitter and 200mA to the flight termination receiver.

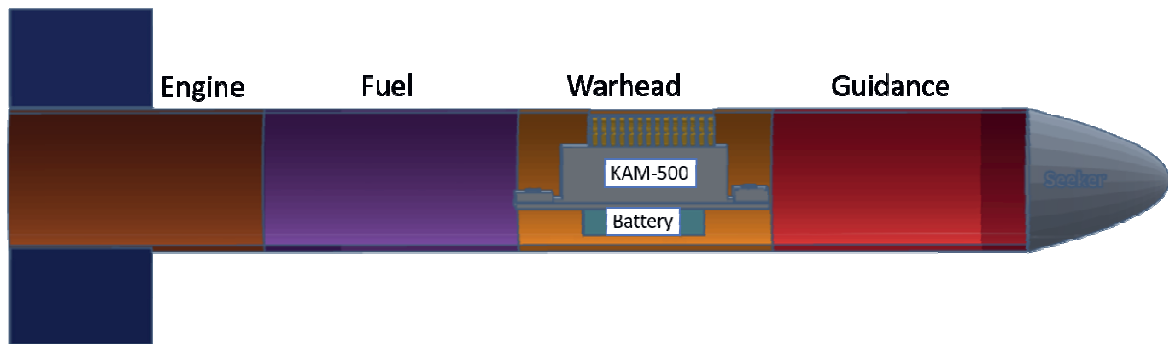
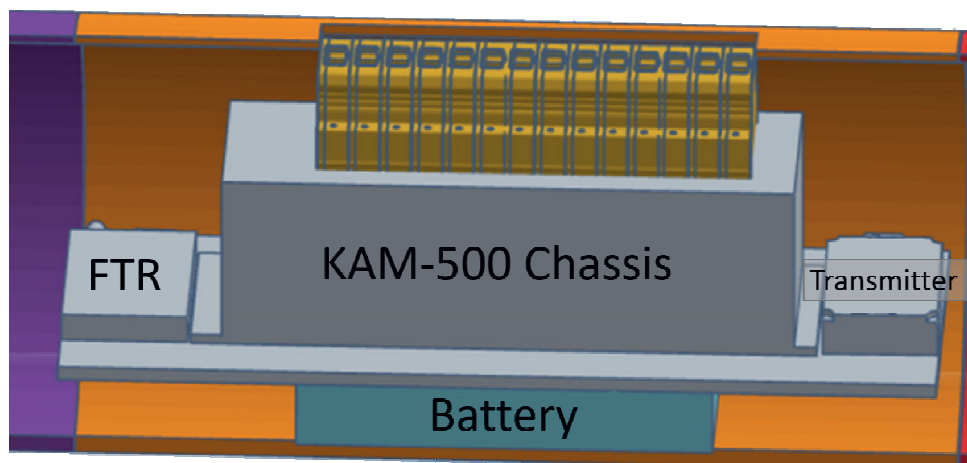


Fig. 2. Generic missile cross section



Warhead Section

Fig. 3. Component parts of missile data acquisition system

This entire Data Acquisition package, including backshells, would require a warhead space of over 220mm.

Option 2: 9 user slot Axon

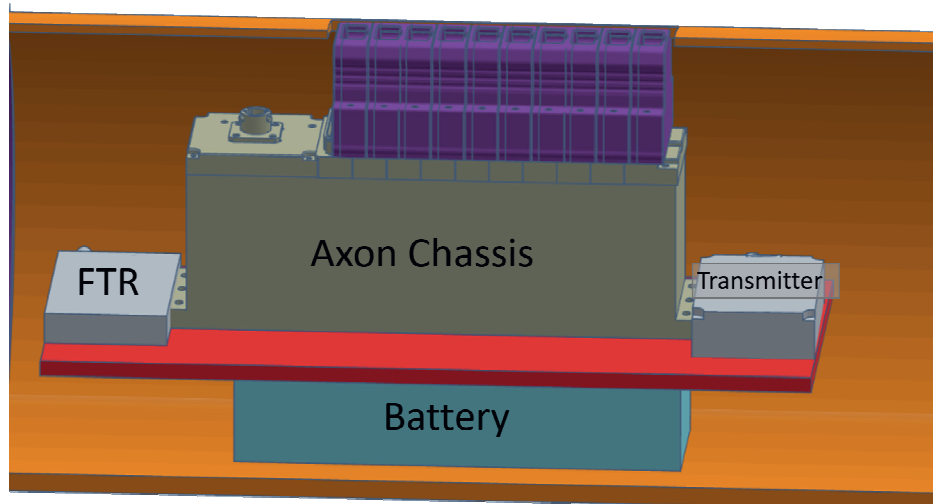
Moving to a 9 User slot Axon chassis offers a 38% saving in volume over the KAM-500 solution and a 52% saving in weight, while still offering flexibility and room to expand to add further measurements modules.

The vibration and accelerometer channels could be combined to one module type, the AXN/ADC/401, an 8 channel flexible analog module that can be configured to handle differential ended, single ended, full bridge, half Bridge, ICP, RTD (2/4 wire), RTD (3 wire), AC coupled, or thermocouple measurements on a channel by channel basis. Users would need two of these to capture the 6 vibration and 6 accelerometer channels, leaving 4 spare channels.

The RTD and thermocouple channels could be combined into a single AXN/ADC/401, with 4 channels configured for RTD inputs (individually selectable RTD types per channel) and 4 channels configured for Thermocouple (individually selectable TC types per channel).

The GPS Data, Honeywell pressure sensors and Seeker data are all RS-232 / RS-422 / RS-485 signaling, but at different rates. These could all be captured by the AXN/UBM/401, a 16 channel RS-232 / RS-422 / RS-485 module which handles data at up to 10 Mbps. Using the above example configuration, there would be 10 free RS-232 / RS-422 / RS-485 channels available for future expansion.

The strain measurements could be captured by either the AXN/ADC/401 or the AXN/ADC/404, a 12 channel bridge module. The 16 voltage measurement inputs could be captured by the AXN/ADC/405, a 24 channel differential ended analog to digital converter module. The video requirements could be met with the AXN/VID/401, a video compression module offering both H.264 and H.265 compression.



Warhead Section

Fig. 4. Axon 9 user slot data acquisition system

This entire data acquisition package, including backshells, would require a warhead space of over 200mm, but with a 52% saving on weight and a 38% smaller DAU.

Option 3: 6 user slot Axon with a transmitter integrated into a module

A standard transmitter is (H x L x W) 33 mm x 83 mm x 57 mm, this includes the casing and power circuitry to turn the 28V aircraft supply into the voltages to run the transmitter. A standard Axon user module is (H x L x W) 12 mm x 65 mm x 52 mm - it is easily conceivable that the transmitter could be modified to take the power off the Axon backplane and fit into a user slot in the Axon chassis. This would save more volume in the overall system and the 100W power available from the Axon PSU is more than capable of driving the transmitter.

Then by taking advantage of the remotely mounted module Axonite chassis, the data acquisition could be moved out of the warhead area, closer to the sensors. Moving to a 6 user slot axon chassis offers a 49% saving in volume over the KAM-500 solution and a 62% saving in weight, while still offering flexibility and room to expand to add further measurements modules.

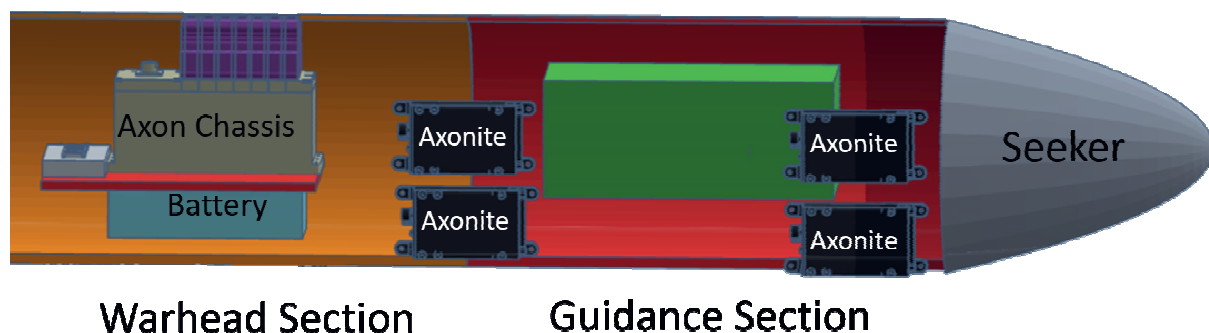


Fig. 5. Axon 6 user slot data acquisition system, transmitter in Axon DAU.

Option 4: 3 user slot Axon with two Axonite extender modules

Taking this a step further, a 3 user slot Axon chassis with two Axonite extender cards, each of which can connect to four Axonites, and the transmitter incorporated into the Axon chassis as before, even further weight and space could be saved in the warhead section.

Moving to a 3 user slot axon chassis offers a 65% saving in volume over the KAM-500 solution and a 71% saving in weight, while still offering flexibility and room to expand to add further measurements modules.

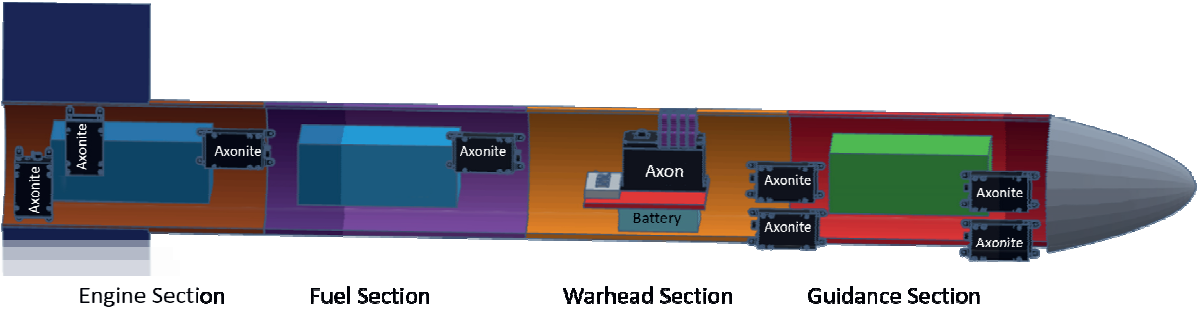


Figure 6: Axon 3 user slot & 8 Axonite data acquisition system, transmitter in Axon

Option 5: Soup can implementation

Taking this to the extremes of what is possible - the extender card (AXN/EXT/404) is a single PCB module requiring 24 pins in the top block to handle all the signal and power for the 4 Axonites. Two of these could be combined into one double PCB card, taking 48 pins in the top block. The encoder card could be placed into the slot where the transmitter card is, making essentially a 2U Axon.

Tailoring the design to fit into the smallest package possible, with the transmitter and battery pack incorporated into a single unit the package size can be greatly reduced. The FTR is still kept separate. The Axon "Soup Can" is a proposal of how, taking advantage of the remotely mounted modules, the Axonites, and incorporating the transmitter and the battery pack, a package can be constructed to fit even the tightest of spaces.

The example below comes in 4 main parts, transmitter, battery pack, front plate and top plate. The top plate holds the Axon controller and the 2 x 4:1 Axonite extender cards. It will contain a specially designed backplane to handle the 2 in one Axonite extender cards.

Using custom designed thermal batteries to provide the required voltages for the flight duration, the need for large DC-DC converters can be removed and a miniature battery pack can be incorporated into the unit. The battery pack is designed to be at the bottom of the unit to offer better centre of gravity.

Figure 7: Axon soup can exploded view

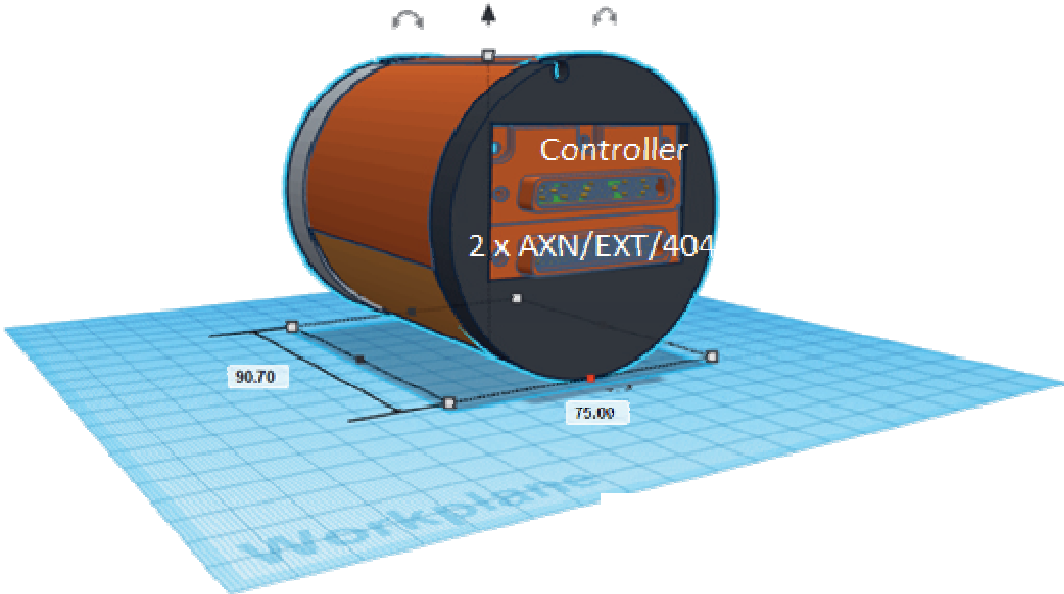


Figure 8: Axon soup can length, 90.7 mm, width, 75 mm

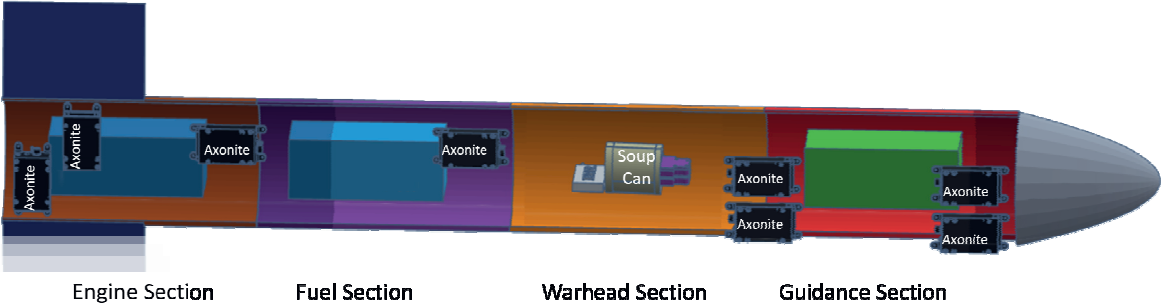


Figure 9: Axon soup can installed

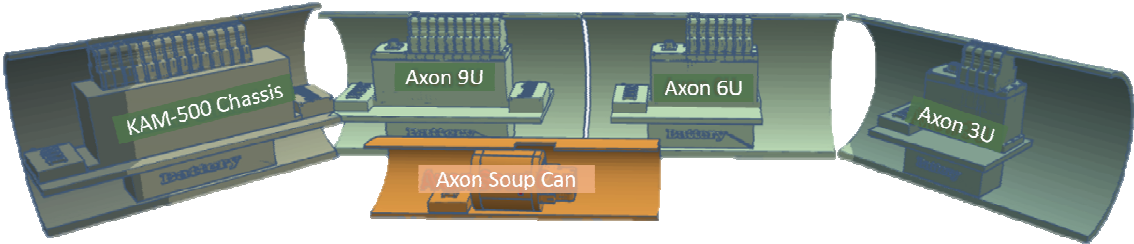


Figure 11: Telemetry pack sizes

Recording

For UAV applications, where space may not be as limited as missile applications and the UAV will be recovered after each test flight, Axon offers the AXM/MEM/401 module. This is an integrated recorder module that records traffic directly off the backplane onto a media card. The card is both removable for data extraction and can be accessed through the Ethernet ports of the controller to download and format the card when the DAU is in accessible. The AXN/MEM/401 can record data in PCAP, iNET-X, IENA, DARv3 and Chapter 10 as required by the program.

However, in missile test, the unit is often not recoverable, so a crash survivable memory module is required. To meet this Curtiss-Wright can offer a Crash Protected Memory Module (CPMM) – used in our Flight Data Recorders (FDR). This is a 64 GB solid state memory array with crash survivability exceeding ED-112A³(the latest regulations), ultra-compact and light weight (1.3 Kg).

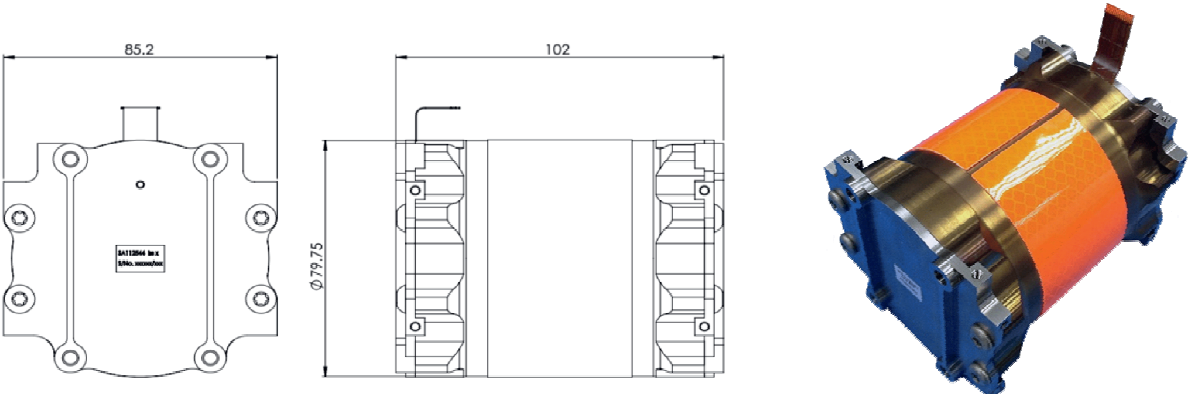


Figure 12: Crash Protected Memory Module

The CPMM adheres to ED-112A defined crash survivability tests, which include

- Fire intensity High: 1100°C for 60 minutes
- Low: 260°C for 10 hours
- Impact shock: 3,400 G for 6.5 ms
- Penetration resistance: 500 lb from 10 ft ¼ inch contact point
- Static crush: 5,000 lb for 5 mins per axis

- Shear/Tensile strength: 6,000 lb for 1 minute each axis
- Fluid immersion: Immersion in aircraft fluids for 24 hr
- Water immersion: 30 day sea water
- Hydrostatic pressure: Equivalent to depth of 20,000 ft

Environmental

The requirements for each individual missile program are unique, so any solution would be tailored to meet these, however these are typically higher than those for standard flight test. Axon is designed to meet the vibration, shock and acceleration levels encountered in such applications.

- Shock: 100g for 11 milliseconds in each direction of the three major axes, terminal peak
 - sawtooth, 12 shocks.
 - 250g for 6ms in each of the three major axes, half sine, 12 shocks.
- Vibration: Sinusoidal: 10g peak
 - Endurance: Random, 0.83g²/Hz peak, 10min/axis
 - Functional: Random, 0.20g²/Hz peak, 60min/axis
- Acceleration: 16.5g for 1 minute in each direction of three mutually perpendicular axes.

Curtiss-Wright have been providing solutions into missile and space applications for many years. Leveraging this experience we know that the below levels are achievable:

- Shock: 120g
- Vibration: 30g
- Acceleration: 50g

Conclusion

This paper shows that significant savings in weight and space can be made when combining the latest technologies in batteries with the next generation of DAUs. Solutions can be tailored to meet the smallest of missile and UAV vessels, without compromising on performance or environmental requirements.

References

-
- ¹ D. Buckley, The Challenges of Data Acquisition in Harsh Remote Places, European Telemetry and Test Conference, Nürnberg, Germany (2016)
DOI 10.5162/ettc2016/4.1
- ² Curtiss-Wright, Online, Available from:
<https://www.curtisswrightds.com/products/flight-test/data-acquisition/acrakam500/kamchs13u.html> (2015)
- ³ EUROCAE, ED-112A – MOPS for Crash Protected Airborne Recorder Systems, Online, (2013), Available from:
<https://eshop.eurocae.net/eurocae-documents-and-reports/ed-112a/>

Design of a minimum weight/space/energy consumption instrumentation system

Florian Mertl, Renaud Urli

Airbus Helicopters Deutschland GmbH, Industriestrasse 4, 86607 Donauwörth, Germany

Florian.Mertl@airbus.com

Renaud.Urli@airbus.com

Abstract

Research platforms require flight test instrumentation systems fulfilling the difficult compromise between minimum weight, space, energy consumption and maximum flexibility combined with a high number of different measurement requirements.

This paper describes the challenges faced during the design of such an instrumentation system, the changes introduced in sequential iterations in the standard architectures of FTI (Flight Test Instrumentation) systems for large AC (aircraft) prototypes, as well as some limits met during the design.

Key words: FTI, Flight Test Instrumentation, Weight, Size, Consumption, Requirements Engineering, demonstrator, research

Introduction

Standard architectures of FTI installations are based on the different functions required in an FTI environment. Therefore each function (e. g. Time Service, Recording, Control) is covered by separate equipment. In addition, the requirement of serving an upmost flexible FTI platform which shall be capable of handling an increasing number of parameters leads to a certain amount of weight, size and of course power consumption of the FTI. Standard test aircraft can cope with non-optimized designs of FTI installations regarding those latter parameters but research platforms or aircraft demonstrators, depending on their mission like e.g. Urban Mobility, will demand a drastically reduced FTI footprint. Several methods shall be used to reach this goal, dealing with both technical and organizational aspects. Despite normal (standard) FTI installations, these contribution factors become high priority elements when designing new aircraft concepts or demonstrators for certain use cases like e. g. urban mobility.

Weight

Weight shall be seen as the most important parameter when building the architecture of a FTI System for a research aircraft. As the optimization of the Payload/AC Weight Ratio already in demonstrator phase is a key element while designing new aircraft concepts, it's obvious that FTI weight must also be reduced

to a minimum. But even if this requirement sounds simple, it has a huge impact on the FTI design. Which steps could help to decrease the FTI weight?

First, do not use LRU (Line replaceable unit) trays. LRU trays offer quick installation/de-installation of the equipment as well as easy access for maintenance and repair. Some trays even provide mechanical damping for protection of tape- or HDD-driven equipment. Removing the tray gives you the benefit of a considerable weight reduction on the one hand, but forces you to provide fix provisions for FTI in the AC's primary structure in the very early design stages of the aircraft.

Second, avoid cut-off connectors. It's obvious that a connection point with plug/receptacle and mechanical support is much heavier than the FTI cable itself in the same area. If sensors are used with pre-assembled cable directly connected at the sensor side, keep in mind to have the cable long enough to route direct from sensor to DAU (data acquisition unit).

As it can be seen in Fig 1, 10cm of a 4wire sensor cable weighs 2.5g. Putting a cut-off connector – assuming a "light" connector type - at this point, it will add a weight of 100g. As a consequence, suppressing cut-off connectors for an medium-sized FTI installation with 100-200 lines will save up to 10-20kg.

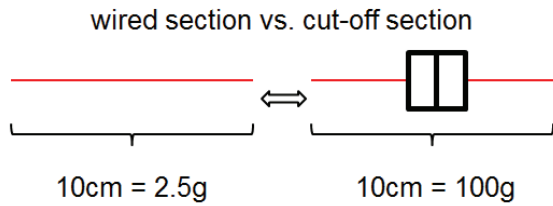


Fig 1 Comparison weight of cable and weight of connection point

Combine functions. As mentioned above, it's common to have one piece of equipment responsible for one function. By combining functions, it's possible to reduce the number of equipment (see Fig 2), ergo reduce weight. For instance, modern FTI systems offer a recording function in the DAU, which makes a separate recorder needless. To achieve this, it's mandatory to determine the necessary recording bandwidth in an early state in order to identify if this combination is possible.

Shift functions. Depending on the test mission, some functions are not needed on board (e. g. TOP Event) while others are required on ground (command and control). These functions shall be therefore covered by the FTI telemetry ground station. This allows the designer to remove the equipment from the aircraft. The constraint is to ensure that these functions can be handled by FTI telemetry ground station.

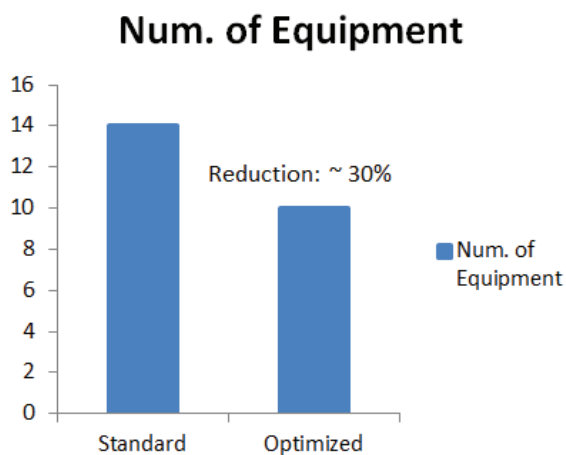


Fig 2 Number of equipment in a medium-sized FTI system; Standard architecture vs. optimized architecture

Total Weight [kg]

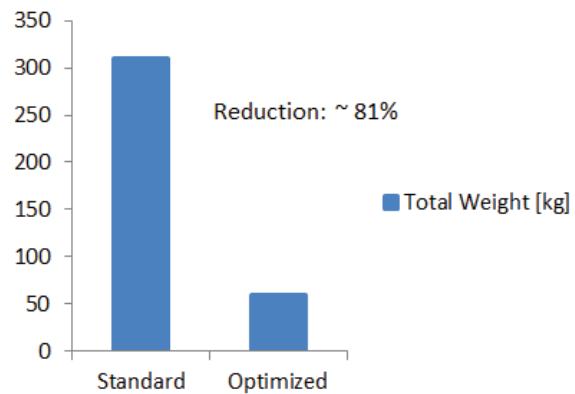


Fig 3 Total Weight of a medium-sized FTI system; Standard architecture vs. optimized architecture

Size

Succeeding in weight reduction is a good basis to focus on the next challenge, reducing the size of the FTI to a minimum. It has to be considered that there's always smaller equipment available on the market. Innovative manufacturers offer new miniaturized DAU's providing higher channel density, more functionality, better performance etc. But in the present context, there will always be a compromise between risk and benefit. Risks to be considered are longer lead time, reduced support quality, late bug fixing, and integration testing issues, release cycle and cost. Accordingly, in most cases the challenge will be to reduce size with the already existing and available equipment.

Decentralize FTI. Usually FTI installations are intended to be installed and de-installed easily. Often a central rack is built in which all – or at least almost all – FTI equipment are installed. This rack is to be fitted in the seat rails and provides connector panels: hence quick to handle, move and maintain. The drawback of this setup is its size. Relocating the FTI equipment to places where free space is available and furthermore shorter cable routes to sensors and tapings are possible, offers size and cable weight reduction.

Avoid cut-off connectors. As mentioned above, cut-off connectors contribute not only to more weight but also to bigger size. Mechanical parts dedicated for FTI often have an impact on the structure design of the aircraft itself. Therefore it degrades the representativeness of the platform compared to the basic design. Substantiations have to be made in order to be able to transfer the obtained data into a qualifiable model. In addition keeping off the cut-off connectors means having a as direct as possible link

between the signal source (sensor, bus) and the DAU.

Avoid spare cabling. To cope with changing demands during testing phases and campaigns, it is common that some spare cabling is foreseen. Doing that, it's possible to react in a flexible way to new needs when operating the aircraft. To fulfill the size reduction requirement, spare cables have to be avoided or, at least, reduced to an absolute minimum. It has to be considered that the success of this process is particularly depending on a disciplined requirement engineering phase. Furthermore, planning a dedicated connection to the bus tapping points from the aircraft systems suppresses duplicated bus distribution modules.

Power Consumption

Reducing the power consumed by FTI equipment is a process with limited opportunities nowadays.

It is essential to identify as exactly as possible the power required by FTI. This postulation leads to a challenging requirement engineering process which has to take place very early, and eventually leads to the reduction of the number of equipment and hence to the power consumption.

Low power transducers like nanotechnology MEMS sensors are not to be easily integrated in current FTI systems as the conditioning equipment is not widely available yet.

Usage of new functions. Modern bus monitor modules in DAU's are capable of gathering data from specific signals (Arinc 429, Serial, Video) only when data are available on the bus. These modules enable a bandwidth reduction by processing and passing the data to the backplane only if an active signal is detected. This leads to an efficient bandwidth usage, improves the recording time as well as the time for data handling in post processing.

Implementation of wireless technology. Although instrumentation requirements are rarely fulfilled by current off-the-shelf wireless systems like IoT ones, their usage shall be evaluated as often as possible. Being usually battery powered, they consequently offer power-free parameters with regard to the aircraft system. On the other hand, their usage provides certain flexibility in the parameter requirement process after the freeze of the FTI architecture, as they can be implemented with

limited impact on the wired FTI system. Last, and especially for the acquisition of rotating parameters, their integration can replace heavier systems based on slip ring or inductive transmission.

Requirements Engineering

The main key to match the size/weight/power consumption requirements as good as possible is to perform a smart, disciplined and focused requirements engineering process. Requirements engineering goes beyond the simple list of parameters to be acquired. For example, knowing the stakeholder for each analogue parameter (strain, pressure...) is one of the most important elements. The analogue parameters are indeed the main driver for defining a FTI architecture whereas bus parameter are less dimensioning.

It is obvious that the parameter with the lowest weight, the smallest size and the less consumed power is the one... which is not required! On the other hand, the most complex, most expensive parameter is the one, which has to be acquired in flight test!

Because of these unpretentiously facts, each parameter has to be challenged: is it really, really necessary to measure it in flight test or can it be acquired during bench testing? Often other MoC (Means of Compliance) like Laboratory Tests, Simulation or Calculation can be used to meet the requirements. The requirements review loops are very time consuming must be done not only once but repeated in iterative steps, with all stakeholders and always have to be very detailed. If done successfully, it leads to the following points which are essential for the success of a project:

- a realistic planning of time and cost is possible.
- The chosen FTI architecture meets the real requirements. Uncertainties can be minimized
- It provides a good visibility of the progress during the requirements engineering phase.

As it can be seen as an example in Fig 4, the requirements engineering process has to be initiated very early and has to be finished at - depending on project size and complexity – approximately one year before the First Flight.

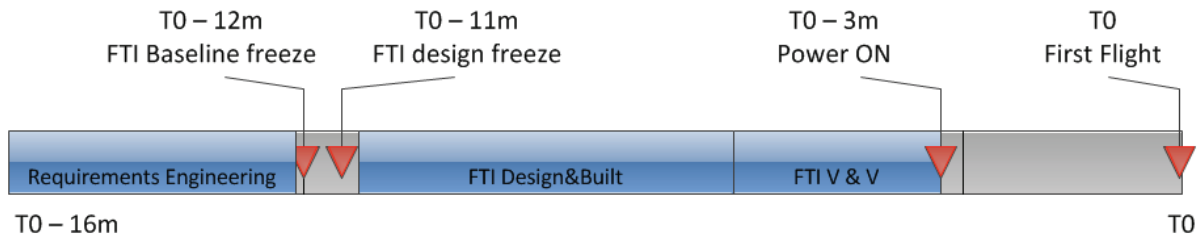


Fig 4 FTI process timeline

Drawbacks and Limits

By following all the steps mentioned above, some drawbacks have to be considered as well. Implementing new technologies and concepts can bring certain risks. Risk assessment is mandatory to mitigate the possible negative impacts. Risk mitigation actions can be backup-scenarios, lab testing. Following the rules mentioned in this article, it has to be noticed that flexibility, being one of the standard significant performance indicator for FTI systems, decreases to near zero. Avoiding cut-off connector and spare cabling, de-centralizing the installation clearly and drastically limit the possibilities to react to changed requirements. It also has to be kept in mind that the FTI platform which will be integrated in such a demanding project will not be re-usable for

other purposes. Brackets, trays, mechanical adaptations are customized for the specific needs. They can't be used anymore after the project has ended.

Summary

This paper discussed the different contribution factors which have to be adjusted in order to meet the requirements for FTI systems used in demonstrator aircraft platforms.

Some key elements were highlighted, with their potential benefits but also the risks which come along with their implementation.

This document showed also that not only technical aspects must be taken into account when designing a new type of such FTI architecture, but also organizational tasks.

Inflight-Measurements of Aircraft Undercarriage Vibration during Deployment

Dr.-Ing. Jan Schwochow¹, Julian Sinske¹, Ralf Buchbach¹

¹ DLR Institute of Aeroelasticity, Bunsenstrasse 10, 37073 Göttingen, Germany,
jan.schwochow@dlr.de

Abstract:

Within the EU funded Project **AFLoNext** (<http://www.aflonext.eu/>) flow-induced vibrations of aircraft components are under investigation. Aerodynamic or structural devices are designed to mitigate the vibration response levels especially of the deployed landing gear doors. The nose landing gear is emitting vorticity which impacts the downstream located main landing doors. To verify the results of unsteady complex flow simulations of the undercarriage conducted by different project partners, flight tests shall provide a database for calibration of numerical investigations and verify the results. Different types of sensors were installed on the undercarriage of the **Advanced Technology Research Aircraft** operated by the German Aerospace Center DLR, comprising accelerometers, strain gauges, travel and pressure sensors. To get detailed knowledge of the dynamic interaction of pressure loads and structural response on the nose and main landing gear doors, the simultaneous data acquisition of all signals at high sample rates up to 2 kHz was mandatory during deployment. In addition, monitoring of critical response levels was essential to stay in defined limits during flight. The presentation will give an overview of the selected Flight Test Instrumentation and the preparation of the test aircraft including the documentation and substantiation to get the flight approval.

Key words: AFLoNext, ATRA, landing gear, distributed DAQ, flight vibration test, flight test instrumentation.

Glossary

A/D	Analog / Digital converter
AFLoNext	Active Flow Loads & Noise Control on Next Generation Wing (EU-Project)
ATRA	Advanced Technology Research Aircraft (AIRBUS A320)
CFD	Computational Fluid Dynamics
DAQ	Data Acquisition
DLR	German Aerospace Center
DO	Design Organisation
EASA	European Aviation Safety Agency
EMA	Experimental Modal Analysis
EMC	Elektromagnetic Compatibility
F/T	Flight Test
FTI	Flight Test Instrumentation

FVT	Flight Vibration Test
GVT	Ground Vibration Test
MLG	Main Landing Gear
NLG	Nose Landing Gear
OMA	Operational Modal Analysis
PtF	Permit to Fly

Introduction

The vibrations on the aircraft undercarriage triggered by unsteady aerodynamics forces are relevant for the design of airframe components. Being generated by unsteady flow around itself or excited by vortices shed from other upstream components, e.g. the nose landing gear (NLG), these vibrations are often present on movable surfaces in the undercarriage area like the main landing gear doors (MLGD) with a potentially significant impact on airframe noise and component fatigue, even though they are open only for a short sequence while the MLGs are in transit. During the years, semi-empirical methods were used to anticipate to flight tests.

Nowadays, high-precision computational fluid dynamics (CFD) simulation tools are becoming available that are capable for predicting unsteady aerodynamic phenomena as well as the dynamic response of the structure prior to F/T. An example result for visibility of the vorticity from [1] is shown in *Figure 1*, which appears, when the LG is in transit (see *Figure 2*). These capabilities allow the thoroughly investigation of the root causes of transport aircraft undercarriage component vibrations and on the other hand the design of small aerodynamic devices, which might impact the flow vorticity to mitigate the excitation levels of the structural response and prevent damages. In best case these devices can be retrofitted to an existing aircraft fleet. Details can be found in [1] and [2].

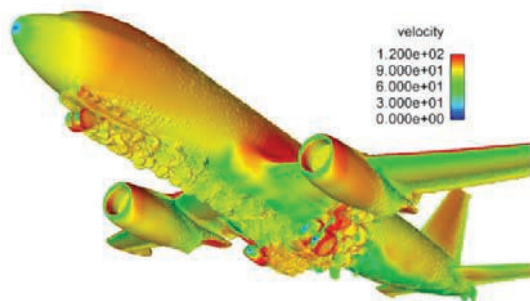


Figure 1. CFD-simulation of undercarriage vorticity from [2].



Figure 2. Landing gear in transit.

The numerical simulation of the vibration level of the undercarriage is associated with uncertainties because of detached flow, vortex shedding and buffet. The unsteady aerodynamic forces of the disturbed flow are exciting the extended gears with opened doors. Again, the oscillating aircraft components influence the kind of aerodynamic characteristics, which results in a coupled aerodynamic and structural interaction. These new multi-disciplinary simulation tools are still in the proving phase, which needs experimental F/T results to check their prediction capabilities.

Consequently, the research activities within the **AFLoNext** project funded by the European Union [3] comprises instrumented F/T with the **Advanced Technology Research Aircraft** (ATRA) operated by the Flight Experiments Department of the German Aerospace Center (DLR) [4]. The ATRA is originally a commercial A320 (see *Figure 3*), which was reconfigured to a research platform equipped with special data acquisition systems to allow comprehensive flight testing for customers.



Figure 3. A320 ATRA - Advanced Technology Research Aircraft, shortly after take-off.

To support the investigations on the undercarriage, a small rugged and customizable data acquisition system (DAQ) was installed outside of the aircraft cabin in the MLG bay containing the signal conditioning and A/D-converters of different type of sensors:

- accelerometers,
- pressure transducer,
- strain gauges, and
- travel sensors.

Furthermore, ground tests on landing gear doors were performed to analyze the dynamic characteristics of the considered door components without aerodynamic disturbances occurring in flight. The landing gears with deployed doors comprise numerous movable cranks and hinges and hydraulics (see *Figure 2*), which is expected to cause nonlinear vibration characteristics due to friction and free-play within the built-in kinematics. To separate between structural phenomena and aerodynamic excitation effects the structural dynamic properties must be identified during a ground vibration test (GVT), where the aircraft is on jacks. By application of experimental modal analysis (EMA), the dominant vibration

mode shapes with natural frequencies can be identified. These modal results will be exploited for calibration and verification of the structural modelling which is applied in numerical simulation.

Besides the clean MLGD configuration, Vortex Generators (VG) on the outer surface of the doors (see *Figure 4*) and aerodynamic deflectors on the inner leading edge (see *Figure 5*) were installed and tested in flight to control the flow with respect to vibration mitigation.



Figure 4. Vortex generators on the MLGD leading edge.

Requirements for Flight Test Instrumentation

To fully understand the aircraft undercarriage phenomena the measurement of the current position of NLG as vortex shedding generator deflection angle of MLG doors, unsteady aerodynamic loads on the MLG doors, the vibration level response were requested by the simulation experts. Supplementary, a camera with high frame rate shall record the MLG and doors in transit.



Figure 5. Aerodynamic deflectors at leading edge of MLGD.

The final Flight Test Instrumentation comprises the following installations:

- position measurement of the NLG leg via travel sensors (string potentiometer) MIDORI CPP45-50 to measure piston stroke at the NLG actuator (see *Figure 6*),
- position measurement of both MLG doors via string potentiometer CPP45-50 at actuator,
- total load measurement of the applied load on each LG door via strain gauges at control rods of NLG + MLG doors (see *Figure 7*),
- vibration level measurement via accelerometers PCB-353B17: 3x tri-axial, 1x bi-axial, 1x uni-axial sensors on each MLG door (see *Figure 8*) and 4x uni-axial on each NLG door (see *Figure 9*),
- aerodynamic load measurement: via pressure transducers KULITE GG835 on in-/outboard surface of left-hand MLG door (see *Figure 8*).

All sensors were glued to the aircraft surface with 3M Scotch-Weld two component epoxy adhesive DP490 [7], which is gap filling and durable down to low temperatures (-55°C). All outboard cables were glued to the aircraft surface with aluminium foil tape 3M 425 [8].

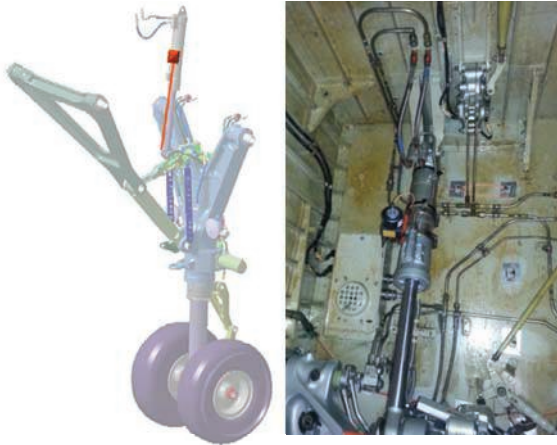


Figure 6. Travel sensor at NLG actuator.

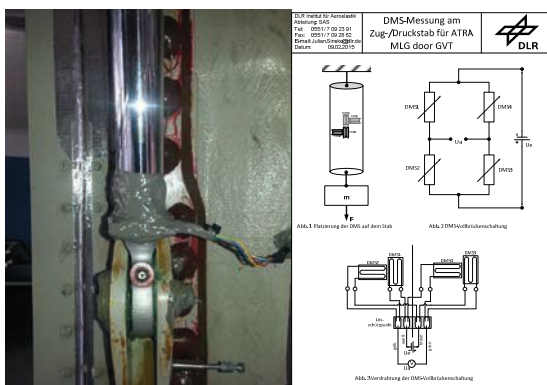


Figure 7. Strain gauge at MLG actuator.

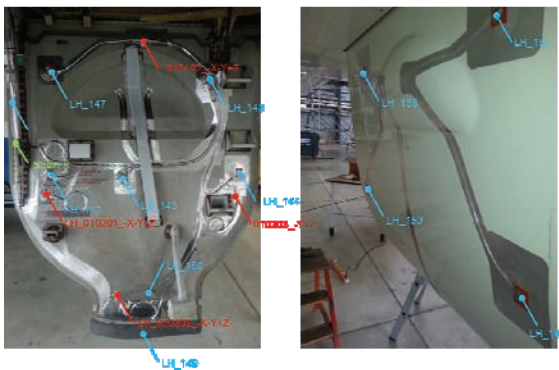


Figure 8. Accelerometers (red) and pressure transducer (blue) on left-hand MLG door.



Figure 9. Accelerometers and strain gauge at right-hand NLG door.

Data Acquisition System

The signals of all different types of sensors must be acquired and logged simultaneously to hard disc to enable the observation of the correlations between the aerodynamic vortex excitation and the acceleration response of the doors. Furthermore, the functionality of online-monitoring of the acceleration response was mandatory to make sure that certain levels are not exceeded during flight.

The available basic DAQ-system in the ATRA has capabilities to record a number of data signals. Since it is installed in the cabin, such a configuration would mean, that all wiring must be routed from outside to the pressurized interior cabin. More than 100 wires would pass a sealed interface located in the fuselage bottom in the MLG bay.

To avoid such an elaborate installation it was searched for an alternative, where the DAQ-system with signal conditioning and A/D-converters is installed outside of the cabin in the MLG bay. Using such a distributed setup, just the power supply and the network connection need to be routed into the cabin, where the system is controlled via a commercial mobile PC, which records the data to hard disk. According to airworthiness specifications simplified verification can be applied for attachment of external masses in fuselage area if the weight limit is below 10kg. The mounting of such device must bear a load factor of 10g, which results to 1kN limit load.

The distributed setup of the measurement units inside and outside the pressurized cabin required an especially robust system. The system had to work reliably at low temperatures and low air pressure in high altitudes. The selected NI cDAQ measuring system, which is very compact and allows online access to the time data, is specified by the manufacturer only up to an altitude of 5000 m and a temperature down to -40°C . This limited specification required a climatic chamber test in which the requirements of a flight profile were simulated, as it would occur during the targeted flight tests. During this climatic chamber test, the measuring system together with the sensors was exposed to a pressure of less than 250 mbar, which simulated an altitude of approx. 11,500 m and a temperature of below -50°C . The measurement system worked perfectly during this 3h test and showed no drifts in the measured signals, no errors or any failure.

The complete setup of the distributed measuring system (see Figure 10) consists of two individual National Instruments chassis of type NI-cDAQ-9188XT [5]. Each contains eight

adaptable signal conditioning modules to support the need of the different sensor types. Both were covered by a rugged protective aluminum case box, which was attached on the keel beam of the aircraft in the MLG bay (see *Figure 10*). The total weight of this LoadDAQ-box is 9.5 kg, while the voltage power supply is 28V. This outboard installation permits considerable shortening of the analog signal routing, which improves the signal to noise ratio and reduces the electromagnetic susceptibility from radio emission of the different communication antennas. A further request for the flight test qualification was a check of electromagnetic compatibility as part of an EMC test in an EMC chamber and later in the installed state on the entire aircraft. These tests intended to exclude the measurement electronics from influencing important components of the aircraft such as radio communication. In several former flight tests the NI-cDAQ-9188XT has proved oneself as robust and reliable system [9].

The architecture of the DAQ-network consists of a central DAQ-PC, which is connected to the local aircraft network and records the data from the two NI-cDAQ chassis with sample rate of 2kHz and at the same time the flight condition parameters comprising flight speed, Mach number, flight altitude, static pressure, angle of attack, yaw angle and other made available by the basic aircraft DAQ-system at sample rate of 10Hz.

This main DAQ-PC distributes these data in the local network, so that further online evaluation and processing can be performed with additional PCs connected to the local network. In *Figure 11* the architecture is summarized. The NI cDAQ-chassis are filled with the following conditioned I/O modules:

- 2x NI 9469 - synchronization of chassis,
- 8x NI 9234 – acceleration with IEPE-signal conditioning +/-5V, 4 channels per module, BNC,
- 3x NI 9234 – pressure transducer, +/-5V, IEPE disabled, 4 channels per module, BNC,
- 2x NI 9237 – +/-25mV/V full bridge analog input with 10V internal excitation and remote sensing, 4 channels per module,
- 1x NI 9239 – ± 10 V simultaneous analog input for travel sensor, 4 channels per module, BNC.

Figure 12 shows the electrical block diagram of the FTI, where the three cable-line connection

from MLG bay into cabin is indicated. The connection between MLG and NLG bay comprises several sensor cables, as shown in *Figure 13*.

Data Acquisition Software

The software to control the measurement system and to acquire the signals is developed with NI LabVIEW 2016. Both NI-cDAQ chassis must be synchronized and all channels must be pre-defined with particular signal conditioning settings. Further, an infrastructure of network-streams is installed to continuously feed several analysis-computers connected to the network with live-data.

The basic data acquisition system of the aircraft supplies the current flight parameters via an additional network stream. These data are collected and stored synchronously with the measurements on the undercarriage.



Figure 10. LoadDAQ box installed on the aircraft keel beam in the MLG bay.

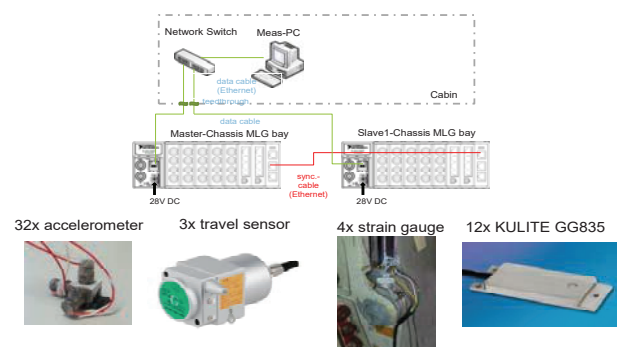


Figure 11. LoadDAQ-System with different sensor types.

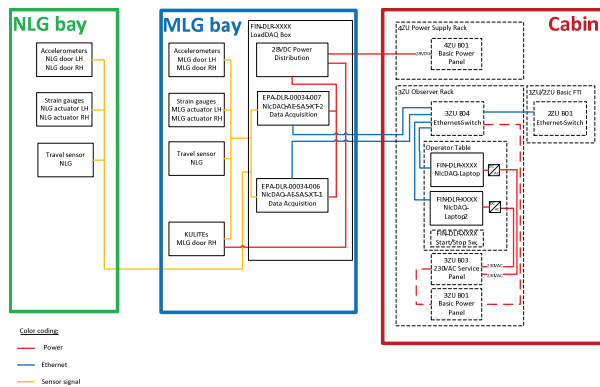


Figure 12. Electrical block diagram of distributed DAQ.



Figure 13. Cable connection to NLG bay.

Qualification for Flight Test

In order to get the permit to fly (Ptf) for the aircraft equipped with FTI several documentation and substantiation reports must be generated and approved if the installation is compliant with the aircraft certification specifications CS-25 published by the European Aviation Safety Agency (EASA) [5]. This approval step guarantees a safe performance of the test flight. The German Aerospace Center (DLR) operates a Design Organisation (DO) to conduct research activities for users from DLR institutes, external research establishments, industry and government authorities / agencies. That comprises the development, type investigation and supplemental type certification of interior and exterior test equipment / attachments or modifications in compliance with applicable airworthiness requirements.

The DO itself grants the supplemental type certification for minor changes within the legally allocated area. Therefore it administrates governmental tasks and acts as part of the administration authority of the Federal Republic of Germany.

The capabilities of the DO are the indispensable prerequisite for the efficient operation of the DLR aircraft fleet in all areas of flight environmental research. In addition to the scientific airplane researches, the main focus lies on the airplanes as a flying laboratory. The application area covers atmospheric research, earth observation and traffic research.

In case of the FTI installation on undercarriage the staff generated compliance reports for the following technical disciplines:

- Electrical substantiation,
- Structural substantiation, and
- Aeroelastic substantiation.

In so-called Special Instructions (SI) the installation procedure is written down step by step, so that the technical staff can follow the instructions and guarantee a qualified installation of the test equipment.

Flight Test Results

In *Figure 14* flight test results are plotted for the deployment sequence of the landing gear at maximum speed of 250kts. The first diagram shows the deflection angles of NLG leg and left-hand MLG door and the total load applied on the door (blue curve) and measured via the strain gauge glued on the actuator rod (see *Figure 7*). The second row contains the accelerations and the third row shows the measured pressures (see *Figure 8*).

The course of the overall load measured by the actuator strain gauge needs some explanation. In the beginning, when the door is closed, the actuator pulls the door against the locking device. This avoids the dropping of the door caused by its own weight, when the locker is suddenly released. At this moment the pulling force is reduced to almost zero and the door opens first by its weight and later when there is gap between door and fuselage bottom by the surrounded aerodynamic forces with tendency to open. When the door is fully deployed – sequence C –, the MLG starts to swing and passes the door. Due to the expulsion of the landing gear wheels additional aerodynamic loading is generated, which pulls the door into the stops. At half deflection angle the force is at its maximum – sequence E –, which represents the static limit load for the door design. Dynamic loads caused by the vibration occur on top of this static condition. So, when the vibration level can be reduced the fatigue loads are decreased as well. This is the reason, why different aerodynamic and structural devices for vibration mitigation are under investigation in

the AFLoNext research project. At the end – sequence G – the door is closed and the actuator pulls against the locker again.

The impact of the NLG as vortex shedding generator can be observed from the comparison of the acceleration level at sequence C, when all doors are open but the NLG is still in the bay, and at the sequence F, when the NLG is down. The same interrelation is observed in the retraction sequence between B and E in *Figure 15*. Here, the maximum speed is limited to 220kts due to the flight manual, which results in slightly lower maximum total loads in the actuator.

The flight test matrix contains several test points at low and high flight speeds and different angles of attack and yaw angles.

These test points were repeated for the checkout flights of the different aerodynamic and structural devices installed on the MLG doors to mitigate the loading and the vibration response.

Finally, a database was filled with experimental flight test results, which serves as the validation reference for the new high-precision CFD-simulation tools to predict unsteady aerodynamic phenomena as well as the dynamic response of the aircraft undercarriage.

Conclusions

The paper presents the preparation, execution and research scope of the AFLoNext flight test campaign dedicated to vibration measurements on the undercarriage of DLR's research aircraft A320 ATRA.

The suitability of the relatively inexpensive NI-cDAQ measuring system for airborne test conditions has been successfully demonstrated during the flight test campaign under real conditions installed in the MLG bay of the ATRA, where the measuring system worked without any failure over the entire duration. The NI-cDAQ system permits customizable signal conditioning for several types of sensor comprising strain gauges, accelerometers, potentiometers and pressure transducer installed on all landing gear doors. The measurement signals can be acquired simultaneously at high sample rates.

The experimental flight test results will serve as a validation database for the upcoming new prediction numerical methods to simulate the dynamics of the overall aircraft undercarriage.

Acknowledgments

The authors would like to thank all partners involved in the AFLoNext Project and the ATRA Team of the DLR Flight Experiments Department in Braunschweig, Germany. Furthermore, the funding of the AFLoNext flight tests by the European Union within FP7 is gratefully acknowledged.

References

- [1] Shia-Hui Peng, Adam Jirasek, Mats Dalenbring, and Peter Eliasson. "Aerodynamic Excitation on MLG Door Exposed to Vortices Emanating from NLG of an Aircraft Model", 34th AIAA Applied Aerodynamics Conference, AIAA AVIATION Forum, (AIAA 2016-4043) <https://doi.org/10.2514/6.2016-4043>
- [2] Maximilian M. Tomac, Arthur W. Rizzi, Dominique Charbonier, Jan B. Vos, Adam Jirásek, Shia-Hui Peng, Andreas Winkler, Alexander Allen, G. Wissocq, Guillaume Puigt, Julien Dandois, and Ramon Abarca-Lopez. "Unsteady Aero-Loads from Vortices Shed on A320 Landing Gear Door: CFD compared to flight tests", 54th AIAA Aerospace Sciences Meeting, AIAA SciTech Forum, (AIAA 2016-0803) <https://doi.org/10.2514/6.2016-0803>
- [3] www.aflonext.eu
- [4] <http://www.dlr.de/fb/en/>
- [5] <http://www.ni.com/data-acquisition/compactdaq/>
- [6] CS-25, <https://www.easa.europa.eu/document-library/certification-specifications>
- [7] <http://multimedia.3m.com/mws/media/827900/dp490-scotch-weld-tm-adhesive.pdf>
- [8] https://www.3m.com/3M/en_US/company-us/all-3m-products/~/3M-Aluminum-Foil-Tape-425/?N=5002385+3293241744&rt=rud
- [9] Sinske, J., Govers, Y., Jelacic, G. et al., "HALO flight test with instrumented under-wing stores for aeroelastic and load measurements in the DLR project iLOADS", CEAS Aeronaut J (2018) 9: 207. <https://doi.org/10.1007/s13272-018-0294-3>

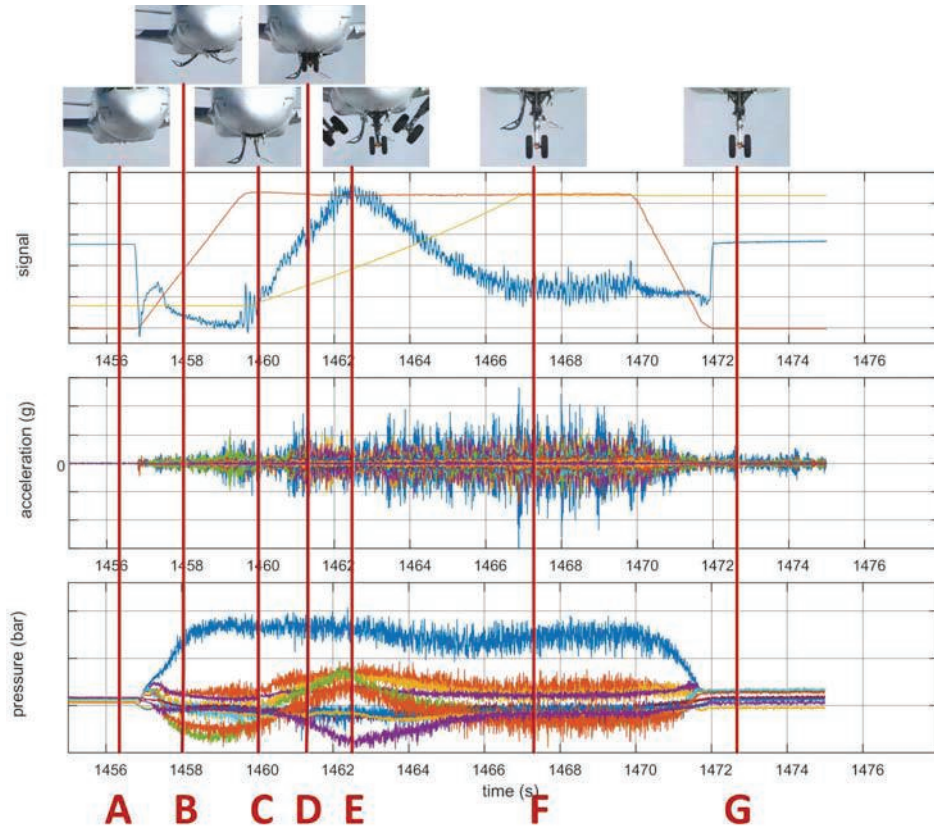


Figure 14. Deployment of LG, acceleration and pressures on left-hand MLG door at 250kts

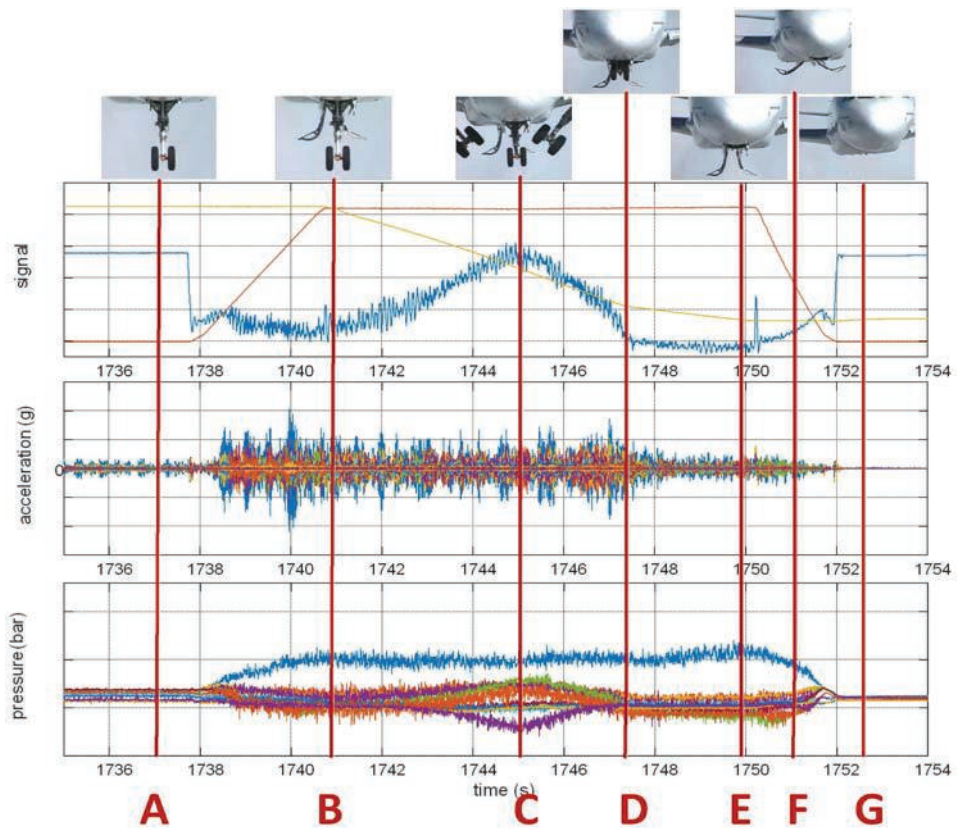


Figure 15. Retraction of LG, acceleration and pressures on left-hand MLG door at 220kts

A400M. Flares trajectories calculation from a chase aircraft

Francisca Coll Herrero¹, Israel Lopez Herreros²

1: Airbus, francisca.coll@airbus.com

2: Airbus, Israel.Lopez@airbus.com

Flight Test – Airbus Defence&Space, Avd. John Lennon s/n, 28906 Getafe (Spain)

Abstract: The A400M defensive aids Sub-System (DASS) includes a radar warning receiver, missile launch and approach warning, and chaff and flare decoy dispensers.

The analysis of the safe separation of flares from A400M within its flight envelope is required as part of the certification process of A400M DASS.

This process includes the validation of the model used by the Aerodynamics Department to calculate the theoretical flare trajectories.

During 2017, it was required to validate the trajectory ejected from dispensers located on the nose of the aircraft, and in this case it was necessary to use external cameras installed in a chase aircraft to cover the completed trajectory.

The aim of this document is to present a methodology used to calculate a real case of flares trajectories on A400M ejected from front dispensers using 2 external cameras installed in a chase aircraft.

Keywords: DASS, safe separation High Speed Cameras, Photogrammetry, HSV, A400M, camera calibration, FollowMe, external cameras.

1 Introduction

The analysis of the safe separation of flares from A400M is required as part of the certification process of A400M DASS (Ref.1).

In order to validate the theoretical model used by the Aerodynamics Department several safe separation flight tests had to be performed.

Initially only dispensers placed in the rear wing fairing (WR 11 & 12) and especially in the rear part of the sponsors (SP 13 & 14) were selected to perform the tests as the most critical ones (Higher risk of impact, HTP) .

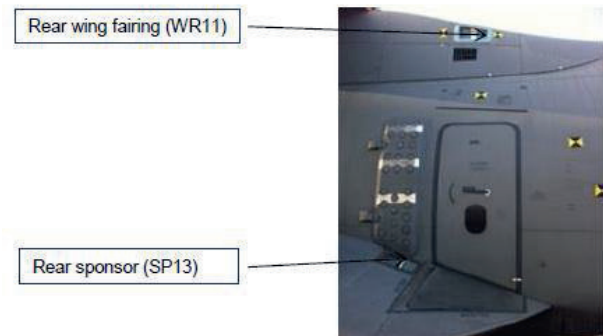


Figure 1. Dispensers

The trajectories are calculated by applying Photogrammetry techniques to the films extracted from onboard High Speed (HSV) cameras (Vannier –AOS, 1024x768 resolution, 200 frames per second).

Four synchronized cameras are needed to cover all theoretical paths, two cameras for the initial part and two for the final part of the path.

- C3S , installed under the left wing, close to the tip
- HS3, installed on a balcony in the place of the last left side window.
- J1S , installed under the left HTP
- HS4 , installed on the left wing- centre fuselage

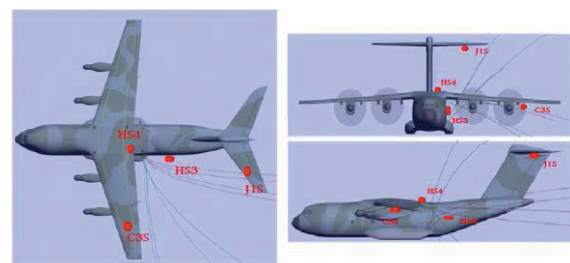


Figure 2. theoretical trajectories

The trajectory is calculated by sections, J1S and C3S for the initial part and HS4 and HS3 for the rest of the path.



Figure 3 :HSV cameras

The Flight Physics Department gives theoretical paths of flares in different flight conditions.

Using the 3D-studio program, the cameras are positioned in order to cover all paths.



Figure 4. Image from J1S using 3D studio



Figure 5. Image from C3S using 3D studio

During 2017, the validation of the flares trajectories from **all the dispensers** has been required.



Figure 6. flares trajectories from all the dispensers

After a detailed study from our team, the following findings were made:

- It is impossible to calculate the trajectories of the flares using the cameras currently installed on the A400M, even changing the orientation of the cameras.
- It is practically impossible to calculate the trajectories of the flares from the dispensers located on the nose of the aircraft with cameras installed anywhere in the aircraft.

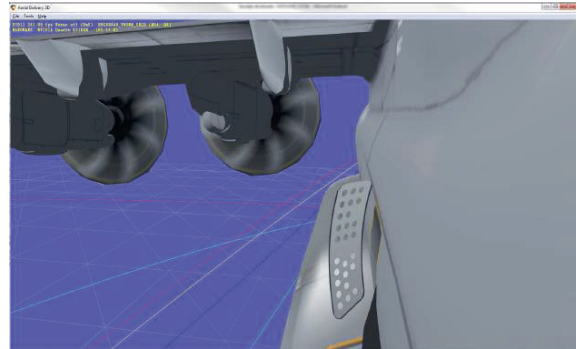


Figure 7. Image from HS3 changing the camera orientation

The aim of this document is to present a new methodology used to calculate a real case of flares trajectories on A400M ejected from front dispensers using 2 cameras installed in a chase aircraft.

During the Flight Tests campaign of safe separation, all the flares will be ejected from the left dispensers due to the symmetry of the aircraft.

The trajectories are calculated using programs developed by FT analysis Tools team of Airbus defense and space.

2 Propose solution by FT Analysis Tools

As mentioned in the previous chapter, it is practically impossible to calculate the trajectories of the flares ejected from the dispensers located on the nose of the aircraft with the cameras installed anywhere in the aircraft.

The solution proposed by FT Analysis Tools department was:

- To use a chase aircraft with 2 synchronized Full HD cameras installed using a tripod, in the right part of the cabin.

- The airplane would fly in parallel to the A400M (security distance around 70 meters) in front of the dispenser to be tested.
- The proposed chase aircraft are the A310 (BOOM), C295 or A400M.



Figure 8. Schematic representation of FT Analysis Tools solution

3 Background .Photogrammetry proces

To calculate the trajectory of an object, photogrammetry proces is divided in to the followings steps: to define Aircraft System Reference, camera calibration, camera positioning and 3D trajectory calculation.

3.1 Aircraft System Reference

In the case of this report, the flares trajectory coordinates are given with respect to A400M coordinate system.

To define this AC coordinate system it is necessary to know the coordinates of at least 3 A400M reference markers, FTI design office provides us with this information.

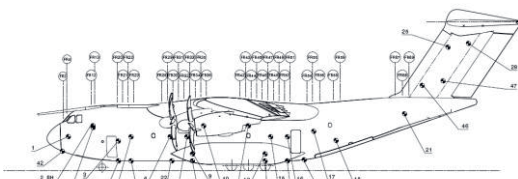


Figure 9.Reference marks on A400M

The figure 10 shows the references marks used in the analysis.

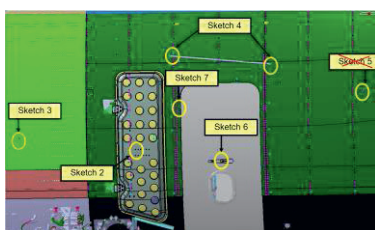


Figure 10.Reference marks used

3.1.1 Tachymeter

The tachymeter will be used to measure the exact coordinates of the reference marks (Ref. 2).

With aid from a telemeter, the positions of the reference points are measured in telemeter coordinates and afterwards, transformed according to aircraft system reference.

Some stickers are used to mark points of interest to be measured with the tachymeter and transform to AC axes system through the reference points.



Figure 11. Aircrfat sistem reference

3.2 Camera calibration

Camera **calibration** , the aim of the calibration process is to obtain the intrinsic optical parameters of the cameras, more specifically of its lens, like focal length, principal point and distortion of the lens.

Matlab® Calibration Toolbox is used to determine the calibration (Ref. 3).

To calibrate a camera, the first step is to take pictures of a checked board (Figure 12). Several shots moving the board to different distances and angles are taken.

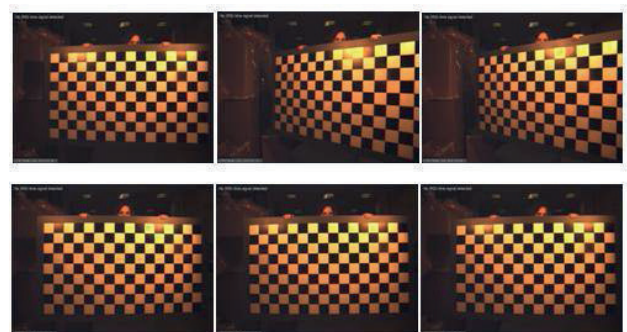


Figure 12.camera calibration

3.3 Cameras positioning

Cameras **positioning**, the aim of this process is to calculate the position (X, Y, Z coordinates) and spatial alignment (roll, pitch, yaw) to respect Aircraft System Reference.

For this process, special stickers are used as reference marks by placing them inside the cameras' visible field.

3.4 3D trajectory calculation

With the information obtained in the previous steps and the 2D coordinates of the object in the image, the 3D object coordinates are calculated using different algorithms for one or two cameras solution.

In the case of flares trajectories, the flares is considered as a point, therefore the algorithm used is two camera solution.

Both the camera position and the flare trajectory are calculated using in-house Software named FollowMe. This software, developed in Matlab®, is based on photogrammetry algorithms and automatic image recognition techniques integrated into a graphical interface to ease the selection of the reference marks.

4 Mathematical solution

Two possible mathematical solutions were considered to calculate the flare's trajectories ejected from nose dispenser.

For each frame of the film, were placed on A400M big stickers to be clearly seen from the chase cameras:

- To calculate the two camera positions to respect A400M System Reference. The flare trajectory is calculated using the two camera solution for mobile cameras.
- To calculate the transformation matrix between both aircrafts (chase and A400M). The flare trajectory is initially calculated to respect chase System reference and finally transformed to A400M System reference using the corresponding transformation matrix. This was the algorithm used in the analysis.



Figure 13. big stickers on A400M

5 Validation and accuracy

The validation was made using FollowMe software to calculate flare 3D trajectory and 3DS Studio Max to study the scenario and the generation of the video/images.

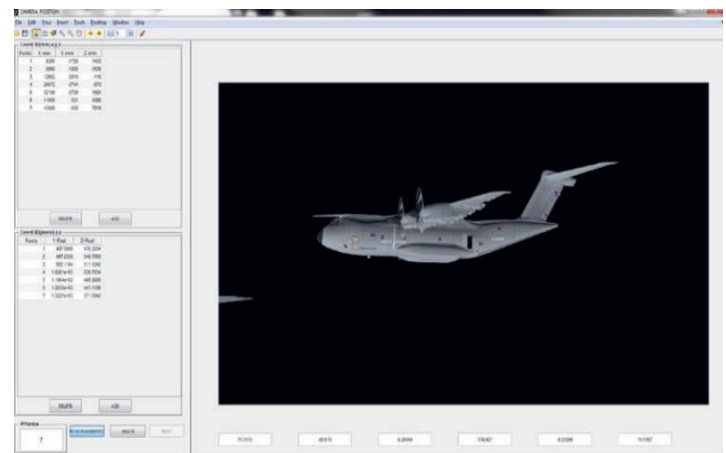


Figure 14. FollowMe software

From the 3D theoretical flares trajectories and the cameras positions, 2D coordinates of the stickers and flares are calculated.

Using these theoretical 2D positions, and applying the algorithm, the obtained 3D trajectory is perfect.

In order to study the accuracy of the algorithm, it is considered 0.3 pixel error in the selection of the stickers and the flare.

In both of the mathematical solutions, the error is less than 0.1 meter, therefore both techniques can be used for the flare trajectory calculation.

6 Pros and Cons

Pros	Cons
Not required additional camera installation in A400M.	Calculate cameras position in each frame or transform matrix.
Recording all left flare trajectories in one flight and one position	Chase aircraft required
COT cameras and easy installation using tripod	
Two cameras for all the flare trajectory	

7 Flight Test campaign

As part of the activities required for validating the A400M flare models of the flare types specified within DASS Certification Plan, a flight test campaign is scheduled in May 2017.

Those tests that consist in ejecting a flare from the rear sponson and wing fairing dispensers have been recorded using onboard high speed cameras, whereas the rest of the tests have been tracked by external means.

The chase aircraft used for the test was A400M-0006 and the flares were ejected from A400M-0002.

7.1 Chase cameras configuration

The chase aircraft A400M-0006 has recorded the flares flying in parallel to A400M-0002.

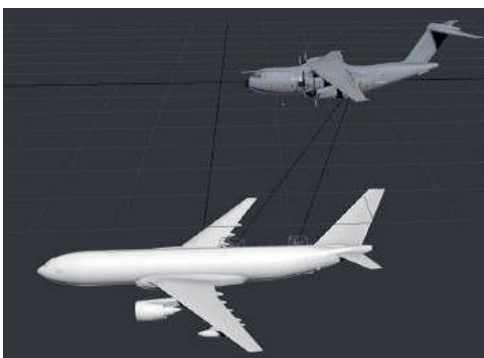


Figure 15. Chase cameras configuration

The two cameras installed are named Front Camera and Rear camera. Figures 16 and 17 show the images captured from these two cameras.



Figure 16. Front Camera



Figure 17. Rear camera

The cameras used in the test were two synchronized Blackmagic Micro Cinema Camera, fullHD (1920X1080 resolution), up to 60 fps.



Figure 18. Blackmagic Micro Cinema Camera

7.2 Analysis Methodology

The flare trajectory is calculated by analyzing the recorded images using FollowMe software.

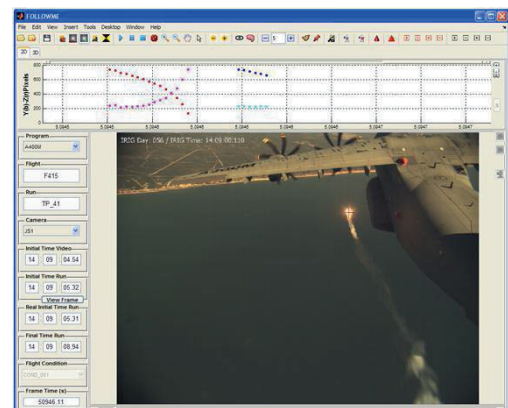


Figure 19. FollowMe interface

The steps are the followings:

- a) The cameras are positioned to respect A400M-0006 Aircraft System Reference (chase AC).
- b) The flares trajectories are calculated to respect A400M-0006 Aircraft System Reference (chase AC).
- c) The final trajectories are transformed from A400M-0002 to A400M-0006 Aircraft System Reference.

The first two steps are the same as the employed for onboard cameras configuration.

In the last step, the algorithm calculates the associated transformation matrix between both aircrafts for each frame.

To do so, the position of at least three points must be known in both axis systems for each instant time.

Several stickers are positioned with the aid of the tachymeter in the A400M-0002 so its coordinates are known in its axis reference system.

Following figure shows the stickers placed in the A400M-0002.



Figure 20. A400M-0002 stickers

With the knowledge of the position of the stickers in both systems, transformation matrix can be calculated and applied to the flares trajectories.

7.3 Trajectory accuracy

Sticker's positions do not change in A400M-0002 axis reference system. This information is used in the trajectory transformation process to obtain the accuracy of this transformation as well as of the photogrammetry tracking.

Next figure shows the stickers position deviation obtained during one flare trajectory.

For each sticker, the difference between the calculated position (X, Y, Z) and the measured with tachymeter (in meters) is represented (< 0.15 m).

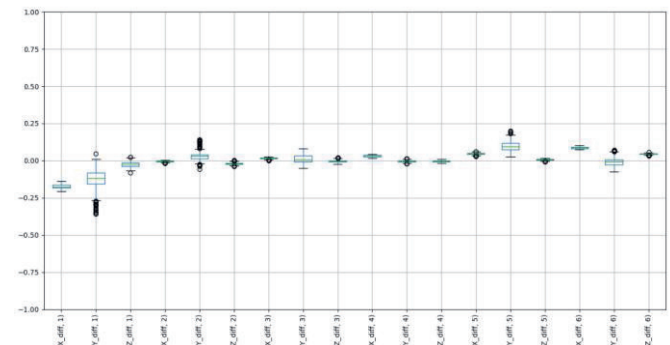


Figure 21. F0988-R025 stickers position deviation in meters

8 Conclusions

A new methodology has been implemented for safe separation analysis using external cameras installed in a chase aircraft.

The used of this technique is necessary when it is not possible to install onboard cameras to cover the entire trajectory.

This methodology has been used during the DASS system certification Flight Test campaign scheduled in May 2017.

9 References

- [1] Coll Francisca , "**A400M DASS. SYSTEM TEST**", SFTE European Chapter Symposium 2015
- [2] GML Lasermesstechnik. 3D Observer Operating Manual. Version 1.1.2005
- [3] Camera calibration toolbox . http://www.vision.caltech.edu/bouguetj/calib_doc

12 Acronyms

DASS	Defensive Aids Sub-System
HSV	High Speed Video cameras

HTP	Horizontal Tail Plane
HS3	Camera installed on the balcony
J1S	Camera installed under the left HTP
HS4	Camera installed on the left wing centre fuselage
WR	Wing firing
SP	Sponsors
AC	Aircraft
FullHD	High Definition (1920X1080) pixels
COT	Camera of things

PARIS - Parallelisation Architecture for Real-time Image Data Exploitation and Sensor Data Fusion

Stephan Blokzyl, Michael Nagler, René Schmidt, Wolfram Hardt
 Computer Science Department, Chemnitz University of Technology, D-09107 Chemnitz, Germany
 {sblo, nagm, renesc, hardt}@hrz.tu-chemnitz.de

Abstract:

The development of visual recognition systems for highly automated, mobile systems is driven by matured electro-optical sensors and application-specific, optimised computational components. Applying good-quality, high-resolution imagery exploited by powerful embedded processors, current computer vision systems provide a detailed representation of system's operational environment and contribute significantly to various perception tasks. However, the exploitation of high-resolution image data is challenging on space-, weight-, and energy-limited mobile systems, especially when respecting real-time and reliability requirements of safety critical functions.

Considering these conditions, this paper introduces a generic parallelisation architecture for real-time image processing using reconfigurable integrated circuits. The architecture supports data and task parallelisation strategies utilising the specific parallelisation capabilities of Field Programmable Gate Arrays. It provides space-, weight-, and energy-efficient parallelisation for image exploitation and information fusion.

The device- and interface-independent architecture maximises parallelism and flexibility of complex image processing applications aboard mobile systems. The modular structure of the proposed architecture enables hardware-acceleration for high-resolution sensor data exploitation, minimises processing latency, and improves the quality of the overall detection result by using multivariate detection methods.

The generic parallelisation architecture will be used for multi-copter-based high voltage transmission line inspection and vision-based localisation of an unmanned aerial vehicle during final approach phase.

Key words: Visual Recognition Systems, Mobile Systems, Parallelisation, Real-time Image Processing, Field Programmable Gate Arrays.

Introduction

The development of computer vision-based measurement and recognition systems is continuously driven by technology progress. Hardware innovations provide more powerful sensors and computing architectures. New methodologies improve sensor data acquisition and signal processing. The growth of interconnection and interaction between computing devices raises heterogeneity and interoperability of advanced computer vision solutions [1].

More powerful sensors with increasing frame rate and resolution generate considerably higher sensor data volumes. High-quality, lossless acquisition, processing, and management of the rising amount of data gets more and more demanding. Especially in automotive, transporta-

tion, avionic, and space applications, which typically realise sensor signal processing on embedded systems, and have to consider safety, reliability, and real-time aspects [2].

Devices like user-programmable integrated circuits (e. g. Field Programmable Gate Arrays, FPGAs) are increasingly popular for embedded, high-performance image data exploitation (brief overview given in [3]). They combine the parallelisation capability and processing power of application specific integrated circuits (ASICs) with the flexibility, scalability, and adaptability of software-based processing solutions. FPGAs provide powerful processing resources due to an optimal adaptation to the target application and a well-balanced ratio of performance, efficiency, and parallelisation.

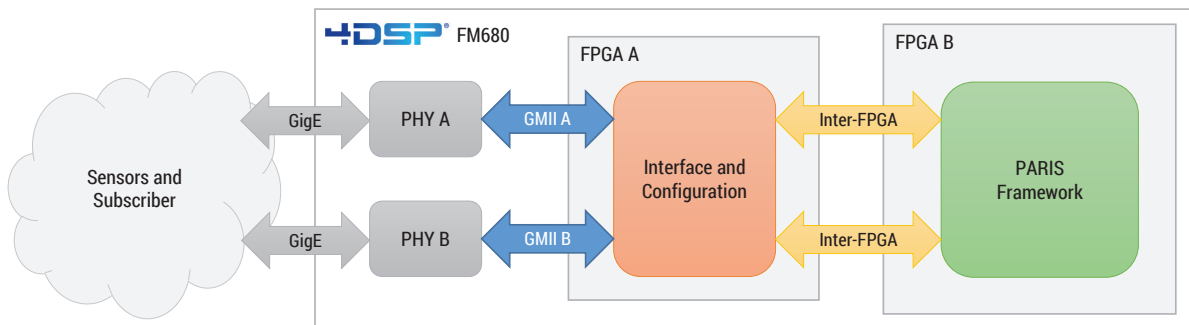


Fig. 1. Ethernet-based interconnection of the PARIS system architecture to the operational environment.

These features are fundamental for the hardware-accelerated real-time image exploitation concept, presented by Blokzyl *et al.* in [4]. With a two-dimensional parallelisation methodology (data vs. task parallelisation), the approach intends to accelerate the image processing procedure and improves the overall processing and result quality. The concept focuses on specific requirements on system components for safety-critical perception applications:

- Flexibility through modularisation and re-configurability
- Result quality enhancement by multi-variate exploitation
- Process acceleration by execution parallelisation
- Result predictability by use of deterministic algorithms
- Determinability of worst-case-execution-time
- Result safety and confidence qualification
- Certifiability for safety-critical applications

The powerful realisation of the two-dimensional parallelisation methodology requires specific attributes of the hosting hardware. Beside flexibility, scalability, and a high degree of parallelisation capabilities, properties like power consumption, energy efficiency, size, and weight play an important role in embedded applications.

Hence, this work introduces the PARIS¹ system architecture, a framework for easy integration of data and task parallelisation for sensor data exploitation, data fusion, system management, data flow, and sensor control (compare Fig. 1).

¹ Parallelisation Architecture for Real-time Image data exploitation and Sensor data fusion

System Architecture

The PARIS system model comprises the following sub-components: Network integration and network management, system and sensor management, as well as image data exploitation and fusion. All elements and their detailed functions are explained in the following sections.

A. Network Integration and Network Management

Network integration and network management includes both physical and logical interconnection of the PARIS system architecture with the operational environment. The PARIS interfaces use Gigabit Ethernet standard to connect all sensors and result subscribers, but the free configurability of FPGAs allows the utilisation of alternative communication standards and protocols (compare Fig. 1).

Popular digital signal processing FPGAs (e. g. XILINX Virtex[®] or Altera Stratix[®] series devices) provide ready-to-use intellectual property (IP) cores for the Data Link layer to enable ease Gigabit Ethernet communication. This IP for Media Access Control (MAC IP) supports Ethernet-based communication without additional user implementation. Layer 1 functions including message transmission (Physical Layer) are realised by external transceivers (see PHY A/B in Fig. 1) and functions of Layer 3 and higher (compare Open System Interconnection Model, OSI model [8]) can be customised with the respect to the target application.

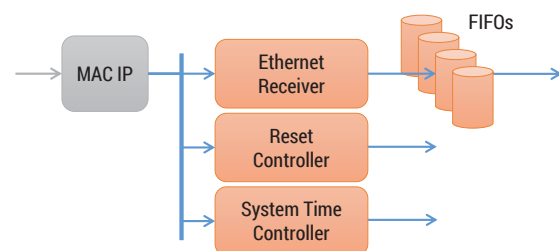


Fig. 2 Basic receiver components of the PARIS system architecture.

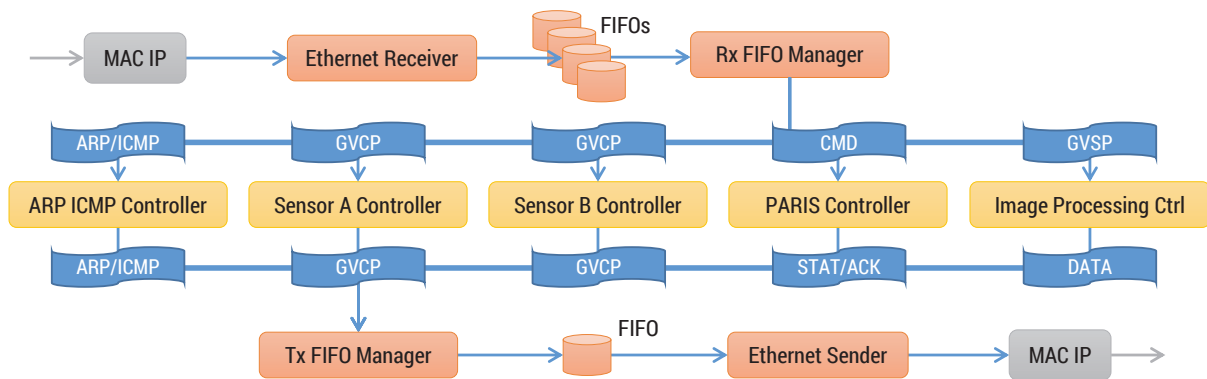


Fig. 3. Overview of receiver, sender, and controller structure of the PARIS system architecture.

The communication between PARIS and PHY transceivers uses the Gigabit Media Independent Interface standard (GMII). GMII is independent from the communication medium and a change from e. g. copper wire-based to fibre-optic transmission does not affect the link between PARIS and the peripherals. Only copper wire-based transceiver modules have to be replaced by devices supporting fibre-optic interconnection. Furthermore, changing Ethernet communication to an alternative technology, like e. g. Peripheral Component Interconnect (PCI) requires the modification of communication IP core only (here MAC IP, Ethernet Receiver in Fig. 2). It has no impact on other system components of the PARIS system model.

This flexibility maximises the integration capability of PARIS in comparison to conventional system architectures. PARIS is not limited to specific FPGA devices or series and can be operated on various boards with arbitrary form factors, physical connections, and interfaces.

PARIS is equipped with two independent Gigabit Ethernet interfaces (A/B) providing a total bandwidth of 2 Gbit/s for sensor data acquisition and result dissemination. As shown in Fig. 2, incoming messages arrive at the MAC IP that extracts the message payload (Ethernet frame) and simultaneously forwards the data to the Ethernet Receiver, Reset Controller, and System Time Controller. The parallelised setup of these three subsequent modules is necessary to ensure global system reset in any error case (e. g. rest of the PARIS is stalled) and to minimise the latency of system time synchronisation. These modules are connected unidirectional to the MAC IP. They have no control access to MAC IP and have to be ready to receive incoming Ethernet frames anytime. Reset and System Time Controller exclusively accept Reset Protocol (RP) respectively Simple Network Time Protocol (SNTP) messages and process these packets in real-time. The Ethernet Receiver accepts all the other message types and

catches them in different receive buffers (First-In-First-Out buffers, FIFOs).

If the MAC IP advises the reception of a new message, the Ethernet Receiver selects an empty receive buffer and saves the minimum packet payload. Destination and checksum information of Ethernet frames is not saved as the PARIS discards misaddressed or damaged incoming messages. Source address data is saved in cases when it is necessary to reply to original sender (e. g. command acknowledge). Saving only minimum payload reduces memory consumption, minimises stall and wait times of concurrently reading modules, decreases processing latency, and prevents data loss.

The application of multiple message buffers allows the parallel processing of incoming data, which accelerates the overall system performance. If only one single buffer was used, the retrieval of large-sized messages would result in longer wait times for non-active parallel modules. Subsequently, already completely received data could not be processed simultaneously because the receive buffer data output is already blocked. As the PARIS predominantly processes image data, the number of large-sized packets is very high. The byte count of image packets (so called jumbo frames) exceeds the 1.5 KB Maximum Transmission Unit (MTU) of standard Ethernet frames. Fetching and exploitation of image jumbo frames takes considerably longer compared to the processing of e. g. small-sized network management messages like Address Resolution Protocol (ARP) or Internet Control Message Protocol (ICMP). Reply and validity times could be neglected. The application of multiple receive buffers reduces this bottleneck and enables parallel data readout and exploitation, which leads to significantly less delay between data reception, processing, and result dissemination.

All error-free frames in the receive FIFOs are forwarded by the System and Sensor Manage-

ment to the appropriate sub-components of the PARIS system architecture (see Fig. 3).

B. System and Sensor Management

As introduced in section A, all received and valid frames are cached in receive buffers (FIFOs) by the Ethernet Receiver. A connected Receive Buffer Manager (Rx FIFO Manager, compare Fig. 3) controls the fetching and distribution of the received data across the PARIS system architecture. The Rx FIFO Manager analyses the message types and distinguishes the following message classes:

1. Address Resolution Protocol (ARP)
2. Internet Control Message Protocol (ICMP)
3. Internet Group Management Protocol (IGMP)
4. GigE Vision Control Protocol (UDP/GCSP)
5. GigE Vision Stream Protocol (UDP/GVSP)
6. System Command Protocol (CMD/UDP)

The Rx FIFO Manager monitors cyclically all receive buffers and checks one buffer at each clock cycle. With e. g. four receive buffers and a system operation frequency of 125 MHz, a new and completely received Ethernet frame is recognised with a maximum latency of 24 ns. According to the message type (indicated by the buffer state), the associated sub-component is connected to the corresponding buffer and starts data readout. The receive buffer is released as soon as the connected module completes data transmission and the Rx FIFO Manager resets the buffer for receiving new data frames. As a result, all messages are forwarded to the different PARIS modules (controllers) depending on their message type:

ARP ICMP IGMP Controller The ARP ICMP IGMP Controller implements the OSI model Layer 3. This module is instantiated two times and manages the network setup and communication parameters (addressing, routing, and traffic control). The two controllers operate the Gigabit Ethernet interfaces of the PARIS system architecture as introduced in section A.

Sensor Controller The Sensor Controllers manage all external imaging devices based on the GigE Vision standard. The GigE Vision standard is an interface and communication standard for Ethernet-based electro-optical sensors (GigE Vision Control Protocol, GVCP). The GVCP has been developed by the Automated Imaging Association (AIA) in the year

2006. As the PARIS framework is equipped with a stereo camera system with two independent electro-optical sensors, two entities of the Sensor Controller exist (A/B). The controllers are duplicable and replaceable with alternatives which enables the application of arbitrary sensors for different recognition and measurement tasks.

PARIS Controller The PARIS Controller monitors and controls the operation of the PARIS system model and handles all incoming CMD messages. The CMD message type contains system configuration data (system parameter) and commands the available work modes. Successful processing of CMD messages is replied by acknowledgement packets (ACK). Continuous status messages (STAT) report the PARIS system (health) and operation status.

Image Processing Controller The Image Processing Controller represents the core module of the PARIS system architecture. The module hosts all image processing units and utilises data and task parallelisation strategies. The Image Processing Controller obtains the image data fragments from the electro-optical sensors (GigE Vision Streaming Protocol, GVSP) and implements pre-processing as well as imagery exploitation (more details given in section B). The result data of the Image Processing Controller is encapsulated in Ethernet frames (DATA) and addressed to the result subscribers. The index of signed in result subscribers is managed by the PARIS Controller.

The processing results of the different controllers (ARP, ICMP, IGMP, GVCP, ACK, STAT, and DATA) are enclosed in Ethernet frames and stored in a wait buffer for sending. A Send Buffer Manager (Tx FIFO Manager) controls the write access to the send FIFO with the help of a token system. If a PARIS sub-component demands write access, it requests a token from the Tx FIFO Manager. The module starts data transmission as soon as the Tx FIFO Manager grants write rights with the help of a handshake mechanism. The module releases the token after transmission completion and a competitive PARIS component can access the send buffer. The send FIFO is realised as singular buffer for each Ethernet interface, because the small lengths and size variances of the outgoing messages lead to significantly less competitive access compared to the receive buffers. An average size of approximately 60 bytes per packet causes a mean wait time of approximately 500 ns until a token is released again².

² With a system operation frequency of 125 MHz.

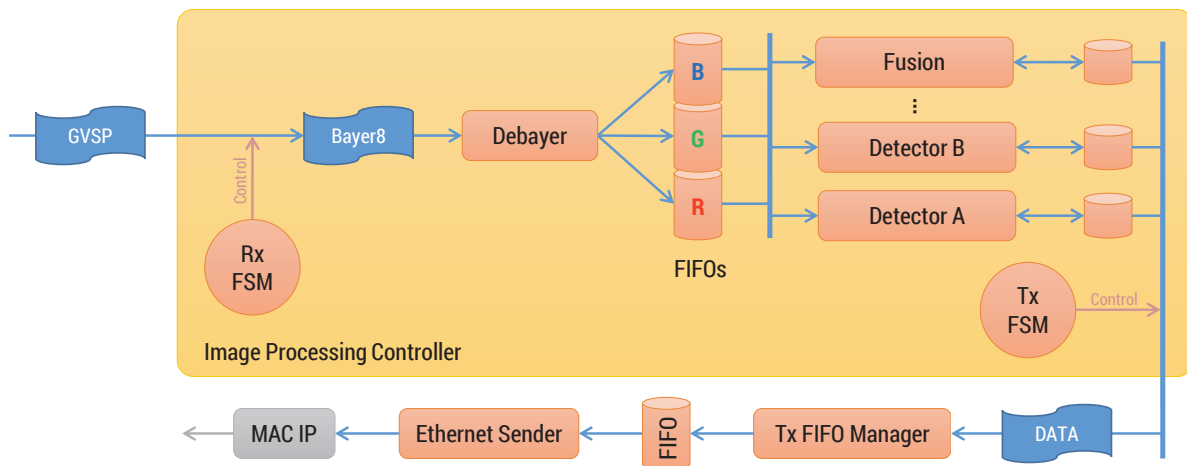


Fig. 4. Data flow and two-dimensional parallelisation inside the Image Processing Controller.

If the PARIS framework hosts applications which generate result data with obviously different-sized result messages, the send buffer can be optionally extended with additional FIFO memories. Multiple send buffers allow simultaneous sending of small, completely cached Ethernet packets while large-sized messages are continuously buffering. This reduces bilateral blocking of PARIS sub-components.

The send buffer status is steadily supervised by the Ethernet Sender. Completely cached Ethernet frames are transmitted to the MAC IP as soon as the MAC IP is ready to accept data and the send medium is free.

C. Image Processing and Fusion

The Image Processing Controller is the core module of the PARIS system architecture. It hosts the parallelisation framework for real-time image data exploitation and fusion. The controller involves all steps for sensor data acquisition, image pre-processing, and image data exploitation. Data acquisition names the (image) payload de-fragmentation of the incoming GVSP messages (image fragments). The extracted raw image stream is typically a Bayer mosaic image that has to be converted to a three-channel colour image, which can be processed by subsequent image processing modules (detectors). The colour image generation is realised by the Debayer module (see Fig. 4). The three resulting partial images represent the image channels Blue, Green, and Red, which are stored in image synchronisation buffer (B/G/R FIFOs).

Parallel image processing modules start execution as soon as enough image data is available in the image synchronisation buffers. The following module with the highest data requirement determines the time to start processing. If one module requires 49 pixels and another

(parallel) module requires only nine pixels to start execution, both modules stall the processing until 49 pixels are available in the image synchronisation buffer (start synchronisation). This earliest start strategy avoids the buffering of the complete image and reduces both processing latency and memory consumption. As result, the image buffer size decreases significantly. The PARIS hardware realisation uses only 12.3 KB of FPGA-BRAM instead of 2,073.6 KB DDR-SDRAM which are required for the software-based processing of two megapixel colour images (high definition resolution). The PARIS system architecture saves more than 99% of image buffer size compared to conventional, software-based image processing solutions.

As shown in Fig. 4, an arbitrary number of various, parallel image processing modules can be connected to the data output bus of the image synchronisation buffer. The different run- and execution times are synchronised by individual result buffers for each image processing module (result synchronisation). This structure qualifies the PARIS framework to use data and task parallelisation strategies as well as static and dynamic in-system-reconfiguration.

Data Parallelisation Multiple instances of independent detectors enable the distribution of incoming sensor data to multiple, homogeneous processing entities. Slow image processing algorithms with a longer execution time compared to the validity time of incoming sensor data (update rate) are accelerated by workload sharing. The detection results of the different image processing modules are aggregated subsequently in a common synchronisation buffer (result aggregation).

Task parallelisation The parallel application of heterogeneous, simultaneously working detec-

tors increases the overall detection result quality. All image segments are analysed by heterogeneous, weak detectors realising different low-level image processing methods on equal image segments. The diverse intermediate results are merged in a subsequent fusion step that generates detections on a higher level of abstraction contributing to the global detection task.

Data Aggregation and Information Fusion All partial and intermediate results are combined in result buffers and validated by a confidence score (compare Fig. 4). This step comprises the synchronisation and aggregation of data parallelisation results and the information fusion of diverse intermediate results from task parallelisation. More details of the concept and the realisation of the fusion approach, including the integration of data from other sources and sensors, are given in [4] and [5].

In-System-Reconfiguration The parallel and modular architecture of the image processing controller enables both static and dynamic reconfiguration without complete deactivation or stalling of the image processing system. The replacement, integration, or exclusion of dedicated detectors enables the PARIS framework to respond to changing recognition conditions and varying detection tasks during run-time. The PARIS is able to adapt the degree of parallelisation inside the image processing core. This guarantees an anytime optimal compromise between energy consumption (power dissipation respectively heat development), computing performance, and acceleration rate.

All partial, aggregation, and fusion results are encapsulated in Ethernet frames after successful processing. The Ethernet messages are pushed to the send buffer (compare section B) which is supervised by the Ethernet Sender. As soon as the send buffer status indicates a completely buffered Ethernet frame and the MAC IP reports readiness to send, the Ethernet Sender transmits the pre-buffered frame to the MAC IP. The MAC IP forwards the message subsequently to the connected PHY transceiver via GMII (see Fig. 4).

Results

The introduced PARIS system architecture is realised on the hardware acceleration board FM680 of the US-American company 4DSP, worldwide leading experts in the area of Commercial-of-the-Shelf (COTS) board-level electronics and FPGA intellectual property. The board is equipped with two XILINX Virtex[®] family FPGAs (see Fig. 1). One Virtex[®]-5 XC5VLX20T FPGA hosts the interface implementation for Gigabit Ethernet communication and manages

the system boot-up process with an external power-on configuration flash memory. The large-scale Virtex[®]-6 XC6VLX550T FPGA with 86,000 slices, 550,000 logic cells, 687,000 flip-flops, and approximately 3.6 Megabyte on-board-RAM [6] realises system and sensor control as well as the sensor signal processing (image data exploitation). These powerful large-scale FPGAs enable high acceleration potential for a wide range of highly parallel image exploitation and data fusion applications.

Logic Resources	Utilisation 6VLX550T <i>PARIS Framework</i>	Utilisation 5VLX20T <i>Interface Device</i>
Slice Registers	9,401 (1.4%)	2,022 (16.2%)
Slice LUTs	13,364 (3.9%)	1,952 (15.6%)
Occupied Slices	4,491 (5.2%)	1,011 (32.4%)
RAM Blocks	44 (2.3%)	4 (15.4%)

Tab. 1 FPGA Utilisation for the PARIS System Architecture

The hardware circuitry of the PARIS system implementation achieves a maximum operation frequency of 125.881MHz with an appropriate logic resource consumption as shown in Tab. 1. The economic, logic resources saving hardware realisation of the PARIS system architecture allows efficient integration of a large number of data and task parallelised image exploitation components and the implementation of complex image processing applications on FPGA devices.

Conclusion and Outlook

The novel PARIS system architecture provides a solution for modular, flexible, and comfortable parallelisation of real-time image data exploitation. The architecture supports both data and task parallelisation strategies, static and dynamic in-system-reconfiguration, and considers fundamental requirements for embedded signal processing architectures like e. g. power consumption, energy efficiency, size, and weight restrictions. The PARIS framework is implemented on a COTS hardware acceleration board, will be proved in a stereo vision-based localisation system of an unmanned aerial vehicle during final approach phase [5][7], and for multi-copter-based high voltage transmission line inspection [9].

Acknowledgment

The results have been supported by the program OPIRA - Open Innovation for Remotely Piloted Aircraft Systems (RPAS), funded by the Federal Ministry for Economic Affairs and Energy, Germany.

Within OPIRA, a collaboration of Airbus Defence and Space, German universities, and research institutes intends to develop holistic solutions to increase air traffic safety and the operation of RPAS for civil applications.

References

- [1] M. Vodel, S. Blokzyl, W. Hardt, Hochauflösende Videodatenanalyse in Echtzeit - FPGA Hardwarebeschleunigung durch Daten- & Task-Parallelisierung, *Proceedings of the 2015 Innosecure 15 - Innovationen in den Sicherheitstechnologien*, April 2015; ISBN: 978-3-86359-299-8
- [2] S. Blokzyl, W. Hardt, Generisches Framework zur Parallelisierung von Echtzeitfähiger Bilddatenauswertung für Rekonfigurierbare Integrierte Schaltkreise, *Proceedings of the Studierendensymposium Informatik 2016 der TU Chemnitz (TUCSIS2016)*, 145-148 (March 2016); ISBN: 978-3-944640-85-3
- [3] S. Blokzyl, W. Hardt, FPGA-basierte Hardwarebeschleunigung für Echtzeitbildverarbeitung und Fusion, *Proceedings of the Informatiksymposium Chemnitz 2012 (TUCSIS2012)*, *Chemnitzer Informatik-Berichte CSR-12-01 (2012)*, 102-105 (July 2012); ISSN: 0947-5125
- [4] S. Blokzyl, M. Vodel, W. Hardt, A Hardware Accelerated Real-Time Image Processing Concept for High-Resolution EO Sensors, *Proceedings of the 61. Deutscher Luft- und Raumfahrtkongress (2012)*, September 2012; DOI: urn:nbn:de:101:1-201211239114
- [5] S. Blokzyl, M. Vodel, W. Hardt, FPGA-based Approach for Runway Boundary Detection in High-resolution Colour Images, *Proceedings of the 2014 IEEE Sensors & Applications Symposium (SAS2014)*, 59-64 (February 2014); ISBN: 978-1-4799-2180-5
- [6] XILINX, Product Specification DS 150 - Virtex-6 Family Overview, August 2015, Available online: http://www.xilinx.com/support/documentation/data_sheets/ds150.pdf
- [7] S. Blokzyl, M. Vodel, W. Hardt, Generischer Ansatz zur kantenbasierten Landebahndetektion in hochauflösenden Farbbildern, *Proceedings of the 62. Deutscher Luft- und Raumfahrtkongress (2013)*, September 2013; DOI: urn:nbn:de:101:1-201312099786
- [8] Study Groups of ITU's Telecommunication Standardization, Information technology - Open Systems Interconnection - Basic Reference Model: The basic model, July 1994; DOI: <http://handle.itu.int/11.1002/1000/2820>
- [9] U. Tudevtagva, S. Blokzyl, B. Battseren, E. Khaltar, The beginning of Unmanned Aerial Vehicle-based Inspection of HVTL, *Power Energy and Engineering Journal*, 23-27 (February 2017); ISBN: 978-99929-73-24-2

Applications of Machine Vision in Flight Test

Phil M. Westhart, Hakima Ibaroudene, Austin J. Whittington, Myron L. Moodie, Ben A. Abbott, Ph.D.
Southwest Research Institute® (SwRI®), San Antonio, TX, USA
fti@swri.org

Abstract:

Machine vision uses cameras, computers, and algorithms to replace human vision in various applications such as factory automation, autonomous vehicles, object recognition, optical character recognition, and many other applications. Existing machine vision technologies can be applied to the flight test domain to solve real world problems, such as extracting data from cockpit displays in real-time. These technologies can reduce installation costs and complexity and may not require aircraft modification to obtain parameter data. This paper explores machine vision techniques for flight test applications and includes a case study of a portable cockpit display video measurement system that reads digital measurements from aircraft instrumentation panels.

Key words: Machine vision, cockpit display, video measurement

Introduction

Machine vision has been leveraged in a variety of domains with many innovative applications. SwRI has been actively performing research in the field of machine vision for over two decades. Some recent machine vision applications include a machine-learning based detection of hazardous chemical spills [1], package sorting in distribution warehouses [2], and enabling autonomous vehicles in GPS degraded environments [3]. Recent efforts have brought this machine vision expertise to approach challenges in the flight test community, specifically targeting increased efficiency in test article preparation.

Due to the increasing complexity of airframes and associated controls for modern aircraft, the test instrumentation is required to be similarly complex, which requires significant investments in manpower and material to prepare an aircraft for test. The developmental flight test of modern commercial aircraft typically requires eight months to a year of test time, in addition to three to six months of planning and installation of instrumentation systems in various locations in the aircraft. While the flight test tools have evolved over time, a constant theme we have observed with all our customers is the need to reduce time and cost required for a test.

Machine Vision Challenges

Flight test environments introduce inherent challenges to traditional machine vision techniques, most notably high vibration and

lighting variation that are driven by the dynamic operating environment of the aircraft. In addition, cost and weight minimization typically requires a single flight test camera covering as large a region as practical which leads to low resolution of features. When flight test cameras are used to capture other active displays such as glass cockpit displays, the unsynchronized frame rates of the displays and cameras produces aliasing and interleaving effects. Traditional approaches must be modified to accommodate for these difficulties.

Since the camera vibrates independently of the observed item, noise is introduced into recorded and live video streams which can negatively affect data extraction. To correct for these errors, landmarks can be identified through calibration and automatically tracked and shifted to ensure they are in the same location. After initial stabilization, vibration is further mitigated by looking at aggregate data across multiple frames of the video feed. This increases the stability of the features to be measured, resulting in more reliable images for data extraction.

While standard machine vision techniques have a variety of feature recognition capabilities, the flight test environment impacts their performance. For example, the performance of standard optical character recognition (OCR) libraries are significantly linked to particular font sets. These approaches often cannot handle font distortions introduced in a flight test environment such as adverse lighting conditions, obliquities in font representation,

and artifacts from interleaved video compression.

We have been able to overcome these limitations by augmenting the machine vision techniques with a combination of calibration-driven image processing techniques. In general, all of the calibration approaches use a form of “template.” That is, imagery that has been collected directly from the display of interest will be used to augment the vision process. This calibration information can then allow the system to “learn” and adapt to the particular setup. For example, the specific distortion to apply is calculated during an initial calibration step and adapted and applied to subsequent data extractions to be able to achieve the necessary measurement accuracy.

Case Study: Cockpit Display Video Measurement

Typically, flight test measurements are acquired through a combination of adding discrete aeromechanical sensors to the structure and tapping into the communication busses between flight control computers. The amount and type of measurement sources depends on a combination of the maturity of the aircraft design under test and what specific test objectives need to be achieved. Historically, smaller test programs (such as testing a modification to an aircraft design that has already been certified in a prior large test program) have simply used a subset of the same instrumentation used for the most involved large test programs. While this minimizes purchasing multiple types of instrumentation equipment, it means that installation effort cannot drop below the minimum required by a subset of that instrumentation technology. Recent industry efforts have focused on leveraging wireless sensing components to remove the cost (install time, cost, and weight) of cabling, but the results have been hampered by practical considerations of power management and batteries.

The growth of storage capacity for flight test data combined with falling costs of video cameras driven by other industries has led to a significant increase in the amount of video acquired from cockpit displays, control surfaces, and actuators. While many other industries have leveraged video cameras with machine vision techniques to monitor and control processes, the flight test industry has largely used the various video sources either as a secondary data source that is only inspected manually when measurements from other sensors conflict, or by manually acquiring

measurements from the video through human inspection.

Seeing this landscape, we have begun to socialize a different strategy to help achieve the goal of reduced time and cost of flight test. Specifically, we feel that if measurement information can be reliably automatically processed from flight test cameras observing cockpit displays, then this instrumentation could potentially reduce or eliminate the need for more traditional instrumentation systems in certain low-instrumentation flight test programs such as supplemental type certificate (STC) or production test.

We have developed a prototype concept demonstration that detects a limited set of numeric display information from cockpit video and begun a dialog with various flight test programs to uncover use cases and requirements which will influence our further research and development. While these demos are far from complete implementations, the results achieved so far and the feedback we have received make us hopeful that a finalized system can provide an effective capability to flight test users.

We have compensated for the constraints of the flight test use case by augmenting traditional machine vision techniques with test-setup specific calibration and additional image processing approaches not typically needed in more controlled machine vision environments. This idea, while a natural fit for the flight test domain, is not common in other industries. Flight test, on the other hand, is comfortable with detailed calibration procedures. We expect that requiring a calibration procedure per install would require less overall setup time than using traditional instrumentation such that the goal of reduced time and cost required for a test is still achieved.

Using the machine vision techniques we have developed, data has been successfully extracted from flight test video of a helicopter’s avionics display. These test case videos were from typical flight test operations with a combination of impairments from vibration, lighting, and momentary blockage by pilot movement. The software requires a video stream that captures the avionics system display, but it is forgiving of camera positioning up to 30 degrees off normal. This video can be either acquired and processed in real-time on a test aircraft or lab bench avionics display, or post-processed from a recorded video file.

The setup calibration approach requires the user to point the camera at the gauge from a distance equivalent to the back of the cockpit

and then mark several features and regions of interest in the image of the gauge. The ability for the algorithms to continually extract measurements without intervention after calibration provides validation of the techniques. Results from the helicopter flight test video extracted using this system have shown >99% fidelity when compared to truth data acquired from available data busses. The results can be seen in Figure 1.

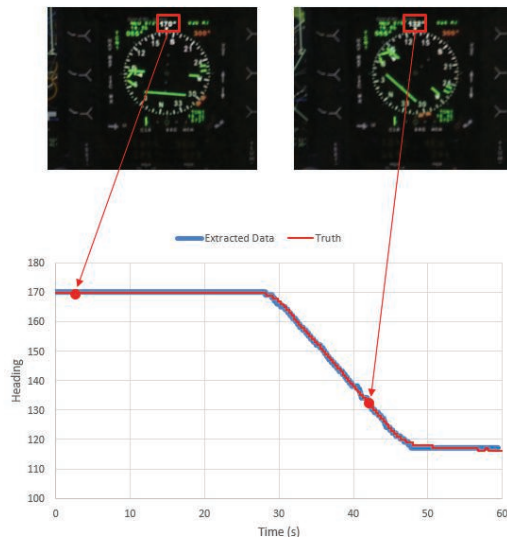


Fig. 1. Measurements extracted from video processing compared to truth data (video courtesy Airbus Helicopters).

The machine vision techniques described here provide a less expensive alternative for gathering and extracting data during a flight test. Traditional methods involve tapping an avionics bus for existing instrumentation, adding the weight and complexity of a bus monitor that must have physical access to the test article's internals.

Machine vision techniques, used to extract data from cockpit displays, provide a bridge between these techniques. The avionics bus data can be reproduced, based on observations of the displays, without requiring the invasive installation of a bus monitor. Detailed knowledge of the bus catalog of the test article, what messages correspond to what values, and in what units, is no longer needed, as engineers can intuitively extract the values of note by associating measurements with the corresponding instrument. The flexibility of the camera is still preserved, as multiple passes can be made post-flight to extract data that had no prior use, but suddenly was relevant in post-processing.

Building on the initial prototype capabilities, we envision the system will ultimately have the capabilities to extract data from a variety of cockpit display types including:

- Alphanumeric text
- Roll/pitch display (i.e. artificial horizon)
- Needle/dial gauges
- Horizontal and vertical bar gauges
- Boolean dashboard indicators

This set of displays covers the set of traditional aircraft instrumentation, including both the instruments for visual flight rules and instrument flight rules. It is also capable of monitoring status of many more advanced, specific instruments presenting data matching these categories and can be customized to specific flight program needs.

Like all measurement systems, consistent time marking is essential. IEEE 1588 PTP time of each acquired video frame is tracked and timestamps are applied to each measurement instance. The system supports adjusting the timestamps by an offset to compensate for video display and camera delays if needed. This provides the data with the timing accuracy necessary for comparative processing with other measurement sources.

Additionally, by utilizing portable and modular software techniques rather than hardware-specific processing, we are able to adapt to a wide variety of platforms from small embedded systems to general purpose PCs. Both the optical and platform components are independent from the software since the calibration process normalizes variations.

In addition to data extraction from avionics displays we see potential in measuring a variety of physical phenomena using similar specialized applications of machine vision. Possibilities include measuring wing deflection, flutter and vibration analysis, ice accumulation measurement, and engine analysis. Expensive and time-consuming installation of sensors could be replaced by the simple installation of a camera, where the nature of the physical event to be measured and the resolution of the camera allow.

Conclusion

This paper has provided a discussion of the challenges associated with using machine vision techniques in a flight test environment. We have had success in enhancing traditional machine vision techniques in order to overcome these challenges, resulting in a solution that has the potential to provide flight test users a rapid-deployment data acquisition capability.

References

- [1] SwRI Smart Leak Detection System Locates Hazardous Chemical Spills,
<https://www.swri.org/press-release/swri-smart-leak-detection-system-locates-hazardous-chemical-spills>
- [2] Blazing a Trail For Smarter, More Agile, Automation,
<https://www.swri.org/sites/default/files/publications/technology-today-summer-2017.pdf>, p4-9
- [3] SwRI's Ranger Localization Technology Allows Precise Automated Driving,
<https://www.swri.org/press-release/swri%E2%80%99s-ranger-localization-technology-allows-precise-automated-driving>

Method and software to perform Pitch Drop

Luiz Eduardo Guarino de Vasconcelos^{1,3}, Nelson Paiva Oliveira Leite², André Yoshimi Kusumoto²,
Leandro Roberto⁵, Cristina Moniz Araujo Lopes^{1,4}

¹ Instituto Tecnológico de Aeronáutica (ITA), Brazil

² Instituto de Pesquisas e Ensaios em Voo (IPEV), Brazil

³ Instituto Nacional de Pesquisas Espaciais (INPE), Brazil

⁴ Instituto de Aeronáutica e Espaço (IAE), Brazil

⁵ Instituto de Estudos Avançados (IEAV), Brazil

du.guarino@gmail.com, epd@ipev.cta.br, andrekusumoto@gmail.com, leandrolr@fab.mil.br,
cmoniz77@gmail.com

Abstract:

Store separation flight tests are considered high risk. Something that precedes the in-flight tests are the pitch drop tests. Pitch drop are fundamental because they allow the static evaluation that the separation meets a minimum degree of safety. A process that has added value to the experimental trials is the use of high data rate acquisition cameras (i.e. greater than 200 fps) and the use of three-dimensional software. In order to reconstruct the 3D separation path with 6DoF from images, 2 or more cameras are required. When using cameras in any activity that requires accuracy in the results, it is necessary to calibrate the optical system used in the tests. In Brazil, the IPEV carried out these tests for years, and the determination of the trajectory of store separation was carried out with a commercial software. In addition, the process was inefficient and costly as it required many weeks of work for the analysis of results and execution of flight tests. To eliminate the use of the commercial tool and to have technical mastery over the entire test, a solution was developed that (1) the construction of a calibration field with depth so that camera calibrations can be performed using a single frame; (2) a method for carrying out pitch drop; (3) and an application that uses computational vision to process the data and generate the results in 6DoF. The benefits of such a solution include better use of resources, minimization of workload, and reduced costs and time. In this paper, the calibration field, the method created for pitch drop, the steps for the development of the computational application and the experiments performed to validate the application are demonstrated.

Key words: image processing; store separation; real time; 3D analysis; camera calibration.

Introduction

The store separation of aircraft is an old story – however the accuracy of the store trajectory during the separation of the aircraft is not so old [1]. Before the 1960s, there were practically no widely used or generally accepted methods for pre-flight prediction of store separation trajectories other than wind tunnel testing techniques. With the advent of modern attack aircraft high-speed, the need arose to carry more and more stores and release them at ever-increasing speeds.

In a military aircraft, each external store (e.g. ammunition, external fuel tank, capsules, bombs, missiles, among others) must be released safely and the launch must be well-planned [2]. To predict the store trajectories, simulation models with six DOF (degrees of freedom) are usually used that describe the movement of the aircraft and the store in relation to one another, as well as the inertial system.

There are two ways of determining flight trajectory data. One is photogrammetry and the other telemetry [3]. Both methods have advantages and disadvantages.

Pitch drop testing is a fundamental step in the store separation testing campaign [4]. These tests are done to establish the aircraft / store configurations required for flight tests. At the IPEV (Flight Testing and Research Institute), pitch drop testing were also essential for the development of a method and software that allows the analysis of store separation. At this time, this analysis is still done post processing. This is of fundamental importance for something that we have been aiming for 5 years, which is the near real-time analysis in the pitch drop testing and store separation flight tests. In this paper, we review some concepts about store separation, store separation analysis, photogrammetry and camera calibration. In addition, we show the use of a photogrammetric

solution developed and used in a real pitch drop testing carried out at IPEV. We also show the implemented method and the pitch drop testing performed.

Store Separation Analysis

The store separation analysis is defined as the determination of position and attitude history of a store after it is deliberately detached or ejected from the aircraft while the store is still under nonuniform aerodynamic interference near the aircraft [2].

The store separation analysis is necessary to redesign the operational limit of store, called envelope [5], in order to analyze the store separation characteristics for various flight conditions.

It is important to note that the main purpose of the store separation test is to collect sufficient data to ensure acceptable separation in terms of safety [6].

Photogrammetry

Photogrammetry is the science of making accurate measurements from photographs [7]. This technique allows to obtain quantitative data of the cameras mounted in the aircraft. Quantitative data are essential to validate the models used in the store separation tests so that they could be used to improve the accuracy of store separation predictions. Usually, high-speed video cameras are used in these tests.

The use of photogrammetry in store separation tests offers significant and unique technical and managerial challenges. When designing the algorithms several factors must be considered, such as camera angle, camera movement, image quality, focal length, lens distortions and environmental conditions. Most of the time, the vapors appear on the images that may decrease the visibility or even obscure the charge. A camera may get engine fluid in its lens or the camera may malfunction and stop working completely.

In addition, store separation tests occur in environments hostile to accurate measurements. The light condition is a major challenge in the use of high-speed cameras [8].

Without photogrammetry, the in-flight test is of a qualitative nature and consists of several flights with store separation approaching the edge of the separation envelope in small incremental steps. This is extremely dangerous.

Pitch Drop Testing

In order to perform this test, the IPEV developed a method that is divided into the following steps: planning, preparation, geometry determination,

camera calibration, test point realization, 2D analysis and 3D analysis with 6DOF..

Planning

As previously stated, a photogrammetric solution to store separation offers significant and unique technical and managerial challenges. At this stage, the planning of the entire test campaign is carried out and the following activities and information are defined: the test period; the teams that will participate in the campaign. Typically, teams from the imaging sector, aircraft maintenance sector, technical support sector, instrumentation and calibration sector, surveying sector; equipment to be used (aircraft, cameras, total station, luxmeter, trigger, targets, tires (Figure 1), power sources, computers, fork-lift, among others).



Fig. 1. Store coupled on the pylon and tires on the ground to cushion the fall.

The target is a circular or square 4 or 6 inch sticker with a bow tie feature (Figure 2). More information is placed close to each target to facilitate identification of the target (i.e. a letter and a number) (Figure 2). This identification facilitates the possible post-processing of the data.



Fig. 2. Example of target used in store separation tests.

At this stage, the scene is still sketched; formal request for support to teams; the definition of the number of test points and their characteristics (some movement determined in the store);

equipments and test site are reserved. Finally, the campaign is formalized - a document with details of the campaign.

Preparation

At this stage, all teams and equipment must be positioned at the test site. The store must be positioned on the aircraft pylon. The tires to cushion the impact of the fall are also positioned. The adhesives are placed on the store, pylon and aircraft. At the IPEV, 20 or more targets are glued to a predetermined pattern on the store, pylon and aircraft to allow more precise photogrammetric analysis of the position of the stores.

The cameras are installed in the photographic POD, positioned, configured and their positions are determined (Figure 3).



Fig. 3. Cameras installed and positioned inside the POD.

The position of the reflectors, the position and the function of each person at the test site are also defined. The synchronism of the cameras is tested. Some releases are made in order to test the ejector, the trigger, the terminology to be used in the test, the capture of the separation by the cameras. Then, the sketch is validated from the scenario.

Geometry Determination

The lateral leveling of the aircraft was done with a Tokyo Theodolite TM20C [9]. The longitudinal leveling (Figure 9) was measured by a Nikon Total Station NPL-632 [10], which guided the height adjustment operation of the hydraulic jacks on which the aircraft was supported. The aircraft leveling reference marks were used for this procedure, which was performed as instructed in the Aircraft Maintenance Manual.

For the survey of the coordinates of the points of interest described, it was necessary to establish a topographical polygon close to the aircraft to base the irradiations of the measurements.

With this information, it was possible to measure the geometry of the store, determine the positioning and attitude of the cameras and the geometry of the aircraft.

A key component in this process is the high-speed digital camera. There are many frame-rates to choose from [1]. However, 200 frames per second is recommended as the best for store separation analysis. A typical charge will travel from its initial captive position to the bottom of the camera view in 0.2 to 0.4 seconds (depending on the distance of the camera and the lens chosen). At 200 frames per second, this will produce 40 to 80 usable frames of data.

In the tests, one Xavante (number 4467) aircraft and two Mikrotron Cube7 high speed cameras were used [11]. The cameras were configured with the acquisition rate at 400 frames per second (fps), mounted externally on the aircraft in a photographic POD to record movements during the release of the store. Two identical cameras were used. This model of camera has the synchronization feature, fundamental in this type of test. This feature allows the cameras to take photos at the same time. Cameras are oriented to maximize overlapping field of view. Because some stores are less than 1.5 m from the camera and measurement volumes are too large, 6 mm and 10 mm lenses are normally used. As a result, optical distortion must be calculated and corrected. For the tests carried out at IPEV, the Kowa 6mm C-Mount lens was used [12]. For the tests, an external fuel tank (store) was also used.

Camera Calibration

There are several approaches for the correction of projective distortion, such as direct linear transformation, polynomial affine transformation, photogrammetric transformation, among others.

As analyzed by [13], the photogrammetric approach is the one that presents the least error, because it uses the camera projection model itself, that is, it considers the principle of the collinearity equations. The problem is that the roll, pitch and yaw (φ , θ , ψ) attitude angles provided by the aircraft system follow the aeronautical definition and are completely different from those used in photogrammetric models. In this sense it is necessary to adapt the reference systems.

The collinearity equations are the mathematical model on which spatial resection is based. They relate the three-dimensional coordinates of the object-space to the corresponding two-dimensional space-image, considering the external orientation of the camera. Does not consider the internal orientation, since it is

defined in the camera calibration process. To do this relationship, these equations consider the location of the camera and its pointing angles, as well as the focal length, not considering the internal geometric distortions of the camera, as shown in Figure 4. In order to arrive at the collinearity equations, besides the change of reference with translations and rotations, a homographic transformation with scale factor should be considered.

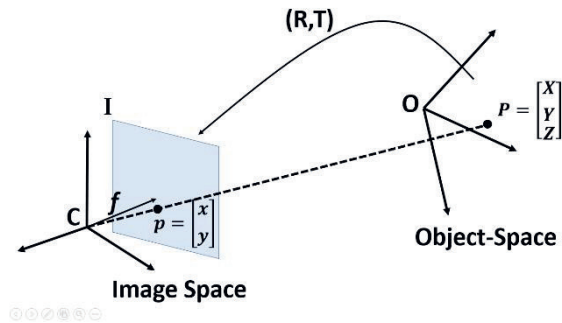


Fig. 4 Change of reference from the system of the object to that of the image.

Where:

C - camera reference system;

I - image reference system;

O - object reference system;

f - focal length;

R - rotation matrix;

T - translation matrix;

P - point in the space of the object;

X, Y, Z - coordinates of point P;

p - point corresponding to P in the image space.

x, y - coordinates of the point p in the image system.

All the points that make up the object can be represented in the two-dimensional image space by the principle of collinearity. For objects sufficiently distant from the camera, the image forms in the focal plane, i.e., the points assume coordinate Z equal to the focal distance f in the camera system. Thus, for a camera aligned to the aircraft, the representation of the coordinates in the image system derives from Equation 1 and is given by Equation 2. This happens when the transformation is made by the aeronautical system, Figure 5a. When done by the photogrammetric system (Figure 5b), use equation 3. The parameters λ_a and λ_m are proportionality factors.

$$\begin{bmatrix} x \\ y \\ z \end{bmatrix} = R \begin{bmatrix} E - Ec \\ N - Nc \\ U - Uc \end{bmatrix} \quad (1)$$

$$\lambda_a \begin{bmatrix} x_a \\ y_a \\ f \end{bmatrix} = A \begin{bmatrix} E - Ec \\ N - Nc \\ U - Uc \end{bmatrix} \quad (2)$$

$$\lambda_m \begin{bmatrix} x_m \\ y_m \\ -f \end{bmatrix} = M \begin{bmatrix} E - Ec \\ N - Nc \\ U - Uc \end{bmatrix} \quad (3)$$

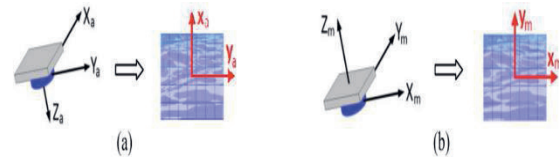


Fig. 5 (a) Image system when using the aeronautical system (b) when using the photogrammetric system.

In the photogrammetric process, the main task is to establish a strict geometric relation between the image and the object, so that information can be extracted from the object only through the image [14]. However, a raw image contains geometric distortions due to the influence of several intrinsic and extrinsic factors on the sensor. Thus, to obtain reliable metric information from images in the various applications, it is essential that the optical assembly (camera-lenses) be calibrated [15].

Calibration

Calibration consists of a process for experimental determination of a series of parameters that describe the process of image formation in the camera, according to an analytical model, which relates the known coordinates of a reference grid, also called the calibration field, with the corresponding in the image [16]. There are several field geometries and several methodologies for calibration [17].

Several factors affect the geometric distortion of the images recorded by a sensor, to a greater or lesser degree depending on the architecture of the sensor and on which platform it is inserted. There are geometric aberrations that affect the quality of the image, but not the position of the objects in the image, namely: aberration of sphericity, astigmatism and curvature of the field [18].

The factors are subdivided into internal and external. The first ones are related to the sensor architecture and their distortions are corrected in the process of internal orientation of the image, known as intrinsic parameters. These parameters are determined in the calibration process. The external factors are related to the medium in which the sensor is immersed and its position and pointing in relation to the object of interest, and corrections are corrected in the process of external orientation of the image, known as extrinsic parameters [19].

Full Calibration Model

A model for camera calibration was developed that considers the pinhole model and the radial [20] and tangential distortions [21], which occur when light rays cross the lens before reaching the sensor. The distortion parameters act on the coordinates (u, v) that have no influence on the intrinsic parameters of the matrix K , defined by equation 4.

$$K = \begin{bmatrix} a_x & s & (c_x - c_c) \\ 0 & a_y & -(c_y - c_l) \\ 0 & 0 & 1 \end{bmatrix} \quad (4)$$

Where:

- $c_c = (C + 1)/2$ (5)
- $l_c = (L + 1)/2$ (6)
- K is the intrinsic matrix.
- s is the skew parameter.
- a_x and a_y the affinity terms.
- c_x and c_y are the principal point lags, in pixels;
- c_c and l_c are the column and row of the central pixel.
- C and L are the number of columns and rows in the image.

Thus, the model construction begins with the isolated representation of the effects of the radial and tangent distortions, as shown in Equation 7. For the understanding, it is necessary to present Figure 6, an image representation, where the definition of the reference systems and some camera parameters.

$$\lambda \begin{bmatrix} u \\ v \\ 1 \end{bmatrix} = M \begin{bmatrix} X \\ Y \\ Z \\ 1 \end{bmatrix} \quad (7)$$

Where:

$$M = [R \quad T] \quad (8)$$

$$T = -R \begin{bmatrix} X_c \\ Y_c \\ Z_c \end{bmatrix} \quad (9)$$

- X, Y, Z are the axes of the reference system of the calibration field.
- X_c, Y_c, Z_c are the coordinates of the camera CP in the field reference system.
- λ is the homographic scale factor.
- M is the reference change matrix.
- R is the rotation matrix.
- T is the translation matrix.

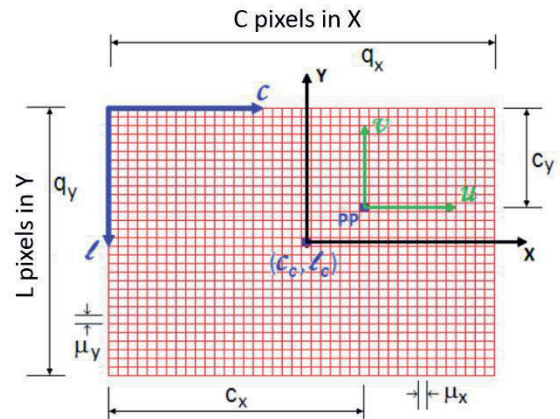


Fig. 6 Reference systems and parameters in the image representation of a camera.

Where:

- x and y are the coordinates in the image system with origin in the central pixel, in pixels.
- c_c and l_c are the column and row of the central pixel.
- u and v are the coordinates in the image system originating from the main point, in pixels.
- PP is the principal point of collimation, point of intersection of the optical axis with the sensor.
- c and l are the axes of the column-row reference system of the image, originating from the upper left pixel.
- c_x and c_y are the lags of the main point, in pixels, measured in the x and y directions in relation to the upper left pixel.
- μ_x and μ_y are the pixel dimensions in the x and y directions.
- q_x and q_y are the dimensions of the sensor in the directions x and y .
- C and L are the number of columns and rows in the image.

For the geometric correction of the images it was necessary to know some parameters of the camera, some extracted from the manual and others calculated. Figure 7 shows the definition of each of them and the following equations express how they were obtained.

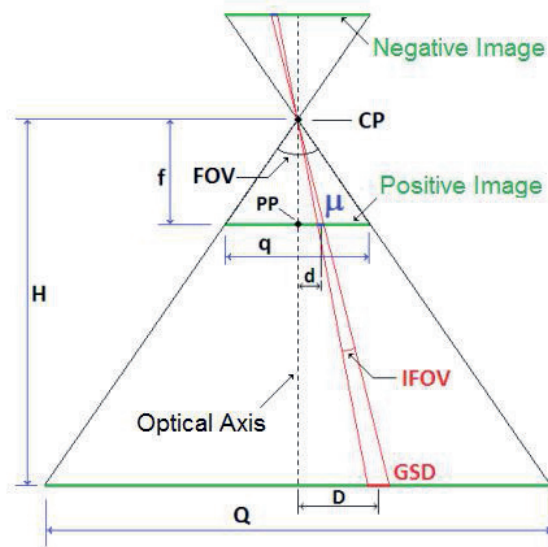


Fig. 7 Geometric parameters of the pinhole camera model.

- f - focal length.
- PP - main point of collimation, intercept of the optical axis with the plane of the image.
- CP - perspective center, point where the light beams that leave the ground and reach the image.
- μ - sensor pixel size.
- q - size of the sensor frame.
- Q - frame size of the projected image on the ground.
- GSD - Ground Sample Distance - pixel size projected on the ground.
- D - size of the object on the ground.
- d - dimension in the image of the object with real dimension D .
- H - projected distance from the CP to the ground, corresponding to the flight height.
- FOV - Field of View - total aperture angle representing the field of view covered by the sensor.
- IFOV - Instantaneous Field of View - aperture angle representing the field of view of a pixel.

From the geometry of the figure can be extracted the mathematical relations to obtain the geometric parameters. Refer to simplified model of pinhole camera free of internal distortion. In order to obtain the coordinates of the pixels in the system X_a, Y_a , or in the X_m, Y_m , from the coordinates in the row-column system, the affine transformation given by Equations 10 and 11, respectively, is used.

$$\begin{bmatrix} x_a \\ y_a \\ f \end{bmatrix} = \mu \begin{bmatrix} -1 & 0 & l_c \\ 0 & 1 & -c_c \\ 0 & 0 & \frac{f}{\mu} \end{bmatrix} \begin{bmatrix} l \\ c \\ 1 \end{bmatrix} \quad (10)$$

$$\begin{bmatrix} x_m \\ y_m \\ -f \end{bmatrix} = \mu \begin{bmatrix} 0 & 1 & -c_c \\ -1 & 0 & l_c \\ 0 & 0 & -\frac{f}{\mu} \end{bmatrix} \begin{bmatrix} l \\ c \\ 1 \end{bmatrix} \quad (11)$$

Calibration Field

As seen, the calibration has the objective of identifying the intrinsic parameters of geometric distortion of the cameras, in order to correct the position of the pixels of the points extracted from the images for the spatial resection.

There are several calibration methods that essentially differ in the type and geometry of the field, the number of necessary photographs, the camera positioning method in the field, the quantity and arrangement of distortion parameters in the mathematical model, the adjustment methodology of the model to identify the parameters, among others. Some studies deal with comparative studies of the different calibration methods [17].

Calibrations that require higher accuracy are usually done in laboratory or controlled environments, where target coordinates are precisely known [22]. In this paper, we used an algorithm, which uses this approach [23].

For this, captures are required in a location with known coordinate references. At the IPEV a geometric calibration field was set up in a room in the X-30 hangar, consisting of a three-dimensional space with 134 targets, according to Figure 18. The targets are cross-shaped in black and white (soil), blue and white (right wall), red and white (left wall) and green and white (ceiling) (Figure 8). The colors are for easy identification and surveying. The targets were constructed with pieces of 5cm of aluminum angle and adhesive with vinyl, each containing the crosshead and its code.

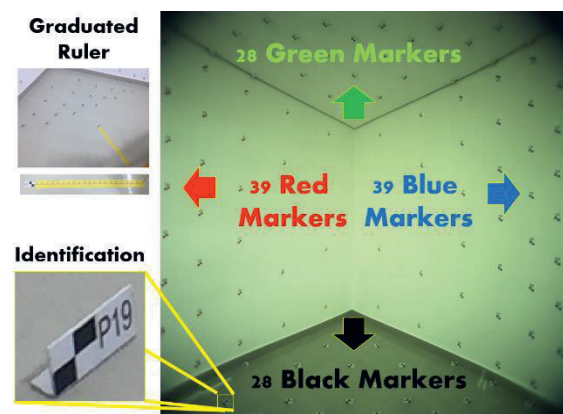


Fig. 8 IPEV Geometric Calibration Field. Detail for identified reference targets and positions marked on the floor for camera positioning.

It was planned to lay out each target in layers of various depths in order to break the linear dependence that occurs between some parameters of the distortion model.

In the calibration process, the exact 3D coordinates of the targets in the field must be known. Thus, a Total Topographic Station [10] was used to determine the three-dimensional Cartesian coordinates of the 134 targets.

Calibration of Cameras

The methodology developed for the calibration in this field provides the knowledge of the external orientation of the camera, that is, its position in relation to the targets and their pointing angles. This favors the convergence in the adjustment of the distortion model and the breakdown of linear dependence between some parameters. Photographic shots were taken with the cameras used in pit drop testing. Later, in each image the line-column coordinates of the reference targets were captured, associating the corresponding coordinates in the field with Total Station, and generating an image indicating the location of the captured targets (Figure 9).

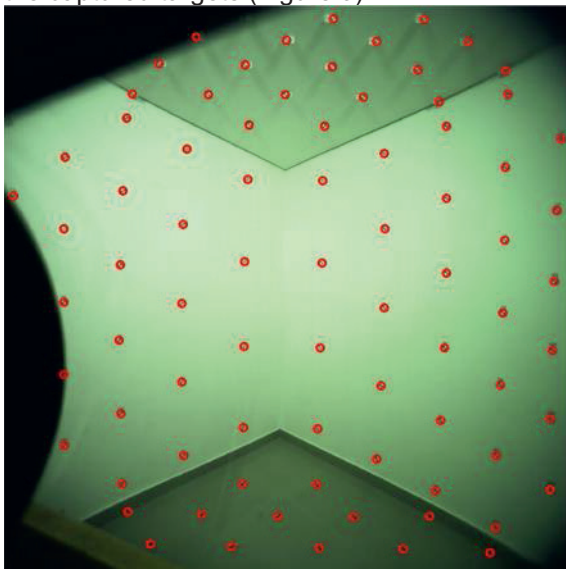


Fig. 9 Examples of captures performed in the IPEV calibration field with the POD rear camera used in the pitch drop testing.

With the three-dimensional Cartesian coordinates XYZ of the calibration field targets and the corresponding line-column coordinates in the captured image, the calibration is performed. The radial distortion was adjusted by a polynomial model of six coefficients, according to Figure 10, obtaining a good adherence.

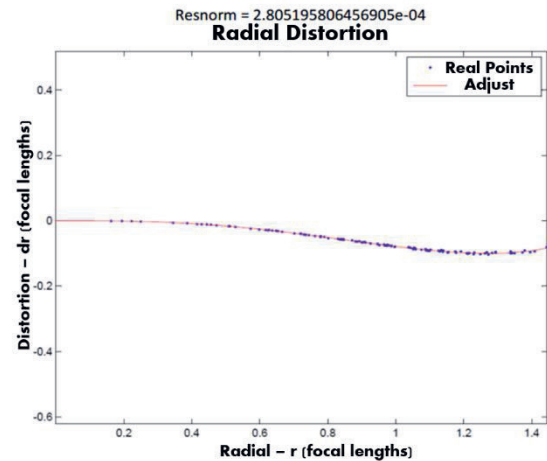


Fig. 10 Radial distortion curve raised in the IPEV field, considering the POD rear camera.

From the parameters identified in the complete distortion model, the reprojection of the reference targets of the calibration field in the two-dimensional image system was performed, compared to the real coordinates obtained in the capture. This allowed for a qualitative evaluation of the adherence of the model, according to Figure 11.

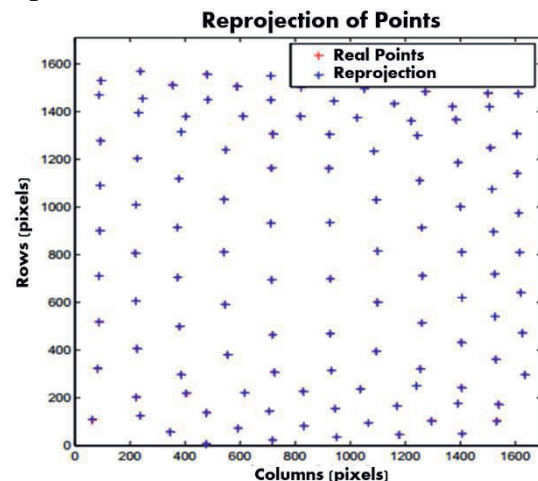


Fig. 11 Reprojection of the reference targets of the calibration field according to the model with the parameters identified for the POD rear camera in the IPEV field.

With the parameters identified in the calibration process, the images generated by the camera, containing geometric distortions, could be re-displayed pixel by pixel to represent the image that would be generated by a pinhole camera, free of distortions.

The method used was the interpolation by the nearest neighbor, maintaining the original size of the pixel.

Realization of Test Points

For testing purposes, all equipment must be in place (i.e. tires, store placed on the pylon,

mounted and attached computers, cameras mounted, connected, configured and synchronized). For each camera there is a computer (notebook) configured. These computers are COTS (Commercial off-the-shelf). As soon as the store is ready for release, the cameras are triggered for recording. After this, a trigger is triggered by the test engineer to determine the start of the test point (frame identification on the cameras). When triggered, after 0.5 second the store is released. After the contact of the store on the tires, the cameras are paused. The videos are then downloaded from the cameras and viewed to determine the validity of the videos. If one of the videos was inappropriate (unsynchronized, lost frames, capture crashes, or any other weather), the videos were discarded. Otherwise, the videos are renamed and stored.

After that, go to the next test point, replacing the store on the pylon.

At the IPEV, 10 valid test points were carried out within 2 hours. At the end of the test day, videos are stored on the IPEV data server.

2D Analysis

After performing the test points on the day, the IPEV photogrammetry team works on information processing.

Video files are transferred to a local computer directory for processing. The computer used for processing is a notebook (COTS).

Each video has, in general, 0.5 second of images that precede the beginning of the separation and 0.5 second of images after the contact of the store in the tires. These images are unnecessary in rendering. Thus, another algorithm was developed to determine automatic recognition for discarding unnecessary images.

The next step is to define the center of each target (store, pylon and wing) so that they can be tracked during separation. To do this, the region of interest is delimited with the aircraft's store and pylon. This is possible because the position of the store and the pylon relative to the camera will not be changed considerably between the separations. The positions of each target are previously known and measured from a total station [10]. An identification algorithm scans the image, looking for corners. It can be observed in Figure 12 that 19 targets were found (red dots) in the store, 7 targets in the pylon and 13 targets in the wing, considering an camera on the left inside the POD.



Fig. 12 Targets identified in store, pylon and wing.

In Figure 13 it is possible to observe the aircraft, pylon and store targets that were tracked during the test point.

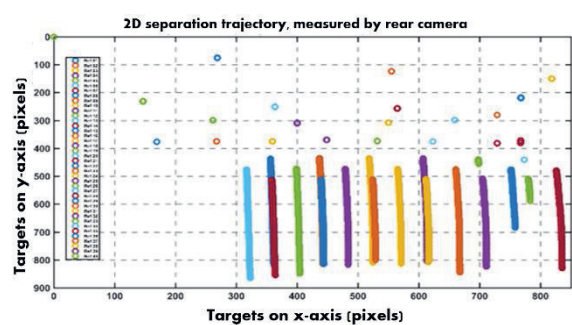


Fig. 13 2D separation trajectory measured by the rear camera.

Given the 2-D frames of each camera, the problem of solving the position (x, y, z) of each target is solved using least squares. Each target is defined by the intersection of two lines, generated by the line of sight of each camera. Each line in space is represented by 2 equations in x, y and z , so that with two straight lines (4 equations), we have an over-determined system, which is solved by least squares (4 equations and 3 unknowns). With a third camera, we have two more equations. It could quickly determine, by means of determinant, if there is intersection between 2 lines in space, which will hardly occur in the experimental measurements. However, a middle ground can be obtained by resolution in the least squares (a point that does not belong to any line but is closest to both simultaneously).

3D Analysis

For the multicamera triangulation algorithm, two or more cameras are used to quantify the error. In the case of POD used, only 2 cameras are possible. After executing the algorithm of 2D Analysis, it is necessary to perform 3D Analysis.

Suppose we are given the coordinates of a number of points measured in two different Cartesian coordinate systems (Fig. 14) [24]. The photogrammetric problem of recovering the transformation between the two systems from these measurements is called absolute orientation [25]. This problem occurs in various contexts.

The transformation between two Cartesian coordinate systems can be thought of as the result of a rigid body movement and can thus be decomposed into a rotation and a translation. In stereophotogrammetry, moreover, the scale may not be known. There are obviously three degrees of freedom for translation. The rotation has another three (direction of the axis on which the rotation occurs plus the angle of rotation around this axis). Scaling adds one more degree of freedom. Three known points in both coordinate systems provide nine constraints (three coordinates each), more than enough to allow the determination of the seven unknowns (3 translations, 3 rotations and 1 scale).

Discarding two of the constraints, seven equations in seven unknowns can be developed to allow the retrieval of parameters.

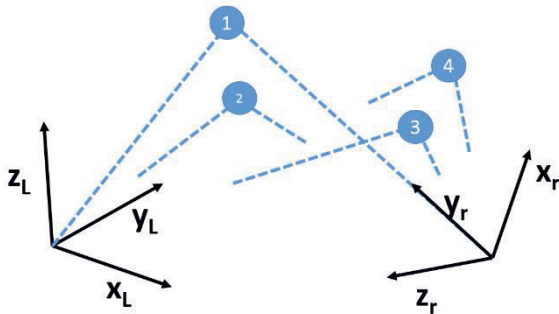


Fig. 14 The coordinates of a number of points is measured in two different coordinate systems. The transformation between the two systems is to be found. Adapted from [24].

The algorithm implemented by [24], uses all available information to obtain the best possible estimate (in a least squares sense). In addition, it is preferable to use it for center point estimation, rather than rely on single-point or single-point measurements. This algorithm is used in this work.

The main purpose of 3D analysis is to obtain 6DoF data. In Figure 15 is shown the example of the view of a test point considering X, Y, Z.

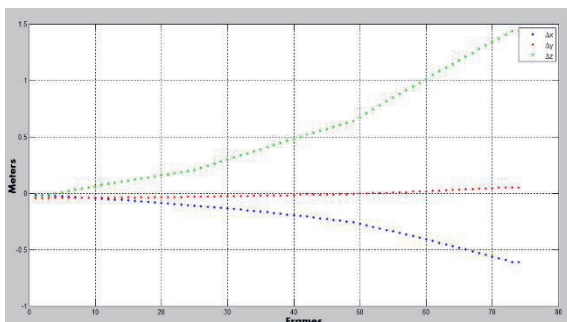


Fig. 15 X, Y, Z data from a test point.

Figure 16 shows the angles (φ, θ, ψ).

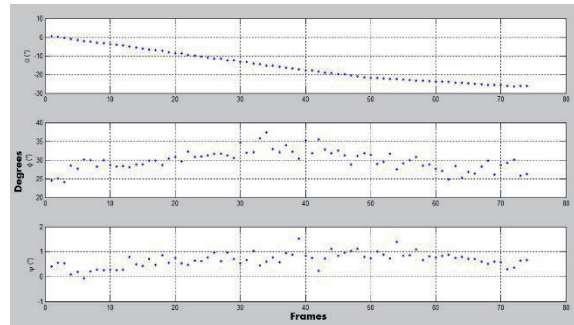


Fig. 16 Data in roll, pitch, yaw of a test point..

Considerations

The objective of this paper was to show the implementation of the method and the photogrammetric solution, developed by IPEV, to perform the analysis of pitch drop tests.

The proposed solution is promising. Both method and solution obtained errors of the order of mm and were considered acceptable for this type of test.

This solution is part of an IPEV development program that aims to perform the real-time analysis in store separation flight tests using photogrammetry.

Suggestions for future work are:

- Validate the information obtained by the photogrammetric solution with another solution widely known in the market (e.g. TrackEye).
- Perform new load separation tests on soil.
- Continue the development of the in-flight test program with real-time analysis.

References

- [1] Arnold, R.J. and Epstein, C.S., AGARD Flight Test Techniques Series on Store Separation Flight Testing. Volume 5. NATO. No.300. Published April 1986. ISBN 92-835-1523-4.
- [2] Persson, I. and Lindberg, A., Transonic Store Separation Studies on the SAAB Gripen Aircraft Using Computational Aerodynamics. SAAB Aerosystems. 26th International Congress of the Aeronautical Sciences. ICAS 2008.
- [3] Cenko, A., Store Separation Lessons Learned During the Last 30 Years, NAVAIR, Patuxent River, MD 20670. 27th International Congress of the Aeronautical Sciences. ICAS 2010.
- [4] Carman, J. B., Hill, D. W., Christopher, J. P., Store Separation Testing Techniques at the Arnold Engineering Development Center. Volume II: Description of Captive Trajectory Store Separation Testing in the Aerodynamic Wind Tunnel (4T). AEDC-TR-79-1, Vol. II (ADA087561). 1980.D

- [5] Cho, H., Kang, C., Jang, Y., Lee, S. and Kim, K., Store Separation Analysis of a Fighter Aircraft's External Fuel Tank. *Int'l J. of Aeronautical & Space Sci.* 11(4), 345–350 (2010). doi:10.5139/IJASS.2010.11.4.345
- [6] MIL-HDBK-1763, Aircraft/Stores Compatibility: Systems Engineering Data Requirements And Test Procedures. Department of Defense USA. 1998.
- [7] Getson, E.S., Telemetry Solutions for Weapon Separation Testing. 33th Annual International Symposium. 2002.
- [8] North Atlantic Treaty Organization, Aircraft/Stores Compatibility, Integration and Separation Testing, STO AGARDograph 300, Flight Test Technique Series – Volume 29. AG-300-V29. Published September 2014.
- [9] LIETZ, Double Center Theodolite TM-20C, 2018. Available in https://cn.sokkia.com/sites/default/files/sc_files/downloads/tm20c_0.pdf. THE LIETZ COMPANY.
- [10] NIKON, Total Station DTM-322 - Instruction Manual, Available in http://www.mcesurvey.com/files/Nikon_DTM-322_Total_Station_Manual.pdf. Version A 1.0.0, Part Number C232E, April 2009.
- [11] MIKROTRON, Mikrotron Cube7, Available in https://mikrotron.de/fileadmin/Data_Sheets/High-Speed_Recording_Cameras/mikrotron_motionblitz_eosens_cube7_datasheet.pdf. 2018.
- [12] KOWA, Lenses 6mm Kowa, Available in <http://www.rmaelectronics.com/content/Kowa-Lenses/LM6HC.pdf>. 2018.
- [13] Lima, S. A.; Brito, J. L. N. S., Estratégias para retificação de imagens digitais. Em: COBRAC 2006 - Congresso Brasileiro de Cadastro Técnico Multifinalitário, UFSC, Florianópolis, 2006. Anais, Artigos, n. 90, p. 1-14, 2006.
- [14] Mikhail, E. M., Bethel, J.S. and McGlone, J.C., Introduction to Modern Photogrammetry. Hoboken: Wiley, 2001. 479p. ISBN 978-81-265-3998-7.
- [15] Gruen, A.; Huang, T. S, Calibration and orientation of cameras in computer vision. Berlin: Springer, 2001. 235 p. ISBN (3-540-65283-3).
- [16] Swapna, P.; Krouglicof, N.; Gosine, R., The Question of Accuracy with Geometric Camera Calibration, St. John's, Newfoundland, pp. 541-546, May 3-6, 2009.
- [17] Clarke, T.A.; Fryer, J.F., The development of camera calibration methods and models, *Photogrammetric Record*, 1998, 16(91): pp 51-66.
- [18] Brito, J.L.N.S.; Coelho, L.C.T.F., *Fotogrametria Digital*, Rio de Janeiro: Ed UERJ, 2007. 196p. ISBN 978-85-7511-114-7.
- [19] Schenk, T., *Digital Photogrammetry*, Ohio, USA: TerraScience, 1ª ed, 1999.
- [20] Heikkila, J., Camera Calibration Toolbox for Matlab. 2000. Available in http://www.vision.caltech.edu/bouguetj/calib_doc/
- [21] Brown, D.C., Decentering Distortion and the Definitive Calibration of Metric Cameras, 29 ed, Washington DC, pp 444-462, March 1965.
- [22] Ladstadter, R.; Gruber, M., Geometric aspects concerning the photogrammetric workflow of the digital aerial camera UltraCamX. In: International Congress for Photogrammetry and Remote Sensing, 21., 2008, Beijing, China. Proceedings... Beijing: International Society of Photogrammetry and Remote Sensing (ISPRS), 2008. p. 521- 526. Vol XXXVII part B1. ISSN (1682-1750).
- [23] Roberto, L., Acurácia do posicionamento e da orientação espacial de veículos aéreos a partir de imagens de câmeras de pequeno formato embarcadas. – São José dos Campos : INPE, 2017. 308p. Dissertação (Mestrado em Sensoriamento Remoto) – Instituto Nacional de Pesquisas Espaciais, São José dos Campos, 2017.
- [24] Horn, B. K. P., Closed-form solution of absolute orientation using unit quaternions, Vol. 4, No. 4/April 1987/*J. Opt. Soc. Am. A*
- [25] Slama, C. C. Slama, Theurer, C., and Henrikson, S.W., *Manual of Photogrammetry* (American Society of Photogrammetry, Falls Church, Va., 1980).

Low Level Flight Monitoring - High performance graphics

A. Rodrigo López Parra¹

¹ Airbus Defence and Space, Sevilla - Spain
rodrigo.l.lopez@airbus.com

Abstract:

Low level flight trials in the A400M require special ad-hoc software with high performance graphic for monitoring and analysis in real time, able to provide insight and analysis as quickly as possible, given the criticality of the maneuvers and the short response time available.

This software provides graphic views in back, side and plan. Showing behaviour and predicting aircraft maneuvers in autopilot mode very close of the terrain, between the mountains.

As well as being able to implements the analysis of tactical functionalities such as, reconnaissance, proximity and visualization of the terrain, guided and planned trajectory for the autopilot, lateral and vertical deviations through safety corridors, dynamic scales of zoom and navigation modes, calculation of maximum performances in real time, compare results for different passes time, generate analysis result already completed, and much more ...

Key words: monitoring, high performance, autopilot, simulate, low level flight, analysis

Introduction

Normally, to follow the tests dedicated to specific tasks, software screens are developed for monitoring the systems on which we want to carry out the test. The most common thing is to design screens for the control of temperatures, pressures, valves, powers, levels, etc ...

They tend to be quite standard and do not consume many graphic resources.

Low level flight tests

However, low level flights in auto-pilot, are one of the most complicated functionalities developed to date in a military aircraft. It is about flying in autopilot at speeds of up to 300 kts at a minimum altitude of 500 ft above the ground, in mountainous terrain.

The objective is to reach the hostile zone without being detected by the radars and to

avoid the defensive ground missile systems, as well as the ground fire.

In order to guarantee the safety of the crew on the test flights, monitoring software has been made for an analysis of the entire maneuver with a high level of detail. Which has required high requirements graphic.

It must be take into account that the flight engineer in charge of the test does not have access to the CDS (Control and Display System) of the pilots.

Therefore, it is necessary to provide a lot of navigation information with an intuitive, smooth, fast and real-time animation. Each one of the maneuvers, each one of the turns, each climb or descent, is critical and there is very short response time for any unforeseen or correction.

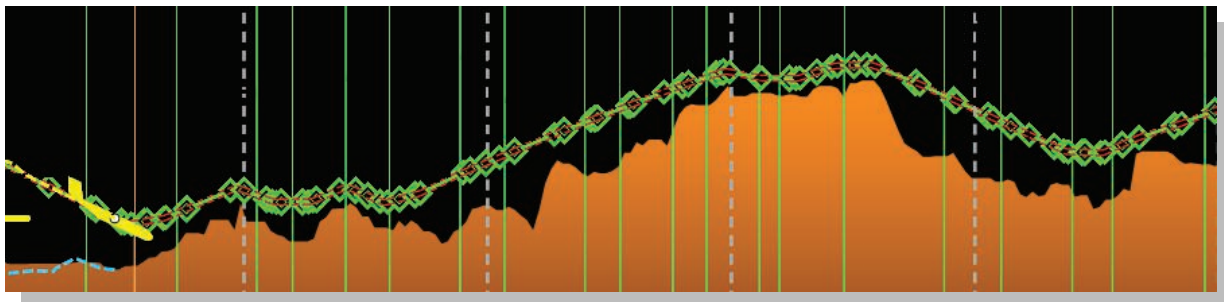


Figure 1. Example Profile of LLF

Design

This ad-hoc software has been divided into three different views of the airplane; plan, side and back. With its position on the terrain, the path to follow and the safety corridors. In addition, another area of performance data with maximum slopes and navigation data has been defined. That tries to collect the limitations of the aircraft for maximum safety conditions.

The software allows us to change and compare between the information provided by the duplicated systems dedicated to calculate the trajectories.

Lateral View	HUD Navigation Extended
Vertical View	Performances

Figure 2. Graphic scheme

The software performs the reconstruction of the trajectories in specific data structures, similar to those of the aircraft navigation equipment, with the aim of making a detailed comparison with the trajectory shown by the aircraft.

Trajectory

If we want to define a trajectory, we need a geographic point of entry, a geographic point of exit, a minimum altitude referenced to the terrain and a speed.

These input data allow the systems to analyze the terrain to fly over and give us two trajectories, a lateral one and a vertical one. Since we move in a three dimensional system.

Plan (Lateral View)

It is a view of the aircraft followed from the sky called lateral view.

The lateral trajectory that the aircraft must follow is shown, defined as a set of segments that they can be straight or curved between geographic coordinates and between well-defined waypoints.

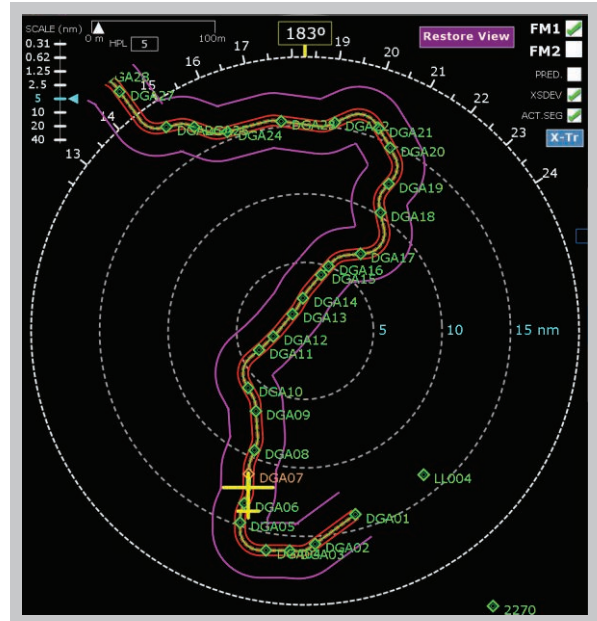


Figure 3. Complete lateral path

We can modify the zoom of distance scales just like the pilot would do in the PFD (Primary Flight Display), in fact we have the same scales as the aircraft itself.

We can explore the complete path and move freely in any direction. In this way, we can see whether the path is right or not in advance.

With smaller zoom levels we can note more useful elements.

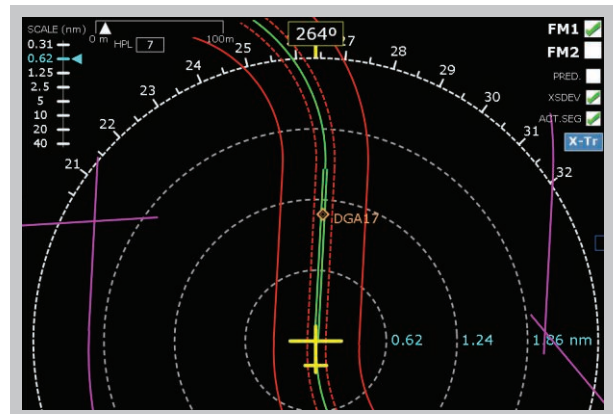


Figure 4. Lateral View

The autopilot must follow exactly the trajectory drawn in green that has been calculated by the systems that analyze the terrain, as the ideal.

To help detect any problem other features have also been developed.

The prediction of the airplane's turn is shown, in the same way that in the aircraft.

The **active segment** of the trajectory located the aircraft by the system.

The **active waypoint** to which we are going.

The **maximum lateral deviation** referenced to the trajectory is shown too.

Three corridor are calculate and drawing from the given trajectory:

- **Excessive desviation corridor.**
There is some problem to keep the aircraft in the path of the trajectory.
- **Safety corridor.**
While we are inside this corridor, we will be safe.
- **Safety altitude corridor.**
It's related to safety altitude.

The safety altitude corridor is drawn for the evasion maneuver.

Also, we can compare the differences in the position of the aircraft between a high precision **DGPS** and the aircraft **GPS**.

Back (Navigation Flight Display)

This is the view that provides to the flight engineer more navigation information, since it reproduces the complete HUD of the aircraft, the navigation modes and monitors the errors that the systems can notify when building the trajectories.

It is possible, for example, that a LLF trajectory is required at a certain speed and that the system that calculate the trajectory notifies that it is not possible to perform it due to an impossible turn or climb for the aircraft's performance.

In addition, the safety graphic U is added. It is a corridor seen from a back of the plane, and of which, the mock-up of the plane should never leave to be safe.

It emulates the presentation of the plane's instruments so that they feel familiar, but all geometric calculations are done internally in real time.

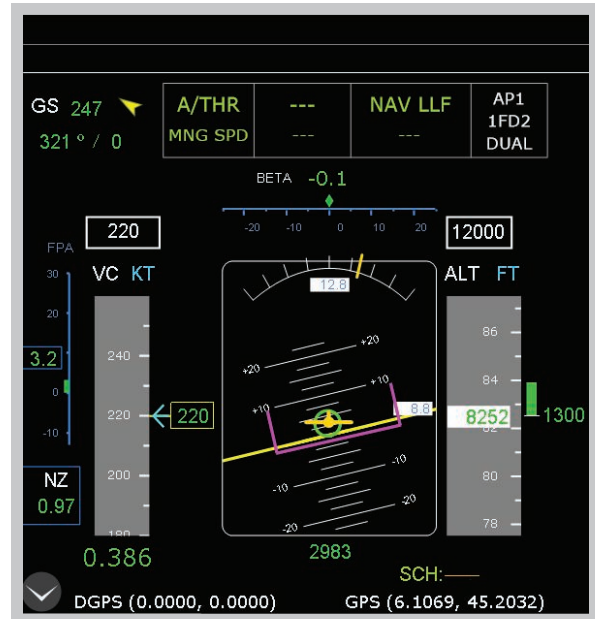


Figure 5. HUD Extended

Performance

This zone collects information of the maximum slope that the aircraft can perform, and the slopes that have the following segments to fly.

The autopilot systems must have verified that all the maneuvers of the LLF path are possible to do, but it never knows, better to check it again.

For the calculation of the performances, the failure of motors can be taken into account for maximum safety.

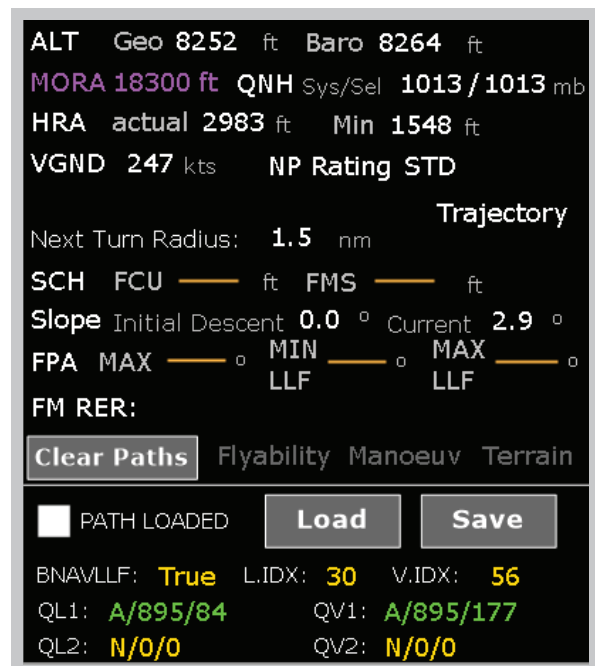


Figure 6. Performances

Side (Vertical View)

This view is the most important of the system, it shows the plane and the terrain from its profile, matching at all times, what is the altitude of the aircraft with respect to the terrain, as well as the trajectory that the autopilot will perform.

At the same time, the path followed by the plane in altitude and radio altimeter is shown and recorded, so you can have a complete trace of the entire aircraft path.

For a vision at all levels we can zoom scales in altitude and distances, apart from moving freely throughout the flight profile.

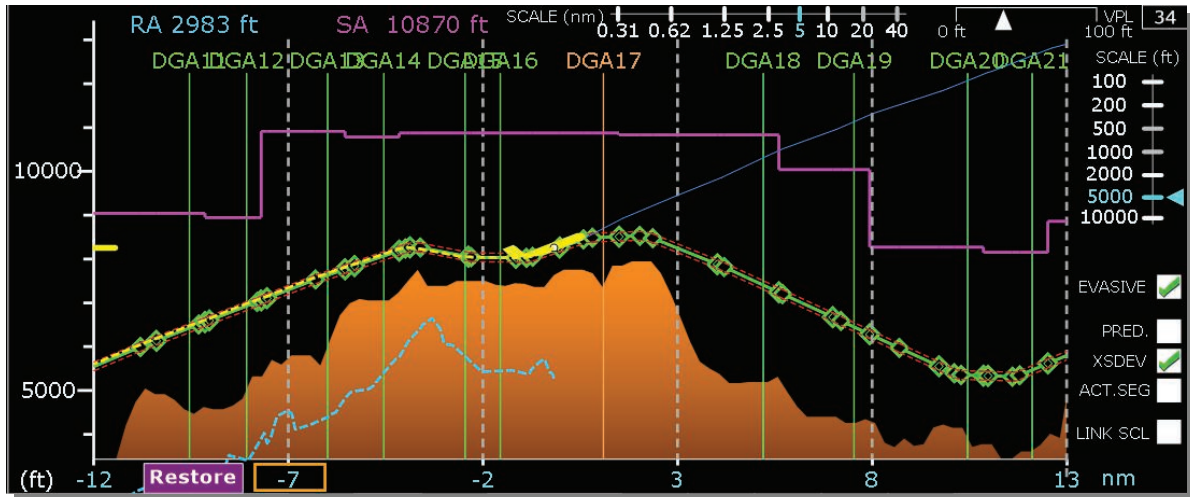


Figure 7. Vertical View

The profile is built as if we were passing a rope for each geographical point that the aircraft is going to fly and we extend it until it is straight. Getting the altitude at each point of that rope.

We can see the A/C mockup how it changes in the climbs and descents through the profile of the mountainous terrain.

The vertical trajectory that the aircraft must follow is defined by a set of straight and curved segments referenced to altitudes and geographic coordinates through the lateral segments of the lateral trajectory.

The vertical predictor of aircraft climb is provided (information extended to the airplane itself).

Starting from the vertical trajectory, we draw the corridor of maximum deviation in altitude and the corridor of safety altitude for the evasive trajectory in case of emergency.

This evasive path is also possible to show at the request of the flight engineer.

In case of any problem following the trajectory, the aircraft will abort the LLF route and perform the evasion maneuver until reaching a safe altitude.

The software automatically saves all the sessions flown in files so that at any time you can display a comparison view with a previous session.

The same session flown on different days will surely give slightly different results if there is no problem. Due to differences in climatic conditions, changes in aircraft performance occur.

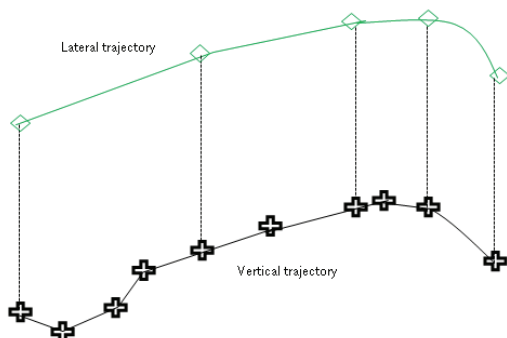


Figure 8. Vertical and lateral segment distribution

We identify the position of the aircraft, reference it to the geographical waypoints, the abscissa of the vertical segments and the exit point of the trajectory.

Rebuilding of the terrain, decoding busses of aircraft

The process to get the terrain has been a new challenge for this software to be really useful. Everything is referenced to this terrain in the vertical view and the most important thing is to know how close the airplane is from the terrain, as we can imagine.

It has had to perform an exclusive research to decode protocol data broadcasted on aircraft busses.

In this way, a lot of valuable information has been obtained (which is not even available for the airplane itself) in order to carry out this software.

The processes have been optimized to avoid the loss of any type of data related to any of the equipment that works in the aircraft autopilot system.

Analysis in real time

The vision and data provided by this software allows a complete analysis and diagnosis of this complicated system, just after the flight.

This software has also been integrated into test benches and simulators, given the enormous support it gives even to preliminary tests on real flights.

Safety critical to Test

Being a very complex system and still in **development**, we must be very careful to the behavior of the systems that are being tested. With this software, you can know how the aircraft will act before it does and anticipate if there is a problem in the definition of the trajectory and/or its route.

The changes with each new standard software in LLF equipment are frequent and this software is in continuous improvement.

References

- [1] German Gallego Garcia, RTF Low Level Flight A400M, 2016 - 2018.

Intelligent Networked Flight Test Instrumentation for a new Fighter Prototype

Guillermo Martínez Morán¹

¹ Airbus Defence&Space, Paseo John Lennon s/n (Getafe-Madrid) – Spain
guillermo.m.martinez@airbus.com

Abstract:

Airbus Defence & Space treasures more than 10 years of expertise in implementing fully network based flight test instrumentations (FTI). The developments accomplished during this long walk have brought to fruition very flexible and versatile FTI. Big platform programs (such as C295, A330-MRTT and A400M) have been taking good advantage from these features.

Transferring these features to a smaller aircraft (such as a fighter) has been the last challenge achieved. Restrictions due to the lack of space and crew onboard had to be overcome by implementing some intelligence onboard. This paper contains description and capabilities of the networked intelligent FTI architecture implemented in a new flight test fighter.

Key words: Intelligent, Network, FTI Architecture, Flexible, Versatile.

Introduction

Flight Test Instrumentations (FTI) architectures based in Pulse Coded Modulation (PCM), and used for decades, have been quite useful in the past and sure will remain with a gold ribbon in the memories of the FTI history.

Nevertheless, the fixed and static nature of the PCM schema derives in rigid and complex architectures, which present many implementation problems in the present context of bigger and bigger FTI installations with more and more data acquired.

This complexity is highly reduced by applying a more flexible schema like the network concept using data packets. Architecture schemas based on Ethernet networks have been widely adopted worldwide in the last 10 years in instrument aircrafts.

Nevertheless, at least in Europe, it has not been applied to fighter instrumentations, maybe due to the fact that data amount is less than the one generated in big aircrafts. However, better features and less cost are possible in fighter installations if the flexibility of the networked schema is used.

This paper presents the new FTI networked architecture for a fighter and compares it to the one used previously.

The presented architecture takes advantage of the flexibility, in order to introduce some intelligent capabilities by adding a basic computing device.

First a brief history of the journey from PCM to Ethernet Networked architectures inside Airbus Defence & Space will be shown.

After that, main FTI systems will be described and compared both for the old and the new architecture. Systems specifically analyzed are: Data Acquisition, Data Distribution, Video, Telemetry, Recording, Time Distribution and Control & Monitoring.

Finally, a detailed description of the intelligent device and its main features will be addressed.

Brief FTI Architecture History

This section contains the description of the evolution of FTI architectures inside Airbus Defence & Space.

Before 2000 all FTI installations used the PCM paradigm to time stamp data acquired. Main advanced related to past installations, where the acquisition system was centralized, was the use of a distributed acquisition system.

This feature allowed to reduce the cabling needed, as all the parameters in one area were grouped in a remote acquisition unit, which was connected to the rest of the system by only two cables (time and data). Previously, each measurement implied a cable being routed from the measuring point to the acquisition system.

Nevertheless, this distributed system used a daisy chain schema, where a master unit must receive all the data coming from the slave units. These slaves were connected following a chain,

with the poor failure resistance provided by this architecture (when a unit fails, all the units behind fails). Additionally, a bottleneck occurs in the data bus connecting all the units, as data are carried to the master unit in a cascade schema.

With the A310-BOOM Flight Test Bed program, in 2002, the new packets paradigm was applied for the first time. However, a parallel installation based on PCM and packets was put in place, in order to validate the new paradigm. For this reason the daisy chain architecture was still used and not all the flexibility and advantages from a real networked architecture were used.

The full networked architecture was for the first time applied in 2005 with the A330-MRTT prototype. After the experience gained with the A310-BOOM program, a fully networked FTI architecture was put in place with satisfactory results. Nevertheless, available technology at that time did not allow acquiring all the

information running through the aircraft buses. It was mandatory to tell the acquisition system which parameters had to be acquired. As a result, managing buses definitions was still highly critical.

With the time the technology evolved and full-acquisition capabilities for buses were introduced in the acquisition systems, reducing the complexity of programming the acquisition system.

Currently, all the new instrumented aircrafts inside Airbus Defence & Space are fully networked and those installed in big aircrafts implements several automatizations and intelligent algorithms running on computers.

The last big step has been done in 2017 with the ultimate test fighter, which includes a fully networked architecture, with full-acquisition capability and intelligence on-board.

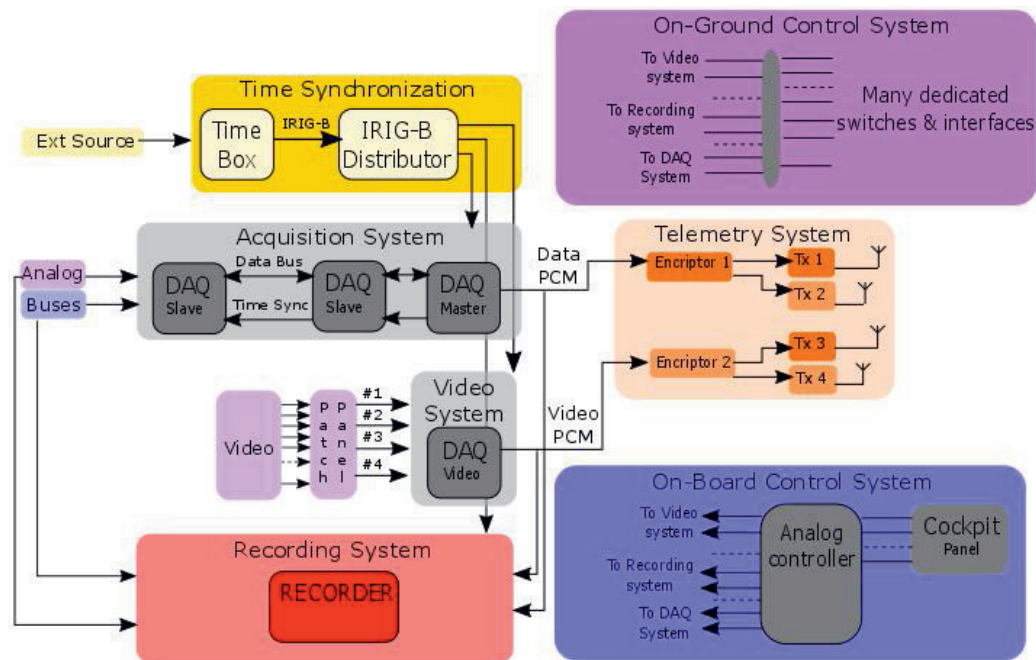


Fig. 1. Legacy Top Level Architecture

Data Acquisition System (DAQ)

In the previous architecture the data acquisition system was based in following main characteristics: PCM output, daisy chain, dedicated time synchronization protocol and parsing acquisition schema.

It was a distributed system with several Remote Acquisition Units (RDAU) acquiring data all around the aircraft. Nevertheless, all acquired data were collected in a master unit which was in charge of building the PCM output with the acquired information. This master unit was connected with the RDAUs through a dedicated

data bus using a serial daisy chain schema (units connected one after another). Main drawbacks of this schema are: poor failure resistance (if one unit fails all the units after it fails), high programming time, no modular programming, limited throughput between RDAUs, complexity to allocate slots for all acquired data in the PCM output.

On the contrary, the new architecture is also a distributed system but based on a star schema, where each RDAU is master of its own acquired data. These data are packetized into an IENA stream, which is sent through Ethernet link to the rest of the system. Main advantages of the

star schema are: better failure resistance (each RDAU operates independently), no bottlenecks to pass data to other RDAUs, less allocation complexity in output stream, a more scalable system (it is easier to add a new RDAU) and in general more flexibility and data throughput.

Additionally, time synchronization of all the RDAUs was performed by using a dedicated time signal implemented in a dedicated bus (also daisy chain based). In the new architecture time synchronization among the RDAUs use a protocol over the data bus (no need for two cables), which is the same protocol of the rest of the FTI system.

Finally, the legacy schema for aircraft buses acquisition was a parsing schema, where certain known data in the buses are extracted and placed into the output stream. This schema implies a perfect knowledge of the aircraft buses definition (ICDs – Interface Control

Document), which is not always simple. Any failure in the ICDs implies a lost of the data, as the data are not acquired in origin. In contrast, the full-acquisition schema of the new architecture acquires all the data from aircraft buses. As soon as any data appears in the bus, is acquired, packetized and sent. Therefore, all data in the bus are acquired, no matter ICD is right or wrong. In case ICD was not correct, data can be interpreted in postprocessing.

Nevertheless, as the amount of acquired data exceeds by far the telemetry data throughput available, a parsing acquisition schema is also programmed in order to send data through the telemetry system. This stream will suffer any ICD issue, but full-acquired recorded data will be safe.

Therefore, DAQ outputs two different data streams: a full-acquisition stream and a filtered (parsed) stream.

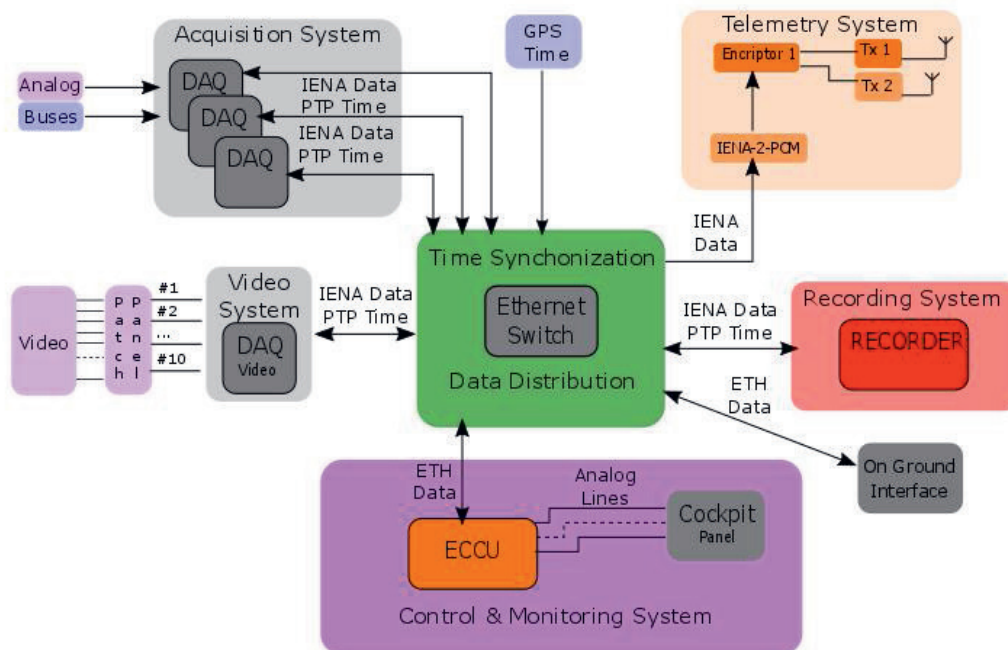


Fig. 2. New Top Level Architecture

Data Distribution System

Legacy architecture data distribution system was based on a point to point connection schema using physical wires connecting each device to another one. The devices could “speak” only with the devices connected to them by a wire.

On the other hand, the new architecture is based in a network schema, where all the devices are physically connected to a central point (Switch) through an Ethernet wire.

This network provides point-to-point communication capability, as each device in the network has a unique address. Each device can speak with any other device in the network, incrementing the working possibilities of the system. This feature is used by the Enhanced Cockpit Control Unit (ECCU) to monitor and control the FTI system.

Additionally, it is possible to send data from one source to many sinks using the multicast capability. It is possible to program in the switch where each data stream must sink. This feature

is widely used in the architecture, as registered in **Error! Reference source not found.**

Moreover, this configuration can be easily changed (even on-the-fly) by configuring the switch accordingly. This feature is used to manage the 10 video data streams, selecting in each flight phase the most appropriate video stream to be shown on ground.

The data distribution system also allows distributing a time synchronization signal based on Ethernet packets to all the connected devices.

Therefore, only one cable per device provides: point-to-point communication with all the system devices, several data streams management and time distribution.

As there are many configuration possibilities is difficult to estimate a maximum throughput the system can handle. Nevertheless, a realistic estimation is up to 100 Mbps per device.

Tab. 1: New Architecture Data Streams

Type	Source	Sink
Full-Acquisition	- DAQ	- REC - ECCU - On-Ground Interface
Telemetry Acquisition	- DAQ	- REC (forensic purposes) - IENA-2-PCM - ECCU
System Status #1	- ECCU	
System Status #2	- DAQ	
Video #1	- Video DAQ	- REC
Video #2		- Some of them to IENA-2-PCM
Video ...		
Video #10		

Video System

In the legacy architecture the video system was able to acquire record and send through telemetry 4 simultaneous video signals. As the possible position cameras were more than 4, a physical patch panel existed in order to plug a fixed camera configuration into the encoders before each test flight.

On the other hand, in the new architecture the system capability have been extended up to 10 simultaneous video encoders. Nevertheless, the physical patch panel still remains as possible position cameras are more than 10.

10 video data streams are always sent to the data distribution system. These data streams

are also IENA streams, so they are managed in the same way as the DAQ data streams.

The switch manages what to do with each video stream. Normally, all the acquired videos are sent to the recording system and a set of them are sent to the telemetry system. Videos sent to the telemetry system can be change on-the-fly, depending on the flight needs, as it is not difficult to change the switch configuration using the ECCU.

Data throughput of each video stream is estimated to be between 1 and 1.5 Mbps, so a total amount of 10-15 Mbps for the video system are used.

Telemetry System

Previous telemetry system consisted of two different telemetry chains: one for video stream and another for data streaming. This fact was imposed by the PCM encoding schema and it forced to install a large number of devices: 2 encryptors, 4 transmitters and 4 antennas. Moreover, the available bandwidth was not interchangeable between data and video, which reduces the flexibility of the system.

By using the IENA packets concept, all data streams can be merged or filtered easily and there is no need to implement two different telemetry chains. Due to this fact, a lot of savings were done both in equipment acquisition and installation costs.

As exposed in the Data Distribution System section, data acquired to be sent through telemetry are acquired in the DAQ following the parsing paradigm in order to adapt the throughput to the available telemetry bandwidth. The selection of the data stream reaching the telemetry chain is done by the switch in the Data Distribution System, but the selection of the information contained in this stream is done by the Acquisition System.

The key part of the new telemetry architecture is the equipment in charge of embedding the IENA packets into a continuous PCM stream suitable to be sent with the current telemetry paradigms. This IENA-2-PCM device follows its own algorithm to do the job and needs a counterpart device on ground, which duty is to convert PCM-2-IENA. Therefore, in the ground segment a replica of the IENA data streams is available to monitor the aircraft.

The telemetry transmitters used in the new architecture are completely digital, so they have inside a premodulation filter, in case a PCM/FM modulation schema is used.

On top of that, all configurations can be done by software: radio frequency, bandwidth and

power, as well as the modulation schema. All the settings are performed through the ECCU, which is also in charge of monitoring the status of the transmitters.

Recording System

The recording system in the previous architecture was devoted to record all the acquired data (video and parameters) and also to provide the total recording of the buses and some high frequency analog parameters.

In the new architecture, the recording system must record all the Ethernet data streams (see Tab.1.): full-acquisition, telemetry acquisition, video and system status.

On the one hand there is no need to perform a total recording, as the DAQ assures all the information in the buses is acquired. On the other hand, the high frequency analog parameters can also be acquired by the DAQ and sent to the data distribution system via a data stream, which will not be sent to telemetry. Therefore there is no need to perform this acquisition.

In the end, the new recording system is an Ethernet network recorder recording all the IENA packets streamed through the switch.

Time Distribution

In the legacy architecture there was a time master, which was loaded with the absolute time before each flight, using a GPS connection or a time box. After this time load, the system runs in free wheel mode affected by the time shifts of the time master. This fact is not critical while the parameters used to analyze the tests come only from the aircraft. Nevertheless, as soon as parameters from on-ground or other aircraft must be analyzed, time differences become critical.

For this reason in the new architecture the system is continuously synchronized through GPS signal. Nevertheless, there is also a way to introduce time into the system in order to operate it inside hangars. The system is able to automatically manage the time source used, following a predefined priority schema. The preferred time source is the GPS; if it is not available an IRIG-B signal is used; lastly, if none of previous signals are available it will relay on the temperature compensated internal oscillator of the time server. In this new architecture, the time master is integrated inside the switch of the data distribution system.

Talking about time distribution protocol, in previous architecture, the time distribution was done using an IRIG-B signal through a point-to-

point schema. This means that one dedicated cable was installed for each device.

In this new architecture the so called Precise Time Protocol (PTP), which operates over Ethernet networks has been used. First main advantage is that there is no need to add any cable as the same data cabling is used to synchronize all the devices in the system (including DAQ which also uses PTP). Moreover, PTP provides a much accurate synchronization of 100 ns, versus tenths of microseconds of the IRIG-B signal.

Control System

The previous architecture did not have a clear defined control & monitoring system. The system was distributed in various dedicated solutions specifically developed for each need.

The onboard control part was mainly performed by using hardware switches connected to a centralized box, which produced the specific hardware signals for each one of the elements being controlled. This solution has been very useful in the past, but it has the problem of being intrinsically rigid and space consuming.

The on-ground control part was based in the same schema, conducting the control & monitor panel to be formed by a lot of different physical interfaces and switches to interact with each one of the devices in the installation.

In the new architecture all control capabilities have been centralized in a dedicated intelligent device called Enhanced Cockpit Control Unit (ECCU). Taking advantage of the networked architecture all the control communications are performed through the same physical interface used to send the data, hence reducing cabling complexity.

Ideally, the control protocol to be used over the network would have been Simple Network Monitoring Protocol (SNMP). Regrettably, not all the devices in the system had the capability to be commanded through SNMP or not all the parameters could be configured. For this reason, we were forced to use a different network protocol in order to configure each one of the devices (i.e. Telnet or proprietary protocols).

Anyway, as the solution is based in a software programmable system is simple to change the parameters controlled or even the way each parameter is controlled.

For those systems, which still don't have a network communication, a dedicated interface has been put in place (i.e. RS-232 bus for telemetry transmitters).

This centralized schema has allowed also substituting all the hardware switches and interfaces by only one dedicated monitoring port in the monitor panel. Through this port, thanks to a dedicated software tool, all the system can be controlled from a single point when the aircraft is on ground.

Monitoring System

As in the control system case, the monitoring system capabilities were also distributed and fully dependent on the possibilities of each device. Some of them did not even have monitoring capability (i.e. telemetry transmitters).

For example, the recording system provided limited amount of information through a dedicated RS-232 bus, which was acquired by the acquisition system and included in the PCM to be sent through telemetry. On the other hand, the acquisition system provided its own status parameters included in the PCM generated by itself.

In the new architecture, almost all the monitoring capabilities have been centralized in the ECCU. In all the cases where it has been possible to monitor the system using SNMP over the network it has been done. On the other hand, some devices were not network connected and for this reason specific interfaces have been put in place.

Current Enhanced Cockpit Control Unit (ECCU) capabilities

This section describes deeply all the functions the ECCU performs inside the new architecture.

System monitoring

The ECCU acts as a centralized monitoring system of all those devices, which does not provide a sufficient level of status report. The ECCU collect status data from those devices and packed them into IENA packets, which are send through the network both to the telemetry and recording system. The data collection schema is a polling one (systems are periodically asked about the parameters).

The telemetry transmitters are one of the devices monitored. Data collection is performed following the specific manufacturer protocol through a RS-232 bus. Parameters extracted are related to configuration control (transmitting frequency, bandwidth, modulation, etc...) and environmental conditions (working temperature).

This is the only device which does not provide a network interface. Nevertheless, thanks to the flexible design of the ECCU it is possible to combine several physical interfaces.

Another monitored system is the recorder. It is monitored using an SNMP client accessing all the relevant information. A big number of working conditions of the main unit are collected: data throughput, recording time remaining, time synchronization status, working temperature, etc... Additionally, all the information related to the input channels being recording is monitored (i.e. Ethernet throughput).

Finally, the network switch is also controlled. As in the recording system, the SNMP protocol through the network connection is used. All the parameters regarding working status (Ethernet port status and data throughput of each port) and environmental conditions (temperature) are polled.

As the switch also acts as time master for the whole system, time synchronization status is also monitored: time source used and synchronization status.

System Own-Care

The monitoring capability can be used in conjunction with the intelligence of the ECCU to take automatic care of all the parameters, which must be monitored to prevent failures in the installation.

As an example, in this aircraft, the ECCU is constantly monitoring telemetry transmitter's temperature to assure it stay below the maximum working environmental. In case, the device gets overheated automatic correction measures are taken by means of modifying the radio-frequency output power.

System control and reconfiguration

The same interfaces used to monitor transmitters, recorder and switch can be used to configure the devices. The telemetry transmitters are configured using the proprietary protocol through RS232 bus, whereas the switch and the recorder are configured using the network interface. Regrettably, the SNMP writing capability has not been implemented neither in the switch nor the recorder. Therefore other means have been used.

Configuration of the recorder has been done through network interface using TMATS commands or some proprietary commands.

On the other hand, configuration of the switch must be done using commands through a Telnet connection.

This configuration capability of the switch is used to select which videos are being transmitted through telemetry. The pilot has

some buttons on the cockpit with which he can select the set of videos to be sent. This set can consist of any combination of the available 10 video sources. The ECCU reads the buttons positions and reconfigure, in real time, the multicast routing table of the switch, changing the videos sent to telemetry.

Moreover, other complex real-time concepts can be implemented. As an example, by combining the use of switch and recorder reconfiguration the real-time access to past measurements can be easily implemented. This concept is explained in the paper “Real-Time access to past measurements using bidirectional communication (TmNS)” included among the papers of this ETTC2018.

System Intelligence

As all the IENA packets containing information acquired by the DAQ runs through the network and are received by the ECCU, it is quite easy to read any parameter contained in those packets and program the ECCU to take an automated action, by reconfiguring any device in the system.

Conclusions

A new flight test instrumentation architecture based on a fully networked concept has been implemented in a new flight test aircraft of an existing fighter. This new concept has allowed a significant reduction in the cabling complexity and in the number of devices needed to be installed on the aircraft.

Additionally, the architecture allows having a more flexible, scalable and capable system.

In terms of capacity, the networked schema provides the possibility to handle much more data (up to 100 Mbps per device).

Flexibility has been improved, by providing better communication possibilities among the devices being part of the system. Additionally, sending the data through IENA packets allow flexibility in the data stream impossible when using PCM schema.

On top of all, an intelligent device has been included, allowing taking advantage of the inherent flexible schema of the networked instrumentation. This intelligent device centralize all the control and monitoring tasks, which provide the capability to easily implement and change any action required in the system. As it also receives all data acquired by the FTI, it is possible to implement automated actions based on data acquired.

Progress and Future Perspectives in Airborne Communication Networking

Kai-Daniel Buechter¹

¹ *Bauhaus Luftfahrt e.V., Willy-Messerschmitt-Str. 1, 82024 Taufkirchen,
kai-daniel.buechter@bauhaus-luftfahrt.net*

Abstract:

A simulation environment was built up to answer questions concerning the availability and performance of aeronautical ad-hoc networks (AAHN). The environment is able to consider base-stations on the ground and satellite communication as internet gateways. Worldwide air traffic, with up to tens of thousands of flights per day can be considered in the simulations. For high data throughput, laser communication is envisioned for aircraft to aircraft communication and potentially also for gateway access. As for telemetry, hybridization is required for node localization and “bootstrapping” of connections. In this contribution, AAHN within a fleet of European aircraft are investigated in the context of air-to-ground and satellite infrastructure available today.

Key words: Aeronautical Ad-hoc Networks, laser communication, air-to-ground (A2G).

Introduction

Current trends in data-driven services in aviation (flight operations management, real-time system monitoring, in-flight connectivity etc.) increase the demands on communication systems, so that state-of-the-art satellite and air-to-ground (A2G) solutions with bitrates on the order of Mbit/s will be strained with regard to throughput, cost, and security in the near future. A complementary technology is free-space optical (FSO) communications, which offers tens of Gbps today (air-to-air / A2A, A2G) without occupying radio spectrum, and with inherent data tapping protection. The prospect of using FSO in the aeronautical context lies in stratospheric communication networks of aircraft or aeronautical ad-hoc networks (AAHN, e.g. [1] [2]), which could provide a throughput far beyond what is available today. Data transmission both in-between aircraft, and to the ground via multi-hop transmission, may be exploited for different types of applications and services. As of today (April 2018), the company Airborne Wireless Network [3] is striving to realize such a network. In this particular case, a hybrid RF-optical approach [4] is pursued; RF is required for signaling while the optical network is used for high-speed throughput. Hybridization may also provide link resilience and redundancy. Base-stations on the ground have also sprung up for mobile communication of civilian aircraft: Gogo has been providing A2G,

in-flight internet in North America since 2008. Solutions based on 4G-technologies are currently being implemented, for example in Europe by Deutsche Telekom in cooperation with Inmarsat and Lufthansa (European Aviation Network or EAN [5]), and by SmartSky in the USA [6]. Around 300 EAN base-stations were set up across all EU member states by Telekom, with a communication radius of “typically” 90 km and bit rates of up to 75 Mbits/s to the aircraft. In this particular approach, ground connectivity, when available, augments S-band satellite communications whenever a fast connection is required. Adding AAHN “on top” could in this case increase the reach of the faster A2G connections by multi-hop transmission, thereby enabling better distribution of available capacities. Therefore, in order to investigate AAHN, several separate systems need to be considered: the air traffic system, the network infrastructure and topology, and the networking and transmission technologies. To this end, Bauhaus Luftfahrt has built up a corresponding simulation environment in order to investigate availability and performance metrics under fleet, infrastructure, and weather considerations. In this contribution, the potentials of AAHN are investigated considering a fleet of aircraft belonging to European airlines. Scenario-based results from the simulations are presented, considering a dense network of base-stations across Europe and the continental USA.

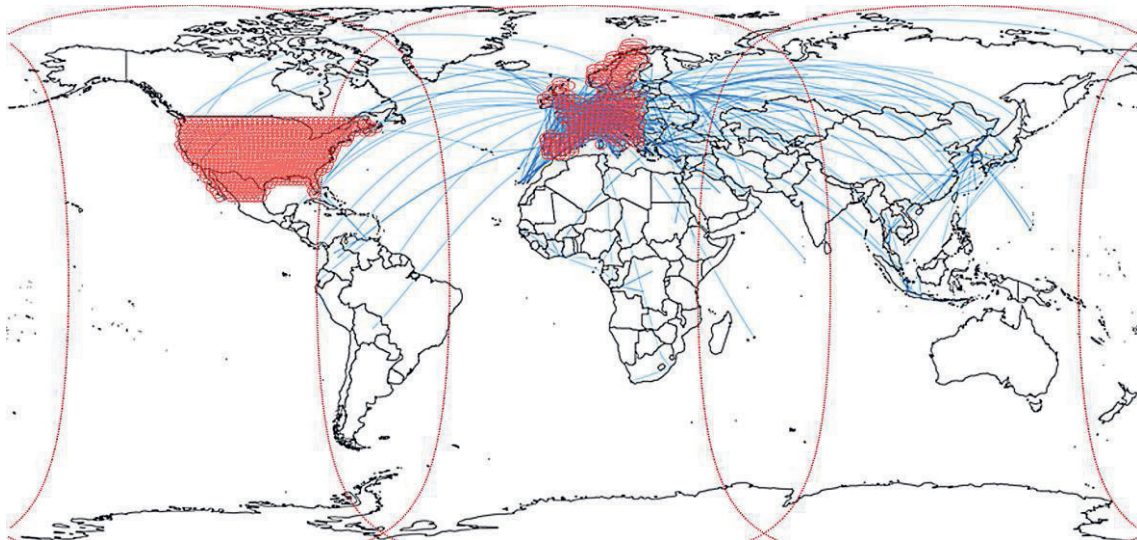


Fig. 1: Depiction of the routes considered in the 24-hour air traffic simulation. The coverage of the assumed telecommunication infrastructure ("footprints" of base-stations and geostationary satellites) is included in red.

Scenario Definition

In the context of this contribution, a fleet of aircraft belonging to European airlines is considered and to this end, the 2016 edition of OAG flight schedule database [7] is used to simulate aircraft movements. The simulated day is October 29, 2016 – we selected the date before as an "average" day in worldwide air traffic [8]. Criteria for selecting flights for the simulations included whether the aircraft belonged to a European airline and whether it had more than 100 seats. Overall, the selection results in 16,862 flights considered overall, within a 24-hour timeframe. The respective routes are shown in Fig. 1.

Infrastructure definition

Base-stations on the ground and satellites are considered as internet gateways and the footprints of either are included in Fig. 1. We assume that base-stations are available across the EU and the USA. To this end, an algorithm places gateways over landmass in the range between 37° and 75° latitude, -15° and 21° longitude (assumption for European infrastructure) and between 25° and 48° latitude, -135° and -60° degree longitude (assumption for US infrastructure). Based on available data on the EAN (about 300 stations covering 4.38 million km²), we estimate that the mean cell radius in Europe is 70 km and assume a maximum communication range of 150 km. The available capacity per cell and

antenna was set to 75 Mbit/s initially, or 225 Mbit/s per base-station, according to current specifications.

In addition to the base-stations, satellites are considered. For the sake of defining a scenario for a satellite capacity estimation, we assume S-band satellites with a transponder bandwidth of 15 MHz in two polarizations. The overall throughput of a single satellite is then assumed to be *channel capacity* \times *polarization* \times *number of spot beams*. We assume that the satellite produces nine spot beams. In order to provide global coverage, we assume that three geostationary satellites are available.

Estimation of communication system performance

As different communication systems are involved, we discuss each type of connection next. An overview of our assumptions is given for A2A, A2G and A2S (air-to-satellite) connections in Tab. 1. Effectively, a 9-m dish and a 50-cm effective aperture are assumed on the satellite and on the aircraft, respectively, for link-budget calculations. The assumed laser aperture is 10 cm in diameter. The number of A2A connections is limited to a maximum of four per aircraft. For the purpose of simplification, we consider unidirectional transmission in the simulation but assume that transmission performance is similar in both directions.

Tab. 1: Definition of communication system performance for the AAHN simulations.

Assumptions:	Air-to-air	Ground-to-air	Satellite-to-air
Carrier wave	FSO: 1.67 μm	RF: 2.1 GHz	RF: 2.1 GHz
Bandwidth	10 GHz (FSO)	15 MHz	15 MHz
Antenna gain (Tx / Rx)	2 x 105 dBi = 210 dBi	15 dBi + 3 dBi = 18 dBi	46 dBi + 21 dBi = 67 dBi
Power	27 dBm (0.5 W)	46 dBm (40 W)	51.5 dBm (140 W)
Additional losses (Tx / Rx)	2 x 14 dB = 28 dB	2 x 3 dB = 6 dB	2 x 3 dB = 6 dB
Atmospheric model (clear sky conditions)	[9]	ITU model, 58% rel. surface humidity	ITU model, 58% rel. surface humidity

According to [10], the feasible communication range for aircraft-to-aircraft communication systems using FSO is between 210 and 380 km, depending on system considerations such as aperture diameter, mean power level and data rate. In practice, as clouds present obstacles to FSO systems, hybridization may be required as a means of mitigation. Our calculations indicate that, under clear-sky conditions, attenuation is small in comparison to free-space losses below 600 km A2A distance. Beyond 600 km aircraft separation, the beam passes through the troposphere and the effect of denser and more contaminated air (water content, aerosols, etc.) dominates overall losses. Earth curvature limits range geometrically beyond 750 km, and clouds restrict practically achievable link lengths further.

Fig. 2, top shows the calculated Shannon capacity for the defined A2A link. In these calculations, the effect of fading losses (due to clear-air turbulence, beam-tracking errors, etc.) and high-altitude atmospheric contaminants (e.g. ice clouds) are not evaluated in detail. However, some system losses are assumed (beam coupling, return losses etc., cf. Tab. 1). Fig. 2, center shows calculated Shannon capacities for ground-to-air links. Assumptions regarding the FSO system are unchanged. As for RF, we assume an S-band carrier frequency of 2.1 GHz with 15 MHz of available bandwidth. The calculated Shannon capacity of approximately 100 Mbit/s at about 100 km distance compares well to EAN specification. In the FSO-case, communication range is less than half that of the A2A scenario and beyond 200 km A2G distance, the performance of the optical link diminishes due to strong attenuation. It is clear that A2G links enjoy less favorable conditions compared to A2A links.

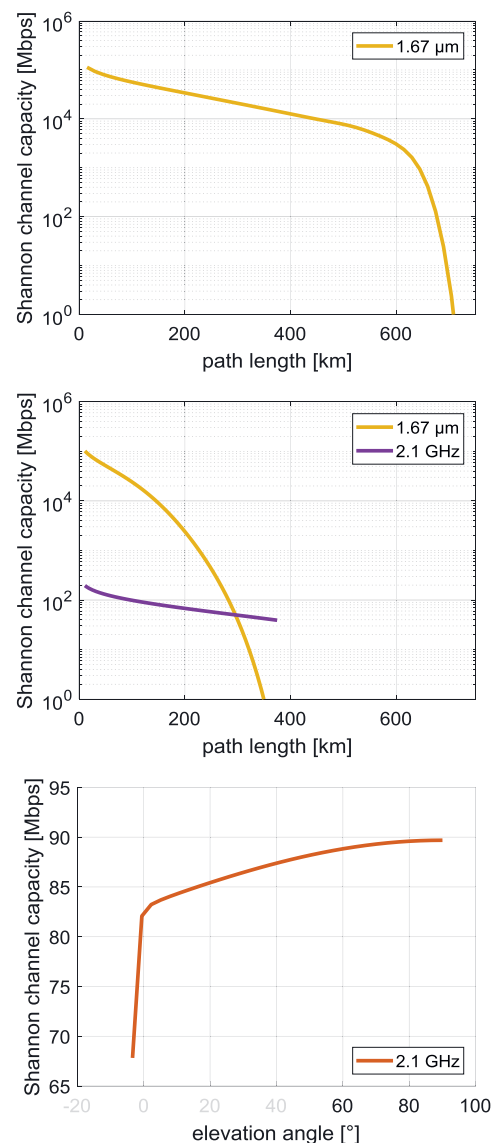


Fig. 2: Calculated Shannon capacities for transmission systems defined in Tab. 1, for A2A (top), A2G (center) and A2S (bottom) connections. Dynamic effects (power fluctuations due to clear-air turbulence, beam tracking etc.) are disregarded.

Tab. 2: Transmission system definition for initial simulations.

Link	Max. link capacity	Max. throughput	Max. range
A2A	1,000 Mbit/s	-	150-600 km
A2G	75 Mbit/s	225 Mbit/s	150 km
A2S	80 Mbit/s	1440 Mbit/s	N.A.

Obscurements by fog, clouds, aerosols and hydrosols as well as higher levels of turbulence restrict FSO availability. Therefore, in the simulations we assume that only RF links to the ground are available.

As for the S-band satellite link (Fig. 2, bottom), a maximum channel capacity of up to 90 Mbit/s is calculated, which we assume doubles with polarization diversity. From the scenario definition, the satellite throughput is defined as 1440 Mbit/s ($2 \times 9 \times 80$ Mbit/s).

Simulation Results: Contemporary Scenario

Assumptions concerning the transmission systems for initial simulations are collected in Tab. 2. For the FSO system (A2A), we specify a capacity of 1 Gbit/s, which is conservative for an optical link. However, as the A2A link is not the bottleneck in the scenario, a capacity increase does not affect the results in this scenario. As for the A2G link, 75 Mbit/s is assumed per cell according to specifications, with a maximum throughput of 225 Mbit/s per base-station (three cells). The maximum capacity for a single link is 75 Mbit/s. As for the satellites, we assume that twice the calculated channel capacity is available per cell with polarization diversity, while the maximum throughput is proportional to the assumed number of beams. The capacity for a single A2S link is limited to 80 Mbit/s. In our simulation model, we assume that the overall bandwidth per gateway (satellite or base-station) is distributed equally among the number of connected clusters. The number of aircraft in flight is shown in Fig. 3. Air traffic peaks at approximately 2800 aircraft. Typically, up to 20% of all aircraft are below clouds. The effect of considering clouds in the simulations is discussed later in the paper. The following results assume that clouds do not have an impact on link availability.

In Fig. 4, top, the percentage of connected aircraft and cluster size statistics are shown, including variances in cluster sizes. Without AAHN ($R_{AC} = 0$ km), 45% of all flights are within range for A2G communication on average. With increasing A2A-range, larger numbers of

aircraft may participate in ad-hoc networking and the rate of aircraft with access to base-stations also increases.

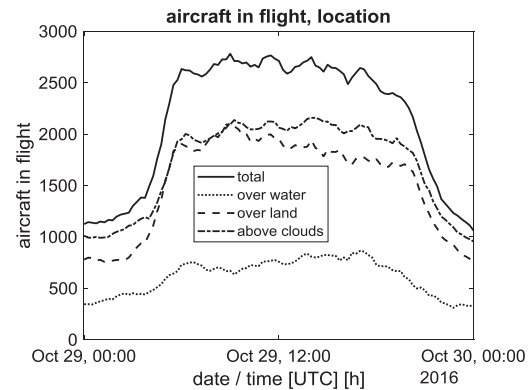


Fig. 3: Absolute number of aircraft in flight. The peak during daytime corresponds mainly to domestic flights.

Adding satellites provides nearly 100% connectivity to all aircraft. In addition, the variance in connectivity reduces with increasing communication range (Fig. 4, bottom: “scenarios” 1 to 10 with varying A2A-range and with or without satellites).

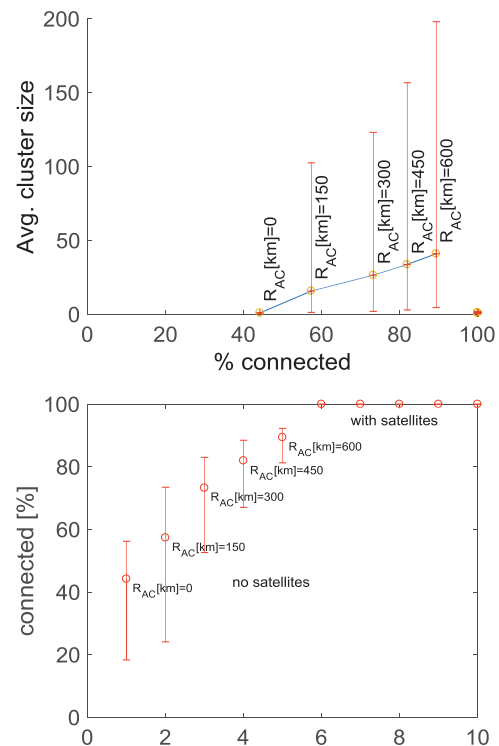


Fig. 4: Percentage of connected aircraft and cluster size statistics for different A2A communication ranges (top). Variance in connectivity for different A2A communication ranges (bottom). With satellites, all aircraft are practically always connected.

During the day, air traffic over Europe is dense and more than 50% of all aircraft in flight connect to the ground directly (Fig. 5, top).

Adding A2A-links enables multi-hop connectivity to the ground via airborne networking, thereby enabling to off-load capacity from the satellites to the base-stations (Fig. 5, bottom). On average, around 40% of aircraft connect via AAHN exclusively in that case.

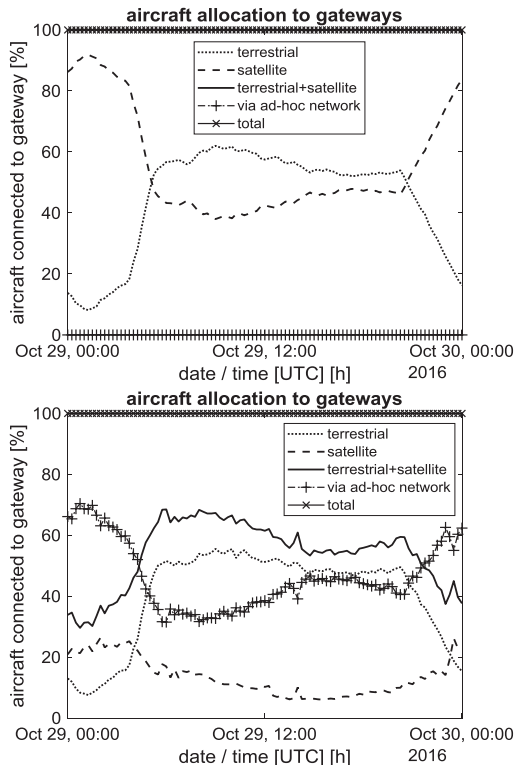


Fig. 5: The fraction of aircraft connected to either satellite or terrestrial gateways (without ad-hoc networking, top) and additionally via AAHN (bottom). In this scenario, especially satellite capacities are relieved as fewer aircraft depend on satellite connectivity (300 km A2A-range assumed in this case). About half the aircraft may use AAHN for A2G connectivity via multi-hop transmission.

Statistics representing the maximum achievable, averaged throughput per aircraft are shown in Fig. 6. Throughput is calculated according to graph flow theory for each connected cluster of aircraft (which may have a size of one) and does not consider overhead due to protocols, retransmission of lost packets, etc. Moreover, it is assumed that each aircraft generates a demand of the full per-link capacity to “flood the network”. The full per-link capacity to the ground is available to only a fraction of all aircraft, as all aircraft within a respective cell share capacity of the base-station without AAHN. With AAHN, the available infrastructure capacity is shared within the respective AAHN-cluster.

In the scenario without airborne networking, about 50% of all flights enjoy bandwidths beyond a few Mbit/s according to the

calculations. This seems reasonable, as roughly 1,000 aircraft have only satellite connectivity available during the air traffic peak (about 40% of 2,500 aircraft in-flight, Fig. 5). With a satellite throughput of 4,320 Mbit/s overall (three satellites with 1,440 Mbit/s each assumed), this results in about four Mbit/s per aircraft on average. Moreover, assuming that roughly 1,500 aircraft do have a ground connection (about 60% of all aircraft in-flight during peak hours), an averaged capacity per aircraft of 45 Mbit/s (= 300 base-stations x 225 Mbit/s / 1,500 aircraft) would be expected for these flights, but considerable variance is evident.

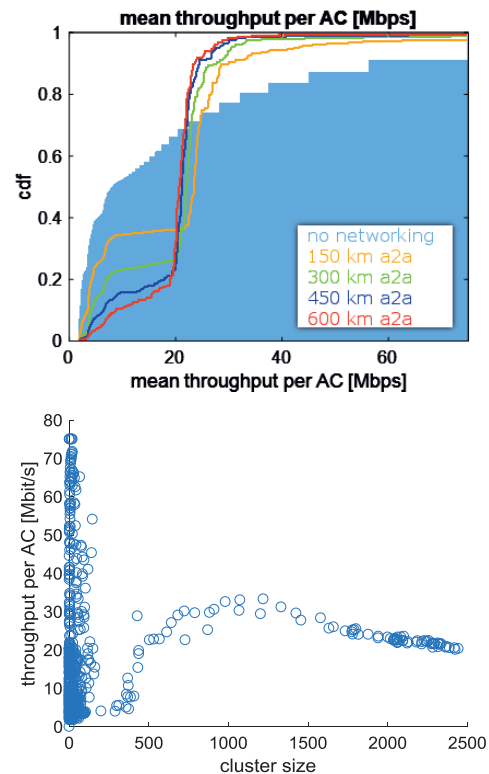


Fig. 6: Cumulative throughput statistics, averaged based on the maximum throughput per cluster of networked aircraft (top). Averaged capacity per aircraft as function of cluster size with 300 km A2A-range (bottom).

When A2A networking is enabled by adding FSO connections, the participating aircraft may share the capacity within their respective mesh cluster, which leads to an equalizing effect in the statistics. Due to the large bandwidth of the FSO connection, the bottleneck to the internet is in the gateway connections. Throughput depends on cluster size and location: over Europe, the mean throughput per aircraft should average out according to air traffic density and cell density. Such an effect is suspected in Fig. 6, bottom: Above a cluster size of about 300 aircraft, the mean throughput peaks at a cluster size of around 1,100 aircraft,

which is of the order of domestic flights over Europe during peak hours in the simulation. In the early morning hours and at night, however, a disproportionate number of flights either converge or diverge over Europe. Therefore, larger fractions of aircraft are beyond the boundaries of the area covered with base-stations, so that fewer aircraft within the mesh provide ground connectivity.

Below a cluster size of 300, the statistics include single aircraft and isolated clusters connected to ground or to satellite, especially beyond the borders of the European territory. Small clusters suffer from a higher volatility, because fewer connections are available with less redundancy but also, the full link capacity is available to some isolated aircraft and clusters.

Simulation Results: Future Scenario

In order to provide a future prospect, the simulation environment is modified in the following way: it is assumed that FSO connections are available to high altitude platforms (HAP) above the clouds. The communication range to HAPs (A2H) is set to 450 km. As optical terminals are point-to-point connections, it is assumed that only a limited number of connections may be formed. Therefore, we assume that the HAPs have four optical connections each, with a capacity of 10 Gbit/s each and a corresponding downlink with 40 Gbit/s. In addition, we assume that satellite laser terminals (SLT) are available to aircraft. Here, we assume that ten connections are available on three geostationary satellites each, with a capacity of 1 Gbit/s. As for the aircraft, we assume a capacity of 10 Gbit/s and 300 km range. Furthermore, we limit demand per aircraft to 1 Gbit/s, corresponding for example to a hundred video streams with 10-Mbit/s each. An overview on the modified assumptions is given in Tab. 3.

Tab. 3: Transmission system definition for future scenario.

Link	Max. link capacity	Max. throughput	Max. range
A2A	10 Gbit/s	-	300 km
A2H	10 Gbit/s	40 Gbit/s	450 km
A2S	1 Gbit/s	10 Gbit/s	N.A.

Simulation results are shown in Fig. 7. The fraction of aircraft which connect through the ad-hoc network is higher than before. Naturally, this is the case, as a limit was imposed on the number of gateway connections. Overall, on

average about 10% of aircraft do not have a connection in this scenario – these could for example use RF satellite resources. However, nearly 80% of all aircraft have an averaged throughput beyond 200 Mbit/s and around 70% of all aircraft even have a throughput of more than 800 Mbit/s.

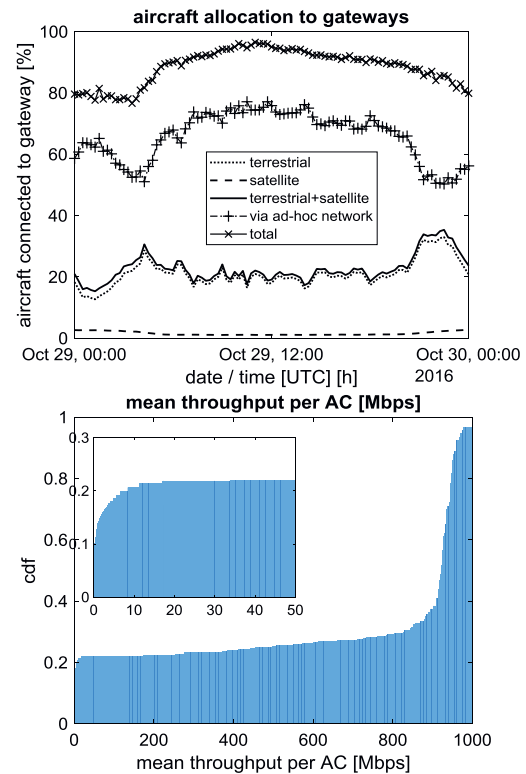


Fig. 7: Scenario with laser connections available between all nodes. As there is a limitation on the available satellite connections, full coverage is not achieved without additional RF satellite links, for example (top). Achievable, averaged bitrates for this scenario. The inset shows the lower left portion of the graph in detail. Around 70% of all aircraft see averaged bitrates of over 800 Mbit/s (bottom).

Finally, when clouds are considered, based on NASA AIRS [11] satellite cloud top pressure data of the simulated day, overall availability suffers as seen in Fig. 8 (result from "future scenario"). In this case, links with a transmission path below or through the cloud top are blocked in the simulation. Chiefly, aircraft during the take-off and landing phases lose their connections. The fraction of aircraft connected directly to infrastructure changes only slightly, as the number of base-station terminals limits the number of connections in the scenario, but some of the gains of the AAHN are lost. Especially the connectivity during peak hours suffers – the main reason is that the frequent short-haul flights over Europe spend a considerable time during their take-off and landing phases below the cloud tops. Some of the losses should be recoverable by

hybridization of the links. Fig. 8, bottom, shows the throughput per aircraft – as the link and infrastructure capacities are higher than the demand per aircraft, throughput approaches the set demand of 1 Gbit/s in this scenario, but doesn't peak as in Fig. 6, bottom.

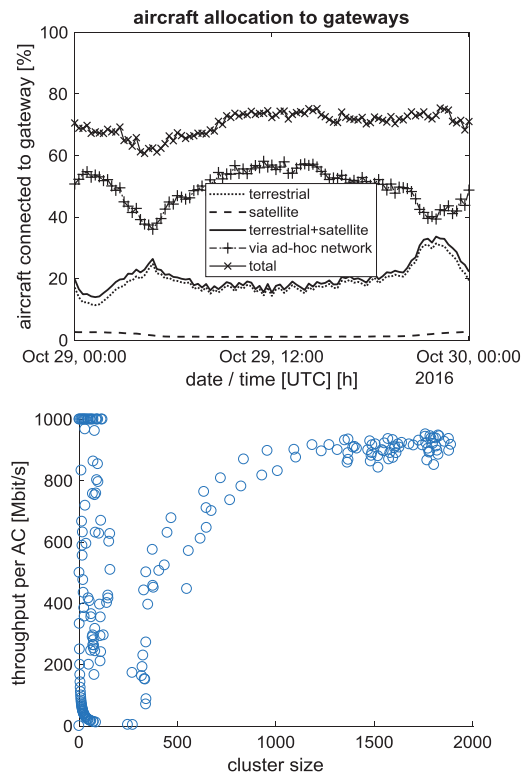


Fig. 8: Scenario above with added cloud top data which impede optical link availability. Mean throughput per aircraft as function of cluster-size is shown in the bottom graph.

Summary and Conclusions

In this contribution, the effect of adding ad-hoc networking capability to the commercial air traffic system was investigated within the context of ground infrastructure and satellite connectivity available today. Certain assumptions and calculations were made based especially on publicly available information on the European Aviation Network. We took certain liberties to represent, to our best knowledge, a feasible, near-future infrastructure perspective in our simulation environment. It was shown that the airborne network enables a redistribution of infrastructure capacities, such that the variance in throughput per aircraft is reduced and more aircraft can be provided with a moderate bandwidth. This is interpreted as a positive overall effect. Moreover, multi-hop communication to the ground frees up satellite capacities, which benefits aircraft without access to base-stations. Peak bandwidths per aircraft are reduced; however, this only affects a fraction of aircraft in-flight. With the

infrastructure available today (as of 2018), adding aeronautical networking could, according to the simulations, provide an averaged throughput of at least 20 Mbit/s to up to 80% of all European aircraft, if these had a free-space optics-based networking capability (overhead not included).

In order to provide a future perspective, the simulation was modified to consider high-speed laser communication to high altitude platforms and satellites, with a limited number of available laser terminals per station, under certain assumptions concerning link capacity and range. Here it was calculated that an averaged throughput of 800 Mbit/s could be provided per aircraft. The total throughput is scalable with the number of gateway connections, demonstrating future growth potentials.

Future work may consider scenarios that evaluate the impact of adding high-throughput satellite connectivity (*ku-/ka-band*), for example, in a refined satellite model. From the perspective of business models, different fleets of airlines and aircraft can be considered with different communication capabilities and communication demands. For a defined fleet, the ratio of equipped aircraft can also be varied for phase-in studies. Adding flights to the simulated fleet improves AAHN availability, so business models should consider incentives for participation. Lastly, the data traffic models may be improved for example to evaluate the "goodput" in the network, and network dynamics may be evaluated for technical feasibility analyses, including for example link acquisition time and the impact on the network. Beyond internet connectivity, also the "inter-mesh" communication capacities may be of interest.

References

- [1] D. Medina, F. Hoffmann, S. Ayaz und C.-H. Rokitansky, Feasibility of an Aeronautical Mobile Ad Hoc Network Over the North Atlantic Corridor, *Proc. Fifth IEEE Conference on Sensor, Mesh, and Ad Hoc Communications and Networks (SECON)*, San Francisco, USA, 2008.
- [2] B. Newton, J. Aikat und K. Jeffay, Concise Paper: Analysis of Topology Algorithms for Commercial Airborne Networks, *IEEE 22nd International Conference on Network Protocols (ICNP)*, Research Triangle Park, USA, 2014.
- [3] „Airborne Wireless Network,“ [Online]. <http://www.airbornewirelessnetwork.com/index.asp>.
- [4] L. B. Stotts, L. C. Andrews, P. C. Cherry, J. J. Foshee, P. J. Kolodzy, W. K. McIntire, M. Northcott, R. L. Phillips, H. A. Pike, B. Stadler

- und D. W. Young, Hybrid Optical RF Airborne Communications, *Proc. of the IEEE*, Bd. 97, Nr. 6, pp. 1109-1127, 2009.
- [5] Deutsche Telekom AG, 2015. [Online]. <https://www.telekom.com/media/company/288250>.
- [6] „SmartSky Networks,“ [Online]. <http://smartsdynetworks.com/>.
- [7] „OAG Aviation Worldwide Limited,“ 2016. [Online]. <http://www.oag.com/>.
- [8] K.-D. Bächter, Availability of Airborne Ad-hoc Communication Network in Global Air Traffic Simulation, *2016 10th International Symposium on Communication Systems, Networks and Digital Signal Processing (CSNDSP)*, Prague, 2016.
- [9] L. Elterman, UV, Visible, and IR Attenuation for Altitudes to 50 km, 1968, *Environmental Research Papers*, Nr. 285, 1968.
- [10] H. Henninger und D. Giggenbach, Avionic Optical Links for High Data-rate Communications, in *25th International Congress of the Aeronautical Sciences*, Hamburg, Germany, 2006.
- [11] E. Fetzer, G. Hulley, E. Manning, J. Blaisdell, L. Iredell, J. Susskind, J. Warner, Z. Wei, W. Blackwell und E. Maddy, AIRS Version 6 Release Level 2 Product User Guide Version 1.1, E. T. Olson, Hrsg., Jet Propulsion Laboratory, Pasadena, CA: Jet Propulsion Laboratory, 2016.

Design and Implementation of a Long Range Autonomous Wireless Critical System and its Application in Remote Hydroelectrical Infrastructure (Water Canals) for Risk Prevention and Hazards in Case of Hydraulic Canals Breaks.

Fco. Javier Fernández Huerta¹, Luis Javier Etayo Pérez², Fco. Javier Alonso Caballero¹

¹ KUNAK Technologies S.L. Pol. Ind. Mocholí, Plaza CEIN 5. 31110, Noáin. SPAIN.

² Acciona Energía S.A. Av. Ciudad de la Innovación 5, 31621, Sarriguren. SPAIN
jfernandez@kunak.es ; luisjavier.etayo.perez@acciona.com ; falonso@kunak.es

Abstract

A new wireless critical system based on Industrial Internet of Things (IIoT) innovations, a combination of different wireless technologies - from mature well known 2G networks to high performance ultra-long range private **169 MHz LoRa** network - and a **cloud distributed architecture** with advanced algorithms is presented to build a critical telemetry system, in this case, applied to real time hydraulic canals monitoring of hydroelectric plants. Thus, sporadic and uncontrolled breaks of hydraulic elements are avoided, decreasing the affection to populations, environment, nearby roads and other infrastructures.

For this pilot deployment 6 different hydraulic canals located in remote sites, some of them without cellular coverage, have been monitored with up to 25 measurement points. The wireless remote terminal units (RTU) have been designed with cutting edge IIoT electronics, enabling **ultra-low power consumption** and autonomous energy harvesting operation with 3W solar panels; allowing 1-minute sampling time and 5 minutes transmission periods to the cloud, where advanced algorithms, requiring the information of every RTU, update the state and health of the infrastructures in real time.

Key words: 169 MHz LoRa Network, Smart Utility Networks, Hydro Electrical Infrastructures, Autonomous Telemetry Devices, Cloud-based telemetry solution.

1. Introduction

ACCIONA SA is a utility company, leader in providing sustainable solutions for infrastructure and renewable energy projects across the world, with 7,254M€ revenues and 37,400 employees. Its offer covers the whole value chain, from design and construction to operation and maintenance, with a presence in more than 65 countries.

KUNAK Technologies SL has designed a disruptive solution to deploy wireless monitoring systems whose ultra-energy efficiency characteristics and end-to-end critical system architecture provide great advantages in isolated, remote and complex environments, guaranteeing the robustness and integrity of 24/7 communications.

ACCIONA is requiring a solution to control more than 300km of hydroelectrical infrastructure for

risk and hazards prevention in case of hydraulic canals breaks. These canals are used to transport the water from a river or dam, across several kilometers, to the forebay tank in order to gain the higher height difference to the power house (turbine) as possible. Some of these infrastructures were built 100 years ago.

Then, it is necessary to find a solution for fast canals breaks detection; reducing their consequences, minimizing canals affections or even predicting the breakages. This will help develop best practices in maintenance of hydroelectrical infrastructures.

This digitalization process had to solve several challenges (see Table 1) such as gathering the data efficiently in remote scenarios with difficult access, coverage problems and lack of power grid; reliable transportation to Internet; mass storage and Cloud computing availability; advanced alarm generation and ease operation and maintenance of the whole system.



Fig.1 Water canal break

In previous attempts realized by ACCIONA to face these challenges, electric power and optical fiber lines were installed, resulting in expensive deployments very difficult to maintain.

Also, other data acquisition systems based on mesh and tree wireless sensor network topologies were tested with no success because of their lack of reliability and robustness.

2. Proposed Solution

Thus, in the following table the problems to be satisfied by the proposed solution are shown as well as how KUNAK's system solve them and the expected benefits for the customer.

Table 1. Problems, Proposed Solution and Benefits for the Customer.

Problem / Pain	Solution	Benefits
Remote infrastructures covering wide mountainous areas	Wireless devices connected to an Internet Cloud Platform	Devices can be connected to the Internet independently of the technology used, while the information is centralized in the Cloud
No Power – deep valleys– Low Solar Radiation area	Ultra-low power consumption electronics + state of the art energy harvesting solutions	Autonomous operation without any additional infrastructure.
Cost	Wireless and autonomous	No wire, no civil works, lower CAPEX and OPEX.
Fast & Easy installation in remote areas	Small and light devices, wireless, autonomous (battery operated), plug & play	Easy to transport, install, configure and operate. Installation ready in less than 1hour.
Reach every infrastructure and place, no matter its remote location	Combined wireless solution. Cellular & Best-in class long range wireless sensor network based on Kunak 169/433/868 MHz LoRa solution.	Long range: Non-Line-of-Sight coverage. (>30Km LoS) Noise and interferences immunity. Wide area coverage in mountainous areas
Reliability and Robustness	IP67 devices with wide temperature range. Wireless Critical System Architecture.	24/7 unattended operation. 10 years autonomous operation without maintenance.
Easy Operation & Maintenance	Bidirectional system with auto health checking, alarms and status	Remote tele-control of sensors and devices. No displacements.
Real-time information on the health of infrastructures.	Advanced algorithms running on the cloud using information from different sensors, devices and data sources.	Any virtual condition, situation or object, can be modeled and presented to the final user in an ease to use dashboard.
Easy integration with third party information systems	Cloud based solution. Open API	Easy integration into SCADAs, information sharing with public bodies and hydrographic basin organizations. Access in mobility from Smartphone Apps.

In order to satisfy the tight requirements explained before, KUNAK proposed an end to end solution, composed by several elements, building a complete autonomous wireless critical system capable of sensing anywhere through the Internet.

The system has the architecture shown in figure 2, with the following components:

- **Sensors:** water level sensors to monitor water height inside the canals.
- **Remote Terminal Units (RTUs):** Small wireless (2G or LoRa) waterproof devices responsible of reading the sensors and send the information to the cloud. The RTUs are provided with an autonomous power supply system (primary or secondary) for long time operation.

- **Gateway:** The base station managing the **169/433/868MHz LoRa** network while maintaining the communication to the Cloud.
- **KunakCloud:** a cloud-based telemetry & telecontrol Software capable of managing the sensors, devices and users, store the information, run complex algorithms in real time, provide intelligent alarms, remote configuration and advanced visualization.
- **Open API:** the open application programming interface allows the solution to interconnect to third party systems and build custom Smartphone Apps for the final customers.

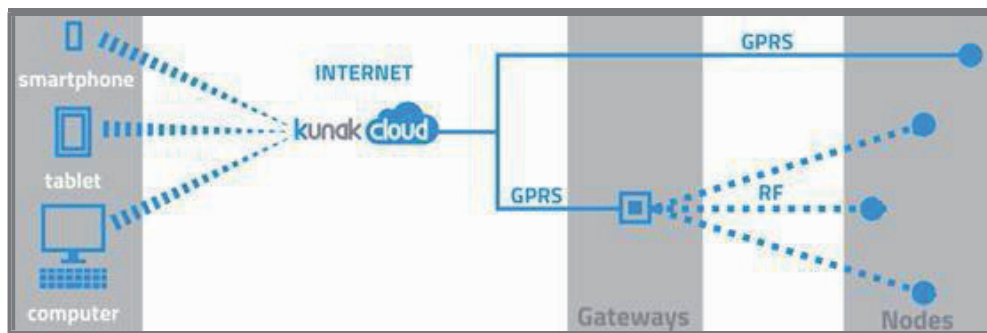


Fig 2. Solution Architecture. Autonomous Nodes using GPRS and Wireless networks based on LoRa modulation are connected to KunakCloud: a Cloud Based Telemetry&Telecontrol Software.

3. Detailed System Description

Sensors: the need of accurately monitoring the water height inside the canals implied the selection of the appropriate sensors capable of measuring the water level with the following considerations:

- Inside the canals, the water is moving, comes from rivers as well as rain falling from the mountains, which make the water to transport mud, leaves...
- Protection from any objet and dirt present in the water as well as to work under extreme environmental conditions.
- Fast response time with low power consumption.
- Low or moderate cost.

For those reasons, radar sensors (high cost, high power consumption), sensors based on conductive and capacitive effects (mud and dirt can influence their readings [1]) and buoys and floats (moving parts that can be obstructed),

were discarded. Thus, hydrostatic pressure sensors, particularly the MA-403 [2], were selected because of their fast response, low power consumption, accuracy and reliability. Also, two ultrasonic sensors from Matbotix (MB7369) [3], were tested and installed next to a hydrostatic pressure sensor to compare both sensors readings over long periods of time and different environmental conditions. Both sensors selected are temperature compensated and the RTUs oversample, average and filter the readings to maximize the accuracy of measurements. One reading is taken every minute to have maximum temporal resolution in this application.

RTUs: cutting edge IIoT technologies were used to design ultra-low power consumption (few μA in sleep mode) devices capable of measuring the sensors, provide independent power supplies from 5 to 19Vdc to them, analyze the readings, store them and transmit, using different wireless technologies, to the cloud. The design has two different power supply systems to guarantee the autonomous

operation depending on the final installation site.

- **Primary Batteries:** devices which were installed underground or in places with no direct sunlight exposure use long life 7.2V, 14Ah lithium primary batteries. These units were configured to send the information to the cloud every 15 minutes to guarantee at least 1-year of autonomous operation.
- **Secondary Batteries:** where small solar panels of 3.5W (6V) can be installed, the units are provided with 3.7V, 10Ah Li-Ion rechargeable batteries. This capacity guarantees at least 4 weeks of autonomous operation without solar charge sending the information to the cloud every 5 minutes. The RTUs are provided with power path and manage the solar charge to avoid batteries overcharge and deep discharge, enhancing batteries life up to 5 years of continuous operation.

The RTUs have different input and output ports: analog (4-20mA, 0-10V), digital (total or partial pulse counters, frequency meters up to 4KHz, ON/OFF state), Modbus RTU-485, relays, etc... which can be easily configured from a computer software enabling their calibration during on field installation.

The electronics and batteries are encapsulated inside 12x12x9cm IP67 polycarbonate enclosures, with IP68 connectors for the sensors, antenna and solar panel. Also, a metallic roof is provided with the system to ease the mast-mount installation, to provide a support for the solar panel and to protect the enclosure from overheating under strong solar radiation during summer, which could reduce the battery life. Finally, external high gain antennas are used to enhance signal strength in remote areas (figures 6 and 7).

Wireless Communications: in order to maintain a continuous bi-directional connection of sensors and RTUs to the cloud, two different wireless technologies have been used. In most of the required monitoring places, even in mountainous valleys, a reliable 2G connection was present which allowed using these cellular networks for data transmission directly to the cloud.

However, there were some infrastructures and areas not covered by any kind of cellular network, which was an enormous challenge for sensing. Satellite technologies were discarded because of their cost and power consumption. That's why, the design of an ultra-long-range

radio frequency sensor network capable of maintaining reliable communications in rural environments with abrupt orography was required to complement the whole system solution and fulfil the customer needs.

Thereby, different sensor networks topologies were evaluated. Mesh and tree topologies (Fig.3) can provide the highest coverage range since each device extends the network by "jumping" the information from one device to another. However, if any *router node* experiences any problem, the whole network will suffer from downtime, not fulfilling the reliable and robustness requirements. The probability of network failures increases with each jump. In fact, in the past, ACCIONA carried out tests with these network topologies undergoing these reliability problems. Besides, as the information must jump across the network, the traffic of the whole system increases as well as its power consumption. Therefore, this kind of networks can suffer from higher duty cycle restrictions, higher latency and much higher power consumption.

For all these reasons, mesh and tree topologies were not considered for high reliability, low latency and low power consumption KUNAK's system architecture in remote scenarios.

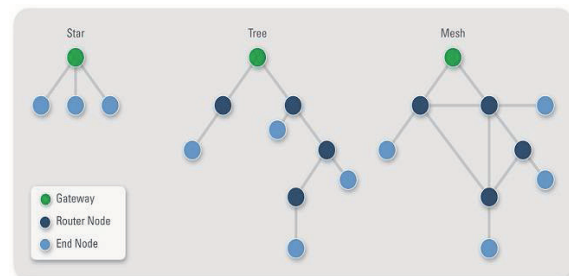


Fig 3. Wireless Sensor Network Topologies.

Star networks are the most reliable as just one point of failure exists, the gateway, that could be redundant to increase robustness in critical applications. Up to date, the main problem of this topology was its coverage since all the end nodes must be within the range of the Gateway and current available modulation techniques within the ISM (industrial, scientific and medical) frequencies (2400/868/433/169 MHz) didn't allow **long range reliable communications distances** of more than few kilometers Line-of-Sight (LoS) and hundreds of meters Non-Line-of Sight (NLoS).

However, new revolutionary modulation techniques in Sub-GHz bands have appeared in the last few years enhancing dramatically the overall performance of wireless networks. Traditional FSK, spread spectrum like LoRa (Long Range, Semtech Trademark), and ultra-

narrowband technologies like Sigfox are available in the Sub-GHz ISM bands.

Some of these technologies, like Sigfox [5], are only present in the 868/900 MHz band which is a limitation for radio propagation in rural mountainous areas (as shown in figure 8). FSK and LoRa Modulation cover the whole Sub-GHz ISM bands, but the outstanding characteristics in terms of link margin; noise and interference immunity; multipath, fading and doppler resistance; and sensitivity [4] of LoRa modulation, makes this technology ideal for ultra-long range wireless communications requiring high reliability and robustness.

The LoRa Alliance [6] develops and promotes the LoRaWAN open standard to enable large scale Low Power Wide Area Networks (LPWAN), based on LoRa modulation, guarantying interoperability between manufacturers. This standard has been mainly designed for large scale networks with thousands of battery operated devices transmitting very few information a day (IoT devices, smart meters). That's why, the standard can't include all the LoRa and FSK modulation schemes since it is focused on high capacity networks excluding very high and very low data rates. Besides, the LoRaWAN is defined for the 868/915 MHz band, which will present problems in applications requiring NLoS communications (hills, mountains, valleys, etc...), excluding other Sub-GHz ISM bands very interesting for remote telemetry systems.

In order to satisfy the requirements of ultra-long range, low power, NLoS telemetry applications, KUNAK has designed a wireless critical system using the LoRa modulation in the 169/433 MHz band. The system can also be configured to work in the 868MHz band for medium range or high throughput, low latency applications (not covered by the LoRaWAN standard: LoRa@37.5Kbps, FSK@300Kbps).

Thus, it has been designed a modem based on the SX1276 transceiver [7] with an ultra-low power Cortex M4 microcontroller running a proprietary stack to set star networks with bidirectional confirmed communications. The modem can be configured through a host microcontroller at any available modulation scheme in the SX1276 transceiver allowing sensitivities down to -149dBm (18bps), high data rates of 300Kbps, output power up to 27dBm and different frequency bands (169/433/868 MHz). Also, interesting features such as Listen Before Talk (LBT), statistics (PER, duty cycle...), as well as automatic acknowledgements are included within the

stack to guarantee packet delivery, network status and health, reduce errors, retransmissions and power consumption.

Finally, a Gateway has been designed to centralize the *end nodes* information, built the start network and send the information to the cloud. This device is based on an embedded Linux platform, running the proprietary gateway stack to manage the previous LoRa modems, with a 4G/3G/2G modem and ethernet connection; everything encapsulated in IP67 enclosure. The gateway requires continuous power supply since no battery back-up is included in this first version.

KunakCloud: a cloud-based platform, hosted on Amazon Web Services (AWS), has been designed, with the architecture showed in figure 4, to manage the devices and sensors, store the information and check the overall system performance and health; from anywhere with Internet access.

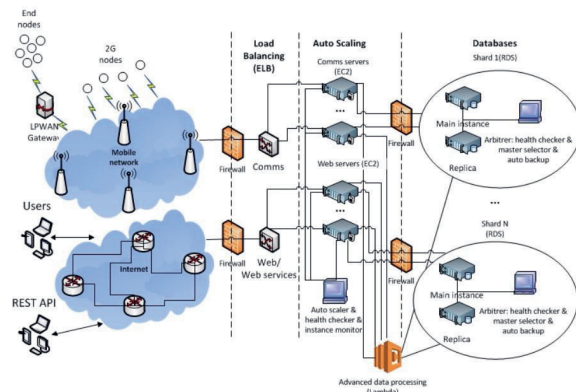


Fig 4: Cloud-platform architecture.

The platform is also responsible of data integrity and interoperability, abstracting the users from any technology involved in the whole system. That is, the user interacts with sensors, devices and configurations such as in a wired system, leaving to KunakCloud the whole responsibility of managing the communications, information, configurations... or automatically recover from any error in communications or servers. RTUs and Gateways has also been designed to automatically recover from any fault, store the information if the communications fail and finally guarantee the delivery of the information to the cloud.

So, all the firmware and software involved in the system is able to handle any errors that may occur and even manage its own recovery. KunakCloud monitors all the control variables, making decisions depending on these, in order to guarantee its integrity based on the boundary conditions.

Thanks to the data model and cloud architecture, new virtual objects, conditions, rules, etc, can be created to model any desired situation with a combination of real time information from different RTUs, external data and advanced calculations. Thus, real time algorithms are running in the cloud to supervise the desired situations. This is used in this project to model the whole hydroelectrical infrastructure and water canals and create intelligent alarms.

4. Field Deployment

The monitoring of six different hydroelectrical infrastructures located in Spain was required within this first pilot deployment, five of them in the Pyrenees and another one in Cantabria. For each infrastructure a deep study was carried out to detect critical points and sections, all the way long of the water canals, where a breakage could produce any risk to human beings, civil works, roads, villages... resulting in 23 hazard points to be monitored.

All these points have access to 2G cellular coverage instead of 3 points of the Betolegui Infrastructure, located in the area of *Selva de Irati* (known for being the second largest beech-fir forest in Europe). Therefore, 20 points were monitored with 2G communications RTUs, and a LoRa star network was deployed in Betolegui to reach this challenging area.

Sensors: Every monitoring point was equipped with a hydrostatic sensor, as previously explained. All of them were installed protected with a PVC tube inside the water canal, as shown in figure 3. In order to evaluate the long-time performance on field of ultrasonic sensors [2], two points were also equipped with this fast response sensors to measure the distance to the water.

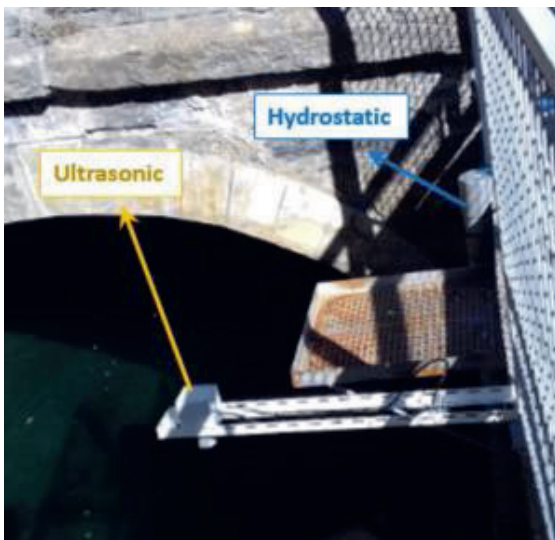


Fig 5. Hydrostatic and ultrasonic sensors installation.

Once the sensors were installed, the operator used the Software Configuration Tool, provided with the RTUs, to configure the sensor's power supply source to one second pre-heating time and to calibrate the 4-20mA sensor output to give the absolute water height inside the canal. Sensor readings were configured at 1-minute sampling interval. In the case of ultrasonic sensor, 2 seconds pre-heating time was used and the pulse width output was read and converted to distance, after being averaged and filtered, by the RTU.

2G Deployments: as mentioned before, 20 points have 2G cellular coverage, 17 of them use solar panels and just 3 of them primary batteries. All of them were installed on the top of 3 meters mast, with 9dBi Yagi directional antenna (figure 6). Installation of those points were easy and fast without any previous coverage study since it was known the existence of cellular signal. On field, the Software Configuration Tool was used to point the antennas to maximize the received signal.



Figure 6: 2G RTUs with 3.5W installed on the top of a 3 meters mast on a water canal side.

LoRa Deployment: in the case of Betolegui infrastructure, a radio coverage study was performed to choose the best frequency and radio configurations and check the viability of this wireless network over the orography.

In the area, a spot with 4G/2G cellular signal and power grid access was located around the middle of the water canal course which could be a good point for the Gateway installation. So, the coverage study started from this point.

First of all, a LoS analysis was realized with the tool included in google earth, checking that there wasn't LoS with any of the monitoring points (Fig. 7). So, the use of 2.4GHz ISM frequency band was impossible with star

networks, almost discarding the use of 868 MHz band without needing any previous study.

However, a simulation with the LoRa System parameters at 868, 433 and 169 MHz was carried out, using the RadioMobile [8] software, to have an approximate performance estimation before field tests. Thereby, it was checked, as shown in figure 8, that the 868MHz frequency didn't reach almost any critical point in the

infrastructure (coverage area in black color); getting an appreciable improvement with the 433MHz band (extended coverage in red). However, some points were still not reached or near the sensitivity values. Finally, thanks to the higher output power available in the 169MHz band and its better propagation behavior, it was possible to provide a reliable coverage to the whole valley as well as most of the places in 100 Km² (extended coverage from previous frequencies in yellow color).

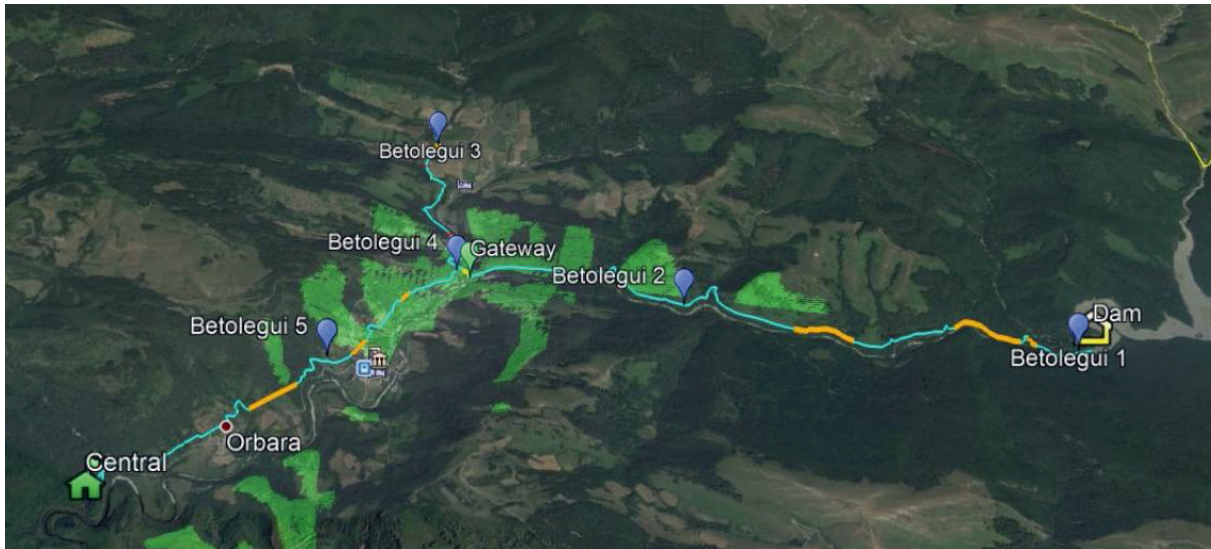


Fig 7. Line of Sight analysis from the Gateway point of view. The water canal and every critical point to be monitored is indicated on the map as Betolegui 1,2,3,4,5. Also the dam and the hydroelectrical plant ("Central").

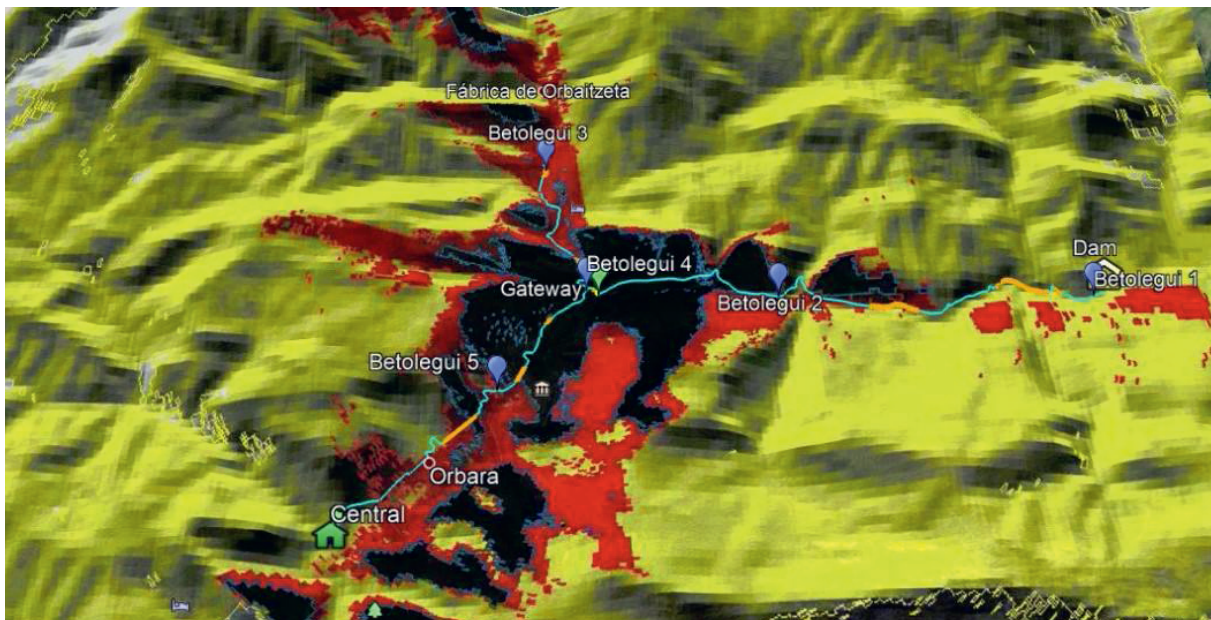


Fig 8: Areas with signal levels above sensitivity (-137dBm) for three different ISM Sub-GHz frequency bands and output EIRP: 14dBm for 868MHz (black), 433MHz (black+red), 27dBm for 169MHz (black+red+yellow)

That's why, it was decided to use the 169 MHz band, with an output EIRP of 27dBm and 41.7KHz bandwidth, to fulfill the European directive requirements. A spreading factor of 10, to have initially a -137dBm sensitivity at

325bps, was chosen to reach the highest link margin as possible without compromising the duty cycle restrictions as just very few devices were going to transmit data once every 5 minutes, corresponding to less than 1% duty

cycle, even with retransmissions under communications failures.

After that, a deeper analysis of every point to point radio link was realized with the same software. Here it is only presented the worst-case point, Betolegui 1, at 4.8Km distance from the Gateway, where the NLoS scenario can be clearly appreciated in Fig 9. An estimation of -114dBm received signal was calculated by the Software. The other points were expected to receive around -100dBm.

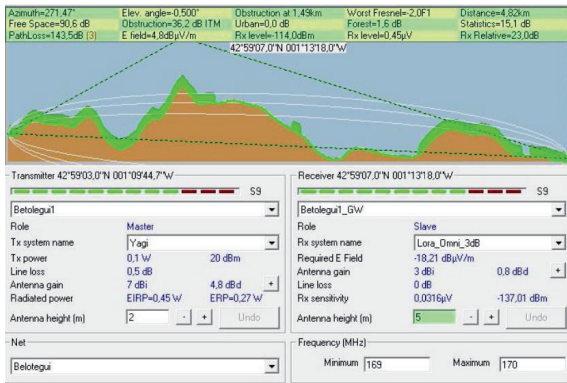


Fig 9. Betolegui 1 to Gateway Radio Link Analysis.

Therefore, it was decided to deploy the LoRa Wireless Sensor Network with the same configuration than the simulations, to have at least 20dB link margin that could hold up any unforeseen once installed. The RTUs were installed with different antennas, in order to test on field their influence in the performance of the system and check the coincidence with the simulations. The gateway was installed with a 3dB omni-directional antenna, Betolegui 1 with a directional 7dB Yagi antenna (Fig. 10) and the other points with 2dB (Fig. 11) and 0dB omnidirectional antennas.



Fig 10. Betolegui 1: 7dB directional Yagi Antenna

The same Software Configuration Tool was used to point the antenna towards the Gateway, and configure the sensors as previously explained.

Cloud-based platform: With all the information being received in a reliable way in the cloud, two different software customizations have been realized:



Fig. 11: Betolegui 3: 0dB omnidirectional antenna.

1. Definition and design of virtual objects (water canals), advanced algorithms, conditions and alarms to model the different infrastructures and supervise their status and health.
2. Specific dashboard for the easy visualization of the water canals status, their parameters and alarms (Fig 12).

In order to automatically supervise the infrastructures health, each canal was split into different sections by using critical checkpoints where the RTUs were installed. Checkpoints were characterized by a series of civil engineering parameters, used as input to calculate flow levels and alarms.

Flow sensors were virtually created based on relations between the civil engineering parameters and the water level measurements. For every water level sensor there was a virtual flow level sensor.

Alarms were triggered on a time basis relation between the flow levels of a checkpoint and the previous one. If a checkpoint has a current flow level higher than the water flow level of the previous one some time ago, it means a possible partial break or partial break. In a similar way, lower level means a possible obstruction or obstruction.

Using these advanced algorithms, it's possible to identify an alarm with a bounded resolution both in time and space.

Thanks to the cloud architecture and its anywhere accessibility, operators could access on site to the data measured by the RTUs, using a Smartphone App, to check the sensor readings, health and status of the RTUs before leaving the installation site. Also, this App helps them to access the information in real time during maintenance works or in case of alarms.

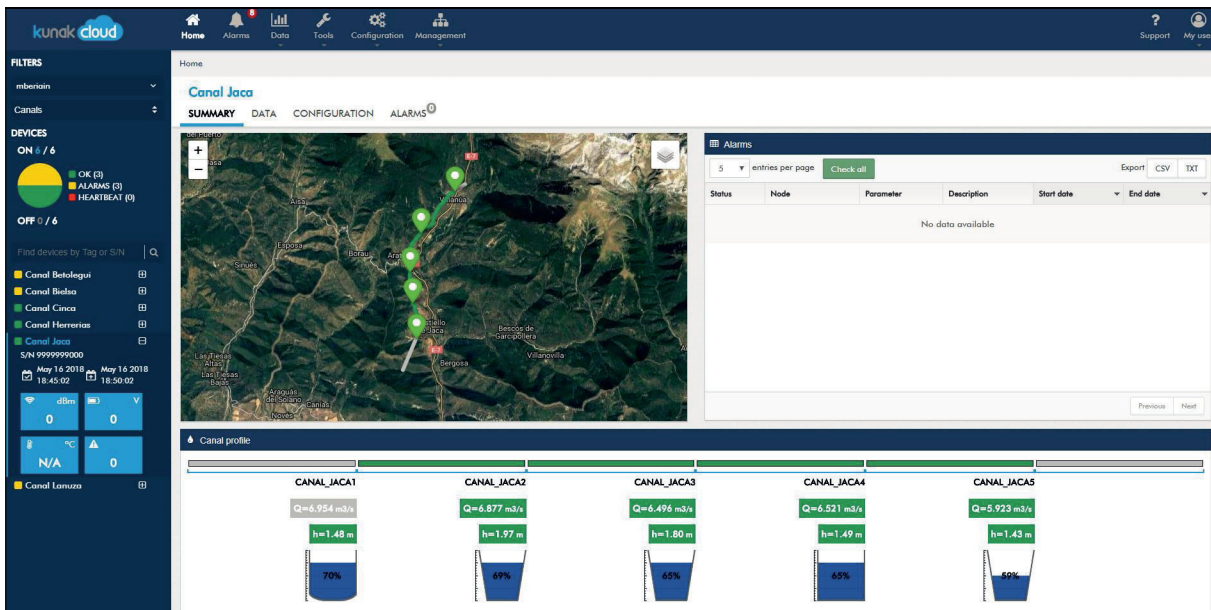


Fig. 12. Customized dashboard visualization. Every critical point is located on the map, dividing the different sections of the canal and reporting a water level and flow values.

5. Field Results

After 10 months continuous operation from the field deployment, the system has shown high reliability and robustness with no fails.

Sensors: hydrostatic pressure sensors have demonstrated great performance on field, with high accuracy and reliability (this application just required 1% accuracy). Comparing to the ultrasonic sensors, the field results show a correlation $R^2=0.99$ with very similar accuracy over the whole environmental conditions (-15 to +40°C). However, in presence of heavy rain, the ultrasonic sensors have shown an increased noise about 1% of the reading, that could be reduced with better filtering and signal processing. Sporadic spikes in the ultrasonic sensor reading have also been appreciated which could also be filtered by improved signal processing.

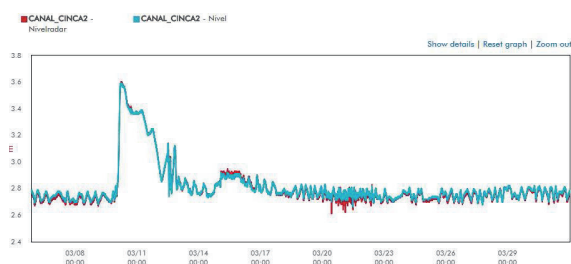


Fig. 13. Hydrostatic vs ultrasonic sensors.

2G Communications: after 10 months operation time, the 2G communications have demonstrated to be very reliable, even in rural environments, with 99% successful communications every 5 minutes (within no more than 1-minute delay). Most of failed communications were solved in the next 5

minutes period with just 0,015% communications problems lasting more than 15 minutes (normally less than 1hour). Most of these communications problems were caused by the base stations that sometimes are battery operated in rural environments, experiencing in one situation 8h continuous downtime. However, the whole information during communications problems was stored in the RTUs and finally transmitted to the cloud once the communication was reestablished.

RTUs: devices have been working from -15°C to +40°C without any problem. Batteries have shown a great performance even on cold, being able to charge below 0°C, achieving a capacity greater than 60% all the time for most of the RTUs.



Fig. 14. RTU after a snowstorm.

LoRa Communications: the wireless sensor network designed has been proven on field, achieving great performance under every environmental conditions. Simulations have shown to be very reliable in 169MHz as the

average signal received by the gateway from Betolegui1 is -113dB (-114dBm simulated) and -110dBm for the other points (10dB worse than expected). This difference could be produced by the antennas installed, resulting in a much better and stable performance of the Yagi antenna than the omnidirectional ones (as expected). Also, the RTU with the Yagi antenna has maintained the same received signal from installation while the RTUs with omnidirectional antennas have shown a deterioration in the received signal of around 10dB.

Hydroelectrical infrastructures: Having accurate information about the water level inside the canals every few minutes provides a great value, since it allows to have a complete control of the evolution of the water level along the whole canal enabling alarms detection when there are unusual levels. Thereby, previously unknown events, like level drops due to dirt or other actions that occur upstream the beginning of the canal, has been detected very easily (Fig. 15)

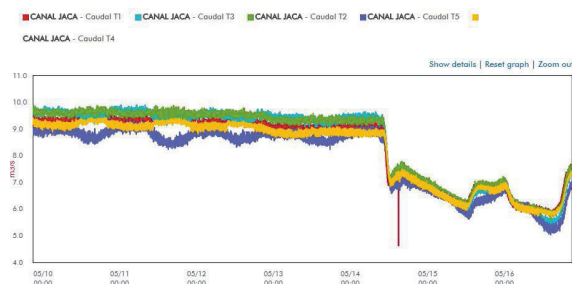


Fig.15. Flow fluctuations in a water canal.

6. Conclusions

Conclusions are presented from the system performance point of view and from the infrastructure digitization results.

System Performance: having a distributed cloud telemetry platform facilitates the deployment of RTUs, sensors and IoT devices anywhere on earth, using Internet as a virtual communications channel that can be extended wirelessly through innovative LPWAN. The system has been globally designed to add very easily new devices on demand, no matter what their location are.

System reliability and robustness has been proven in this deployment, enabling real time information with autonomous RTUs as if it was a wired solution.

Low power consumption ultrasonic sensor has been tested on field with very good results comparing to hydrostatic sensors. Thus, they offer an alternative for applications where 1-3% accuracy is allowed.

Finally, a new multi-band LoRa star network has been designed and tested at 169MHz on field, achieving incredible performance in terms of coverage and reliability, reaching remote locations where before it was not possible to monitor. The use of Yagi antennas is recommended for these deployments, resulting in higher received signal stability reaching similar values than those simulated with RadioMobile.

Hydroelectrical infrastructures digitization: Before this project, ACCIONA didn't have the possibility of gathering real-time data from difficult access isolated points, losing the control of the health and events in the canals.

Thanks to this project, the operations have been digitized enabling data-informed decisions with real-time intelligence.

Unknown behaviors of the water canal levels have been evidenced in parts with non-uniform geometries as well as variations in the inflow rate due to upstream affections. But most important, the high frequency of data has allowed to generate alarms for the early anomalies detection in the cloud and hence the reduction of affections by rapid action.

Overall, the presented solution implements real operational intelligence turning real-time data into actionable results; with an easy to deploy and operate software solution that connects sensor-based data, structures, and people to generate real-time, geo-located insights.

Acknowledgements: The authors wish to thank the whole KUNAK Team for their commitment and work, specially Mikel Beriáin and Asier Galech, for their collaboration with the cloud platform and the LoRa gateway design, and Jacopo Soffritti, for his help with the simulations. Also, the whole ACCIONA team for their support and professionalism on field installation.

References

- [1] Instrument Engineers' Handbook, Fourth Edition, Volume One.
- [2] Datasheet MA-403: <http://www.inst-apli.com/>
- [3] Datasheet MB7369: <https://www.maxbotix.com/>
- [4] <https://www.semtech.com/uploads/documents/an1200.22.pdf>
- [5] <https://www.sigfox.com/en/sigfox-iot-technology-overview>
- [6] <https://LoRa-alliance.org/>
- [7] <https://www.semtech.com/products/wireless-rf/LoRa-transceivers/SX1276>
- [8] <http://www.ve2dbe.com/english1.html>

Real-Time access to past measurements using bidirectional communication (TmNS)

Heiko Körtzel¹, Guillermo Martínez Morán², Christian Buechner¹

¹ Airbus Defence and Space GmbH, Manching (Germany)

² Airbus Defence and Space S.A.U., Getafe (Spain)

heiko.koertzel@airbus.com, guillermo.m.martinez@airbus.com, christian.buechner@airbus.com

Abstract:

A fundamental principle of the **Telemetry Network System** (TmNS) approach is to enhance, rather than replace, today's telemetry systems by providing significant improvements in order to revolutionize how flight tests are executed. One of the highlight is the capability to **access in real-time past measurements** (onboard recorded data, while still recording new data) by using the **bidirectional communication of a TmNS**. This paper outlines the approaches taken to implement such a function on an airborne/ground network.

Key words: Telemetry Network System, TmNS, bidirectional communication, record, replay

Introduction

One key element in flight tests is a measurement data recording capability onboard. Here data is collected from several sources like sensors, data busses, data acquisition systems and video systems through suitable interfaces and stored on storage media within the aircraft under test. Beside this data recording capability a data downlink telemetry capability is another key element in classical flight tests and it is obvious that in most cases the sustained data throughput is very different for those both data sinks. For example data recording bandwidths onboard can be hundred times higher (or even more) than data downlink telemetry bandwidths used for flight tests. In classical flight tests the reduced data set to be transmitted over the downlink telemetry channel is predefined pending on the test purpose and achieved by filtering the data onboard before routing them to the telemetry channel and for backup reason also to the onboard recording system.

Within an Airbus Defence and Space internal R&T project called "Interactive Bidirectional Telemetry (IBT)" the establishing of a bidirectional communication should be analyzed as well as several use cases of interest and necessary functions needed in the airborne and ground network. Furthermore the approach should be aligned with the Telemetry Network System (TmNS) featuring selected highlights intended to be reached with TmNS. Among different kind of use cases one out of them is the dynamic change of the data set which is

transmitted over the downlink on request of the flight test engineers. Based on the limitation in bandwidth of the telemetry downlink channel two main reasons for this need are predominant. First, pending on the test purposes or pending on unexpected system behavior during a flight different sets of filtered data could become necessary to be transmitted. Second, due to possible telemetry interruption a retransmitting of data could become necessary rather than wait till access to the onboard storage media can be get (e.g. after aircraft landing).

Guidelines and Requirements

There are several conditions which has to be followed for an implementation of a retransmission function in a flight test instrumentation (FTI) system.

Architectural:

Since all measurements are stored onboard a replay back into the downlink transmission system of a past time slice would be a suitable way to retransmit data. In order to achieve this, switching functions in the airborne instrumentation architecture would become necessary to reroute the data flow. Further the recording system has to provide a controllable and dynamical access to the stored data which shall be compatible to the mentioned switching function. Moreover in any case a continuous onboard recording of the whole data set has to be assured. Another architectural guideline can be the constancy of the telemetry channel. So for a seamless operation between live data and

replayed data the data framing and key figures of the channel should remain identical.

Operational:

Since the need for access of past measurement data may arise unpredictable, the flight test engineers, as the main users of the telemetry data, need a way to change the onboard system into a replay mode on their request. This request has to contain at least start time and end time or duration of the replay and should be given through a suitable user interface.

Safety:

Since the telemetry data are a primary source of information of the state of all aircraft systems and as such a basis for decision even for safety aspects a clear situational awareness shall be present all the time during the execution of a flight test. Therefore a clear indication if the displayed data is a replay content or a live content is needed to all involved persons following the flight test. Furthermore an automatic switch back to a safe state has to be implemented onboard.

Architecture

An Ethernet based onboard architecture including a central manageable network switch allows a flexible data routing implementation. Such a central network switch with at least 6 ports can receive UDP data from a FTI data acquisition system (DAS) on port 1, route them over port 4 and 5 to recording ports on a recorder and over port 6 to a telemetry bridge. While port 2 is used for receiving control commands, port 3 is used to configure the recorder. The recorder itself shall provide 2 Ethernet recording ports to receive UDP data. The first one to receive high bandwidth data for post flight analysis and the second one to receive low bandwidth telemetry data for a later replay. Furthermore the recorder shall provide a general Ethernet port for configuration and control purpose as well as for streaming out recorded data in the replay case. Not mandatory, but for a more simple architecture a IRIG106 Chapter 7 telemetry bridge inside the recorder is desirable (see Fig. 1).

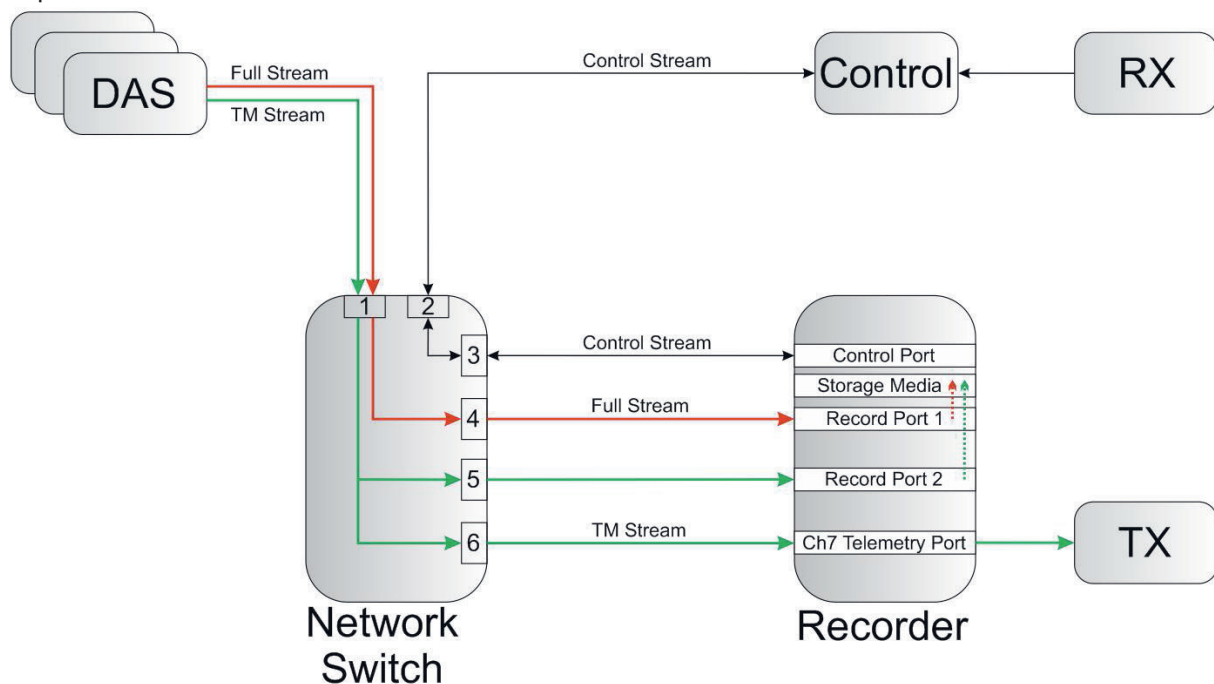


Fig. 1. Architecture with data flow in case of live data telemetry

An uplink RX system receives control commands. Those commands are analyzed and validated by a control system which also initialize on request a reconfiguration of the switch and the recorder. After such a reconfiguration for a data replay, the switch

stops the routing of live telemetry data from port 1 to port 6 and routes instead replay data from port 3 to port 6. While the recorder is reconfigured to replay data of the previously recorded telemetry data stream over its control port to the port 3 of the switch (see Fig. 2).

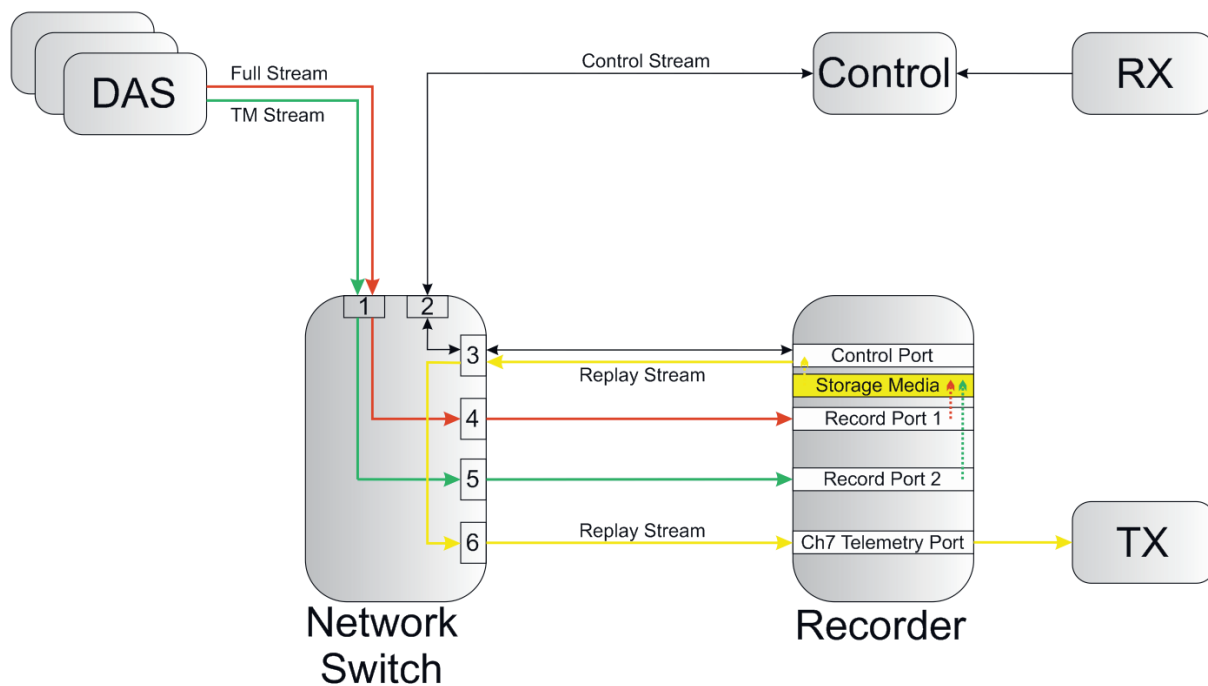


Fig. 2. Architecture with data flow in case of replay data telemetry

Implementation

Within the setup of the Airbus Defence and Space internal R&T project, the DAS generates a MPEG-TS video Ethernet stream, that is recorded and streamed according to the configuration of the network switch to a Remote Control Application, that is capable to decode the video Ethernet stream provided by the DAS or the recorder. The implementation of this R&T project can be divided into a hardware part and into a software part.

On the one hand the hardware part within the FTI architecture with dedicated connections to control the network switch and recorder. On the other hand the software part, which is part of the control unit to receive and translate data coming from a remote control application (see Fig. 2 – RX and TX block)

Hardware:

For this R&T project following hardware was used:

Control Unit

The control unit is a standalone device equipped with an Ethernet TCP/IP interface provided by i.e. a microcontroller, PC, etc. The control unit is connected to the network switch directly and to the recorder over the network switch (see Fig. 2.).

Remote Control Device

As Remote Control Device a standard PC is used, running the Remote Control Application on it (Fig. 2 – RX and TX block).

Network Switch

A NSW-12GT-1 twelve port Gigabit airborne network switch provided by Teletronics Technology Corporation (TTC) was used [1].

Data Acquisition System

The DAS system consist of an ACRA KAM-500 chassis equipped with a KAD/BCU/140 Ethernet backplane controller (IENA/iNET-X) and a KAD/VID/106 video module, provided by Curtiss-Wright [2]. The captured video is distributed by the Ethernet backplane controller via TCP/IP encapsulating iNET-X and MPEG-TS frames.

Recorder

As data recorder a Zodiac Data Systems MDR-8shRC equipped with an Ethernet module (METH2) and data storage provided by ZODIAC AEROSPACE was used. [3]

Software:

The software itself is also sub-divided in two parts. First the remote control application, that is sending control commands to the control unit and decoding the Ethernet telemetry data stream. Second the application running on the control unit, which receives control commands from the remote control application and configures the network switch and recorder according to the received remote control data. As programming language Python 3.x with QT framework was used.

Control Unit Application

The control unit application is a stand-alone application that can be executed without a graphical user interface and no user interaction. The software architecture can be splitted in three parts. The first part is a TCP/IP server awaiting data from the remote control application. If data is received it is processed according to the command (start/stop replay). The second part controls the network switch configuration. To configure the network switch, a TCP/IP Telnet connection between the switch and control unit is established.

Afterwards, in case of configuring the switch to route replay data from the recorder, the dedicated IP routing table for the specific port is changed. Now replay data provided by the recorder, available at switch port 3 is routed to port 6 and transmitted by the IRIG106 Ch7 telemetry module within the recorder (see Fig.2). If a stop command is processed by the control unit, the network switch is reconfigured by TCP/IP telnet commands to route telemetry data coming from the DAS to the IRIG106 Ch7 telemetry module again (see Fig.1). Within the network switch only the routing table for the involved switch ports are modified, that only specific multicast IP Ethernet streams are blocked or not blocked for involved ports.

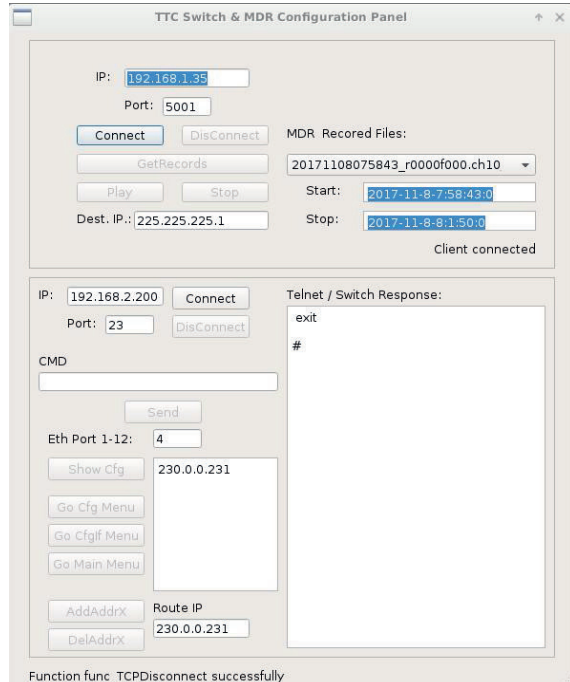


Fig. 3. GUI Control Unit Application

Just after the network switch configuration, the third part of the control unit application is initiated and directs the recorder. The recorder provides three different control modes:

- IRIG-106 remote commands (serial connection)

- Simple Network Management Protocol (SNMP) commands (by TCP/IP)
- UDP remote access (by TCP/IP)

The control unit application uses the UDP remote access for recorder communication.

In the first step the control unit application queries the name and start/stop time of all recordings from the recorder. Afterwards the recording file is selected that matches the start/stop time for replay data (start/stop time is retrieved from the remote control application).

bits	15 (msb)	8	7	(lsb) 0
bytes	+0		+1	
+0	max_udp_size (uint16)			
+2	tmats_interval (by default = 0) (uint16)			
+4	op_mode (uint8)		speed_mode (uint8)	
+6	speed (uint16)			
+8	reserved1 (0) (uint16)			
+10	reserved2 (0) (uint16)			
+12	reserved3 (0) (uint16)			
+14	reserved4 (0) (uint16)			
+16	start_year (uint16)			
+18	start_month (uint8)		start_day (uint8)	
+20	start_hour (uint8)		start_minute (uint8)	
+22	start_second (uint8)		start_10ms (uint8)	
+24	stop_year (uint16)			
+26	stop_month (uint8)		stop_day (uint8)	
+28	stop_hour (uint8)		stop_minute (uint8)	
+30	stop_second (uint8)		stop_10ms (uint8)	
+32	{			
...	file_name (512 bytes)			
...	}			
+542	}			
+544	mcb			
+546	nof_subcomponents (uint32)			
...	lcb			
+0	{			
+2	destination_ip (by default = 11.59.31.255) (uint32)			
...	lcb			
+4	mcb			
+6	destination_port (default = 2000) (uint32)			
...	lcb			
+8	mcb			
+10	nof_channel_ids (uint32)			
...	lcb			
+0	{			
+2	channel_id (def = -1 for no filter) (uint16)			
...	reserved5 (0) (uint16)			
...	}}			

Fig. 4. Recorder UDP Start Replay command [4]

Afterwards a specific UDP control frame (see Fig. 4) is send to initiate replay data from the recorder. The main settings in this control frame are filename, start-/stop time for replaying and multicast destination IP address and port. From now on replay data is streamed by the recorder in IRIG-106 chapter 10 format, encapsulated in a UDP Ethernet frame. If replay data streaming has stopped a command is received from the remote application and the IP routing table of the network switch is changed to route data coming from the DAS to the telemetry gateway again.

Remote Control Application

The Remote Control application (see Fig. 2 – combination between RX and TX block) provides a graphical user interface (GUI), with all parameters that are necessary to start data replay of specific recorded data. The main functionality of this application is to establish a TCP/IP Ethernet connection to the server provided by the Control Unit application. The Remote Control application encapsulated a start/stop command combined with start/stop time for the data replay and transmits this data to the Control Unit where this data is extracted and starting or stopping replay data is initiated. Another functionality of the application is detecting UDP Ethernet data provided by the Recorder or DAS. If data replay has finished, a stop command is transmitted to the control unit application to initiate reconfiguration of the network switch to route the DAS TM (telemetry) data stream to the recorder IRIG106 Ch7 telemetry gateway module again.

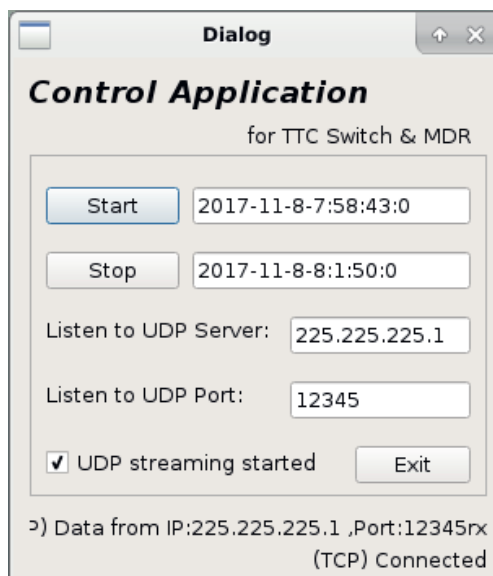


Fig. 5. GUI Remote Control Application

To decode a telemetry Ethernet data stream, the application must handle different Ethernet frame formats encapsulated in each other. For example a video Ethernet data stream provided by DAS can consist of following encapsulation:

ETH/IP (UDP (IENA/iNET-X (MPEG-TS)))

If this data is replayed by the recorder the encapsulation of this stream will increase to following framework:

ETH/IP (UDP (IRIG-106 Ch10 (IENA/iNET-X (MPEG-TS))))

For evaluation purposes the Remote Control Application running on a dedicated PC is connected to the network switch directly to pass the IRIG106 Ch7 telemetry gateway module

and to extract encapsulated data without the need to decode IRIG-106 Ch7 header.

Summary

This first implementation of a real-time access function to past measurements shows a seamless operation between transmitting live data and replay of stored data. All architectural and operational guidelines were implemented and the final implementation of safety guidelines should be easily feasible with the Control Unit Application. Furthermore this implementation can be considered as a practical use of some features emphasized by the TmNS Standard as followed [5]:

“The IP network foundation of the TmNS brings with it features including routing, Quality of Service (QoS), and congestion control. The following list highlights some of the capabilities that IP networking brings to telemetry.

- *Addition of Bidirectional Communications to Telemetry: bidirectional communications is one of the most fundamental enhancements provided by the TmNS. It enables the following capabilities.*

- o *Real-Time Access to Test Article (TA) Measurements: Provides a mechanism for real-time access to current and past measurements on the TA both directly from the sensors and from the recorder(s).*

- o *PCM Backfill: Provides the ability to retrieve measurements from the TAs in near real time that were dropped in the Serial Streaming Telemetry feed (PCM dropouts).”*

References

- [1] Teletronics Technology Corporation, NSW-12GT-1 Manual, Revision D, 8/29/16
- [2] Curtiss-Wright, ACRA KAM-500 Databook, HW/BK/0002, 12/04/2017
- [3] Zodiac Data Systems GmbH, Technical Specification HEIM DATaRec 4 MDR-8s/MDR-8sf, Doc. 56024102

Zodiac Data Systems GmbH, Technical Specification METH2, METH2A, Doc. TS_METH2_METH2A_160419_HD5620041R018 35.fm
- [4] Zodiac Data Systems GmbH, DATaRec® 4 Series, Programming Manual, Version 1.41, 4/4/2017
- [5] Telemetry Standards, RCC Standard 106-17 Chapter 21, July 2017

System for Aircraft Data Value Demonstration

Stanislas Martin

AIRBUS Operations SAS, 316 route de Bayonne 31060 Toulouse, France
stanislas.martin@airbus.com

Abstract:

In the frame of the Skywise data avionics platform, an end-to-end prototype was developed, certified and deployed in airlines, with the objective to demonstrate the value of aircraft data.

This on-board connectivity system is composed of existing flight test means to acquire massive data on board and of standard industrial components to transmit data directly to Airbus data lakes after each landing via standard 4G infrastructure.

These data were then analysed by a Smart Data Analytics plateau to develop algorithms, in order to improve maturity of the aircraft or give recommendations to better operate the aircraft.

Thanks to a strong commitment and a trans-functional and trans-national team work, it has been possible to design, manufacture and certify the Skywise-demonstrator in a very short time frame (five months).

The system has been installed on in-service aircraft by the team and is operating in real airline operations. Since its entry into service in December 2016, the demonstrator has sent over 10 Terabytes (TB) of in-service data from five airlines worldwide. More than 100 algorithms have been developed and validated by Airlines, thus demonstrating the value of aircraft data analysis.

Key words: Data, connectivity, value, prototype, certification.

Context

For several decades, aircraft include a high number of avionics systems which are exchanging data between each other. However, on many aircraft, most of these data remains "inside" the aircraft and is accessible neither by the airline nor by the manufacturer. This is particularly the case for the Single Aisle aircraft family (A319/A320/A321) which initial conception did not integrate the capability to retrieve a high amount of aircraft internal data. Indeed, standard systems allow retrieving a few hundreds of parameters amongst the 24,000 really present.

Yet, it was strongly foreseen that accessing to more in-service data could bring great benefits to all parties. It would indeed be a way to improve knowledge on how aircraft are operated all along their life and in their real commercial environment.

The assumption was therefore that analyzing more in-service aircraft data would lead to:

- Improving the design of the aircraft (in addition to the flight test data traditionally used for this purpose)
- Enhancing services and recommendations to operate the aircraft more efficiently

- Solving in-service issues quicker and/or more efficiently

While launching a long-term activity to develop a data collector and connectivity system that could be installed on the whole Single Aisle aircraft fleet, it was decided to quickly develop an in-service demonstrator to:

- Run this scenario on a few in-service aircraft in order to confirm these benefits. In other words, to demonstrate data value.
- De-risk the industrial solution, by better identifying the pain points and upcoming difficulties.

This in-service demonstrator was also the opportunity to develop partnership with some airlines by addressing some concrete use cases at an early stage, thus allowing more efficient work with common interest between Airbus and its clients.

This article will describe the chosen solution for the embedded part of this demonstrator. It will then explain how it has been implemented, focusing on the challenges encountered and the success key factors. Finally, general results will be given.

It should be noted that it is not in the perimeter of this document to address legal and financial topics.

Technical solution

Considering a strong timing constraint, the opportunity to use already existing systems was essential. Consequently, the solution was built

on systems already used on flight test aircraft, and completed with commercial-of-the-shelf (COTS) systems.

The on-board system consists in two main functions described below:

- Acquisition of on-board data
- Automatic wireless transmission from board to ground

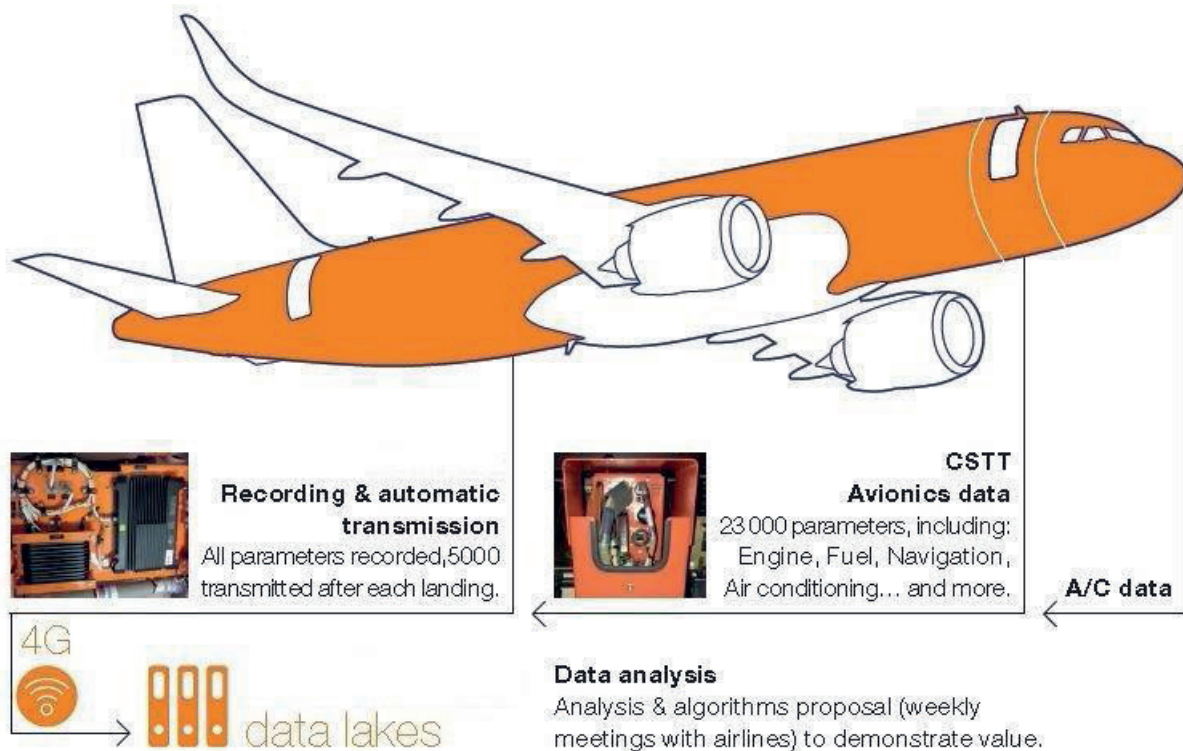


Fig. 1. General architecture principle of the demonstrator

The first function – acquisition of on-board data – is ensured by an acquisition unit already largely used for the flight tests of the production aircraft. This system is called PATS (Production Aircraft Test System) for its use in a flight test context, and is called CSTT (Customer Support Test Tool) in its certified version. It consists in a 4-MCU ARINC-600 chassis which can easily be installed in the electronic bay (in identified available slots) and connected to the aircraft avionics ARINC-429 buses. The CSTT system then automatically and continuously receives and acquires the complete avionics data: every sample of every label on all the buses, which corresponds to a set of approximately 24,000 parameters. The system then merges those parameters on a single Ethernet wire.



Fig. 2. Acquisition unit (CSTT system)

The second function – Automatic wireless transmission from board to ground – is ensured by a connectivity system built around COTS components (an industrial 4G router and its antenna, and ruggedized computing unit) associated with FTI units for managing power conversion. These units are installed on a

support plate specifically designed which is installed in the forward cargo area of the aircraft.

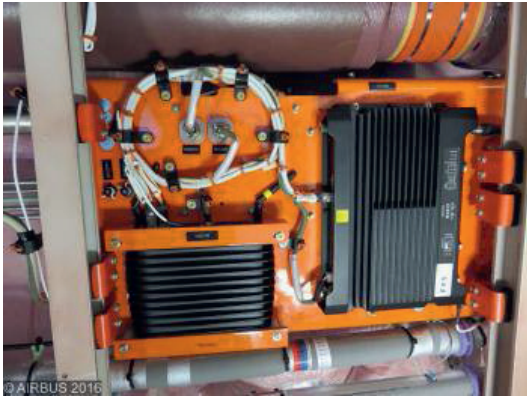


Fig. 3. Pre-equipped plate with connectivity system

All the CSTT data are sent over an Ethernet connection to the computing unit which records them. A part of these data is processed in real-time to allow automatic management of the different operational modes. It can therefore automatically detect the aircraft flight phases and act accordingly. In particular, by commanding the 4G router, the computing unit automatically activates (resp. deactivates) the 4G communication when the aircraft is on ground (resp. in flight). In doing so, after each landing, a large set of data acquired during flight (approximately 5,000 parameters selected amongst the 24,000) is automatically downloaded from the aircraft to the ground. The 4G link indeed allows sending the data directly from the aircraft to data lakes inside the Airbus network in a secured way over the standard telecommunication infrastructure.

An internal community of Airbus specialists can then access this high amount of data and proceed to various analyzes in very different technical fields.

Challenges and success key factors for quick implementation

One of the main challenges encountered was the time constraint. The target at start of the very beginning of the project was to install such a demonstrator on an in-service aircraft within a few months whereas traditionally, developing and certifying in-service aircraft equipment is generally a matter of years.

First, a quick development has been possible as it was built on existing components. Lab and flight tests were then also done in a short time frame. As for certification, it focused on safety aspect, ensuring that the system could be installed and operated on aircraft – for a limited period of time – in a safe way. Long-term

reliability of the functional aspect was not deeply demonstrated (aircraft can fly safely at its full capability even if the Skywise demonstrator system cannot ensure its function).

The very special team spirit around this project has been a key factor for its success. Efficiency was achieved thanks to a reduced team – with an “agile” spirit – of people coming from many different Airbus domains: flight test instrumentation, engineering, information technologies, certification, design, manufacturing, customer support, safety, environmental and electrical qualification. All stakeholders were directly involved and strongly supported by internal sponsors. Direct communication channels were used to allow quick decision when needed.

Thanks to this, certification was reached 5 months after project start. It was installed on the first in-service aircraft one month later. Finally, to this date, 11 aircraft (5 different airlines over 4 continents) have flown with such a system since December 2016.

Technical difficulties encountered

Many technical challenges have been encountered during the project. Some of them are exposed hereafter.

One objective was to make the installation of the system as easy as possible, in particular to allow installation on already operating aircraft without generating service interruption. A pre-equipped plate and a harnesses kit were designed to this end. Thanks to this, and to the installation concept of CSTT (use of an available slot in the electronic bay), an installation over one to two nightshifts is generally possible thus allowing installation of the system directly in the airline facilities in its home base airport.

Another challenge was to ensure a 4G worldwide coverage. Many tests were done – in particular across borders – to secure automatic configuration of the 4G router so that connection can be established in any country. A special roaming contract was signed with a telecommunication operator to allow 4G (or 3G as a fallback option) in every region of the world and in most countries.

Next technical issue relates to the management of data downloading to the ground. Whereas the nominal use case is to record data during flight and download all of it directly after landing, some technical risks were indeed to be anticipated. Typically, there could be poor communication (or even no communication at all) in some airports and/or during some time

slots (e.g. 4G not deployed yet, overcrowded network). Therefore, the system needed to be robust against interruption and low download speeds. Algorithms were put in place to manage download interruptions without losing data. Additionally, the number of downloaded parameters has been adjusted (typically 5,000 parameters) to avoid backlog increase and internal storage in the on-board system was ensured to allow saving the data for approximately 1 month in case of difficulties.

Results and benefits

After 18 months of operations on 11 aircraft, more than 10 Terabytes of data have been collected.

Meetings have been held with engineering staff from airlines to target key topics and then propose analysis and algorithms using these data.

This led to a very good feedback from customers and concrete results. For example, the root cause of certain abnormal deteriorations could be quickly identified and appropriate recommendations given to the operator. It also led to a better understanding on how some avionics systems are used, and allowed proceeding to predictive maintenance on some components.

An additional benefit was the ability to know the real 4G heat map on more than 200 aircraft worldwide by monitoring and precisely correlating the aircraft geographical position, the signal level and type, and the resulting bitrate. Indeed, whereas 4G seems to have become the standard nowadays, it is not yet reality everywhere or may have very different performance levels, making this type of information very valuable.



Fig. 4. Heat map for connectivity on European airports



Fig. 5. Heat map for connectivity on an airport

Conclusion

The systems reached its targets by confirming the value of acquiring and analyzing more aircraft data, validating the strategic vision held by the Skywise project. It also allowed to de-risk the industrial solution and to work in partnership with a set of customers which expressed a very good feedback.

Consequently to this new “in-service demonstration” approach, the project has been internally awarded in 2018.

Glossary

COTS	<i>Commercial-of-the-shelf</i>
CSTT	<i>Customer Support Test Tool</i>
FTI	<i>Flight Test Instrumentation</i>
PATS	<i>Production Aircraft Test System</i>
SA	<i>Single Aisle</i>
TB	<i>Terabyte(s)</i>

How to connect a sensor to the Internet

Dipl.Ing. Thomas Schildknecht , Schildknecht AG, 71711 Murr , thomas.schildknecht@schildknecht.ag

Summary

The task of connecting sensors to the Cloud sounds trivial at first. It must be clarified whether a sensor is located within a company network (vertical network) or outside (horizontal network). Within a company network, it is quite simple, it can be very expensive if you cannot access an Internet access infrastructure such as Ethernet & WLAN for technical and / or organizational reasons. The lecture describes which organizational requirements can be found in practice and which technical methods have been proven so far.

1 Mega trends Cloud, Internet of things (IoT) and Industry 4.0

The buzzwords stated above stand for the trend of digitization. Within a corporate network digitization is nothing really new and has been state of the art for many years. Remote maintenance for facilities that are not local is also being used successfully. This application reduces travel times and costs, since in the event of an error access via a so-called VPN (Virtual Private Network) connection is possible. However, VPN connections are reaching their limits when it comes to continuously transferring data from a large number of devices. If these devices are also distributed worldwide, e.g. in an industrial application with pumps, VPN is not scalable and very expensive. Another hurdle is the availability of Internet access technology at on site. Even if a network with Internet access is available to an end customer using the pump, there is little chance that a supplier could also use it to connect its sensor. The security requirements of companies usually do not allow this. This means that in the context of this lecture alternative Internet access technologies will be discussed for these kind of tasks.

2 Connectivity

2.1 LoRa, Sigfox & Cellular Radio 2G-4G

Possible Internet access technologies are LoRa, Sigfox and cellular radio, to name a few. LoRa and Sigfox are only available in a few places. Sigfox relies on a provider to operate a base station on site. LoRa also uses the royalty SRD band at 868MHz, but anyone can operate a base station. The range is in practice between max. 300 to max. 1km, depending on the antenna of the sensors. The technology aims at very cost-effective data transfer of a few euros per year. Data can only be transferred in small packages of a few bytes per day.

Cellular Radio (2G-4G) are available throughout the world. Using this technology, one has to rely on a contract with a mobile service provider who provides and maintains the network and sets a fee for it. Cellular phone contracts have not been offered to date for IoT device requirements. In international deployment, there are also completely new tasks. Roaming functionalities are limited for SIM cards meaning that they are switched off automatically after a certain. Furthermore, roaming partners in the country of use are not guaranteed including network coverage at the site. Previous contracts for M2M (machine to machine) communication are also limited by the data volume and are usually more expensive than end customer contracts. Thus, the industrial user must know at the time of delivery in which country the system will be used later. So far, these limitation limit successful usage of cellular radio technology. The lecture describes a new generation of M2M - IoT SIM cards and contracts with many new possibilities such as eSIM, unseetered roaming and role-based management.

2.2 Cloud Portal

In order to send data from a sensor to the Internet, you need a data storage with an IP address that can be reached worldwide and a software that handles the many different involved. This is called a cloud or data portal.

Currently, more than 700 data portals are available on the market. Data portals from the best-known providers are SAP HANA, Microsoft Azure, Amazon Iot, IBM Siemens Mindsphere, Software AG Cumolocity etc. These portals are almost exclusively data portals that store, process and visualize data. They can be operated within the company network or hosted publicly in a professional data center. In contrast, there are a few device portals that can handle the management of the connected devices, update the operating system over-the-air (OTA), and coordinate users' access rights to devices, etc. One of the most well-known device Portals is iCloud from Apple. Here, the connected "devices" are managed by Apple. This includes the update management of the operating system

and the programs (APPs). This function is also required for IoT devices. The data cloud and the device cloud exchange data through a standardized software interface, the RESTful API.

2.3 Interfaces to the process

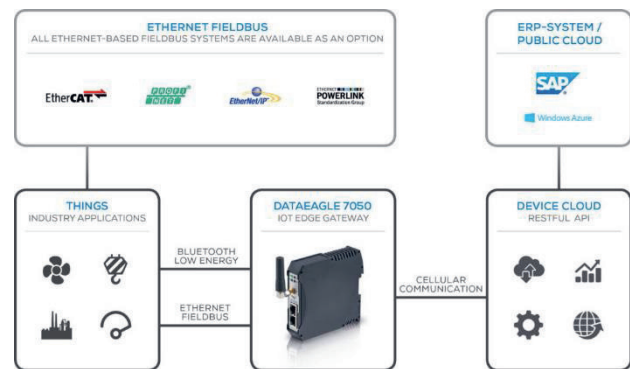
Typical data sources in industrial applications are sensors or machines and their control units. These have partially completely different hardware and software interfaces. These range from 0-10V / 4-20mA analog sensor signals, SPI, RS232 / 485 to fieldbus connections using Profibus, Profinet, or Powerlink etc. Also wireless sensor connections like EnOcean, 802.15.4 (6LowPan), Wifi or Bluetooth Low Energy is already available on the market. These interfaces and protocols are not suitable for data transmission to a data cloud. For this reason, gateways (another term is IoT Edge Gateway) are needed.

2.4 IoT Edge Gateway

Gateways take over the interfaces and protocol conversion from the sensor to the data cloud. Mostly they are stand-alone devices, as this functionality cannot be directly integrated into a sensor (yet). When using one or more wireless interfaces (e.g., Bluetooth for sensor interfacing and cellular for worldwide connectivity), it needs to be considered that every radio system in Europe needs to be certified according to RED (Radio Equipment Directive). Often, this procedure is not economically feasible for sensors as well as time consuming.

IoT edge gateways have a pre-processing functionality, which reduces the received sensor data volume according to application-specific needs. This is needed in order to minimize costs for the data transmission or to increase the service life of the battery during battery operation. In addition to the operating system of the gateway, it must also be possible to transfer new applications such as the rules for pre-processing or the measurement intervals to the gateway. This should preferably be done over-the-air (OTA), so persons are needed locally.

2.4.1 Integration of an IoT Gateway



Picture 1 From „Thing“ to Cloud

3 Conclusion

With horizontally connected data networks a variety of new tasks, from process knowhow, selection of suitable sensors, the connection to control units, connectivity, IT protocols within the Internet communication, complex security requirements up to the contract design with the mobile radio providers arise. Thus, the goal is to integrate all these functions into a gateway and device cloud, that provide standard interfaces to the sensor and to many data clouds through the device cloud.

Real Time Data Validation Embedded System for Flight Test Using Common Portable Devices

A. MSc. Andre Yoshimi Kusumoto¹, B. Eng Wagner Oliveira Lima¹, C. Dr. Nelson Paiva Oliveira Leite¹
 Instituto de Pesquisas e Ensaios em Voo (IPEV)
 Pça Mal. Eduardo Gomes nº 50, Vila das Acácias, São José dos Campos, SP
 12.228-901 - Brazil - +55 12 3947-7957
 kusumotoayk@ipev.cta.br {A}, cti-e@ipev.cta.br {B}, epd@ipev.cta.br {C}

Abstract:

The flight test data acquisition and data storage process require the integration of a dedicated Flight Test Instrumentation (FTI) for gathering accurate measurement. In a given test flight are performed several test points, which validation requires strict compliance with various predetermined conditions (e.g. 10s speed stabilization at 230kts \pm 2kts @1 σ). Furthermore, for several test flights the validation of a given test point carried out at the Fixed Telemetry Ground Station (FTGS) doesn't solve entirely the problem, because in some cases, the pilot needs additional information (e.g. Command forces), which are not displayed in the aircraft cockpit instruments, to control the execution of a given test point. For small aircraft (e.g. AT-29) there is no available space for FTI and data processing system installation and this precludes the integration of advanced crew information systems. However, the computing power grows of new mobile systems (e.g. Tablets) opens new horizons for the development of such advanced information systems. Therefore, the Instituto de Pesquisas e Ensaios em Voo (IPEV) developed and integrated an airborne ultra-compact information system to be used for real-time test flight management and decision-making or test data processing, validation, displaying and data reduction analysis. Flight tests conducted by EFEV (i.e. Brazilian Flight Test School) 2017 class students were used to evaluate the software and the results were considered satisfactory.

Key words: flight test, real time, data acquisition, data validation, mobile devices.

Introduction

Nowadays, mobile devices usage in flight tests campaigns has increased due to the availability of Flight Test Instrumentation (FTI) wireless components (e.g. IEEE 802.11 - Wireless LAN).

Wireless sensors and Wireless Data Acquisition System (DAS) are offered by companies as a solution for acquisition and validation of flight tests data [1].

In a fighter aircraft where its inherent limited space is a major constraint for installing FTI components, the conventional wired network can be exchanged for wireless network.

Beside the WLAN, there is several other wireless network technologies such as Bluetooth (i.e. IEEE 802.15), but in all cases, the challenges to be surpassed are latency, synchronization and package delivery reliability.

As a general trend, the wireless environment seems to be a reality for the Flight Test community. However, flight safety and data accuracy issues must always be considered for the solution development.

Mobile devices can be used for image acquisition and flight test data processing (e.g. ground weather reference system for Air Data Computer - ADC calibration Flight Tests Campaign) [2].

Another possible solution is the development of a real-time airborne test data visualization application for test point validation.

The implemented solution should consider the current availability of Consumer Off-the-Shelf (COTS) devices. However, the agility in implementing solutions (e.g. apps - application development) and its mobility are attributes that help its integration with legacy DAS.

The availability of real-time data through applications developed under Android environment to be installed in mobile devices for visualization by the Test Pilot is very relevant, because in some cases the Test Crew needs additional information (e.g. command forces), which are not displayed on the aircraft dials, to control the execution of a given test point.

Such feature improves flight test efficiency because it guarantees a successful execution of all test point, mostly when such trials should be performed within a predetermined range of several control parameters (e.g. Stick displacement).

On large aircraft (e.g. KC 390) a complete flight test data acquisition, processing and validation system can be installed within the aircraft. In this case, the necessary information for the correct execution and/or validation of the test point could be easily presented for the Test Pilot and Engineer. On the other hand, on a small aircraft (e.g. A-29 Super Tucano) the space constraints avoids the installation of FTI along with the data processing system.

So in this case, there is no possibility to integrate advanced information systems into the Test Bed. However, the computational capacity evolution of advanced processing devices opens new horizons for the development of such ultra-compact airborne information systems.

The objective of this paper is to discuss the development of a compact airborne system for FTI data processing to aid the Test Pilot in flight trials for the determination of aircraft static and dynamic stability parameters. To do that, FTI data was sent via UDP (User Datagram Protocol) to an airborne computer installed into the A-29B aircraft.

Such system has the function of processing the income data stream using a customized application program. After processing, the data is sent over the wireless network to be accessed by mobile devices installed in the front and rear seats of the test bed.

Specific applications were developed on mobile devices to receive and display data to the test crew. The data presentation software was designed to display numerical values and specific graphic elements, to allow real-time analysis of the test results, for test point validation, and continuous verification of limits, to avoid the occurrence of risk condition, for enhancing flight safety levels.

The application was validated by the 2017 class students of the Brazilian Flight Test Course carried out by EFEV (i.e. Brazilian Flight Test School) and the results were considered satisfactory.

System Architecture

The goal of this project is to provide a way to allow the Test Pilots and Engineers to visualize real-time data inside the aircraft cockpit. In order to accomplish this purpose, it's needed to:

1. Acquire raw data from the FTI;
2. Convert raw data to Engineering Units (EU) data; and
3. Send data for the users.

To accomplish that an airborne Single-Board Computer (SBC) equipped with two Ethernet Interfaces is used to acquire, process and distribute live FTI data. In this application the first LAN port is used for acquiring FTI data over UDP protocol. The second port should send EU data for the users. The selected SBC should comply with MIL-STD-810 standards for shock and vibration [3].

For Test Pilot data visualization, it is used a mobile device with maximum 5 inches screen due to space constraints inside the cockpit.

At the rear seat, to display test data for the engineers, a device with 8 inches screen attached to his leg was considered the best choice. In both cases, crew jettison possibility avoid the usage of any wired solution.

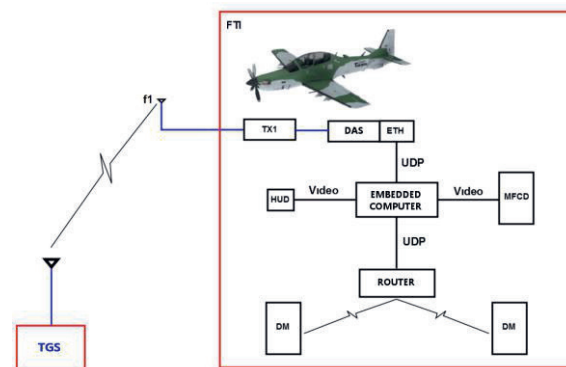


Figure 1. System Architecture

As presented, system architecture was proposed considering its usage for Flight Tests Campaigns and its integration into the A-29B aircraft (Figure 1).

All flight data are provided by the FTI to the airborne SBC through an UDP connection. The computer acquires, translate, pack and send all data to mobile devices via an WIFI router to make any selected data set available over the WIFI network inside the cockpit.

Two applications were developed in this project as follows:

1. The first one is an embedded program who acquires data from FTI, convert to engineering units and send the results to mobile devices. This application is composed by 3 modules (Figure 2) as follows:

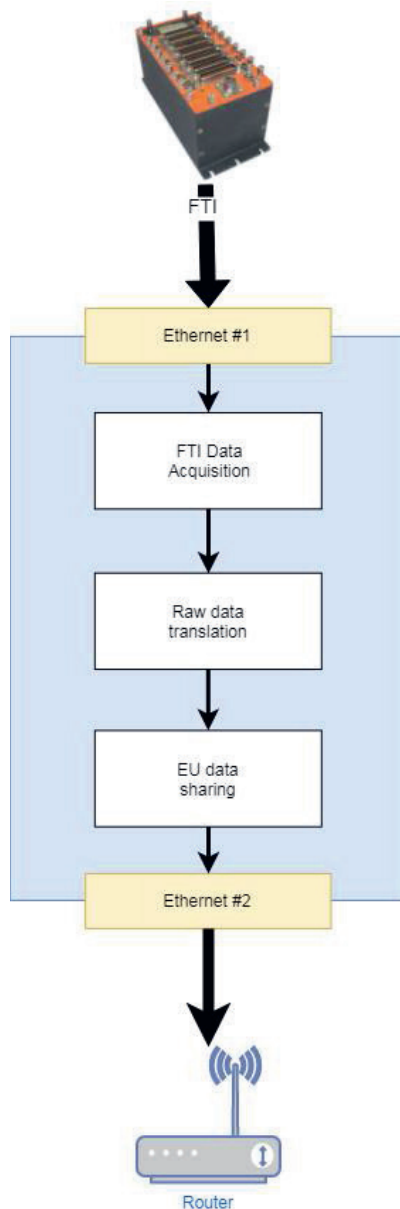


Figure 2. Component Diagram of embedded processing application

- a. Data acquisition module who gets all data from FTI through an UDP connection using embedded computer Ethernet interface #1. The module read a XML (Extensible Markup Language) file that contains all FTI configuration, such as IP address, port and UDP packets structure.
- b. The processing module that converts raw data to EU. Such software It is a compiled Matlab[®] function and it provides controlled and updated calibration information that assures an exact data conversion.

c. The distribution module, thought an UDP connection using Ethernet interface #2, shares all EU converted data to the WIFI network.

2. A second application was developed to get all data provided by the embedded application thought the WIFI network and display them to the Test Crew. This application is required to display data in numeric and graphic formats (i.e. gauges and strip-charts), change gauges and strip-charts configuration and group data by maneuvers.

System Integration

The A-29B aircraft FTI was changed to comply with specific needs to this project for the inclusion of UDP connection and additional hardware installation. The SBC and router installation is depicted in Figure 3.



Figure 3. Embedded computer and router installation

As presented, the SBC was installed in the aircraft trunk and the router in the cockpit.

The Mobile Device used by the pilot was installed next to aircraft front panel, on the Head-Up Display (HUD) left side.

The engineer tablet was installed in a specific base over his leg using a COTS flying clipboard (Figure 4).



Figure 4. Pilot and engineer mobile device installed

The pilot device was kept in pilot's field of view to allow external and HUD visual references visualization information during flight the execution of test point and data reading. This setup provides feedback information to help the pilot to correctly apply the flight techniques and to properly control and maintain the Test Bed within the required flying conditions providing a

concise situational awareness to assure a safe flight. Furthermore, the device position allows ease and user-friendly access so the Test Crew could also change displays pages and device configuration during the flight.

Ground and Flight Tests Execution

For flying a modified aircraft due to the FTI and the proposed system installation into the test bed, it is required the issuing of a Special Flying Permit by Instituto de Fomento e Coordenação Industrial (Industrial Fostering and Coordination Institute - IFI) who is the Brazilian Military Certification Authority. So for the verification of the modified aircraft compliance it was performed several ground tests that includes electromagnetic compatibility and interference, physical and critical cabin compliance.

All results were considered satisfactory and there was no significant WIFI network interference on the aircraft systems.

The equipment installation ergo metrics was considered satisfactory by test crew and the inspectors of certification authority.

At the end the Special Flying Permit was issued, and the system evaluation Flight Test Campaign was executed for system final validation.

For system verification, it was selected the A-29 static and dynamic flight qualities syllabus of the 2018 class, of the Brazilian Flight Test Course, carried out by EFEV. Such evaluation was composed by several Test Points as depicted in Table 1.

Table 1. Selected System Validation Tests Points

Point	Zp Ref (ft)	Vc Ref (kt)	Configuration
Flight controls check (PAL check)	-	-	-
Take off	-	-	TB/FDN
Stabilization	10.000 12.000	130 160	TR/FR
Mechanical characteristics of the Flight Command System (MCFCS)			
Longitudinal static stability and acceleration & deceleration			
Short-period			
Dutch roll			
Phogoid			
Steady sideslip approach			
Maneuverability			

In addition to the listed Test Points (Table 1), crew staff performed cabin critique to evaluate the tool operation during the execution of the flight tests. It was also verified the tool suitability for test data presentation, its update rates,

scales and graphic elements to follow and control the execution of test points.

Finally, system operation evaluation was performed based on implemented functionalities and configurations.

Results

While on the ground, for the execution of the flight controls checkpoint procedures (i.e. PAL check), the application was considered very useful for adjusting and validating the pilot command inputs.

During the tests it was also possible to display the evolution of command position values, as the pilot advanced with command inputs.

While in operation, it was also possible to perform a FTI parameter check before the aircraft take off. Such procedure improves FTI data reliability and reduces the occurrence of refly because this tool easily indicates the occurrence of any parameter degradation to allow an early FTI data non-compliance detection.

Several evaluation reports indicates that this system improves Test Crew situational awareness because it enables the continuous monitoring if the actual aircraft flight condition is within its cleared flying envelope, to avoid unnecessary violations. Moreover, it also helps the crew to properly execute the test points as required by the test order.

Another relevant point to be reported is the fact that test points are often performed outside ideal conditions or even in non-valid conditions because in the aircraft cabin the pilot and test engineer do not have access to all control parameters involved in the test.

This fact implies the undesired repetition of test flights and it causes direct impacts to the execution of the flight test program increasing its execution time and associated costs.

However, with the use of this application, it was possible to verify in real-time the actual flying conditions from the beginning to the end of all executed test points.

Such feature allows a careful evaluation of the test results by the Test Crew and therefore the validation of test points while the aircraft is still flying. This enhancement improves flight test campaign efficiency.

As an example, for the execution of the Dutch Roll and Short-Period test points, the Test Pilot needs to excite, the dynamic modes of the aircraft over its longitudinal and directional axes.

The recommended flight technique for evaluating such flight qualities is dependent of the pilot amplitude and frequency inputs on flight controls.

As reported the developed application played a key role though the validation of the curves plotted at the mobile device of the command and surface positioning parameters.

Such validation process allow the Test Engineer to warn the test pilot when he needs to adjust the maneuver.

Moreover, after the excitation, it is also possible to verify if the aircraft responded accordingly and to view the test results on the mobile device screen.

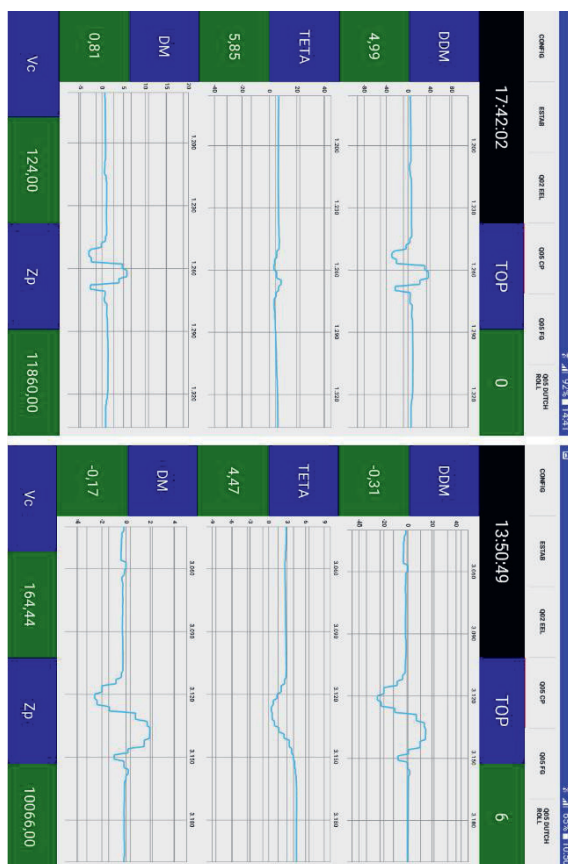


Figure 5. Doublet inputs: (a) not valid; (b) valid

Figure 5 shows an example of a Short Period with Doublet input for longitudinal axis excitation as follows.

1. The first chart (i.e. Figure 5a) depicts an asymmetric and short duration input therefore the dynamic modes were not properly excited. Such conclusion could be verified by the TETA (i.e. Angle of Attack) parameter trace.
2. The second chart (i.e. Figure 5b) depicts a valid input where the modes are properly excited resulting in a

greater amplitude response of the TETA parameter.

As presented with the introduction of this new tool, it was possible for the test crew to analyze and evaluate the validation condition of the test point and to eliminate false perceptions. It should be noticed that such conclusion would not be possible using only data presented in the original cockpit displays and dials of the aircraft.

The test crew also reported that the devices did not interfere with the regular aircraft piloting so the flight was still safe with such equipment installed into the cockpit.

Finally, the observed results were considered satisfactory by the 2018 class Flight Test Course pilots, engineers and instructors for the execution of instruction Test Flights and real Flight Test Campaigns. In addition, the use of the tool was very well accepted by IPEV's testing community that foreseen the possibility of using it in several other flight tests applications.

Conclusion

Mobile devices can be very useful in the development of airborne applications, because they are built with well integrated resources such as cameras and accelerometers. In addition, its easiness for development, validation and integration of new software on the Android environment speedup the process of implementing innovative and/or customized solutions.

In this development it was demonstrated the safe and reliable use of these types of devices for flight test applications.

In addition, the presented results were validated during the instructions flights of the 2018 class of the Brazilian Flight Test Course.

Future developments should encompass, the integration of the tool with the aircraft Multi-Function Color Display (MFCD) and HUD.

Such development may also approach the development of new facilities for test data presentation and insertion of graphical aids for the Test Crew (e.g. flight director, specific excess power) aiming the correct execution of the testing techniques, improving Flight Test efficiency and safety.

Acknowledgement

We wish to thank the unconditional support provided by the Instituto de Pesquisas e Ensaios em Voo (IPEV). Also we like to thank FINEP under agreement 01.12.0518.00 that funded the development of this tool and the presentation trip.

References

- [1] COLLINS, D. **Wireless Data Acquisition in Flight Test Networks**. Proceedings of the European Test and Telemetry Conference ETTC 2016, Nuremberg: ETTC 2016.
- [2] VASCONCELOS, L. E. G.; KUSUMOTO, A. Y.; LEITE, N. P. O.; **Development of an Image Processing Application for Air Data System Calibration using iOS Mobile Devices**, Proceedings of the European Test and Telemetry Conference ETTC 2013, Toulouse: ETTC 2013.
- [3] UNITED STATES. Department of Defense. **MIL-STD-810G**: Environmental Engineering Considerations and Laboratory Tests. Aberdeen, 2008.
- [4] GOOGLE DEVELOPERS. **Android Introduction**. 2018.
<<https://developer.android.com/guide/>>
- [5] IEEE Std 802.11. **IEEE Standards for Local and metropolitan area networks**.

A case study in creating flexible FTI configuration software

Alan Cooke
Curtiss-Wright, Dublin, Ireland,
acooke@curtiswright.com,

Abstract

This paper presents a case study in designing flexible, future-proofed FTI configuration software. It starts by outlining the challenges posed to software in supporting the combined FTI and related product lines of two historically disjoint customer bases that differ in their software user experience but still have the same high expectation levels when it comes to customer support. The paper then describes how Aerospace Instrumentation (AI) used this opportunity to reconfigure two software products to not only support historically separate product lines, but also to create greater choice for their customers in addition to providing greater flexibility and options for the future.

Key words: FTI, Software

Introduction

In an ideal world, Flight Test organizations could use hardware from multiple vendors to pick and choose the best solution. However, there are many issues that prevent this – one of which is the need to use different software suites to configure and manage the hardware. This paper outlines how software from two formally separate businesses are being adapted to allow customers to take full advantage of the vast product portfolio from their combined product lines. It also describes how this change has further enhanced the flexibility and options now available to its customers.

Integration Problems

Flight test programs require Data Acquisition Systems (DAS) to collect and process valuable data. These DAS consist of many elements including sensors, data acquisition units, recorders, switches and transmitters. Setting up these components is achieved through software. There are several vendors that supply some or all of these components and they all have their own software to support them. In an ideal world, engineers would be able to cherry pick equipment from multiple vendors, and re-use whatever equipment they have from previous programs, to build the system they need. However, trying to do this will typically result in integration problems because of the need to use multiple software suites. This means they are very likely to encounter incompatibility issues, for example, with data

formats and time synchronization. Even if they can find ways to work around these issues, there is increased work associated with using multiple software suites. It also increases the risk of time delays as the system will be more complex with more things to go wrong.

While initiatives such as iNET are setting standards that should facilitate cross vendor hardware support in several different software packages, it will likely be some time before such standards are widely in use. Various other standards, such as XidML and MDL, have the potential to be part of the solution but without all vendors buying into working towards a universal software platform, engineers will still need to use separate software packages.

In the meantime, engineers in the field must contend with workarounds that reduce efficiency and add risk to a program by adding another layer of complication to a system that may result in delays. Vendors themselves can help here by integrating some equipment with their own prior to delivery. This is an effective solution, but it may add delays in delivery of systems, add cost and is not as flexible. This approach works best when there is limited equipment being integrated as more equipment from more vendors adds overhead to the integration effort.

Possible Solutions

A common scenario in many flight test facilities and at aircraft OEMs is to try and persist with one vendor as long as is practical. This circumvents the problems associated with integrating multi-vendor systems and it also allows the re-use of database and visualization systems as well as negating the need for new product training and processes. The disadvantage is that organizations can find they are getting 'locked in' to certain product lines and may be selecting equipment not because it is the best fit for the job but because it is the most convenient overall.

Case Study

Background

Curtiss-Wright recently acquired Teletronics Technology Corporation (TTC) – a leading supplier of DAS. Curtiss-Wright was already a leading DAS supplier so it now has a combined product range that no other FTI vendor can hope to match. This provides an unprecedented opportunity for customers, but poses a significant challenge to Curtiss-Wright's TTCWare and DAS Studio configuration software.

Individually, both software packages are extremely flexible, each optimized to maximize the productivity of its users. They can both be used to configure Data Acquisition Units (DAU), Recorders, Switches, High-speed Cameras and much more. However, both applications take a different approach to configuring a system. Furthermore, each application has a large, well-established and loyal user base, making it undesirable to simply choose one of these applications as the sole configuration software for the Aerospace Instrumentation product range.

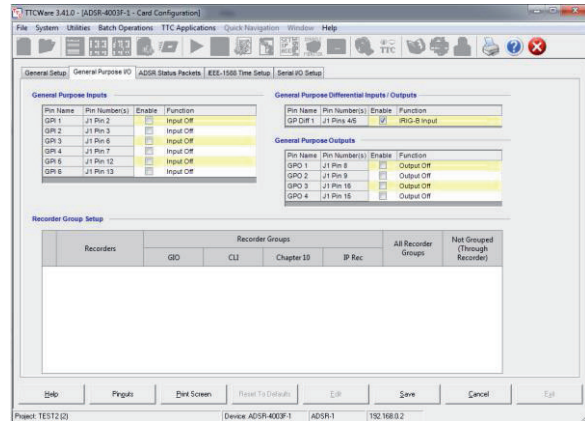
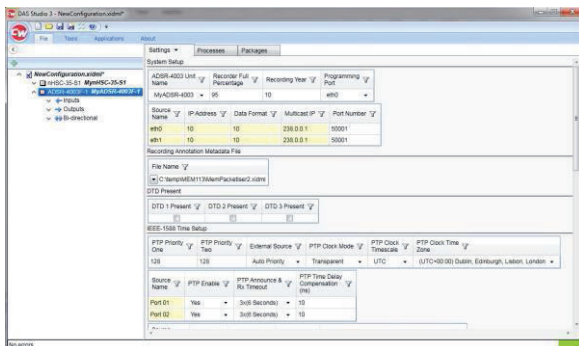


Figure 1 - TTCWare and DAS Studio are both highly capable, but they take different approaches

Without steps to effectively integrate their functionality, customers would have to use two separate pieces of software, maintain two different processes to configure hardware and be forced to support different configuration file formats. This is far from ideal for customers and the issues are similar to those faced by many Flight Test Organizations utilizing equipment from two or more DAS vendors.

Curtiss-Wright therefore initiated an integration effort that was aimed at avoiding the issues encountered when integrating equipment from two separate product lines. The initiative also aimed to allow users to benefit from more choice, greater equipment reuse and ultimately to provide greater overall flexibility.

Flexible Software

As part of the reconfiguration of Aerospace Instrumentation's configuration software a number of constraints were imposed.

Design Constraints

A number of constraints were imposed on the reconfigured software.

1. The software must facilitate the existing processes and expectations of previously distinct customer bases.
2. Users should be given the choice of either using DAS Studio or TTCWare
3. The software should provide both GUI and Command line interfaces
4. Both configuration software needed to support hardware from both business units
5. The software must maintain the highest level of quality and reliability possible

In addition to these requirements the following objectives needed to be met

1. Add support for new Data Acquisition Cards as quickly as possible
2. Be able to extend the functionality of the software over time. As more and more capabilities are added to combined product line the software needs to be easily able to support these features without major rewrites
3. The ability to grow to meet (the perhaps unanticipated) future needs of customer. This could potentially include new Bus and Transmission protocols, new synchronization mechanism, sensor types, and so on.
4. All or some of the core functionality of both TTCWare and DAS Studio may need to be ported to other platforms (such as mobile devices or different Operating systems) or distributed across multiple platforms
5. Some or all of the core functionality may need to be incorporated into third party software
6. Support emerging and future standards such as iNET

There was also an implicit assumption that the software will need to be constantly reconfigured over time in unanticipated ways. In summary, the reconfigured software needed to be designed for *maximum flexibility*.

Building Flexible Software

The design constraints dictated a flexible design but what exactly is meant by flexible software and how can flexible software be built? From a software architecture point of view, software requirements fall in to two categories, *functional* and *non-functional* requirements. Flexibility is a *non-functional* requirement, and maps to what is known as a *Quality Attribute* [1]. Quality Attributes are used to guide the design of software, they generally do not specify specific technologies or functional features and essentially describe certain properties that a software design must possess.

The Quality Attribute of Flexibility, given the constraints described above can be further refined into other Quality Attributes. There exists a set of well know techniques that are designed to meet any given set of Quality Attributes.

Table 1 lists these.

Table 1 – The Quality Attributes associated with flexible software and techniques used to meet them

Attribute	Description
Modularity	Using reusable components to build software. It helps to maintain the flexibility by enforcing the separation of concerns between different functionally and semantically similar blocks of code. This better enables the reuse of different functionality across multiple pieces of software
Extensibility	This is the ability to easily extend the functionality of the software and to greatly reduce the fragility of the software. This is greatly helped by building software using semantically coherent Modules/Components
Portability	Software portability to multiple platforms i.e. different hardware platforms and OS
Reusability	The ability to reuse some or all of the functionality across multiple pieces of software
Testability	This is the ability to test automatically test the functionality of the software. This is a necessary to maintain the existing quality of software by automatically detecting regression issues in the software
Attribute	Example Techniques
Modularity	Code to Interfaces: Using this technique, code implement a specific public interface or “contract”. Other code relies on or codes to these published interfaces and is ignorant of how the code is actually implemented behind the published interfaces Semantic Coherence: This is the practice of co-locating functionally related software in the same library or component.
Extensibility	Dependency Injection: The ability to “inject” functionality into other pieces of code, generally done by passing a module that implements a specific “Interface” into dependent code. Specifying in an external configuration file increase flexibility. Loose coupling: For maximum flexibility and to reduce the fragility of the software the various components/modules that compose a system should not be aware of each other. Specifically, the software should be design so that modules/communicate with each other using either a message based system such as a message broker, be event driven or perhaps some combination of both. Product Line Architectures: This technique can be used if variants of the same product are required. This is can be achieved using configuration files and is greatly eased by using some or all of the techniques discussed above [2] Plugins: This allows functionality that implements or conforms to specific interfaces to be automatically discovered and integrated at specific locations in the software
Portability	Layered Architecture: Where software is composed into two or more layers that increasingly abstract the software functionality from the physical platform or OS. A layered architecture combined with the use of loosely coupled, modular components in each layer also aid portability.
Reusability	APIs and SDKs: Creating a set of APIs and SDKs, accompanied by clear documentation can greatly increase the reusability of software. Using semantically coherent software modules helps to partition software into reusable units. Coding to Interfaces helps to isolate the specific implementation details from the software using the modules.
Testability	Coding to Interfaces help in the testing and verification of software by allowing test code to use “Mocking” techniques ¹ to test code and to automate unit testing ² Using layered architectures greatly increases the testability of software by allowing the various layers of the software to be tested separately. In particular, it allows the software that does not interact with hardware to be tested more easily.

¹ See https://en.wikipedia.org/wiki/Mock_object and <https://github.com/Moq/moq4/wiki/Quickstart>

² See https://en.wikipedia.org/wiki/Unit_testing and <http://nunit.org/>

Results

The following sections outline the results of the reconfiguration effort within Curtiss-Wright, Aerospace Instrumentation.

One software, Two User Interfaces

Both DAS Studio and TTCWare have been reconfigured to use a common functional core

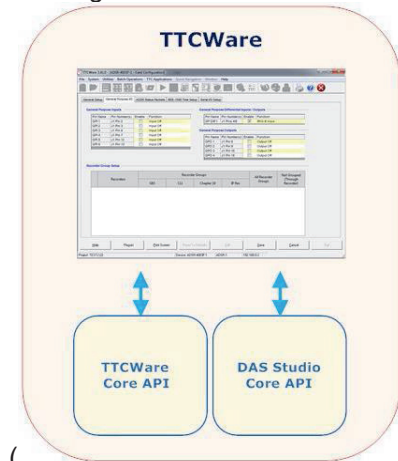


(Figure 2).

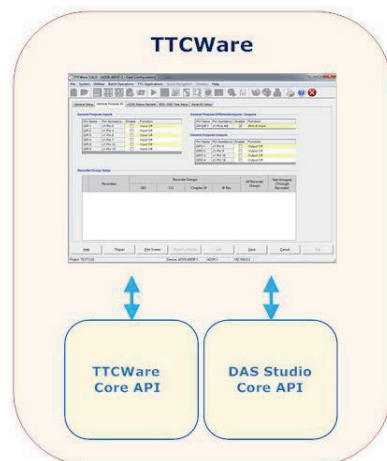
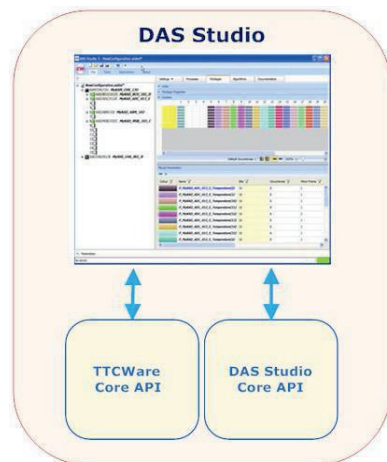


Figure 2 - Both TTCWare and DAS Studio use a common functional core

Specifically, the core business logic for both DAS Studio and TTCWare have been wrapped in separate APIs, and these in turn have been separated from the user interface layers. This permits support for hardware from either company to be added to either application with minimal effort. The approach also allows existing and future customers to use either TTCWare or DAS Studio as their preferred Graphical User Interface (GUI).

Discover & Program

The reconfigured software makes it easy to program mixed systems, for example, DAS Studio can communicate with, discover and configure equipment using native hardware protocols that would have formally only been achievable with TTCWare³ (Figure 3).

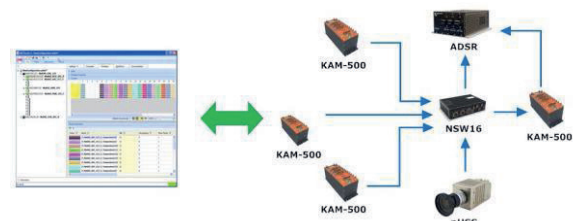


Figure 3 - Using DAS Studio to program a variety of equipment from formally different product lines

Similarly, TTCWare can discover and program equipment using native protocols that would have previously required DAS Studio (Figure 4).

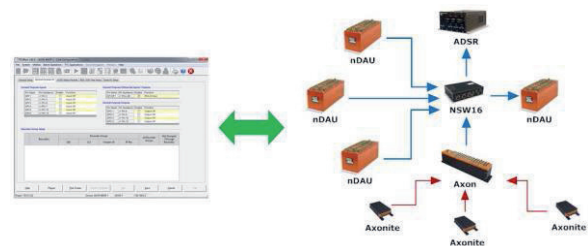


Figure 4 - TTCWare being used to program an Axon along with a variety of TTC equipment

This organizations will be able choose a wider mix of hardware than before and the choice of either a DAS Studio of TTCWare as their configuration software

Enhanced Flexibility

The common functional core also facilitates a greater choice for customers in how they choose to configure their systems.

³ Such as TDDP protocol used to discover TTC equipment

Support for Industry metadata standards

Aerospace Instrumentation engineers are very active on industry standard groups such as the RCC and iNET, and in particular, have made key contributions to the development of MDL (Measurement Definition Language). They are also founding members of the XidML community.

This expertise means that both TTCWare and DAS Studio offer unrivalled flexibility in how customers choose to describe their data acquisition systems. Customers can now use TTC XML, XidML and eventually MDL to define the structure of their data acquisition networks and how they are configured.

Command line programming

Many customers store their configuration data in company databases and other proprietary formats. They then process the data in these systems and convert it to file formats required by specific vendor FTI equipment.

To facilitate this approach, Aerospace Instrumentation provides a set of well-documented command line tools for both verifying configuration file formats and for using them to program their systems. This application takes a XidML file as input and can be used to verify the configuration and/or program one product line or a mix of the two product lines. The command line interface will also take an MDL file as input once the standard has been finalized and published.

Powerful APIs

In addition to giving customers the choice of which application to use (TTCWare, DAS Studio or Command Line Interface) a set of powerful APIs are also available as shown in Table 2.

XidML & XdefML APIs	Customers can use these APIs to create, manipulate and validate XidML and XdefML files. These APIs are used extensively in DAS Studio and TTCWare to generate configuration screens.
TTCWare Core API	This API gives users direct access to the core TTCWare functionality. It can be used by customers to discover and program TTCWare hardware, in addition the ability to define configurations and save/read them to/from TTC XML files.

DAS Studio Core API	This API gives customers direct access to the core DAS Studio business logic and functionality. It can be used by to discover and program DAS Studio hardware, in addition the ability to define configurations and save/read them to/from XidML files.
RESTful API	For extra flexibility, combined core API functionality is also accessible via a common RESTful interface.

Table 2- Available APIs

Together, these APIs provide a level of flexibility and choice that are not provided by other FTI vendors.

Built for the Future

The reconfiguration of TTCWare and DAS Studio was also carried out with an eye to the future. In particular, it was anticipated that customers may need the flexibility to deploy the software to different platforms and operating systems

Linux

All of the core APIs can now be run on the Linux operating system.

All command line interfaces are also capable of running on Linux, allowing customers to create and validate configuration files, in addition to programming both product lines.

Browser-based configuration

The RESTful API provides a mechanism for browser-based user interfaces (Figure 5) to configure and program hardware. As a result, the core functionality can now be hosted on individual DAUs and or even if required on company networks offering further flexibility to Aerospace Instrumentation customers.

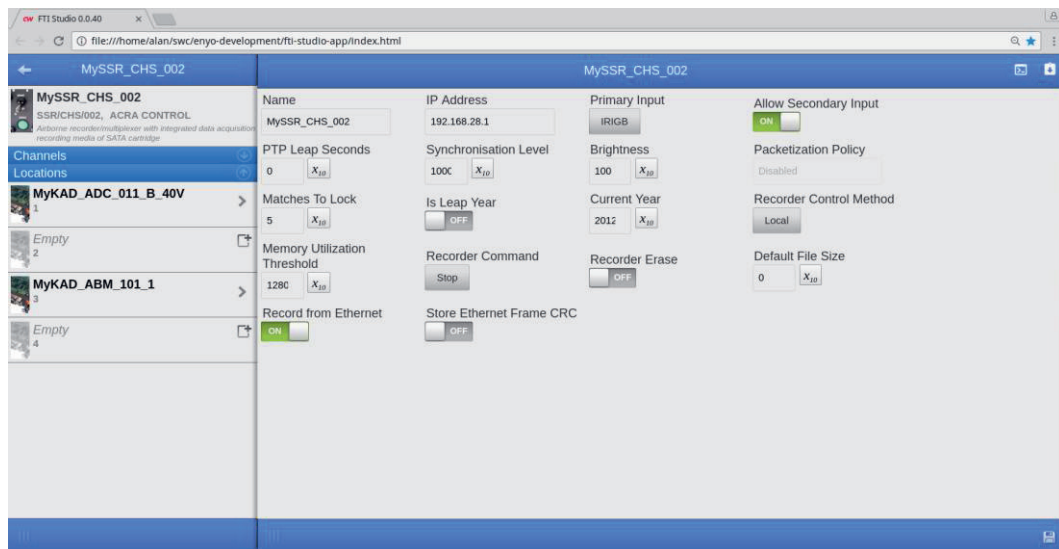


Figure 5 - Browser-based FTI configuration software

Mobile devices

Native Android, iOS and Windows Phone apps can also leverage the RESTful API to configure and program systems. In this scenario, the native mobile app connects to individual DAUs that host and run the RESTful FTI configuration services allowing users to adjust the configuration of the DAU.

Conclusion

Curtiss-Wright's full data acquisition product lines, under the umbrella of Aerospace Instrumentation, provide an unrivalled portfolio of products. This offers customers an unprecedented level of flexibility and choice but also presented a challenge to TTCWare and DAS Studio, the configuration software used for the product lines, as both applications have a wide and varied user base.

To address this challenge both TTCWare and DAS Studio have been reconfigured to allow equipment from either product line to be added to both configuration applications with minimal effort. This was achieved through the creation of a common functional core that is incorporated into both DAS Studio and TTCWare. The end result is that users will have the choice of using either TTCWare or DAS Studio for configuring system comprised of mixed hardware.

The reconfiguration of the software has also allowed Aerospace Instrumentation to offer even greater flexibility for customers by providing a set of powerful APIs and command line tools, support for multiple configuration file formats such as MDL, TTC XML and XidML, in addition to creating a pathway to future software support on multiple platforms and operating systems.

References

- [1] L. Bass, P. Clements and R. Kazman, "Software Architecture in Practice (SEI Series in Software Engineering (Hardcover))," Addison-Wesley Professional; 3rd edition (September 25, 2012).
- [2] P. Clements and L. Northrop, "Software Product Lines," Addison-Wesley Professional; 3rd edition (August 30, 2001).

A Process Model for the Discovery of Knowledge in Sensor-Based Indoor Climate Data

Dominik Gruedl¹, Thomas Wieland¹

¹ *Fraunhofer Anwendungszentrum Drahtlose Sensorik, Sonntagsanger 1, 96450 Coburg, Germany*
gruedldk@iis.fraunhofer.de, thomas.wieland@iis.fraunhofer.de

Abstract:

Sensors in office spaces collect data about the indoor climate in order to monitor and control HVAC-systems to ensure a constant air quality. The quality of indoor climate is dependent on various aspects, such as carbon dioxide, temperature, and humidity.

Approaches on searching patterns in this sensor data by using data mining techniques rarely explicitly apply established process models like KDD (knowledge discovery in databases) or CRISP-DM (cross industry standard process for data mining). These process models describe data mining as one of multiple steps in the whole process of extracting patterns from data. Other steps include the preprocessing of the data as well as the evaluation of the extracted patterns after the data mining.

This paper analyzes these aforementioned approaches and compares them to the established process models before deriving a process model that can be widely applied to data mining projects searching for patterns in sensor-based indoor climate data. The derived process model puts more emphasis on understanding the data and its context as preliminary steps to the extraction of patterns via data mining. In addition to facilitating new research on indoor climate data, the derived process model also allows to understand research in this field of study more easily.

Key words: CRISP-DM, Data mining, knowledge discovery in databases, process model, sensor-based indoor climate data

Introduction

The indoor climate in offices influences the health, productivity and comfort of the employees ([19], [20]). Indoor climate data collected by sensor networks can be used, among other things, to react to changes in the indoor climate. For example, if a threshold value of carbon dioxide is exceeded, a warning lamp can be switched on to indicate the increased value to the persons in the room.

In addition, various data mining methods have already been applied to detect patterns in sensory indoor climate data ([1], [4], [5], [6], [7], [11], [14], [17], [22]).

The research work mentioned above is mainly concerned with the testing of various data mining methods. However, this application is only one step towards the discovery of knowledge in large databases, for example described by the process models KDD (knowledge discovery in databases) [9] or CRISP-DM (cross industry standard process for data mining) [18]. The purpose of these process models is the standardized approach to discover novel, potentially useful, understandable and statistically valid patterns in

the analyzed data [9]. In addition to data mining, this comprises, for example, cleaning the data of noise and inconsistencies and transforming the data for the respective data mining procedure by standardization or discretization.

Lack of reference to clearly defined process models makes it difficult to reproduce the results of research work in which data mining is used to determine knowledge in sensor-based indoor climate data. Furthermore, it is difficult to get an overview of research work with similar contents on the subject of data mining.

Methodology

This paper aims to define a process model that is particularly suitable for the discovery of knowledge in sensor-based indoor climate data.

First, the most commonly used process models for discovering knowledge in large data sets are described. These process models are examined to see to what extent they are suitable for describing research work that has already discovered knowledge in sensor-based indoor climate data.

Based on these investigations a process model is derived which takes the advantages and disadvantages of the established process models into consideration.

Subsequently, process models are discussed which were described and applied in two of the investigated research projects.

Established Process Models

Various process models exist which are intended to standardize the approach of data mining projects. The most commonly used non-proprietary process models are CRISP-DM and KDD [15] (Fig. 1).

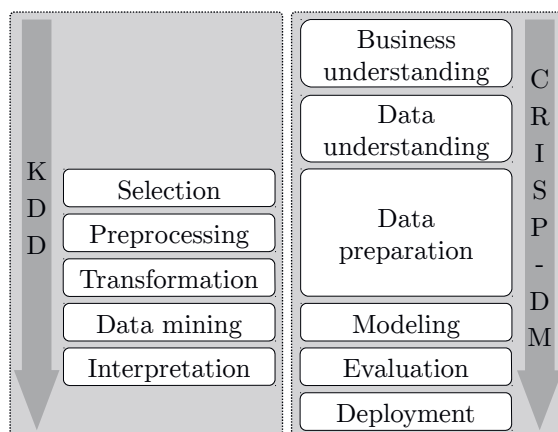


Fig. 1: Comparison of the process models KDD and CRISP-DM

These process models partly overlap. The KDD process model focuses mainly on data preparation and data analysis. The CRISP-DM process model, on the other hand, comprises steps for integrating data mining project into a business context. Nevertheless, the process models share several process steps ([3], [10], [21]).

The steps business understanding, data understanding and deployment of the process model CRISP-DM are not available in the process model KDD. These steps are very project- and company-dependent and therefore usually different for each data mining project. The step data preparation of the process model CRISP-DM comprises the steps selection, preprocessing, and transformation in the process model KDD [3].

Sensor-based Indoor Climate Data

Data mining as such is a very versatile toolset that can be applied to a plethora of situations. A typical use case is deducing information from data measured by distributed sensors, e.g. in buildings.

The presence of people in a room is an important information for the effective and efficient management of temperature and ventilation control devices [22]. Up to 16 % of energy is wasted due to increased energy requirements in unoccupied rooms [13]. Although the number of present persons could be determined through monitoring the persons in the room, this monitoring would be an intrusion into the privacy of the employees. Numerous research groups ([5], [6], [7], [11], [14], [17], [22]) therefore tried to determine with the help of data mining whether there are correlations between indoor climate data recorded by sensors and the presence of the persons in the room.

Opening and closing windows significantly influence the climate in a room ([2], [16]). Furthermore, natural ventilation is the most frequently used form for changing the room climate [8]. In [4], the authors investigated the causes of people's behavior with regard to opening and closing windows using data mining.

The climate and construction properties of a building have a major influence on its energy consumption and CO₂ emissions. For example, by using certain materials, the waste heat from direct sunlight could be used for more efficient temperature management [12]. So-called intelligent buildings are supposed to be able to be both comfortable and energy-efficient for the people present. In [1], the relationship between the optimization of energy consumption and the comfort of people in the room was scrutinized. According to [1], a room is perceived as comfortable if it is both thermally comfortable and optimally lit. Based on the data from these two aspects, classifiers were trained to identify energy-efficient and comfortable rooms.

Suitability of KDD

With the help of the highly detailed preparation of the data, consisting of the steps selection, preprocessing and transformation, corresponding modifications to the collected data can be traced very well (Fig. 2). In the research work examined, these steps of the KDD process model were applied in various degrees of detail.

Not all processing steps may be necessary for the discovery of knowledge in sensor-based indoor climate data. For example, if uniform sensors are used, the data selection step for this data can be omitted. Alas, not only specially collected sensor data, but also the data of third parties are used for the discovery of knowledge. Therefore an integration of the

sensor data and the third-party data is necessary. However, this integration was not described in the research work examined. Due to the lack of these explanations, it is difficult to understand the subsequent steps.

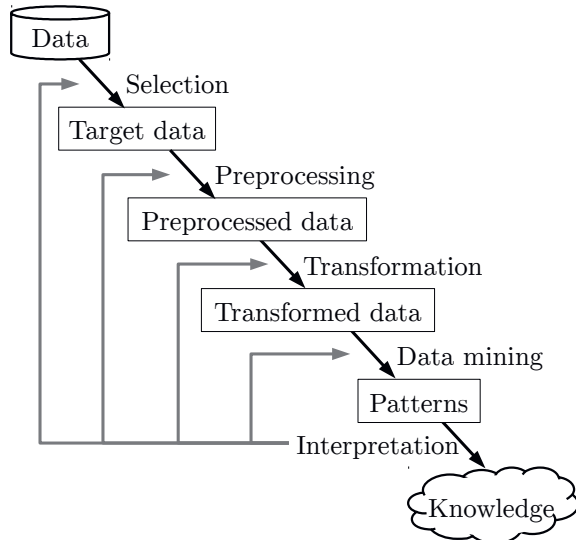


Fig. 2: Process model KDD [9]

Due to the technical conditions for wireless sensor networks, data collection errors may occur. If data is missing or faulty, e.g. due to defective sensors or problems in wireless communication, the data stock must be cleaned up before data mining. In addition, average values were often calculated for the indoor climate data to reduce the amount of data. These tasks are summarized in the data preprocessing step of the process model. This step of the KDD process model is particularly necessary when using feature selection and feature learning.

When selecting the data mining method, in most cases process-dependent data transformations must be carried out on the indoor climate data. Among other things, this process step includes the calculation of new attributes that are necessary for classification procedures. Smoothing can also be used as a method to remove peaks in the indoor climate data.

It may be very difficult to differentiate between the process steps data preprocessing and data transformation. For example, both process steps describe the aggregation as an instrument of the respective preparation. In addition, identical tasks are described with different names. This concerns, for example, the measures for removing noise during the data preprocessing and smoothing the data as part of the data transformation.

In the research work examined, the necessary domain knowledge is explained first. These preliminary considerations, which were made in almost all the research work examined, are not the subject of the process model KDD. In contrast to the CRISP-DM process model, business understanding, data understanding and deployment are not discussed in the KDD process model. The KDD process model therefore focuses on the purely technical aspects of data mining.

Suitability of CRISP-DM

The CRISP-DM process model is designed for data mining projects that take place in an industrial context. This means that the integration of the respective project into the operational processes is of particular importance (Fig 3.).

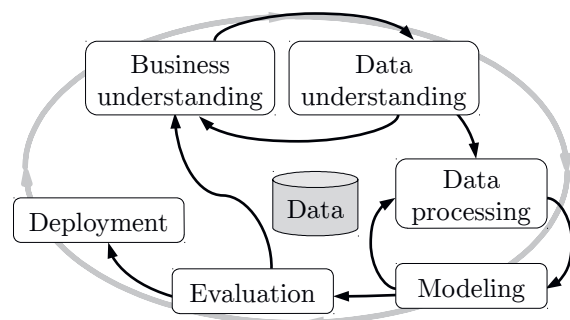


Fig. 3: Process model CRISP-DM [18]

For this reason, the facts and the existing data basis are first examined before working with the data. Furthermore, the deployment of the generated models after their evaluation is an integral part of this process model.

In the beginning of the research work examined, the context of the respective work was always described in great detail. The domain knowledge explained here is indispensable for understanding the following steps. The clarification of legal questions prior to data collection is also crucial before taking further action. If indoor climate data should be investigated in an operational context using data mining, financial or project planning questions could also be very important.

In the same way as the facts, the data which are to be examined are always thoroughly described. In addition to their description, the collection of the data was also discussed in detail.

According to the definition, data collection is not part of the CRISP-DM process model. The CRISP-DM process model is designed to examine data that already exists in the company. The purpose of data collection is therefore not primarily the discovery of knowledge, but the handling of operational processes. For example, delivery and invoice data is collected in order to track the flow of goods and money. Only during a data mining project this data is used for knowledge discovery. However, in the research work examined, the specified indoor climate data were collected exclusively for analysis by means of data mining.

The process step of data preparation combines the steps selection, preprocessing and transformation of the process model KDD. This summary makes it more difficult to trace the exact steps taken to prepare the data.

In the context of the research work under investigation, the deployment of the generated models was only discussed with the aim of optimizing them.

Defining the Ideal Process Model

Based on the investigations carried out, a process model can be derived, which is particularly suitable for the discovery of knowledge in sensor-based indoor climate data (Fig. 4).

The investigated process models KDD and CRISP-DM show specific weaknesses which exclude the general recommendation of one of these process models for application to the investigated research work.

However, in addition to these weaknesses, specific aspects of the process models could be identified, which very well describe the actual procedures of the investigated research work. In addition, some authors carried out measures, which are not intended as process steps in the process models examined.

By merging the benefits of the established process models and the best practices, almost all necessary process steps of the actual procedures can be represented in a unified and optimized process model.

This process model is ideal for understanding research work analyzing sensor-based indoor climate data as well as for planning and performing new research on this kind of data.

The steps of this process model can be summarized as follows:

1. Business understanding: The purpose of this process step of the CRISP-DM process model is to understand the task to be solved and the respective context ([3], [21]). The research work examined focuses exclusively on scientific issues that are almost exclusively located in the context of the energy efficiency of buildings. To deal with these questions, a high degree of domain knowledge from several areas of expertise is required, e. g. indoor climate, sensor technologies, human factors and architecture. In addition, there are relationships between the various domains. Changes in human behavior or the weather, for example, have an effect on the indoor climate.

Also part of this process step is the clarification of legal questions. E. g., the collection of the ground truth by means of cameras is prohibited under labor law.

2. Data understanding: This process step is used to determine the required data and to analyze the available data for its suitability for data mining ([3], [21]). For each context examined, different context data is required. For example, the context data for determining the presence differs greatly from the context data for determining the comfort of persons in the room.

3. Data collection: Data collection is not a process step of the examined process models. The required indoor climate and context data

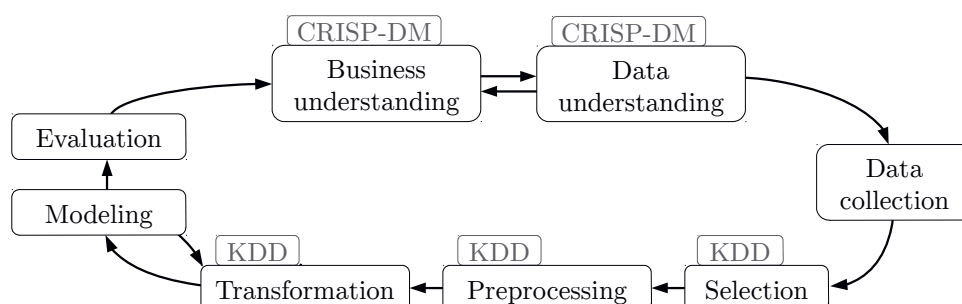


Fig. 4: Optimized process model for the discovery of knowledge in sensor-based indoor climate data

are collected based on the information from the previous process steps. This includes, among other things, the selection and installation of the sensors required for measuring the necessary room climate and context data, as well as the rooms provided for this purpose.

4. Selection: The aim of this step is to select and merge the data to be examined using all collected data ([3], [10]).

5. Preprocessing: During the preprocessing, the previously selected and integrated data is to be prepared for the data mining ([3], [10], [21]). This step is independent of the used data mining method. Part of this process step is the so-called data cleansing, i. e. the information-neutral removal of errors in the data. Another part of data preprocessing is the data reduction. In this process, subsets of the selected are formed in order to reduce the calculation effort during the data mining.

6. Transformation: The transformation step is used to prepare the data for a specific data mining method ([3], [10]). This step can be used, for example, to create new attributes that are required as class labels for classification methods.

7. Modeling: Various methods can be used to detect patterns in the processed indoor climate data. In most of the research work examined, classification was used to search for patterns in the respective indoor climate data. Although different forms of classification were used for this purpose, the basic procedure for generating classifiers was retained. This means that for training and testing the classifiers, corresponding training and test data was generated ([3], [10], [21]). When generating this training and test data, attention was also paid to ensure that the data was split according to both stratification and cross-validation. Only the authors of [4] performed both cluster and association analysis. The results of the cluster analysis were used for the creation of association rules.

8. Evaluation: Various metrics can be calculated to compare the results obtained from the previous data mining step ([3], [10], [21]). In all research work that used classification to search for patterns in the indoor climate data collected, the accuracy of the respective results was calculated. [4] evaluated the cluster quality using the Davies-Bouldin index and the quality of the association rules using support and confidence.

9. Repetition: The examined research work concludes with the identification of open

problems or the formulation of new research questions. I. e. it is not the immediate use of the results obtained in an industrial context that is proposed, but rather the optimisation of the respective model by means of further scientific studies.

Discussion

Two of the investigated research projects applied specially defined process models. This section discusses to what extent these process models are suitable for the discovery of knowledge in sensor-based indoor climate data.

The process model of [1] is based on the process model CRISP-DM. However, it does not cover all steps of the original process model (Fig. 5).

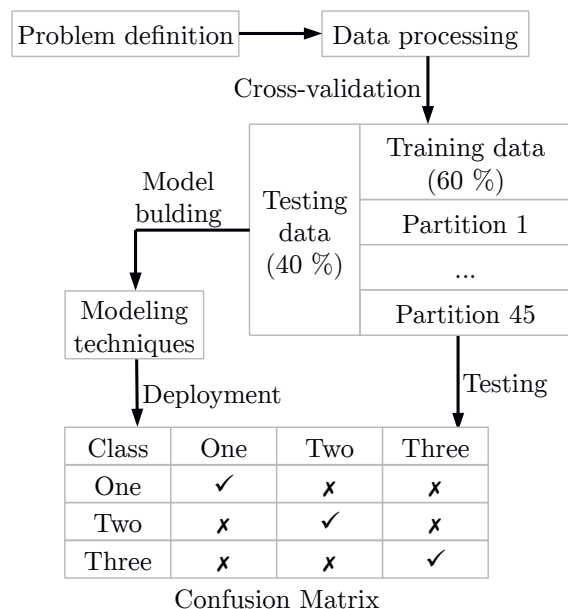


Fig. 5: Applied process model by [1]

For example, the steps data understanding and data preparation are combined in the step data processing.

As with all other research work, the description of the facts is given directly at the beginning of [1]. However, in the first step of its process model, [1] will limit itself to describing the problem to be solved. The process model proposed by [1] does not reflect the actual course of the data mining project.

[1] assigns the data collection to the second process step. This measure, though, is not part of the original process model CRISP-DM. Splitting the data records using cross-validation is part of the modeling according to the original definition of the process model and not to be seen as a separate step.

Furthermore, [1] is limited to classification procedures for the generation of models. Thus

the use of a confusion matrix is sufficient for the evaluation of the classifiers. If other data mining methods are used in future investigations, the process model must be adapted accordingly..

Furthermore, the process model does not indicate any jumpbacks to previous process steps.

The authors of [4] described in their research work a process model with three steps (Fig. 6).

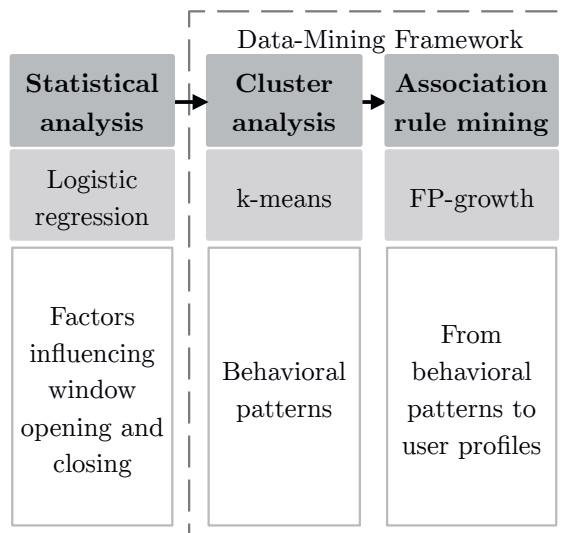


Fig. 6: Applied process model by [4]

Similar to the KDD process model, the process model in [4] mainly describes measures for data preparation and analysis. In contrast to the CRISP-DM process model, business understanding and data understanding deployment are not part of the process model.

The first step of the process model in [4] is to reduce the amount of data to be analyzed. Thereby, those indoor climate data sets are determined, which have the greatest influence on the investigated context. This reduction in data volume is independent of the subsequent data mining procedures.

The second and third steps of the process model of [4] are summarized as a "data mining framework". These process steps deal with the actual modeling by using clustering and association analysis. In the established process models, this procedure would be described as a return to a previous process step.

The process model of [4] does not provide for the evaluation of the generated model. Nevertheless, [4] conducted such an evaluation during their research.

Due to the fixed procedures for data preparation and analysis, the process model of [4] cannot easily be applied to other research work.

Conclusion

Within this paper, a process model was proposed that is suitable for the discovery of knowledge in sensor-based indoor climate data.

The established process models could only be mapped to the research work examined in accordance with their focal points. The process model KDD is particularly suitable for describing data preparation, whereas the process model CRISP-DM is particularly suitable for describing the situation.

The derived process model contains the process steps of the established process models most frequently used in the research work under investigation. In addition, data collection was added as a process step. This process model not only allows new data mining projects to be carried out transparently and comprehensively in indoor climate data recorded by sensors, but also makes it easier to understand work already carried out in this area.

In the next step, the process model should be tested and refined by its practical use in data mining projects. Furthermore, the comparison of the process model with less known process models, which were not used for this study, would be conceivable.

References

- [1] A. Ahmed, N. E. Korres, J. Ploennigs, H. Elhadi, K. Menzel, Mining building performance data for energy-efficient operation, *Advanced Engineering Informatics* 25(2), 341–354 (2011); doi: 10.1016/j.aei.2010.10.002
- [2] R. Andersen, V. Fabi, J. Toftum, S. P. Corgnati, B. W. Olesen, Window opening behaviour modelled from measurements in Danish dwellings, *Building and Environment* 69, 101–113 (2013); doi: 10.1016/j.buildenv.2013.07.005
- [3] J. Cleve, *Data Mining*, 2nd ed., Berlin, De Gruyter (2016)
- [4] S. D'Oca, T. Hong, A data-mining approach to discover patterns of window opening and closing behavior in offices, *Building and Environment* 82, 726–739 (2014); doi: 10.1016/j.buildenv.2014.10.021
- [5] B. Dong, B. Andrews, K. P. Lam, M. Höynck, R. Zhang, Y.-S. Chiou, D. Benitez, An information technology enabled sustainability test-bed (ITEST) for occupancy detection through an environmental sensing network, *Energy and Buildings* 42(7), S. 1038–1046 (2010); doi: 10.1016/j.enbuild.2010.01.016.
- [6] A. Ebadat, G. Bottegal, D. Varagnolo, B. Wahlberg, H. Hjalmarsson, K. H. Johansson, Blind identification strategies for room occupancy estimation, *IEEE*, 1315–1320 (2015)

- [7] T. Ekwevugbe, N. Brown, V. Pakka, D. Fan, Realtime building occupancy sensing using neural-network based sensor network, 2013 7th IEEE International Conference on Digital Ecosystems and Technologies (DEST), IEEE, 114–119 (2013)
- [8] V. Fabi, R. V. Andersen, S. Corgnati, B. W. Olesen, Occupants' window opening behaviour: A literature review of factors influencing occupant behaviour and models, *Building and Environment* 58, 188–198 (2012); doi: 10.1016/j.buildenv.2012.07.009
- [9] U. M. Fayyad, *Advances in knowledge discovery and data mining*, Menlo Park, AAAI Press (1996)
- [10] J. Han, M. Kamber, J. Pei, *Data mining: Concepts and techniques*, 3. ed., Amsterdam, Elsevier/Morgan Kaufmann (2012)
- [11] C. Jiang, M. K. Masood, Y. C. Soh, H. Li, Indoor occupancy estimation from carbon dioxide concentration, *Energy and Buildings* 131, 132–141 (2016); doi: 10.1016/j.enbuild.2016.09.002
- [12] A. M. Khudhair, M. M. Farid, A review on energy conservation in building applications with thermal storage by latent heat using phase change materials, *Energy Conversion and Management* 45(2), 263–275 (2004); doi: 10.1016/S0196-8904(03)00131-6
- [13] R. J. Meyers, E. D. Williams, H. S. Matthews, Scoping the potential of monitoring and control technologies to reduce energy use in homes, *Energy and Buildings* 42(5), 563–569 (2010); doi: 10.1016/j.enbuild.2009.10.026
- [14] T. H. Pedersen, K. U. Nielsen, S. Petersen, Method for room occupancy detection based on trajectory of indoor climate sensor data, *Building and Environment* 115, 147–156 (2017); doi: 10.1016/j.buildenv.2017.01.023
- [15] G. Piatetsky-Shapiro, CRISP-DM, still the top methodology for analytics, data mining, or data science projects (2014)
- [16] I. A. Raja, J. F. Nicol, K. J. McCartney, M. A. Humphreys, Thermal comfort: Use of controls in naturally ventilated buildings, *Energy and Buildings* 33(3), 235–244 (2001); doi: 10.1016/S0378-7788(00)00087-6
- [17] S. H. Ryu, H. J. Moon, Development of an occupancy prediction model using indoor environmental data based on machine learning techniques, *Building and Environment* 107, 1–9 (2016); doi: 10.1016/j.buildenv.2016.06.039
- [18] C. Shearer, The CRISP-DM Model: The New Blueprint for Data Mining, *Journal of Data Warehousing* 5(4), 13–22 (2000)
- [19] P. Wargocki, D. P. Wyon, J. Sundell, G. Clausen, P. O. Fanger, The Effects of Outdoor Air Supply Rate in an Office on Perceived Air Quality, Sick Building Syndrome (SBS) Symptoms and Productivity, *Indoor Air*, 222–236 (2000)
- [20] P. Wargocki, D. P. Wyon, Ten questions concerning thermal and indoor air quality effects on the performance of office work and schoolwork, *Building and Environment* 112, 359–366 (2017); doi: 10.1016/j.buildenv.2016.11.020
- [21] I. H. Witten, C. J. Pal, E. Frank, M. A. Hall, *Data mining: Practical machine learning tools and techniques*, 4. ed., Cambridge (2017)
- [22] Q. Zhu, Z. Chen, M. K. Masood, Y. C. Soh, Occupancy estimation with environmental sensing via non-iterative LRF feature learning in time and frequency domains, *Energy and Buildings* 141, 125–133 (2017); doi: 10.1016/j.enbuild.2017.01.057

Machine Learning-Driven Test Case Prioritization Approaches for Black-Box Software Testing

Remo Lachmann
 IAV GmbH, Rockwellstraße 16, Gifhorn, Germany,
 remo.lachmann@iav.de

Abstract

Regression testing is the task of retesting a software system after changes have occurred, e.g., after a new version has been developed. Usually, only a subset of test cases is executed for a particular version due to restricted resources. This poses the problem of identifying important test cases for testing. Regression testing techniques such as test case prioritization have been introduced to guide the testing process. Existing techniques usually require source code information. However, system testing of complex applications often restricts access to the source code, i.e., they are a black-box. Here, a large set of test cases is manually executed. In previous work, we proposed a test case prioritization technique for system testing using supervised machine learning. We designed our approach to prioritize manually executed test cases, i.e., it analyzes meta-data and natural language artifacts to compute test case priority values. In this paper, we apply further machine learning algorithms and an ensemble learning approach. In addition, we evaluate our approach on three different data sets in total, which all stem from the automotive industry and, thus, represent real life regression testing data sets. We analyze the results of our approach in terms of its failure finding potential. Our findings indicate that black-box testing can be improved using machine learning techniques.

Key words: Test Case Prioritization, Black-Box Software Testing, Regression Testing, Machine Learning, System Testing

1. Introduction

Modern software systems have to fulfill a large set of requirements due to their complexity and longevity. Thus, in the crucial phase of software testing in a software engineering project, the correspondence of the program behavior to its requirements is assessed. The more complex the system under test, the higher is the testing effort, which takes up to 50% of all project resources in software engineering [13].

While testing is an important task that is part of most professional projects, it still has its limitations. As the testing effort is larger than available testing resources, testing has to be focused on important aspects of the application, which are likely to fail or are of high importance for the overall functionality. However, especially in black-box testing, the identification of important test cases is non-trivial due to the lack of source code availability [26]. White-box test techniques are able to identify changes in the software on code level, which can guide the tester to changes, which should be retested in regression testing.

In contrast, black-box testing is focused on the integrated system [2]. Source code is not available due to various reasons, e.g., contract

issues or the usage of precompiled components such as libraries or components developed by 3rd party companies such as suppliers [26]. One prime example of component-based development is the automotive industry, where different companies implement electronic control units, which are later integrated as a whole. Most regression testing techniques focus on source code to select or prioritize test cases [29,16,5]. This reduces their applicability in black-box testing.

To tackle the issue of black-box regression testing, we introduced a regression testing technique based on supervised machine learning in previous work [19]. Our approach prioritizes black-box test cases written in natural language with the aim to emulate test experts and, preferably, find failures as early as possible in the testing process. It uses machine learning (ML) algorithms to find patterns in existing data. Previously, we evaluated our test case prioritization approach using two case studies, one from the automotive industry and one from academia.

In this paper, we diversify and extend our approach using additional ML algorithms to prioritize black-box test cases, i.e., we introduce

the application of neural networks [12], k-nearest neighbor (KNN) [27] and logistic regression [14]. We further extend our concept by combining the output of several ML algorithms to create an *ensemble learner* [27]. Furthermore, we extend our evaluation to a total of three complex industrial systems to make a more general assumption about the effectiveness of our approach. In total, we apply these techniques to three industrial case studies, which provide different features.

In summary, we make the following contributions in this paper:

1. We extend our existing test case prioritization approach by means of additional ML algorithms, which are used in isolation and as an ensemble. We are able to show that our approach is flexible in terms of applied algorithms.
2. We investigate the effectiveness of our technique on three industrial, real-life subject systems. While each system is a software testing project, they are different in nature. Our evaluation results indicate that our approach is indeed applicable to a wide range of projects.

The remainder of this paper is structured as follows: We explain necessary background knowledge in Section 2. Section 3 gives an overview of our general test case prioritization concept. In Section 4, we briefly introduce the machine learning algorithms we apply in this paper to perform a test case prioritization approach. In Section 5, we describe our case evaluation setup and results. We discuss related work in Section 6. We conclude this paper and give insights on future work in Section 7.

2. Background

In modern software engineering, testing is one of the most important aspects to ensure software quality [13]. Testing should commence as early as possible and is an important part of each step in the software development process [2]. Especially regression testing is of importance as software development is not stopped after a version has been finished, but rather developed in a continuous fashion, going from one version to the next [20]. Regression testing focuses on the retest of already tested parts of a software system to ensure that changes do not influence previously implemented functionality [21]. To ensure the correct behavior of a system after a change, a full test is necessary, i.e., the execution of each defined test case for each version under test. However, full testing of a software version is not feasible due to restricted resources and complex software systems [7, 29].

To cope with limited testing resources, different regression testing techniques have been developed to reduce the number of test cases to be executed. Most techniques are categorized into *test case prioritization*, *test case selection* and *test case minimization* approaches [29]. All of these techniques are used to guide the focus of the testing efforts. Each approach computes a priority of each individual test case for a particular software version under test based on different criteria, e.g., changed code coverage [16, 29]. While test case selection and minimization aim to reduce the set of executed test cases, e.g., by identifying redundancies, test case prioritization aims to sort the test cases according to their priority.

Prioritization of test cases has one advantage over a selection: it allows continuous testing until resources are exhausted or all test cases are executed, while always focusing on the most important test cases [22]. Test case selection, on the other hand, still requires the full execution of the selected set, which might still be very large. Thus, we will focus on test case prioritization in this paper. In particular, we aim to improve the test case prioritization for black-box testing, where no source code is available. This makes regression testing far more difficult, as traditional techniques analyze source code changes to identify important test cases [7, 16, 29].

To tackle black-box regression testing, we introduced a test case prioritization technique [19] which is based on ML. ML describes techniques which are able to learn from a given data set to extract information which is then applicable to other data instances [11, 27]. ML techniques are in particular useful for optimization tasks, where a certain optimization goal shall be reached in an efficient manner. ML algorithms are plenty and usually require large data sets to learn from, as this deduction step generates the knowledge required to perform the desired tasks on unknown data.

Different types of ML techniques exist. Two main categories to distinguish algorithms are *supervised* and *unsupervised* ML approaches [27]. Both rely on the notion of *training data*, i.e., data instances provided to extract knowledge. However, in supervised learning these instances contain a *label*, i.e., their corresponding correct output is pre-assigned, e.g., the correct class. For instance, supervised ML techniques can perform classification tasks, e.g., in spam detection [3]. In contrast, unsupervised techniques use unlabeled data. Clustering is one type of an unsupervised approach, where instances are grouped into clusters according to their features [27].

These types of ML approaches have been investigated for decades, and a wide range of specific algorithms have been created to perform specific ML tasks [11, 27]. To apply a specific ML algorithm, the input data is converted into a *feature vector representation*. Each feature is a distinct characteristic, e.g., the sender of a spam mail. The set of all features is a representation of a specific data instance. Based on the feature representation, ML algorithms aim to detect patterns in the data. Examples are similarities between instances, or the prediction of values, e.g., to predict the cost of a house based on its given features and the costs of other houses, which is an example for a regression task.

ML algorithms can also be used together as an *ensemble learning* approach [27]. Here, either different types of algorithms can be combined (*stacking*) or the same type of algorithm can be trained with different input to create a *boosting* approach using weak learners.

This paper focuses on supervised learning as we aim to learn from expert knowledge to predict the importance of new test cases. We also introduce forms of ensemble learning for test case prioritization.

3. Concept

The test case prioritization concept of this paper is an extension of our previous work [19]. Fig. 1 illustrates a schematic overview of the main phases of our test case prioritization approach. We give a brief overview of the main steps of the test case prioritization approach in the following.

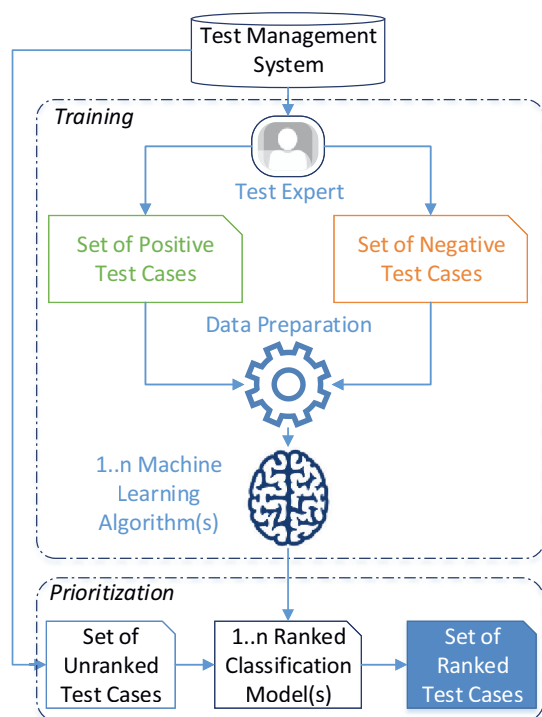


Fig. 1. Main Concept of the Black-Box Test Case Prioritization using Machine Learning

As shown in Fig. 1, the data we use to perform a test case prioritization is stored in a data management system. We are not restricted to specific types of data, database or system domain. However, we assume to have access to a defined set of *test cases*, a defined set of *requirements* and a set of *revealed failures*. In theory, each test case is linked to at least one requirement, e.g., how a certain function shall work. Failures, which have been revealed by a test case, should be linked accordingly. However, in practice this traceability is not always given. For our approach, we assume that the authors keep the data up to date and provide traceability between related artifacts.

A test expert has to select a training set for the ML algorithm. In particular, we require the expert to select a set of *positive test cases*, i.e., test cases which are of high importance, used regularly or are for some other reason important for the current version under test. To complement this step, the expert provides a set of *negative test cases*. These are of low importance, e.g., as the particular functionality has not been changed for many versions or is of low risk. Our approach is based on the idea of expert knowledge. Thus, we do not further restrict this step, but let the tester decide about the importance of particular test cases. While this is a manually performed step, we only require the expert to select a subset of test cases.

The training data is used as input for a machine learning algorithm. Our approach is compatible to various ML algorithms, which have to fulfill the following requirements:

- Supervised, as we want to emulate the decisions made by test experts based on two classes: *to test* and *not to test*
- Able to cope with large feature spaces with sparse data
- Result is a ranked classification model, i.e., an input value is provided with an output value, representing its priority

After the training data is selected, we extract features for test cases based on their meta-data, e.g., title, number of linked requirements or execution duration. In addition, we parse their textual description, a novelty among regression testing techniques [19]. Based on the latter, we compute a dictionary of all words contained in the test cases. We prepare the dictionary using natural language processing [6], i.e., tokenization [25], stemming and removal of stop words [28]. Each word represents a feature, which makes the preprocessing useful to reduce the vector space.

We are able to extract the following information for black-box test case prioritization:

- Test case description (natural language)
- Test case age
- Number of linked requirements
- Number of linked defects (history)
- Severity of linked defects
- Test case execution cost (*time*)
- Project-specific features (e.g., market)

Furthermore, we can apply our approach to an arbitrary set of features, which are used by the human expert for test selection. Thus, the set of features, which are considered as input for the machine learning, is selected by an expert before the learning phase commences. This is important for project-specific features.

After the training data is transformed into a feature representation, the ML algorithm computes a ranked classification model. Afterwards, we use this model to prioritize arbitrary, unknown test cases. The result is an ordered list of test cases according to their priority value. The goal is to identify important test cases with a higher likelihood to find failures.

4. Applied Algorithms

In this paper, we analyze the effectiveness of four different supervised ML algorithms. In this section, we give a brief overview of the applied algorithms, but refer the reader to additional literature on ML for a more in-depth understanding of their inner workings, which is out of scope for this paper [11, 27].

First, we apply *ranked support vector machines (SVM Rank)* [15] to solve the test case prioritization problem. We used this technique in our previous work [19]. SVM Rank is able to compute a ranked classification model even for large feature vectors and provided good results in previous work for black-box regression testing [19]. Similar to normal SVMs, the algorithm computes a hyperplane in the n -dimensional feature vector space to create maximized margin between two given classes according to their labels.

The second algorithm we apply is *K-Nearest-Neighbor (KNN)* [27]. KNN computes distances between neighbor instances and computes a value according to their labels. The constant k defines the number of neighbors, which are considered when computing the class of an unknown instance. For our approach, we set k to 5 and use Euclidean distance as these parameters provide the best results.

Third, we apply *logistic regression (Log Reg)* [14]. This technique computes the probability that a given entity belongs to a certain class by fitting a logistic regression curve to the data and performing a maximum likelihood estimation. We use two classes, i.e., to test or not to test. Test cases are ordered according to their probability that they belong to the former category.

The fourth ML algorithm we apply are *neural networks* [12]. They imitate the human brain and contain *neurons*, which are connected with each other in a layered form. Each neuron might fire given a certain input. We use two hidden layers to solve black-box test case prioritization.

Our approach is able to use all of these algorithms to compute priority (or probability) values for an arbitrary set of test cases, which indicate its importance for the particular system under test. The higher the computed value, the earlier the test case execution.

In addition to an isolated execution of the ML algorithms, we define two more approaches based on the idea of *ensemble learning* [27]. Here, the idea is to combine the results of different algorithms or classifiers to create an even more powerful ML approach. Hence, we introduce *historical* and *combinatorial ensemble learning*. Fig. 2 shows how n ML algorithms are used to regression test m software versions under test (VUT). The dotted lines represent samples for our ensemble learning concepts.

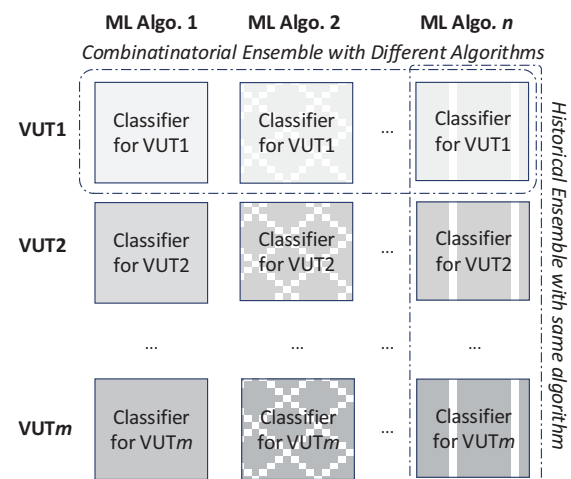


Fig. 2. Schematic Overview of Historical and Combinatorial Ensemble Approaches

First, we introduce the idea of *historical ensemble learning* of classifiers as indicated by the vertical dotted line in Fig. 2. Assuming that a software application is tested over the course of several versions. For each version, a new classifier can be trained by testers based on previous findings. Thus, several classifiers exist. Instead of always using the newest classifier, we propose to combine the classifiers of the n latest

versions to combine their results and improve the prioritization quality. Similar to the concept of *boosting* [27], we use classifiers of the same type, e.g., only neural networks. Consequently, old classifiers are not dispensed but reused. The impact on the result could be identical or decline with their age, i.e., version number.

Our second ensemble learning approach is to consider a set of classifiers for the same version as indicated by the vertical line in the first row in Fig. 2. Here, we combine the results of (a subset of) n different algorithms, e.g., neural networks, SVM, KNN and logistic regression. This combinatorial approach is similar to the concept of *stacking* [27]. When classifying test cases with each of these classifiers, we are able to combine the given priority values for a given test case and compute its average priority value. This provides an overall list for all test cases, which is adjusted according to all classifiers involved. This technique is flexible in terms of what classifiers to apply.

5. Evaluation

One of the main aspects of this paper is an analysis of the practical applicability of our test case prioritization approach. We implemented a prototype using the *Dlib.net* ML framework [17] and the *Accord.Net* ML framework [23].

In this paper, we extend our previous evaluation to a total of three industrial subject systems, dropping the academic system. To perform a structured quality assessment, we first describe our research question. Next, the subject systems are explained. Afterwards, we go into detail about the evaluation methodology. Next, we present and discuss the results for all three systems. An assessment of potential threats to validity concludes this section.

5.1 Research Questions

For our evaluation, we formulate the following three research questions, which we aim to answer in this paper:

RQ1: What is the impact of the test case description features on the quality of the different algorithms?

RQ2: Is there one particular ML algorithm, which is the best choice for black-box test case prioritization?

RQ3: Is it possible to train the system without the help of an expert to achieve satisfying results?

5.2 Subject Systems

In total, we assess our approach using three different subject systems. All three systems stem from the automotive domain. Compared to our previous work, we are able to assess the

technique's applicability for real-life data on a larger scale. Due to legal restrictions, we refer to the systems as *System A*, *B* and *C*. Each system describes different types of software testing projects and they involve different authors and stakeholders. We give a basic overview of the size of the three systems in Tab. 1. The table contains the number test cases, which are available for each project, the number of positive (*#Pos TC*) and negative (*#Neg TC*) test cases used for training, the number of failures (*#F*) linked to the training set as well as the vector size, i.e., the number of features extracted. We only use the linked failures in the training data later for evaluation.

Tab. 1. Subject System Overview

ID	#Total TC	#Pos TC	#Neg TC	#F	Vector Size
A	~1700	111	115	133	~1500
B	~2400	493	278	86	~3150
C	>10.000	213	133	26	~6400

The three subject systems focus on different software systems and are written by different persons, leading to a high variety on data quantity, quality and content. They even vary in their provided meta-data, i.e., some have user-defined features such as "release market". Our test case prioritization approach is able to handle different data artifacts, i.e., types of meta-data [19]. Thus, we are still able to apply the prioritization to these different projects, even though they do not provide the same features.

5.3 Methodology

Our technique aims to provide priority values to perform a guided test case prioritization. Thus, we aim to assess if our technique is indeed able to improve regression testing in terms of effectiveness. In science, this is measured using one particular metric: *Average Percentage of Faults Detected (APFD)* [22]. It computes how fast a set f of m failures is covered by n test cases. It returns a value between 0 and 1, whereas 1 is the theoretical optimum and, thus, the best value. In other words, a higher value indicates that failure revealing test cases are executed first according to the computed priority.

Formally, APFD is defined as follows [22]:

$$APFD = 1 - \frac{\sum_{i=1}^m TF_i}{n \cdot m} + \frac{1}{2n}$$

We measure APFD for all three different subject systems explained in the previous subsection. In particular, for system B and C, we let a test expert provide the required training data, i.e., a

set of positive and negative test cases. We do not guide the tester in this process. The test experts are only given the information about a desired set size of at least 100 test cases for both sets and that both, positive and negative test sets should be of similar quantity. For *system A*, no expert was available and we had to provide training data on our own, which we further explain in the discussion for RQ3.

As we use static data, i.e., are provided with a static set of test cases, requirements and failures, we are not able to detect new failures as test cases are not executed after prioritization. Hence, to compute an APFD value, we have to prepare the data set as follows: We split the set of failures in two subsets according to their age. Old failures are used for training, i.e., the failure content is available as features. New failures are used for testing, i.e., they are used for APFD computation only. The split is done in an uniform fashion, i.e., we split the failures in two sets of similar size where both sets contain about 50% of all failures. This allows us to test the approach based on unknown failures without influencing the trained model.

To perform a more precise analysis of our approaches, we perform a *k-fold cross validation* [27] on our data sets. In particular, we split the set of test cases (comprising both positive and negative test sets) in $k=10$ folds. While $k-1$ folds are used for training, one fold is used for testing. The testing fold is the one used for APFD computation. Only failures linked to test cases, which are in the testing fold, are considered for APFD computation. Thus, we can make sure that for each repetition of our experiments a new set of “unknown” failures is used for APFD, which reflects the usage of our approach in a real-life scenario. The experiment is repeated k times, where the testing fold differs for each repetition to increase confidence in the results.

We compute a random ordering of test cases 100 times for each fold of our cross-validation as comparison. We average the results.

5.4 Results and Discussion

Results for RQ1. We analyze the performance of our test case prioritization approach using the APFD metric. In particular, we run a k -fold analysis for our three subject systems to assess the effectiveness of our approach compared to a random prioritization.

For the first research question, we investigate how APFD is influenced when using the test case description feature in all combinations with other features compared to those feature combinations, which do not include the test case description.

To give a more detailed sample, we show particular APFD results for all algorithms for system C in Fig.3 and Fig.4. Both figures show boxplots for the different runs of feature-combinations for each technique. The plots show the median value (line in the middle of the box), the average value (only in Fig. 4, cross marker) and upper and lower quartiles (boxes above and below median) as well as the upper and lower boundary of APFD values achieved by each ML algorithm.

In particular, the figures show a boxplot for the random approach, SVM rank (SVM), K-nearest neighbor (KNN), Logistic Regression (*Log Reg*), Neural Networks (*Neural*) and an ensemble of all four ML algorithms. We use boxplots as we repeated each technique for all different feature combinations, once with test case description (cf. Fig. 3) and without (cf. Fig. 4).

The first thing we notice is that a random ordering produces an APFD of ~ 0.5 . In contrast, most of the ML techniques produce better results. To answer our question, we first analyze the effectiveness when using the test case description feature as seen in Fig. 3. Here, logistic regression performs best of the isolated ML algorithms with an average APFD of 0.69. However, KNN only produces an average APFD of 0.44, which is worse than the random ordering. The best overall result is achieved when combining all four approaches, boosting yields an average APFD of ~ 0.71 , i.e., it achieves the highest failure finding potential for this system.

When analyzing the results displayed in Fig. 4, we notice that feature combinations, which do not include the test case description features do worse than their counterparts. For KNN, the APFD even drops below a random ordering. When the test case description is not available to the ML algorithms, the quality decreases. No algorithm was able to increase its average APFD without using the test case description.

Tab. 2 shows an overview of all average APFD values achieved for all subject systems using the ML algorithms. We split the results for the feature combinations, which included the test case description and for those without. In addition, the average APFD value for each ML algorithm is shown. We mark the best APFD values for each system in bold font. As the results show, the results observed for system C reflect the results we gathered for all subject systems. While a random ordering was not able to produce good results, our applied ML approaches benefit from the usage of the test case description features significantly and are, sometimes, not effective without access to the description (e.g., KNN).

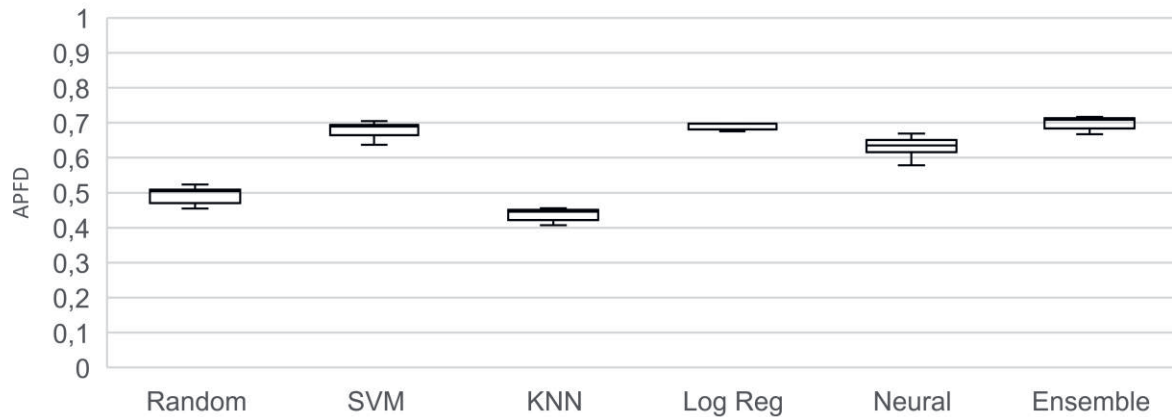


Fig. 3. APFD Values for Evaluation Repetitions for System C with Description-Related Features

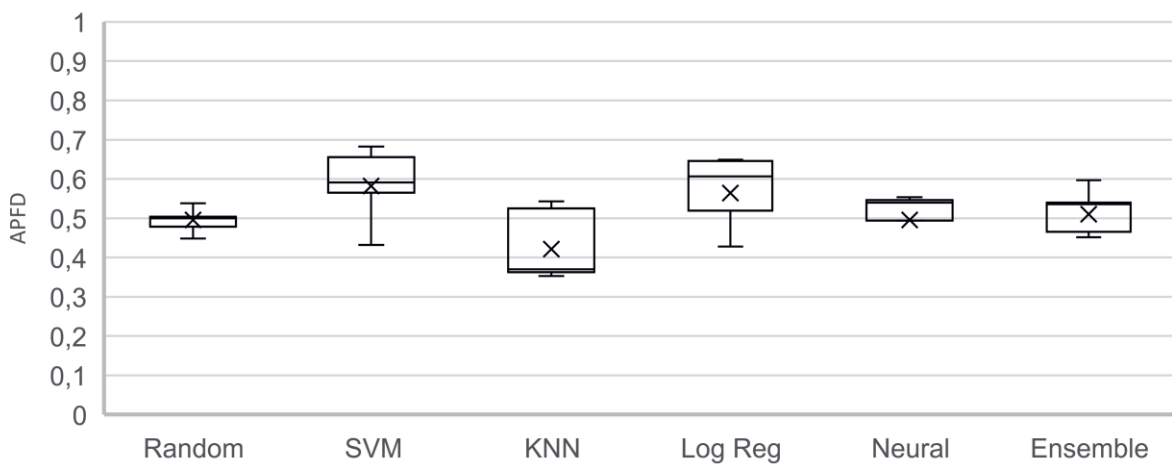


Fig. 4. APFD Values for Evaluation Repetitions for System C without Description-Related Features

Tab. 2. APFD Overview for all three Subject Systems and their Overall Average Value

System	Average APFD value with description				
	SVM	KNN	Log Reg	Neural	Boost.
A	0.68	0.69	0.75	0.7	0.72
B	0.64	0.52	0.66	0.56	0.57
C	0.68	0.44	0.69	0.63	0.7
Avg.	0.67	0.55	0.7	0.63	0.66
Average APFD value without description					
A	0.44	0.27	0.47	0.48	0.4
B	0.53	0.5	0.58	0.55	0.56
C	0.58	0.42	0.56	0.5	0.51
Avg.	0.52	0.4	0.54	0.51	0.49

In terms of *efficiency*, the most demanding ML algorithm is neural network. For all features selected for our largest system (System C), we measure a training time of ~17.3 seconds. KNN is the fastest with about 2.1 seconds. SVM produces a result after ~6.1 seconds and KNN takes 2.3 seconds. The subsequent prioritization is fast for either approach, it only takes milliseconds for each algorithm. These observations are equivalent for all subject systems. The test case description feature has the largest impact on the computational time due to the fact, that each word is a feature increasing the vector space up to 6400 features (cf. Tab. 1).

Overall, logistic regression seems to be the best choice in when investigating effectiveness and efficiency in combination.

Results for RQ2. To investigate research question 2, we apply all algorithms and their ensemble to all three subject systems. Tab. 2 shows the average APFD results of all algorithms. We notice that logistic regression outperforms the other applied ML algorithms in System A and B in terms of effectiveness and is

the second best choice in system C. This is the case for all combinations, i.e., with natural language artifacts and without. This shows that the performance of this algorithm is stable and, thus, the logistic regression seems to be a good choice for the test case prioritization approach.

The boosting approach using all four algorithms at once outperforms the logistic regression only in *System C* with an average APFD of 0.7. Thus, the overhead of computing all four approaches seems not worth the effort compared to running logistic regression in isolation. However, it might be worth to investigate a *weighted ensemble approach*, where certain classifiers have a higher impact due to their produced quality [27].

Results for RQ3. While we had access to test experts for two subject systems, we had to train *System A* without the help of an expert, which is a restriction to our approach. Therefore, we aim to answer research question 3 using this system.

To provide a meaningful training set without the help of an expert, we select test cases, which have found failures in the past to be of positive impact and, thus, be in the positive test set. The negative set contains only test cases without failures. Furthermore, for this particular project, each test case has a priority and severity value assigned on the 3-level scale by the designers. While these values are sufficient for test case selection, they are too coarse-grained to be used for prioritization. Thus, we use test cases with particular low priority and severity values as negative test cases.

As the results in Tab. 2 indicate, the machine learning was able to produce a sophisticated test case order for *System A*, which outperforms the random ordering. Thus, we validate research question 2. It is possible to train our system without detailed expert knowledge. In particular, the logistic regression algorithm was able to produce good results, with an average APFD value of 0.75.

We notice that it is necessary to provide certain data for training data without expert knowledge. Risk-based data, such as failure severity and impact, is useful to guide the training process, without focusing on experience. This is similar to risk-based testing [10].

5.5 Threats to Validity

We aim to mitigate any negative effects, which might influence our evaluation results. While we have developed the tool on our own, which could have caused some faults in the code, we performed intense testing to ensure the correct functionality of our prototype and its parameterization.

To increase the confidence in our results, we use three different case studies. Still, they all stem from the automotive industry, which could influence our findings. However, as different authors and testers maintain these systems and use them in a different context, we argue that our results show that our approach is applicable for different projects to improve a prioritization. Furthermore, we increase the trust in our results using k-fold cross validation.

For our evaluation, we only use a subset of ML algorithms applicable to our problem. Other algorithms might improve the test case prioritization quality even further. To tackle this issue, we used four popular techniques, which already produce desirable results. While further improvement is possible, our algorithm selection already shows the potential of the test case prioritization concept in real-world testing scenarios.

6. Related Work

Regression testing has been widely discussed in literature. Yoo and Harman [29] provide a complex survey of minimization, selection and prioritization techniques. Khatibsyarbini et al. [16] show in their survey that the set of test case prioritization publications is still growing in recent years. However, the main focus of most test case prioritization approaches is still a code analysis for priority computation [16].

Machine learning has been used to improve white-box testing in the past. Analyzing the code leads to a wide range of fault prediction approaches, which has been surveyed by Catal [5]. However, white-box approaches require code access, e.g., to analyze modified code snippets for their test relevance. As code access is not available, we have to investigate black-box regression testing approaches in more detail.

In terms of black-box regression testing, our previous work on black-box test case prioritization is most related to the concept presented in this work [19]. We used SVM Rank to compute priority values for natural language test cases. Khatibsyarbini et al. [16] show in their survey, that history and requirements-based approaches, which fall in the category of black-box related techniques, still only share 18% of the total number of publications in novel test case prioritization approaches until 2017. Fazlalizadeh et al. [9] present a greedy technique to prioritize test cases based on system level test data, such as failure history. Engström et al. [7] have extended this approach by using, among others, static priority values. However, they could not find a significant improvement compared to the previous approach. Agarwal et al. [1] use two different ML

techniques as automated oracles in black-box testing. Their findings show that the quality is based on the amount of available data. In contrast to this work, they use program input and output as features. Bhasin and Khanna [4] use neural networks for black-box testing. Here, test cases are defined as module state diagrams. Thus, their approach is model-based in nature and not applicable in a system testing scenario without providing the necessary graphs. De Souza et al. [24] present a multi-objective test case prioritization based on two objectives: minimization of execution costs and requirements coverage. They apply *particle swarm optimization* to achieve their goal. Their results outperform a random approach. In previous work, we defined a multi-objective test case selection approach for black-box testing [18]. We define seven different objectives to be optimized using genetic algorithms. The approach is able to achieve good precision and recall for certain objective combinations. Yoo et al. [30] introduce a clustering approach for test case prioritization. They use dynamic execution traces as input. Human experts prioritize these clusters, which is similar to our idea to incorporate expert knowledge in the process of regression testing.

7. Summary and Future Work

Conclusion. In this paper, we present different ML-driven approaches for test case prioritization in black-box testing. We extend our previous technique [19] by including other ML algorithms beside SVM Rank [15]. Furthermore, we discuss the idea of ensemble learning-based test case prioritization, i.e., combining the output of different ML algorithms for one version or the output of one algorithm for several versions.

We evaluated our approaches on three different subject systems, which stem from the automotive industry. We ran all four ML algorithms on all three systems and evaluated their effectiveness and efficiency. As baseline, we compared their performance against a randomized ordering. We are able to show that the natural language description of a test case is an important feature for test case prioritization, as it is able to increase the average APFD value for all ML algorithms on all subject systems. We also notice that, given certain meta-data, we are able to train the system without help of an expert.

In total, we are able to state that our test case prioritization approaches are able to outperform a random ordering significantly. The best performance is achieved when using logistic regression [14], which is used for the first time in this paper to solve the test case prioritization problem based on natural language artifacts.

Future Work. In our evaluation, we noticed a partial lack of traceability between artifacts, e.g. the link between failures and test cases is not always provided. The main reason for this issue is explorative testing, where testers do not strictly follow a protocol but rather test in a use-case driven environment. An example for this are test drives in the automotive industry, where testing is performed in an ad-hoc fashion.

The issue of missing traceability is reducing data quality and, therefore, the potential of our machine learning-driven test case prioritization approaches. Thus, we are investigating techniques, which are able to improve traceability in a semi-automatic fashion. By analyzing failures, we want to create automatic links to suitable test cases, which might have produced this failure. This improves data quality, test case coverage analysis and the potential for automatic test case prioritization. Furthermore, we want to investigate the potential of our historical ensemble approach to prioritize test cases. This requires a long-term evaluation setup, where different versions are tested in a live testing environment.

Acknowledgements

The author thanks Antony Beno Louison Jayapathy for fruitful discussions and his help with the realization of the presented concept.

References

- [1] D. Agarwal, D. E. Tamir, M. Last and A. Kandel. "A Comparative Study of Artificial Neural Networks and Info-Fuzzy Networks as Automated Oracles in Software Testing," in IEEE Transactions on Systems, Man, and Cybernetics - Part A: Systems and Humans, vol. 42, no. 5, pp. 1183-1193, 2012; doi: 10.1109/TSMCA.2012.2183590
- [2] P. Ammann and J. Offutt. Introduction to Software Testing (1 ed.). Cambridge University Press, New York, NY, USA, 2008. ISBN: 978-0521880381
- [3] F. Benevenuto, G. Magno, T. Rodrigues, V. Almeida. Detecting Spammers on Twitter. Proceedings - Collaboration, Electronic messaging, Anti-Abuse and Spam Conference (CEAS), 2010. doi:10.1.1.297.5340
- [4] H. Bhasin and E. Khanna. Neural network based black box testing. SIGSOFT Softw. Eng. Notes 39 - 2, 2014, pp. 1-6. doi: 10.1145/2579281.2579292
- [5] C. Catal, Software fault prediction: A literature review and current trends, Expert Systems with Applications, Volume 38, Issue 4, 2011, pp. 4626-4636, doi:10.1016/j.eswa.2010.10.024
- [6] G. G. Chowdhury. Natural language processing. Annual review of information science and technology, 37(1), 2003, pp. 51-89. doi: 10.1002/aris.1440370103

- [7] E. Engström, P. Runeson and A. Ljung, "Improving Regression Testing Transparency and Efficiency with History-Based Prioritization -- An Industrial Case Study," 2011 Fourth IEEE International Conference on Software Testing, Verification and Validation, 2011, pp. 367-376. doi: 10.1109/ICST.2011.27
- [8] G. Erdogan, Y. Li, R.K. Runde et al. *Int. Journal on Software Tools Technology Transfer*, 2014, 16: 627. doi: 10.1007/s10009-014-0330-5
- [9] Y. Fazlalizadeh, A. Khalilian, M. A. Azgomi and S. Parsa, "Prioritizing test cases for resource constraint environments using historical test case performance data," 2009 2nd IEEE International Conference on Computer Science and Information Technology, 2009, pp. 190-195. doi: 10.1109/ICCSIT.2009.5234968
- [10] M. Felderer and I. Schieferdecker. 2014. A taxonomy of risk-based testing. *Int. J. Softw. Tools Technol. Transf.* 16 - 5, 2014, pp. 559-568. doi:10.1007/s10009-014-0332-3
- [11] A. Géron. *Hands-on machine learning with Scikit-Learn and TensorFlow: concepts, tools, and techniques to build intelligent systems*. O'Reilly Media, Inc., 2017. ISBN: 978-1491962299
- [12] I. Goodfellow, Y. Bengio, A. Courville, "Deep learning". Vol. 1. Cambridge: MIT press, 2016. ISBN: 0262035618
- [13] M. J. Harrold, *Testing: a roadmap*. In *Proceedings of the Conference on The Future of Software Engineering (ICSE)*, 2000, ACM, pp. 61-72. doi: 10.1145/336512.336532
- [14] D. W. Hosmer Jr., S. Lemeshow, and R. X. Sturdivant. *Applied logistic regression*. Vol. 398. John Wiley & Sons, 2013. doi:10.1002/9781118548387
- [15] T. Joachims, "Optimizing search engines using clickthrough data". In *Proceedings of the eighth ACM SIGKDD international conference on Knowledge discovery and data mining (KDD '02)*. ACM, pp. 133-142. doi: 10.1145/775047.775067
- [16] M. Khatibsyarhini, M. Adham Isa, D. N.A. Jawawi, R. Tumeng, *Test case prioritization approaches in regression testing: A systematic literature review*, *Information and Software Technology*, Vol. 93, 2018, pp. 74-93. doi: 10.1016/j.infsof.2017.08.014
- [17] D. E. King. 2009. Dlib-ml: A Machine Learning Toolkit. *J. Mach. Learn. Res.* 10 (December 2009), pp. 1755-1758. doi: 10.1145/1577069.1755843
- [18] R. Lachmann, M. Felderer, M. Nieke, S. Schulze, C. Seidl, and I. Schaefer. *Multi-objective black-box test case selection for system testing*. In *Proceedings of the Genetic and Evolutionary Computation Conference (GECCO '17)*. ACM, 2017 pp. 1311-1318. doi: 10.1145/3071178.3071189
- [19] R. Lachmann, S. Schulze, M. Nieke, C. Seidl and I. Schaefer, "System-Level Test Case Prioritization Using Machine Learning," 2016 15th IEEE International Conference on Machine Learning and Applications (ICMLA), 2016, pp. 361-368. doi: 10.1109/ICMLA.2016.0065
- [20] M. M. Lehman, "Programs, life cycles, and laws of software evolution," in *Proceedings of the IEEE*, vol. 68, no. 9, 1980, pp. 1060-1076. doi: 10.1109/PROC.1980.11805
- [21] H. K. N. Leung and L. White, "Insights into regression testing (software testing)," *Proceedings. Conference on Software Maintenance*, 1989, pp. 60-69. doi: 10.1109/ICSM.1989.65194
- [22] G. Rothermel, R. H. Untch, Chengyun Chu and M. J. Harrold, "Prioritizing test cases for regression testing," in *IEEE Transactions on Software Engineering*, vol. 27, no. 10, pp. 929-948, 2001. doi: 10.1109/32.962562
- [23] C. R. Souza, "The Accord.NET Framework," <http://accord-framework.net>. São Carlos, Brazil. 2014.
- [24] S. de Souza, Luciano & Miranda, Péricles & Prudêncio, Ricardo & Barros, Flávia. *A Multi-Objective Particle Swarm Optimization for Test Case Selection Based on Functional Requirements Coverage and Execution Effort*. *Proceedings - International Conference on Tools with Artificial Intelligence, ICTAI*. pp. 245-252, 2011. doi: 10.1109/ICTAI.2011.45.
- [25] J. J. Webster and C. Kit. *Tokenization as the initial phase in NLP*. In *Proceedings of the 14th conference on Computational linguistics - Volume 4 (COLING)*, Vol. 4., 1992, pp. 1106-1110. doi: 10.3115/992424.992434
- [26] E. J. Weyuker, "Testing component-based software: a cautionary tale," in *IEEE Software*, vol. 15, no. 5, pp. 54-59, 1998. doi: 10.1109/52.714817
- [27] I. H. Witten, E. Frank, and M. A. Hall. 2017. *Data Mining: Practical Machine Learning Tools and Techniques (4th ed.)*. Morgan Kaufmann Publishers Inc. ISBN: 978-0-12-804291-5
- [28] Z. Yao and C. Ze-wen, "Research on the Construction and Filter Method of Stop-word List in Text Preprocessing," 2011 Fourth International Conference on Intelligent Computation Technology and Automation, Shenzhen, Guangdong, 2011, pp. 217-221. doi: 10.1109/ICICTA.2011.64
- [29] S. Yoo and M. Harman, *Regression testing minimization, selection and prioritization: a survey*. *Softw. Test. Verif. Reliab.*, 22: pp. 67-120, 2012. doi:10.1002/stvr.430
- [30] S. Yoo, M. Harman, P. Tonella, and A. Susi. *Clustering test cases to achieve effective and scalable prioritisation incorporating expert knowledge*. In *Proceedings of the eighteenth international symposium on Software testing and analysis (ISSTA)*. ACM, pp. 201-212, 2009. doi: 10.1145/1572272.1572296

Improving the efficiency of T&E for Aircraft and Mission Systems with more effective modeling and simulation

Jeff Baxter

Analytical Graphics Incorporated, 220 Valley Creek Blvd. Exton, PA 19341 U.S.A,

Abstract:

As technology advances, aircraft and mission systems continue to increase in capability and complexity while at the same time, the urgency has never been greater to deliver these systems in a timely manner. In order to maintain this balance, effective modeling and simulation tools are critical.

Modeling and simulation tools have continued to mature in order to meet the growing complexity and urgent timelines. According to a RAND report on **Test and Evaluation Trends and Costs for Aircraft and Guided Weapons [1]**, "Virtually all test programs now incorporate modeling and simulation."

Effective modeling and simulation tools enable flexible and interactive virtual environments that can be used to rapidly design flight routes. Sets of candidate test-point combinations in the assembly of test-cards can be virtually modeled to iteratively arrive at a test mission plan that is more efficient and more robustly designed than by more traditional methods.

Here we will review the application of modeling and simulation for dynamic planning, execution, and post-flight quick-look that has proven able to increase test-point density and more often ensure achievement of test-point objectives. Modeling application and iteration methods used to achieve more optimal test-flight designs will be discussed and contrasted with traditional contemporary methods.

Final consideration and discussion will describe the overall areas of positive T&E execution phase impact including practitioners' operations efficiency, flight effectiveness & efficiency, post-flight quick-look and forensics analysis and flight safety.

Key words: AGI, T&E, COTS, M&S, STK, Test and Evaluation Tool Kit.

Introduction

There is significant benefit to using a common modeling and simulation environment for evaluating aircraft performance and measures of mission effectiveness across all portions of the program lifecycle; from concept and engineering, through test and evaluation to training and operations.

Using a commercial modeling and simulation package maintains consistency in asset performance models, environments, and mission goals throughout the various phases of the project or program lifecycle. This ensures reliability and comparability in mission objective assessment. Additional efficiency gains are found through sharing models defined in early stages and passing them along to groups engaged in subsequent phases of product development. This reduces the amount of work to recreate models as well as lowers the risk of introducing errors due to mismatched modeling between applications.

Another benefit of commercial modeling and simulation tools is that they continue to advance in capabilities indefinitely as they're in continual use among many programs, whereas many custom, program-specific tools get terminated as their specific program ends or their authors move on.

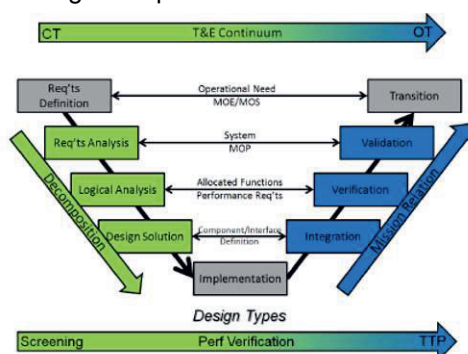


Fig. 1. Illustration of Decomposition and Mission Relation for Test Planning.

Additionally, having an extendable interface and open API allows for customization of workflows to fit the needs of each phase while continuing to use a consistent toolset.

This paper will emphasize the advantages of using commercially available modeling and simulation packages by highlight the use of the commercial-off-the-shelf software package Systems Tool Kit (STK), and the T&E focused extension called Test and Evaluation Tool Kit (TETK), produced by Analytical Graphics Incorporated (AGI).

Support of the Aircraft Project Lifecycle

Every project or program progresses through a series of stages to go from concept to implementation. For the purpose of this paper, we will address the following phases: CONOPS and Engineering, Procurement, Training and Simulation, and Test Validation and Operations.

Each phase has different requirements for modeling, analysis and visualization but having a single tool capable of participating in all phases will significantly reduce schedule risk and internal tool usage training requirements.

STK provides specific capabilities to evaluate aircraft systems and mission performance across all phases of development ranging from simplified or conceptual aircraft and sensor performance modeling, to detailed modeling in iterative trade study evaluations for engineering and testing of high fidelity mission models for test and evaluation or operational mission planning.

Commercial Modeling and Simulation Software

AGI's commercial off-the-shelf (COTS) software Systems Tool Kit (STK) is a time-based 2D and 3D modeling environment for evaluating land, sea, air and space system performance. This environment incorporates terrain data and radio frequency attenuation models, complex vehicle and sensor/payload dynamic behaviors, and the ability to compute relationships between objects based on those dynamics, terrain presence, and RF environment models. Such relationships between objects include (but are not limited to) relative position and orientation, line of sight (including obscuration from terrain), and communication link and radar signal quality.

Engineers, mission analysts, operators and decision makers can model complex aircraft and mission systems, from the aircraft performance to the payloads they carry and even the supporting assets on the ground or in space, all within the context of the mission and operating environment. System performance can be evaluated in real or simulated time, with reports, graphs and 3D visualizations to convey easily understandable results.

STK also provides an open API and software development kits for a variety of customization options. This includes analytical plugin points which are provided to allow users to augment any calculation or to compute custom measures of effectiveness in process with STK's other metrics. Alternatively, the engine behind the STK application can be used as an embeddable component in custom application development

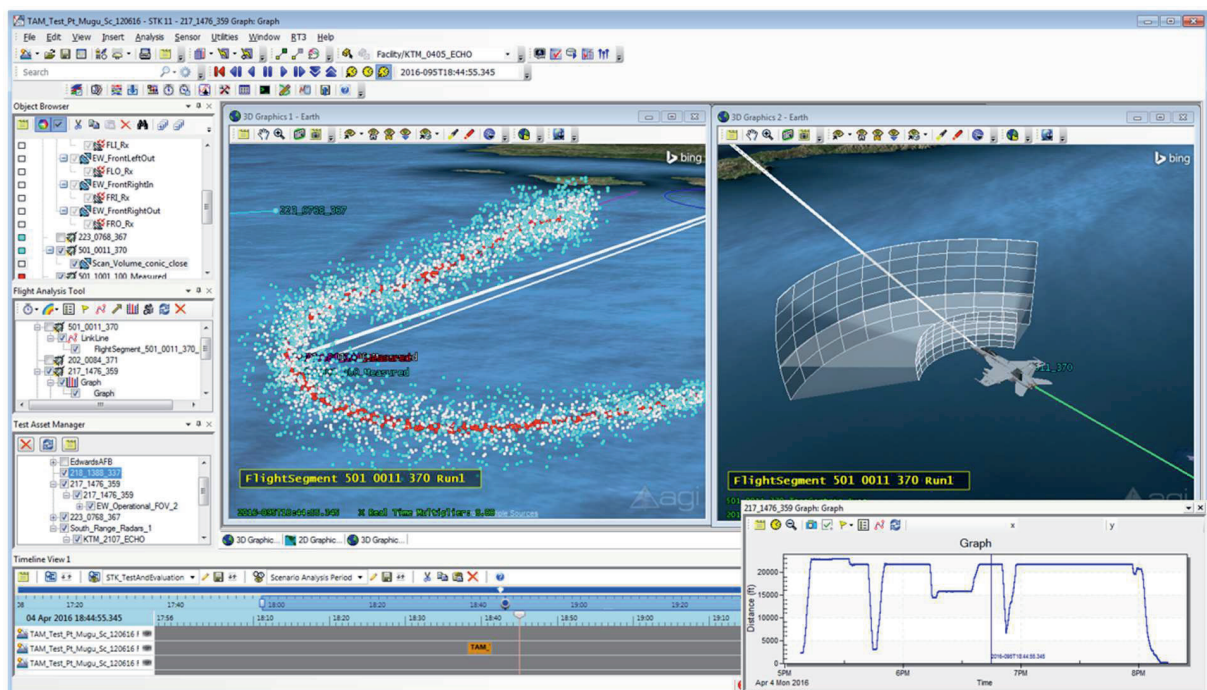


Fig. 2. Systems Tool Kit T&E Tool Kit Application

for desktop and mobile applications as well as server and web-based architectures.

This flexibility makes STK a great choice for customizing solutions for the high-fidelity needs of aircraft system test and evaluation program lifecycles.

CONOPS and Engineering

It is critical to create a realistic depiction of both the conceptual systems in question as well as provide a method for allowing invested engineering development of those systems.

Modeling and simulation environments can provide the capability to simulate flights based on true or conceptual performance parameters in a wide variety of mission profiles. Modeling end-to-end scenarios for mission threads and vignettes allows users to quickly assess measures of performance/measures of effectiveness (MOPs/MOEs) for missions such as ISR, strike, air defense, close air support (CAS), electronic warfare, and more. This gives analysts the ability to play out a series of concepts to evaluate performance of the design and then make adjustments and reevaluate.

Another critical feature is the basis for aircraft modeling to incorporate a 6 degree of freedom simulator to ensure accurate mission planning and modeling capabilities. This takes in aircraft configuration data (aerodynamic lift and drag curves, propulsion thrust properties, climb, cruise and landing characteristics) and propagates position and attitude through a series of user defined waypoints, holding patterns (circular, racetrack, raster search) and maneuvers (push/pull accelerations, rolls, loops). Missions adhere to the aircraft performance model with realistic bank and flight path angles, turn radii, climb rates and aircraft velocity. This provides the capability to evaluate the design's ability to perform missions and combat maneuvers or to out maneuver and accelerate away from combatants or ground targets.

Utilizing a wide variety of flight profile metrics helps aid in determining design effectiveness such as fuel state over a mission, thrust required to sustain maneuvers (including environmental characteristics like wind speed and direction), load factor and thrust/power remaining throughout maneuvers. Using these data sets, analysts can determine the feasibility of mission profiles and answer questions about the mission such as: 'can the aircraft design achieve the required climb rates?', 'does the proposed aircraft have the required range or endurance?',

'does the selected propulsion system provide the required thrust?'

This provides flight planning relative to other objects in the simulated scenario including the mission environment and the local terrain profile. This allows for easily designing formation flying maneuvers, sensor pointing and weapons drops on stationary or moving targets, low altitude terrain-following maneuvers and inflight refueling, just to name a few. Incorporating GIS data also provides the ability to establish flight corridors and no-fly zones to aid in mission planning.

In addition to flight performance is the need to manage a wide variety of additional mission system models and performance metrics which



Fig. 3. Flight Plan Editing in STK

provides context to the mission plan. Modeling the other subsystems, payloads and objects in the mission (communications, electronic countermeasures, weapons performance, ground based radars, communications packages and refueling capabilities) can help create a full understanding of the aircraft's capabilities such as range and endurance, the ability to avoid detection while closely approaching adversary radars, and kill chain efficiency.

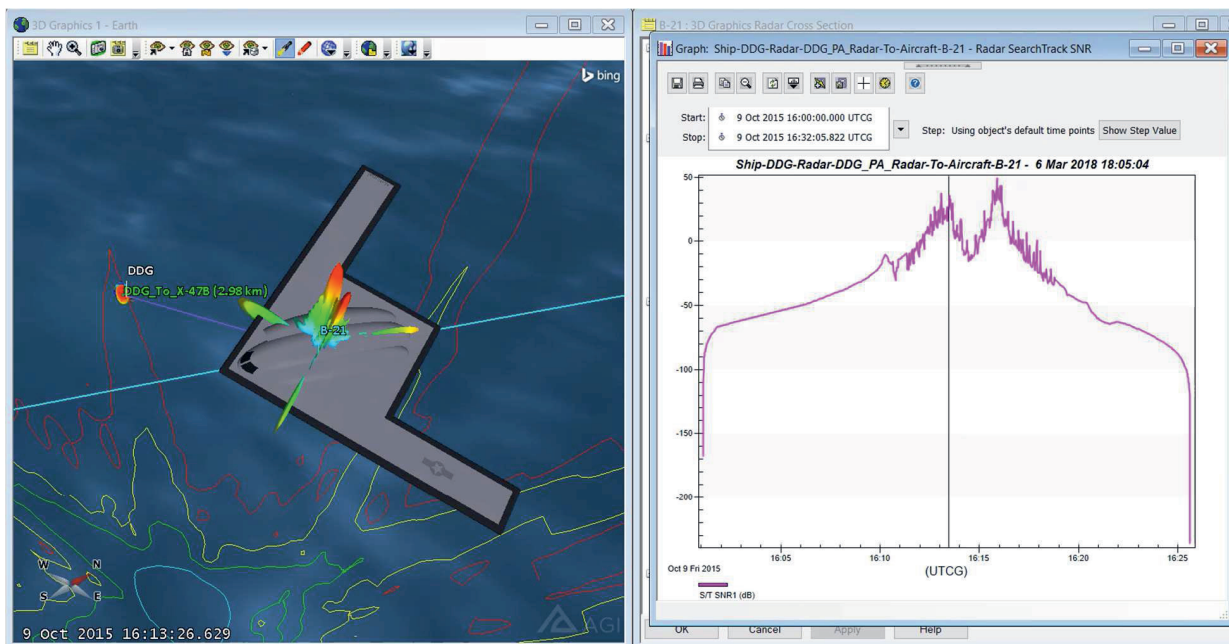


Fig. 4. Calculated Radar Detection of Simulated Target – Showing Signal to Noise Ratio (SNR)

An example of a mission evaluation might be determining how bank angles during fighter maneuvers may exceed sensor gimbal limits or field of regard causing loss of line of sight between sensors and targets, or understanding the minimum number of aircraft required to perform ISR coverage of various size regions dependent upon fighter performance and launch/recovery locations.

Taking into account attitude changes in aircraft throughout flight plans provides relative orientation between all other objects and reference frames in the modeled scenario. When an aircraft climbs or banks, the attached payloads rotate appropriately. For example, with a series of receiver antennas mounted about the aircraft, the antenna gain patterns maintain their orientation with respect to the rolling aircraft frame which translates to a reorientation in the Earth fixed reference frame. Knowing how the range and angles between other transmitters and the rolling aircraft change over time allows software simulations to determine which antenna and what part of its gain pattern is receiving the incoming signal and therefore how the link budget changes during the maneuver. Using information like this, engineers can design or select more appropriate antennae and determine the appropriate number and location of antennae to optimize link availability during expected operations of the aircraft.

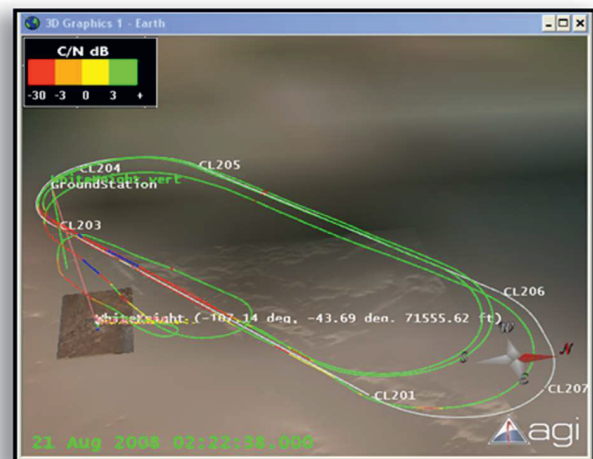


Fig. 5. Flight Plan in STK Showing Predicted Communications Link Quality via Path Colorization

With regards to the fighter kill chain (the time to find, fix, track, target, engage and assess), having the ability to model all the various sensors, weapons and timing of events in tandem with the fighter and target performance (stationary or moving) allows for the entire process to be simulated and evaluated early on in the project development. Sensor fields of view can be modeled, detection and tracking algorithms can be integrated, GPS receivers and position accuracy can be evaluated, and even weapon guidance modes can be simulated. Bringing all these together allows for trade studies to be conducted to find weaknesses and assess solutions to improve kill chain effectiveness.

Having these capabilities exist in a simulated software environment provides analysts with the tools to iterate through a series of trials (changing aircraft performance characteristics and sensor details or moving the targets and adversary aircraft) and having the flight path automatically update for the new mission parameters. This makes it possible to efficiently evaluate a large mission deck and determine either how well a specific aircraft design will perform in a series of missions or what the requirements need to be to achieve the goals of each mission, such as wing loading, thrust and sensor/payload requirements.

Acquisition

Proposed system designs can be explored within modeling and simulation packages and results can be compared and constrained to requirements, effectively determining whether or not the suggested system is capable of accomplishing the mission goal. For procurement of new systems, there is often the option to trade out various components (sensors/radars, weapons, etc.) and software simulation provides an analytical environment for direct comparison of component choices and their relative performance in current and future missions.

Aircraft performance models can be established for all platform choices such that each platform can be run through the same mission profiles and evaluated. Beyond the base platform, the simulated communications and radar capabilities provide ways to evaluate the effectiveness of various payload options and their effect on the overall mission performance of the aircraft and its systems under consideration. This provides a simple way to investigate the feasibility of different system designs in both measures of performance as well as implementation complexity or even overall system cost. For example, if a weapon has its own radar and is capable of guiding itself to an intended target, how much quicker can the aircraft be re-tasked rather than the aircraft's radar being required to guide the weapon to its target? Or for electronic countermeasures, which systems significantly improve an aircraft's ability to avoid being tracked by ground radars or incoming missiles?

By employing a robust modeling and simulation environment, these system design options can easily be linked to acquisition decisions and give designers and decision makers a common tool for validating and verifying design decisions.

Test and Evaluation

Modeling aircraft in a simulation environment prior to testing helps maximize the number of tests a vehicle can perform per flight such that fewer flights overall are required, and ultimately contributes to saving time and money. The use of an end-to-end modeling and simulation package such as STK ensures a higher probability of having a successful flight, again reducing the number of required flights to accomplish a full evaluation of aircraft subsystems. The same models used in the design phase can easily be passed along to test and mission planners so that all of the high fidelity design work can be used to optimize flight planning.

These pre-mission simulation activities provide the ability to coordinate many objects and their interactions and intended behaviors. The time-dynamic nature of STK provides the tools to synchronize position and orientation of all assets to maximize test efficiency.

This concept was proven to help avoid flights for F-35. One of the test flights called for exercising all sensors for one of their subsystems in the same flight. Because STK could model all of the sensors and their fields of view, along with the aircraft routes and orientations, one of the test flight engineers simulated the flight and determined that it wouldn't achieve the desired test point. Instead, he modified the route in STK which called for an additional maneuver, and saved the test flight. Not only did this save a lot of money by not flying a poorly designed test, but it also saved a lot of time since they didn't have to wait for the data to come back from the real flight before realizing it wouldn't work.

Simulating the test with supporting assets beforehand can also reveal the potential to fill white space with additional test points. For example, resetting a formation may also result in a flight path that presents an easy opportunity to test a given set of antennae at no extra cost.

Having the test plan plotted in a time-dynamic simulation environment then provides the ability to conduct pretest rehearsals or make quick changes on the day of the test. Rather than putting pilots in a real time simulator and flying the entire mission just to determine whether or not test metrics are collected as expected, operations can be simulated in faster-than-real-time to generate test metrics and evaluate test quality. Moving this process further up the chain also yields significant time savings if test planners can evaluate each test procedure before even constructing the test mission deck, long before test pilots are involved.

On the day of the test, if flight conditions change, for example excessive winds that require the test aircraft to crab into the wind altering the geometry of the plan, a decision can be made as to whether or not adjustments to the flight plan can compensate for the crab angle or if the test is infeasible. This makes for a much more informed go-or-no-go decision, potentially saving both time and operational testing costs.

In addition to pretest planning, STK is also used for post mission playback and test validation. It provides the capability to plot the flight path, play back the mission at faster or slower than real time, visually inspect specific events and add visual indicators for test results such as colorized flight paths, communication link indicators and dynamic data displays. Test result scenarios can then be shared as images, movies or hosted web-based visualizations.

Northrop Grumman Integrated Systems used the STK desktop application to evaluate communications systems for airborne platforms. They were specifically concerned with performance based on antenna placement on the aircraft. After modeling the gain pattern, location and orientation of the antenna, multiple flight profiles were evaluated to understand the coverage and blockages they would encounter during the test. By modeling the communications system and selecting optimal flight profiles before their test flights they were able to save millions of dollars in reduced number of flight tests as well as allowing them to deliver on schedule. One of the Northrop Grumman engineers, Bruce MacDougall, referred to the process as “valid flight testing at your desk”.

Operations

Moving beyond the test phase and into operations, an end-to-end modeling and simulation package can continue to provide performance evaluation in mission planning and real time operations.

Because STK offers a fully documented application programming interface (API), custom applications can be created on the same foundation as the engineering and planning tools. These custom interfaces can provide a simplified workflow which is tailored to the specific operator’s needs, only providing the features required for mission planning with the fewest number of inputs. This allows for individuals to take advantage of all the high fidelity analysis provided by the software, but without the need to learn the workflow for the detailed engineering tools available in the commercial desktop version of the application. This same API makes it possible to embed

specific capabilities into existing applications. Since many operational systems cannot be fully replaced due to cost of development and time to retrain all of the operators, plugins can be integrated to augment current capabilities and provide additional functionality without building from scratch or having to change well known workflows.

In areas of real time operations, STK supports live data feeds such as DIS, HLA, and other custom data feeds as necessary to form a complete Common Operational Picture (COP). Entity tracks for all vehicles and resources involved in the operation can be imported into this same environment exposing the ability to compute relationships in real time: who can see whom, where communications are available, where the areas of interest are and what assets are closest to them, and other mission critical information. Decision makers can intelligently sift through the vast amounts of data to issue well-informed commands.

Summary

The commercial maturity of computer based modeling and simulation software packages provides a depth and breadth of capabilities to engineering activities, and an ease of integration within overall flight test and evaluation efforts. These modeling methods enable the evaluation of systems at reduced risk, and with significantly reduced cost.

Software capabilities are perfectly aligned for concepts development, mission analysis, and engineering design of systems under study while providing an invaluable tool in the study and development of design considerations and requirements in preparation for acquisition activities.

Leveraging COTS modeling and simulation software provides unparalleled support across multiple aspects of the operational system program life cycle from system development to operational deployment.

References

- [1] RAND Corporation. (2004). Test and Evaluation Trends and Costs for Aircraft and Guided Weapons. Retrieved from https://www.rand.org/content/dam/rand/pubs/monographs/2004/RAND_MG109.pdf

169 MHz LoRa Network	11.3	exchange format	3.1
3D analysis	10.4	experimental tests	2.1
A400M	10.1	external cameras	10.1
Acceleration Sensors	1.1	Ferroelectric Ceramics	1.1
accuracy estimation	7.2	fibre Bragg gratings	7.3
Aeronautical Ad-hoc Networks	11.2	Fibre Channel	6.1
Aeronautical Mobile Telemetry	8.3	Fibre Optical	6.1
AFLoNext	9.5	Field Programmable Gate Arrays	10.2
AGI	12.5	FISINT	6.2
air-to-ground (A2G)	11.2	flap deflection	7.3
analysis	10.5	Flexible	11.1
animal tracking	5.2	flight test	12.1
Artificial Intelligence	9.1	Flight Test Instrumentation	9.4, 9.5
ATRA	9.5	flight vibration test	9.5
Autonomous Telemetry Devices	11.3	FollowMe	10.1
autopilot	10.5	FTI	9.2, 9.4, 12.2
Beamforming	4.1	FTI Architecture	11.1
BeiDou III satellites	4.3	GNSS	5.1
Best Source Selection	2.3	GPS	6.2
bi-directional	8.1	GPS/GNSS locations	5.3
bidirectional communication	11.4	Hardware-/Software Partitioning	4.1
biodiversified forests	5.2	high lift wing	7.3
biotelemetric system	5.2	high performance	10.5
Black-Box Software Testing	12.4	hot-wire anemometer	7.1
blade deformation	7.4	HSV	10.1
camera calibration	10.1, 10.4	Hydro Electrical Infrastructures	11.3
certification	11.5	ICP®	1.1
Cloud-based telemetry solution	11.3	image processing	10.4
cockpit display	10.3	iNET	8.4
coding	2.2	Integrated Solutions	9.3
Cognitive State	9.1	Intelligent	11.1
compression	3.3	interference signal environment	5.3
connectivity	11.5	IPCT	7.2, 7.4
Consumption	9.4	IRIG 106	2.2
Correlating Best Source Selectors	2.3	IRIG-106	8.4
COTS	12.5	Jamming	6.2
CRISP-DM	12.3	JSON	3.3
DAS	3.2	knowledge discovery in databases	12.3
DASP	9.2	landing gear	9.5
DASS	10.1	laser	2.4
Data	11.5	laser communication	11.2
Data Acquisition	2.3, 9.3, 12.1	laser vibrometer	7.1
Data Acquisition Configuration	9.2	link availability	2.2
Data Bus	6.1	Load	1.4
Data mining	12.3	LoRa	5.1
data quality metric	2.2	LoRa systems	5.2
data validation	12.1	low level flight	10.5
Database	9.2	Low Pass Filter	1.1
decline	4.2	Low Power	5.1
deformation measurement	7.2	Low Temperature Coefficient (LTC)	1.1
demonstrator	9.4	M&S	12.5
distributed DAQ	9.5	Machine Learning	9.1, 12.4
diversity	2.2	Machine vision	10.3
DQDS	2.1	MDL	3.2
DQE	2.3	MEMS	1.7
dynamic	8.1	metadata	3.3
encryption	3.3	MIL-STD-1553B	6.1
Energy Harvesting	5.1	MIL-STD-1760	6.1
errors and vulnerabilities	5.3	Miniature-DAU	9.3

Missile Test	9.3	Smart Utility Networks	11.3
mobile devices	12.1	Software	12.2
Mobile Systems	10.2	Spectrum Efficiency	8.3
monitoring	10.5	Spectrum Efficient Technologies & Applications	8.2
Network	11.1	Spectrum Encroachment	8.3
Network Based Telemetry	8.2	Spectrum loss & Encroachment	8.2
Network Environment	8.2	Spectrum Sharing	8.3
Networking	8.4	Spoofing	6.2
object-oriented	3.3	steerable directional antennas	2.1
Open Standards	3.2	stereoscopic imaging	7.4
Optical fibre sensors	7.3	STK	12.5
optical measurements	7.4	store separation	10.4
optimization	2.4	Stress Level	9.1
optoelectronics system	7.2	System on Chip	4.1
OTX	3.1	System Testing	12.4
Overload	1.1	T&E	12.5
Parallelisation	10.2	telemetry	4.3, 6.2, 8.1, 8.2
Parallelization	4.1	Telemetry Network System	11.4
Photogrammetry	7.2, 10.1	Test and Evaluation	8.2
Plug-in	9.2	Test and Evaluation Tool Kit	12.5
process model	12.3	Test Case Prioritization	12.4
propagation calculation	4.2	Test Infrastructure	8.2
propeller aerodynamics	7.1	test knowledge	3.1
prototype	11.5	test language	3.1
Quality of Service	8.3	Test Resource Management Center	8.2
quasi-real time	5.2	test technology	1.7
Radio Frequency (RF) Spectrum	8.3	Time synchronization	1.4, 1.7
RCC	8.4	TmNS	8.4, 11.4
real time	10.4, 12.1	transhorizon NLoS propagation	2.1
real-time	8.1	tunnel	4.2
Real-time Image Processing	10.2	two-layer	4.3
Real-Time Position Tracking	5.1	UAV Test	9.3
record	11.4	UHF frequency	4.2
record and replay systems	5.3	UHT-12 TM	1.1
Regression Testing	12.4	unattended test	2.4
replay	11.4	USV	2.1
Requirements Engineering	9.4	value	11.5
research	9.4	vehicle diagnostics	3.1
RF amplifier	4.2	Versatile	11.1
rocket-ground wireless interface	2.4	vibration	1.7
rotating camera	7.4	video measurement	10.3
Rotor system	1.4	Visual Recognition Systems	10.2
safe separation High Speed Cameras	10.1	Weight	9.4
safety in autonomous driving	5.3	wind tunnel	7.3
sensorbased indoor climate data	12.3	Wireless	8.2
serial	8.1	wireless network	1.7
shedding frequencies	7.3	Wireless Transmitting	1.4
short message service	4.3	XdefML	3.2
short message terminal	4.3	XidML	3.2
simulate	10.5	XML	3.2, 9.2
Size	9.4		